DFG Schwerpunktkolloquium

IODP - ICDP

GEOMAR, Kiel

7.3. - 9.3. 2012

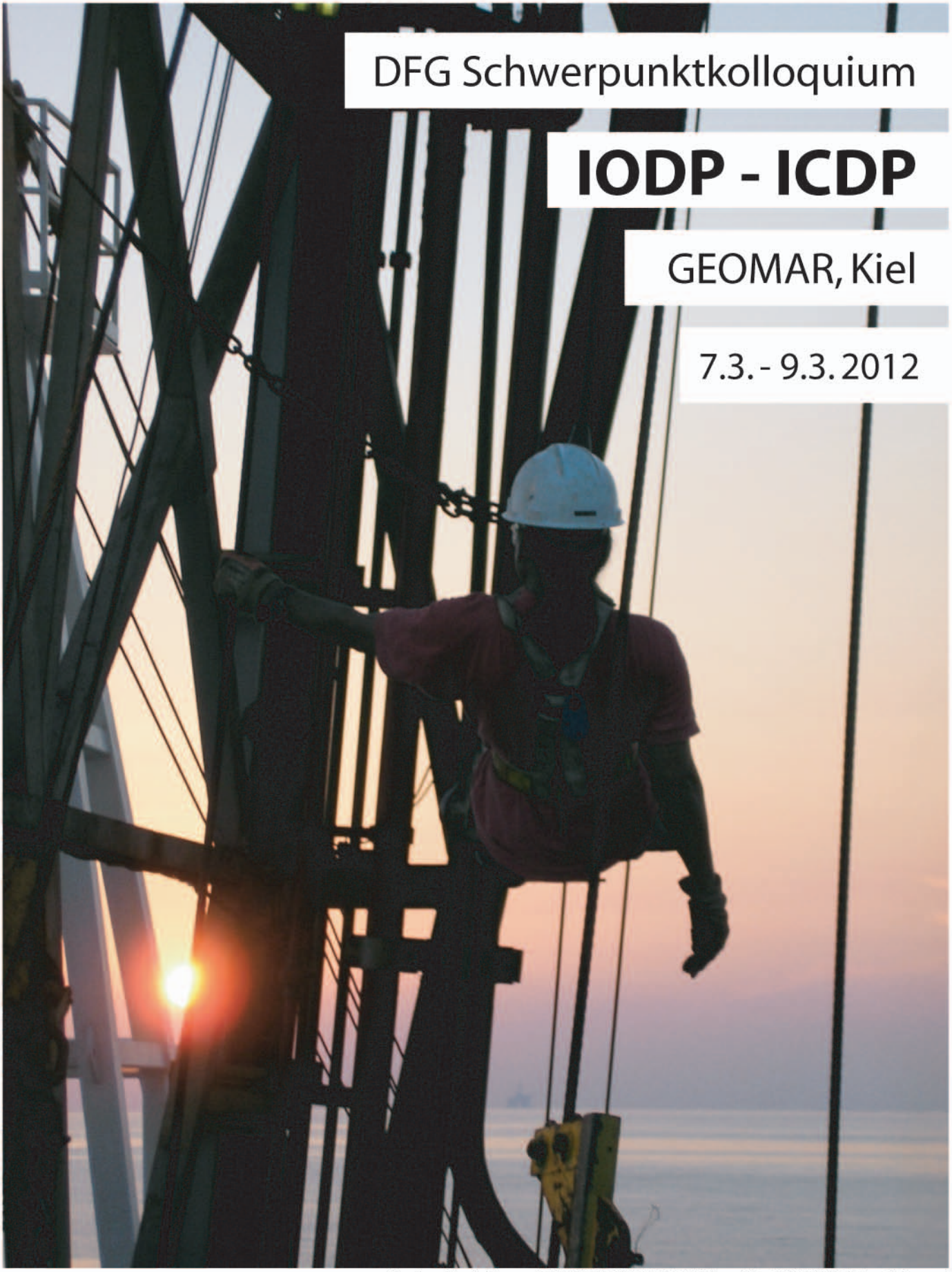

Roughneck im Bohrturm auf R/V JOIDES RESOLUTION, IODP Expedition 308, Juli 2005 (Foto: J. Behrmann)

icdp Deutschland

IODP
INTEGRATED OCEAN DRILLING PROGRAM

GEOMAR

Teilnehmerliste

Name	Vorname	Institution und Ort
Almeev	Renat	Institut für Mineralogie, Leibniz Universität Hannover
Andreev	Andrej	Institut für Geologie und Mineralogie, Universität Köln
Antz	Benny	Universität Heidelberg
Assis Fernandes	Vera	Museum für Naturkunde, Leibniz-Institut für Evolutions- und Biodiversitätsforschung, Humboldt-Universität Berlin
Bach	Wolfgang	Universität Bremen
Bahr	André	Institut für Geowissenschaften, Goethe-Universität Frankfurt
Barckhausen	Udo	Bundesanstalt für Geowissenschaften und Rohstoffe (BGR), Hannover
Baumann	Karl-Heinz	Universität Bremen
Beermann	Oliver	Institut für Geowissenschaften, Christian-Albrechts-Universität Kiel
Behrens	Harald	Institut für Mineralogie, Leibniz Universität Hannover
Behrmann	Jan	Helmholtz-Zentrum für Ozeanforschung Kiel (GEOMAR)
Beier	Christoph	GeoZentrum Nordbayern, Universität Erlangen-Nürnberg
Betzler	Christian	Geologisch-Paläontologisches Institut, Universität Hamburg
Blöthe	Marco	Bundesanstalt für Geowissenschaften und Rohstoffe (BGR), Hannover
Böhm	Evelyn	Universität Heidelberg
Böhm	Florian	Helmholtz-Zentrum für Ozeanforschung Kiel (GEOMAR)
Bolte	Torsten	Institut für Mineralogie, Leibniz Universität Hannover
Bornemann	André	Institut für Geophysik und Geologie, Universität Leipzig
Bosch	Frank P.	E.ON Energy Research Center, RWTH Aachen
Botcharnikov	Roman	Institut für Mineralogie, Leibniz Universität Hannover
Brandl	Philipp	GeoZentrum Nordbayern, Universität Erlangen-Nürnberg
Bräuer	Karin	Helmholtz-Zentrum für Umweltforschung (UFZ), Halle
Brauer	Achim	Helmholtz-Zentrum Potsdam, Deutsches GeoForschungsZentrum
Breuker	Anja	Bundesanstalt für Geowissenschaften und Rohstoffe (BGR), Hannover
Brumsack	Hans	Institut für Chemie und Biologie des Meeres (ICBM), Carl von Ossietzky Universität Oldenburg
Buske	Stefan	Institut für Geophysik und Geoinformatik, TU Bergakademie Freiberg
Contreras	Lineth	Institut für Geowissenschaften, Goethe-Universität Frankfurt
Conze	Ronald	Helmholtz-Zentrum Potsdam, Deutsches GeoForschungsZentrum
Cukur	Deniz	Helmholtz-Zentrum für Ozeanforschung Kiel (GEOMAR)
Dählmann	Anke	Department of Geotechnology, TU Delft
De Campos	Christina	Ludwig-Maximilians-Universität München
de Schepper	Stijn	Department of Earth Science, University of Bergen
Dersch-Hansmann	Michaela	Hessisches Ministerium der Justiz, für Integration und Europa, Wiesbaden
Deutsch	Alex	Universität Münster
Diester-Haaß	Liselotte	Universität des Saarlandes, Saarbrücken
Drath	Gabriela	IODP, Bundesanstalt für Geowissenschaften und Rohstoffe (BGR), Hannover
Dullo	Christian	Helmholtz-Zentrum für Ozeanforschung Kiel (GEOMAR)
Dultz	Stefan	Institut für Bodenkunde, Leibniz Universität Hannover
Dupont	Lydie	MARUM Universität Bremen
Ehmann	Sebastian	Institut für Geophysik und extraterristrische Physik, Technische Universität Braunschweig
Engelen	Bert	Institut für Chemie und Biologie des Meeres (ICBM), Carl von Ossietzky Universität Oldenburg
Engelhardt	Tim	Institut für Chemie und Biologie des Meeres (ICBM), Carl von Ossietzky Universität Oldenburg
Erbacher	Jochen	IODP, Bundesanstalt für Geowissenschaften und Rohstoffe (BGR), Hannover
Erzinger	Jörg	Helmholtz-Zentrum Potsdam, Deutsches GeoForschungsZentrum
Fallahi	Mohammad	Universität Leipzig
Fanara	Sara	Institut für Mineralogie, Leibniz Universität Hannover
Fehr	Annick	E.ON Energy Research Center, RWTH Aachen
Felis	Thomas	MARUM Universität Bremen
Fiebig	Jens	Institut für Mineralogie, Leibniz Universität Hannover
Förster	Verena	Universität Köln
Francke	Alexander	Institut für Geologie und Mineralogie, Universität Köln
Frank	Ute	Helmholtz-Zentrum Potsdam, Deutsches GeoForschungsZentrum
Friedrich	Oliver	Institut für Geowissenschaften, Goethe-Universität Frankfurt
Fütterer	Dieter	Alfred-Wegener-Institut für Polar- und Meeresforschung (AWI), Bremerhaven
Gärtner	Claudia	Westfälische Wilhelms-Universität Münster
Gebhardt	Catalina	Alfred-Wegener-Institut für Polar- und Meeresforschung (AWI), Bremerhaven
Geldmacher	Jörg	Helmholtz-Zentrum für Ozeanforschung Kiel (GEOMAR)
Gischler	Eberhard	Institut für Geowissenschaften, Goethe-Universität Frankfurt
Glomb	Vera	Institut für Geophysik und Geoinformatik, TU Bergakademie Freiberg
Gohl	Karsten	Alfred-Wegener-Institut für Polar- und Meeresforschung (AWI), Bremerhaven
Götze	Hans-Jürgen	Institut für Geowissenschaften, Christian-Albrechts-Universität Kiel
Grevemeyer	Ingo	Helmholtz-Zentrum für Ozeanforschung Kiel (GEOMAR)
Griess	Juliane	Alfred-Wegener-Institut für Polar- und Meeresforschung (AWI), Potsdam
Groeneveld	Jeroen	Universität Bremen
Grützner	Jens	Alfred-Wegener-Institut für Polar- und Meeresforschung (AWI), Bremerhaven
Grunert	Patrick	Institut für Erdwissenschaften, Universität Graz
Gussone	Nikolaus	Institut für Mineralogie, Westfälische Wilhelms-Universität Münster
Haase	Karsten	GeoZentrum Nordbayern, Universität Erlangen-Nürnberg
Hahn	Annette	GEOPOLAR, Universität Bremen
Hammerschmidt	Sebastian	MARUM Universität Bremen
Harjes	Hans-Peter	Institut für Geophysik, Ruhr-Universität Bochum
Harms	Ulrich	Helmholtz-Zentrum Potsdam, Deutsches GeoForschungsZentrum
Hathorne	Ed	Helmholtz-Zentrum für Ozeanforschung Kiel (GEOMAR)
Hauffe	Torsten	Justus Liebig Universität Giessen
Heide	Klaus	Universität Jena
Heldt	Matthias	IODP, Bundesanstalt für Geowissenschaften und Rohstoffe (BGR), Hannover
Henrich	Rüdiger	Universität Bremen
Hepp	Daniel	MARUM Universität Bremen
Herrle	Jens	Institut für Geowissenschaften, Goethe-Universität Frankfurt
Hess	Kai-Uwe	Ludwig-Maximilians-Universität München
Hesse	Reinhard	Earth & Planetary Sciences, McGill University, Montreal
Heydolph	Ken	Helmholtz-Zentrum für Ozeanforschung Kiel (GEOMAR)
Hinz	Karl-Heinz	Verwaltungsunion Hannover

Hockun	Katja	MARUM Universität Bremen
Hoernle	Kaj	Helmholtz-Zentrum für Ozeanforschung Kiel (GEOMAR)
Höfig	Tobias	TU Bergakademie Freiberg
Hofmann	Peter	Institut für Geologie und Mineralogie, Universität Köln
Hohmann	Timo	Helmholtz-Zentrum für Ozeanforschung Kiel (GEOMAR)
Holbourn	Ann	Institut für Geowissenschaften, Christian-Albrechts-Universität Kiel
Holtz	François	Institut für Mineralogie, Leibniz Universität Hannover
Holzheid	Astrid	Institut für Geowissenschaften, Christian-Albrechts-Universität Kiel
Horsfield	Brian	Helmholtz-Zentrum Potsdam, Deutsches GeoForschungsZentrum
Hötzel	Sebastian	MARUM Universität Bremen
Hunze	Sabine	Leibniz-Institut für Angewandte Geophysik (LIAG), Hannover
Husen	Anika	Institut für Mineralogie, Leibniz Universität Hannover
Ikari	Matt	MARUM Universität Bremen
Jöns	Niels	Universität Bremen
Jung	Claudia	Institut für Geowissenschaften, Goethe-Universität Frankfurt
Kahl	Wolf-Achim	Universität Bremen
Kallmeyer	Jens	Universität Potsdam
Karas	Cyrus	Institut für Geowissenschaften, Goethe-Universität Frankfurt
Keyser	Matthias	Bundesanstalt für Geowissenschaften und Rohstoffe (BGR), Hannover
Khélifi	Nabil	Helmholtz-Zentrum für Ozeanforschung Kiel (GEOMAR)
Kirchner	Clemens	Institut für Mineralogie, Leibniz Universität Hannover
Klügel	Andreas	Universität Bremen
Knebel	Carola	Helmholtz-Zentrum Potsdam, Deutsches GeoForschungsZentrum
Koch	Mirjam	Institut für Geowissenschaften, Goethe-Universität Frankfurt
Koepke	Jürgen	Institut für Mineralogie, Leibniz Universität Hannover
Kopf	Achim	Universität Bremen
Kotthoff	Ulrich	Geologisch-Paläontologisches Institut und Museum, Universität Hamburg
Krastel	Sebastian	Helmholtz-Zentrum für Ozeanforschung Kiel (GEOMAR)
Küchler	Rony	MARUM Universität Bremen
Kuhnt	Wolfgang	Institut für Geowissenschaften, Christian-Albrechts-Universität Kiel
Kukkonen	Maaret	Institut für Geologie und Mineralogie, Universität Köln
Kukowski	Nina	Institut für Geowissenschaften, Friedrich-Schiller-Universität Jena
Kunze	Sabine	IODP, Bundesanstalt für Geowissenschaften und Rohstoffe (BGR), Hannover
Kutterolf	Steffen	Helmholtz-Zentrum für Ozeanforschung Kiel (GEOMAR)
Lazarus	David	Museum für Naturkunde, Leibniz-Institut für Evolutions- und Biodiversitätsforschung, Humboldt-Universität Berlin
Leduc	Guillaume	Christian-Albrechts-Universität Kiel
Lehnert	Oliver	GeoZentrum Nordbayern, Universität Erlangen-Nürnberg
Lindhorst	Katja	Helmholtz-Zentrum für Ozeanforschung Kiel (GEOMAR)
Lorenschat	Julia	Institut für Umweltgeologie, Technische Universität Braunschweig
Lücke	Andreas	Forschungszentrum Jülich
Lückge	Andreas	Bundesanstalt für Geowissenschaften und Rohstoffe (BGR), Hannover
Lüniger	Guido	Deutsche Forschungsgemeinschaft (DFG), Bonn
Mackensen	Andreas	Alfred-Wegener-Institut für Polar- und Meeresforschung (AWI), Bremerhaven
Maronde	Dietrich	Universität Bonn
März	Christian	School of Civil Engineering and Geosciences, Newcastle University
Mayr	Christoph	Institut für Paläontologie und Geobiologie, Ludwig-Maximilians-Universität München
McAnena	Alison	Institut für Geologie und Mineralogie, Universität Köln
Meinhardt	Ann-Kathrin	Institut für Chemie und Biologie des Meeres (ICBM), Carl von Ossietzky Universität Oldenburg
Meinhold	Guido	Georg-August-Universität Göttingen
Meyer	Christian	Institut für Geologische Wissenschaften, Freie Universität Berlin
Meyers	Philip A.	Department of Earth and Environmental Sciences, The University of Michigan
Möbius	Iris	Institut für Geowissenschaften, Goethe-Universität Frankfurt
Mohnke	Oliver	E.ON Energy Research Center, RWTH Aachen
Montinaro	Alice	Universität Münster
Morgavi	Daniele	Ludwig-Maximilians-Universität München
Mousavi	Sima	Universität Leipzig
Müller	Tim	Institut für Mineralogie, Leibniz Universität Hannover
Müller-Michaelis	Antje	Alfred-Wegener-Institut für Polar- und Meeresforschung (AWI), Bremerhaven
Mullick	Nirjhar	Institut für Geophysik und Geoinformatik, TU Bergakademie Freiberg
Naafs	David	Alfred-Wegener-Institut für Polar- und Meeresforschung (AWI), Bremerhaven
Neugebauer	Ina	Helmholtz-Zentrum Potsdam, Deutsches GeoForschungsZentrum
Niedermann	Samuel	Helmholtz-Zentrum Potsdam, Deutsches GeoForschungsZentrum
Nowak	Marcus	Institut für Geowissenschaften, Eberhard Karls Universität Tübingen
Nürnberg	Dirk	Helmholtz-Zentrum für Ozeanforschung Kiel (GEOMAR)
Oberhänsli	Roland	ICDP, Universität Potsdam
O'Connor	John	GeoZentrum Nordbayern, Universität Erlangen-Nürnberg
Oehlerich	Markus	Ludwig-Maximilians-Universität München
Ohlendorf	Christian	GEOPOLAR, Universität Bremen
Osborne	Anne	Helmholtz-Zentrum für Ozeanforschung Kiel (GEOMAR)
Pabich	Stephanie	Institut für Mineralogie, Westfälische Wilhelms-Universität Münster
Palamenghi	Luisa	Universität Bremen
Pickarski	Nadine	Universität Bonn
Piller	Werner E.	Institut für Erdwissenschaften, Universität Graz
Pletsch	Thomas	Bundesanstalt für Geowissenschaften und Rohstoffe (BGR), Hannover
Preu	Benedict	Universität Bremen
Preuss	Franziska	Institut für Chemie und Biologie des Meeres (ICBM), Carl von Ossietzky Universität Oldenburg
Preuß	Oliver	Institut für Mineralogie, Leibniz Universität Hannover
Pross	Jörg	Institut für Geowissenschaften, Goethe-Universität Frankfurt
Raddatz	Jacek	Helmholtz-Zentrum für Ozeanforschung Kiel (GEOMAR)
Raschke	Ulli	Museum für Naturkunde, Leibniz-Institut für Evolutions- und Biodiversitätsforschung, Humboldt-Universität Berlin
Rausch	Svenja	Universität Bremen
Reimold	Wolf Uwe	Museum für Naturkunde, Leibniz-Institut für Evolutions- und Biodiversitätsforschung, Humboldt-Universität Berlin
Reischmann	Thomas	Hessisches Landesamt für Umwelt und Geologie, Wiesbaden
Renaudie	Johan	Museum für Naturkunde, Leibniz-Institut für Evolutions- und Biodiversitätsforschung, Humboldt-Universität Berlin
Röhl	Ulla	MARUM Universität Bremen
Sarnthein	Michael	Institut für Geowissenschaften, Christian-Albrechts-Universität Kiel
Schäbitz	Frank	Universität Köln
Schindlbeck	Julie	Helmholtz-Zentrum für Ozeanforschung Kiel (GEOMAR)

Schmincke	Hans-Ulrich	Helmholtz-Zentrum für Ozeanforschung Kiel (GEOMAR)
Schreck	Michael	Alfred-Wegener-Institut für Polar- und Meeresforschung (AWI), Bremerhaven
Schreiber	Kirstin	Justus Liebig Universität Giessen
Schulz	Hartmut	Institut für Geowissenschaften, Eberhard Karls Universität Tübingen
Schumann	Kai	Helmholtz-Zentrum für Ozeanforschung Kiel (GEOMAR)
Shishkina	Tatiana	Institut für Mineralogie, Leibniz Universität Hannover
Shumilovskikh	Lyudmila	Georg-August-Universität Göttingen
Simonyan	Anna	Institut für Mineralogie, Leibniz Universität Hannover
Smolka	Peter P.	Westfälische Wilhelms-Universität Münster
Spieß	Volkhard	Universität Bremen
Stein	Rüdiger	Alfred-Wegener-Institut für Polar- und Meeresforschung (AWI), Bremerhaven
Steinke	Stephan	MARUM Universität Bremen
Stipp	Michael	Helmholtz-Zentrum für Ozeanforschung Kiel (GEOMAR)
Strack	Dieter	International Oil & Gas Consultant, Ratingen
Strauch	Gerhard	Helmholtz-Zentrum für Umweltforschung (UFZ), Halle
Sumita	Mari	Helmholtz-Zentrum für Ozeanforschung Kiel (GEOMAR)
Teichert	Barbara	Institut für Geologie und Paläontologie, Westfälische Wilhelms-Universität Münster
Teschner	Claudia	Helmholtz-Zentrum für Ozeanforschung Kiel (GEOMAR)
Timmerman	Martin Jan	ICDP, Universität Potsdam
Uenzelmann-Neben	Gabriele	Alfred-Wegener-Institut für Polar- und Meeresforschung (AWI), Bremerhaven
Vallé	Francesca	MARUM Universität Bremen
Virgil	Christopher	Institut für Geophysik und extraterristrische Physik, Technische Universität Braunschweig
Voges	Kevin	Institut für Mineralogie, Leibniz Universität Hannover
Voigt	Janett	Helmholtz-Zentrum für Ozeanforschung Kiel (GEOMAR)
Voigt	Silke	Institut für Geowissenschaften, Goethe-Universität Frankfurt
Wagner	Dirk	Alfred-Wegener-Institut für Polar- und Meeresforschung (AWI), Bremerhaven
Wallrabe-Adams	Hans-Joachim	MARUM Universität Bremen
Weber	Michael	Institut für Geologie und Mineralogie, Universität Köln
Wegler	Ulrich	Bundesanstalt für Geowissenschaften und Rohstoffe (BGR), Hannover
Wenau	Stefan	Universität Bremen
Wille	Michael	Universität Köln
Winkelmann	Daniel	Helmholtz-Zentrum für Ozeanforschung Kiel (GEOMAR)
Wittig	Volker	Geothermie-Zentrum, Universität Bochum
Wohlenberg	Jürgen	RWTH Aachen
Wonik	Thomas	Leibniz-Institut für Angewandte Geophysik (LIAG), Hannover
Zhu	Jiayun	Forschungszentrum Jülich
Zirkel	Jessica	Institut für Geowissenschaften, Goethe-Universität Frankfurt

Weber, M.E., Clark, P.U., Ricken, W., Mitrovica, J.X., Hostetler, S.W., Sprenk, D., Kuhn, G.	Bipolar synchronicity for the termination of the Last Glacial Maximum	IODP	168
Westerhold, T., Röhl, U., Edgar, K., Lyle, M., Pälike, H., Wilkens, R., Wilson, P., Zachos, J.	New insights on Middle to Late Eocene Carbon Cycle Dynamics from high-resolution geochemical records (IODP Exp 320/321 and ODP Leg 199)	IODP	169
Wille, M., Schäbitz, F., and the PASADO science team	Comparison of pollen profiles with the dust proxy from the Antarctic ice core EPICA Dome C since 51.1 ka cal BP	ICDP	171
Zhu, J., Lücke, A., Wissel, H., Mayr, C., Ohlendorf, C., Zolitschka, B., and the PASADO science team	Environmental instability at the last Glacial – Interglacial transition in Patagonia, Argentina: the stable isotope record of bulk sedimentary organic matter from Laguna Potrok Aike	ICDP	173
Zirkel, J., Herrle, J.O., Pälike, H., Liebrand, D.	Deciphering Oligocene climate dynamics using benthic and planktic foraminifera from Site U1334 (IODP Expedition 320)	IODP	175
Zolitschka, B., Ohlendorf, C., Buylaert, J.-P., Gebhardt, A.C., Hahn, A., Kliem, P., Mayr, C., Wastegård, S., and the PASADO Science Team	Hydrological variability of the last 50 ka recorded in Laguna Potrok Aike (Pali Aike Volcanic Field, Argentina)	ICDP	176

Fahrtberichte

IODP Expedition 330 Louisville Seamount Trail - Implications for geodynamic mantle flow models and the geochemical evolution of primary hotspots - Preliminary Results

C. BEIER[1], S. RAUSCH[2], S. EHMANN[3], IODP EXPEDITION 330 SCIENTISTS[4]

[1]GeoZentrum Nordbayern, Universität Erlangen-Nürnberg, Schlossgarten 5, D-91054 Erlangen
[2] Fachbereich Geowissenschaften, Universität Bremen, Klagenfurther Straße (GEO), 28359 Bremen
[3]Institut für Geophysik und extraterrestrische Physik, TU Braunschweig, Mendelsohnstr. 3, 38106 Braunschweig
[4]Integrated Ocean Drilling Program, Texas A&M University, College Station, TX.

The existence and origin of mantle plumes has been the subject of many studies where geophysical, geochemical and geodynamical approaches have all been used to increase our understanding of where and how mantle plumes originate and what controls their melting behaviour. Thus, understanding the nature of mantle plumes and the extend to which they are stationary in the Earth's mantle is fundamental for modern models of mantle convection and plate tectonics. Contrasting the Wilson-Morgan fixed mantle plume hypotheses (Morgan, 1971; Wilson, 1963), palaeomagnetic evidence collected during ODP Leg 197 to the Emperor Seamount Chain (Duncan et al., 2006) implies that the Hawaiian hotspot has moved southward between 81 and 47 Ma on the order of 10-40 mm/yr (Tarduno, 2007). Thus, comparison of long-lived seamount chains is of fundamental importance to determine if hotspots move coherently or not.

The Hawaiian-Emperor and Louisville Seamount Trails in the Pacific preserve a more than 70 Ma history of age-progressive volcanism where the geological evolution of the Hawaiian-Emperor chain is relatively well know from drilled and dredged samples. Contrastingly, the Louisville Seamount Trail is much less well sampled and only few data are available. The Louisville Seamount Trail is approximately 4200 km long extending southeastward from Osbourn Seamount, which is currently being subducted into the Tonga Trench to a seamount which is located about 300 km west of the Pacific Antarctic Rise (Fig. 1). The youngest sample associated with the Louisville Seamount Trail from this seamount has an age of 1.11 Ma (Koppers et al., 2004) and ages increase westwards. Lithosphere to the west of the West Wishbone Scarp formed at the Osbourn Trough spreading centre which became extinct at ~90 Ma (Downey et al., 2007), while lithosphere to the east of East Wishbone Scarp formed at the Pacific Antarctic Rise.

The primary scientific objectives of IODP Expedition 330 to the Louisville Seamount Trail were a) to determine the paleolatitude change over time for the Louisville hotspot, b) determine the volcanic history of individual seamounts and the overall age progression of the Louisville Seamount Trail and c) determine the magmatic evolution of the Louisville Seamount Trail and the associated mantle source by geochemistry. Secondary objectives of this expedition were a) to determine if the submarine Ontong Java Plateau was formed during the initial arrival of the Louisville mantle plume around 120 Ma, b) to estimate the potential temperatures and degrees of melting of the Louisville Seamount Trail sources and c) to provide paleoceanographic and paleoclimate data at 40°-50°S paleaolatitudes in the southern ocean from Louisville pelagic sediments.

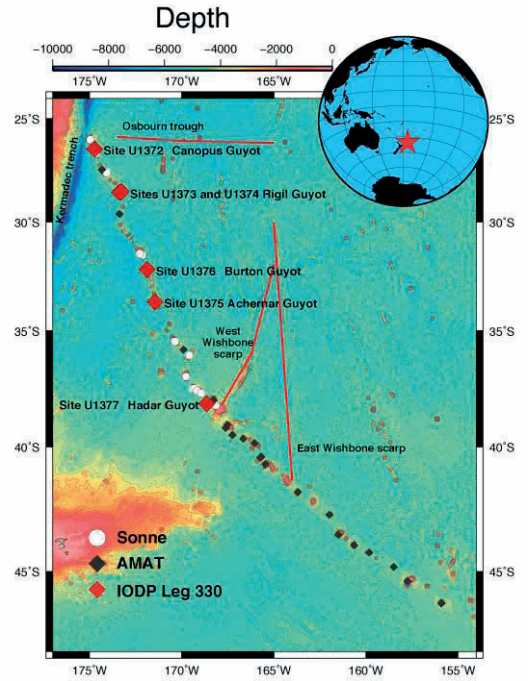

Fig. 1: Map of the Louisville Seamount Chain using GMT (Wessel and Smith, 1991). AMAT02RR samples are from site survey expedition (Koppers et al., 2012), Sonne samples are from SO 167 (Beier et al., 2011; Stoffers et al., 2003).

IODP Expedition 330 used the drilling strategy of ODP Leg 197 in order to target seamounts that have similar ages compared to those drilled along the Emperor Seamount Trail (Detroit, Suiko, Nintoku and Koko) (Fig. 1; Expedition 330 Scientists, 2011). In total six sites on five guyots were drilled (Canopus, Rigil, Burton, Archenar and Hadar) in an attempt to sample as many in-situ lava flows as possible. A total of 1114 m of sediment and igneous basement was drilled, and 806 m was recovered (average recovery = 72.4%). At Site U1374 on Rigil Guyot, a total of 522 m was drilled, with a record-breaking 87.8% recovery.

Several Louisville sites drilled may give evidence for subaerial conditions on the top reaching into shallow submarine and submarine conditions with increasing hole depths, however, even though the flat-topped Louisville guyots likely once were volcanic islands the drill samples only provided sparse evidence for subaerial volcanism.

Almost all Expedition 330 core material is characterized by low degrees of alteration (see also below), providing a large quantity of samples of well-preserved to slightly altered basalt, containing, pristine olivine crystals with melt inclusions, fresh volcanic glass, unaltered plagioclase, various micro- and macrofossils, and, in one case, mantle xenoliths and xenocrysts.

The bulk of the sediments drilled on the guyot tops consist of sequences of volcanic sandstones and basalt breccia or conglomerate often intercalated by lava flows and tephra of submarine eruptions and auto-brecciated lava flows or peperites.

At Site U1376 on Burton Guyot a ~15m thick algal limestone reef was cored while, on three other seamounts, condensed pelagic limestone units were drilled (< 30 cm thickness). These limestones will provide insights into the paleoclimate record at higher southern latitudes (~50°) since Mesozoic times. The igneous basement consists of a large number of in situ lava flows, pillow basalts, auto-brecciated lava flows, intrusive sheets or dikes, hyaloclastites, and peperites. The two oldest seamounts drilled (Canopus and Rigil Guyots, Fig. 1) revealed a large number of in situ lava flows adequate to average out paleosecular variation and yield eruption ages estimated to be on the order of 78 and 73 Ma, respectively. At all drill sites large quantities of hyaloclastites, volcanic sandstones and basalt breccias were recovered, which in many cases show consistent paleomagnetic inclinations compared to neighbouring lava flows. Site U1374 on Rigil Guyot revealed a magnetic polarity reversal in the cored sequence.

Downhole logging has been conducted at site U1374 and U1376, using the triple combination (triple combo) tool string, the Formation MicroScanner (FMS)-sonic tool string, the Ultrasonic Borehole Imager (UBI), and the third-party Göttingen Borehole Magnetometer (GBM) provided by the Institute for Geophysics at TU Braunschweig. The UBI tool string was only run at site U1374, the other tool strings were run at both sites. Lithological and structural features were imaged in good quality and will be used to identify lithological boundaries in sections with little or no core recovery.The reoriented borehole images are used to reorient selected core samples back to geographic coordinates to improve paleomagnetic analyses.The GBM recorded high quality three component magnetic data, deriving important information on the declination of the remnant magnetisation of the drilled in situ lava flows contributing to the determination of the paleolatitude history of the Louisville Seamount chain.

On-board major and trace element analysis of the igneous rocks by inductively coupled plasma–atomic emission spectroscopy (ICP-AES) indicates that, at a lot of the drilled sites, alteration has not obscured magmatic signatures significantly, with the exception of K2O in some samples. The data indicate that most samples are alkalic basalt, although several are transitional basalt. Their compositions overlap those measured for dredge samples from other sites along the Louisville Seamount Trail (Beier et al., 2011) but cover a smaller range of variation (see also Beier et al., this volume). Much of the chemical variation in the seamounts appears to be the result of variable amounts of crystal fractionation involving different amounts of olivine, clinopyroxene and plagioclase.

Although generally well preserved, the igneous sections have some degree of secondary alteration by low-temperature water-rock interaction and weathering. In total three alteration phases were distinguished: carbonates, clay minerals, and other secondary phases. Site U1372 shows two main intervals of different dominant colors of alteration (green and red), than can directly be related to the oxidation state of the alteration processes. Cores from Site U1374 display abundant carbonate veins, as well as vesicles and voids filled with carbonates within the first 300 meters below seafloor (mbsf). The igneous rocks are altered under subzeolite to zeolitefacies conditions, indicating that the carbonates formed from seawater-derived hydrothermal fluids at relatively low temperatures of < 100°C. With increasing depth, zeolite abundance increases and a succession of zeolites, from phillipsite to analcite and possibly to stilbite, implies an alteration temperature gradient from 40-80°C up to 140°C in accordance with published drill core data (Eastern Iceland: Walker, 1951; Kerguelen Island: Giret et al., 2003; East Greenland: Neuhoff et al., 2011).

More than sixty microbiology samples collected from the four seamounts represent one of the largest collection from any hard rock expedition, most of which have focused particularly on young mid-ocean ridge settings. The occurrence of fresh volcanic glasses in almost all drill sites will allow to investigate the activity and boring patters of glass-metabolizing microorganisms (Fisk et al., 1998; Furnes et al., 2001) in the largely unstudied seamount subsurface environment.

Overall, the large quantity and excellent quality of the material drilled during IODP Expedition 330 will allow to address all of the scientific objectives of this expedition and beyond.

References:

Beier, C., Vanderkluysen, L., Regelous, M., Mahoney, J.J. and Garbe-Schönberg, D., 2011. Lithospheric control on geochemical composition along the Louisville Seamount Chain. Geochem. Geophys. Geosyst., 12: Q0AM01.

Downey, N.J., Stock, J.M., Clayton, R.W. and Cande, S.C., 2007. History of the Cretaceous Osbourn spreading center. Journal of Geophysical Research, 112: B04102.

Duncan, R., Tarduno, J.A., Scholl, D.W. and Davies, T., 2006. Leg 197 Synthesis: Southward motion and geochemical variability of the Hawaiian Hotspot. Proceedings of the Ocean Drilling Program, Scientific Results.

Expedition 330 Scientists, 2011. Louisville Seamount Trail: implications for geodynamic mantle flow models and the geochemical evolution of primary hotspots. IODP Preliminary Report, 330.

Fisk, M. R., Giovannoni, S. J., and Thorseth, I. H., 1998. The extent of microbial life in the volcanic crust of the ocean basins, Science, 281, 978–980.

Furnes, H. , Staudigel, H., Thorseth, I., Torsvik, T., Muehlenbachs, K., and Tumyr, O., 2001. Bioalteration of basaltic glass in the ocean crust, Geochem. Geophys. Geosyst., 2, 1049.

Giret, A., Weis, D., Grégoire, M., Mattiellli, N., Moine, B., Michon, G., Scoates, J., Tourpin, S., Delpech, G., Gerbe, M.C., Doucet, S., Ethien, R., and Cottin, J-Y., 2003. L'Archipel de Kerguelen: les plus vieilles îles dans le plus jeune océan. Géologues, 137: 15-23.

Koppers, A.A.P., Duncan, R.A. and Steinberger, B., 2004. Implications of a nonlinear 40Ar/39Ar age progression along the Louisville seamount trail for models of fixed and moving hot spots. Geochem. Geophys. Geosyst., 5(6): Q06L02.

Koppers, A.A.P. et al., 2012. New location of the present-day Louisville Hotspot based on 40Ar/39Ar geochronology. Geochemistry Geophysics Geosystems.

Morgan, W.J., 1971. Convection plumes in the lower mantle. Nature, 230: 42-43.

Neuhoff, P.S., Watt, W.S., Bird, D.K., and Pedersen, A.K., 2011. Timing and structural relations of regional zeolite zones in basalts of the East Greenland continental margin. Geology, 25:803-806.

Stoffers, P. et al., 2003. Cruise Report SONNE 167 Louisville Louisville Ridge: Dynamics and Magmatism of a mantle plume and its influence on the Tonga-Kermadec subduction system, Institut für Geowissenschaften, Universität Kiel, Kiel.

Tarduno, J.A., 2007. On the motion of Hawaii and other mantle plumes. Chemical Geology, 241(3-4): 234-247.

Walker, G.P.L., 1951. The amygdale minerals in the Tertiary lavas of Ireland. I. The distribution of chabazite habits and zeolites in the Garron plateau area, County Antrim'. Am. Min., 29:773.

Wessel, P. and Smith, W.H.F., 1991. Free software helps map and display data. EOS, 72: 441.

Wilson, J.T., 1963. A possible origin of the Hawaiian Islands. Canadian Journal of Earth Sciences, 41: 863-870.

Report from Expedition 334: The Costa Rica Seismogenesis Project (CRISP)

M. STIPP[1], U. BARCKHAUSEN[2], S. KUTTEROLF[1], I. ARROYO[1], P. VANNUCCHI[3], K. UJIIE[4], AND EXPEDITION 334 SCIENTIFIC PARTY

[1] Marine Geodynamik, Helmholtz-Zentrum für Ozeanforschung Kiel (GEOMAR), Wischhofstr. 1-3, 24148 Kiel, Germany
[2] Bundesanstalt für Geowissenschaften und Rohstoffe, Stilleweg 2, 30655 Hannover, Germany
[3] Earth Science Department, University of Florence, Via La Pira 4, 50121 Firenze, Italy
[4] Graduate School of Life and Environmental Sciences, University of Tsukuba, 1-1-1 Tennodai, Tsukuba 305-0006, Japan

IODP expedition 334 drilled into the upper and middle slope of the Costa Rican forearc of the continental Caribbean plate and into the incoming oceanic Cocos plate offshore Osa Peninsula. The western coast of Costa Rica represents a characteristic erosive margin consisting of continental basement and a small frontal sediment wedge. Material from the overriding continental plate is eroded at the front and from below by the subducting oceanic plate. This subduction erosion and the related extensional tectonics cause a continuous thinning of the forearc and an upward and landward migration of the plate boundary. The eroded upper plate material represents much of the filling of the subduction channel between the two plates.

Subduction erosion has been found to be active over a long time period in Costa Rica starting at least in the mid-Miocene. Evidence for that is indirectly given from the subsidence record of the forearc sediments caused by forearc thinning (e.g., Vannucchi et al., 2001; 2004). Initiation of subsidence can be related to a change in subduction erosion rates, which is probably caused by a plate kinematic reorganization of the Cocos plate and shallowing of the subduction angle (e.g., Ranero et al., 2000; Vannucchi et al., 2004).

The incoming Cocos plate is highly fractured and contains a large number of seamounts. Their subducted counterparts have been seismically imaged beneath the forearc wedge. They contribute significantly to the strong wedge deformation up to the mid-slope region and maybe even further. The sediment cover on the incoming plate offshore Osa Peninsula is thin due to the young age of the plate and the vicinity of the Cocos Ridge. The Cocos Ridge subduction is the main reason why the updip limit of the seismogenic zone is at only 5 - 5.5 km depth, i.e. within reach of modern ocean drilling technique. Additionally the intensive pre-investigation of the Central American active margin, and the relatively high level of seismicity are the main reasons why the CRISP location was chosen as primary target to penetrate the zone of active seismic slip in an erosive subduction zone to better understand large earthquake nucleation and rupture propagation. Expedition 334 was dedicated to investigate the upper plate material, to quantify subduction channel thickness and subduction erosion, to characterize fluid/rock interaction, to measure the stress field in the forearc region, and to investigate effects of ongoing ridge subduction.

Expedition 334 cored four drilling sites, carried out logging while drilling (LWD) at two of them and accomplished two holes for high-resolution geochemical and microbiological sampling as well as in-situ temperature measurements. At the upper slope site U1379, 949 mbsf were drilled. The forearc sediments are mainly composed of consolidated clay, clayey silt with intercalated calcareous concretions, tephra layers, and fining- and coarsening-upward sequences of silty sands and sandstone. Facies and calcareous microfossil analyses indicate rapid deepening from a beach sand to shelf sediments and to upper slope sediments followed by a rapid shallowing back to a shallow water environment.

The transition to the seismically depicted forearc basement occurs at 882 mbsf. The basement unit consists of a breccia with clasts of limestone, basalt, and mudstone in a sandy matrix intercalated with basalt. The basement occurs below a sequence of sandy and clayey siltstone as recovered in the 66 m long core section. The lithological change at the basement transition can be related to a considerable porosity reduction from ~40% to 20%, a density increase from ~2.0 g/cm3 to 2.3 g/cm3, and a resistivity increase from ~1.3 Ωm to 2.5 Ωm of the LWD data. Hence the underlying sedimentary basement shows a remarkably higher grade of consolidation than the upper slope-apron sediments. However, the rocky basement of the Caribbean plate, which was expected to be found based on the reflection seismic images was not present at the drillsite.

Structural measurements of the bedding planes indicated two angular discordances, one at approximately 600 mbsf from gently to more steeply dipping orientations within the forearc sediments and the second at the transition to the basement from the steep orientation back to more gently dipping bedding planes. In the lower part of the forearc sedimentary sequence, the fault population increases and four major fault zones occur, which are characterized by brecciated zones in the fault core and decreasing brittle deformation features towards the rim. Normal faults are predominant. Different fault generations can be distinguished when analyzing overprinting relations and the occurrence of healed and open faults. The uppermost fault zone at 642 - 653 mbsf corresponds to a low density and high-porosity interval identified by LWD.

Drilling at the middle slope sites U1378 and U1380 did not reach the acoustically-defined basement due to unfavorable hole conditions at 524 mbsf and 482 mbsf, respectively. The sedimentary sequence is dominated by dark greenish gray terrigenous silty clay intercalated with fining- and coarsening-upward sequences consisting of lithic sands and tephra layers. The bedding at the middle slope sites shows shallow to moderate dip angles. There are steep healed and open faults with dominant normal sense of shear and sediment-filled vein structures indicate paleoseismic activity. Similar to site U1379, several meter-wide major faults with brecciated and fractured zones could be described.

Incoming plate site U1381 was cored to 164 mbsf. A 96 m-thick sequence of clay, silty clay, and silicic and calcareous ooze covers the basaltic oceanic lower crust. The sediments are characterized by gently dipping bedding planes. No brittle deformation features were observed in the sediment cores, while the basalts display different generations of open and mineralized fractures.

First results of leg 334 show a slope sedimentary sequence in the forearc of the Costa Rica active margin indicative of forearc basin development. Rapid subsidence is followed by a record of shallowing water conditions indicative of rapid sedimentation rates. The acoustically-defined basement could be sampled and characterized.

Whether these rocks correspond to the Osa mélange exposed onshore needs to be further investigated. Subsidence is due to subduction erosion and contemporaneous forearc extension causing a thinning of the overriding continental Caribbean plate. The main principal stress direction as determined from fault analysis and borehole breakouts is extensional at the upper slope and compressional at the middle slope corresponding to the present-day plate convergence. The transition from compression to extension probably marks the onset of subduction erosion between the two slope sites. The downgoing oceanic Cocos plate shows a thin pelagic sedimentary cover on top of a basaltic sequence as originally determined from reflection seismic pre-site surveys. Further investigations on fluid flow, stress state, the quantification of subduction erosion and the evolution of the magmatic arc are on the way.

References:

Ranero, C.R., von Huene, R., Flueh, E., Duarte, M., Baca, D., and McIntosh, K., 2000. A cross section of the convergent Pacific margin of Nicaragua. Tectonics 19(2), 335–357.

Vannucchi, P., Galeotti, S., Clift, P.D., Ranero, C.R., and von Huene, R., 2004. Long-term subduction-erosion along the Guatemalan margin of the Middle America Trench. Geology 32(7), 617–620.

Vannucchi, P., Scholl, D.W., Meschede, M., and McDougall-Reid, K., 2001. Tectonic erosion and consequent collapse of the Pacific margin of Costa Rica: combined implications from ODP Leg 170, seismic offshore data, and regional geology of the Nicoya Peninsula. Tectonics 20(5), 649–668.

Cruise Report: IODP Expedition 335 "Superfast Spreading Rate Crust IV"

J. KOEPKE[1] AND IODP EXPEDITION 335 SCIENCE PARTY

[1] Institut für Mineralogie, Leibniz Universität Hannover, Callinstrasse 3, 30167 Hannover; e-mail: koepke@mineralogie.uni-hannover.de

Introduction

Expedition 335, "Superfast Spreading Rate Crust IV", started at the 13th April, 2011 in Puntarenas (Costa Rica) and ended at 3rd June, 2011 in Balboa (Panama). It is the fourth part of a multi-cruise program to drill a complete section of the upper oceanic crust into the underlying gabbros. This section is regarded as reference for fast-spreading oceanic crust.

Hole 1256D (6.736°N, 91.934°W) was initiated during Ocean Drilling Program Leg 206 in the eastern equatorial Pacific in 15 Ma crust that formed at the East Pacific Rise (Fig. 1) during a period of superfast spreading (~220 mm/y). This site was chosen to exploit the inverse relationship between spreading rate and the depth to axial low-velocity zones, thought to be magma chambers now frozen as gabbros, observed from seismic experiments.

During Integrated Ocean Drilling Program (IODP) Expedition 309 in Jul-Aug 2005, Hole 1256D was deepened to a total depth of 1255 meters below seafloor (mbsf). Expedition 312 returned to Hole 1256D and deepened it to 1507 mbsf. After completing Expedition 312, the hole extended through 810 m of extrusive normal mid-ocean-ridge basalt, 345.7 m of sheeted dikes, and 100.5 m into plutonic rocks, completing the first penetration of an intact section of the upper oceanic crust. Gabbros were encountered at 1406.6 mbsf, precisely within the depth range predicted from the extrapolation of multichannel seismic results at modern mid ocean ridges to this superfast spreading rate.

IODP Expedition 335 returned to ODP Hole 1256D in order to deepen the previous penetration of intact ocean crust about several hundred meters with the aim to reach cumulate gabbros. The major objectives of IODP Expedition 335 were: (1) to test/modify models on the mechanisms of the magmatic accretion at fast spreading ocean systems; (2) to identify the way of hydrothermal circulation proceeding in the lower crust and to quantify the amount of hydrothermal cooling; (3) to determine the geological rationale behind the Layer 2-3 boundary at Site 1256 estimated by seismic methods; (4) to estimate the contribution of lower crustal gabbros to marine magnetic anomalies. It was anticipated that even a shortened IODP Expedition could deepen Hole 1256D a significant distance (300 m) into cumulate gabbros.

Operations

Expedition 335 reentered Hole 1256D more than five years after the completion of last expedition 312 to Site 1256. The expedition was faced with a series of significant engineering challenges, never experienced before in the history of IODP drilling, although difficulties and engineering problems were not unexpected in case of drilling in a deep, uncased, marine borehole into igneous rocks. The first major problem was a major obstruction at a depth of 920 which prevented reentry of the dill pipe into the deeper parts of the hole. Finally, due to outstanding, persistent efforts of the drilling crew, the obstruction was successfully cleared.

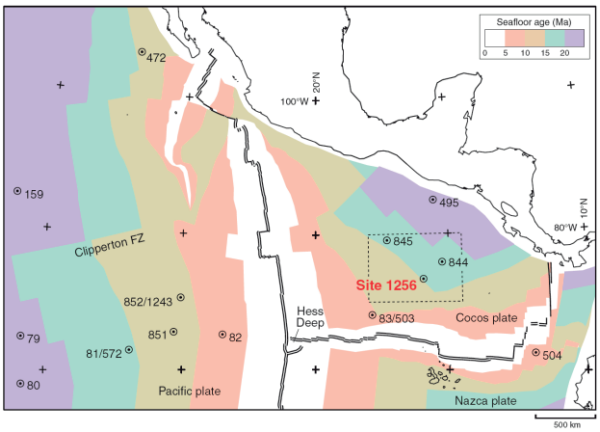

Fig. 1. Age map of the Cocos plate and corresponding regions of the Pacific and Nazca plates. Isochrons at 5 m.y. Selected DSDP and ODP sites that reached basement are indicated by circles (Site 1256 in red). The wide spacing of the 10 to 15 m.y. isochrons to the south reflects the extremely fast (200–220 mm/y) full spreading rate. From Expedition 335 Scientists (2011).

Extremely critical was a subsequent major problem at the bottom of the hole where extreme hard basalts metamorphosed to granulite-facies hornfelses, the so-called granoblastic basalts, are exposed that caused already serious trouble during the previous Expedition 312. Although the thickness of the zone of hornfelsic rocks was estimated to be only a few decameter, their extreme toughness once more prevented drilling progress, expressed in the grinding down a coring bit into a smooth stump (Fig. 2).

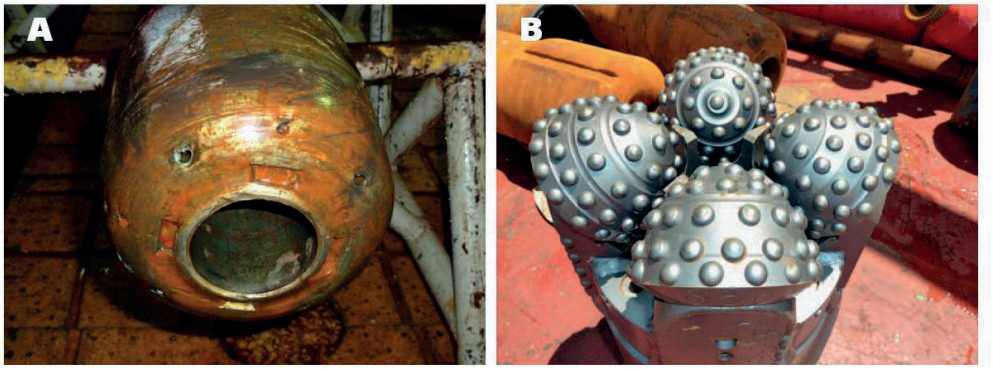

Fig. 2. A: Remains of the Ulterra C9 RCB coring bit used during Run 9. The bit was probably used for ~10 h after it was significantly destroyed and abraded, something never seen before by the drill crew. B: For comparison a new drilling bit of the same type. Modified from Expedition 335 Scientists (2011).

In the following 17 days a survey for cleaning, milling, and reaming was undertaken in order to clear the bottom of the hole of metal debris from the destroyed coring bit and of an incredible amount of drilling cuttings. This effort forced the innovative use of hole-clearing equipment (e.g., the use of Bowen full-flow reverse circulation junk basket; use of large magnets) and involved about 240 km of drilling pipe deployments (trips) down into the hole and back on deck. During these operations, hundreds of kilograms of rocks and drill cuttings have been recovered. Included were large, up to five kg blocks of the granoblastic basalts, which were previously recovered only very poorly by coring. Included were also a limited number of gabbroic blocks, implying that the bottom of the whole was close to breaking through into the gabbroic layer.

Results

The engineering challenges encountered during Expedition 335 operations resulted in a major loss of time from the coring and wireline program initially planned for Expedition 335. Coring on this Expedition deepened Hole 1256D only modestly, from 1507.1 to 1521.6 mbsf at low rates of penetration and recovery (0.9 m/hr, 11% respectively).

The hole clearing operations at the bottom of Hole 1256D recovered a unique collection of rock boulders, large cobbles, angular rubble and fine cuttings of mostly strongly to completely recrystallized granoblastic basalt including small amounts of gabbroic rocks and evolved plutonic rocks. The granoblastic basalts are interpreted as previously hydrothermally altered basalts of the sheeted dikes which were metamorphosed under granulite facies conditions. There is evidence that hydrothermal alteration occurred both before and after the formation of granoblastic textures. The petrographic record include both primary magmatic features (dike-dike contacts; the presence of microphenocrists), as well as effects of hydrothermal alteration before the metamorphic overprint (pre-cursor textures of hydrothermal breccia formation; formation of hydrothermal veins metamorphosed to pure orthopyroxene veins). The large blocks exhibit intrusive, structural and textural relationships, and overprinting and cross-cutting hydrothermal alteration and metamorphic paragenetic sequences that hitherto have not been observed due to the one dimensional nature of drill cores and the very low rates of recovery of the granoblastic dikes during Expedition 312 (<7% recovery). Textural and contact relationships imply that the rocks recovered during Expedition 335 represent a ~15 m interval of the upper crust – lower crust transition, located below the ~90 m section drilled by Expedition 312 consisting of two gabbroic intrusions and an intercalated "Dike Screen 1" – a mixed zone of granoblastic basalts and fine-grained rocks with a plutonic character. The total vertical thickness of granoblastic basalts is over 114 m, and Dike Screen 2 is now about the same thickness (so far) as Dike Screen 1.

The recovered Dike/Gabbro transitions is a very complex zone, where magmatic processes interfere with metamorphic and hydrothermal processes: below, the axial melt lens filled with a basaltic magma at a temperature of ~1200°C, and above, the seawater hydrothermal cells operating at temperatures of max. 400-500°C, representing one of the highest (quasi) steady-state thermal gradient of a crustal system described on our planet. Theoretical models predict that the heat of the axial melt lens is exchanged across a thin (<100 m), hot (>650 °C), impermeable conductive boundary layer (CBL) sandwiched between the axial melt lens and the sheeted dikes. Thanks to Expeditions 312 and 335, now the first in-situ samples from such a CBL zone are available: The 114 m-thick zone of granoblastic basalts, representing granulite-facies metamorphosed previously hydrothermally altered basalts of the sheeted dike complex, in which beside felsic lithologies variegated, heterogeneous gabbros were intruded. These gabbros are interpreted as frozen remnants of a deeper continuous axial melt lens, not yet reached by drilling.

Although the extensive engineering problems during Expedition 335 prevented major progress in deepening Hole 1256D, significant progress was made in improving the borehole. The engineering efforts on Expedition 335 have repaired and prepared Hole 1256D for further deep drilling, following 5 years of non-activity. Hole 1256D is 1500 m of hard rock coring closer to cumulate gabbros than any other options in intact ocean crust. Hole 1256D is dedicated to answer fundamental questions about the formation of new crust at fast spreading mid-ocean ridges, best achieved by a timely return to Site 1256.

References:

Expedition 335 Scientists (2011) Superfast spreading rate crust 4: drilling gabbro in intact ocean crust formed at a superfast spreading rate. IODP Prel Rept 335: doi: 10.2204/iodp.pr.335.2011

Report from IODP Expedition 336: Microbial Processes at North Pond (22°46'N, 46°05'W) Initiation of Long-term Coupled Micro-biological, Geochemical, and Hydrological Experimentation within the Seafloor

W. BACH[1], K.J. EDWARDS[2], A. KLAUS[3], EXPEDITION 336 SCIENCE PARTY

[1]University of Bremen, Klagenfurter Str., 28359 Bremen, Germany, wbach@uni-bremen.de
[2]University of Southern California, Los Angeles, USA, kje@usc.edu
[3]IODP, Texas A&M University, College Station, USA, aklaus@iodp.tamu.edu

The upper ~500 m of basaltic ocean crust is fractured and permeable, harboring the largest hydrologically active aquifer on Earth. Below at least 60% of the seafloor, the oceanic crust is hydrologically active with a fluid flux through the crust that rivals global riverine input to the oceans. Solutes, colloids (including microbes) circulate actively through the crustal aquifer, but the extent to which microbes colonize, alter, and evolve in subsurface rock is not known. A large fraction of ocean crust remains uncovered by sediments for millions of years on the flanks of Mid Ocean Ridges (MORs), before being blanketed in the abyssal plains of the ocean, and eventually subducted at trenches. These basement outcrops serve as "breathing holes" through which seawater can ventilate the ocean crust. Fluid flow within the crust is focused in specific areas, where permeability is increased, usually at the contacts of lava flows or in brecciated. In these intervals, the extent of rock alteration is increased, suggesting elevated intensity of seawater-rock interaction. Most of this alteration is believed to take place within the first 10-15 Ma of crustal evolution. It is well known that the geochemical changes associated with basalt alteration in the uppermost oceanic crust play an important role in setting ocean chemistry. It is unknown, however, what the role of microorgansims is in mediating this seawater-ocean crust exchange. Expedition 336 sucessfully initiated subseafloor observatory science to examine the linkages between hydrological, geochemical, and microbiological in a young mid-ocean ridge flank setting.

All sites are located in the North Pond at 22°45'N, 46°05'W in 4414 to 4483 m water depth. This area was known from previous ocean drilling and site survey investigations as a site of particularly vigorous circulation of seawater in permeable 8 Ma basaltic basement underlying a <300 m thick sedimentary pile. Understanding how this seawater circulation affects microbial and geochemical processes within the uppermost basement was the primary science objectives of Expedition 336.

Basement was cored and wireline-logged in Holes U1382A and U1383C. Upper oceanic crust in Hole 1382A, which is only 50 m west of Hole 395A, was cored between 110 and 210 m below seafloor (mbsf). 31% of the penetrated basement were recovered, producing different volcanic flow units with distinct geochemical and petrographic characteristics. Intercalated between two flow units is a sedimentary breccia, containing clasts of basalt, gabbroic rocks, and mantle peridotite; this unit was interpreted as a rock slide deposit. Hole 1383C recovered 50.3 m of core from an interval between 69.5 and 331.5 mbsf. The basalts are aphyric to highly plagioclase-olivine phyric tholeiites that fall on a liquid line of descent controlled by olivine fractionation. They are fresh to moderately altered, with clay minerals (saponite, nontronite, celadonite), Fe-oxyhydroxide, carbonate, and zeolite as secondary phases replacing glass and olivine to variable extents.

Sediment thickness was about 90 m at Sites 1382 and 1384 and varied between 38 and 52 m at Site 1383. The sediments are predominantly nanofossil ooze with layers of coarse foraminiferal sand and occasional pebble size clasts of basalt, serpentinite, gabbroic rocks, and bivalve debris. The lowermost meters of the APC-cored sections feature brown clay. XCB-coring at the sediment-basement interface recovered <1 m of brecciated basalt with micritic limestone. Sediments were intensely sampled for geochemical porewater analyses and microbiological work. Shipboard determination of dissolved oxygen concentrations in the pore waters indicate pronounced C-shaped profiles, indicating diffusion of oxygen into the sedimentary pile from both interfaces and oxygen consumption by aerobic microbial activity within the sediments.

Major strides in ridge flank studies have been made by employing CORK subseafloor observatories, as they facilitate combined hydrological, geochemical, and microbiological studies and facilitate controlled experimentation within the subseafloor. Expedition 336 installed fully functional observatories in two newly drilled holes (U1382A and U1383C) and placed an instrument and sampling string in an exisiting hole (395A). While the CORK wellhead at Hole 395A broke of and another Hole (U1383B) was abandoned after a bit failure, these holes and installations in them will be convenient for future observatory science targets. The CORK observatory in Hole U1382A has a packer seal in the bottom of the casing and monitors/samples a single zone extending from 90 to 210 mbsf. Hole U1383C was equipped with a three-level CORK observatory which separates a zone of thin basalt flows with intercalated limestone (~70-146 mbsf) from one within glassy, thin basaltic flows and hyaloclastites (146-200 mbsf) and a lowermost zone (~200-331.5 mbsf) of more massive pillow flows with occasional hyaloclastite in the upper part.

Operations during Expedition 336 were successful in laying the foundation for long-term monitoring, experimentation, and observations by subsequent ROV or submersible dive expeditions. CORKs will be used as perturbation and monitoring points for single- and cross-hole experiments, and will use recently developed novel in-situ microbiological experimentation system. The first ROV cruise to the North pond observatories will take place in April/May of 2012 (ROV Jason2 operated from RV MSM Merian).

Preliminary Results of IODP Expedition 339 „Mediterranean Outflow“

A. BAHR[1], F.J. HERNÁNDEZ-MOLINA[2], D. STOW[3], D. HODELL[4], C. ALVAREZ ZARIKIAN[5] AND EXPEDITION 339 SCIENTISTS[6]

[1]Institut für Geowissenschaften, Universität Frankfurt
[2]Departmento Geociencias Marinas, Universitad de Vigo
[3]Institute of Petroleum Engineering, Heriot-Watt University, Edinburgh
[4]Godwin Laboratory for Palaeoclimate Research, University of Cambridge
[5]Integrated Ocean Drilling Program, Texas A&M University, College Station, TX
[6]: IODP Expedition 339 Scientists: Acton, G., Bahr, A., Balestra, B., Ducassou. E., Flood, R., Flores, J-A., Furota, S., Grunert, P., Hodell, D., Jimenez-Espejo, F., Kim, J. K., Krissek, L., Kuroda, J., Li, B., Llave, E., Lofi, J., Lourens, L., Miller, M., Nanayama, F., Nishida, N., Richter, C., Pereira, H., Roque, C., Sanchez Goñi, M., Sierro Sanchez, F., Singh, A., Sloss, C., Takashimizu, Y., Tzanova, A., Voelker, A., Williams, T., Xuan, C.

The main target of IODP Expedition 339 (starting in Ponta Delgada, Azores, on 17 November 2011, and ending in Lisbon on 17 January 2012) was the contourite depositional system in the Gulf of Cádiz and off the West Iberian margin as a key location for the investigation of the Mediterranean Outflow Water (MOW) and its influence on North Atlantic circulation and climate. The Gulf of Cádiz is the world's premier contourite laboratory and presents a unique opportunity to test current models of contourite formation. It is also a prime target for understanding the effects of tectonic activity on the evolution of the Strait of Gibraltar and on margin sedimentation.

Overall, IODP Exp. 339 had five major objectives:

Understand the opening of the Gibraltar Gateway and onset of MOW.

Determine MOW paleocirculation and global climate significance.

Establish a marine reference section of Quaternary climate change.

Identify external controls on sediment architecture of the Gulf of Cadiz and Iberian margin.

Ascertain synsedimentary tectonic control on architecture and evolution of the contourite depositional system.

To meet these objectives, five sites were drilled in the Gulf of Cádiz (U1386, U1387, U1388, U1389, and U1390) and two sites off the West Iberian margin (U1385 and U1391) (Fig. 1), with the deep Site U1385 located outside the main core of the MOW. A total of 5447 m of core were recovered (86.4% recovery), and downhole logging was performed in all but two sites (U1385 and U1388).

Based on the shipboard stratigraphy, Miocene sediments have been penetrated at two different sites, implying the strong presence of MOW in the sedimentary record following the opening of the Gibraltar Gateway. Contourite deposits have been identified from ~4.2 to 4.5 Ma, although affected by downslope sedimentation processes and hiatuses. Post-cruise research will establish whether this dates from the first onset of MOW. Pliocene sequences have been recovered at four sites, all of which imply relatively low bottom current activity and generally weak MOW, with evidence for a slow increase in current speed through the late Pliocene. Significant hiatuses present at all sites are interpreted as a consequence of enhanced bottom currents related to intensified MOW flow. Quaternary sediments are generally dominated by contourite deposition and drift development. Two successive periods of current intensification have been noted during the Quaternary period, based on the increase of sandy and silty contourites. These are separated by a regional hiatus of variable duration.

The contourite deposits recovered are quite uniform in composition and texture. Remarkable is the absence of primary sedimentary structures and an intense bioturbation. Characteristic are bi-gradational sequences with a large range of partial sequence types in accord with contourite formation models. Unexpected was the quantity and extent of well-sorted and clean contouritic sands. These sands represent a previously unrecognized exploration target for oil and gas reservoirs. However, complex interactions between contourite and turbidite processes have been documented that are not incorporated into current contourite models. Further studies will allow us to resolve outstanding issues of depositional processes, drift budgets and the recognition of fossil contourites in the ancient record onshore.

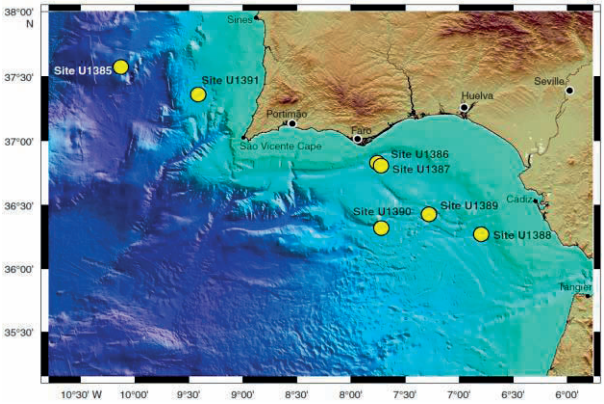

Figure 1 Expedition 339 sites in the Gulf of Cádiz and West Iberian margin

For the investigation of orbital and millennial climate fluctuations, Site U1385 ("Shackleton Site") has been successfully drilled with four holes down to ~150 mbsf allowing the construction of two complete splices dating back to ~1.4 Myr. The seminal work of Nick Shackleton and co-workers (e.g. Shackleton et al., 2000, 2002) have demonstrated the great potential of Iberian Margin sediment cores for high-resolution paleoceanographic and paleoclimatic reconstructions as they can be confidently tied to Antarctic and Greenland ice core records as well as to European terrestrial archives. A comprehensive post-cruise sampling effort is planned to generate a high-resolution reference record which will greatly improve the precision with which marine sediment records of climate change can be correlated to ice cores and other terrestrial archives. It furthermore appears from shipboard measurements that the same climatic cycles preserved in Site U1385 sediments are also evident in all contourite drift sites, albeit with a 3 – 10 fold higher sedimentation rate. This will provide the base for even more detailed sampling of these sites aided by a very robust stratigraphic correlation with Site U1385. This excellent stratigraphic control will moreover allow indentifying and precisely dating hiatuses in the contourite records.

The drilling enabled the dating of major unconformities and minor discontinuities identified on seismic reflection profiles, which is important in order to calibrate the existing seismic stratigraphic framework. The study of the sedimentary architecture of the contourite depositional system is pivotal to distinguish between external controls such as climate, sea level and local tectonics in order to establish a refined sequence stratigraphic model for contourite deposits. Aside from climate variations, tectonic activity appears to have exerted a strong control on margin development, downslope sediment transport and contourite drift evolution. This is particularly valid for the time interval from the closure of the Atlantic-Mediterranean gateways in Spain and Morocco just over 6 Ma and the opening of the Gibraltar Gateway at 5.3 Ma. Based on the timing of events major tectonic pulses are identified in the sedimentary record, linked with asthenosphere activity. These pulses are related to the closure of Atlantic-Mediterranean connections, opening and subsequent deepening of the Gibraltar Gateway, continental margin instability, basin subsidence, local uplift and diapiric intrusion. These processes influenced the strength and nature MOW flow and, hence, sedimentation processes in the Gulf of Cadiz. The material gathered during IODP Exp. 339 and subsequent post-cruise research will greatly improve our understanding of the timing of these processes and feedbacks involved.

References:

Shackleton, N.J., Chapman, M., Sánchez-Goñi, M.F., Pailler, D., Lancelot, Y., 2002. The classic Marine Isotope Substage 5e. Quaternary Research 58, 14-16.

Shackleton, N.J., Hall, M.A., Vincent, E., 2000. Phase relationships between millennial-scale events 64,000-24,000 Years Ago. Paleoceanography 15, 565-569.

Abstracts:

ICDP

Late Quaternary environmental changes in ancient Lake Ohrid – correlating sediment record, dated fossils, and genetic information

C. ALBRECHT[1], T. HAUFFE[1], K. SCHREIBER[1], H. VOGEL[2], B. WAGNER[2], T. WILKE[1]

[1] Department of Animal Ecology and Systematics, Justus Liebig University Giessen, Heinrich-Buff-Ring 26-32 (IFZ), 35392 Giessen, Germany.
[2] Institute of Geology and Mineralogy, University of Cologne, Zülpicher Str. 49a, 50674 Köln, Germany.

Ancient Lake Ohrid - a transboundary lake in the central Balkans - is probably of early Pleistocene or Pliocene origin and amongst the few lakes in the world harbouring an outstanding degree of endemic biodiversity (Albrecht & Wilke, 2008). The ultimate reasons for the accumulation of the observed elevated levels of biodiversity and endemicity are not well understood, but are now targeted in the ICDP project SCOPSCO (Scientific Collaboration on Past Speciation Conditions in Lake Ohrid). A major goal of the SCOPSCO project is to study the interplay of geological/limnological and biological evolution by combining data obtained from sediment core analyses and the fossil record as well as ecological investigations and DNA sequencing of recent organisms.

Sediment cores & fossils – no signs of species assemblage change yet

Although there is a long history of evolutionary research in Lake Ohrid, particularly on molluscs (summarized in Albrecht & Wilke, 2008), a mollusc fossil record has been missing until very recently. For the first time, gastropod and bivalve fossils were reported by Albrecht et al. (2010) from the basal, calcareous part of a

Figure 1. Pairwise comparison of representative fossil mollusc specimens of core Co1200 (left specimens) and recent analoga from Lake Ohrid (right specimens). Scale bar is 2 mm.

2.6 m long sediment succession (core Co1200) from the north-eastern part of Lake Ohrid. Electron spin resonance dating of mollusc shells from the same stratigraphic level yielded an age of 130 ± 28 ka. Lithofacies III sediments, i.e., a subdivision of the stratigraphic unit comprising the basal succession of core Co1200 between 181.5-263 cm,

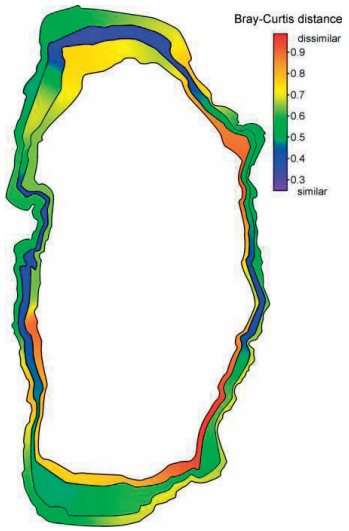

Figure 2. Similarity map of the thanatocoenosis of core Co1200 and recent gastropod communities in ancient Lake Ohrid. Three habitat zones are shown: Surface Layer (0–5 m), Intermediate Layer (5–25 m) yielding the highest average similarity with the fossil assemblages, and Deep Layer (25–50 m).

appeared solid, greyish-white. It consisted almost entirely of silt-sized endogenic calcite ($CaCO_3$ > 70 %) and, indeed, intact and broken mollusc shells. We compared the faunal composition of the thanatocoenosis with recent mollusc associations in Lake Ohrid. A total of 13 mollusc species (9 gastropod and 4 bivalve species) could be identified within Lithofacies III sediments (Figure 1). The value of sediment core fossils for reconstructing palaeoenvironmental settings was evaluated and the agreement between sediment and palaeontological proxies was tested. The combined findings of the ecological study and the sediment characteristics suggest deposition in a shallow water environment during the Last Interglacial. The fossil fauna exclusively included species also found in the present fauna, i.e., no extinction events are evident for this site since the Last Interglacial. The thanatocoenosis showed the highest similarity with recent Intermediate Layer (5-25m water depth) mollusc assemblages of Lake Ohrid (Figure 2).

Ecological analyses – evolutionary history matters

Environmental fluctuations such as consecutive changes of lake-level low- and highstands are believed to trigger biological evolution. Preliminary studies have revealed lake-level fluctuations of Lake Ohrid of up to 60 m during the last glacial-interglacial cycle (Lindhorst et al., 2010), climate dependent occurrence of micro algae (Reed et al., 2010), and spatial variation of sediment features (Vogel et al., 2010). We were using presence-absence data from the most species-rich group in Lake Ohrid, the Gastropoda and identified biodiversity hotspots in the lake basin, e.g., near lacustrine springs and spring fields. These areas are known to be most affected by lake-level changes during the last glacial-interglacial cycle. Spatial heterogeneous distribution of biodiversity is not only determined by different degrees of long-term

environmental stability, but also by processes based on a species´ habitat requirements such as present day climate and neutral processes like speciation, extinction or dispersal limitation of species. Our studies (Hauffe et al., 2011) showed a strong correlation between present day environmental drivers acting on two hierarchical levels: Large scale effects such as lake depth resulted in broad

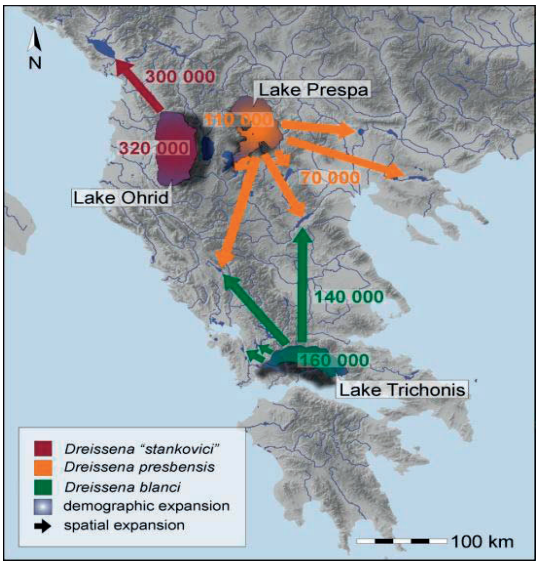

Figure 3. Map of the southwestern Balkans showing the mean estimated times of demographic and spatial expansion models in native Dreissena spp. based on mismatch analyses of the COI gene. red – Dreissena stankovici; orange – D. presbensis; green – D. blanci; color gradient within lake – demographic expansion of the respective Dreissena sp. in the lake with the respective time before present; arrow – spatial expansion of the respective Dreissena sp. with the respective time before present.

differences in gastropod assemblages. Small scale effects like environmental gradients caused minor differences in biodiversity distributions on a smaller spatial scale. However, a significant proportion of gastropod community variation in Lake Ohrid seems to be driven by a largely independent neutral process, i.e., the evolutionary history of a species (Figure 3).

Molecular analyses – population history explained by information from sediment records

Evolutionary events such as past population expansions inferred from molecular data of living molluscs can be linked to observed environmental fluctuations form proxies such as the sediments records obtained from drilling campaigns. This approach was used in a comprehensive study on zebra mussels (Dreissena spp.) in Balkan lakes including Lake Ohrid (Wilke et al., 2010).

Due to the continuous lack of relevant paleolimnological data, we were unable to provide an explanation for the massive population expansions in Dreissena "stankovici" some 300 000–320 000 years ago in Lake Ohrid (Figure 4). However, the demographic expansion of D. presbensis in Lake Prespa, the sister lake of Lake Ohrid, 110 000 years ago (Figure 4) well corresponds to the end of the Eemian interglacial and was therefore possibly caused by environmental and climatic fluctuations that were inferred for the Ohrid-Prespa region during the last glacial-interglacial cycle (Lézine et al., 2010; Lindhorst et al., 2010; Vogel et al., 2010; Wagner et al., 2010). Interestingly, while these affects are apparent in Lake Prespa, they did not leave traces in the demographic history of D. "stankovici" in Lake Ohrid. In fact, the new fossil record shows that D. "stankovici" already had a dominant position in the benthic invertebrate assemblages of the latter lake during the Last Interglacial (Albrecht et al., 2010; Figure 1). These observations lead to the hypothesis that regional environmental changes may have had pronounced effects on the population histories of Dreissena spp. in the Balkans, though the high buffer capacity of Lake Ohrid (deep oligotrophic lake with a considerable water input coming from sublacustrine springs) may have mitigated these effects.

SCOPSCO - Perspectives for linking of sedimentological, ecological and molecular data

The new mollusc fossil record opens a valuable biological perspective for palaeolimnological and evolutionary reconstructions, particularly in respect to the role of environmental stability in generating biodiversity. Lake-level and associated habitat changes can cause community changes. This is obviously not the case for Lake Ohrid molluscs, at least not for the time frame since the Last Interglacial. The same holds true for the ostracode record (Belmecheri et al., 2009).

In the future, lake-level fluctuations and potential associated faunal changes in the Ohrid basin could be traced using additional (older) sediment records from sites outside or inside the recent lake. The most promising

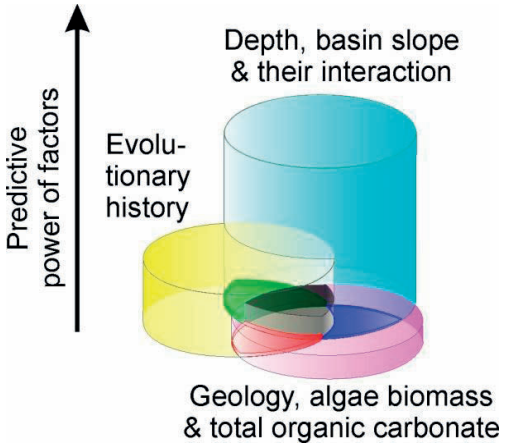

Figure 4. Venn-diagram showing the partitioning of the explained variance of gastropod community compositions in Lake Ohrid into fractions of predictors and their combinations. The figure indicates that environmental predictors alone can explain most of the similarity among gastropod associations. Purely spatial patterns of community similarity are most likely caused by the evolutionary history and limited dispersal capacities of species and do play a major role in explaining the structure of gastropod assemblages.

information can be expected from foreset and terrace structures in the southern part of the basin dating back several 100 ka (Lindhorst et al., 2010). Besides the many environmental proxies expected, these structures may provide potential fossil mollusc records for investigations of community changes, which may date back to the earliest stages of lake formation. The methodology recently used would also be applicable to such old records (Albrecht et al. 2010).

The demonstrated existence of a mollusc fossil record in Lake Ohrid sediment cores also has great significance for the upcoming SCOPSCO deep drilling project. It can be hoped that a more far reaching mollusc fossil record as

well as other proxies will then be obtained, enabling insight into the early evolutionary history of Lake Ohrid.

References:
Albrecht, C., Vogel, H., Hauffe, T., and Wilke, T.: Sediment core fossils in ancient Lake Ohrid: testing for faunal change since the Last Interglacial, Biogeosciences, 7, 3435-3446, 2010, doi:10.5194/bg-7-3435-2010.
Albrecht, C. and Wilke, T.: Lake Ohrid: biodiversity and evolution, Hydrobiologia, 615, 103–140, 2008.
Belmecheri, S., Namiotko, T., Robert, C., von Grafenstein, U., and Danielopol, D. L.: Climate controlled ostracod preservation in Lake Ohrid (Albania, Macedonia), Palaeogeography, Palaeoclimatology, Palaeoecology, 277, 236–245, 2009, doi: 10.1016/j.palaeo.2009.04.013.
Hauffe, T., Albrecht, C., Schreiber, K., Birkhofer, K., Trajanovski, S., and Wilke, T.: Spatially explicit analysis of gastropod biodiversity in ancient Lake Ohrid, Biogeosciences, 8, 175-188, 2011, doi:10.5194/bg-8-175-2011.
Lindhorst, K., Vogel, H., Krastel, S., Wagner, B., Hilgers, A., Zander, A., Schwenk, T., Wessels, M., and Daut, G.: Stratigraphic analysis of lake level fluctuations in Lake Ohrid: an integration of high resolution hydro-acoustic data and sediment cores, Biogeosciences, 7, 3531-3548, 2010, doi:10.5194/bg-7-3531-2010.
Reed, J. M., Cvetkoska, A., Levkov, Z., Vogel, H., and Wagner, B.: The last glacial-interglacial cycle in Lake Ohrid (Macedonia/Albania): testing diatom response to climate, Biogeosciences, 7, 3083-3094, 2010, doi:10.5194/bg-7-3083-2010.
Vogel, H., Wessels, M., Albrecht, C., Stich, H.-B., and Wagner, B.: Spatial variability of recent sedimentation in Lake Ohrid (Albania/Macedonia), Biogeosciences, 7, 3333-3342, 2010, doi: 10.5194/bg-7-3333-2010.
Wagner, B., Vogel, H., Zanchetta, G., and Sulpizio, R.: Environmental change within the Balkan region during the past ca. 50 ka recorded in the sediments from lakes Prespa and Ohrid, Biogeosciences, 7, 3187-3198, 2010, doi: 10.5194/bg-7-3187-2010.
Wilke, T., Schultheiß, R., Albrecht, C., Bornmann, N., Trajanovski, S., and Kevrekidis, T.: Native Dreissena freshwater mussels in the Balkans: in and out of ancient lakes, Biogeosciences, 7, 3051-3065, 2010, doi: 10.5194/bg-7-3051-2010.

ICDP

Late Pliocene/Early Pleistocene environments of the north-eastern Siberian Arctic inferred from Lake El'gygytgyn pollen record

A.A. ANDREEV[1], V. WENNRICH[1], P.E. TARASOV[2], J. BRIGHAM-GRETTE[3], N. R. NOWACZYK[4], M. MELLES[1]

[1]Institute of Geology and Mineralogy, University of Cologne, Germany
[2]Free University Berlin, Institute of Geological Sciences, Palaeontology Branch, Berlin, Germany
[3]Department of Geosciences, University of Massachusetts, Amherst, USA
[4]Helmholtz-Zentrum Potsdam, Deutsches GeoForschungsZentrum, Potsdam, Germany

The Arctic is known to play a crucial, but not yet completely understood, role within the global climate system. Therefore, the development of possible scenarios of future climate changes is a major scientific challenge. However, reliable climate projections for the Arctic are hampered by the complexity of the underlying natural variability and feedback mechanisms. An important prerequisite for the validation and improvement of the climate projections is a better understanding of the long-term climate history of the Arctic. .On the Arctic borderland, the formation of continuous, non-interrupted paleoenvironmental records was widely restricted due to repeated glaciations, thus limiting information predominantly to the Holocene and in a few cases to the last glacial/interglacial cycles (e.g. Andreev et al., 2011 and references therein). Continuous sequences that penetrates the entire Quaternary and further into the Pliocene, with a temporal resolution at least as good as the marine record, is highly desired from the terrestrial Arctic. For example, with such record at hand we can validate the absolute temperature rise during the mid-Pliocene that was proposed by former studies. Such a record has now become available from Lake El´gygytgyn located in northeastern Siberia (67°30' N, 172°05' E). The lake lies within a meteorite impact crater located 100 km to the north of the Arctic Circle in Chukotka Peninsula, northeastern Russia. The crater was created nearly 3.6 Myr ago in volcanic target rocks. The impact formed an 18 km wide hole in the ground that then filled with water. The modern lake is 170 m deep and has a roughly circular shape with a diameter of 12 km. The retrieved lake sediments are trapped pollen from a several thousand square-kilometer source area and potentially provide reliable insights into regional and over-regional millennial-to-century-scale history of vegetation and climate changes of this part of the Arctic since the Pliocene.

The German-Russian-American ''El´gygytgyn Drilling Project“ of ICDP has completed three holes (ICDP site 5011: holes 5011-1A, 5011-1B, 5011-1C) in the center of the lake between October 2008 and May 2009, penetrating about 318 m thick lacustrine sediments and about 200 m of the impact rocks below (see for details Melles et al., 2011). Because of its unusual origin and high-latitude setting, scientific drilling at Lake El´gygytgyn offered unique opportunities for paleoclimate research, allowing the time-continuous reconstruction of the climatic and environmental history of the terrestrial Arctic back into the Pliocene for the first time. We obtained the first continuous pollen record reflecting paleoenvironmental and paleoclimate changes during the Late Pliocene and transition to the Early Pleistocene inferred from the lower 200 m of Lake El'gygytgyn lacustrine sediments.

Initila pollen studies show that lacustrine sediments accumulated in Lake El´gygytgyn are an excellent archive of vegetation and climate changes since ca 3.55 Myr BP. Studied pollen assemblages can be subdivided into 25 pollen zones which are well reflecting the main paleoenvironmental fluctuations in the region during the late Pliocene and Pleistocene. Climate conditions in the study area were the warmest about 3.5-3.35 Myr BP. Spruce-fir-hemlock-larch-Pseudotsuga forests dominated the vegetation in nowadays treeless tundra area. Temperatures were at least 15° C higher than modern. After ca 3.4 Myr BP dark coniferous taxa gradually disappeared from the vegetation cover. The very pronounced environmental changes are revealed about ca 3.35-3.275 Myr BP when treeless tundra and steppe like Poaceae-Cyperaceae-Artemisia-Selaginella rupestris habitats dominated the area. Large amounts of coprophilous fungi spores point to a permanent presence of numerous grazing herds around the lake. It is noticeable that according to the paleomagnetic geochronology this episode occurred at the Mammoth subchron during the Gauss chron. The dry and cold climate conditions were similar to those during the Late Pleistocene. Temperatures were close to the modern. We may assume that area was under permafrost condition. Larch-stone pine forests with some spruce changed again to treeless and shrubby environments at the beginning of the Pleistocene, ca 2.6 Myr BP. The Early Pleistocene sediments contain pollen assemblages reflecting alternation of treeless intervals with cold and dry climate and warmer intervals when larch

forests with stone pine were also common in the region. Very dry environmental conditions are revealed after ca 2.175 Myr BP. High amounts of green algae colonies (Botryococcus) point to a shallow water conditions ca 2.55, 2.45, and ca 2.175 Myr BP.

The further high-resolution palynological study of the sediment core are important to reveal climate fluctuations inside the main glacial/interglacial intervals and will give the first continuous and detailed scheme of environmental changes for the whole Arctic.

References:

Andreev, A., Schirrmeister, L., Tarasov, P., Ganopolski, A., Brovkin, V., Siegert, C., Hubberten, H.-W. (2011). Vegetation and climate history in the Laptev Sea region (arctic Siberia) during Late Quaternary inferred from pollen records, Quaternary Science Reviews 30, 2182-2199.

Melles, M., Brigham-Grette, J., Minyuk, P., Koeberl, C., Andreev, A., Cook, T., Gebhardt, C, Haltia-Hovi, E., Kukkonen, M., Nowaczyk, N., Schwamborn, G., Wennrich, V. & El'gygytgyn Scientific Party. (2011). The Lake El'gygytgyn Scientific Drilling Project – Conquering Arctic Challenges in Continental Drilling, Scientific Drilling 11, 29-40.

ICDP

Paleogeophysical characterization of a climate archive based on downhole logging in the ICDP project PALEOVAN

H. BAUMGARTEN, T. WONIK, S. HUNZE

Leibniz-Institute for Applied Geophysics (LIAG), Stilleweg 2, 30655 Hannover

Lake Van (eastern Anatolia, Turkey) is the 4th largest terminal lake worldwide and is located at a key climatic position. Past climate changes have been recorded in the sensitive hydrological system of Lake Van, which is evident from terraces around the lake. The lake sediments archives approximately 500,000 years of climate history. The ICDP project PALEOVAN aims to enhance the understanding of the paleoclimatic and paleoenvironmental conditions of the Middle East.

Investigations (shallow coring, surface geophysics) have been started in 1970's and a deep drilling campaign has been executed in summer 2010. Two boreholes with total depth of 140 m (Northern Basin) and 220 m (Ahlat Ridge) were drilled; the core recovery was about 91 % (Ahlat Ridge) and 71 % (Northern Basin). The Ahlat Ridge site is located in a deep basin of Lake Van (water depth: 375 m). Results from a geophysical survey indicate, that an undisturbed sedimentary sequence is preserved. The lithology consists mainly of clayey silt and tephra deposits, which originates from several volcanoes in the surrounding of Lake Van.

A continuous dataset of downhole data (spectral gamma ray, magnetic susceptibility, dipmeter, and resistivity) as well as partly sonic data have been achieved at both sites. Spectral gamma ray, resistivity, and susceptibility data have been interpreted by applying multivariate statistics (cluster analysis). The logs have been subdivided into cluster units based on similarities in their physical properties. The lithological information from the visual core description has been taken into account and associated lithological units have been derived.

The tephra deposits at the Ahlat Ridge drillsite are characterized by strong differences in their physical properties. The tephra differ mainly in their natural radioactivity and susceptibility values.

Depth trends can be observed. Tephra with higher susceptibility and lower natural radioactivity occur frequently at the deeper part of Ahlat Ridge whereas tephra tends to have lower susceptibility and higher natural radioactivity values at the shallower section. This suggests compositional changes of the tephra deposits (basaltic – rhyolithic) in time. In cooperation with other PALEOVAN working groups, not only differentiation but also linking with different volcanic sources and eruption phases is possible.

IODP

Hydrothermal alteration of Site 1309 gabbro during experimental conditions beyond the critical point of seawater

O. BEERMANN[1], D. GARBE-SCHÖNBERG, A. HOLZHEID

[1]CAU Kiel, Institut für Geowissenschaften, Ludewig-Meyn-Str. 10, 24118 Kiel; mail: ob@min.uni-kiel.de

Submarine hydrothermalism with extensive alteration of oceanic crust is a major process governing energy and mass fluxes from Earth's interior into the oceans. New estimates suggest that about fifty percent of hydrothermal crust alteration occurs along slow and ultra-slow spreading ridges in the deep sea (1). Hydrothermal systems in water depths >3000 m can run at extreme temperatures under pressure (p) and temperature (T) conditions above the critical point of seawater (298 bar and 407 °C [2]) if enough heat from magma injections is provided. Exactly this type of submarine hydrothermalism has recently been discovered [3]: a high-pressure system in 3000 m water depth at 5°S on the Mid Atlantic Ridge (MAR) emanating extremely hot fluids (>400°C), which contain high to very high concentrations of dissolved hydrogen, methane, transition metals (e.g., Cu, Fe) and exhibit a unique rare earth element (REE) chemistry with LREE and HREE depletion and no Eu-anomaly ('special REE-signature') [4]. New results from 2- and 3-D phase models indicate that these high-pressure systems run very stable for long time periods without compositional fluctuations as known from the East Pacific Rise (EPR) in <2500 m water depth [5, 6].

There is a large deficiency in experiments studying changes in chemistry of fluid and original rocks from the oceanic crust, e.g. MOR basalt and gabbro, during hydrothermal alteration by seawater at p-T-conditions typical for deep water slow-spreading ridges. However, hypotheses exist to explain the chemical composition of the high p-T MAR 5°S fluids, (1) one explains MAR 5°S fluids being the result of re-dissolution of anhydrite previously formed in the sub-seafloor, (2) another hypothesis points towards the involvement of a 'reaction zone fluid' originating from the leaching of oceanic crust at p-T-conditions of the two phase seawater field [3, 4].

Improvement of parameters controlling the fluid chemistry during high p-T seawater-MORB alteration requires experimental investigations of element partitioning (including REEs) between MORB and both, single phase seawater fluid or brine and vapor. Therefore, in situ sampling of single phase fluid as well as coexisting liquid and vapor- or brine and vapor phases - the latter being stable only at experimental p-T conditions - is essential.

Therefore, we refined the Au reaction cell system by inserting two individual Ti-sampling tubes into an Au

reaction cell. This set-up allows in situ sampling of both, single or two phase fluids below or above the critical p-T conditions of seawater. The entire reaction cell system is enclosed by a hydrothermal vessel (PARR® reactor), which can be externally heated.

The p-T conditions inside the vessel imposed by isochoric heating up to 490°C and 485 bar using distilled water are - within an uncertainty of ± 2 bar and ± 2°C - in agreement with the equations of state for H_2O [7]. First in situ sampling tests using the Au reaction cell filled with 25 ml of 3.2 wt.% NaCl(aq) at 430°C and 427 bar (conditions of the two phase seawater field) revealed high saline fluid/brine (~19 wt.% NaCl) and low saline vapor (~0.5 wt.% NaCl), which have been extracted separately. In total ~3 ml of brine was sampled first without any changes in p, while during extraction of vapor (in total ~2 ml with respect to the volume of condensed vapor) p decreased by ~15 bars. However, NaCl concentrations of both, brine and vapor, were in good agreement to the values given by the solvus for the system NaCl-H_2O at prevailed p and T [8, 9]. In the following seawater-MORB alteration experiments will be performed by using fine-grained unaltered gabbro as starting rock (a core sample from MAR 30°N, Site U1309D, Atlantis Massif, IODP expedition 305) and natural bottom seawater collected at MAR 5°S as well as synthethic NaCl(aq)-liquids as starting fluid.

References:
[1] German et al. (2009) Geochim. Cosmochim. Acta 73, A428 (Goldschmidt Conf. Abstracts).
[2] Bischoff & Pitzer (1985) EPSL 25, 385-397
[3] Koschinsky et al. (2008) Geology 36, 615-618
[4] Schmidt et al. (2010) Geochim. Cosmochim. Acta 74, 4058–4077
[5] Coumou et al. (2008) Geochim. Cosmochim. Acta 72, A184 (Goldschmidt Conference Abstracts).
[6] Coumou et al. (2009) J. Geophys. Res. 114, B03212.
[7] Wagner & Pruss (2002) J. Phys. Chem. Ref. Data, 31, 387-535.
[8] Bischoff & Pitzer (1989) Am. J. Sci. 289, 217-248.
[9] Driesner & Heinrich (2007) Geochim. Cosmochim. Acta 71, 4880–4901.

IODP

Geochemical constraints on the evolution of the Louisville Seamount Trail

C. BEIER[1], A.R.L. NICHOLS[2], P.A. BRANDL[1], H. BRÄTZ[1], IODP EXPEDITION 330 SCIENTISTS[3]

[1]GeoZentrum Nordbayern, Universität Erlangen-Nürnberg, Schlossgarten 5, D-91054 Erlangen
[2] Institute for Research on Earth Evolution (IFREE), Japan Agency for Marine Earth Science and Technology (JAMSTEC), 2-15 Natsushima-cho, Yokosuka, Kanagawa, 237-0061, Japan
[3] Integrated Ocean Drilling Program, Texas A&M University, College Station, TX.

The geochemical changes observed in long-lived seamount chains can be used to test models of the origin of oceanic intraplate volcanism and the evolution of magmas within a single seamount. The along-chain (temporal) variations in lava composition may arise from variations in the composition of the mantle sources, changes in the melting process, and/or vari- ability in the thickness of the underlying lithosphere, which influences the degree and depth of melting beneath intraplate volcanoes. Small scale variations within a single seamount may reflect variations in fractional crystallisation and assimilation. Samples recovered during drilling at various sites along long-lived seamount chains provide the easiest way to evaluate all of these variations. The Hawaiian-Emperor Seamount Chain and Louisville Seamount Trail, both in the Pacific Ocean, preserve more than 70 Ma of age-progressive volcanism.

The geochemical evolution of the Hawaiian-Emperor Seamount Chain is relatively well known from drilled and dredged samples. In contrast, the Louisville Seamount Trail is much less well sampled and only few geochemical data are available (Beier et al., 2011; Cheng et al., 1987; Hawkins et al., 1987). The Louisville Seamount Trail is approximately 4200 km long, extending southeastward from Osbourn Seamount, which is currently being subducted into the Tonga Trench, to a seamount located about 300 km west of the Pacific Antarctic Rise. The youngest sample from the Louisville Seamount Trail, with an age of 1.11 Ma (Koppers et al., 2004), was recovered from this seamount and ages increase westward. Lithosphere to the west of the West Wishbone Scarp formed at the Osbourn Trough spreading centre, which became extinct at ~90 Ma (Downey et al., 2007), while lithosphere to the east of East Wishbone Scarp formed at the Pacific Antarctic Rise. As a result, the thickness of the lithosphere underlying the older end of the Louisville Seamount Trail decreases from south to north, while seamount ages increase.

During IODP Expedition 330 six sites on five different seamounts along the westermost 1500 km of the Lousiville Seamount Trail were drilled. Here, we present preliminary major (including Cl, F, S), trace and volatile element data for glass measured by electron microprobe, laser ablation inductively coupled mass spectrometry (LA-ICP-MS) and Fourier-transform infrared (FTIR) spectroscopy, respectively, from the four seamounts in which glass was recovered. All glass samples analysed are alkalic, in agreement with published dredge samples (Beier et al., 2011; Cheng et al., 1987); most are basalts to tephrites, with a few trachybasalts, and their MgO and SiO_2 contents range from 3.5 to 7.3 wt.% and 44.46 to 50.17 wt.%, respectively. Major and trace elements for volcanic glasses along the westernmost end of the Louisville Seamount Trail imply that volcanism was geochemically extremely uniform from ~85 Ma to 50 Ma both along-chain and within a single seamount. The glasses provide no evidence for a tholeiitic shield building stage in the Lousiville seamounts, contrary to what is generally observed in the Hawaiian volcanoes.

Incompatible element ratios (e.g., Nb/U, Ce/Pb) imply that the glasses are fresh and, unlike published whole rock data (Beier et al., 2011), display no evidence for significant alteration despite the relatively large age range covered. Rare earth element (REE) ratios (e.g., Ce/Yb, Sm/Yb) from the deepest site drilled during IODP Expedition 330, U1374 at Rigil Seamount, imply that older glasses from deeper than 245 meters below seafloor may have been derived from smaller degrees of partial melting than the younger lavas. However, these changes are small (<1-2% difference in degree of partial melting). La/Yb and Zr/Nb of the Louisville Seamount Trail glasses are homogeneous over a period of at least 35 Myr while other intraplate volcanic settings display much greater variability on much shorter timescales (e.g., Hawaii shows more than twice the variability of the Louisville Seamount Trail in these ratios over <5 Ma (Shafer et al., 2005; Yang et al., 1996)). The immobile trace element ratios (e.g. Nb/Zr, La/Yb) increase and become more variable from the oldest (U1372) to the youngest (U1377) site and imply decreasing degrees of

partial melting. Volatile concentrations (H_2O, CO2, Cl, F, S) indicate that most samples have degassed, suggesting eruption near or above sea level. Assuming saturation, the H_2O contents from the youngest seamount drilled (Site U1377) indicate that these samples were erupted in the deepest water (~300 meters below sea level). The deeper eruption depths recorded by the younger seamount suggest that the seamounts that erupted on younger lithosphere subsided faster than the older seamounts erupted on older lithosphere. This reflects the greater flexibility of oceanic lithosphere <50 Ma, while lithosphere >50 Ma is more rigid and thus less affected by the overlying seamount.

Beier, C., Vanderkluysen, L., Regelous, M., Mahoney, J.J. and Garbe-Schönberg, D., 2011. Lithospheric control on geochemical composition along the Louisville Seamount Chain. Geochem. Geophys. Geosyst., 12: Q0AM01.

Cheng, Q. et al., 1987. Isotopic evidence for a hotspot origin of the Louisville seamount chain, Seamounts, islands, and atolls. American Geophysical Union, Washington, DC, United States, pp. 283-296.

Downey, N.J., Stock, J.M., Clayton, R.W. and Cande, S.C., 2007. History of the Cretaceous Osbourn spreading center. Journal of Geophysical Research, 112: B04102.

Hawkins, J.W., Lonsdale, P.F. and Batiza, R., 1987. Petrologic evolution of the Louisville seamount chain. In: B.H. Keating (Editor), Geophysical Monograph Series. AGU, Washington D.C., pp. 235-254.

Koppers, A.A.P., Duncan, R.A. and Steinberger, B., 2004. Implications of a nonlinear $^{40}Ar/^{39}Ar$ age progression along the Louisville seamount trail for models of fixed and moving hot spots. Geochem. Geophys. Geosyst., 5(6): Q06L02.

Shafer, J.T., Neal, C.R. and Regelous, M., 2005. Petrogenesis of Hawaiian postshield lavas: Evidence from Nintoku Seamount, Emperor Seamount Chain. Geochem. Geophys. Geosyst., 6(5): Q05L09.

Yang, H.-J., Frey, F.A., Rhodes, J.M. and Garcia, M.O., 1996. Evolution of Mauna Kea volcano: Inferences from lava compositions recovered in the Hawaii Scientific Drilling Project. Journal of Geophysical Research, 101: 11747-11767.

IODP

The Neogene monsoon and oceanic currents in the Indian Ocean: The Maldives archipelago

C. BETZLER[1], C. HÜBSCHER[1], T. LÜDMANN[1], J. REIJMER[2], G. EBERLI[3], D. KROON[4], A. DROXLER[5], M. TIWARI[6], E. GISCHLER[7]

[1]University Hamburg (Germany)
[2]VU University Amsterdam (Netherlands)
[3]RSMAS Miami (USA)
[4]University Edinburgh (UK)
[5]Rice University Houston (USA)
[6] National Centre For Antarctic & Ocean Research Goa (India)
[7]University Frankfurt (Germany)

New seismic data from the Maldives show that the Neogene of the Maldives carbonate edifice image large drift deposits controlled by Indian monsoon-triggered currents. The stacking pattern of depositional sequences through the Lower to Middle Miocene traces variations of accommodation space, which are proposed to be primarily governed by fluctuations of relative sea level. During the late Middle Miocene, this system was replaced by a twofold configuration of bank development. Bank growth continued synchronously with partial bank drowning and associated deposition of giant sediment-drifts. Drowned banks show shapes attesting the occurrence of strong surface currents. Therefore, this turnover is attributed to the onset and/or intensification of oceanic currents and related upwelling. Drift sediments, characterized by offlapping geometries, formed as large-scale prograding complexes. Our drilling plan for IODP includes seven proposed drill sites in water depths of 370-540 m in the central Inner Sea realm.

The overall development of shape and relief of the modern/Quaternary Maldive atolls presumably also relates to the monsoon current pattern. It is true that development of Quaternary reef geomorphology is largely attributed to the interplay of reef growth during Pleistocene sea-level rise and highstands and to dissolution (karst) during sea-level fall and lowstands. However, the typical circular shapes formed by sand and reef growth seen in both marginal and internal platforms, so unique to the Maldives, strongly suggests changing current control as major additional factor. In order to test this hypothesis we propose one drill site on a marginal island of South Maalhosmadulu Atoll within the framework of ICDP, in the vicinity of the seven IODP sites. In order to keep logictics at a low level, we propose to drill from one location vertically into the reef margin proper and inclined into each the fore reef and the platform lagoon (3 cores).

Findings are not only expected to be applicable to other examples of Neogene platforms in the Indo-Pacific region but also to other carbonate platforms in the geological record. Onset, type and variations of drift deposits in the platform edifice further provide not only a new and valuable proxy for the reconstruction of the oceanic currents around the Maldives but also for the development of the associated large-scale oceanographic current system with a world-wide impact. Additionally, the sedimentary record of the drift deposits may represent an excellent archive of the Indian monsoon history. The overall aim of the project thus is to place the Maldives current system into the larger scale development of the global oceanographic current system by integrating results from other ODP and IODP expeditions like the south Atlantic, the Mediterranean outflow, or the Bahamas expeditions. Apart from pure scientific aspects, the analysis of Quaternary reef and platform accretion patterns will contribute to the important socioeconomic aspect of mid-ocean island development in the light of climate change and sea-level rise, which affects >50 million people worldwide in the small island developing states (SIDS).

IODP

Reconstruction of the Atlantic Circulation back to the Last Interglacial by a combined proxy approach from ODP Leg 172 Site 1063 sediments

E. BÖHM[1], J. LIPPOLD[1], A. MANGINI[1], M. GUTJAHR[2], F. WOMBACHER[3]

[1]Academy of Sciences, Heidelberg, Germany
[2]National Oceanography Centre Southampton, UK
[3]University of Köln, Germany

The Atlantic Meridional Overturning Circulation (AMOC) plays a key role in the global climate system due to the transport of heat energy and CO_2. Thus, it is crucial to reconstruct the past distribution of water masses and circulation strengths in order to assess its future impact on global climate.

εNd and $^{231}Pa/^{230}Th$ from deep sea sediments are two promising proxies to derive the origin of water masses respectively to the past strength of ocean circulation. In preceding projects the high accumulating sediment core ODP Leg 172 Site 1063 has been proved as an appropriate

location for the application of both proxies (Gutjahr and Lippold, 2011; Lippold et al., 2009). In this study the existing data set has been extended in high temporal resolution back to the last Interglacial (Eemian). It is assumed that temperatures during the Eemian were partly higher than during the Holocene (Kaspar et al., 2005). Thus, in regard to a recent global warming, these reconstructions of the past ocean circulation may serve to anticipate future developments.

Fig. 1: Comparison of Eemian εNd (black) to Holocene εNd (grey) and to SPECMAP (δ18O)

Numerous measurements of $^{231}Pa/^{230}Th$ have already been performed in the time range from 65 to 143 ka with a high temporal resolution (1 ka or less; Fig. 2). First results show that the 231Pa/230Th method reaches its detecting limit at 125 ka due to the short half life of 231Pa (T1/2=33 ka). Beyond this age the lithogenic background and the ingrow from the authigenic fraction become too high in relation to the excess fraction. In the time span from 125 to 137 ka the proportion of 231Paxs within the total 231Pa is in the range of 10 - 20 % causing unreliable data. The time span between 95 and 125 ka displays strong fluctuations (231Pa/230Th =0.046 to 0.079) with one pronounced peak at 119 ka (231Pa/230Th =0.095). This is consistent with (Bauch et al., 2011) who found a short cold event with near-glacial surface ocean summer temperatures in MIS 5.5.

This study is the first which use synergetic effects of both εNd isotope and $^{231}Pa/^{230}Th$ ratio measurements from identical samples on a timescale back to the Eemian Interglacial. The time interval of the planned measurements (35 ka back to 130 ka) spans several severe climate incidents like Heinrich Events (HE-4 to HE-6), numerous Dansgaard-Oeschger Cycles, the Last Glacial Inception and the last Interglacial.

Several measurements of the water mass source proxy εNd have been accomplished already within the time range from 60 to 154 ka with a temporal resolution of averaging 3 ka. The transition from MIS 6 to MIS 5.5 is marked by a distinct drop in the εNd values from -11,5 to -14 (Fig. 1, switch from Southern Sourced Water (SSW) to Northern Sourced Water). This is consistent with εNd results from (Gutjahr and Lippold, 2011) obtained from the same core at the transition from MIS 2 to MIS 1.1 and from a neighbouring core (Roberts et al., 2010) (Fig. 1, grey lower x-axis). The radiogenic εNd during MIS 6 to MIS 6.4 displays the presence of SSW while unradiogenic εNd values at the beginning of MIS 5.5 indicates an active deep water formation in the north comparable to the Holocene. The similar temporal behaviour of εNd during Termination I and II implies recurring millennial-scaled identical processes converting the AMOC from a Glacial mode into an Interglacial mode. The post-Eemian Glacial Inception displays generally unradiogenic εNd with two surprisingly extreme low values around 93 ka and 100 ka.

To the assess the potential influence on $^{231}Pa/^{230}Th$,

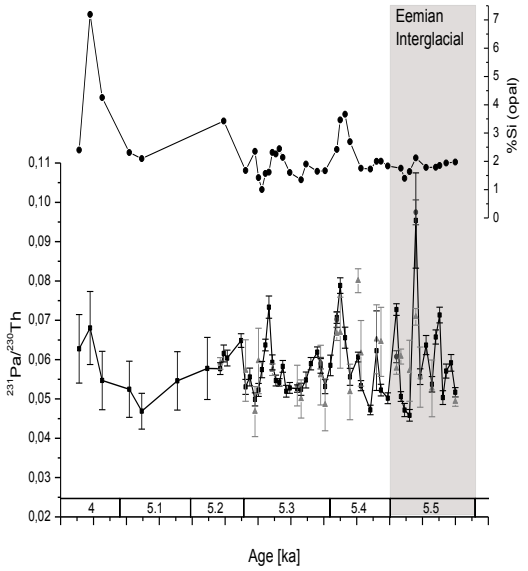

Fig. 2: Comparison of $^{231}Pa/^{230}Th$ and biogenic opal measurements

measurements of biogenic opal have been performed. Biogenic opal effects the 231Pa/230Th ratio because 231Pa has a strong affinity for this type of particles (Bradtmiller et al., 2007; Chase et al., 2002; Geibert and Usbeck, 2004; Lippold et al., 2009). This may result in high 231Pa/230Th despite of an active AMOC. In this case, opal flux and 231Pa/230Th would be correlated. The opal content in the measured samples does not exceed 5 % apart from one data point at 69 ka with 7 % (Fig. 2). This very small biogenic opal content in combination with the absence of significant correlation implies that local variations in opal flux at ODP Site 1063 do not affect 231Pa/230Th. Therefore, the variations in 231Pa/230Th may rather attributed to AMOC variations.

References:

Bauch, H.A. et al., 2011. Climatic bisection of the last interglacial warm period in the Polar North Atlantic. Quaternary Science Reviews, 30(15-16): 1813-1818.

Bradtmiller, L.I., Anderson, R.F., Fleisher, M.Q. and Burckle, L.H., 2007. Opal burial in the equatorial Atlantic Ocean over the last 30 ka: Implications for glacial-interglacial changes in the ocean silicon cycle. Paleoceanography, 22(4): PA4216.

Chase, Z., Anderson, R.F., Fleisher, M.Q. and Kubik, P.W., 2002. The influence of particle composition and particle flux on scavenging of Th, Pa and Be in the ocean. Earth and Planetary Science Letters, 204(1â€“2): 215-229.

Geibert, W. and Usbeck, R., 2004. Adsorption of thorium and protactinium onto different particle types: experimental findings. Geochimica et Cosmochimica Acta, 68(7): 1489-1501.

Gutjahr, M. and Lippold, J., 2011. Early arrival of Southern Source Water in the deep North Atlantic prior to Heinrich event 2. Paleoceanography, 26(2): PA2101.

Kaspar, F., Kühl, N., Cubasch, U. and Litt, T., 2005. A model-data comparison of European temperatures in the Eemian interglacial. Geophys. Res. Lett., 32(11): L11703.

Lippold, J. et al., 2009. Does sedimentary 231Pa/230Th from the Bermuda Rise monitor past Atlantic Meridional Overturning Circulation? Geophys. Res. Lett., 36(12): L12601.

Roberts, N.L., Piotrowski, A.M., McManus, J.F. and Keigwin, L.D., 2010. Synchronous Deglacial Overturning and Water Mass Source Changes. Science, 327(5961): 75-78.

IODP

Stable Strontium and Calcium Isotopes of Low Temperature Alteration Carbonates from Ocean Crust Basalts

F. BÖHM[1], A. EISENHAUER[1], S. RAUSCH[2], W. BACH[2], A. KLÜGEL[2], A. NIEDERMAYR[3], J. TANG[4], M. DIETZEL[5]

[1]Helmholtz-Zentrum für Ozeanforschung Kiel (GEOMAR), Germany
[2]Geoscience Department, University of Bremen, Germany
[3]Institut für Geologie, Mineralogie und Geophysik, Ruhr-Universität Bochum, Germany
[4]Department of Earth & Environmental Sciences, Tulane University, New Orleans, USA
[5]Institute of Applied Geosciences, Graz University of Technology, Graz, Austria

The calcium carbonate minerals calcite and aragonite frequently form during low temperature alteration (LTA) of ocean crust basalts (Staudigel et al., 1981). LTA carbonates represent a sink for carbon and calcium that plays a significant role in global budgets (Alt & Teagle, 1999). They further can provide records of the chemical composition of seawater (Sr/Ca, Mg/Ca ratios) on multi-million year timescales (Coggon et al., 2010). However, the latter application is still debated (Creech et al., 2010; Broecker & Yu, 2011; Coggon et al., 2011).

Stable isotopes of calcium and strontium in LTA carbonate minerals may allow to evaluate the quality of the seawater chemistry records. Kinetic processes during mineral formation and diagenetic alteration during deep burial in the ocean crust can modify the composition of the LTA carbonates. These processes are expected to influence both element and isotope ratios. We therefore started recently to investigate radiogenic strontium isotopes ($^{87}Sr/^{86}Sr$), stable strontium isotopes ($\delta^{88/86}Sr$) and calcium isotopes ($\delta^{44/40}Ca$) of LTA calcites and aragonites from DSDP and ODP cores of the Atlantic and Pacific Ocean. Additional sampling of Indian Ocean cores is planned to complement the sample set.

Studies of paired strontium and calcium isotope analyses of calcite and aragonite grown in laboratory experiments using CO_2 diffusion techniques (Tang et al., 2008; Niedermayr, 2011) provide a baseline for interpretation of isotope effects observed in the LTA samples. The experimental precipitation studies revealed a strong positive correlation of $\delta^{88/86}Sr$ and $\delta^{44/40}Ca$ of calcite resulting from kinetic isotope fractionation controlled by precipitation rates (Böhm et al., submitted). Aragonite, in contrast, displays rate dependent fractionation for calcium isotopes (Niedermayr, 2011), but not for strontium isotopes.

Calcium isotopes of most LTA calcites are significantly heavier compared to the LTA aragonites. Some young LTA calcites are heavier than the experimental calcites. This is probably a result of the slow precipitation in isotopic quasi-equilibrium in cold deep-ocean water. LTA aragonites preferentially take up light calcium, showing more depleted values than experimental aragonites. In analogy with the rate dependent fractionation effects of calcite, this observation indicates a significantly lower equilibrium calcium isotope fractionation for aragonite than for calcite. The LTA calcites with the lowest Ca isotope values in our data set formed in warm basement fluids (25 to 55°C) and may have incorporated light calcium from ocean basalt.

Strontium isotopes of most LTA samples plot in a very narrow range slightly lighter than the modern seawater value. LTA aragonite might be slightly heavier than LTA calcite and is significantly heavier than experimental aragonite. LTA calcites are slightly enriched in heavy Sr compared to experimental calcite. There is no correlation between Ca and Sr isotopes of the LTA calcites, which is in obvious contrast to the experimental calcite results. The lack of correlation largely excludes rate effects as an explanation for the light Ca isotope signatures of the LTA calcites that formed in warm basement fluids. More likely light basaltic Ca was enriched in these warm fluids.

Most remarkably, some samples show significant enrichment of heavy Sr relative to modern seawater. This observation can not yet be explained with the available preliminary data and current fractionation models.

With the available data we do not observe any $\delta^{88/86}Sr$ trend that can be correlated with geological or geochemical parameters (including sample formation age, formation temperature, depth in basement, $^{87}Sr/^{86}Sr$, Sr/Ca ratios). More data are necessary to explain the significant variability observed in stable Sr isotope fractionation of LTA calcites and aragonites.

References:

Alt J.C., Teagle D.A.H. (1999) The uptake of carbon during alteration of ocean crust. Geochimica et Cosmochimica Acta 63: 1527-1535.

Böhm, F., Eisenhauer A., Tang J., Dietzel M., Krabbenhöft A., Kisakürek B., Horn C. (submitted) Strontium isotope fractionation of planktic foraminifera and inorganic calcite.

Broecker W.S., Yu J. (2011) What do we know about the evolution of Mg to Ca ratios in seawater? Paleoceanography 26: doi:10.1029/2011PA002120.

Coggon, R.M., Teagle, D.A.H., Smith-Duque, C.E., Alt, J.C., Cooper, M.J. (2010), Reconstructing past seawater Mg/Ca and Sr/Ca from mid-ocean ridge flank calcium carbonate veins. Science 327, 1114-1117.

Coggon R.M., Teagle D. A. H., Dunkley Jones T. (2011) Comment on "What do we know about the evolution of Mg to Ca ratios in seawater?" by Wally Broecker and Jimin Yu. Paleoceanography 26: doi:10.1029/2011PA002186

Creech J.B., Baker J.A., Hollis C.J., Morgans H.E.G., Smith E.G.C. (2010) Eocene sea temperatures for the mid-latitude southwest Pacific from Mg/Ca ratios in planktonic and benthic foraminifera. Earth and Planetary Science Letters 299: 483-495.

Niedermayr, A. (2011) Effects of magnesium, polyaspartic acid, carbonate accumulation rate and temperature on the crystallization, morphology, elemental incorporation and isotopic fractionation of calcium carbonate phases. Doctoral Thesis, 158pp., Graz University of Technology, Graz.

Staudigel H., Hart S., Richardson S. (1981) Alteration of the oceanic crust: Processes and timing. Earth and Planetary Science Letters 52: 311-327.

Tang J., Dietzel M., Böhm F., Köhler S. J., Eisenhauer A. (2008) Sr2+/Ca2+ and 44Ca/40Ca fractionation during inorganic calcite formation: II. Ca isotopes. Geochimica et Cosmochimica Acta 72: 3733-3745.

ICDP

Evolution of magma storage conditions of Yellowstone hotspot, an experimental study focused on magmatic water content (DFG project HO1337/22)

T. BOLTE[1], F. HOLTZ[1], R. ALMEEV[1], B. NASH[2]

[1]Institute of Mineralogy, Leibniz University of Hannover
[2]Department of Geology and Geophysics, University of Utah

The Snake River Plain Yellowstone Hotspot volcanic province (SRPY) elongates from the border triangle of Oregon, Nevada and Idaho in northeast direction through the northwest of the USA, to the Yellowstone Plateau at the

border between Wyoming and Idaho, the currently active element of YSRP. The continental crust of the North American plate moved more than 600km in west-southwest direction over the Yellowstone hotspot during the last 15 Ma and induced a bimodal (rhyolitic – basaltic) magmatism (Morgan & McIntosh, 2005; Camp & Ross, 2004). This volcanism partly produced large volume eruptions (up to 3000km³) (Christiansen *et al.*, 2002) of high-silica rhyolites with ash fall tuffs and ignimbrites, and hence is one of the Earths largest active silicic-dominated volcanic system.

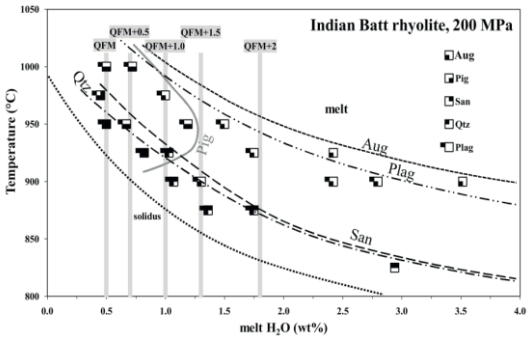

Figure 1. Phase diagram with phase stability fields for the experimental run of IBR composition at 200MPa. Lines show estimated stability fields as a function of temperature and water content in the melt. Note that Pigeonite is always present in the natural rocks and that the pre-eruptive conditions are within the stability field of this mineral (H_2O content < 1.5 wt%).
Abbreviations of phase symbols: Plag = plagioclase, Aug = augite, Pig = pigeonite, San = sanidine, Qtz = quartz, grey verticals = calculated redox conditions relative to QFM.

In addition to implications for paleo-climate and paleo-environmental change, the general aims of the scientific drilling project in the Snake River Plain (SRP) are the characterization of the chemical and isotopic composition of the basalts and rhyolites through time at each drill site to constrain the effects of fractionation, recharge, and assimilation, the effects of the underlying lithosphere on magma compositions, and the changes in these processes with time. The variation of chemical and isotopic compositions of basalts and rhyolites between drill sites will be compared to characterize the role of age and composition of the underlying lithosphere. Information of ages and compositions of rhyolitic caldera complexes that underlie the eastern SRP will be useful to determine their origin (crustal melts, mantle fractionates) and to constrain the timing of eruption and rate of plume movement.

The drilling activity has just finished. The first drilling started in September 2010 at Kimama. The drilling moved to Kimberly in January 2011. The third drilling at Mountain Home has been finished in July 2011. Actually the open hole logging and the preparation for longterm loggings is running at Mountain Home drill site (Shervais et al, 2005).

Among the general questions mentioned above, this proposal focus mainly on the evolution of magma storage conditions of rhyolites and basalts in space and time. In this report we present results obtained in the first 14 months of the project. Analytical and experimental work has been conducted to trace the evolution of magma storage conditions in space and time, by using natural samples from different eruptive centers across the Snake River plain. The ages of the collected natural rhyolite samples vary from 10.5 Ma to 0.6 Ma. In a first stage, particular attention is given to 12.7 to10.5 Ma rhyolitic eruptive events (Bruneau Jarbidge eruptive center) and 6.6 to 4.4 Ma events (Heise eruptive center). The natural rhyolites of all sample locations range from low to high silica, medium to high K_2O and display classical characteristics of A-type granites.

Analytical work: Bulk analysis (commercial) and microprobe analyses of glasses, glass inclusions and of the main mineral phases (Pl+San+Aug+Pig+Mt+Ilm+Qtz±Fa) have been used to determine crystallization temperatures using various geothermometers (two-pyroxene thermometer; Ilmenite-magnetite pairs; Ti-in-quartz; zircon saturation). The two-pyroxene results obtained for the Bruneau Jarbidge eruptive center (975°C to 994°C) confirm the temperatures determined by Cathey and Nash (2004) from two-pyroxene thermometry. The calculated temperatures for the different units are also in good agreement with previous published observations (Nash & Perkins, 2005; Nash et al, 2006; Christiansen & McCurry, 2008; Watts, 2010). Our measurements of Ti concentrations in quartz minerals indicate similar high temperatures (982 to 995 °C at 260 – 270MPa) using the recent Ti-in-quartz thermobarometer of Huang & Audetat (2011). Pressure estimations using the Ti-in-quartz method are in the range of 260 – 270MPa. The dataset obtained so far for Bruneau Jarbidge eruptive center, Heise eruptive center and other recent rhyolites indicate that the magma storage pressure is lower for low temperature magmas (down to 140 MPa for temperatures of ~ 850 °C) and higher for high temperature magmas (up to 280 MPa for temperatures of ~ 950-1000 °C). Additional analytical work is currently conducted on natural sample materials from the Heise eruptive center used for high pressure experiments. Attempts have been made to determine the water concentration in glass inclusions with infrared techniques, but this approach failed (inclusions too small, very low water concentrations) and the results cannot be used to constrain water activities.

Experimental work: A first experimental study was carried out to constrain phase relations representative for the older Bruneau Jarbidge eruptive center (BJ). Two different samples were selected as representatives of explosive and effusive stages of silicic volcanism (Cathey & Nash, 2004). The explosive, high evolved Bruneau Jarbidge Rhyolite (BJR) sample is ~ 10.5 Ma old, crystal poor (5-15%) and characterized by the anhydrous phenocryst assemblage including Pl, San, Aug, Pig, Qtz, Mt, Ilm, fayalite (Fa), and accessory zircon (Zir) and apatite (Ap). These sample is selected from Unit 9j of the Cougar Point Tuff (Cathey and Nash, 2004). The effusive, less evolved Indian Batt rhyolite (IBR) sample is ~ 8.2 – 9.5 Ma old and contains the same ammount of crystalls and mineral assemblage than BJR(Cathey and Nash, 2009). ssure vessels (CSPV) at 800-850°C, and at 50, 200 and 500MPa in internally-heated pressure vessels (IHPV) at 850-1025°C. The run duration varied from 7 to 40 days. The water activity (aH2O) of the experimental charges was varied by adding a fluid composed of a mixture of H2O and CO_2. In CSPV the oxygen fugacity was monitored by adding a solid Ni-NiO oxygen buffer, whereas in IHPV experiments were conducted at intrinsic oxygen conditions, corresponding to NNO+2.6 under H_2O-saturated and to

~QFM at nominally dry conditions. Additional experiments were conducted at reduced oxygen conditions down to QFM -4.5 by adding Hydrogen into the IHPV. Partial Hydrogen pressure was monitored by Shaw membrane technique to calculate oxygen fugacity. Water concentrations in most of the experimental glasses were determined using infrared spectroscopy (FTIR) or Karl Fischer Titration (KFT) (Holtz et al, 2001).

In general, our crystallization experiments support that crystal fractionation is the dominating mechanism responsible for chemical variations in rhyolite from the Bruneau-Jarbidge eruptive center. This is illustrated by the good overlap of natural petrochemical trends (lava flows, ignimbrites, air fall glasses) with experimentally determined liquid lines of descent. Furthermore the anhydrous character of the magmas from the Bruneau Jarbidge eruptive center, published by previous investigations (e.g. Honjo et al., 1992; Perkins & Nash, 2002), is verified by our experiments. Water contents of less than 1.5wt% H_2O are necessary to reproduce natural phase assemblage. The occurrence of iron-phases (magnetite, ilmenite) in the system is strongly dependent on oxygen fugacity; however, changes in oxygen fugacity do not affect significantly LLDs and the stability of phases because of the low Fe content of the systems.

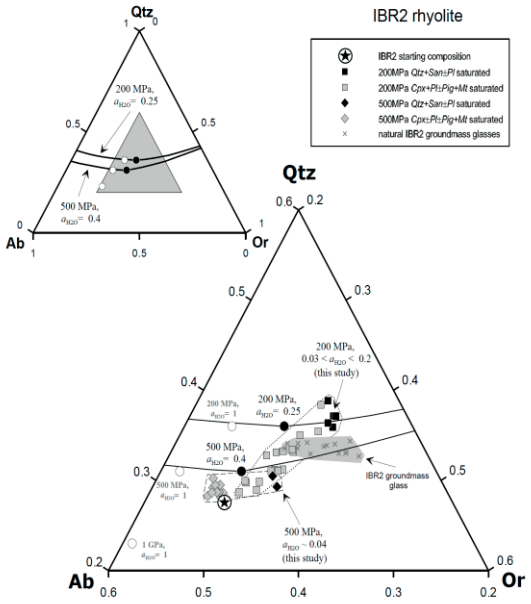

Figure 2. Ternary Qz-Ab-Or diagram with selected glass compositons of IBR experiments compared to natural glasses. Plotted are 200 and 500MPa experiments in addition to experimentally determined cotectic lines of the synthetic haplogranitic system (Holtz *et al*, 1992). The circles are minimum und eutectic compositions for water-saturated conditions; the black dots are minimum compositions for reduced water activities. The grey field and crosses display the range of natural matrix glass compositions. The Qz-Ab-Or contents have been corrected for Ca using the calculation method of Cashman and Blundy (2000).

The experimental results obtained at 200 MPa have been submitted for publication to Journal of Petrology (positive review with minor changes). Data obtained for IBR are shown exemplary in the phase diagram in Fig. 1. Results for BJR at other pressures are not shown here but are used for the general implications. The comparison of the composition of natural and experimentally synthesized phases confirms that high temperatures (> 900 °C) and extremely low melt water contents (less than 1.5 wt% H2O) are required to reproduce the natural mineral assemblages. In melts containing ~ 0.5 to 1.5 wt% H2O, the liquidus temperature of the more evolved composition BJR is ~940 – 1000 °C and is at least 30 °C lower than that of the IBR sample (970-1030 °C). At 200 and 500 MPa, a minimum temperature of 920°C is necessary to reproduce the main phases in IBR. At 200 MPa, the pre-eruptive water content of the melt for IBR is constrained in the range 0.7 – 1.3 wt% at 950°C and 0.3 – 1.0 wt% at 1000°C, assuming a pressure of 200 MPa. For the same ranges of water concentration, at 500 MPa, the respective pre-eruptive temperatures are slightly higher (by ~ 30 to 50°C). It was difficult to constrain pre-eruptive conditions for BJR because one of the main natural phases, plagioclase, could only be synthesized at conditions close to the solidus. However, the compositions of natural and synthetic glasses indicate that the pre-eruptive temperature of plagioclase-free rhyolite is at least 900°C. The composition of the clinopyroxene and pigeonite pairs can only be reproduced for water contents below 1.5 wt% H2O at 900°C, or even lower water contents if the temperature is higher.

The experimental results are used to explore possible proxies to constrain the depth of magma storage. The crystallization

sequence of tectosilicates is strongly dependent on pressure between 200 and 500 MPa. In addition, normative Qtz-Ab-Or contents of glasses quenched from melts coexisting with quartz, sanidine and plagioclase depend on pressure and melt water content, assuming that the normative Qtz and Ab/Or content of such melts is mainly dependent on pressure and water activity, respectively (Holtz et al. 1992). The composition of experimental glasses (melts) obtained in experiments at 200 and 500 MPa and the position of cotectic lines for the haplogranite system are reported in Fig. 2, together with the composition of natural groundmass glasses. Clearly, the experimental melts coexisting with Pl+San+Qtz have normative Qz-contents close to those of the cotectic lines at the corresponding pressure (black diamonds at 500 MPa; black squares at 200 MPa), indicating that the synthetic Qz-Ab-Or system can be used to interpret the composition of the natural rhyolitic systems.

Since the composition of the natural matrix glasses from IBR are between the cotectic lines for 200 and 500 MPa (Fig. 2), a pre-eruptive pressure of ~ 300-400 MPa can be estimated from the glass composition. This pressure estimations is in good agreement with the Ti-in-quartz method indicating a quartz crystallization pressure of ~260MPa (assuming a temperature of 980°C). Using the same approach for BJR composition, a pre-eruptive pressure of 200-300 MPa can be deduced. Finally, it is emphasized that the petrological approach to determine pressure from the composition of glasses coexisting with cotectic assemblages(feldspar +Qtz) which has been tested for the Snake River Plain rhyolites using experimental data may be useful for a variety of rhyolitic magmas, considering that it is extremely difficult to use geobarometers in amphibole-free rhyolitic systems.

Further objectives

Further experimental and analytical studies will focus on the Heise volcanic field. Natural rhyolite samples from 4.45 Ma Kilgore Tuff have been selected to reproduce the phase assemblage and to test if the estimated temperatures are 100 -150°C lower than those of the Bruneau-Jarbidge eruptive center, as already suggested by petrological studies. Additional melt inclusion analyses of selected samples from Bruneau-Jarbidge and Heise eruptive centers should the evolution of melt composition (and possibly P and T) in magma-chamber(s). It is also planed to apply and optimize the approach using the ternary Qz-Ab-Or system to determine pre-eruptive pressures in Yellowstone rhyolites. Finally, the recently proposed Ti-in-quartz thermometer will be used and experiments are planed to calibrate the thermobarometer for the investigated compositions.

Petrological investigations of basaltic rocks from the Snake River plain are planed and crystallisation experiments are planed to be conducted for compositions collected from the ICDP drilling. Samples with no or very little alteration have been drilled and will be selected. The analytical and experimental studies will focus on the conditions under which differentiation took place in the basaltic systems (P, T, volatile activities).

References:

Camp, V. E. and M. E. Ross (2004): Journal of Geophysical Research, 109 (B8).

Cashman, K. and J. Blundy (2000): Philosophical Transactions: Mathematical, Physical and Engineering Sciences 358(1770): 1487-1513.

Cathey, H.E., & Nash, B.P. (2009): Journal of Volcanology and Geothermal Research 188, 173–185

Cathey, H.E., & Nash, B.P. (2004): Journal of Petrology, 45, 27-58.

Christiansen, R. L., Foulger, G. R. & Evans, J. R. (2002): Geological Society of America Bulletin 114, 1245-1256.

Christiansen, E. & McCurry, M., (2008): Bulletin of Volcanology, 70(3): 251-267.

Holtz, F., Johannes W., Tamic N. & Behrens H. (2001): Lithos 56: 1-14.

Holtz, F., H. Behrens, et al. (1992): Chemical Geology 3-4: 289-302.

Honjo, N., Bonnichsen, B., Leeman, W.P., and Stormer, J.C. (1992): Bulletin of Volcanology, 54(3), 220-237.

Huang, R. & Audetat, A. (2011): Goldschmidt 2011 conference abstract.

Morgan, L.A. & McIntosh, C.M. (2005): GSA Bulletin,117, 3/4, 288 - 306.

Nash, B. P. & Perkins, M. E. (2005): Geochimica et Cosmochimica Acta 69, A142.

Nash, B.P., Perkins, M.E., Christensen, J.N., Der-Chuen Lee, Halliday, A.N. (2006): Earth and Planetary Science Letters 247, 143-156.

Perkins, M.E., and Nash, B.P. (2002): Geological Society of America Bulletin, 114(3), 367-381.

Shervais, J. W., Kauffman, J. D., Gillerman, V. S., Othberg, K. L., Vetter, S. K., Hobson, V. R., Zarnetske, M., Cooke, M. F., Matthews, S. H. & Hanan, B. B. (2005): In: Pederson, J. & Dehler, C. M. (eds.) Interior Western United States, 1-26, doi: 10.1130/2005.fl d1006(1102).

Watts, K. E., Bindeman, I. N. et al. (2010): Journal of Petrology 52(5), 857-890.

IODP

Microfossil response to the PETM at DSDP Site 401 (eastern North Atlantic)

ANDRÉ BORNEMANN[1], RAYK WALTHER[1], SIMON D'HAENENS[2], CHRISTIAN JOACHIM[3],

ROBERT P. SPEIJER[2], JÖRG MUTTERLOSE[3], RICHARD D. NORRIS[4]

[1] Institut für Geophysik and Geologie, University Leipzig, Germany,
[2]Department of Earth and Environmental Sciences, KU Leuven, Belgium,
[3] Institut für Geologie, Mineralogie und Geophysik, Ruhr-Universität Bochum, Germany,
[4] Scripps Institution of Oceanography – University of California San Diego, USA.

The Paleocene–Eocene Thermal Maximum (PETM; 55.8 Ma) is the most prominent of a number of global transient warming events during the Paleocene and Eocene epochs. This so-called hyperthermal has been studied in numerous sites with deep and shallow marine sediments as well as in terrestrial archives. Nearly all of these sections show indications of substantial warming based on temperature-sensitive geochemical proxies and a pronounced negative carbon isotope excursion accompanied by biotic changes. However, only few complete deep-sea records exist from the North Atlantic region. In the Bay of Biscay at DSDP Site 401 the PETM is well developed and consists of a fairly thick sequence of clay-rich sediments providing well preserved calcareous microfossils. So far foraminiferal calcite has been used to compile high resolution carbon and oxygen isotope records for the sea-floor and the surface ocean from this site. Carbon isotopes represent the typical asymmetric, negative anomaly of about 2 per mil; oxygen isotope data suggest high rates of freshwater supply into the Bay of Biscay resulting in enhanced water column stratification during both the core of the carbon isotope excursion and the recovery phase.

In this contribution we combine detailed assemblage records of planktic and benthic foraminifera as well as calcareous nannofossils studied from the same sample material in order to reconstruct the biotic response to this severe warming event. This allows us to detect differences and similarities between these microfossil groups that represent different life habitats and trophic strategies.

All three microfossil groups show distinctive changes within the course of the PETM. The quantitative benthic foraminiferal record shows the well-known extinction of several Paleocene taxa. However, a closer look at (the core of) the PETM reveals that the diversity remains relatively high and that the specific benthic taxa and their abundances differ substantially from known records such as Walvis Ridge and Maud Rise in the South Atlantic. Also the two plankton groups reveal major assemblage shifts. Calcareous nannofossils show the typical Fasciculithus/Zygrhablithus cross-over close to the base of the PETM, in addition certain taxa increase significantly in abundance during the CIE core. The oligotrophic-photosymbiotic acarinids introduce the PETM and are subsequently followed by high abundances of Morozovella subbotinae, which is the dominant taxon troughout the CIE core. The meso- to eutrophic chiloguembelinids increase in abundance after the CIE onset, specifically during the two recovery phases. This may indicate high nutrient supply

rates probably related to enhanced run-off from the continent.

Moreover, the preservation of none of the three studied calcareous microfossil groups as well as the detailed planktic foraminiferal fragmention index suggest severe dissolution at the onset of PETM as it is usually the case in other deep-sea records. This is in agreement with the sedimentary carbonate contents which drops from 70 to 30 wt% across the CIE onset, but never reaches values close to zero percent.

ICDP

Spatial and temporal variations of the fluid signatures with regard to ongoing magmatic and different earthquake swarm activity beneath the Cheb basin/CZ

K. BRÄUER[1], G. STRAUCH[2]

[1]helmholtz Centre for Environmental Research – Ufz, Department Catchment Hydrology, Theodor-Lieser-Str.4, 06120 Halle, karin.braeuer@ufz.de

[2]helmholtz Centre for Environmental Research – Ufz, Department Hydrogeology, Permoserstraße 15,04118 Leipzig, gerhard.strauch@ufz.de

Our investigation area is part of the European Cenozoic rift system and located at Czech-German border close to the earthquake swarm region Nový Kostel. This region is the locus typicus for the term "earthquake swarm"; since 1985/86 the largest numbers of earthquake swarms in the Vogtland/NW Bohemia have occurred in the Nový Kostel focal zone. Comprehensive isotopic studies of free fluids (CO_2, He) have been started 20 years ago and have in particular included three extended chemical and isotope monitoring studies lasting for several years each. Seismically induced changes in fluid characteristics could be proved at selected locations, based on unique weekly sampling campaigns (Bräuer et al., 2003, 2008). As a result of the detailed isotopic studies due to the 2000 earthquake swarm an increase of mantle-derived helium were observed at degassing locations in the eastern part of the Cheb basin before this swarm (Bräuer et al., 2005). The finding of mantle-derived free fluids marked by $^3He/^4He$ ratios within the subcontinental mantle range, as well as the fault-related increase of upper mantle-derived helium contributions associated with high gas fluxes as a whole confirm the assumption of channel-like degassing on very deep reaching faults. Superimposed to this long-time trend the results of our detailed fluid monitoring close to the active fault zone have shown local, three month-lasting $^3He/^4He$ anomalies indicating the occurrence of dike-like mantle-derived magma intrusions. For the first time, a hidden magmatic process in a non-volcanic region has been traced and may improve our knowledge about the connection between intraplate seismicity and repeated magma injections (Bräuer etal., 2009). Between May 2005 and June 2008 the mantle-derived degassing has been studied monthly at four locations within the Cheb Basin degassing centre, and at the Wettinquelle spring to the north on the edge of the Cheb Basin. The Bublák and U Mostku locations are on the Počatky Plesná Fault Zone (PPZ) while the Kopanina and Dolni Častkov locations are on the Mariánské Lázně Fault (MLF). Only micro-seismicity occurred during this monitoring period but seismically triggered geochemical anomalies were repeatedly observed at the locations close to the focal zone (Bräuer et al., 2011).

The aim of the current project is the comprehensive interpretation of the gas and isotope composition which were recorded up to December 2011 in relation to the strong earthquake swarm from October 2008.

As a result of the fluid studies started in 1992 in the Vogtland/ NW Bohemia region it seems to be evidently that the fluids function as a mediator between a magmatic driven process and swarm earthquake seismicity. Mantle-derived fluid migration through the lithosphere, its interrelation to swarm earthquake seismicity and fault-related magma/fluid transport in the crust are in focus of the studies. The project is based on gas and isotope time series data which have been recorded at eight different degassing locations of the Cheb basin and its northern periphery up to December 2011 due to ongoing magmatic activity and three different strong swarm earthquake periods occurred between 1994 and 2008.

First of all we aim to evaluate the temporal and spatial occurrence of fluid anomalies after the strong earthquake swarm 2008 related to Mariánské Lázně and the Počatky-Plesná fault zone. The data recorded between May 2005 and June 2008 (Bräuer et al., 2011) at two locations at the PPZ and two locations at the MLF during seismic quiescence form the basis of this part of the project.Thus an evaluation of the behaviour of the mantle-derived fluids migrationg on two different faults close to the Nový Kostel focal zone in relation to the same swarm is possible for the first time.

Moreover, we want to compare seismically triggered fluid anomalies of the strong swarms 2000 and 2008 in relation to the different seismic properties of the swarms and explore the progressive spatial and temporal increase of mantle-derived helium fractions at locations close to the focal zone. Furthermore, we will look for isotopic indications due to ascending magma from a deeper reservoir by detailed analysis of helium, carbon isotope time series since 1994 at Bublák - the location with the highest gas flux and the highest $^3He/^4He$ ratios. The final interpretation of all data will provide assistance in the interpretation of temporal and spatial anomalies observed in geophysical studies pointing to isotopic time-series studies as useful tool for the evaluation of geodynamic processes. As a whole the results will supply essential information to find an optimal ICDP drilling location in the western Eger rift area.

References:

Bräuer K., Kämpf H., Strauch G. Weise S. (2003) Isotopic evidence ($^3He/^4He$, $^{13}C_{CO2}$) of fluid-triggered intraplate seismicity J.Geophys. Res. 108, doi:10.1029/2002JB002077.

Bräuer K., Kämpf H., Niedermann S., Strauch G. (2005) Evidence for ascending upper mantle-derived melt beneath the Cheb basin, central Europe. Geophys. Res. Lett. 32, doi:10.1029/2004GL022205.

Bräuer K., Kämpf H., Koch U., Niedermann S., Strauch G.(2007) Seismically induced changes of the fluid signature detected by a multi-isotope approach (He, CO_2, CH_4, N_2) at the Wettinquelle, Bad Brambach (central Europe). J.Geophys. Res. 112, doi:10.1029/2006JB004404.

Bräuer K., Kämpf H., Niedermann S., Strauch G. Tesař T. (2008) Natural laboratory NW Bohemia: Comprehensive fluid studies between 1992 and 2005 used to trace geodynamic processes. Geochem. Geophys. Geosys. 9, doi:10.1029/2007GC001921.

Bräuer K., Kämpf H., Strauch G. (2009) Earthquake swarms in non-volcanic regions: What fluids have to say. Geophys. Res. Lett. 36, doi:10.1029/2009GL039615.

Bräuer K., Kämpf H., Koch U., Strauch G. (2011) Monthly monitoring of gas and isotope compositions in the free gas phase at degassing locations close to the Nový Kostel focal zone in the western Eger Rift¸ Czech Republic. Chem. Geol. 290, 163-176.

IODP

Tracing the evolution of the upper mantle using ancient MORB glasses

P. A. BRANDL[1]*, M. REGELOUS[1], K. M. HAASE[1], C. BEIER[1]

[1] Lehrstuhl für Endogene Geodynamik, GeoZentrum Nordbayern, FAU Erlangen-Nürnberg, Schlossgarten 5, D-91054 Erlangen
correspondence: philipp.brandl@gzn.uni-erlangen.de

Formation of the oceanic crust at mid-ocean ridge spreading centres and its subsequent evolution has an important influence on sea-level, the carbon cycle and seawater chemistry over timescales of 10-100 Ma. Changes in the rate of production of oceanic crust (due to either variations in average spreading rate or mantle temperature) with time could therefore result in global sea-level change over long time periods. Oceanic crust covers approximately 60 % of the Earth's surface area, and preserves a valuable record of mantle melting processes at mid-ocean ridges, and possible changes in mantle composition and temperature since the Middle Jurassic. Oceanic crust older than about 20 Ma is generally covered by sediment and only accessible by drilling, but although many DSDP-ODP-IODP sites have penetrated more than 100 m into 'normal' oceanic basement up to 170 Ma in age, there has been no systematic geochemical study of these samples

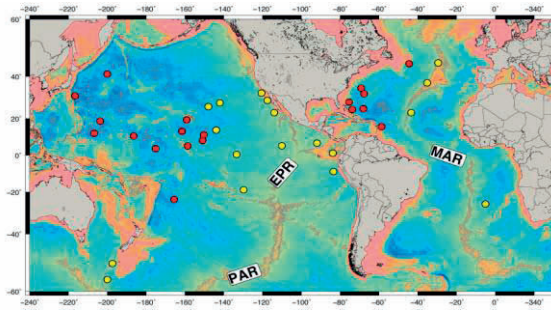

Figure 1. Location of DSDP-ODP-IODP Sites drilled into ancient oceanic crust in the Atlantic and Pacific Ocean which were sampled in this study. Sites younger 80 Ma are marked in yellow, sites older 80 Ma are marked in red.

using modern analytical techniques.

Previous geochemical studies of ancient MORB (e.g. Humler et al., 1999; Fisk and Kelley, 2002) reported an apparent difference between fractionation-corrected Fe and Na contents of Cretaceous mid-ocean ridge basalt (MORB) and young MORB from active spreading centres, and this difference was interpreted as the result of a 50-60°C higher upper mantle temperature in the Jurassic-Cretaceous. However, the use of MORB compositions to infer mantle temperature has been questioned by Niu and O'Hara (2008), who proposed that variations in mantle composition are largely responsible for differences in fractionation-corrected MORB compositions. If so, a mantle overturning or 'superplume' event, perhaps linked to the formation of the widepread mid-Cretaceous oceanic plateaus and resulting in a change in upper mantle composition at that time may better explain the apparent temporal changes in MORB chemistry reported by Humler et al. (1999). Clearly it is important to distinguish between these alternatives.

We present new major and trace element data, measured using electron microprobe and LA-ICPMS techniques, for more than 360 glasses from 30 DSDP-ODP-IODP drill sites (Figure 1) from the Atlantic (9 sites) and Pacific (21 sites). The age of the oceanic crust at these sites ranges from 6 Ma up to 160-170 Ma, and all sites were drilled into normal oceanic crust far from hotspots. We have analysed exclusively fresh volcanic glasses, because the whole-rock samples used in previous compilations of ancient oceanic crust composition (Humler et al., 1999), may be compromised by alteration and accumulation of phenocrysts, in which case they do not represent melt compositions. For comparison we have compiled a dataset of zero-age MORB glasses (~3000 samples) from ridges far from hotspots (based on

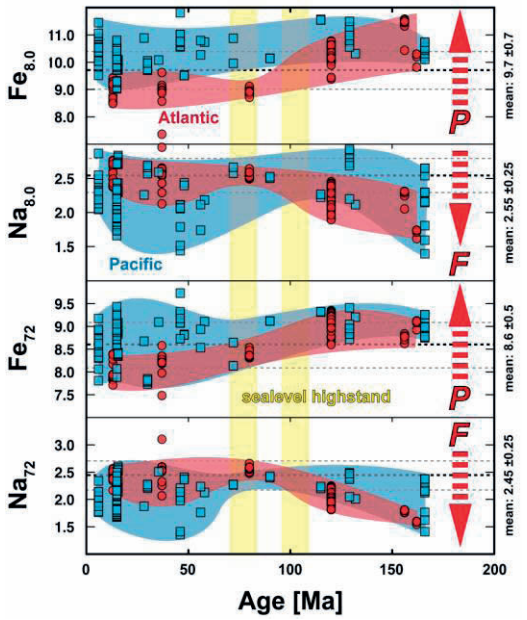

Figure 2. Plot of melting sensitive major elements versus age for glasses analysed in this study: Fe is sensitive to the average pressure (depth) of melting, whereas Na is sensitive to the degree of melting. Means for present-day normal MORB (K_2O/TiO_2 < 0.15; compiled from PetDB) are shown for comparison. Subscripts indicate the method of fractionation correction: 8.0 indicates re-calculation of major element concentration to a MgO concentration of 8.0 wt. % (following Klein and Langmuir, 1987), 72 indicates re-calculation to a common Mg# of 72 following the method of Niu and O'Hara (2008). The two periods of Cretaceous sea-level highstand are shown in yellow. Red arrows indicated with P and F display direction of increasing pressure of melting and degree of melting, respectively.

K_2O/TiO_2 < 0.15 and geographic position) using the PetDB database.

A complex problem when comparing and interpreting major element data from different sites with different MgO concentrations is the way of calucation a correction for fractional crystallisation. Our data display differences in the slope of the liquid line of descent (LLD) along which magma becomes differentiated by crystal accumulation (predominantly olivine, clinopyroxene and plagioclase). Klein and Langmuir (1987) and Niu and O'Hara (2008) provide the best methods for data correction to a 'primary' magma composition, since most of our sample suites

simply do not fractionate enough to calculate regression parameters for every distinct LLD's.

Data from the Pacific does not convincingly show temporal variations in melting sensitive major elements; Fractionation corrected FeO^t ($Fe_{8.0}$ and Fe_{72}) may indicate slightly higher values (melting starts deeper) before ~80 Ma, but this difference is still at the upper range of variation observed from ocean drilling sites. Large variations but no significant trend is observed in $Na_{8.0}$ or Na_{72}. An important observation is that the chemical variation within a single site is as large or even exceeds that observed over tens of millions of years. In the Atlantic, a more convincing trend of higher $Fe_{8.0}$, lower $Na_{8.0}$ (higher average pressure and degree of melting) for older MORB. Since a similar effect is not seen in the Pacific, this may be well explained by the existence of plumes at the initial stages of ocean spreading even in the Central Atlantic (where most of the old seafloor sites have been drilled) which has been proposed by Janney and Castillo (2001). We will test this hypothesis by trace element data.

It is remarkable that data from ocean drilling seem to differ from data (means with 1SD in Fig. 2; data from PetDB) dredged along the global mid-ocean ridges at present day. Since drillcores preferentially sample the uppermost flows at a given location, a possible explanation is that the youngest flows, emplaced on the ridge flanks, tend to have low $Na_{8.0}$, high $Fe_{8.0}$ than those erupted along the ridge axis which are sampled by dredging. This could explain the apparent difference between young and ancient MORB noted by Humler et al. (1990), since they compared only drillcore samples older than 90 Ma with zero-age MORB glasses dredged from the ridge axes. Another major complication is the existence of a highly heterogeneous mantle underneath the Pacific which also affects the major element compositions of mantle melts (e.g. Haase et al., 2011; Brandl et al., in press). The large chemical variations within single cores in the Pacific (and probably with age, too) may thus best be explained by source heterogeneity rather than major and short term varaiations in the melting regime. In that case it would be difficult to draw conclusions from fractionation corrected FeOt or Na_2O on differences in the melting regime and potential mantle temperature. If this would be true, then the observed trend in the Atlantic could either represent cooling of the upper mantle underneath the Mid-Atlantic Ridge or a subsequent change in source composition. Further study of our trace element data and advanced modelling will be necessary to test this hypothesis. Several studies have suggested that two global sea-level highstands occured in the Cretaceous: one between 110 to 95 Ma and a second between 85 and 70 Ma before present. These high sea-levels are related to major changes in the oceanic spreading system and not predominantly to the emplacement of large igneous provinces (LIP) in the ocean basins (Müller et al. 2008; Seton et al., 2009). Since the cumulative length of the mid-ocean ridge system is relatively constant on long-term (except for a major increase in the Early Cretaceous), and if changes in mantle temperature over time are insignificant, then the absence of ice-sheets, changes in sea-level may be primarily driven by changes in the crustal production rate, which controls the average age of the oceanic lithosphere. Crustal production rate has decreased by about a third from 4x106km$^{2/}$Ma during the Late Cretaceous less than 3x106km2/Ma in the late Tertiary. This results in an increase in the average age of oceanic lithosphere from 42 Ma to about 64 Ma to about 64 Ma and a significant deepening of the ocean basins (Müller et al., 2008, Secton et al., 2009).

A correlation between spreading rate and degree of melting underneath the spreading-rate is not straightforward. Ridge segments can have different rates of magma supply even at same spreading rate. Nevertheless we would expect that changes in the average seafloor spreading rate on the magnitude of 30 % would also affect the average degree of mantle melting and thus crustal thickness. Seismic experiments (e.g. compilations by White et al., 1992 and Nagihara et al., 1996) have revealed differences in crustal thickness of about 1 km even if the timing when these changes occured or whether these are gradual processes are not well constrained. Humler et al. (1999) argued from these data that oceanic crust before 80 Ma (7.4 ±1.0 km) is substantially thicker than young oceanic crust (6.6 ±0.8 km). Rubin and Sinton (2007) showed that compared to MORB from fast-spreading ridges, those from slow-spreading ridges tend to have more variable, and less evolved compositions.

Work is in progress to compare lavas from ancient Atlantic and Pacific ocean crust in order to see whether differences between slow-spreading and fast-spreading ridges also existed in the past. Nine of the sites we sampled penetrated more than 100 m into the oceanic crust and we are examining the chemical stratigraphy of individual boreholes in order to test models for crustal accretion (e.g. Hardarson and Fitton, 1997, etc.).

References:

Brandl, P.A., Beier, C., Regelous, M., Abouchami, W., Haase, K.M., Garbe-Schönberg, D., Galer, S.J.G. Off-axis volcanism along the East Pacific Rise: Quantiative constraints on mantle heterogeneity and melting processes. Chem. Geol. (in press).

Fisk, M. and Kelley, K.A. Probing the Pacific's oldest MORB glass: mantle chemistry and melting conditions during the birth of the Pacific Plate. Earth Planet. Sci. Lett. 202 (2002) 741-752.

Haase, K.M., Regelous, M., Duncan, R.A., Brandl, P.A., Stroncik, N., Grevemeyer, I. Insights into mantle composition and mantle melting beneath mid-ocean ridges from post-spreading volcanism on the fossil Galapagos Rise. Geochem. Geophys. Geosys. 12 (2011) Q0AC11

Humler, E., Langmuir, C., Daux, V. Depth versus age: new perspectives from the chemical compositions of ancient crust. Earth and Planetary Sience Letters 173 (1999) 7-23.

Janney, P.E., Castillo, P.R. Geochemistry of the oldest Atlantic oceanic crust suggests mantle plume involvement in the early history of the Central Atlantic Ocean. Earth and Planetary Science Letters 192 (2001) 291-302.

Klein, E.M. and Langmuir, C.H. Global correlations of ocean ridge basalt chemistry with axial depth and crustal thickness. Journal of Geophysical Research 92 (1987) 8089-8115.

Müller, R.D., Sdrolias, M., Gaina, C., Steinberger, B., Heine, C. Long-term sea-level fluctuations driven by ocean basin dynamics. Science 319 (2001) 1357-1362.

Nagihara, S., Lister, C.R.B., Sclater, J.G. Reheating of old oceanic lithosphere: Deductions from observations. Earth and Planetary Science Letters 139 (1996) 91-104.

Niu, Y. and O'Hara, M.J. Global correlations of ocean ridge basalt chemistry with axial depth: a new perspective. Journal of Petrology 49 (2008) 633-664.

Rubin, K.H., Sinton, J.M. Inferences on mid-ocean ridge thermal and magmatic structure from MORB compositions. Earth and Planetary Science Letters 260 (2007) 257-276.

Seton, M., Gaina, C., Müller, R.D., Heine, C. Mid-Cretaceous seafloor spreading pulse: Fact or fiction? Geology 37 (2009) 687-690.

White, R.S., McKenzie, D., O'Nions, R.K. Oceanic crustal thickness from seismic measurements and rare earth element inversion. Journal of Geophysical Research 97 (1992) 19683-19715.

IODP

Microbiology of deep stratified sediments on the New Jersey shallow shelf (IODP Exp. 313)

A. BREUKER, S. STADLER, A. SCHIPPERS

Bundesanstalt für Geowissenschaften und Rohstoffe, Stilleweg 2 D-30655 Hanover, Germany

The USGS AMCOR drilling in 1976 discovered a large freshwater lens beneath the Atlantic coastal plain and underlying the New Jersey shelf. The New Jersey shallow shelf sediments were drilled in summer 2009 to elucidate their geological and biological properties. Drilling was performed up to a depth of 757 meters below seafloor (mbsf) at three locations 45–67 km offshore. Chemical analysis revealed at least one big freshwater lens (1). The aim of our study was the microbiological analysis of the drilled sediments. Total cell counts, real-time PCR-data, cloning and sequencing revealed a microbial community typical for marine sediments: Logarithmically decreasing total cell numbers with depth with good accordance to bacterial and archaeal 16S rRNA gene copy numbers (Fig. 1). A detailed analysis of archaeal 16S rRNA gene sequences in four depths performed with the phylogenetic program ARB based on the latest SILVA database (SSURef_108_SILVA_09_09_11_opt.arb, www.arb-home.de) revealed a stratified microbial community (Fig. 2; Table 1). The rarefaction curves calculated with the mothur software (www.mothur.org) (2) for operational taxonomic units for archaeal 16S rRNA gene sequences indicated a good sampling of archaeal sequences with decreasing diversity with depth (not shown). In all analyzed depths crenarchaeotic sequences provided the major part of the microbial community. Interestingly, in a depth of 17 mbsf no euryarchaeotic sequences were detected. Within the Crenarchaeota, the MCG (Miscellaneous Crenarchaeotic Group) was the dominating group. The MCG is found in a wide range of habitats (3). In addition to the MCG, the Group C3 is the only other group found in 17 mbsf depth. The members of Group C3 seem to be restricted to marine or terrestrial water ecosystems and are mostly found in marine sediments such as mangrove sediments and deep sea sediments. The MBG-B (Marine Benthic Group B) was only found in 7 mbsf, the shallowest analyzed depth. This finding is in accordance with the analysis of Teske and Sørensen (3) who described that MBG-B Archaea were amongst others detected by several researchers in different habitats such as surficial marine sediments of the North Atlantic (4), and e.g. hydrothermal vent sites (5). The biologic properties of these Archaea remain so far unclear. Some sequences belonging to the deeply branching THSCG (Terrestrial Hot Spring Crenarchaeotic Group) were detected as well. A screening of the ARB database revealed very different isolation sources such as hot springs, hypersaline groundwater, marine sediments from the tropical western Pacific, hydrothermal fluids, sulfide chimneys, and mangrove soils. Some members of the MG1 (Marine Group 1) could be exclusively found at 13 mbsf. The detected sequences are closely related to Nitrosopumilus maritimus, the first cultivated ammonia-oxidizing crenarchaeum (6). The numbers of the sequences of MG1 seem to be inversely related to those of the MCG. This supports the assumption that members of the MCG group live in anaerobic sediments or anaerobic niches in contrast to the possibly aerobic living MG1 members. Regarding the Euryarchaeota, some sequences of small subgroups like Group 20a-9 were found in particular depths of 9 and 13 mbsf. The numbers of clone sequences of the Marine Benthic Group D and the DHVEG1 (Deep Sea Hydrothermal Vent Euryarchaeotal Group 1), found in marine and freshwater ecosystems, the widespread SAGMEG (South African Gold Mine Group), and the DSEG (Deep Sea Euryarchaeotal Group) were highest at 13 mbsf. In summary, we found a high diversity of archaeal groups with fluctuating numbers of sequences with depth. Further fine-tuned phylogenetic analysis including the calculation of different trees and qPCR of functional genes are in progress. Or aim is to identify which geochemical properties e.g. availability of oxygen, ammonia etc. define the microbial diversity.

References:

Mottl, M.J., Stadler, S. Hayashi, T. (2009). Fresh and salty: chemistry of sediment pore water from the New Jersey Shallow Shelf: IODP Exp. 313. Eos, Trans. Am. Geophys. Union, 90(52)(Suppl.): PP31A-1293. (Abstract).

Schloss, P.D., Westcott, S., Ryabin, T., Hall, J.R., Hartmann, M., Hollister, E.B., Lesniewski, R.A., Oakley, B.B., Parks, D.H., Robinson, C.L., Sahl, J.W., Stres, B., Thallinger, G.G., Van Horn, D.L., Weber, C.F. (2009). Introducing mothur: open source, platform-independent community-supported software for describing and comparing microbial communities. Appl. Environ. Microbiol. 75, 7537-7541.

Teske, A.P., Sørensen, K.B. (2008). Uncultured archaea in deep marine marine subsurface sediments: have we caught them all? The ISME J. 2, 3-18.

Vetriani, C., Jannaschm H.M., MacGregor, B.J., Stahl, D.A., Reysenbach, A.L. (1999). Population structure and phylogenetic characterization of marine benthic archaea in deep–sea sediments. Appl Environ Microbiol 65: 4375-4384.

Takai, K., Horikoshi, K. (1999). Genetic diversity of the archaea in deep sea hydrothermal vent environments. Genetics 152, 1285-1297.

Könnecke, M., Bernhard, A.E., de la Torre, R., Walker, C.B., Waterbury, J.B., Stahl, D.A. (2005). Isolation of an autotrophic ammonia-oxidizing marine archaeon. Nature 437, 543-546.

ICDP

Probing of Intra-continental magmatic activity-drilling the Eger Rift (PIER-ICDP):current project status and future plans

S. BUSKE[1], N. MULLICK[1], M. KORN[2], M. FALLAHI[2], S. MOUSAVI[2], S. SHAPIRO[3], P. WIGGER[3], U. WEGLER[4], M. KEYSER[4], B. RŮŽEK[5], J. HORÁLEK[5], P. HRUBCOVÁ[5], T. FISCHER[6]

[1]TU Bergakademie Freiberg, Institute of Geophysics and Geoinformatics, 09596 Freiberg, nirjhar.mullick@geophysik.tu-freiberg.de

[2]Universität Leipzig, Institute of Geophysics and Geology, Talstr. 35, 04103 Leipzig

[3]Freie Universität Berlin, Department of Geophysics, Malteserstrasse 74-100, 12249 Berlin

[4]Bundesanstalt für Geowissenschaften und Rohstoffe, Stilleweg 2, 30655 Hannover

[5]Institute of Geophysics of the Academy of Sciences of the Czech Republic, Boční II/1401, 141 31 Prague 4, Czech Republic

[6]Institute of Hydrogeology, Engineering Geology and Applied Geophysics, Charles University, Albertov 6, 128 43 Praha 2, Czech Republic

The western Eger rift area is dominated by ongoing magmatic processes in the intra-continental lithospheric mantle. These processes take place in absence of any presently active volcanism at the surface. However, they are expressed by a series of phenomena distributed over a relatively large area, like occurrence of repeated earthquake

swarms, surface exhalation of mantle-derived and CO_2-enriched fluids, mofettes, mineral springs and enhanced heat flow, among others. At present this is the only known intra-continental region where such deep-seated, active lithospheric processes currently occur. The geodynamic nature and the implications of these processes are far from being understood, and a series of open questions remain: Is magmatic activity taking place in the upper mantle or in the lower crust ? Is it a developing large-scale fault zone or a zone of developing volcanism ? What is the geodynamic role of fluids in general and of CO_2 in particular ? What is the geodynamic relationship between geophysical and geochemical signatures of these magmatic processes ?

On the other hand, continuous seismic monitoring, active seismic surveys, fluid and groundwater level monitoring as well as GPS measurements have been carried out in this region for many years. It is therefore an excellent location for an ICDP drilling project targeted to a better understanding of the crust-mantle interaction in an area of active magmatic underplating. The PIER-ICDP initiative has been established to address these questions, to create a common geophysical and geochemical frame between the former KTB site and Eger Rift, bounded at its Western and Eastern endings by scientific drilling data, and in that way to significantly contribute to understanding the intra-continental mantle-crust interaction in a broader scale.

The currently running projects within PIER-ICDP perform a profound geophysical characterization of the crust and mantle with the focus on the topic of "fluids triggering lithospheric activity":
Seismic and seismologic features of the Vogtland-Bohemia earthquake swarms:
the reprocessing of reflection seismic data (9HR profile) has revealed interesting features with respect to the structure of the upper and lower crust and in particular with regard to the relationship between the location of earthquake swarms and fluid-indicating bright spots in the reflection image (see poster by Mullick et al.)
Spatial and temporal seismic imaging of fluid migration through the crust in the W-Bohemia/Vogtland earthquake swarm region:
an average 1-D velocity model is derived by traveltime inversion using local earthquakes (see poster by Sima et al.), bambient noise surface wave tomography yields a 3D velocity model down to depths of about 15 km (see poster by Fallahi et al.), the temporal changes of seismic velocity due to swarm earthquake activity is investigated by coda-wave- interferometry (see poster by Keyser et al.)

This poster summarizes the relationship between the results achieved so far and gives an overview about the planned further investigations (network of shallow boreholes, new reflection seismic profiles, etc.). The final goal will be to develop a Czech-German observatory at depth consisting of an array of several drill holes suitable for long-term monitoring experiments to shed light on the ongoing geodynamic processes in that area as a whole.

IODP

Early Eocene vegetation and climate on Antarctica: insights from IODP Site U1356 (Wilkes Land margin)

L. CONTRERAS[1], J. PROSS[1], P. K. BIJL[2], , U. RÖHL[3], S.M. BOHATY[4], L. TAUXE[5,] C.E. STICKLEY[6], S. SCHOUTEN[7], H. BRINKHUIS[2]

AND IODP EXPEDITION 318 SCIENTISTS.

[1]University of Frankfurt, Germany
[2]Utrecht University, Utrecht, The Netherlands
[3]MARUM - Center for Marine Environmental Sciences, University of Bremen, Bremen, Germany
[4]National Oceanography Centre, University of Southampton, UK
[5]Scripps Institution of Oceanography, La Jolla, USA
[6]Department of Geology, University of Tromsø, Tromsø, Norway
[7]Department of Marine Organic Biogeochemistry, NIOZ Royal Netherlands Institute of Sea Research, Den Burg, The Netherlands

The terrestrial climate conditions on Antarctica prior to the development of large-scale glaciation around the Eocene/Oligocene transition is still poorly known due to the obliteration or coverage of potential archives by the Antarctic ice sheet. Available data, which are mainly from the Antarctic Peninsula, are only partially representative of the climate on the Antarctic mainland. The core material drilled during IODP Expedition 318 (Wilkes Land margin), yielding sediments of Early Eocene to Quaternary age, documents ~53 m.y. of Antarctic climate history. Notably, IODP Site U1356 yielded a shelfal succession of early and middle Eocene strata with excellent chronostratigraphic control, representing early Eocene (53.9-51.9 Myr ago) greenhouse conditions and, separated by a ~2 Myr-long hiatus, an interval of presumed latest early Eocene to middle Eocene (49.3-46 Myr ago) cooling.

Based on this material, we carried out palynological (pollen and spores) and organic geochemical (MBT/CBT paleothermometry) analyses on the Eocene of IODP Site U1356 in order to obtain the first continental climate reconstructions for Antarctica for the peak of the early Eocene greenhouse world. Our palynological data indicate that the early Eocene vegetation along the Wilkes Land margin was highly diverse and contained thermophilous elements that today are restricted to tropical and subtropical settings. In combination with our MBT/CBT paleotemperature results, they provide strong evidence for near-tropical warmth at least in the coastal lowlands along the Wilkes Land margin. At the same time, vegetation elements that today prefer cool temperate settings are consistently present, suggesting that a vegetation zonation by altitude and/or coastline distance. In contrast, the middle Eocene pollen and spore record indicates a dominance of a cool temperate, low-diversity forest vegetation dominated by Nothofagus (southern beech) and conifers, and thermophilous elements are consistently absent; lower temperatures are also suggested by the MBT/CBT data.

ICDP

Structural and stratigraphic analysis of the Lake Van, Eastern Turkey: An integration of high resolution seismic and drilling data

D. CUKUR[1], S. KRASTEL[1], D. WINKELMANN[1], T. LITT[2], PALEOVAN SCIENTIFIC TEAM

[1]GEOMAR| Helmholtz Center for Ocean Research, Wischhofstrasse 1-3, 24148 Kiel, Germany
[2]Steinmann-Institut für Geologie, Mineralogie und Paläontologie, Rheinische Friedrich-Wilhems-Universität Bonn, Nußallee 8, 53115 Bonn, Germany

Lake Van in Eastern Anatolia (Turkey) is the fourth largest terminal lake in the world (with a surface area of 3,574 km², a volume of 607 km³, a maximum depth of 450 m, and a maximal length of 130 km WSW-ENE (Fig. 1). In summer 2010, Lake Van was chosen for scientific drilling in the framework of the International Continental Drilling Program (ICDP) aiming to recover long paleoclimate and paleoseismic archives. Two sites (Ahlat ridge and Northern basin) were successfully drilled based on seismic data collected during a pre-site survey in 2004. Here we present a joint interpretation of the seismic

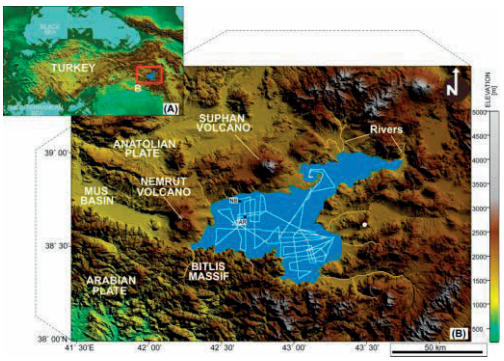

Fig. 1. Location of Lake Van as well as seismic reflection profiles and drilled wells.

and drilling data.

Interpretation of seismic reflection and drill data from Lake Van reveal extensive details about the structure, stratigraphy, lake level fluctuations, and the evolution of the lake basin. Seismic data reveals the main structural features inside the lake, including the Northern basin, Tatvan basin, Ahlat sub-basin, and Deveboynu basin (Fig. 2). These basins are separated by basement ridges such as Northern and Ahlat ridges. Seventeen seismic sequence boundary including the top of the acoustic basement (SB1 to SB17 from oldest to youngest) in the deep basin were interpreted and mapped (Fig. 3). The time-structure maps were converted into depth using the time-depth relationship constructed from seismic-to-well tie at the Ahlat ridge well. The structure maps of the sequence boundaries exhibit tilting to west, suggesting that the sequences were deposited with greater subsidence in the west. NE-trending normal faults are dominant; E-W oriented thrust faults are seen locally.

At least seventeen sequences, S1 to S17 from oldest to youngest, were identified in the deep sedimentary section, based on the seismic reflection configuration (Fig. 3). Sediments in the lake appear to have been sourced mainly from east; maximum sediment thickness is estimated to be more than 400 m in the deepest part of the lake. The seismic sequences in basins are dominated by an alternation of well-stratified and chaotic reflecting layers. The chaotic seismic facies are interpreted as mass-flow deposits (up to ~50 m thick), most probably triggered by

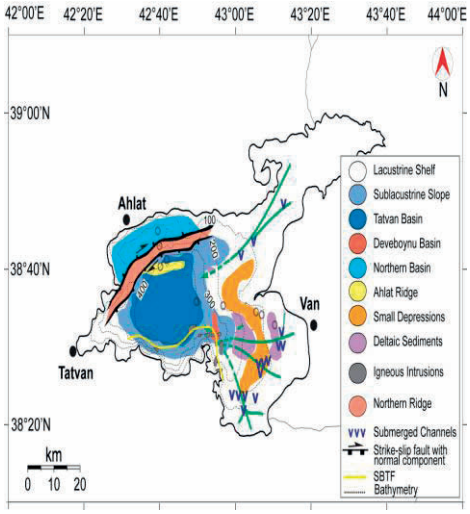

Fig. 2. Main structural and stratigraphic features of Lake Van interpreted from seismic data.

earthquakes and/or rapid lake level fluctuations.

The absence of mass flows in Ahlat sub-basin indicate that most mass flows originate close to the southern shore of Lake Van and that Ahlat ridge is likely to have acted as a structural barrier for these mass flows. The moderate-to-high-amplitude, well-stratified facies seen in the deeper parts of the basins are interpreted as lacustrine deposits and tephra layers. Core-to-seismic correlation supports this interpretation; strong high-amplitude reflections on seismic data correlate well with thick (~2 m) tephra layers.

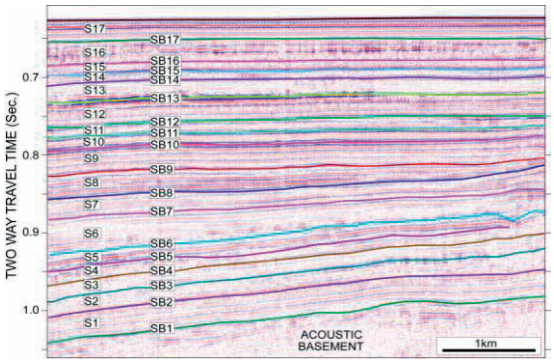

Fig. 3. Seismic reflection profile showing seismic sequences (S1 to S17, from oldest to youngest) and bounding seismic surfaces (SB1 to SB17) identified in the study area.

Seismic data suggest Lake Van has a minimum age of 500 ka, consistent with the preliminary results of core dating. Since then, lake level fluctuations reaches an amplitude of more than 500 m (up to 450 m deeper and 80 m higher than the present lake level) but the deep basins were permanently filled with water. Evidence for lake level fluctuations in the seismic data includes clinoform packages, erosional unconformities and sublacustrine channels. Seismic data also reveal evidence of shallow gas, such as gas seepages, gas plumes, acoustic blanking, and enhanced reflections.

ICDP

ICDP-NL: A new platform in the Netherlands

A. DÄHLMANN AND THE ICDP-NL COMMUNITY[1]

[1]ICDP-NL, c/o Anke Dählmann, TU Delft, Stevinweg 1, NL-2628 CN Delft; a.dahlmann@tudelft.nl

Starting 2011, the Netherlands are a member country of the International Continental Scientific Drilling Program. The Dutch community, ICDP-NL, is an open platform that intends to bundle the expertise of (sometimes rather small) research groups and specialists. ICDP-NL represents all relevant groups of the geosciences in the Netherlands. Its aim is to support Dutch researchers in their ambition towards ICDP projects and to keep efficient contact with the funding agencies.

Research institutions currently involved and their expertise are:
Utrecht University, Faculty of Geosciences: palaeomagnetism, petrology, strategraphy & paleontology, geochemistry, palaeo-ecology, marine palynology, tectonics
VU University Amsterdam, Faculty of Earth and Life Sciences: climate change & landscape dynamics, hydrology & geo-environmental sciences, petrology, sedimentology & marine geology, isotope geochemistry
TU Delft: geotechnology, luminescence dating
University of Amsterdam: Paleo-ecology
Leiden University: Archeology
TNO - Geological Survey of the Netherlands: basin evolution, regional tectonics, burial history, climate change and related sea level movement, biostratigraphy and sedimentary processes

General Dutch research interests in ICDP:
High-resolution, multi-proxy record of climate change
Correlation of various climate records
Driving mechanisms of environmental and climatic change
Expand geological time scales (Milankovitch cycles)
Comparitive methodology of age-model development
Changes in / links between biotic and geological systems
Early Earth processes, Archean hydrothermal environments
Earth monitoring and process-oriented modeling
Integration of different spatial and temporal scales for the interplay between tectonics and climate

Selection of Dutch past and present involvement in ICDP:
Chicxulub Scientific Drilling Project
Barberton Drilling Project: Peering into the Cradle of Life
Colorado Plateau Coring Project
Scientific Collaboration On The Past Speciation Conditions in Ohrid
Hominin Sites and Paleolakes Drilling Project
Barberton Greenstone Belt Drilling Project
Climate evolution in Central Asia during the past few million years: A case study from Lake Issyk-Kul

IODP

Testing the veracity of productivity proxies: a comparison of geochemical and faunal data.

LISELOTTE DIESTER-HAASS, KATHARINA BILLUPS,

l.haass@mx.uni-saarland.de kbillups@udel.edu

Marine biological productivity, more specifically the ocean's biological pump, is an important criterion in studies focusing on the global carbon cycle and climate change. The basic premise is that the higher the productivity, the stronger the biological pump, i.e. the higher the export productivity, the more particulate organic carbon can be sequestered in sediments and withdrawn from the global carbon pool.

Several proxies have been used to infer temporal changes in carbon transfer through the water column using geochemical approaches , such as accumulation rates of silica, carbonate, organic matter, biogenic Barium (Ba), and Phosphorous (P), P/Ba ratios. Micropaleontological proxies for paleoproductivity include benthic foraminiferal species assemblages, the number of benthic foraminifera per gram of sediment (noBf) and benthic foraminiferal accumulation rates (BFAR) (e.g.Herguera and Berger, 1991; Herguera, 2000). Each proxy alone suffers from a characteristic set of uncertainties that may be related to, for example, carbonate or opal dissolution, diagenesis, sediment focusing, and sedimentation rates. Thus paleoproductivity reconstructions benefit from a multi-proxy approach..

Here we test the hypothesis whether the large variations in productivity described for Paleogene sediments (60-30Ma) of the Southern Ocean (ODP Sites 738, 689 and 690) by Faul and Delaney (2010) derived from geochemical proxies also leave a signal in faunal derived productivity. Specifically, we compare productivity reconstructions based on numbers of benthic foraminifera per gram of sediment with the geochemical proxies P and Ba µmol and MAR's, and P/Ba ratios of Faul and Delaney(2010). P is considered to be related to organic carbon buried flux, whereas Ba reflects export productivity (op.cit.). The ratio of reactive P to Ba is considered as a proxy to reconstruct the fraction of organic C buried relative to export productivity.

Variations in noBf mirror variations in PMAR and Pµmol. The two data sets, noBf and Pµmol -which are both independent of the age model- show a very good correlation at Site 738 and 689 (r = 50 and 67). At Site 690, however, an anoxic sediment unit between 52 and 56 Ma shows very low noBf when Pµmol was elevated affecting the correlation. Variations in the P/Ba ratio covary with changes in noBf at Site 738 and 689 (except for the 35-25Ma interval at Site 689, when opal sedimentation set in and led to an increase in noBf in parallel with Ba and related decrease of the P/Ba ratio) confirming the basic

assumption: more organic carbon buried means more food for benthic foraminifera and increase in the noBf.

This correspondence of geochemical and faunal productivity reconstructions underlines the validity of the benthic foraminiferal number method as a tool in studying changes in the global carbon cycle.

References

Herguera, J.C., and Berger, W.A., (1991). Paleoproductivity from benthic foraminifera abundance: glacial to postglacial change in the west-equatorial Pacific, Geology, 19, 1173-1176, 1991.

Herguera, J.C., (2000). Last glacial paleoproductivity patterns in the eastern equatorial Pacific: benthic foraminifera records, Mar.Micropal., 40, 259-275.

Faull,K.L. and Delaney,M.L.,(2010). A comparison of early Paleogene export productivity and organic carbon burial flux for Maud Rise, Weddell Sea, and Kerguelen Plateau, south Indian Ocean. Paleoceanography, 25, PA3214,doi:10.1029/2009PA001916.

IODP

Three-component magnetic downhole measurements during IODP Expedition 330

S. EHMANN[1], L. ANDERSON[2], A. HÖRDT[1], M. LEVEN[3], C. VIRGIL[1] AND EXPEDITION 330 SCIENTISTS[4]

[1] IGEP, TU Braunschweig, Braunschweig, Germany
[2] Department of Geology, University of Leicester, Leicester, UK
[3] Institute of Geophysics, University of Göttingen, Göttingen, Germany
[4] Integrated Ocean Drilling Program, Texas A&M University, College Station, TX, United States

The Louisville Seamounts, a 4300km long chain of submarine volcanoes formed during the last 80 million years, are a counterpart to the Hawaiian-Emperor seamount chain, which was formed above a different Hotspot but on the same tectonic plate. Measurements taken during ODP Leg 197 revealed that the Hawaiian Hotspot is not stationary relative to the mantle, but moved southward by about 15° between 81 and 47 Ma. To determine wheter both Hotspots move independently or whether they form a common reference frame for the Pacific Plate, a total of six drill holes on five different seamounts of ages comparable to already examined seamounts of the Hawaiian-Emperor chain were drilled during IODP Expedition 330.

The Göttingen Borehole Magnetometer (GBM) was run three times in two different boreholes during Expedition 330. It comprises three orthogonal fluxgate magnetometers and three orthogonal fibre optical gyros, which enable reorientation of the recorded magnetic field to the geographic reference frame.

There are two main sources of errors during the reorientation procedure. First, the gyros exhibit a temperature dependent drift that has to be removed before the gyro data can be used to reorient the magnetic field data. This drift has been determined in calibration measurements and is lowest in the temperature range between 40°C and 50°C. Therefore the gyros are actively heated to keep their drift as low as possible. However, due to the cold marine environment, the temperature of the gyros dropped as low as 30°C during the measurements during Expedition 330. Second, due to their principle of operation, the gyros record the rotation of the Earth. To be able to remove this influence, the orientation of the tool at the beginning of each measurements has to be known. This is easily possible on land, but can be fairly challenging on board of a moving ship.

To be able to account for any unknown drifts, a new algorithm has been developed that uses the inclinations of the tool recorded by two pendulum inclinometers inside the GBM. These inclinometers have a lower resolution and accuracy than the gyros and are very sensitive to mechanical shocks and vibrations, but on average they measure the total tilt of the tool and their errors don't accumulate during the course of a measurement. The new algorithm calculates a drift that reduces the differences between the tilt of the tool determined using the gyros and the tilt measured by the inclinometers. Reorienting the magnetic field using this additional drift significantly reduces differences between down- and uplog of the measurements.

Using the reoriented magnetic field and magnetic suceptibility data from the drill cores, the magnetization of the drilled volcanic rocks can be determined by inverse modelling. In particular, the declination of the magnetization can be determined, which is not possible when measuring the magnetization of unoriented core samples. Assuming that the direction of the remanent magnetization equals the direction of the magnetic field at the place and time of formation of the rocks, paleopole positions (e.g. the position of the north pole at the time of formation of the rocks relative to their current position) can be calculated and used to determine the history of movement of the Hotspot.

The values of the calculated magnetizations are strongly dependent on the values of the background field used for the modelling. An aluminium sinker bar, specifically manufactured for Expedition 330, was used as a spacer to seperate the GBM from ferromagnetic and possibly magnetized parts of the tool string. Measurements and simulations done before Expedition 330 showed that this siginficantly reduces errors in the recorded magnetic field, but especially the vertical component of the recorded magnetic field remains sensitive to exterior magnetic distortions. A remaining influence of the tool string/wireline or possibly long wave magnetic anomalies in the surroundings of the drill site can't be excluded, so care has to be taken when choosing the background field values. Errors of this kind can be reduced by comparing magnetizations determined by inverse modelling of the downhole date to magnetizations measured on drill cores and by (iteratively) adjusting the values chosen for the background field.

First results show a good quality of the reoriented magnetic field data, which correlate with the lithology determined from drill cores and enable a first estimate of the remanent magnetization.

IODP

Quantification of temperate Rhizobiophages and associated host populations in subsurface sediments of ODP Leg 201 by quantitative PCR

T. ENGELHARDT[1], H. CYPIONKA[1], B. ENGELEN[1]

[1] Institut für Chemie und Biologie des Meeres, Carl-von-Ossietzky Universität Oldenburg, Carl-von-Ossietzky Straße 9-11, D-26111 Oldenburg, Germany, www.pmbio.icbm.de

Bacteriophages were found to be a numerically abundant part of microbial communities in various marine deep sediments. Direct counting of virus-like particles has shown that the number of viruses typically exceeds the total cell counts. Furthermore, the ratio between viruses and cells increased with depth, indicating ongoing viral production in these sediments. Viruses might be the main predators in highly compacted and mostly anoxic subsurface sediments, as grazers are most likely absent.

To get a better understanding of the origin of these viruses and their influence on the microbial life in the marine subsurface, we started investigations on phage-host systems. By analysing a phylogenetically diverse selection of bacterial isolates obtained from ODP Leg 201 sediments we found about 50% among them carrying prophages (Engelhardt et al., 2011). The phages isolated during these experiments showed a high morphological and genetical diversity. In the frame of the Marine Phage Genome Sequencing Project, five of these phages were subjected to whole-genome sequencing.

Rhizobium radiobacter as an model host for the analysis of viral communities in subsurface sediments

A population of Rhizobium radiobacter was used to analysed viral communities in marine deep sediments. R. radiobacter was shown to contribute up to 5% to the total microbial community in the Mediterranean subsurface (Süß

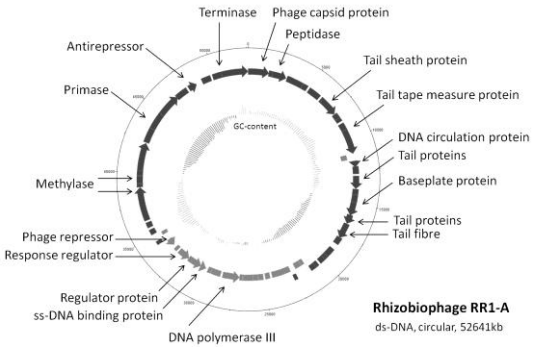

Figure 1: Map of the whole genome of Rhizobiophage RR1-A is shown. The annotation of genes is given in the figure.

et al., 2006). For ODP Leg 201 sediments, their relative amount of the bacterial community was up to 7.5%. Our culture collection from these sediments comprises 36 different strains of R. radiobacter. Genome fingerprints by ERIC-PCR have shown that the population of R. radiobacter formed site-specific subpopulation. Stimulation experiments to induce prophages have identified all 36 strains to be lysogens. Analysis of the phage genomes by pulsed-field gel electrophoresis indicated that two different phages were present in the analysed host population. The genome sizes were determined to be 52kb and 34kb, respectively. Several strains occurred to have multiple prophage infections. Thus, lysogeny appears to be a typical feature of the deep subsurface isolates of R. radiobacter.

Development of a specific detection system for temperate Rhizobiophages

Based on the whole genome information of

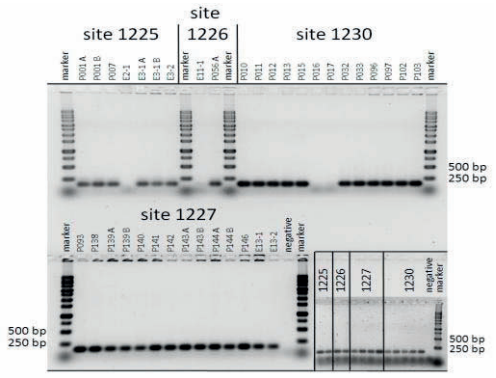

Figure 2: Primer specificity for prophage antirepressor gene of Rhizobiophage RR1-A was verified by PCR. Genomic DNA of 36 R. radiobacter isolates and purified viral DNA extracts from various sediment samples (small box) from ODP Leg 201 were used as templates.

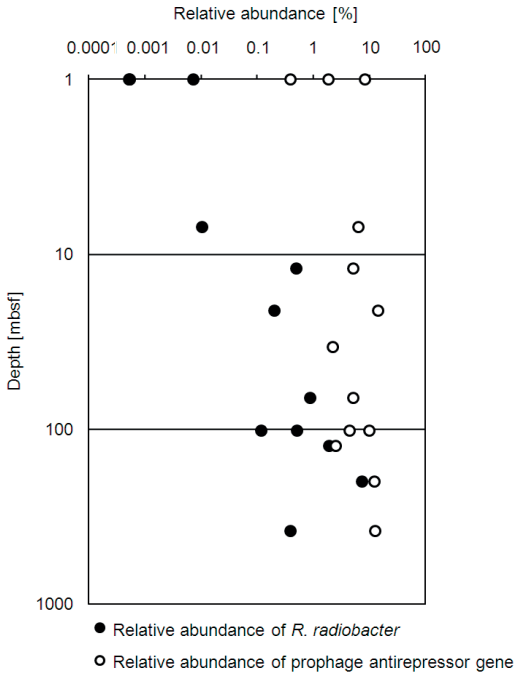

Figure 3: The relative abundance of R. radiobacter (black cycles) and copies of the prophage antirepressor gene of Rhizobiophage RR1-A (open cycles) are shown for subsurface sediments of ODP Leg 201 sediments (combined plot for ODP sites 1225, 1226, 1227, 1230).

Rhizobiophage RR1-A, primer sets were developed to target the antirepressor gene (Fig. 1). This gene is involved in the switch between lysogeny and the lytic cycle and is specific for temperate phages. The specificity of the detection system was verified by testing the primer sets on all available isolates of R. radiobacter and additionally on viral DNA extract from sediment samples of various sampling sites and depths of ODP Leg 201 sediments. For

the isolates as well as the environmental samples, no unspecific amplification was observed (Fig. 2). However, it has to be considered that the detection of known Rhizobiophages in the sediments might be underrated. Even if antirepression-mediated induction of prophages was supposed to be a common mechanism, we missed any prophage that uses a different regulation system for lysogeny.

Quantification of Rhizobiumphages in ODP Leg 201 sediments by quantitative PCR

Quantitative PCR was applied on purified viral DNA extracts obtained from various sites and depths to quantify the number of antirepressor gene copies in these sediments. Gene copy numbers of prophage antirepressor gene accounted for 10^5 to 10^6 genes cm^{-3} of sediment. The number of phages containing this gene varied with depths, but constituted no clear trend. However, the relative amount of temperate Rhizobiophages in relation to the total virus counts was generally higher in deeper sediment layers (Fig. 3). Phages containing the targeted antirepressor gene contributed up to 12.4% (ODP site 1225, 198mbsf) to the total virus abundance.

Lysogeny as an important feature for microbial populations in subsurface sediments

Rhizobium radiobacter is an abundant and frequently isolated organism in ODP Leg 201 sediments. The increasing relative abundance with depth in comparison to the total bacterial community points towards an adaptation to the environmental conditions present in the deep subsurface. The constant degradation of organic matter during sediment accumulation leads to a limited substrate availability for indigenous microorganisms. Thus, metabolically versatile species such as R. radiobacter (Batzke et al., 2007) might take advantage on this situation. Furthermore, the prophages found in all isolates might also function as an adaptation factor. Genes carried by prophages can affect host cell metabolism and might provide new metabolic facilities that help to increase survivability.

The occurrence of lysogeny as a typical feature among *R. radiobacter* is reflected by the high amount of temperate Rhizobiophages found in the investigated deep subsurface sediments. Furthermore, an ongoing production of phages can be assumed due to the general high amount of phages in deeper sediment layers. As the mobility of phages and host cells is limited in highly compacted sediments, it appears unlikely that lytic viral reproduction is a dominant mechanism for viral proliferation. Furthermore, the host cell density might be too low to support a lytic phage reproduction. Thus, the production of phages may result more likely from natural induction of prophages, which in strongly supported by the presence of the high amount of temperate phages in subsurface sediments. Our results show that phages are an active component in marine deep sediments and indicate lysogeny as an important feature of microbial communities in the marine subsurface.

References:

Batzke A., Engelen B., Sass H., Cypionka H. (2007) Phylogenetic and physiological diversity of cultured deep-biosphere bacteria from equatorial Pacific Ocean and Peru Margin sediments. Geomicrobiol. J.24, 261-273.

Engelhardt T., Sahlberg M., Cypionka H., Engelen B. (2011) Induction of prophages from deep-subseafloor bacteria. Environm Microbiol Rep 3:459–465.

Süß J., Schubert K., Sass H., Cypionka H., Overmann J., Engelen B. (2006) Widespread distribution and high abundance of Rhizobium radiobacter within Mediterranean subsurface sediments. Environ. Microbiol. 8, 1753-1763.

ICDP

Ambient noise surface wave tomography in NW-Bohemia/Vogtland region

M.FALLAHI[1], M. KORN[1], CH. SENS-SCHÖNFELDER[2]

[1]Insitut für Geophysik und Geologie, Universität Leipzig, Talstraße 35, 04103 Leipzig

[2]Deutsches Geoforschungszentrum Helmholtz-Zentrum Potsdam

The NW-Bohemia/Vogtland region at the border between Germany and Czech republic is a place of presently ongoing geodynamic processes in the intra-continental lithosphere, which results in the occurrence of repeated earthquake swarms, mantle-derived fluid exhalations, mofettes, mineral springs and enhanced heat flow. It is a key site to study the mantle-crust interaction in an active magmatic environment, and has been proposed as a site for scientific drilling. Fluid reservoirs have been proposed for the upper crust as well as for the crust-mantle transition zone, but their direct observation is still missing.

Here we investigate the crustal seismic structure of W-Bohemia/Vogtland based on the methodology of ambient-noise surface wave tomography. Continuous recordings of the permanent seismic station networks of Germany and Czech Academy of Sciences as well as temporary seismic stations that had been deployed during the BOHEMA and PASSEQ experiments in W-Bohemia/Vogtland. Ambient noise cross-correlations are performed on the data recorded between 2002 and 2003 for BOHEMA experiment and between 2007 and 2008 for the other stations.

Group velocity dispersion curves are obtained by time-frequency analysis of the cross-correlation functions between all possible station pairs. This yields a much better ray path coverage of the region of interest than could be ontained by surface wave tomography from natural events and therefore has the potential of higher resolution. We test and implement a signal-to-noise ratio (SNR) selection method for producing one-sided cross correlograms, which yields better-defined dispersion ridges than the standard two-sided averaging approach.

Travel times of the extracted Rayleigh waves were measured between station pairs for different frequencies between 0.1 and 1 Hz, and tomographically inverted to provide independent 2D group velocity maps corresponding to different sampling depths, and thus together giving an indication of the velocity variations in 3D extending to a depth of 15 km.

ICDP

Pre-eruptive conditions of the Campanian Ignimbrite eruption: Experimental constraints from phase equilibria and volatile solubility studies.

S. FANARA, R.E. BOTCHARNIKOV, A. HUSEN, J. BUDDENSIEK AND H. BEHRENS

Institute of Mineralogy, Leibniz University of Hannover, Callinstr. 3, 30167 Hannover, Germany, (h.behrens@mineralogie.uni-hannover.de)

The Campanian Volcanic District is located in the middle-southern part of the Campanian Plain and comprises the unrest Campi Flegrei Volcanic Field and the Monte Somma-Vesuvio strato-volcano. The Phlegrean Volcanic District (PVD) includes three volcanic fields: the Campi Flegrei caldera and the volcanic islands of Ischia and Procida. Two main eruptions formed the Campi Flegrei: the 39 ka Campanian Ignimbrite (CI) super-eruption yielding > 200 km^3 dense rock equivalent with trachytic-phonolitic composition (Civetta et al., 1997; Arienzo et al., 2009) and the 14 ka Neapolitan Yellow Tuff (Deino et al., 2004). Nowadays, more than 2 milion people live within this high risk volcanic region. Therefore, eruption forecasting and hazard assessment at Campi Flegrei Caldera using geophisical, stratigraphical, volcanological, structural, petrological and experimental data are essential.

Natural samples were collected on Procida Island

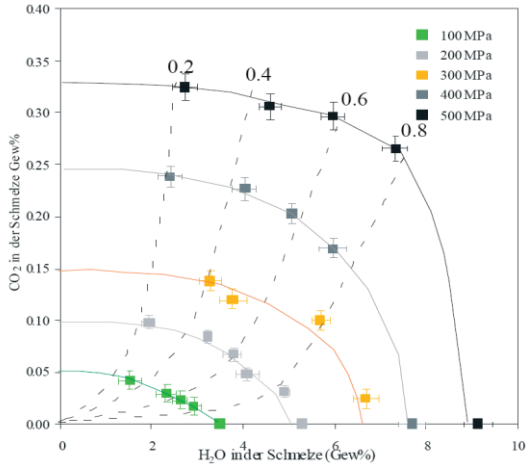

Fig. 1. Solubility of H_2O and CO_2 in the trachy-basaltic melt of Solchiaro at different pressure and X_{H2O}

during a field excursion in 2010 organised by the University of Hannover and in collaboration with the University of Rome (Prof. Danilo M. Palladino). Procida island is particularly suitable for stratigraphic reconstruction and sampling due to the thick pyroclastic sequence exposed on the costal cliffs.

Samples of the four different juvenile products (obsidian clasts, sputter clasts, white crystal-rich pumices and gray crystal-rich pumices) as well as the pyroclastic flow matrix from the CI were collected, being the CI the most-evolved member of the PVD (Arienzo et al., 2009). The youngest products of Procida island coming from the Solchiaro eruption were also sampled, being the least evolved of the PVD area and considered as the mafic end-member for the Campi Flegrei magmatism (Mormone et al., 2011). Thus, they may provide information on the source of more evolved magmas associated with this volcanic system.

Samples collected during the field trip in Procida were investigated with optical microscope and electron microprobe analyses in three bachelor theses (Güttler 2010, Krull 2010, Mozar 2010). The chemical composition, the mineral association, the water content and the oxidation state in pumices, ashes and obsidians belonging to the Breccia Museo Unit (CI) and Solchiaro deposits were examined. The CI pumices show a high-porous vitrophyric structure, with 30 to 60 vol% bubbles. The glass matrix presents micro-crystals (probably Titano-magnetite). As phenocrysts, alkali-feldspar (mostly sanidin), plagioclase, clino-pyroxene (diopside) and biotite were identified, in agreement with the findings of Fabbrizio et al. (2008) and Civetta et al. (1997). The common mineral association of the Solchiaro products consists in feldspars, clinopyroxenes, biotite and opaque minerals (probably Titano-magnetite). The samples collected near the eruptive center contains also olivine as the first crystallizing phase and show a relatively high amount of Mg in the glass matrix compared to the distal products.

A trachy-basaltic glass was prepared from the collected natural pumices and ashes of Solchiaro deposits. The natural samples were crushed in powder and double melted

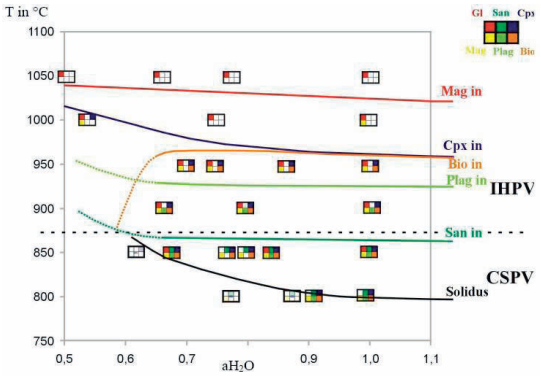

Fig.2. Phase diagram with estimated stability fields of the mineral phases for CI trachytic melts at 200 MPa. Filled squares show presence of the phase. Gl=glass, San=sanidine, Cpx = clinopyroxene, Mag = magnetite, Plag = plagioclase, Bio = Biotite.

at 1600°C for 10 h in Pt crucibles in a conventional muffle furnace. A synthetic trachyte reproducing the least evolved composition of CI (Triflisco OF17c1; Civetta et al., 1997) was prepared by melting of mixtures of oxides and carbonates at the same conditions and using the same procedure as for the trachybasalt. Bulk compositions and homogeneity of the produced glasses were tested by electron microprobe CAMECA SX100.

H_2O and CO_2 solubilities were investigated in the trachybasaltic melt of Solchiaro at 1200°C and at pressure from 100 to 500 MPa for approx. 24 h in an Internally Heated Pressure Vessel (IHPV) (Fig.1) (Buddensiek, 2010). It was found that solubility of water increases with pressure in a range from 3.49 wt% at 100 MPa to 9.15 wt% at 500 MPa with X_{H2O}=1 and shows a non linear dependence on X_{H2O} in the whole pressure range. The solubility of CO_2 increases with increasing pressure as well from 400 ppm at 100 MPa to 3200 ppm at 500 MPa with

X_{H2O}=0.8, showing a linear dependence at 100 and 200 MPa but deviating from linearity for higher pressures. The solubility behavior of volatiles in trachybasaltic magma resembles that of tholeitic basalt (Shishkina et al., 2010), but the CO_2 solubility is much lower than found for phonotephritic melts (Behrens et al., 2009). At constant

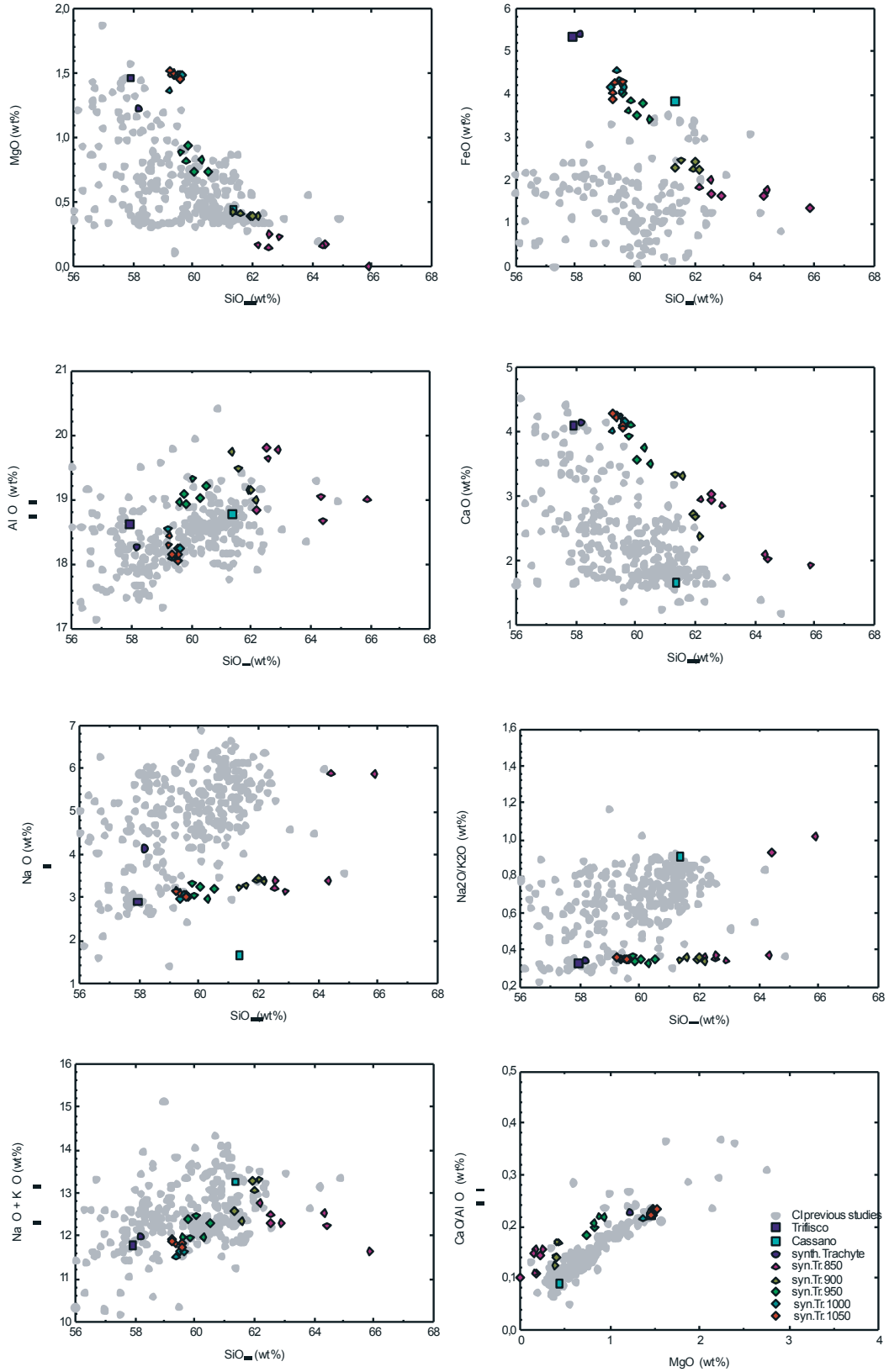

Fig. 3. Harker diagrams show compositional evolution of the melt. SiO2 content is used as a parameter for the degree of differentiation.

pressure, the maximum H_2O solubility is by a factor 30 - 60 higher than the maximum CO_2 solubility in trachybasaltic melts.

The redox state of iron in the glasses was analyzed after dissolution using the colorimetric method (Schüssler et al., 2008). It was evidenced that the samples after the experiments were strongly reduced and that the Fe^{2+}/Fe_{total} content was not influenced by pressure. Instead, with increasing the water activity and the water content, the conditions became oxidizing and the Fe3+ content increases.

To investigate the differentiation of the magma, tracing the evolution of the melt composition, the different mineral phases and their stability field, the less evolved end-member of the CI was used. Crystallization experiments at 200 MPa and at temperatures from 850 to 1050°C with X_{H2O} fluid between 1 and 0.5 were run in Cold Seal Pressure Vessel (CSPV) and IHPV. Run products were analysed by microscope, electron microprobe and spectroscopic techniques. The phase relationships at 200 MPa pressure under relatively oxidizing conditions are shown in Fig. 2 (Husen, 2010). The liquidus for the investigated system lays between 1050°C and 1000°C with magnetite as the first crystallising phase and pyroxene as second phase appearing between 1050°C and 950°C. Biotite crystallizes between 1000°C and 950°C and plagioclase between 900°C and 850°C. The last phase is the sanidine which appears below 900°C.

In Fig. 3 the melt evolution of the experimental samples is plotted in Harker diagrams and compared with the natural whole rock composition from previous studies.

It is demonstrated that a simple differentiation path cannot explain the complexity of magma compositions of the CI, consistent with the hypothesis in previous studies that the variety of magmas is due to mixing between magma reservoirs and accumulation of host rock material.

Lately, viscosities of shoshonitic and latitic melts, relevant to the Campi Flegrei Caldera magmas, have been experimentally determined at atmospheric pressure and at 0.5 GPa, temperatures between 567°C and 1600°C and water contents from 200 ppm to 3.30 wt%, by Vetere et al. (2010, 2011).

Further solubilities studies involving the trachytic and phono-trachytic compositions of the CI are planned to design and interpret better decompression experiments (this work will be done in cooperation with the group of M. Nowak in Tübingen). The equilibrium concentrations of volatiles as function of pressure will be measured from 20 to 500 MPa not only for H_2O and CO_2, but also for Cl and S, in the way to develop and to improve degassing scenarios for Campi Flegrei volcanos.

Taking into account the results of the solubility experiments, it is planned to systematically study the phase equilibria of the CI`s most evolved trachytic melts and of the parental trachy-basaltic Solchiaro´s melt as a function of temperature, pressure, redox conditions and volatile content of the system. The proposed pressure range of the study covers the suggested depth of the shallow magma chamber (2 – 6 km; 50 – 150 MPa) to that of the possible deeper reservoir (8 – 9 km, 200 – 250 MPa).

In addition to equilibria with H_2O-CO_2 fluids we plan to study selectively the influence of other volatiles (Cl and S) that turned out to be of larger importance (Webster et al., 2011). Furthermore, H_2O-undersaturated experiments, where the same water content in the melt will be adjusted as in experiments with mixed H_2O-X fluids (X = CO_2, Cl or S), will be performed. Comparison of both types of experiments will allow us to distinguish the effect of changing water fugacity from specific effects of other fluid components. A possible set of capsules in an experiment could involve systems with fluids composed by 100% H_2O, 75% H_2O – 25% CO_2, 50% H_2O – 50% CO_2, 75% H_2O – 25% Cl, 75% H_2O – 25% S plus an additional capsule with 75% of the expected H_2O content at water saturation of the melt. The experiments will be carried out at relatively oxidizing conditions. Such conditions are consistent with suggested relatively high oxygen fugacities in the CI magma chamber.

References:

Arienzo, I., Civetta, L., Heumann, A., Wörner, G., and Orsi, G. (2009) Isotopic evidence for open system processes within the Campanian Ignimbrite (Campi Flegrei-Italy) magma chamber. Bull Volcanol 71: 285-300.

Behrens H., Misiti V., Freda C., Vetere F., Botcharnikov R.E., Scarlato P. (2009) Solubility of H_2O and CO_2 in ultrapotassic melts at 1200 and 1250 °C and pressure from 50 to 500 MPa. Am. Mineral. 94, 105–120.

Civetta. L., Orsi, G., Pappalardo, L., Fisher, R.V., Heiken, G., and Ort, M. (1997) Geochemical zoning, mingling, eruptive dynamics and depositional processes - The Campanian Ignimbrite, Campi Flegrei caldera, Italy. J Volcanol Geotherm Res 75:183–219.

Deino, A.L., Orsi, G., de Vita, S., and Piochi, M. (2004) The age of the Neapolitan yellow tuff caldera-forming eruption (Campi Flegrei caldera, Italy) assessed by 40Ar/39Ar dating method. J Volcanol Geotherm Res 133: 157–170.

Fabbrizio, A., and Carroll, M.R. (2008) Experimental constraints on the differentiation process and pre-emptive conditions in the magmatic system of Phlegraean Fields (Naples, Italy) J Volcanol Geotherm Res 171: 88-102

Lesne, P., Scaillet, B., Pichavant, M., and Beny, J.M. (2011) The carbon dioxide solubility in alkali basalts: an experimental study. Contrib. Mineral. Petrol. 162, 153-168.

Mormone, A., Piochi, M., Bellatreccia, F., De Astis, G., Moretti, R., Della Ventura, G., Cavallo, A., and Mangiacapra, A. (2011) A CO_2-rich magma source beneath the Phlegrean Volcanic District (Southern Italy): Evidence from a melt inclusion study. Chem. Geol. 287, 1-2, 66-80.

Schlüssler, J.A., Botcharnikov, R.E., Behrens, H., Misiti, V., and Freda, C., (2008) Amorphous Materials: Properties, structure and Durability: Oxidation state od iron in Hydrous phono-tephritic melts. Am. Mineral. 93, 1493-1504.

Shishkina, T., Botcharnikov, R.E., Holtz, F., Almeev, R.R., and Portnyagin, M. (2010) Solubility of H_2O and CO_2-bearing fluids in tholeiitic basalts at pressures up to 500 MPa. Chem. Geol. 277, 115-125.

Vetere, F., Behrens, H., Holtz, F., Vilardo, G., and Ventura, G. (2010) Viscosity of crystal-bearing melts and its implication for magma ascent. J. Mineral. Petrol. Sc. 105, 151-163.

Vetere, F., Botcharnikov, R., Holtz, F., Behrens, H., and De Rosa, R. (2011) Solubility of H_2O and CO_2 in shoshonitic melts at 1250°C and pressure from 50 to 400MPa: Implications for Campi Flegrei magmatic system. J. Volc. Geoth. Res. 202, 251-261.

Webster, J.D. (2011) Distribution of Sulfur between melt and fluid in S-O-H-C-Cl- bearing magmatic systems at shallow crustal pressures and temperatures. Rev. Mineral. Geoch. 73, 247-283.

IODP

Thermophysical properties derived from lab measurements and downhole logging at New Jersey Shallow Shelf (IODP Expedition 313)

A. FEHR[1], R. PECHNIG[2], J. INWOOD[3], J. LOFI[4], F.P. BOSCH[1], C. CLAUSER[1]

[1] Applied Geophysics and Geothermal Energy GGE, EON Energy Research Center, RWTH Aachen University, Aachen, Germany
[2] Geophysica Beratungsgesellschaft mbH, Aachen, Germany
[3] Department of Geology, University of Leicester, Leicester, United Kingdom
[4] Géosciences Montpellier, Université Montpellier, Montpellier, France

The IODP drilling expedition 313 New Jersey Shallow Shelf was proposed for obtaining deep sub-seafloor samples and downhole logging measurements in the crucial inner shelf region. The inner to central shelf off-shore New Jersey is an ideal location for studying the history of sea-level changes and its relationship to sequence stratigraphy and onshore/offshore groundwater flows. The region features rapid depositional rates, tectonic stability, and well-preserved, cosmopolitan age control fossils suitable for characterizing the sediments of this margin throughout the time interval of interest. Past sea-level rise and fall is documented in sedimentary layers deposited during Earth's history. In addition, the inner shelf is characterised by relatively fresh pore water intervals alternating vertically with saltier intervals (Mountain et al., 2010). Therefore, three boreholes were drilled in the so-called New Jersey/Mid-Atlantic transect during IODP Expedition 313 New Jersey Shallow Shelf. Numerous questions have arisen concerning the age and origin of the brackish waters recovered offshore at depth. Here we present an analysis of thermophysical properties to be used as input parameters in constructing numerical models for future groundwater flow simulations.

Our study is based mainly on Nuclear Magnetic Resonance (NMR) measurements for inferring porosity and permeability, and thermal conductivity. We performed NMR measurements on samples from boreholes M0027A, M0028A and M0029A and thermal conductivity measurements on the whole round cores prior to the Onshore Party. These results are compared with data from alternative laboratory measurements and with petrophysical properties inferred from downhole logging data.

We deduced petrophysical properties from downhole logging data and compared them with results obtained with laboratory measurements. In water saturated samples, the number of spins in the fluid is proportional to sample porosity. NMR porosities were calculated from the zero amplitudes of the transverse relaxation measurements by normalizing the CPMG (Carr, Purcell, Meiboom, Gill) amplitudes of the measured samples to the amplitudes measured on a pure water cylinder which is equivalent to a porosity of 100 %. The NMR porosities fit well with porosities determined by Multi Sensor Core Logger (MSCL) and porosity measured on discrete samples using a helium gas pycnometer.

Using log interpretation procedures, the volume fraction of different rock types and their porosity can be derived. From the volume fraction of each rock type and its porosity, continuous profiles of thermal conductivity can be derived by using a suitable mixing law, e.g. such as the geometric mean. In combination with thermal conductivity measurements on cores, these continuous thermal conductivity profiles can be calibrated, validated and finally used to provide reliable input parameter for numerical models.

The porosity values from NMR seem to correlate well with porosities deduced from other measurements. In order to compare NMR permeabilities, we need permeability determined by an alternative method. The thermal conductivity derived from logs correlates with the measurements performed on cores.

In a next step, a numerical model will be set up and the measured thermophysical properties will be implemented in order to study transport processes in passive continental margins. This numerical model will be based on existing geological models deduced from seismic data and drillings.

References:
Mountain G. M., Proust J.-N. and the Expedition 313 Science Party (2010): The New Jersey Margin Scientific Drilling Project (IODP Expedition 313): Untangling the Record of Global and Local Sea-Level Changes, in Scientific Drilling No. 10, September 2010, p. 26-34. DOI 10.2204/iodp.sd.10.03.2010

IODP

Coral records of climate change since the Last Glacial Maximum - IODP Expedition 325 to the Great Barrier Reef

T. FELIS[1], A.L. THOMAS[2], Y. YOKOYAMA[3], J.M. WEBSTER[4], AND EXPEDITION 325 PALEOCLIMATE AND DATING GROUPS

[1]MARUM – Center for Marine Environmental Sciences, University of Bremen, Bremen, Germany
[2]Department of Earth Sciences, University of Oxford, Oxford, United Kingdom
[3]Atmosphere and Ocean Research Institute, The University of Tokyo, Tokyo, Japan
[4]School of Geosciences, The University of Sydney, Sydney, Australia

Integrated Ocean Drilling Program (IODP) Expedition 325 "Great Barrier Reef Environmental Changes", designed to investigate the fossil reefs on the shelf edge of the Great Barrier Reef in the western tropical South Pacific, was the fourth expedition to utilize a mission-specific platform and was conducted by the European Consortium for Ocean Research Drilling (ECORD) Science Operator (ESO) (Webster et al., 2009; Expedition 325 Scientists, 2010; Webster et al., 2011). The objectives of Expedition 325 are to establish the course of sea level change, to define sea-surface temperature variations, and to analyze the impact of these environmental changes on reef growth and geometry for the region over the period of 20–10 ka. Expedition 325 complements Expedition 310 "Tahiti Sea Level" (Camoin et al., 2007) that in 2005 recovered postglacial coral reef material from the flanks of the island of Tahiti in the central tropical South Pacific in depths ranging from 41 to 117 meters below sea level and ages spanning from ~16 to ca. 8 ka, but also from the penultimate deglaciation.

To meet the Expedition 325 objectives, a succession of fossil reef structures preserved on the shelf edge seaward of the modern Great Barrier Reef were cored at three geographic locations from the dynamically positioned vessel Greatship Maya in February–April 2010 (Expedition

325 Scientists, 2010; Webster et al., 2011). A total of 34 boreholes across 17 sites were cored in depths ranging from 42 to 167 meters below sea level. The cores were described during the Onshore Science Party (OSP) at the IODP Bremen Core Repository (Germany) in July 2010, where minimum and some standard measurements were made (Expedition 325 Scientists, 2010; Webster et al., 2011). Preliminary dating of core catcher samples was undertaken, between drilling and the OSP, to confirm that coral reef material ranging in age from >30 to 9 ka was recovered during Expedition 325. High-quality fossil coralgal frameworks are found in a number of horizons of different cores thus recording high energy reef settings, which is crucial for precise reconstructions of sea-level and sea-surface environmental change. The late Pleistocene sections appear diagenetically unaltered and comprise coralgal boundstone, coralgal-microbial boundstone, skeletal grainstone and rudstone, and unconsolidated sand.

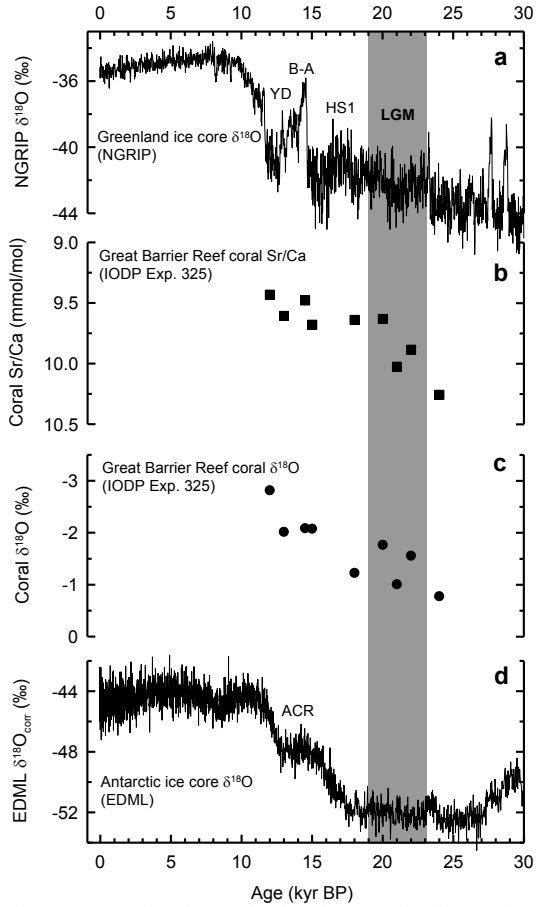

Figure 1. Records of Greenland and Antarctic climate change and Great Barrier Reef coral Sr/Ca and 18O (IODP Expedition 325). (a) Greenland ice core 18O (North Greenland Ice Core Project, NGRIP) (NGRIP members, 2004) (GICC05 age scale relative to AD 1950). Younger Dryas (YD), Bølling-Allerød (B-A), Heinrich Stadial 1 (HS1) and Last Glacial Maximum (LGM, grey bar) are indicated. (b) Preliminary results of Great Barrier Reef mean coral Sr/Ca values, based on ultra-high resolution analysis of individual fossil coral colonies (Isopora, Acropora). (c) Preliminary results of Great Barrier Reef mean coral 18O values, based on ultra-high resolution analysis of individual fossil coral colonies (Isopora, Acropora). (d) Antarctic ice core 18O (EPICA Dronning Maud Land, EDML) (EPICA Community members, 2006). Antarctic Cold Reversal (ACR) is indicated. All ice core ages are relative to AD 1950. Coral ages are approximate ages based on U-series and radiocarbon analyses of Expedition 325 core catcher samples (Expedition 325 Scientists, 2010; Webster et al., 2011).

The preliminary chronology, combined with the recovered depths of the core catcher samples, is particularly exciting as it clearly demonstrates that Expedition 325 recovered coral reef material from key periods of interest for sea level change and environmental reconstruction, including the Younger Dryas, the Bølling-Allerød, meltwater pulse 1A (MWP-1A), the 19 ka-MWP, the Last Glacial Maximum (LGM) and Heinrich stadials 1 and 2 (Figure 1a). Given that there are so few fossil coral records spanning these intervals, and even fewer from stable, passive margin settings far from the confounding influence of ice sheets, highlights further the importance of the new Expedition 325 cores. Further postcruise research on samples taken during the OSP is expected to fulfil the objectives of the expedition.

Scleractinian coral colonies can monitor sea-surface temperatures and other oceanographic parameters (e.g., salinity and sediment run-off), and fossil corals can be used as recorders of past variations in these parameters. The ultra-high resolution analyses of Sr/Ca and δ18O ratios in fossil corals recovered by IODP Expedition 325 will provide sub-seasonally resolved reconstructions of temperature and hydrologic balance at the sea surface for time windows of several years. These coral records will allow quantifying changes in the amplitude of seasonality and perhaps interannual climate variations in the tropical southwest Pacific that occurred since the LGM. Moreover, the mean coral Sr/Ca and δ18O values of a large number of fossil corals will provide information on mean changes in temperature and δ18O seawater during the last deglaciation. In addition to fossil Porites corals that are typically used for high-resolution paleoclimate studies in the Indo-Pacific region IODP Expedition 325 has recovered a large number of massive Isopora and corymbose branching Acropora corals.

As modern proxy calibrations for these coral genera

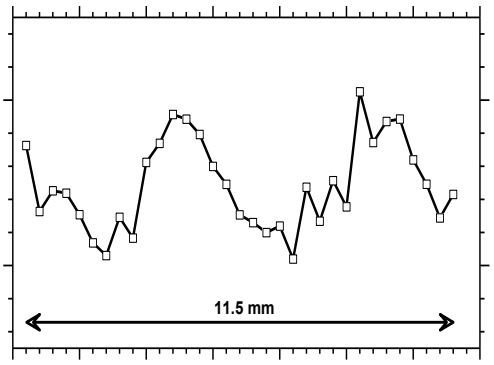

Figure 2. Ultra-high resolution Sr/Ca record of a ~24 kyr BP fossil Acropora coral recovered by IODP Expedition 325. The preliminary results suggest that 2.5 annual cycles are present in this near-monthly resolution record of the coral Sr/Ca temperature proxy.

are not available, such calibrations are currently being developed within the IODP Expedition 325 Paleoclimate group. The DFG funded project "Seasonal to interannual climate variability in the tropical southwest Pacific during the last deglaciation - Monthly resolved reconstructions from Great Barrier Reef corals" (FE 615/4-1) is part of the international effort to reconstruct past climate change from

fossil corals recovered by IODP Expedition 325. Preliminary mean Sr/Ca values of individual coral colonies generated within this project indicate the expected trend toward warmer sea surface temperatures (SST) since the LGM (Figure 1b). Similarly, the corresponding mean coral δ18O values indicate the expected trend toward more negative δ18O since the LGM, reflecting the combined signal of temperature and δ18O of seawater (Figure 1c). Moreover, it was possible to generate a short ultra-high resolution Sr/Ca-based record of past SST variations from a fossil Acropora coral that has an approximate age of ~24 kyr BP, probably reflecting 2.5 annual cycles in near-monthly resolution (Figure 2). These initial results are consistent with those generated by other members of the Expedition 325 Paleoclimate group. Approximate coral ages are based on U-series and radiocarbon analyses of Expedition 325 core catcher samples (Expedition 325 Scientists, 2010; Webster et al., 2011), which are currently being improved by the Expedition 325 Dating group.

References:
Camoin, G.F., Iryu, Y., McInroy, D.B., and the Expedition 310 Scientists, 2007. Proceedings IODP, 310: Washington, DC (Integrated Ocean Drilling Program Management International, Inc.). doi:10.2204/iodp.proc.310.2007.
EPICA Community members. One-to-one coupling of glacial climate variability in Greenland and Antarctica. Nature 444, 195-198 (2006).
Expedition 325 Scientists, 2010. Great Barrier Reef environmental changes: the last deglacial sea level rise in the South Pacific: offshore drilling northeast Australia. IODP Preliminary Report, 325. doi:10.2204/iodp.pr.325.2010.
North Greenland Ice Core Project members. High-resolution record of Northern Hemisphere climate extending into the last interglacial period. Nature 431, 147-151 (2004).
Webster, J.M., Yokoyama, Y., Cotterill, C., and the Expedition 325 Scientists, 2011. Proceedings IODP, 325: Tokyo (Integrated Ocean Drilling Program Management International, Inc.). doi:10.2204/iodp.proc.325.2011.
Webster, J.M., Yokoyama, Y., and Cotterill, C., 2009. Great Barrier Reef environmental changes: the last deglacial sea level rise in the South Pacific: offshore drilling northeast Australia. IODP Scientific Prospectus, 325. doi:10.2204/iodp.sp.325.2009.

ICDP

Detailed 40Ar/39Ar step heating study of Chesapeake Bay crater impactites: tektites and impact melt from USGS-ICDP drill core Eyreville-B

V. A. FERNANDES[1,2], J. HOPP[2], W. SCHWARZ[2], M. TRIELOFF[2] AND W. U. REIMOLD[1]

[1]Museum für Naturkunde, Leibniz Institute, Humboldt Univ. Berlin, Berlin, Germany;
[2]Institut für Geowissenschaften, Univ. Heidelberg,Heidelberg, Germany;

Introduction: Current radiometric age determination for the Chesapeake Bay crater (located in Atlantic Coastal Plain centered near the present mouth of Chesapeake Bay in eastern Virginia, U.S.A.) of 35.3±0.1 Ma [1-4] is based on total fusion $^{40}Ar/^{39}Ar$ and K-Ar age determination of the North America (NA) tektites (i.e., distal impact glasses), bediasites and georgiaites. In preliminary ^{40}Ar-^{39}Ar work, we have shown that precise Ar ages on these tektites cannot be acquired by total fusion experiments but require step heating measurements [5]. $^{40}Ar/^{39}Ar$ total fusion and K-Ar ages are based on the assumption that tektites are pure quenched glass, i.e., all NA tektites did not gain or lose any Ar after formation. Particularly, it has been assumed that during the 900 to 2300 km travel through the atmosphere, the melt did not retain any relict ^{40}Ar, or the tektites did not lose any ^{40}Ar from the in situ ^{40}K decay after formation (e.g., weathering). However, careful inspection of tektites using SEM, EMPA and optical microscopy shows that these samples are heterogeneous and composed not only of quenched glass but also of clasts and voids/bubbles. The current DFG-ICDP project is focused on a systematic petrographic, geochemical and radiometric study of the first impact melt rocks found in the USGS-ICDP drill core Eyreville-B obtained from the Chesapeake Bay impact structure [6&7] and to refine the ^{40}Ar-^{39}Ar ages for the related NA tektites.

Sample	aliquot	% ^{39}Ar	Age (Ma)	Total # heating steps
Be281-Ac2	core	91	33.57±0.49	17
Be281-Ar2	rim	56	33.14±0.29	21
Be281-Bc2	core	83	34.39±0.35	20
Be283-1	bulk	96	34.48±0.27	16
Georgiaite	bulk	79	34.76±0.36	20

Table 1 Summary of the 40Ar/39Ar step-heating results for three bediasites and one georgiatite (2σ). Aliquots of core and rim are shown.

Samples and methodology: To better re-evaluate the age of North American tektites and implicitly the Chesapeake Bay crater, material from rim and core areas of three bediasites (Be281-A, Be281-B and Be283) were irradiated at the Sacavém Reactor in Lisbon, Portugal for 17hours. Samples and 10 aliquots from each neutron fluence monitors, Fish Canyon sanidine (FCs-2) and Bergell granodiorite biotite (HD-B1), were loaded into vacuum sealed pure-silica vials. Argon was extracted from samples by using a high-frequency induction furnace at the Univ. of Heidelberg. All data were corrected for background, blank, interference and decay.

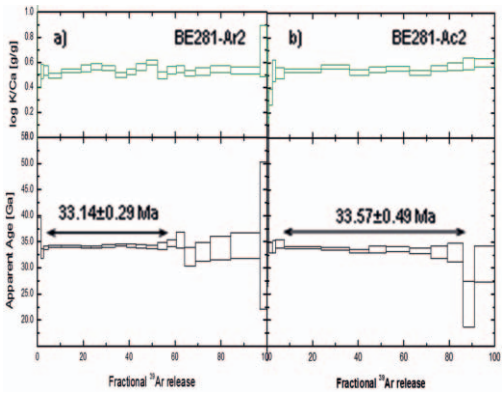

Figure 1 Resuls for Bediasite Be281-A: a) Apparent age spectrum and K/Ca vs. fraction of 39Ar release for rim aliquot Be281-Ar2. b) Apparent age spectrum and K/Ca vs. fraction of ^{39}Ar release for core aliquot Be281-Ac2.

$^{40}Ar/^{39}Ar$ step heating results: Bediasite rim and core material was studied separately in order to evaluate gain or loss of Ar by the tektites. To date, a total of five aliquots have been analyzed for $^{40}Ar/^{39}Ar$ release over 16 to 21 heating steps (Table 1; Figs. 1). Included in the irradiation batch was a pair of rim and core fractions from one bediasite and also undifferentiated material from a

georgiaite. Overall, the initial 5-10 % ^{39}Ar released are characterized by high apparent ages associated with argon having atmospheric ^{40}Ar/^{36}Ar ratios (Fig. 1). For all 5 samples, the following age plateaux comprising most of the ^{39}Ar release (90-95%) vary from 33.14±0.29 Ma (youngest aliquot) to 34.76±0.36 Ma (oldest aliquot) (errors 2σ), Table 1. The logK/Ca plot shows constant ratios of ~0.4 to ~0.6 over the entire ^{39}Ar release (e.g., Fig.1). For tektite Be281-A, samples from rim (Be281-Ar2) and core (Be281-Ac2) were analyzed (Fig.1). The age obtained for each sample is within error the same (Table 1). However, the relatively large error shown by the core sample makes it difficult to determine if there is actually a difference among an individual tektite. To evaluate this, further duplicate runs are in progress. In an inverse isochron diagram, all

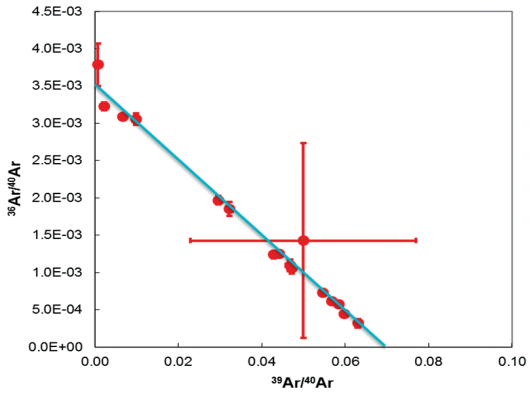

Figure 2 39Ar/40Ar vs. 36Ar/40Ar for bediasite core material Be281-Ac2

heating steps form a mixing line between trapped atmospheric argon with a ^{40}Ar/^{36}Ar value of ~295.5 and a radiogenic ^{40}Ar component (Fig. 2).

Summary: ^{40}Ar/^{39}Ar data acquired from NA tektites suggest that total fusion ages obtained from individual fragments (however performed on samples smaller than those used for step heating, and likely permiting a higher spatial resolution) should be cross-checked by step heating age spectra in order to evaluate a reliable age, together with careful neutron flux determination and petrographic/geochemical inspection using SEM and EMPA. The release pattern of the spectra obtained provided evidence that the samples, whose data is presented here, did neither contain excess ^{40}Ar, nor experienced secondary loss of radiogenic ^{40}Ar. Some minor redistribution effects by ^{39}Ar recoil seem possible. Presently acquired data suggest that the age of the Chesapeake Bay impact structure is probably slightly younger than the 35.3 Ma reported by [1-4].

Current and future work: ^{40}Ar/^{39}Ar analyses on tektites and the first impact melt found [8] within the USGS-ICDP drill core Eyreville-B are in progress. This includes further rim and core material from all 3 bediasites and respective duplicates. To evaluate the possible presence of excess argon or mass-fractionated atmospheric argon in voids and bubbles, non-irradiated tektite material will be crushed under vacuum conditions with subsequent analyses of the gas. Furthermore, SEM and EMP investigations will be finalized to characterize the clasts observed within the different NA tektites. Moreover, within the sample package batch sent for irradiation at the Sacavém Reactor, there were included a total of 20 aliquots of age monitors: 10 FCs-2 aliquots and 10 HD-B1 aliquots. Considering the given uncertainty for the FCs-2 monitor [9-12], which was used during irradiation for preliminary ^{40}Ar/^{39}Ar analyses by [5], the current aim in using two age monitors in the same irradiation package is to cross-check the monitor ages and to verify the flux gradient of the Sacavém reactor.

Acknowledgements: Dr. Ingo Leya, Dr. Axel Wittmann and Mr. Hal Povenmire provided material for this study. Dr. Paul Renne facilitated access to the 40Ar/39Ar instrument at the Berkeley Geochronology Center for preliminary analyses by VAF. Financial support to VAF has been provided by DFG-ICDP FE 1211/1-1.

References: [1] Glass B. P., Muenow D. W., and Aggrey K. E. (1986) Meteoritics 21, 369-370 (abstr.). [2] Glass B. P., Koeberl C., Blum J. D., Senrle F., Ize G. A. , Evans B. J., Thorpe A. N., Povenmire H. and Strange R. L. (1995) Geochim. Cosmochim. Acta 59, 4071-4082. [3] Albin E.F. and Wampler J.M. (1996) Lunar and Planet. Sci. Conf. XXVII, 5-6 (abst). [4] Horton J. W., and Izett G. A. (2004) In Studies of the Chesapeake Bay Impact Structure, USGS Prof. Paper 1688, E1-E30. [5] Fernandes et al. (in preparation). [6] Wittmann A., Schmitt R.T., Hecht L., Kring D.A., Reimold W.U. and Povenmire H. (2009a) Geol. Soc Amer. Special Papers 458, 377-396. [7] Wittmann A., Reimold. W.U., Schmitt R.T., Hecht L. and T. Kenkmann (2009b) Geol. Soc Amer. Special Papers 458, 349-376. [8] Wittmann et al. (2009) Geol. Soc. Amer. Special Papers 458, 377-396. [9] Renne et al., (1998) Chem. Geol. 145, 117–152. [10] Jourdan and Renne (2007) Geochim. et Cosmochim. Acta 71, 387-402. [11] Hilgen and Kuiper (2009) Geol. Soc. of Amer. Spec. Paper 452, 139- 148. [12] Rivera et al. (2011) Earth Planet. Sci. Lett. 311, 420-426.

ICDP

The Chew Bahir project, southern Ethiopia: Towards a reconstruction of Late Quaternary climate shifts in the cradle of humankind

V.FOERSTER[1], A. JUNGINGER[2], A. ASRAT[3], M. UMER[4], H.F. LAMB[4], T. GEBRU[1], V. WENNRICH[6], M. WEBER[6], J. RETHEMEYER[6], N. NOWACZYK[5], U. FRANK[5], M. C. BROWN[5], M. TRAUTH[2], F. SCHAEBITZ[1]

[1]University of Cologne, Seminar for Geography and Education; Gronewaldstrasse 2; 50931 Cologne; Germany
[2] University of Potsdam, Institute of Earth and Environmental Science; Germany
[3] Addis Ababa University, Department of Earth Sciences; P. O. Box 1176, Addis Ababa, Ethiopia
[4] Aberystwyth University, Institute of Geography and Earth Sciences, Aberystwyth SY23 3DB, U.K.
[5] Helmholtz-Zentrum Potsdam, Deutsches GeoForschungsZentrum – GFZ, 14473 Potsdam; Germany
[6] University of Cologne, Institute of Geology and Mineralogy; Zülpicher Str.49A; 50674 Cologne; Germany

Chew Bahir, today a playa in a tectonically-bounded basin in southern Ethiopia, forms the transition zone between the Main Ethiopian Rift to the north and the Omo-Turkana basin to the southwest. This close proximity to the world class paleoanthropological site of the Omo Kibish, where the oldest known anatomically modern human fossils were found, makes the about 5 km thick sediment infill a unique archive as it can provide sedimentary records for reconstructing paleoenvironments in the source region of modern man. Out of the close interrelationship between climate and human evolution and dispersal, the necessity evolves to understand the character, including timing, amplitude, synchronicity and abruptness of dry-wet-dry cycles in East Africa as they are thought to have paced and controlled human dispersal significantly.

The Chew Bahir project focuses on these rapid dry-wet variations and their impact on the biosphere and is part of the ICDP "Hominid Sites and Paleolakes Drilling Project" (HSPDP), because the project's objective is to reconstruct the East African paleoenvironments in the timeframe of human evolution. Moreover the project is associated to the CRC-806 programme "Our Way to Europe" that studies the dispersal of anatomical modern humans into Eurasia.

The new data from the Chew Bahir project we present here are based on six cores (9-18 m depth) that were drilled in a NW-SE transect across the basin and provide a continuous record of the dry-wet-dry alternations during the last 45 ka. Our sedimentological, geochemical, geophysical, magnetic, macro- and microfossil analyses as well as a suite of AMS radiocarbon dates show that especially moisture availability has been subjected to major and partly abrupt fluctuations in the Chew Bahir basin.

Age control and the sedimentation rates were determined by a series of calibrated radiocarbon ages. The radiocarbon ages of biogenic carbonates (shells of the

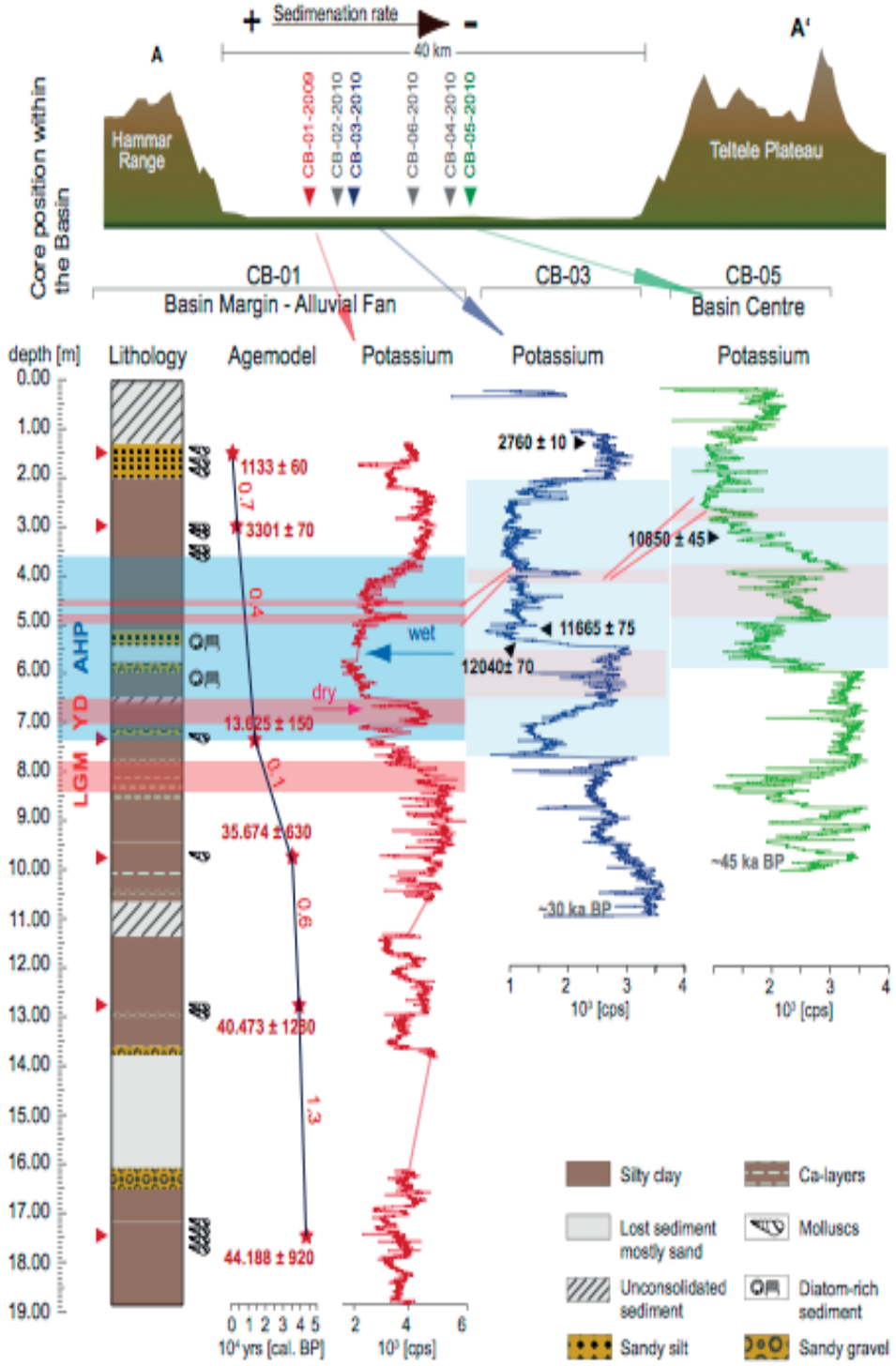

Figure 1: Lithology, age-depth model and results of geo-chemical and physical investigations of the pilot core CB-01 and CB-03, CB-05, illustrating from left to right the decrease of sedimentation rate towards the basin center; Potassium (K) indicates marked amplitudes with noticeably abrupt transitions; high K values show dry conditions; stars represent C14 ages and numbers along the agemodel indicate sedimentation rates in mm/year.

abundant Melanoides tuberculata) and bulk sediment samples are consistent, showing no reversals. However, charcoal samples (fossil wood) are currently picked to approach an estimation of a possible reservoir effect in the basin and its variation through time. This approach will shed light on the reliability of the radiocarbon chronology. Furthermore, with special emphasis on the Holocene, the agemodels have been improved by a collaborative paleomagnetic study at the GFZ Potsdam. Based on the age models (Fig. 1), interpolated ages were calculated for every centimeter, revealing that the sediment cores have recorded the environmental history of the Chew Bahir from ~44 to 1.0 ka cal BP therewith including the Last Glacial Maximum times, the African Humid Period (AHP ~15-5 ka cal BP) and ending with the onset of the Medieval Warm Period (700-1,000 cal BP).

Besides the other measured chemical elements such as Ti/Fe, Ca/Sr, and Mn, the most striking paleoenvironmental indicator seems to be potassium as a proxy for aridity in the catchment of the Chew Bahir. Following the potassium curve of our pilot record, demonstrating humidity with decreasing values, it becomes clear that during the time interval between ~15-5 ka the basin has been subdued to humid conditions. These resulted in an enlarged lake with fresh water diatoms and a dominance of fluvial fine grained input, outlining a prominent and clearly defined wetter period, known as the insolation controlled AHP with a remarkable abrupt onset and a rather gradual termination. The AHP frames a sharply defined arid phase (12.8-11.6 ka cal BP) that has been associated with the Younger Dryas chronozone.

The pilot core CB-01 was drilled at the western margin of the Chew Bahir basin on the foot of an extensive alluvial fan, which is activated during strong rainfall events, washing in feldspar minerals from the Hammar range. These contain potassium bearing minerals, which is expressed in partly sharp increases of this element in the sediment record, reflecting the onset of dry conditions on millennial or even centennial timescales. All components of gneiss, like quartz, mica and mainly feldspars, dominate the mineral assemblage throughout the whole core as first XRD investigations on the pilot core reflect. Therewith it is not surprising to find higher potassium values for the deduced arid phases, as the feldspars coming from the Hammar range are eroded easier during dry phases with a sparse vegetation cover and then washed in during heavy rains. During wetter phases however, fluvial input dominates, diluting the potassium content and depositing material from a more diverse catchment. So, given low potassium values indicate wetter conditions, also the latest XRF results of CB-03 and CB-05, which are located at the basin centre and in an intermediate site, show this shift to incresed moisture availabilty interupted by significant dry-spells. Sedimentation rates support this by increased deposition values during wet phases (Figure 1).

The latest results of the new cores CB-02 to CB-06 show that within the basin itself variations concerning sedimentation rates, material composition and diatom assemblages can be noted, which are most likely attributed to changes in the dominating input mechanisms and basin morphology. Based on our results a clearly decreasing sedimentation rate towards the center of the basin can be deducted as illustrated in Figure 1. Consequently, this will enable us to reach even further back in time by drilling in the center of the Chew Bahir basin as proposed in the ICDP-HSPDP project. Thus, Chew Bahir not only represents a suitable climate archive with well datable lacustrine deposits and reacts sensitively towards even minor climate signals in this highly variable environment, but also could in fact reveal the nature, causes, and impact of climate changes in the cradle of humankind.

ICDP

SCOPSCO: Preliminary results of new cores from Lake Ohrid

A. FRANCKE[1], B. WAGNER[1], H. VOGEL[1]

[1]University of Cologne, Institute for Geology and Mineralogy, Zülpicher Str. 49a, 50674 Cologne

Lake Ohrid, located at the boarder of Macedonia and Albania, is supposed to be the oldest lake in Europe. Formed about 3 to 5 million years ago (Albrecht and Wilke, 2009), the lake provides a valuable terrestrial paleoclimate record back to the Pliocene, probably showing important climatic links to marine records of the Mediterranean Sea. Furthermore, the lake accommodates more than 200 endemic species (Stankovic, 1960). The combination of paleoenvironmental information with modelled speciation events based on molecular clock analysis can help to better understand the mechanism triggering evolution. Until today, only relative short cores spanning the last glacial-interglacial cycle are available from Lake Ohrid (Wagner et al., 2008; Vogel et al., 2010). In order to reconstruct the complete climatic history of Lake Ohrid, a full proposal (Scientific Collaboration On Past Speciation Conditions in Lake Ohrid: SCOPSCO) was submitted to the International Continental Scientific Drilling Program (ICDP) in 2009. The scientific goals outlined in the proposal comprise 5 primary drill sites and the recovery of a 680m long sediment sequence from the deepest part of the lake ("DEEP"-site). Beside new outcomes about climate variability and biodiversity, this project also aims to reveal precise information about the age and origin of the lake as well as about tectonic and volcanic activity in the Mediterranean region. Funding by ICDP and other national and international funding agencies will likely allow a start of the deep drilling operation in 2012.

In 2011, we carried out a joint field campaign with the CRC 806 project "Our way to Europe". The aim of the field campaign was to recover sediment cores from lakes Dojran (Macedonia, Greece), Prespa (Macedonia, Greece, Albania), and Ohrid. Within the scope of the SCOPSCO project, undisturbed surface sediments at the "DEEP"- site were cored and can be used for the establishemnt of a core composite with the cores to be recovered during the deep drilling campaign in 2012. Secondly, site #5 in the SCOPSCO proposal, the "LINI"-site, was cored in 2011. This site was chosen to obtain more information about active tectonics and mass wasting. The target depth at the "LINI"-site (260 m water depth) was 20 m. However, technical problems and severe winds did not allow duplicate coring and led to a complete loss of the coring equipment. Despite the technical problems, we were able to recover a 10 m long sediment sequence, which includes at least one mass wasting event between 310 cm and 110 cm field depth. Preliminary results indicate that the mass wasting event is characterized by homogenous grey

sediments and a distinct sand layer with an erosional basis at 310 cm field depth. The combination of information obtained from the seismic surveys of Lake Ohrid and the timing of the mass wasting event can provide valuable information to the tectonic activity in the basin.

Ongoing studies also indicate that the major part of the "LINI" core is composed of Holocene deposits. Below approximately 800 cm field depth, the color of the sediment is grey-olive to grey and sand lenses are common. Younger deposits are charchterized by a brown- or olive-grey color, a relatively high organic matter content and by indications of bioturbation. Based on former studies of sediment cores from Lake Ohrid (Wagner et al., 2008; Vogel et al., 2010), the shift in sedimentological characteristics at 800 cm field depth corresponds with the Pleistocene/Holocene transition. If subtracting the 200 cm of mass wasting deposits between 310 cm and 110 cm field depth, the remaining Holocene sediments suggest sedimentation rates at least twice as high compared to the existing records from the lake. This will allow obtaining a high-resolution record of Holocene environmental changes, which can be compared to the surface sediments recovered from the "DEEP" site and to other records from the region, such as from lakes Prespa or Dojran.

Particularly the record gained from Lake Dojran in summer 2011 could become an excellent counterpart to the "LINI" sequence, as this record is supposed to have a similar thickness of Holocene deposits. As Lake Dojran is relatively shallow for its size (maximum of 7 m water depth and a surface area of 40 km^2), the sediment record could provide an amplified signal of hydrological changes in the region. A high variability of the carbonate content and the grain-size as well as the occurrence and absence of shells and their fragments indicate significant variations in the Holocene environmental settings at Lake Dojran. Very poorly sorted clayey silt with sand lenses and dropstones at the very bottom of the Lake Dojran sequence probably indicates a significant lake level lowstand at the end of the Pleistocene, which probably correlates with hiati in the existing records from Lake Ohrid (Wagner et al., 2008; Vogel et al., 2010).

References:

Albrecht, C. and Wilke, T. (2009): Ancient Lake Ohrid: biodiversity and evolution: Developments in Hydrobiology 205: 103-140.

Stankovic, S. (1960): The Balkan Lake Ohrid and Its Living World, Den Haag, Monographiae Biologicae, 357 p.

Vogel, H., Wagner, B., Zanchetta, G., Sulpizio, R., and Rosén, P. (2010): A paleoclimate record with tephrochronological age control for the last glacial-interglacial cycle from Lake Ohrid, Albania and Macedonia: Journal of Paleolimnology 44: 295-310.

Wagner, B., Lotter, A. F., Nowaczyk, N., Reed, J. M., Schwalb, A., Sulpizio, R., Valsecchi, V., Wessels, M., and Zanchetta, G., 2008, A 40,000-year record of environmental change from ancient Lake Ohrid (Albania and Macedonia): Journal of Paleolimnology 41: 407-430.

Wagner, B., Vogel, H., Zanchetta, G., and Sulpizio, R., 2010, Environmental change within the Balkan region during the past ca. 50 ka recorded in the sediments from lakes Prespa and Ohrid: Biogeosciences 7: 3187-3198.

IODP

Millennial-scale sea-surface temperature variability in the late Pliocene to early Pleistocene North Atlantic

O. FRIEDRICH[1], P.A. WILSON[2], C.T. BOLTON[3], R. SCHIEBEL[4]

[1]Institut für Geowissenschaften, Goethe-Universität Frankfurt, Altenhöferallee 1, Germany
[2]National Oceanography Centre Southampton, University of Southampton, European Way, UK
[3]Facultad de Geologia, Universidad de Oviedo, Jesus Arias de Velasco, Spain
[4]BIAF, Université d'Angers, 2 bd Lavoisier, France

While the late Pleistocene is typically characterized by large-amplitude millennial-scale temperature fluctuations, their occurrence and significance under a warmer climate is highly debated. Several recent studies show millennial-scale climate fluctuations also during the warmer intervals of the late Pliocene and earliest Pleistocene. The occurrence and especially the amplitude of this kind of suborbital climate variability in terms of surface-water temperatures (SST), however, is rather unknown and high-resolution, millennial-scale SST records for this time interval are still missing.

Here we present a new late Pliocene to earliest Pleistocene high-resolution (~400 yr resolution) SST record from Integrated Ocean Drilling Program Site U1313 (North Atlantic Ocean, 41°N). We used Mg/Ca-derived paleotemperature estimates of the planktic foraminifer Globigerinoides ruber to investigate changes in summer SST on orbital to millennial time scale. Reconstructed summer SST shows temperatures up to 3°C above present day for interglacials of the late Pliocene to earliest Pleistocene (2.9 to 2.4 Ma). Glacials are characterized by summer temperatures between 18°C and 21°C. Millennial-scale SST variability over the first large-amplitude glacial-interglacial cycles that occur after initiation of northern hemisphere glaciation (spanning marine isotope stages MIS 101 to 95) reveal small-amplitude variability in summer SST at periodicities of ~1.9 kyr and ~2.2 kyr. This variability prevailed regardless of glacial or interglacial state and shows no amplification during glacials, questioning the crossing of an ice-sheet threshold for amplification of millennial-scale climate fluctuations during the late Pliocene to earliest Pleistocene glacials. Furthermore, the reconstructed summer SST at Site U1313 contradicts results of former studies proposing a significant weakening and/or southern shift of the North Atlantic Current, supposed to trigger cooling of the northern hemisphere and intensified ice-sheet formation.

ICDP

Detrital zircon geochronology and provenance analysis for Paleoproterozoic siliciclastic sediments of the Fennoscandian Shield

C. GÄRTNER[1], H. BAHLBURG[1] , A. MARTIN[2], D.J. CONDON[2], A.R. PRAVE[3], A. LEPLAND[4] J. BERNDT[5], A. GERDES[6]

[1]Institut für Geologie und Paläontologie, Westfälische Wilhelms-Universität Münster, Germany
[2]NERC Isotope Geosciences Laboratory, British Geological Survey, Keyworth, UK
[3]School of Geography and Geosciences, University of St. Andrews, UK
[4]Geological Survey of Norway, Trondheim, Norway
[5]Institut für Mineralogie, Westfälische Wilhelms-Universität Münster, Germany
[6]Institut für Geowissenschaften, Goethe-Universität Frankfurt /Main, Germany

The Archaean-Paleoproterozoic transition (2.5-2.0 Ga) marks a period of several environental changes and plate tectonic reorganisations in Earth's history. Volcano-sedimentary rock successions in Russian Fennoscandia contain deposits related to some of those upheavals and were drilled during the Fennoscandian Arctic Russia – Drilling Early Earth Project (FAR-DEEP), which is part of the International Continental Scientific Drilling Program

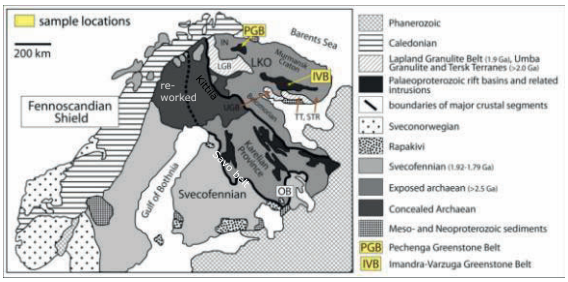

Fig. 1: Map of Fennoscandia, Northern Europe, with sample locations. Different provinces and terranes in Fennoscandia reflect potential source areas of detrital zircons (after Daly et al., 2001). IVB: Imandra-Varzuga Greenstone Belt, PGB: Pechenga Greenstone Belt, LKO: Lapland-Kola-Orogen/Kola Province, OB: Onega Basin, ST: Strelna Domain, TT: Tersk Terrane, IN: Inari Terrane, LGB: Lapland Granulite Belt, UGB: Umba Granulite Belt.

(ICDP). The successions represent 500 Ma recovered in rocks from the Pechenga and Imandra-Varzuga Greenstone belts (Kola Province) and the Onega basin (Karelian Province, Fig. 1, Melezhik et al., 2005). This study focuses on siliciclastic sedimentary rocks from the two greenstone belts, whose successions have a correlative stratigraphy (Fig. 2). U-Pb geochronology by laser ablation inductive coupled plasma mass spectrometry (LA ICP-MS) was applied on detrital zircons to improve age constraints on the duration of the Huronian glaciation and the Lomagundi-Jatuli Event, upheavals that characterize the Archaean to Palaeoproterozoic transition. Furthermore, the provenance of the rocks is being investigated using Hf isotope and whole rock geochemical analysis.

The Huronian Glaciation was the first known presumably worldwide glaciation and occurred from 2.45-2.22 Ga as three glacial events (Young et al., 2001). The Lomagundi-Jatuli Event took place in the aftermath of the glaciation from 2.3-2.06 Ga (Karhu & Holland, 1996; Shields & Veizer, 2002, Melezhik et al., 2007) and is marked by a large positive excursion of $\delta^{13}C$ in sedimentary carbonates. Three formations in the Pechenga (Neverskrukk, Kuetsjärvi, Kolasjoki Formation) and two formations in the Imandra-Varzuga greenstone belt (Seidorechka, PolisarkaKolasjoki, Fig. 2) were sampled. Seventeen samples containing sandstones, siltstones, greywackes and tuffs were analysed, chosen due to their stratigraphic position below or above characteristic successions like glacial diamictites and isotopically heavy carbonates.

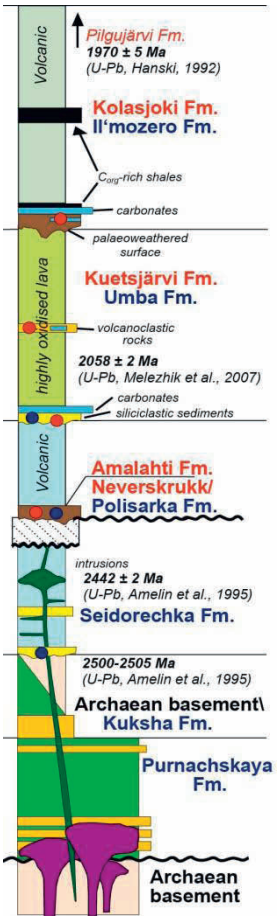

Fig. 2: Combined stratigraphic profile for the Pechenga (red) and Imandra-Varzuga (blue) greenstone belts (after Melezhik et al., 2005).

To determine the maximum depositional ages of the host rocks we were interested in the youngest zircon ages of the samples. Analyses with high contents of common lead (>1.5%) were excluded for interpretation concerning the maximum depositional ages, as this effects the reliability of the U-Pb ages, just as discordant zircons (<90%, >102%). Nevertheless, the discordant zircons are still used to assess a timing of Pb-loss, indicating a metamorphic overprint around 550 Ma or crystallization ages of c. 2.5 Ga. Selected zircons with youngest ages determined by LA-ICPMS analysis were subsequently analysed by isotope dilution-thermal ionisation mass spectrometry (ID-TIMS) to assess concordance and accuracy of dates to be used as stratigraphic constraints.

The obtained detrital zircon ages range from 3.5 to 1.85 Ga with one prominent age group between 2.9-2.6 Ga in all but two samples (Fig. 3). The youngest zircons from individual samples vary due to their stratigraphic position. To constrain the duration of the Huronian glacation

siliciclastic sediments from the Seidorechka and Polisarka Sedimentary Formation (Sed. Fm.) of the Imandra-Varzuga Greenstone belt have been analysed, as glacial diamictites have been observed in the Polisarka Sed. Fm. Isotopically heavy sedimentary carbonates related to the Lomagundi-Jatuli Event occur in the Kuetsjärvi Fm., overlying the Neverskrukk Fm. (Melezhik et al., 2005; Fig. 2). Youngest age data of 2.43 Ga for the Seidorechka Sed. Fm., reproduced by ID-TIMS analysis, and 2.34 Ga for the Polisarka Sed. Fm. (Fig. 3), are interpreted to reflect the maximum depositional ages for these formations. This indicates a maximum duration of the glacial event on the isotopic excursion in Fennoscandia. This coincides with previous age constraints of 2.36 Ga reported by Shields & Veizer (2002) and is supported by the maximum depositional age for the Neverskrukk Fm. Youngest ages of c. 2.4 Ga for the overlying Kuetsjärvi Sed. Fm. imply that the deposition occurred later than the formation of its detrital zircons so these is not applicable to be used for time constraints (Fig. 3). The Kuetsjärvi Volcanic Fm., overlying the Kuetsjärvi sediments, yielded a clear age peak from 2.1 to 2.0 Ga, with an average of 2.06 Ga, reproduced by ID-TIMS analysis (Fig. 3), which would be coinciding with Melezhik et al. (2007). Youngest zircons

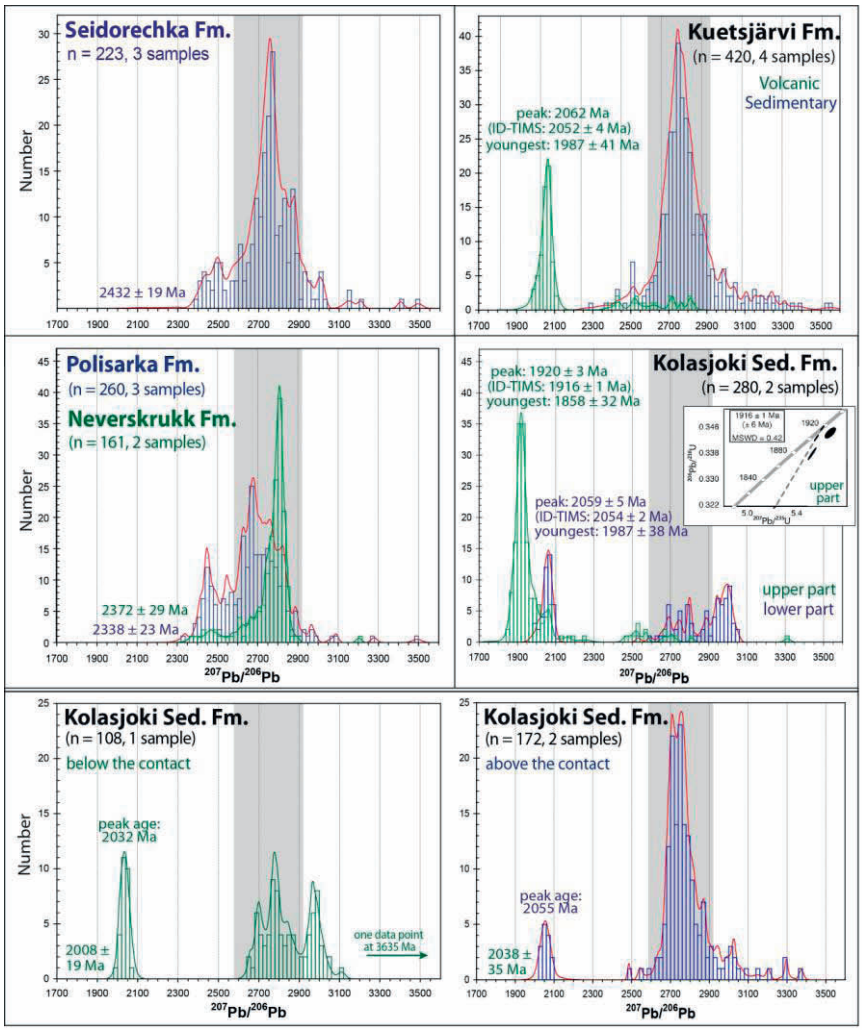

Fig. 3: Histograms showing U-Pb ages for all formations with peak ages, analysed by LA ICP-MS. The main age group of 2.9-2.6 Ga is marked by grey colours. The small rectangle shows young ages of 1.92 Ga from the Kolasjoki Sedimentary Fm. specified by ID-TIMS analysis.

Fennoscandian Shield during this time frame, consistent with age constraints for the second glacial event from the Pretoria Group in South Africa (Hannah et al., 2004). For the Neverskrukk Fm. (Pechenga Greenstone Belt), which is correlative to the Polisarka Sed. Fm., maximum depositional ages of 2.37 Ga (Fig. 3) also match with these previously obtained ages.

The end of the Huronian glaciation also describes the beginning of the subsequent Lomagundi-Jatuli Event, hence, the age of 2.34 Ga from the Polisarka Sed. Fm. is also a maximum constraint for the onset of the carbon of 1.99 ± 0.04 Ga indicate a slightly younger deposition, but considering the error they still point to a similar duration.

To further constrain the end of this event in the Kolasjoki Sed. Fm., two samples have been analysed. They derive from above isotopically heavy carbonates and are separated by a carbonate succession. The detrital zircon age distributions yielded remarkable differences, showing age groups of 2.0-1.85 Ga (peak age: 1.92 Ga, youngest zircon: 1.86 ± 0.03 Ga) for the upper part (above carbonates) and 2.1-1.98 Ga (peak age: 2.06 Ga, youngest zircon: 1.98 ±

0.04 Ga) for the lower part (below carbonates, Fig. 3). This indicates different maximum depositional ages and considering the error, the lower part and also the youngest zircon ages are in accordance with the middle Kuetsjärvi Volcanic Fm. The LA-ICPMS analysis on the Kolasjoki Sed. Fm. were repeated by ID-TIMS analysis. Age results of 2.054 ± 0.002 and 1.916 ± 0.001 Ga for the lower and upper part, respectively, verified the different age peaks (Fig. 3). As Hanski (1992) presented U-Pb zircon data of 1.97 ± 0.005 Ga for a felsic tuff from the overlying Pilgujärvi Volcanic Fm. (Fig. 2), this difference within the Kolasjoki Sed. Fm. seems to reflect a disturbance in the hitherto established stratigraphy. Hence, additional field samples from above and below a potential unconformity, between the first two dated samples, were analysed. The results showed age peaks of 2.032 and 2.055 Ga (Fig. 3), which are interpreted as maximum depositional ages and are similar to those of the lower Kolasjoki Sed. Fm. This indicates that this unconformity does not display the change in the detrital zircon age spectra. Further samples will unravel the zircon age distribution in the Kolasjoki Sedimentary Fm. in more detail.

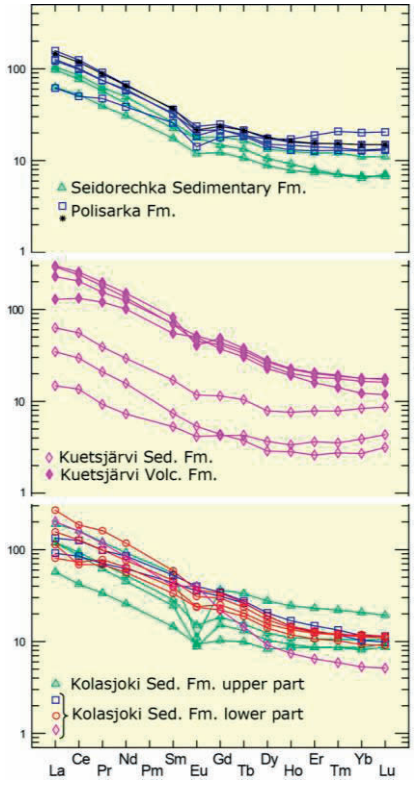

Fig. 4: Rare earth element distributions from samples from all dated formations. Normalized to chondrite (Taylor & McLennan, 1985).

To define the provenance areas for the detrital zircons and siliciclastic sedimentary rocks, in addition Hf isotope and whole rock geochemical analysis were applied. Detrital zircon age results form several similar age groups in the different formations, indicating similar provenances. Furthermore, geochemical and isotopic data point to several phases of crustal growth during the developing Fennoscandian Shield and support a more detailed determination of the source areas:

>3.1-2.9 Ga and 2.9-2.6 Ga: Most of the samples and 73 % of all dated zircons yielded ages in this time interval. They indicate a provenance of the siliciclastic sedimentary rocks in the surrounding Archean provinces, e.g. Kola and Karelian Province and Murmansk Craton (Fig. 1). Mostly positive εHf isotope values point to a source of juvenile Archean crust from the cratonic interior and Archean basement, which was partly reworked during the generation of the Fennoscandian Shield, e.g. during the Saamian (3.1-2.9 Ga) or Lopian (2.9-2.6 Ga, Gaal & Gorbatschev, 1987) orogenies and by accretion of Neoarchean cratons around 2.7 Ga forming the supercontinent Kenorland.

2.6-2.4 Ga: This time interval represents the onset of rifting of Archean crust, initiated by increased instrusive actvity, which later led to the break-up of Kenorland (Daly et al., 2006). The time span from 2.4-2.2 Ga was characterized by ongoing rift processes and non-orogenic quiescence, which caused a marked decrease in the abundance of detrital zircons at that time (<2% of dated zircons). Hf isotope data for zircons having ages around 2.4 Ga indicate reworked Archean material from craton regions and Archean basement.

2.1-1.85 Ga: This time span is divided into two age groups at c. 2.1-2.0 Ga (Kuetsjärvi Volcanic Fm., lower Kolasjoki Sed. Fm.) and c. 2.0-1.9 Ga (upper Kolasjoki Sed. Fm.). These geochronological data already indicate different or additional provenances, which is corroborated by Hf isotope data that obtained different results than the Archean zircons and the two age groups within as well. Hence, detrital zircons from the lower part with negative εHf isotope values might be derived from reworked Archean crust and/or additionally reworked crust that has been contaminated by younger juvenile crust. Zircon grains from the upper part of the Kolasjoki Sed. Fm. differ from the rest as they show positive εHf isotope values. This also indicates a different source for these zircons. Furthermore, the REE contents of the upper Kolasjoki Sed. Fm. show pronounced negative Eu-anomalies, which are not present in older samples and sets this samples aside again (Fig. 4). Potential source areas for the samples are the Lapland-Kola orogen and/or micorcontinents accreted during the Svecofennian orogeny, including the Umba Granulite Belt, Strelna Domain, Inari and Tersk Terrane, and juvenile arcs, e.g. Kittilä and Savo arc (Lahtinen et al., 2009; Fig. 1).

Geochemical results for most samples yielded REE distributions showing characteristics of typical Archean sandstones and greywackes with increased LREE and lower HREE contents and weakly developed or absent negative EU anomalies (except upper Kolasjoki Sed. Fm., Fig. 4). This supports an Archean source for the siliciclastic sediments. Decreased REE contents of the Kuetsjärvi Sed. Fm. point to even more evolved material as a source. Additionally, crucial trace element ratios including Th/Sc point to input from Archean as well as Paleoproterozoic sources (after Taylor & McLennan, 1985). This is also reflected in the varying detrital zircon age spectra, including both Paleoproterozoic and Archean grains.

References:

Amelin, Y.V., Heaman, L.M., Semenov, V.S. (1995): U-Pb geochronology of layered mafic intrusions in the eastern Baltic Shield: implications for the timing and duration of Paleoproterozoic continental rifting. Precambrian Reseach, 75, p. 31-46.

Daly , J.S., Balagansky, V.V., Timmerman, M.J., Whitehouse, M.J., de Jong, K., Guise, P., Bogdanova, S., Gorbatschev, R., Bridgwater, D. (2001): Ion microprobe U-Pb zircon geochronology and isotopic evidence for a trans-crustal suture in the Lapland-Kola Orogen,

northern Fennoscandian Shield. Precambrian Research, 105, p. 289-314.
Daly, J.S. Balagansky, V.V., Timmerman, M.J., Whitehouse, M.J. (2006): The Lapland-Kola orogen: Palaeoproterozoic collision and accretion of the northern Fennoscandian lithosphere. In: Gee, D.G. & Stephenson, R.A. (eds): European Lithosphere Dynamics. Geological Society, London, Memoirs, 32, 561–578.
Gaal G. & Gorbatschev, R. (1987): An outline of the Precambrian evolution of the Baltic Shield. Precambrian Research, v. 35, p. 15-42.
Hannah, J.L., Bekker, A., Stein, H.J., Markey, R.J., Holland, H.D. (2004): Primitive Os and 2316 Ma age for marine shale: implications for Paleoproterozoic glacial events and the rise of atmospheric oxygen. Earth and Planetary Science Letters, v. 225, p. 43-52.
Hanski, E.J. (1992): Petrology of the Pechenga ferropicrites and cogenetic, Ni-bearing gabbro-wehrlite intrusions, Kola Peninsula. Geological Survey of Finland Bulletin, v. 367, 192 p.
Karhu, J.A. & Holland, H.D. (1996): Carbon isotopes and rise of atmospheric oxygen. Geology, v. 24, p. 867-870.
Lahtinen, R., Korja, A., Nironen, M., Heikkinen, P. (2009): Palaeoproterozoic accretionary processes in Fennoscandia, The Geolocigal Society, London, Special Publications, v. 318, p. 237-256.
Melezhik , V.A., Huhma, H., Condon, D.J., Fallick, A.E., Whitehouse, M.J. (2007): Temporal constraints on the Paleoproterozoic Lomagundi-Jatuli carbon isotopic event. Geology, v. 35, no. 7, p. 655-658.
Melezhik, V.A., Kump, L., Strauss, H., Fallick, A.E., Hanski, E., Hawkesworth, C.J., Lepland, A., Prave, A., Philippov, N. (2005a): Fennoscandian Arctic Russia - Drilling Early Earth Project (FAR – DEEP). Full proposal to the International Continental Scientific Drilling Program.
Shields, G. & Veizer, J. (2002): Precambrian marine carbonate isotope database: Version 1.1. Geochemistry, Geophysics, Geosystems, v. 3, p. 1-12.
Taylor, S.R. & McLennan, S.M. (1985): The Continental Crust: Its Composition and Evolution. 312 pp.
Young G.M., Long, D.G.F., Fedo, C.M., Nesbitt, H.W. (2001): Paleoproterozoic Huronian basin: product of a Wilson cycle punctuated by glaciations and a meteorite impact. Sedimentary Geology, 141-142, p. 233-254.

ICDP

Lake Issyk-Kul, Kyrgyzstan: Seismic investigation of the lacustrine sediments

A. C. GEBHARDT[1], M. DE BATIST[2], L. NAUDTS[3], L. DE MOL[4]

[1]Alfred Wegener Institute of Polar and Marine Research, 27568 Bremerhaven, Germany
[2]Renard Centre of Marine Geology, University of Gent, 9000 Gent, Belgium

Lake Issyk-Kul is located in an intramontane basin of the Tien Shan mountains in Kyrgyzstan, Central Asia. It has formed in a tectonically active region with W-E striking major thrust zones north and south of the lake. The lake's modern surface level is at 1607 m above sea level, maximum depth in the central basin of the lake is roughly 670 m, and the total water volume is around 1736 km3. The lake is elongated with 180 km in west-east and 60 km in south-north direction. With a surface area of 6232 km2, Lake Issyk-Kul is the second largest lake in the higher altitudes (De Batist et al., 2002). The lake is characterized by two large delta areas at its western and eastern end, with the deltaic area being as wide as up to 60 km in the eastern and 40 km in the western part, and by steep slopes at the northern and southern shore. The lake contains the sediments of the past up to several million years, and has been proposed as a future target for deep drilling within ICDP.

Three seismic surveys by Russian and Belgian groups in 1982, 1997 and 2001 revealed a thick sediment infill in Lake Issyk-Kul. At both the western and the eastern end of the lake, large delta systems were formed by actual and previous inlets, namely the Tyup and Djyrgalan rivers in the eastern part of the lake (still active) and the Chu River at the western end of the lake (currently bypassing the lake). Large sub-aquatic channel systems are visible in the lake's bathymetry in the shallower part of the delta systems close to the river mouths. They were quite likely formed by these rivers during a former lake level lowstand. The delta system consists of stacked prograding delta lobes with a characteristic topset-foreset-bottomset configuration. These lobes together with sub-aerial terraces found at several spots around the lake witness lake level fluctuations of up to >400 m (Naudts, 2002; De Mol, 2006). Many of the delta lobe sequences show internal sediment geometries that point at small lake level oscillations of higher frequency that are superimposed on the long-term lake level fluctuations. Using sequence stratigraphy techniques, the stacked delta lobes together with their internal sedimentary structures will allow the detailed reconstruction of lake-level changes.

The sediments in the central plain of Lake Issyk-Kul are mainly well-layered with many turbiditic sequences intercalated with pelagic background sedimentation. Sediments are slightly inclined towards south with increasing angles with depth. This clearly shows that the lake basin is a halfgraben structure. A fault is found in the southern part of the lake sediments and can be followed for several kilometers.

Mass transport deposits such as debris flows are a common feature close to the steeper flanks around the central plain. They are often associated with smaller channels incised into the slopes that funnel sediment transport downslope.

The southern flank is rather steep and characterized by many small terraces that might have formed during earlier lake-level lowstands and by several canyons that are related to small inlets at the southern shore. The northern flank, however, shows a small, shallow shelf area of 25 to 30 m water depth. This area is characterized by glacial outwash sediments that were brought to the lake by small rivers that drain the large end moraines that are located north of the lake on the foot of the Kunghei Range.

References:

De Batist, M., et al., 2002. Bathymetry and sedimentary environments of Lake Issyk-Kul, Kyrgyz Republic (Central Asia): a large, high-altitude, tectonic lake. In: J. Klerkx and B. Imanackunov (Editors), Lake Issyk-Kul: Its Natural Environment. NATO Science Series, Series IV: Earth and Environmental Sciences. Kluwer Academic Publishers, Dordrecht, pp. 101-123.
De Mol, L., 2006. Reconstructie van meerspiegelschommelingen in het Issyk-Kul Meer (Kirgizië) op basis van de geomorfologische en seismostratigrafische analyse van rivierdelta's. M.Sc. Thesis, University of Gent, Gent, 144 pp.
Naudts, L., 2002. Seismisch-stratigrafische interpretatioe van een complex deltasysteem in het Issyk-Kul Meer, Kyrghyzstan. M.Sc. Thesis, University of Gent, Gent, 133 pp.

IODP

Evidence for influence of the Galápagos hotspot on the East Pacific Rise MORB composition during times of superfast spreading

J. GELDMACHER[1], T. HÖFIG[1,2], F. HAUFF[1], K. HOERNLE[1], D. GARBE –SCHÖNBERG[3],D.S. WILSON[4]

[1]GEOMAR, Helmholtz-Zentrum für Ozeanforschung Kiel, Wischhofstr. 1-3, 24148 Kiel, Germany
[2]Department of Mineralogy, TU Bergakademie Freiberg, Brennhausgasse 14, D-09596 Freiberg, Germany
[3]Institut für Geowissenschaften, Christian-Albrechts Universität Kiel, Ludewig-Meyn-Str. 10, 24118 Kiel, Germany
[4]Dept. Earth Science, UCSB, Santa Barbara, CA 93106-9630, USA

The Cocos-Nazca Spreading Center (CNS) in the Eastern Equatorial Pacific is one of the best-investigated examples for interaction with an off-axis mantle plume, the Galápagos hotspot. The Gálapagos hotspot lies ~200 km south of the CNS, which was initiated by the break-up of the Farallon Plate about 23 m.y. ago (e.g., Meschede and Barckhausen, 2001) and joins the East Pacific Rise spreading center about 1100 km west of the hotspot.

Today, the influence of the Galápagos hotspot on mid-ocean ridge basalt composition can only be seen along the CNS but Galápagos plume material may have reached the East Pacific Rise (EPR) in the past. The question if Galápagos plume material has reached the EPR is of particular importance for the interpretation of data from oceanic crust at ODP/IODP Site 1256, which was formed ~15.2 m.y. ago at the EPR during a period of superfast spreading (Wilson, 1996). Hole 1256D, which was initiated during ODP Leg 206 and meanwhile re-occupied and deepened by three successive IODP expeditions, is considered to be a reference site for oceanic crust formed at fast spreading ridges. A possible Galápagos influence could put the geochemical representativeness of Site 1256 basalts into question. To address this question, basaltic crust samples from several DSDP, ODP, and IODP drill sites that formed along the East Pacific Rise between 3ºS and 7ºN and between 9 and ≥23 Ma were studied to determine the effect of the Galápagos hotspot on their geochemistry.

Mid-ocean ridge basalt (MORB) lavas from sites formed between 11 and ≤23 Ma show moderately enriched, Galápagos plume-like Pb (double-spike) and Nd isotope ratios compared to lavas created shortly before or after this interval. Despite their more enriched isotopic composition, their incompatible element data indicate source depletion. The abundances of highly incompatible to less incompatible elements, e.g., La/Yb, Tb/Lu, Ce/Yb, Zr/Y, Ce/Sm of N-MORB formed between 11 and 18 Ma is lower than MORB formed after 11 Ma and today's EPR N-MORB and is shifted in the opposite direction from the Galápagos field. In contrast, the <11 Ma lavas fall within the compositional range of today's N-MORB.

The combined incompatible trace element depletion and isotopic enrichment of the 11 to ≤23 Ma lavas can be explained by derivation from a Galápagos plume source that experienced melt extraction while ascending under previous Galápagos Islands before entering the EPR or during its transport along the ridge system. The (more fertile) trace-element and isotopically enriched components of a heterogeneous plume (as Galápagos is characterized, e.g.,White et al., 1993; Hoernle et al., 2000) will get progressively exhausted through ongoing melt extraction leaving the more refractory and isotopically less enriched plume matrix behind.

The arrival of this material at the East Pacific Rise took place immediately after formation of the Cocos-Nazca Spreading Center, which provided a direct channel for hot plume material to flow into the main ridge network. The interval of Galápagos plume influence correlates with the beginning and end of superfast spreading at the equatorial East Pacific Rise, indicating a causal relationship such as increased "ridge suction" due to the greatly enhanced spreading rate.

References:

Hoernle K., Werner R., Morgan J.P., Garbe-Schönberg D., Bryce J., Mrazek J. (2000) Existence of complex spatial zonation in the Galápagos plume for at least 14 m.y. Geology 28, 435-438

Meschede M. and Barkhausen U. (2001) The relationship of the Cocos and Carnegie ridges: age constraints from paleogeographic reconstructions. Int. J. Earth Sciences 90, 386-392

Wilson D.S.(1996) Fastest known spreading on the Miocene Cocos-Pacific plate boundary. Geophys. Res. Lett. 23, 3003-3006

White W.M., McBirney A.R., Duncan R.A. (1993) Petrology and geochemistry of the Galápagos islands: Portrait of a pathological mantle plume. J. Geophys. Res. 98, 19,533-19,563

ICDP

Seismic site characterization for the Deep-Fault-Drilling-Project Alpine Fault

V. GLOMB[1], S. BUSKE[1], D. PEIKERT[1], O. HELLWIG[1], F. HLOUSEK[1], A. KOVACS[2], A. GORMAN[2] , D. SCHMITT[3]

[1]Institute of Geophysics and Geoinformatics, TU Bergakademie Freiberg, 09596 Freiberg, vera.glomb@geophysik.tu-freiberg.de
[2]Department of Geology, University of Otago (NZ)
[3]Department of Physics, University of Alberta (CA)

The Alpine Fault in New Zealand (South Island) is one of the largest active plate-bounding continental fault zones on earth. Earthquakes with a magnitude of 7.9 occur every 200-400 years, the last ruptured in 1717 thus implying a sginificant geohazard potential. Additionally the Alpine Fault is a globally significant natural laboratory because of its surface exposure and the shallow depth of mechanical and chemical transitions. Within the ICDP Deep-Fault-Drilling-Project Alpine Fault (DFDP-AF; https://wiki.gns.cri.nz/DFDP) a drill hole shall give insight into the geological structure of the fault zone and its evolution to understand the related deformation and earthquake processes.

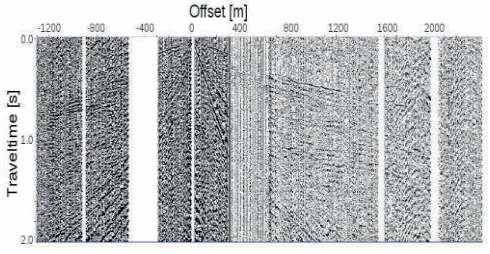

Fig. 1: Example shot gather acquired in 2011along Whataroa River across the potential DFDP drill site location.

With the help of advanced seismic imaging techniques the shallow structure of the Alpine Fault will be imaged to find the most suitable drill site location. A new seismic reflection profile has been acquired in 2011 by the WhataDUSIE project team consisting of partners from the University of Otago (New Zealand), TU Bergakademie Freiberg (Germany) and the University of Alberta (Canada). The reflection profile, located in the Whataroa river valley, has a total length of about 5 km with up to 643 geophones and spacings between 4-8 m, recording approximately 100 shots along the profile line. First data examples of single shot gathers and preliminary processing results will be presented. Further processing will enable a seismic site characterization providing important information for the selection of the borehole location. Additionally the high resolution seismic images will allow a better understanding of the tectonic and geodynamic settings. These information will also be important as a basis for other researchers investigating e.g. the geohazard of the area.

IODP

Drilling in the Amundsen Sea Embayment: Reconstructing West Antarctic Ice Sheet dynamics (IODP 784-Full proposal)

K. GOHL[1], J.B. ANDERSON[2], T. BICKERT[3], C.D. HILLENBRAND[4], M. KONFIRST[5], G. KUHN[1], F.O. NITSCHE[6], F.R. RACK[7], U. SALZMANN[8], R. SCHERER[9], M. SCHULZ[1], G. UENZELMANN-NEBEN[1], E. WEIGELT[1], J.S. WELLNER[10]

[1]Alfred Wegener Institute for Polar and Marine Research, Dept. of Geosciences, Bremerhaven, Germany; contact: karsten.gohl@awi.de
[2]Rice University, Earth Science Dept., Houston, TX, USA
[3]MARUM - Center for Marine Environmental Sciences, University of Bremen, Bremen, Germany
[4]British Antarctic Survey, Cambridge, UK
[5]Byrd Polar Research Center, Ohio State University, Columbus, USA
[6]Lamont-Doherty Earth Observatory, Palisades, NY, USA
[7]University of Nebraska, Dept. Earth & Atmospheric Sciences, Lincoln, NE, USA
[8]University of Northumbria, [8]Department Geography & Environment, Newcastle Upon Tyne, UK
[9]Northern Illinois University, Dept. of Geology and Environmental Geosciences, USA
[10]University of Houston, Dept. Earth & Atmospheric Sciences, Houston, TX 77204-5007, USA

The West Antarctic Ice Sheet (WAIS), which is grounded below present sea level and, thus, is highly sensitive to climatic changes, is likely to have had a very dynamic history over the last several million years. Its collapse would result in a global sea-level rise of 3-5 m over present levels yet the world's scientific community is not able to predict how it might behave in the future, nor is much known of how it has behaved in the past. The reconstruction and quantification of partial or complete WAIS collapses in the geological past are needed in order to provide necessary constraints for ice sheet models predicting future WAIS behaviour and its potential contributions to global sea-level rise. Large uncertainties exist regarding the chronology, extent, rates, and spatial and temporal variability of past advances and retreats of the WAIS across the continental shelves. These uncertainties are mainly due to the fundamental lack of data from drill core. A series of drill sites are proposed for the Amundsen Sea Embayment shelf where seismic data reveal oceanward dipping sedimentary sequences that span the time from the pre-glacial depositional phase to the youngest glacial periods. Our drilling strategy is to target a transect from the oldest sequences close to the bedrock-basin boundary in the south to the youngest sequences in the north of the western and eastern Amundsen Sea Embayment continental shelf. This transect will yield a detailed history of the glacial cycles in the Pine Island-Amundsen Sea region and allow correlations to the WAIS history known from the Ross Sea. In addition, deep-water sites on the continental rise of the embayment are selected for recovering continuous records of glacially transported sediments and the details of climatic and oceanographic changes throughout glacial-interglacial cycles.

IODP

Lessons to be learned from the Costa Rica seismogenesis (CRISP) drilling project and the 2002 Osa earthquake sequence

I.GREVEMEYER[1], ROBERT HARRIS[2], IVONNE ARROYO[1], ERNST R. FLUEH[1], J. BEHRMANN[1]

[1]GEOMAR | Helmholtz Zentrum für Ozeanforschung Kiel, Wischhofstraße 1-3. 24148 Kiel, Germany (igrevemeyer@geomar.de)
[2]College of Oceanic and Atmospheric Sciences, Oregon State University, Corvallis, Oregon, USA

On March 11, 2011 the most powerful known Japanese earthquake hit NE Japan off the Tohoku province. In contrast to the concept put forward by scientists, the earthquake's major slip occurred near the trench axis, an area generally believed to be characterized by stable sliding rather than seismic coupling. This concept holds at least for accretionary subduction zones. However, after the Tohoku earthquake this concept might be challenged for erosive margins. Offshore of Central America IODP may help to answer some of the questions, as the Costa Rica Seismogenesis Project (CRISP) is designed to explore the processes involved in the nucleation of large interplate earthquakes at erosional subduction zones. CRISP is a three stage drilling project. CRISP-A was drilled in 2011 and CRISP-B will be drilled in late 2012. However, will CRISP-C ever be able to reach the seismogenic zone? The June 16, 2002 magnitude Mw=6.4 earthquake and its aftershocks may have the answer.

Unfortunately, global event locations present uncertainties too large to prove that the event actually occurred at a location and depth reachable by riser drilling. We have compiled a database including foreshocks, the main shock, and ~400 aftershocks, with phase arrival times from all the seismological networks that recorded the 2002 Osa sequence locally. This includes a temporal network of ocean-bottom seismometers (OBS) that happened to be installed close to the area at the time of the earthquake. The coverage provided by the marine network allowed us to better constrain the event relocations, and to further analyze the seismicity in the vicinity of Osa for the six months during which they were deployed. Moreover, we used teleseismic waveform inversion to provide additional constraints for the centroid depth of the 2002 Osa earthquake, allowing further study of the focal mechanism.

Along the Costa Rican seismogenic zone, the 2002 Osa sequence is the most recent. It nucleated in the SE region of the forearc where this erosional margin is underthrust by a seamount covered ocean plate. A Mw=6.9 earthquake sequence occurred in 1999, co-located with a subducted ridge and associated seamounts. The Osa mainshock and first hours of aftershocks began in the CRISP area, ~30 km seaward of the 1999 sequence. In the following two weeks, subsequent aftershocks migrated into the 1999 aftershock area and also clustered in an area updip from it. The Osa updip seismicity, however, apparently occurred where interplate temperatures are ~100°C or less. These temperature estimates are based on surface heat flow and thermal modelling. CRISP-A drilling confirmed the low temperatures – again challenging older concepts of seismogenesis at erosive margins.

The state-of-the-art presented here is based on a refined 1-D velocity model for Costa Rica and its offshore domain. In the future, we like to derive a 3-D velocity model of Costa Rica and its Pacific margin from a unique dataset of several temporary deployments of OBS and land stations that will allow us to provide much lower error bounds for the location of the Osa seismic sequence. Along with results from CRISP-A and B, the proposed study will help us to understand the properties controlling earthquake nucleation and rupture propagation at erosive margins.

ICDP

Methanogenic communities and their response to Holocene and Middle to Late Pleistocene climate changes in arctic environments

J. GRIESS[1,2], K. MANGELSDORF[2], D. WAGNER1 AND THE EL'GYGYTGYN SCIENTIFIC PARTY

[1] Alfred Wegener Institute for Polar and Marine Research, Research Unit Potsdam, Telegrafenberg A45, 14473 Potsdam, Germany
[2] Helmholtz Centre Potsdam, GFZ German Research Centre for Geosciences, Telegrafenberg B423, 14473 Potsdam, Germany

Arctic regions are sensitive key regions to monitor processes related to climate change (McGuire et al., 2009). Northern high latitude regions are especially pronounced by observed warming effect and future models predict further warming trends in soil and atmospheric temperature especially for this area (IPCC, 2007). Furthermore, according to latest estimations 50 % of the belowground carbon (1672 Pg (10^{15} g) are stored in northern permafrost regions (Tarnocai et al., 2009). Additionally, lakes represent deposits of produced or stored organic matter and the anaerobic conditions in the anoxic sediments provide suitable conditions for the metabolic activity of a variety of microorganisms. Organic matter in lake sediments or permafrost deposits can be degraded to acetate, hydrogen (H_2) and carbon dioxide (CO_2) by a consortium of heterotrophic microorganisms and subsequently metabolized to methane by methanogenic archaea.

A temperature increase in these regions can result in the emissions of considerable amounts of greenhouse gasses such as carbon dioxide and methane, having a positive feedback effect on earths' atmospheric temperature ('polar amplification'). Methane emissions are of particular interest as their effect on climate is reported to account 18 % of the green house effect (IPCC, 2007). By an increase in the ground temperature, the bioavailability of soil organic matter and microbial activity including methanogenic processes will be triggered.

To predict the risk for future climate and estimate the global atmospheric carbon budget, it is important to understand the microbial driven methane dynamics of the Siberian Arctic and their response to climate changes in the past. Therefore, a combination of quantitative and qualitative analyses of recent and fossil methanogenic communities was performed to characterize methanogenic communities in various arctic settings and reveal their variations in scope of glacial-interglacial climate changes. In the following, a comprehensive study was conducted, comprising archives of past microbial activity and recently active microorganisms in terrestrial permafrost deposits recovered from central Lena Delta and lake sediments in Chukotka, NE-Russia.

Terrestrial permafrost deposits were recovered within a Russian-German expedition in central Lena Delta. The Lena River Delta is the largest delta within the circum arctic land masses with an area of about 29 x 10^3 km. The entire Lena Delta is located in the zone of continuous permafrost, where the permafrost reaches thicknesses of about 500-600 m. During summer 2002 a permafrost core

Figure 1: Location of the study sites in the Russian Arctic (map modified after H. Lantuit, AWI)

of 23 m length was drilled in the depression of a low-centered ice-wedge polygon within the scope of the Russian-German expedition LENA 2002 on Kurungnakh Island (N 72°20, E 126°17).

Additionally, this study comprises terrestrial permafrost deposits and lake sediments recovered 2008/2009 in scope of the ICDP-project 'Scientific drilling in Lake El'gygytgyn' (Melles et al., 2011). The following abstract will present results of both study site, however the terrestrial permafrost deposits of lake El'gygytgyn will not be considered.

Methanogenic communities in terrestrial permafrost on Kurungnakh Island, Lena Delta

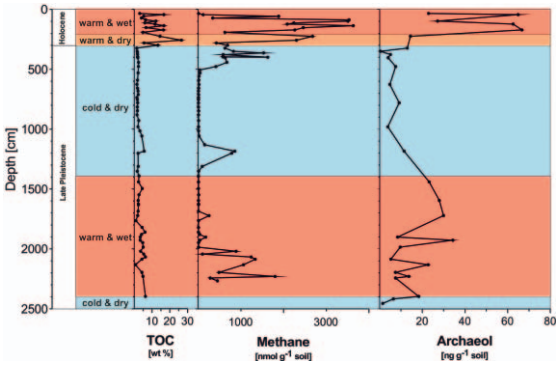

Figure 2: Organic carbon, methane and archaeol along the Kurungnakh permafrost sequence

The Kurungnakh permafrost core was sectioned into 5 units (Figure 2) according to the respective paleoclimate reconstruction done by Wetterich et al. (2008) for this site. The permafrost deposits are characterized by changing abundances of organic carbon and methane along the core. However, a spatial correlation of these two parameters along the core could be shown. Total organic carbon content varied between 1.5 and 26.5 wt%. The sequence is characterized by relatively high amounts of TOC at the bottom with up to 6 wt%. The TOC decreases slightly to relatively constant values of about 2% in between 1700-300 cm, showing a slight peak at 1200 cm

In this context the question occurs, whether the methane found in terrestrial permafrost deposits (i) is produced in situ by currently or recently active methanogenic archaea in permanently frozen ground or (ii) was produced and trapped during times of sedimentation in the respective deposits during the Late Pleistocene and Holocene? Therefore, this study focussed on the analysis of fossil lipid biomarker as well as biomarker for viable or recently living microbial communities.

To reconstruct fossil methanogenic communities, archaeol was used as a biomarker that is characteristic for methanogenic archaea and stable in geological times. Generally, the concentration of archaeol in the Kurungnakh permafrost sequence seem to be linked to warm and particularly wet climate conditions during the Late Pleistocene and Holocene in the Siberian Arctic (Figure 2). This suggests an increased abundance of methanogenic archaea in terrestrial permafrost during these intervals and a climate driven response of the involved methanogenic archaea. However, colder climate conditions conversely caused decreasing in the abundance of methanogenic archaea as can be seen in the declining amount of archaeol as well as a change in the community composition as was shown with genetic fingerprints retrieved from methanogenic archaea.

However, our studies also revealed living and potentially active methanogenic archaea in surface near and surprisingly, deeper layers of frozen ground. Phospholipids are considered as suitable life markers for microbial communities as the degradation of these membrane compounds would rapidly take place after cell death of the source microorganisms. A variety of phospholipid ester (PLFA) and ether (PLEL), being life markers for bacteria and archaea, respectively, could be detected along the permafrost sequence (Figure 3). Holocene deposits were especially pronounced, but archaeal life markers were also pronounced at an interval around 17 m depth. Additionally, a varied fingerprint pattern of methanogenic archaea could be shown for this intervall. The abundance of living and potentially active cells was furthermore confirmed by incubation experiments indicating a significant methane production in samples of this depth.

These findings suggest that the observed methane profile can be the result of both past and modern methane production in perennially frozen sediments. It is furthermore shown, that permafrost deposits are a suitable archive to reconstruct past microbial communities and their response to climate changes in Late Pleistocene and Holocene. Past warming phases have led to enhanced occurrence of methanogenic archaea and considerable

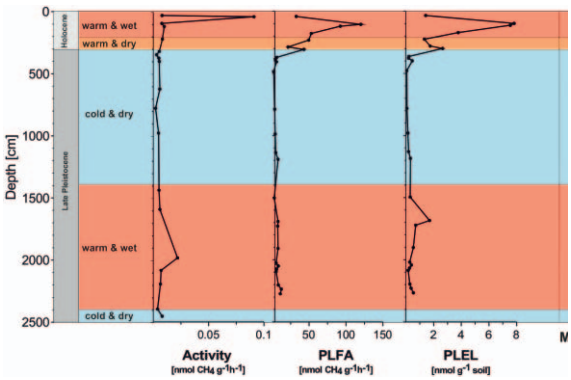

Figure 3: Indications for living microbial communities in the Kurungnakh permafrost sequence

amounts of methane emitted and stored during past warming events as was reconstructed from previous warming events.

Microbial communities in Middle to Late Pleistocene deposits of Lake El'gygytgyn

Anaerobic turnover of organic matter in lake sediments is of particular interest as deeper sediments of limnic systems are yet unexplored, in particular in arctic environments. However, studies on the quantification and spatial distribution of bacteria and archaea in deeper and thus, older lake sediments are currently missing. The El'gygytgyn Crater Lake represents a unique archive due to its age, size and high-latitude setting and is one of the best conserved impact structures (Layer, 2000; Melles et al., 2011). Thus, lake sediments, recovered in scope of the 'Lake El'gygytgyn Scientific Drilling Project' (Melles et al., 2011) as part of the 'International Continental Scientific Drilling Programm (ICDP)', provide the exceptional opportunity to study microbial communities in Middle – to Late Pleistocene sediments with a special focus on methanogenic archaea. In scope of this study, the vertical distribution of archaeal and bacterial communities could be described initially for Arctic lake sediments deposited in Middle- to Late Pleistocene.

Our data show a spatial correlation of lipid biomarker, gene copy numbers of bacteria and archaea and the abundance of organic carbon (Figure 4). Layers with high amounts of TOC are also characterized by high numbers of bacteria or archaea as can be seen in the respective lipid marker and quantification of the respective genes. This

indicates substantial numbers of microorganism in Middle – to Late Pleistocene sediments of the El'gygytgyn Lake. This supports the importance of belowground biosphere habitats in terms of biomass and cycling of organic matter.

Furthermore, by characterizing the involved methanogenic communities, this study advances our understanding for methane cycling processes and anaerobic cycling of carbon for arctic lakes. Archaeol was used as characteristic marker to show changes in the abundance of methanogens with depth (Figure 5). The abundance of methanogenic archaea differs with depth. A correlation to large scale paleoclimate conditions is suggested, as amounts of archaeol are most pronounced during glacial intervals MIS 8 and 10. This indicates a higher abundance of methanogenic archaea during colder climate conditions and suggests the existence of psychrophilic methanogens in the lake sediments. In contrast, the amounts of archaeol and therefore, the abundance of methanogenic archaea during times of deposition decreases during warmer climate conditions of MIS 9 (interglacial). This interval is characterized by high amounts of organic carbon. However, we suggest it was less suited for methanogenic

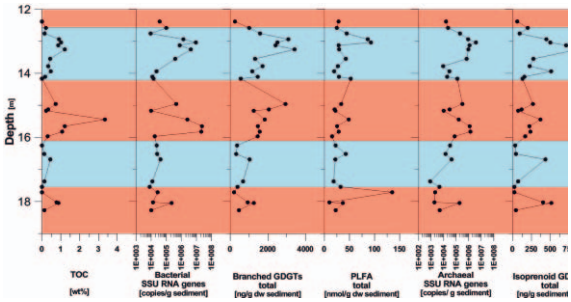

Figure 4: Spatial correlation of the abundance of organic carbon and bacterial and archaeal lipid marker and gene copy numbers of the respective micro-organisms.

metabolism at the time of deposition.

Genetic analysis driven on the community composition of methanogenic showed a correlation with the abundance of organic matter. Intervals of increased organic carbon content provide sufficient substrate for heterotrophic bacteria, as can be seen in the increased gene copy numbers and lipid biomarker amounts for bacteria in the respective samples (Figure 4). The degradation of complex organic matter subsequently provides suitable substrate for a divers methanogenic community (Figure 5). It is suggested, that the less divers methanogenic communities in the remaining depths are due to limitation of organic substrates. Thus, a rather limited, but specialised methanogenic community with few, but dominant members might have developed.

Generally, we could show that the amount of organic carbon is the main driver of differences in abundance as well as the diversity of microbial communities with depth. However, we suggest an influence of glacial-interglacial climate changes on temperature sensitive parts of the methanogenic community as was shown for members related to Methanocellales and Methanomicrobiales, whereas members of Methanosarcinales seem to remain rather unaffected and were abundant throughout the core.

Incubation experiments show that methane production rates throughout the examined sequence were higher in younger deposits and decreased with depth. However, significant methane production could also be measured in samples of 400 ka. Furthermore, eco-molecular analyses showed that methanogenic DNA must have originated from intact cells. This indicating the potential of methanogenic archaea to obtain a metabolic activity in the sediments despite deposited a thousand years ago.

The results of the presented study are of enormous importance to advance our understanding of microbial

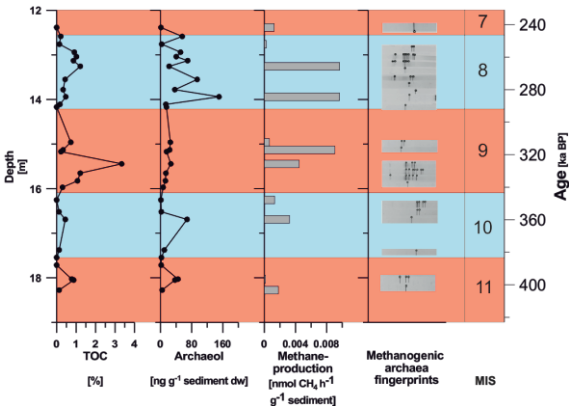

Figure 5: Spatial distribution, potential methane pro-duction rate and genetic diversity of methanogenic archaea along the examined lake sediment sequence.

turnover of organic matter in arctic habitats. These regions are especially characterised by the abundance organic substrates and in particular affected by an increase in atmospheric temperature in scope of the on-going climate change.

References: IPCC -Contribution of Working Group I to the Fourth Assessment Report of the Intergovernmental Panel on Climate Change (2007) Cambridge University Press, Cambridge. Melles et al., Scientific Drilling 11: 29. Mc Guire et al., Ecol Monogr 79: 523. Tarnocai et al.,. GBC, 23: GB2023. Wetterich et al., Quaternary Science Reviews 27: 1523.

IODP

Pliocene Marine Isotope Stage (MIS) M2: Was it caused by a hiccup in the closure of the Panamanian Gateway?

J. GROENEVELD[1], S. DE SCHEPPER[2], B.D.A. NAAFS[3] , M.J. HEAD[4], J. HENNISSEN[5], C. VAN RENTERGHEM[6], S. LOUWYE[6], R. TIEDEMANN[3]

[1]Institute of Geosciences, Bremen University, Germany
[2]University of Bergen, Norway
[3]Alfred Wegener Institute, Bremerhaven, Germany
[4]Brock University, Canada
[5]University of Toronto, Canada
[6]University of Ghent, Belgium

The mid-Pliocene was an episode of prolonged global warmth and strong global thermohaline circulation, interrupted briefly at ca. 3.30 Ma by a global cooling event corresponding to Marine Isotope Stage (MIS) M2. This glaciation has often been referred to as a failed attempt towards the Northern Hemisphere Glaciation (NHG), which is often associated with major changes in the closure of the Panamanian Gateway. Here, we present ongoing work on a series of high-resolution records from six (I)ODP/DSDP sites along a transect which runs from the east Pacific (Site 1241), via the Caribbean (Site 999) and the Gulfstream (Site 603) along the subtropical gyre (Site

U1313) to Sites 610 and U1308 in the North Atlantic Current (NAC). The aim is to reconstruct in high-resolution the sequence of events leading into MIS M2 and the following deglaciation into the mid-Pliocene warm period, often referred to as the PRISM-interval. The two major scientific questions include firstly if a short-lived re-opening of the Panamanian Gateway led to interruption of the Gulfstream allowing the ice build-up on Greenland for MIS M2; and secondly if the deglaciation from MIS M2 into the PRISM-interval, i.e. the last time Earth's climate was significantly warmer than today, can be taken as an analogue for modern day global warming.

The proxies which are being used aim to reconstruct changes in sea surface temperature (SST), relative sea surface salinity (SSS), and overall water mass characteristics. To reconstruct changes in SST we used alkenones and Mg/Ca on Globigerina bulloides for the North Atlantic sites, and Mg/Ca on Globigerinoides sacculifer (surface) and Neogloboquadrina dutertrei (thermocline) for the East Pacific and Caribbean. Changes in relative salinity are determined by combining stable oxygen isotopes of the planktonic foraminifer species with the reconstructed temperatures to result in $\delta 18O_{water}$. Faunal assemblages of dinoflagellates for the North Atlantic and around Panama (in progress) are used to reconstruct changes in water mass characteristics not necessarily related to just temperature and/or salinity. Benthic δ18O records were used to tune the age models from all sites to each other and to fit them with the global benthic δ18O stack LR04.

The results show that the major changes leading into MIS M2 are starting significantly earlier than would initially be expected from the benthic δ18O stack. Just after the height of the preceeding interglacial MG1 a major decline in the presence of dinoflagellate cyst Operculodinium centrocarpum, which is a modern day indicator for the NAC, suggests nearly a shutdown of the overturning circulation, accompanied by decreasing SSTs. Interestingly, SSTs in the Caribbean also start to decrease well before M2. Considering the present day situation on both sides of Panama the much shallower mixed-layer in the East Pacific would give cooler temperatures for the habitat of G. sacculifer than the deeper mixed-layer in the Caribbean. And thus, the SST decrease during MIS MG1 in the Caribbean could be interpreted as an inflow of relatively cold Pacific water due to a re-opening of the Panamanian Gateway, either due to the sea level highstand during MIS MG1 and/or a short-lived tectonic event. The cessation of warm and salty water into the North Atlantic would then have have been the trigger to allow massive ice build-up on Greenland into MIS M2.

The deglaciation of MIS M2 into the PRISM-interval could potentially been considered as the change from present day climate towards a warmer state of climate. As such, reconstructing this change could help us to understand what changes we can expect in the future. On the other hand, the results show the deglaciation is not a typical one in that SSTs in the Caribbean started to warm up already when ice volume reached its maximum. Most likely the increase in ice volume caused the Panamanian Gateway to close again cutting off the cool East Pacific water from entering the Caribbean. This led to a recovery of the Carribean Warm Pool and re-invigorated the Gulfstream and the NAC, indicated by the re-appearance O. centrocarpum, such that MIS M2 did not lead to NHG but bounced back up into the warm PRISM-interval.

IODP

New data on the Stilostomella-event in the North Atlantic from IODP Expedition 339

P. GRUNERT[1], F. J. HERNÁNDEZ-MOLINA[2], D. STOW[3], C. ALVAREZ-ZARIKIAN[4] AND IODP EXPEDITION 339 SCIENTISTS[5]

[1]Institute for Earth Sciences, University of Graz, Austria; patrick.grunert@uni-graz.at
[2]Departmento Geociencias Marinas, Universidad de Vigo, Facultad de Ciencias del Mar, Vigo, Spain
[3]Institute of Petroleum Engineering, Heriot-Watt University, Edinburgh, Scotland, United Kingdom
[4]Integrated Ocean Drilling Program, Texas A&M University, College Station, Texas, USA; zarikian@iodp.tamu.edu
[5]IODP Expedition 339 Scientists: Acton, G., Bahr, A., Balestra, B., Ducassou. E., Flood, R., Flores, J-A., Furota, S., Hodell, D., Jimenez-Espejo, F., Kim, J. K., Krissek, L., Kuroda, J., Li, B., Llave, E., Lofi, J., Lourens, L., Miller, M., Nanayama, F., Nishida, N., Richter, C., Roque, C., Sanchez Goñi, M., Sierro Sanchez, F., Singh, A., Sloss, C., Takashimizu, Y., Tzanova, A., Voelker, A., Williams, T., Xuan, C.

The "Stilostomella-event" refers to the step-wise extinction of deep-sea benthic foraminifera with elongate, cylindrical tests (Stilostomellidae, Pleurostomellidae and some Nodosariidae) during the Mid-Pleistocene Transition (1.2-0.6 Ma; Hayward, 2002; Kawagata et al., 2005). The event has been described from the Atlantic, Indian and Pacific Oceans and is considered one of the major turn-over events in benthic foraminiferal communities during the Cenozoic. The timing and underlying causes of this global event are still a matter of debate. Shipboard data collected from Pleistocene sediments during IODP Expedition 339 further document the extinction event in the North Atlantic and allow the comparison of foraminiferal records from different water depths.

Initial analysis of the foraminiferal assemblages reveal clear differences in the abundance of various stilostomellid, pleurostomellid and nodosariid species between the deeper sites along the Western Iberian Margin (1085-2289m) and the shallower sites in the Gulf of Cadiz (577-991m). Consequently, different patterns of extinction can be observed in the two areas. Stratigraphic constraints from calcareous nannoplankton and magnetostratigraphy as well as calculated sedimentation rates suggest that the extinction datum falls within the time-span of ca. 0.5-0.8 Ma at all sites. This estimate is in good agreement with previous reports from the ODP sites 980 and 982 in the North Atlantic (Kawagata et al., 2005).

More detailed post-cruise work on the foraminiferal assemblages, paleoceanographic proxies and stratigraphy of the sites cored during Expedition 339 will improve our understanding of the timing and the underlying causes of the observed extinction patterns.

References

Hayward, B.W., 2002. Late Pliocene to middle Pleistocene extinctions of deep-sea benthic foraminifera ("Stilostomella extinction") in the southwest Pacific. J. Foram. Res., 32: 274-307.

Kawagata, S., Hayward, B.W., Grenfell, H.R., and Sabaa, A., 2005. Mid-Pleistocene extinction of deep-sea foraminifera in the North Atlantic Gateway (ODP sites 980 and 982). Palaeogeogr., Palaeoclim., Palaeoecol., 221: 267-291.

ICDP

Seismic images of the tremor region at the San-Andreas-Fault system around Cholame (USA)

S. GUTJAHR[1], S. BUSKE[2]

[1]Freie Universität Berlin, Department of Geophysics, Malteserstrasse 74-100, 12249 Berlin, stine@geophysik.fu-berlin.de
[2]TU Bergakademie Freiberg, Institute of Geophysics and Geoinformatics, 09596 Freiberg, buske@geophysik.tu-freiberg.de

We present seismic images of the Coast Ranges and the San-Andreas-Fault system in Central California including the non-volcanic tremor region around Cholame. The seismic images have been obtained by applying advanced seismic imaging techniques (Fresnel volume migration, Buske et al., 2009) to the industry seismic reflection data set WSJ-6. The reflection profile was acquired in 1981 over a distance of about 180 km from Morro Bay to the Sierra Nevada foothills running across several prominent fault systems, e.g. the Rinconada fault in the western part as well as the San Andreas fault in its central part. The latter includes the region of increased non-volcanic tremor activity near Cholame, as reported by several authors.

We are able to image the crust and the uppermost mantle down to approximately 40 km depth by recorrelating the original field data to 26 seconds two-way traveltime. A 3D tomographic velocity model derived from local earthquake data (Thurber et al., 2006, Lin et al., 2010) was used. The imaging technique was implemented in 3D taking into account the true shot and receiver locations of the crooked profile line. The imaged subsurface volume itself was divided into three separate parts to correctly account for the significant kink in the profile line near the San Andreas fault. The most prominent features in the resulting images are areas of high reflectivity down to 30 km depth in particular in the central western part of the profile corresponding to the Salinian Block between the Rinconada fault and the San Andreas fault. Southwest of the San Andreas fault surface trace a broad zone of high reflectivity is located at depths between 20 km to 35 km. Non-volcanic tremor events that were located by Nadeau et al. (2009) appear southwest of the San Andreas fault below the seismogenic zone down to depths of approximately 30 km. Most of the tremor locations correlate well with zones of high reflectivity southwest of the San Andreas fault zone.

In the area of the San Joaquin Valley along the eastern part of the profile line slightly west dipping sediments show up between depths of 2 km to 10 km. These sediments are folded and faulted below the region of the Kettleman Hills. Steeper west dipping reflectors can be identified below the uppermost sedimentary layers down to depths of approximately 20 km.

The resulting images are compared to existing interpretations (Trehu and Wheeler, 1987; Bloch et al., 1993) and discussed in the frame of the suggested non-volcanic tremor locations in that area.

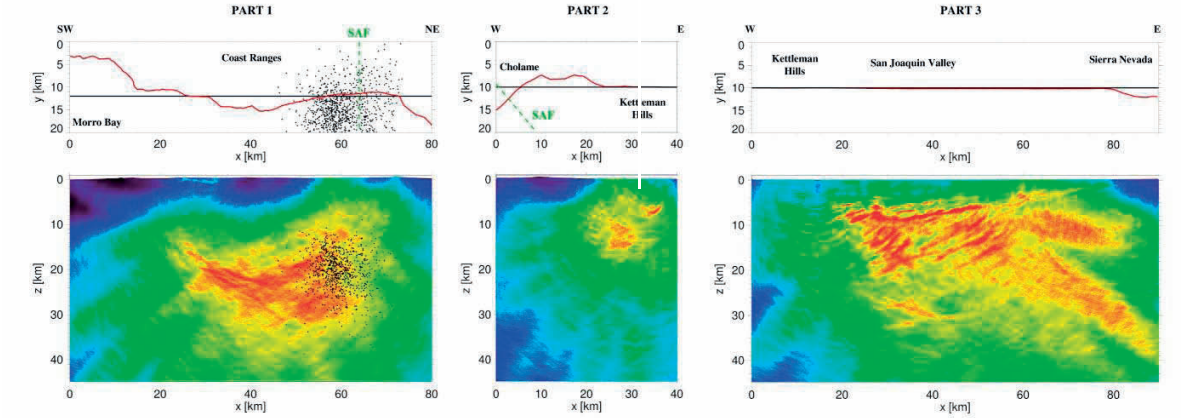

Fig. 1: Top: Map view of each part of the receiver line (red), green dashed line marks location of San Andreas fault surface trace, black line gives y- position of depth -section below ; Bottom: obtained seismic reflection images and tremor locations (black dots in part 1).

References:

Bloch, R. B., von Huene, R., Hart, P. E.,Wentworth, C.M. (1993). Style and magnitude of tectonic shortening normal to the San Andreas fault across Pyramid Hills and Kettleman Hills South Dome, California. Bull. Seism. Soc. Am., 105, p.464–478.

Buske, S., Gutjahr, S., Sick, C. (2009). Fresnel Volume Migration of single-component seismic data. Geophysics, Vol.74, No.6, WCA47-WCA55.

Lin, G., Thurber, C. H., Zhang, H., Hauksson, E., Shearer, P. M., Waldhauser, F., Brocher, T. M., Hardebeck, J. (2010). California Statewide Three-Dimensional Seismic Velocity Model from Both Absolute and Differential Times. Bull. Seism. Soc. Am., 100, pp.225-240.

Nadeau, R. M., Guilhem, A. (2009). Nonvolcanic Tremor Evolution and the San Simeon and Parkfield, California Earthquakes. Science, Vol325.

Thurber, C., Zhang, H., Waldhauser, F., Hardebeck, J., Michael, A., Eberhart-Phillips, D. (2006) Three-Dimensional Compressional Wavespeed Model, Earthquake Relocations, and Focal Mechanisms for the Parkfield, California Region. Bull. Seism. Soc. Am., 96,S38-S49

Trehu, A. M., Wheeler, W. H. (1987) Possible evidence in the seismic data of profile SJ-6 for subducted sediments beneath the Coast Ranges of California, USA. Open-File Report 87-73

ICDP

Geochemical characterization of the 51 ka Laguna Potrok Aike sediment sequence using high-resolution X-ray fluorescence core scanning data (southern Patagonia, Argentina)

A. HAHN[1], P. KLIEM[1], C. OHLENDORF[1], B. ZOLITSCHKA[1] AND THE PASADO SCIENCE TEAM[2]

1 Geopolar, Institute of Geography, University of Bremen, Germany (anhahn@uni-bremen.de)
2 PASADO Science Team as cited at: http://www.icdp-online.org/front_content.php?idcat=1494

During the lake deep drilling campaign PASADO in 2008 (ICDP expedition 5022) more than 500 m of lacustrine sediment was recovered from the maar lake Laguna Potrok Aike (PTA), Argentina. From Site 2 a composite profile (5022-2CP) with a total length of 106 m was assembled. The major element composition was assessed with a spatial resolution of 5 mm using an ITRAX XRF core scanner (COX analytical systems, Croudace et al., 2006). Prior to the interpretation of XRF-scanning data, some methodological aspects have to be taken into consideration.

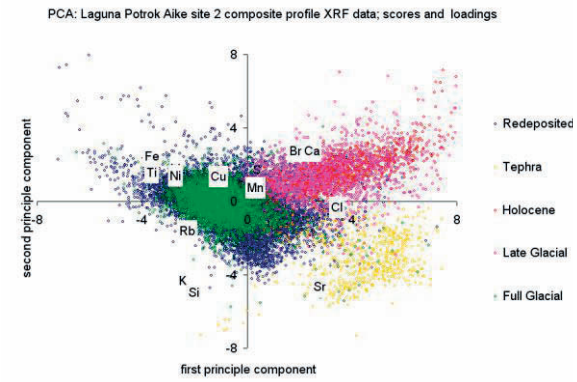

Fig. 1 - The location (scores indicated as colored circles for each measurement point) of redeposited, tephra, Holocene, Late Glacial and Full Glacial sediments in the PCA of PTA 2CP XRF data. Loadings (indicated with the element symbols) show which elements are responsible for the distribution of the data points in the PCA. The PCA gives information about data quality; elements with noisy profiles show scores close to 0.

Principal component analysis (PCA) is a useful tool for analyzing large datasets like element counts from XRF-scanning and this approach helps to reduce noise and/or element-specific biases (Shanahan et al. 2008; Fig. 1). A PCA was applied to normalized counts of all elements if their profiles contain an interpretable geochemical signal. Wet continous measurements were compared to dry powder measurements in order to asses the quality of the data and select the best standardization technique for data processing.

Tephra layers have a very distinct geochemical signature and are therefore excluded from further analysis. The sharp boundary between the carbonate-bearing and the carbonate-free depositional systems at 15,600 cal. BP or 18.82 m composite depth (mcd) dominates the PCA of 5022-2CP marking the transition from the Glacial to the Late Glacial. Holocene and Late Glacial sediments can easily be distinguished by elements that are indicative of organic-rich sediments (Br, Cl) or of calcite (Ca). Ca in the Holocene sediments of PTA can be attributed to calcite precipitation (Haberzettl et al. 2005). Br and Cl have been related to organic sediment components (Br) containing Cl-bearing pore water (Thomson et al. 2006). For PTA a correlation is detected between TOC and Br (R^2 = 0.64). Glacial sediments are characterized by elements that represent terrigenous sediment fluxes (Fe, Zn, Al, Si, K, Ti, Zr, Mn, Cu) (Cohen 2003).

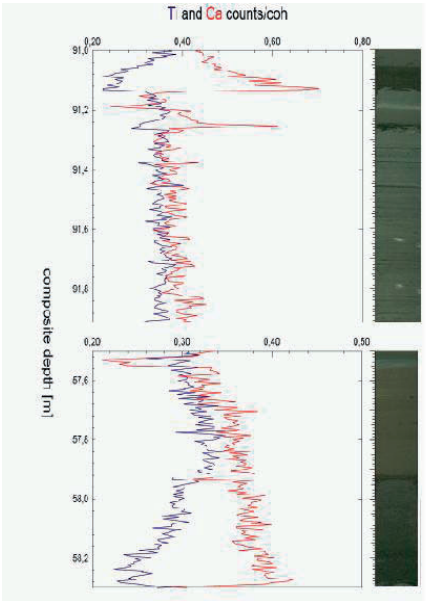

Fig. 2 - Core images and XRF data show the correaltaion between the coarse grainsize fraction and high Ca content.

Geochemical variations of the clastic glacial sediments have been explored by excluding all data points from the PCA that are linked to the sediments above 18.82 mcd. As expected, elements indicative of clastic input (Fe, Zn, Al, Si, K, Ti, Cu) are responsible for positive scores in the first component and indicators of organic matter (Br) and calcite (Ca) have little importance. The accumulation of Mn along with the bulk of elements related to clastic input was probably inhibited by reducing conditions during glacial high lake levels conditions (Haberzettl et al. 2005). Ca and Sr are purely clastic signals in the carbonate-free glacial deposits. However, they do not correlate with the bulk of indicators for terrigenous input, instead they dominate the second principal component (PC2). This component becomes especially important in glacial sediments and is assumed to be a signal of grainsize and basaltic provenance. Visual core inspection shows that peaks in Ca counts correspond to sediments that are coarse grained and dark colored (Fig. 2). Ca and Sr are abundant in plagioclases of volcanic rocks. A possible source for this material is the basalt outcrop located in the direct proximity of the lake that is cut by the primary inflow and eroded directly by wave action during lake level highstands. Occurrence at the base of turbidites as well as in discrete layers suggest multiple transport modes. Once event-deposits are removed from the composite profile, the sediment sequence mainly consists of clays and silts and therefore should lack any grainsize and water content effects and thus be suitable for paleoenvironmental studies. Haberzettl et al. (2007) used TIC content as a primary

proxy for climate reconstructions of the past 16ka. For the carbonate-free older sediments we propose the scores of PC1 as a summarizing indicator for climate-related variations in depositional conditions. High scores in PC1 reflecting clastic sediments are thought to have been been formed under cold unproductive probably windy, low lake level conditions. Low scores in PC1 are assumed to reflect warm conditions with high lake levels (melt water inflow). These conditions could increase the production and conservation of organic material. Therefore low scores in PC1 roughly correspond to high TOC values and C/N ratios. All three proxies point to a link with periods of warming (A events) in Antarctica suggested by the EPICA ice core record (EPICA, 2004; Fig. 3).

References

Cohen A.S., (2003), Paleolimnology – the history and evolution of lake systems. Oxford University Press, Oxford.

Croudace, IW, Rindby, A. & Rothwell, R.G., (2006), ITRAX: description and evaluation of a new multifunction X-ray core scanner. In: Rothwell, R.G. (ed.) New Techniques in Sediment Core Analysis. Geological Society, London, Special Publications, 267, 51–63.

EPICA community members, 2004. Eight glacial cycles from an Antarctic ice core. Nature 429, 623–628.

Haberzettl, T., Fey, M., Lücke, A., Maidana, N., Mayr, C., Ohlendorf, C., Schäbitz, F., Schleser, G. H., Wille, M., and Zolitschka, B. (2005). Climatically induced lake level changes during the last two millennia as reflected in sediments of PTA, southern Patagonia (Santa Cruz, Argentina). Journal of Paleolimnology 33, 283-302.

Haberzettl, T., Corbella, H., M. Fey, S. Janssen, A. Lücke, C. Mayr, C. Ohlendorf, F. Schäbitz, G.-H. Schleser, E. Wessel, M. Wille, S. Wulf, B. Zolitschka (2007). A continuous 16,000 year sediment record from Laguna Potrok Aike, southern Patagonia (Argentina): Sedimentology, chronology, geochemistry. The Holocene, 17: 297-310.

Kliem, P., D. Enters, A. Hahn, C. Ohlendorf, A. Lisé-Pronovost, G. St-Onge, S. Wastegård, B. Zolitschka and the PASADO science team (2012). Lithology, radiocarbon chronology and sedimentological interpretation of the lacustrine record from Laguna Potrok Aike, southern Patagonia. Quaternary Science Reviews, submitted.

Shanahan, T. M., J. T. Overpeck, J. B. Hubeny, J. King, F. S. Hu, K. Hughen, G. Miller, and J. Black (2008), Scanning micro-X-ray fluorescence elemental mapping: A new tool for the study of laminated sediment records, Geochem. Geophys. Geosyst., 9, Q02016, doi:10.1029/2007GC001800.

Thomson, J., Croudace, I.W. & Rothwell, R.G., (2006), A geochemical application of the ITRAX scanner to a sediment core containing eastern Mediterranean sapropel units. In: Rothwell, R.G. (ed.) New Techniques in Sediment Core Analysis. Geological Society, London, Special Publications, 267, 65–77.

IODP

Two million year history of the Indian Monsoon

E.C. HATHORNE[1]

[1]Helmholtz-Zentrum für Ozeanforschung Kiel (GEOMAR), Wischhofstr. 1-3, 24148 Kiel, Germany

Over 3 billion people live in the area influenced by the Asian monsoon, the rains of which provide vital water resources while posing a risk to human life through flooding. Despite the importance to so many the monsoon is difficult to predict and model, making its future development in a changing global climate uncertain. To help improve models and predictions, histories of monsoon variability beyond the instrumental record are required. Many records of the East Asian monsoon have been generated from China and the South China Sea while past variability of the Indian Monsoon is mostly known from records of monsoon wind strength over the Arabian Sea. Here we propose to use the unique long sediment core obtained by the IODP vessel JOIDES Resolution in the Andaman Sea to examine the past variability of Indian Monsoon precipitation on the Indian sub-continent and directly over the ocean. Our multi-proxy approach will reveal changes in continental weathering, runoff and direct precipitation on orbital timescales for the last 2 million years filling a fundamental gap in our understanding of the Indian Monsoon in the past. More detailed studies will examine variations on millennial timescales for the last glacial and deglaciation, and the novel application of single foraminifera shell geochemistry will allow variability on inter-annual and seasonal timescales to be investigated for selected intervals.

IODP

Transgressional-regressional erosion on Canterbury Basin, NZ: Estimation of "missing strata" from one-axial consolidation tests

D. A. HEPP[1], S. KREITER[1], D. OTTO[1]

[1]MARUM – Center for Marine Environmental Sciences and Faculty of Geosciences, University of Bremen

Because of its proximity to the uplifting mountain chain, the Southern Alps, and strong ocean currents coupled to the Antarctic Circumpolar Current the Canterbury Basin, on the eastern margin of the South Island of New Zealand, provides an opportunity to study the complex interaction of these tectonical and erosional processes with glacioeustatic global sea level change which results in a high-frequency sedimentary record of depositional cyclicity from the late Miocene to recent.

Within these sedimentary record nineteen seismostratigraphic sequence boundaries were recognized along a continental margin transect. The interpretation of these erosional unconformities is limited due to the poorly defined time gaps comprising the missing sediment intervals. However, a nearly continuously sedimentary record is crucial for, e.g., age-depth estimation, correlation with lithological sequences among each site, and two dimensional backstripping. In intervals with poor core recovery where "missing strata" were indicated, an underestimation of sedimentation rates and thicknesses of lithological sequences is unavoidable. This again constrains the potential of the interpretation of sedimentary processes in controlling continental margin sedimentary cycles on the basis of a reconstructed initial sedimentary record.

An approach to bridge these gaps in the sedimentary record is the reconstruction of these "missing strata" using the reaction of clayey sediments to changing overburden stresses. The compaction characteristics of clayey sediments are determined by the maximum effective overburden stress, they experienced since their deposition. This allows constraining the former overburden and ultimately the thicknesses of "missing strata" from geotechnical tests, e.g. from one-axial consolidation tests performed in oedometers.

In this study we performed one-axial consolidation tests with 56 whole-round samples from four sites along a shelf-slope transect (Site U1353, U1354, U1351, U1352) which were collected during IODP Expedition 317 (Fulthorpe et al., 2011). The measurements are time consuming. Each sample was loaded by 13 to 19 loading steps at which each loading step takes approximately 24 hours. The pre-consolidation stress was estimated using the graphical procedure after Casagrande (1936). However, this method is limited because (1) it requires that the

transition from the reloading curve to the virgin compression curve is well defined on the semilogarithmic plot of void ratio vs. effective stress, (2) the pre-consolidation stress is potentially underestimated, and the pre-consolidations >800 kPa are potentially untrustworthy (Sauer et al., 1992).

In addition, shipboard measurements of sediment strength (fall cone penetrometer, automated vane shear), whole-round logging data (magnetic susceptibility, natural gamma radiation) and moisture and density analyses were used to constrain the interpretation of the geotechnical tests and lithological and sequence analyses. Since for Site U1354 no shipboard moisture and density or borehole logging data are available we calculated bulk density with wet weight of the sample in a defined volume. A comparison with known shipboard data shows that the calculated results are slightly underestimated but reliable.

The results from the one-axial consolidation tests show that the compaction history can be traced horizontally across a shelf-slope transect and vertically down to a sediment depth of up to 150 m. This sediment interval comprises the uppermost three unconformities. The reconstructed thicknesses of "missing strata" for the first three sequence boundaries vary about 10 to 30 m. The data in the uppermost parts, with overconsolidation ratios between 2.3 and 3, are strongly overconsolidated and may lead to an overestimation of the thicknesses. For deeper sediment intervals the maximum effective overburden stress of the recent sediment is higher than the calculated past effective overburden stress of the "missing strata" so that the calculation of their thicknesses is not reliable. While the recent shelf topography is dipping toward the shelf edge, the reconstructed paleo-shelf topography with paleo-sediment thicknesses reflect nearly horizontal erosion for shelf Sites U1351, U1353 and U1354 which points to transgressional-regressional erosion.

The study shows that the maximum past effective overburden stress can be used to estimate the thicknesses of "missing strata".

References:

Casagrande A. 1936. The determination of the pre-consolidation load and its pratical significance. In Proceedings of the first International Conference on Soil Mechanics and Foundation Engineering: Cambridge; 60-64.

Fulthorpe CS, Hoyanagi K, Blum P, Expedition 317 Scientists. 2011. Canterbury Basin sea level: Expedition 317 of the riserless drilling platform, Townsville, Australia, to Wellington, New Zealand, Sites U1351-U1354, 4 November 2009-3 January 2010. Proceedings of the Integrated Ocean Drilling Program, Expedition Reports 317: 10.2204/iodp.proc.317.2011

Sauer EK, Egeland AK, Christiansen EA. 1993. Preconsolidation of tills and intertill clays by glacial loading in southern Saskatchewan, Canada. Canadian Journal of Earth Sciences 30: 420-433.

IODP

The origin of the Shatsky Rise: Isotope geochemistry (Sr, Nd, Pb, Hf) of volcanic rocks from IODP Site U1347A

K.HEYDOLPH[1], J.GELDMACHER[1], K. HOERNLE[1]

[1]GEOMAR | Helmholtz-Zentrum für Ozeanforschung Kiel, Wischhofstr. 1-3, 24148 Kiel, Germany

Why drill the Shatsky Rise?

The submarine Shatsky Rise plateau is a unique large igneous province (LIP) situated in the northwest Pacific Ocean ca. 1500 km east of Japan. In contrast to other large oceanic LIP's (e.g., Ontong-Java, Manihiki and Hess Rise) which formed during the Cretaceous normal superchrone (122-84 Ma), it is the only large intraoceanic plateau, which formed during the Late Jurassic to Early Cretaceous at a time period with numerous reversals of the Earth's magnetic field. These magnetic reversals, combined with bathymetric data, allow a detailed reconstruction of the original tectonic setting and subsequent evolution and approximate seafloor age from the magnetic record (e.g. Nakanishi et al., 1999). Accordingly, the three main

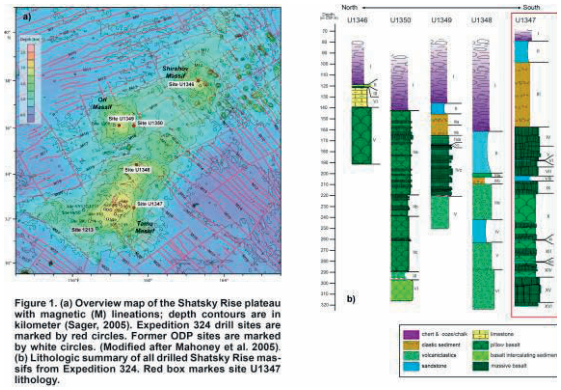

Figure 1. (a) Overview map of the Shatsky Rise plateau with magnetic (M) lineations; depth contours are in kilometer (Sager, 2005). Expedition 324 drill sites are marked by red circles. Former ODP sites are marked by white circles. (Modified after Mahoney et al. 2005). (b) Lithologic summary of all drilled Shatsky Rise massifs from Expedition 324. Red box markes site U1347 lithology.

volcanic edifices Tamu, Ori, and Shirshov massifs formed by massive volcanism during a short time span along a southwest - northeast trending, rapidly spreading triple junction. During the time of deposition the initially voluminous volcanism, which created the Tamu massif, waned to less voluminous phases creating the Ori and then the Shirshov massif. The different phases of volcanism could represent the transition from a plume head to tail.

According to Nakanishi et al. (1999) and Sager et al. (1999) the magnetic and bathymetric data suggest that Shatsky Rise formed through the interaction of a mantle plume head with a ridge. However, drill and dredge samples from former cruises to Shatsky Rise, show trace element and isotopic characteristics similar to Pacific mid-ocean-ridge basalt (MORB) (e.g. Tatsumi et al., 1998; Mahoney et al., 2005). Additionally, there has been a ~30° rotation of the Pacific-Izanagi Ridge at the time of Shatsky Rise formation (Sager et al., 1988). While it has been shown, that plate motion is primarily controlled by subduction (e.g., Lithgow-Bertolloni and Richards, 1998), it is not clear how a mantle plume could affect the velocity of a plate by acting on the trailing boundary of the ridge. Therefore the reorientation of the plate may imply a plate tectonic origin instead of a plume head. Therefore, the Shatsky Rise shows characteristics of both ridge-control

and involvement of a plume-head.Consequently one main objective of this expedition was to test both hypotheses (plume head versus ridge-control) for plateau genesis. Another goal of this project is to better understand the evolution of the Shatsky Rise using Ar-Ar age dating of volcanic rock samples from all suitable lithological units from all drill sites, which is being carried out in close collaboration with fellow scientists from Oregon State University.Drilling results and Site U1347 samples isotopic geochemistry.

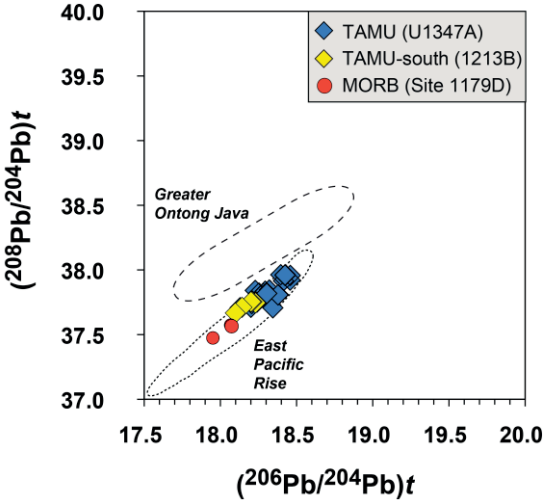

Figure 2: Thorogenic lead isotopic variation diagram for Tamu massif volcanic rocks and contemporary MORB reference site. Data for East Pacific Rise field after Mahoney et al. (2005) and for Greater Ontong Java after Mahoney et al. (2005) and Hoernle et al. (2010).

During the expedition five sites on the three different massifs were drilled and successfully sampled, with one site (U1346) on the summit of Shirshov Massif and two sites on Ori (U1349 and U1350) and on Tamu (U1347 and U1348) respectively (Fig.1a). All sites (except for site U1348) revealed basaltic lava flows, which occur as packages of pillow basalt and massive inflation units, frequently interbedded with volcaniclastic sediments. The largest massive inflation flows have a maximum thickness ~ 23m and the thickest occur on Tamu Massif, comparable to massive flows cored on Ontong Java Plateau during ODP Leg 192. Massive flows are also found at Sites U1349 and U1350, on Ori Massif summit and flank, respectively, though an entire ~50 m succession of igneous rocks from Site U1346 (Shirshov Massif summit) consists of pillow lavas (Fig.1b). Ori Massif flow units are generally thinner than on Tamu Massif, presumably indicating that the average eruptions become smaller and less effusive from Tamu to Ori to Shirshov massifs. Cores from site U1348 contained a thick sequence (~120 m) of highly altered volcaniclastic sediments with shallow-water carbonaceous sandstones on top (Fig.1b). The cored basaltic lava flows range from relatively fresh (Sites U1347 and U1350) to moderately to highly altered (Sites U1346 and U1349). Additional recovered basement rocks from two summit sites (U1346 and U1349) showed the most severe alteration, whereas rocks from Sites U1347 and U1359 are apparently less affected by alteration.

We present new Sr, Nd and Pb (double spike) and the first Hf isotope data from volcanic rocks of relatively fresh basaltic lava flows from recent Site U1347 and ODP Leg 198 Site 1213 both located on Tamu massif the southernmost (oldest) volcanic edifice of Shtasky Rise (Fig.1a). We calculated the initial (144Ma) isotopic values for all samples to show their isotopic composition at the time of deposition.

Initial $^{176}Hf/^{177}Hf$ and $^{143}Nd/^{144}Nd$ isotopic compositions from site U1347 are fairly uniform throughout the entire hole ranging between 0.283076 to 0.283100 ($^{176}Hf/^{177}Hf$) and 0.512903 to 0.512981 ($^{143}Nd/^{144}Nd$) respectively, showing neither distinct MORB nor intraplate (plume) affinity. Site 1213 samples are slightly less radiogenic in Nd and Hf isotopic compositions. Relatively unradiogenic $^{87}Sr/^{86}Sr$ data from site U1347 range from 0.70276 to 0.70296 and mostly overlap with Pacific MORB like values. In a Nd vs Hf isotope plot site U1347 form a tight cluster at the edge of the Pacific MORB field below the present-day Hf-Nd mantle array. Site 1213 samples have less radiogenic Nd and Hf isotopic compositions. Although initial Pb double spike $^{206}Pb/^{204}Pb$ and $^{208}Pb/^{204}Pb$ isotopic compositions for Site U1347 range from 18.13 to 18.46 and 37.71 to 37.96 respectively and overlap with MORB-like compositions, they trend towards more radiogenic, intraplate-like values (Fig.2).

In general, our data from the southern (site 1213) and eastern (U1347) Tamu massif show a very homogeneous and relatively depleted isotopic composition. These could be consistent with an origin of the initial (oldest) phase of Shatsky volcanism from an arriving plume head characterized by large degrees of melting (Farnetani and Hoffman, 2011). To test this hypotheses, isotope measurements from lavas from the younger Shatsky Massifs (Ori and Shirshov) are underway. If these younger edifices represent the transition from plume head to plume tail, we expect that these lavs show a more heterogeneous isotopic composition (possesing both more enriched and possible even more depleted isotope ratios) reflecting a more pure endmember signal, undiluted due to the lesser degree of melting.

References:

Farnetani, C.G., and Hofmann, A.W. (2011) Mantle plumes. Encyclopedia of Solid Earth Geophysics.

Hoernle, K., Hauff, F., Bogaard, P.v.d., Werner, R., Mortimer, N., Geldmacher, J., Garbe-Schönberg, D., and Davy, B. (2010). Age and geochemistry of volcanic rocks from the Hikurangi and Manihiki oceanic Plateaus. Geochim. Cosmochim. Acta, 74, 7196-7219,

Lithgow-Bertelloni, C., and Richards, M.A. (1998) The dynamics of Cenozoic and Mesozoic plate motions. Rev. Geophys., 36(1): 27-78.

Mahoney, J.J., Duncan, R.A., Tejada, M.L.G., Sager, W.W., and Bralower, T.J. (2005) Jurassic-Cretaceous boundary age and mid-ocean-ridge-type mantle source for Shatsky Rise. Geology, v. 33, p. 185-188.

Nakanishi, M., Sager, W. W., and Klaus, A. (1999) Magnetic lineations within Shatsky Rise, northwest Pacific Ocean: Implications for hot spot-triple junction interaction and oceanic plateau formation. J. Geophys. Res. 104.

Sager, W.W., Handschumacher, D.W., Hilde, T.W.C., and Bracey., D.R. (1988) Tectonic evolution of the northern Pacific plate and Pacific-Farallon Izanagi triple junction in the Late Jurassic and Early Cretaceous (M21-M10). Tectonophysics, 155(1-4): 345-364.

Sager, W. W., Kim, J., Klaus, A., Nakanishi, M., and Khankishieva, L. M. (1999) Bathymetry of Shatsky Rise, northwest Pacific Ocean: Implications for ocean plateau development at a triple junction. J. Geophys. Res. 104.

Tatsumi, Y., Shinjoe, H., Ishizuka, H., Sager, W.W., and Klaus, A., (1998) Geochemical evidence for a mid-Cretaceous superplume: Geology, v. 26, p. 151-154.

ICDP

Southern Patagonian climate during the last 55,000 years: insights from lipid biomarkers and their isotopes

HOCKUN K.[1]; SCHEFUSS, E. [1;] MOLLENHAUER G. [1,2]

[1] MARUM – Zentrum für Marine Umweltwissenschaften, Universität Bremen, Leobener Straße, 28359 Bremen
[2] Alfred Wegener Institute, Am Handelshafen 12, 27570 Bremerhaven

For predicting the future response to climate change, we need to understand the environmental changes in the past. It is of major importance to improve high resolution climate reconstruction by using reliable and well calibrated proxies from the marine and terrestrial realms, in particular in areas with strong climatic gradients highly sensitive to climate change, i.e. the high southern latitudes. The PASADO ("Potrok Aike Maar Lake Sediment Archive Drilling Project") Lipids project aims at providing new insights into the climate history of southern South America by using organic-geochemical proxies based on molecular fossils, i.e. lipid biomarkers from terrestrial and aquatic plants/organisms (n-alkanes, n-fatty acids) and their compound-specific isotope composition (δD) as well as from microbial membranes (glycerol dialkyl glycerol tetraethers, GDGTs). The overarching goal is to establish quantitative reconstructions of changes in temperature and hydrology in southern Patagonia over the last 55,000 years.

First regional calibrations of GDGT distributions from microbial membranes and an identification of suitable lipid biomarker tracers are needed for paleo-climatic reconstruction. Soil samples from a W-E transect as well as a series of lake surface sediments have been analysed to establish a regional calibration of GDGT-based proxy parameters (MBT/CBT, methylation ratio/cyclization ratio of branched tetraethers) to determine their dependence on soil temperature and soil pH in southern Patagonia. Furthermore, the lipid biomarker signatures of lake surface sediments and various organic source materials (aquatic and terrestrial plants) from the study site, Laguna Potrok Aike (51°58´S, 70°23´W), will be analyzed to identify the major contributors to organic matter in the sediments and find suitable tracers for paleo-reconstructions. Differences between compound-specific δD values of biomarkers from aquatic and terrestrial sources are expected to reflect hydro-climatic conditions of the lake system.

In order to reconstruct regional climate changes from Laguna Potrok Aike and its vicinity, samples from the 100 m long PASADO core will be analyse by these proxies to extend the investigations to the past 55.000 year. Together with published data, we aim at developing an improved mechanistic understanding of the coupling of terrestrial climatic conditions and oceanic climate changes in the Southern Hemisphere.

IODP

Late Neogene vegetation change of the south west african tropics (Namibia)

S. HOETZEL[1]& L. DUPONT[1]

[1]MARUM Center for Marine Environmental Sciences, University of Bremen, Leobener Straße Bremen D - 28359

The Miocene-Pliocene is the period of the major savanna grassland expansion in Africa and is followed or accompanied by the expansion of the so-called C_4 plants (Edwards et al., 2010; Strömberg, 2011), which are adapted to dry warm conditions. The driving forces for this expansion are still unknown. Increased climatic seasonality, increasing general aridification, cloud cover, intense herbivory, and fire abundance are discussed to play important roles (Osborne, 2008; Beerling & Osborne, 2006). It is mostly believed that strong upwelling attended with decreasing sea-surface temperatures played a major role in the desiccation and hydrology changes on the African continent (Dupont *et al.*, 2005, 2011). However, direct evidences for this link have been rarely reported so far and it is still poorly known how the tropical vegetation changed in southern Africa and, especially, how the tropical savannas developed.

The main scientific objective of this study is to to gain insights in the variability of the tropical vegetation with emphasis on the expansion of the grasslands and its driving forces. Therefore, the current study focuses on the continous tropical marine sediment sequence of ODP Site 1081, offshore Namibia (19°37'S, 11°19'E, 794 m water depth).

So far the period from 9.2 to 2.8 Ma has been studied for its pollen, spores, and charcoal content. The results suggest relative hunid conditions with a rather strong signal of woodlands and mountain vegetation between 9.2 and 8.3 Ma. From 8.3 Ma on, there is a gradual change to drier conditions recorded by a strong increase of grass pollen indicating that savanna grasslands replaced woodlands. This increase represents the major savanna grassland expansion in southern west Africa during the studied period. At 7.2 Ma large amounts of charred particles indicate stronger fire activity. This increased fire activity is propably related to the establishement of the savanna grasslands providing large amounts of fuel for bushfires. At 5.1 Ma the sedimentation pattern indicates higher fluvial input represented by higher pollen influx rates and the presence of swamp and lake indicators, such as Typha and Nympheaceae pollen. This might be related to a change in the course of the Cunene River, which fed the Lake Cunene during Late Miocene and Pliocene times (today visible as Etosha pan). The Cunene River discharge to the Atlantic Ocean probalbly began during late Pliocene times when the inland Lake Cunene started to dry out (Hipondoka, 2005).

Additionally, these data will be compared with results from biogeochemical studies and dinoflagellate cyst counts to unravel further land/sea linkages.

References:

Beerling, D.J. & Osborne, C.P. (2006) The origin of the savanna biome. Global Change Biology, 12, 2023-2031.

Dupont, L.M., Donner, B., Vidal, L., Pérez, E.M. & Wefer, G. (2005) Linking desert evolution and coastal upwelling: Pliocene climate change in Namibia. Geology, 33, 461-464.

Dupont, L.M., Linder, H.P., Rommerskirchen, F. & Schefuß, E. (2011) Climate-driven rampant speciation of the Cape flora. Journal of Biogeography, 38, 1059-1068.
Edwards, E.J., Osborne, C.P., Strömberg, Caroline A.E., Smith, S.A., Bond, W.J., Christin, P.-A., Cousins, A.B., Duvall, M.R., Fox, D.L., Freckleton, R.P., Ghannoum, O., Hartwell, J., Huang, Y., Janis, C.M., Keeley, J.E., Kellogg, E.A., Knapp, A.K., Leakey, A.D.B., Nelson, D.M., Saarela, J.M., Sage, R.F., Sala, O.E., Salamin, N., Still, C.J. & Tipple, B. (2010) The origins of C_4 grasslands: integrating evolutionary and ecosystem science. Science 328, 587-591.
Hipondoka, M. (2005) The Development and Evolution of Etosha Pan, Namibia, Thesis Julius-Maximilian-Universität, Würzburg.
Osborne, C.P. (2008) Atmosphere, ecology and evolution: what drove the Miocene expansion of C_4 grasslands? The Journal of Ecology, 96, 35-45.
Strömberg, C. (2011) Evolution of Grasses and Grassland Ecosystems. Annual Review of Earth and Planetary Sciences, 39, 517-544.

IODP

The radiogenic lead (double-spike) isotope record of Neogene-Quaternary Eastern Equatorial Pacific sediment cores and its implications for lead sources and paleoceanography in the circum-Caribbean region

T. HÖFIG[1,2], K. HOERNLE[1], F. HAUFF[1], M. FRANK[1], S. DUGGEN[1], A. KLÜGEL[3]

[1]GEOMAR | Helmholtz Centre for Ocean Research, Wischhofstr. 1-3, D-24148 Kiel, Germany
[2]Department of Mineralogy, TU Bergakademie Freiberg, Brennhausgasse 14, D-09596 Freiberg, Germany
[3]University of Bremen, Department of Geosciences, Klagenfurter Str. 2, D-28359 Bremen, Germany

For more than three decades, there has been increasing awareness of the importance of radiogenic isotopes as (paleo)-oceanographic proxies. Lead (Pb) isotopes serve as an especially powerful tool, because there are three radiogenic Pb isotope ratios that can be used to trace the variety of sources and pathways of Pb in the oceans (see Frank (2002) for a recent review). Bulk sediment trace metal isotope records are poorly known, which is mainly linked to their heterogenous sediment composition compared to pristine seawater precipitates. However, bulk sediment archives in marine cores provide a window into the past. In this study, we characterize the Pb isotopic composition of bulk sediments of the thickest (ca. 475 m) and most continuous sediment column considered so far. Our primary questions were what are the sources of Pb in marine carbonate and pelagic sediments, are there systematic temporal changes of the Pb isotopic composition in the section, and if so, why.

To address these questions, the Pb DS (double-spike) isotope compositions of DSDP Site 495 and ODP/IODP Site 1256 sediment packages, located on Cocos Plate crust in the tetonically and volcanically vigorous area of the Eastern Equatorial Pacific Guatemala Basin (Fig. 1), were determined. Both sites show a wide range of values ($^{206}Pb/^{204}Pb$: 18.28–18.80, $^{207}Pb/^{204}Pb$: 15.51–15.63, $^{208}Pb/^{204}Pb$: 37.93–38.71) forming excellent linear arrays (Fig. 2) with increasingly radiogenic Pb isotope ratios with decreasing age in both cores over a combined period of 20 million years from the Lower Miocene to Late Pliocene (Fig. 3). We interpret these arrays to reflect mixing of Pb from two primary sources. The sediments directly above the igneous ocean crust in both cores have isotopic compositions that fall within the East Pacific Rise (EPR) mid-ocean ridge basalt (MORB) field, indicating that the Pb in these sediments is predominantly derived from hydrothermal fluids being expelled at the spreading center into the surrounding seawater. As the crust moved away from the EPR spreading center, the hydrothermal

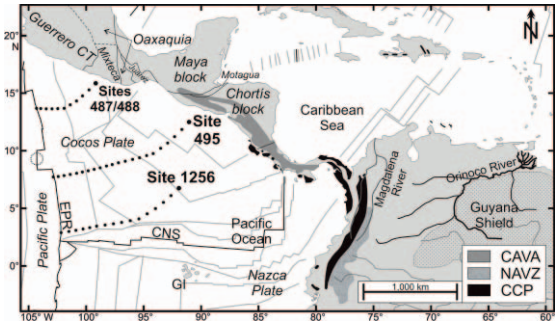

Fig. 1: Map of the Eastern Equatorial Pacific showing major plate tectonic units and geographic features mentioned in the text (locations of DSDP Site 495 and ODP/IODP Site 1256 are indicated). Present location of drill sites and reconstructed "flow lines" are calculated with the software GPlates (http://www.gplates.org). Small black dots along flow paths mark 1 m.y. increments. Additionally, present-day ridges and 5 m.y. isochrones are depicted. Location and boundaries of Middle American terranes (Maya block, Chortís block, etc.) according to Keppie (2004). Position of the Central American Volcanic Arc (CAVA; Early Miocene to Quaternary in age) according to Hoernle et al. (2008). Location of the Caribbean-Colombian Plateau (CCP; uplifted Caribbean Large Igneous Province fragments) after Hauff et al. (2000). Position of the Northern Andean Volcanic Zone (NAVZ) according to Hart and Miller (2006). South American river courses and Guyana Shield location after Hoorn et al. (2010). EPR = East Pacific Rise, CNS = Cocos-Nazca Spreading Center, GI = Galápagos Islands. Sample area of reference EPR MORB is displayed with stippled circle and marked by drilled Cocos Plate basement locations of Sites 487,

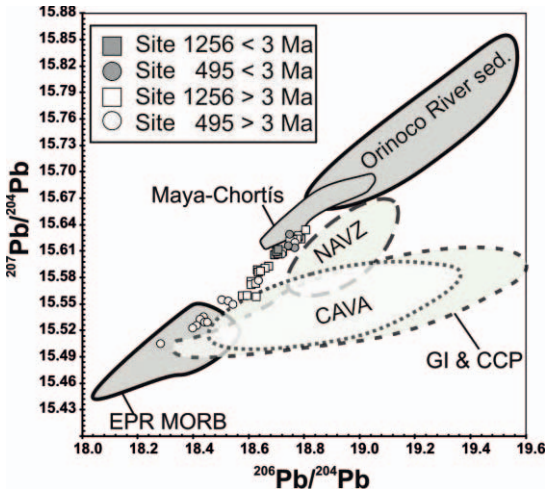

Fig. 2: $^{207}Pb/^{204}Pb$ vs. $^{206}Pb/^{204}Pb$ plot showing a two-component mixing line established by Sites 495 & 1256 sediments with low-radiogenic EPR MORB and high-radiogenic cratonic sources. Note that ever since its existence the (proto-)Orinoco River has drainaged the northern part of the Amazonian Craton termed Guyana Shield (data from White et al., 1985; Carpentier et al., 2008). EPR MORB data from Verma (2000), Sims et al. (2002), Sadofsky et al. (2009), and Waters et al. (2011). Maya and Chortís block data from Cumming et al. (1981). CAVA (Central American Volcanic Arc), CCP (Caribbean-Colombian Plateau), GI (Galápagos Islands), and NAVZ (Northern Andean Volcanic Zone) data are taken from the GEOROC database.

component decreased systematically in the sediments and the Pb isotopic composition becomes systematically more radiogenic. Surprisingly, the thorogenic and uranogenic Pb isotope diagrams show that the active continental volcanic arcs and uplifted tectonic ridges of Central America and NW South America do not come into consideration as sources for the radiogenic Pb isotope component, since

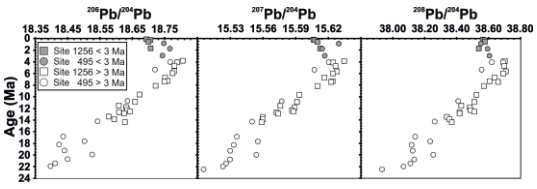

Fig. 2: Age versus Pb isotopes plots showing clear temporal trends for Pb isotope ratios of both sediment cores studied. This trend to more radiogenic values with decreasing age terminates at c. 3.5 Ma. Subsequently, the ratios drop down reflecting changing oceanographic conditions likely related to the closure of the Panama Seaway.

they do not fall on the mixing array (Fig. 2). Hence, volcanic input via explosive eruptions seems to be too discontinuous to establish an enduring signal in the cores. The upper endmember of the mixing array, however, displays a clear continental signature (Fig. 2). These samples represent one of the most radiogenic oceanic sediments discovered thus far. Therefore, solely a cratonic source comes into consideration for the radiogenic endmember. Such a source is ubiquitous in the vicinity of the Eastern Equatorial Pacific, since Mexico and Central America are made up of ancient terranes of Neoproterozoic to Mesozoic age amalgamated together during several convergence phases and now crop out in proximal areas to the coast (see Keppie (2004) for a review). Here, riverine input and subsequent surface ocean current transport are the most likely pathways. However, this straightforward observation is challenged by cessation of the temporal radiogenic trend after 3.5 Ma. Although, both sites still approach Central America, the Pb isotope ratios of the youngest sediments of Site 1256 drop down to lower values after 3.5 Ma (Fig. 3). It is suggested that this change is related to the closure of the Panama Seaway, which took place at c. 3.5 Ma (see Schmidt (2007) for a detailed review). Therefore, either a cratonic source similar to the Central American basement originating from the other side of the gateway was effectively blocked (Guyana Shield signal delivered by proto-Caribbean Current) or different ocean currents derived from an area within the Pacific Ocean basin led to a dilution of the Central American radiogenic signal reaching Site 1256.

In summary, the Neogene-Quaternary sedimentation sequences studied represent a remarkably steady-state, long-lasting Pb isotope record for the Eastern Equatorial Pacific, showing a systematic temporal trend over more than 20 million years. This trend only requires two types of endmembers: a mid-ocean ridge hydrothermal component which dominates near the ridge and a cratonic component that dominates near the continents. Interestingly there is no evidence that volcanic ash from Central America, South America or the Galápagos have significantly influenced the Pb isotopic composition of the sediments. Future studies should focus on more bulk sediment Pb isotope records from other DSDP/ODP/IODP drilling sites in a global scale in order to address the question whether systematic temporal trends are an omnipresent feature in oceanic lead isotope chemistry.

References:

Carpentier, M., Chauvel, C., Mattielli, N. (2008): Pb–Nd isotopic constraints on sedimentary input into the Lesser Antilles arc system. Earth and Planetary Science Letters, 272: 199–211.

Cumming, G.L., Kesler, S.E., Krstic, D. (1981): Source of lead in Central American and Caribbean mineralization, II. Lead isotope provinces. Earth and Planetary Science Letters, 56: 199–209.

Frank, M. (2002): Radiogenic isotopes: Tracers of past ocean circulation and erosional input. Reviews of Geophysics, 40: 1–37.

Hart, D., Miller, D.J. (2006): 19. Analysis and correlation of volcanic ash in marine sediments from the Peru margin, Ocean Drilling Program Leg 201: Explosive volcanic cycles of the North-Central Andes. In Jorgensen, B.B., D`Hondt, S.L., and Miller, D.J. [eds.]: Proceedings of the Ocean Drilling Program, Scientific Results, Vol. 201.

Hauff, F., Hoernle, K., van den Bogaard, P., Alvarado, G., Garbe-Schönberg, D. (2000): Age and geochemistry of basaltic complexes in western Costa Rica: Contributions to the geotectonic evolution of Central America. Geochemistry, Geophysics, Geosystems, 1, doi:10.1029/1999GC000020.

Hoernle, K., Abt, D.L., Fischer, K.M., et al. (2008): Arc-parallel flow in the mantle wedge beneath Costa Rica and Nicaragua. Nature, 451: 1094–1098.

Hoorn, C., Wesselingh, F.P., ter Steege, M., et al. (2010): Amazonia through time: Andean uplift, climate change, landscape evolution, and biodiversity. Science, 330: 927–931.

Keppie, J.D. (2004): Terranes of Mexico revisited: A 1.3 Billion year odyssey. International Geology Review, 46: 765–794.

Meynadier, L., Allègre, C., O'Nions, R.K. (2008): Plate tectonics, radiogenic isotope tracers and paleoceanography: The case of the manganese crusts in the Pacific. Earth and Planetary Science Letters, 272: 513–522.

Sadofsky, S., Hoernle, K., Duggen, S., Hauff, F., Werner, R., Garbe-Schönberg, D. (2009): Geochemical variations in the Cocos Plate subducting beneath Central America: implications for the composition of arc volcanism and the extent of the Galápagos Hotspot influence on the Cocos oceanic crust. International Journal of Earth Sciences, 98: 901–913.

Schmidt, D.N. (2007): The closure history of the Central American seaway: evidence from isotopes and fossils to models and molecules. In: Williams, M., Haywood, A.M., Gregory, F.J., Schmidt, D.N. [eds.]: Deep-time perspectives on climate change: Marrying the signal from computer models and biological proxies. The Micropalaeontological Society, Special Publications, 427–442.

Sims, K.W.W., Goldstein, S.J., Blichert-Toft, J., et al. (2002): Chemical and isotopic constraints on the generation and transport of magma beneath the East Pacific Rise. Geochimica and Cosmochimica Acta, 66: 3481–3504.

Verma, S.P. (2000): Geochemistry of the subducting Cocos plate and the origin of subduction-unrelated mafic volcanism at the volcanic front of the central Mexican Volcanic Belt. In: Delgado-Granados, H., Aguirre-Díaz, G., and Stock, J.M. [eds.]: Cenozoic tectonics and volcanism of Mexico: Boulder, Colorado. Geological Society of America Special Paper 334, 195–221.

Waters, C.L., Sims, K.W.W., Perfit, M.R., Blichert-Toft, J., Blusztajn, J. (2011): Perspective on the genesis of E-MORB from chemical and isotopic heterogeneity at 9–10°N East Pacific Rise. Journal of Petrology, 52: 565–602.

White, W.M., Dupré, B., Vidal, P. (1985): Isotope and trace element geochemistry of sediments from the Barbados Ridge–Demerara Plain region, Atlantic ocean. Geochimica et Cosmochimica Acta 49: 1875–1886.

IODP

Deep-water formation in the Bering Sea? Insights from Nd isotopes for site U1341 (Bowers Ridge, IODP 323)

T. HOHMANN, C. L. BLANCHET AND M. FRANK

GEOMAR | Helmholtz Centre for Ocean Research Kiel, Wishhofstrasse 1-3, 24148 Kiel
thohmann@geomar.de, cblanchet@geomar.de

Changes in North Pacific Deep Water ventilation are prone to greatly affect global climate through storage/release of CO_2. However, past dynamics of this water mass are not well understood as paleorecords provide contradictory

evidence. Today, no deep water forms in the North Pacific due to low sea surface salinities. During glacial times however, enhanced sea-ice formation and resulting higher sea-surface salinity in the Bering Sea might have favored formation of intermediate water, as suggested by Horikawa et al. [2010]. Furthermore, the neodymium isotopes signature of sediments deposited south of the Bering Sea hints toward enhanced deep-sea outflow from the Bering Sea during glacial stages, so perhaps deep convection [VanLaningham et al., 2009]. Based on these results, we aim at reconstructing the dynamics of deep-water masses in the southern Bering Sea during the Quaternary, in order to understand their role in the CO2 budget. During Integrated Ocean Drilling Program (IODP) campaign 323, a series of sediment cores was retrieved on Bowers Ridge, near the location where Horikawa et al. [2010] reported formation of intermediate water during the last glacial maximum. For this study, we selected IODP site U1341, which was retrieved at 2177 m water-depth, at a site that is presently bathed by Bering Sea Deep Water, in order to test whether deep-water convection also occurred during glacial stages. According to the preliminary age model [Expedition 323 Scientists, 2009], site U1341 covers the past 5 Ma but we will focus on the past 1 million years, for which samples were collected every 50 cm to provide a 5 kyr-resolution. We analysed the neodymium (Nd), strontium (Sr) and lead (Pb) isotope composition of ferromanganese coatings formed on sediment particles during early diagenesis, in order to reconstruct past seawater isotopic composition. Preliminary Nd and Sr results for the past 140 kyr suggest that the leaching protocol applied is successful in recovering past sea-water signature. The Nd isotopes varry following changes in paleoclimate, with higher values (up to 1.3 εNd units) during cold periods and lower values (-0.3 to-0.8 εNd units) during warm periods. This observation is in accordance with results previously obtained and might indicate the occurrence of deep-water formation in the Bering Sea during cold intervals of the last glacial cycle. Such a process might involve brine formation, as already suggested by Horikawa et al [2010]. Further work is needed to confirm this first observation, and notably the Nd isotope composition of foraminifera will help assessing present and past deep water isotopic composition. Finally, the Nd, Sr and Pb signature of bulk sediments and specific grain-size fractions will be performed in order to reconstruct past changes in sediment delivery to the core site (e.g., sediments transported by sea ice, icebergs…).

References:

Expedition 323 Scientists. Bering Sea paleoceanography: Pliocene-Pleistocene paleoceanography and climate history of the Bering Sea. IODP Preliminary Report 323, Integrated Ocean Drilling Program, 2009.

K. Horikawa, Y. Asahara, K. Yamamoto, and Y. Okazaki. Intermediate water formation in the Bering Sea during the glacial periods: Evidence from neodymium isotope ratios. Geology, in press, 2010. doi: 10.1130/G30225.1.

S. VanLaningham, N. G. Pisias, R. A. Duncan, and P. D. Clift. Glacial-interglacial sediment transport to the Meiji Drift, northwest Pacific Ocean: Evidence for timing of Beringian outflow. Earth and Planetary Science Letters, 277:64–72, 2009.

IODP

Impact of late Miocene cryosphere expansion on Pacific meridional overturning

A. HOLBOURN[1], W. KUHNT[1], S. CLEMENS[2], W. PRELL[2], N. ANDERSEN[3]

[1]Institute of Geosciences, Christian-Albrechts-University, D-24118 Kiel, Germany
[2] Department of Geological Sciences, Brown University, Box 1846, Providence, RI 02912, USA
[3] Leibniz Laboratory for Radiometric Dating and Stable Isotope Research, Christian-Albrechts-University, D-24118 Kiel, Germany

Although past climates are not exact analogues for the modern world, understanding long-term variations is critical for unravelling the main drivers of climate change and for interpreting current trends and predicting future change. The relatively warm late Miocene period potentially offers a close analogue to understand future climate developement. During the Neogene, Earth slowly transitioned from Greenhouse to Icehouse conditions, culminating with development of extensive Pleistocene ice sheets over the northern high latitudes. However, the mechanisms controlling these transient climate modes are still poorly understood, largely due to the scarcity of continuous, high-resolution climate series that can be calibrated to an astronomical time scale. A major challenge is that late Miocene isotope records show relatively low amplitude variability (often ~0.5 ‰ or less), making it difficult to resolve climate signals from „noise“ and to constrain the timing of events. Additionally, deep marine records are often plagued by pervasive horizons of carbonate dissolution over the interval known as the „Carbonate Crash“ (~9-11 Ma, Lyle et al., 2008).

We present high-resolution (2-3-kyr time resolution) benthic foraminiferal oxygen ($\delta^{18}O$) and carbon ($\delta^{13}C$) isotope data in a continuous sedimentary succession recovered at Ocean Drilling Program (ODP) Site 1146 in the South China Sea (19° 27.40’ N, 116° 16.37’ E, water depth: 2092 m). A free connection existed between the South China Sea and the West Pacific during the middle and most of the late Miocene, as the modern Bashi Strait (sill depth ~2600 m) only formed between Luzon and Taiwan at ~6.5 Ma, as a result of the Luzon Arc collision (Wang, Prell and Blum et al., 2000). The continuous, hemipelagic succession recovered from multiple holes in this site exhibits relatively constant sedimentation rates (2-3 cm/kyr), thus providing an exceptional archive of climate variability spanning the middle to late Miocene. Our astronomically-calibrated benthic isotope records closely track changes in the deep ocean over the interval 12.9-8.4 Ma and provide direct evidence that the development of Pacific meridional overturning was tightly coupled to Antarctic cryosphere expansion.

Methods

We measured $\delta^{18}O$ and $\delta^{13}C$ in epifaunal benthic foraminifers (Planulina wuellerstorfi and Cibicidoides mundulus). Well-preserved tests were broken into large fragments, cleaned in alcohol in an ultrasonic bath, then dried at 40°C. Measurements were made with the Finnigan MAT 251 mass spectrometer at the Leibniz Laboratory, Kiel University. The instrument is coupled on-line to a Carbo-Kiel Device (Type I). Samples were reacted by individual acid addition (99% H_3PO_4 at 73°C). Standard

external error is better than ±0.07 ‰ and ±0.05 ‰ for $\delta^{18}O$ and $\delta^{13}C$, respectively. Replicate measurements on ~4 % of samples indicate mean reproducibility better than ±0.09 ‰ for $\delta^{18}O$ and $\delta^{13}C$. Results were calibrated using the National Institute of Standards and Technology (Gaithersburg, Maryland) carbonate isotope standard NBS 20 and NBS 19 and 18, and are reported on the PeeDee belemnite (V-PDB) scale.

sheet melting in Antarctica, whereas cool summers during low obliquity would favour ice-sheet growth, and (2) that a low summer insolation gradient between low and high latitudes during high obliquity would decrease poleward moisture transport, inhibiting ice-sheet buildup (Loutre et al., 2004).

Amplitude and frequency of climate fluctuations (12.9 to 8.4 Ma)

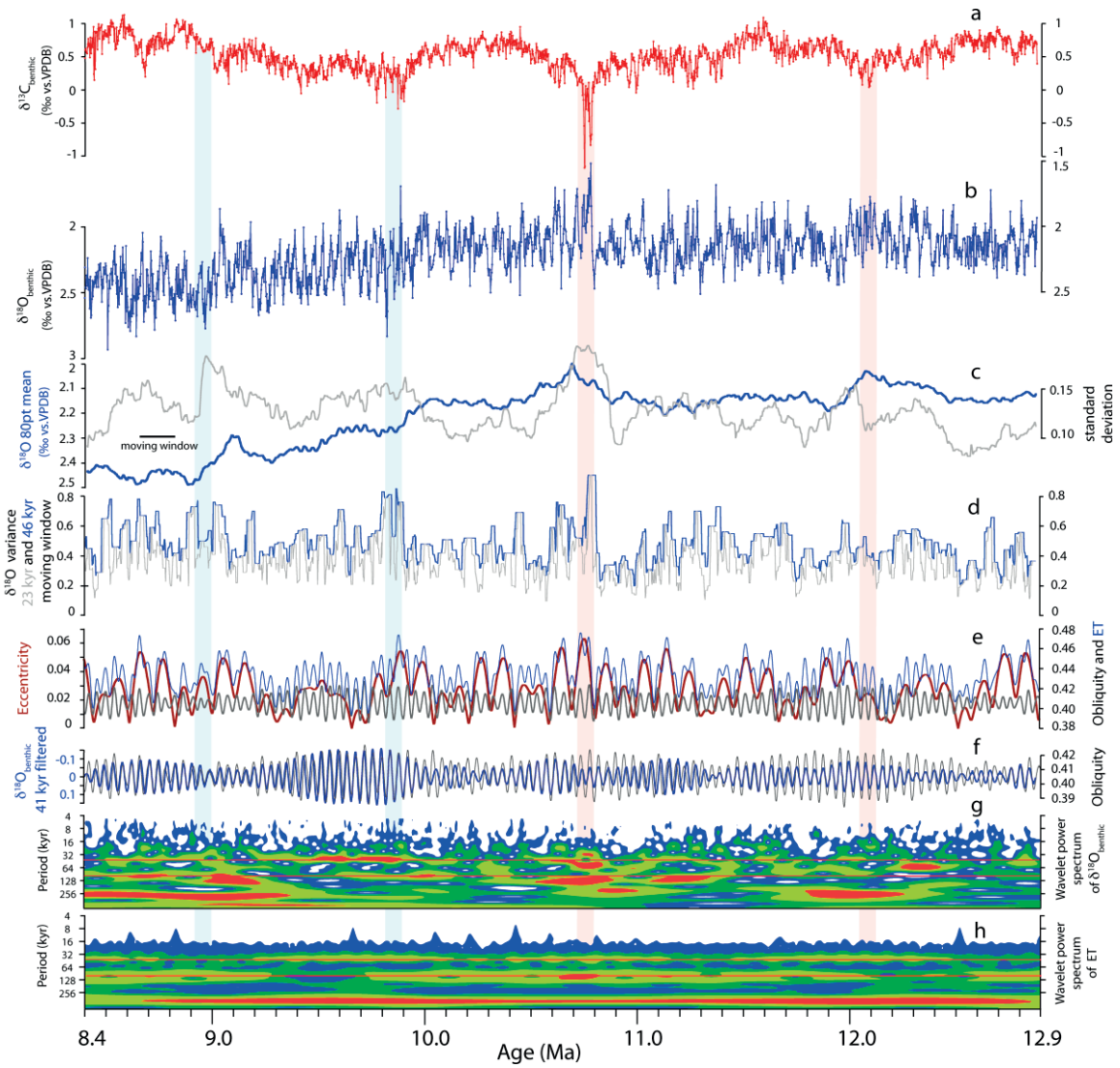

Figure 1. Benthic stable isotope records from ODP Site 1146; a. δ13C; b. δ18O; c. 80 point moving window mean and standard deviation of δ18O; d. Amplitude variance in d18O (23 kyr and 46 kyr moving windows); e. Eccentricity, obliquity and ET from Laskar et al. (2004); f. 41 kyr filter of δ18O and orbital obliquity using Gaussian filter with bandwidth of 0.004 centered at frequency of 0.0243; g. wavelet power spectrum of δ18O using a Morlet wavelet with 6 parameters, scale width of 0.01, and start scale of 2, contour levels represent more than 75% (red), 50% (yellow), 25% (green), and 5% (blue) of wavelet power; h. wavelet power spectrum of ET (same settings as in g). Blue bands mark glacial expansions, orange bands indicate warming events.

We generated a new chronology in ODP Site 1146 by correlating the benthic foraminiferal $\delta^{18}O$ record to variations of the Earth's orbit (obliquity and eccentricity in Laskar et al., 2004). The benthic isotope signals are well resolved and preserved original spectral characteristics in the depth domain, allowing us to apply a minimal tuning strategy in order to avoid artificial changes in sedimentation rates. We constructed an eccentricity-tilt composite (ET) with no phase shift and tuned $\delta^{18}O$ minima to obliquity maxima, since we assumed (1) that relatively warm summers during high obliquity would promote ice-

In both depth and time domains, the 1146 δ18O and δ13C series are characterized by high-frequency fluctuations that broadly correspond to variations in the Earth's orbit (Figure 1). The δ13C series shows prominent ~41 and ~100 kyr variations that are superposed on lower frequency oscillations approximating the 400 kyr long eccentricity cycle. Mean δ13C values generally fluctuate between 0 and 1 ‰, except for two abrupt negative excursions reaching ~-0.8 and ~-1.2 ‰ at 10.8-10.7 Ma. The δ18O curve in ODP Site 1146 reveals a long-term glacial expansion and deep water cooling with most of the

δ18O increase occurring in two distinct steps at 9.9 and 9.0 Ma (Figure 1). From 12.9 to 9.9 Ma, mean $\delta^{18}O$ values oscillate between 2.1 and 2.2 ‰, showing transient decreases to < 2.0 ‰ at 12.1 and 10.8 Ma. Mean $\delta^{18}O$ then exhibit two successive marked increases at 9.9 Ma and 9.0 Ma, after which maximum values are sustained at 2.3-2.4 ‰ and 2.4-2.5 ‰, respectively. Based on the δ18O signal, we identify two distinct phases of climate evolution. Between 12.7 and 9.9 Ma benthic $\delta^{18}O$ exhibits marked changes in amplitude variability (variance: 0.2 to 0.9 ‰) that point to substantial variations in ice volume and deep water temperature, although no long-term glacial expansion is evident over this interval. A distinct cooling step at 9.9 Ma initiated a new mode of climate variability with enhanced sensitivity to obliquity forcing between 9.8 and 9.2 Ma during a protracted interval of low eccentricity variability. A change back to high-amplitude eccentricity after 9.2 Ma led to a transient warming followed by renewed global cooling after 9.0 Ma. Comparison of $\delta^{18}O$ data over the interval 16.5 to 12.9 Ma in ODP Sites 1146 and 1237, which are located in different water depths and oceanographic settings, supports that the 1146 record represents a Pacific deep-water signal, directly coupled to Antarctic climate and ice volume fluctuations (Holbourn et al., 2007).

Global warming event at 10.8 Ma

A most intriguing feature in the 1146 $\delta^{13}C$ series is the massive decline (~1 ‰) closely coinciding with an abrupt $\delta^{18}O$ drop of ~1 ‰ at 10.8 Ma, marking a prominent episode of global warming (Figure 2). A second, even more

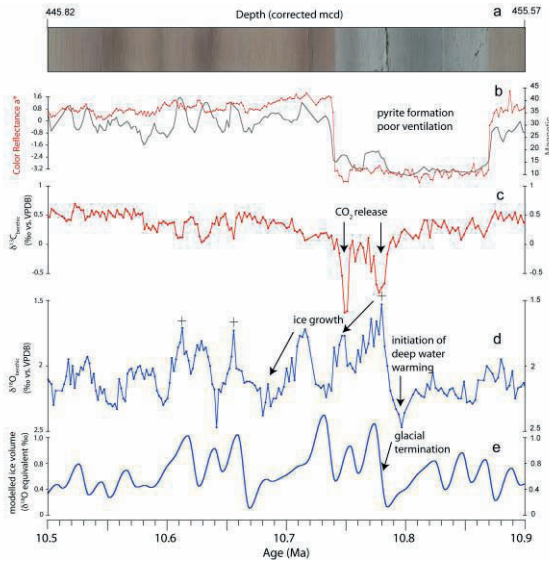

Figure 2. Details of benthic isotope and carbonate dissolution data across global warming event; a. digitized core photograph; b. color reflectance a* (red-green) and magnetic susceptibility; c. $\delta^{13}C$; d. $\delta^{18}O$ independently tuned to ET; e. ice volume model of Imbrie and Imbrie (1980) forced by 75° S insolation. Model setup for Pleistocene Northern Hemisphere ice sheets, prescribing 17 kyr time lag of minimum ice volume to maximum insolation and 4:1 ratio between glacial growth and melting.

pronounced $\delta^{13}C$ negative excursion (~-1.2 ‰) corresponds to a further sharp decrease in $\delta^{18}O$ following a temporary recovery lasting ~30-40 kyr. The magnitude of the $\delta^{13}C$ decreases preclude that they are solely driven by local export flux and remineralization of particulate organic matter. In fact, these $\delta^{13}C$ spikes also occur in the deeper (water depth 3294 m) South China Sea Site 1148 (Tian et al., 2008), and appear related to episodes of ocean wide $\delta^{13}C$ depletion. In Site 1146, sedimentological evidence indicate that a prolonged period of reduced deep-water ventilation with pyrite formation at the seafloor preceded the unusual warming event at 10.8 Ma. We infer that increased deep water stratification after ~10.9 Ma due to weaker meridional overturning, promoted widespread storage of dissolved inorganic and organic carbon and acidification of the deep ocean. This long-term trend was only reversed after two intense warming pulses led to enhanced ocean mixing and CO_2 release to the atmosphere, further fuelling warming and ice decay at peak insolation. The striking similarity of benthic $\delta^{18}O$ to modelled ice volume (Figure 2) supports that variations are driven by Antarctic ice dynamics. This climatic sequence is reminiscent of $\delta^{18}O$ and $\delta^{13}C$ negative excursions (~1 ‰) during the middle Miocene „Greenhouse“ climate phase (~16.4 to 14.7 Ma). These extreme events probably represent episodes of rapid deep water warming causing massive CO_2 release from the poorly ventilated abyssal ocean. In the deep SE Pacific Site 1237 (water depth 3212 m) the $\delta^{18}O$ decreases correspond to intense dissolution horizons paced by short eccentricity, suggesting major decreases in deep ocean alkalinity during periods of maximum warmth. These deep water warming and acidification episodes bear resemblance to „hyperthermal“ events, linked to rapid CO_2 release from the oxidation of dissolved organic carbon in the abyssal deep ocean reservoir during older, warmer intervals of Earth history (Sexton et al., 2011).

Impact of late Miocene glacial events on Pacific circulation

The sustained benthic $\delta^{18}O$ increase after 9.9 Ma (~0.2 ‰ mean) marks a new threshold in Miocene glacial expansion and ice sheet dynamics. Between 9.8 and 9.4 Ma, benthic $\delta^{18}O$ and $\delta^{13}C$ show enhanced sensitivity to obliquity forcing and glacial-interglacial $\delta^{18}O$ cycles exhibit a more pronounced asymmetry, indicating a change

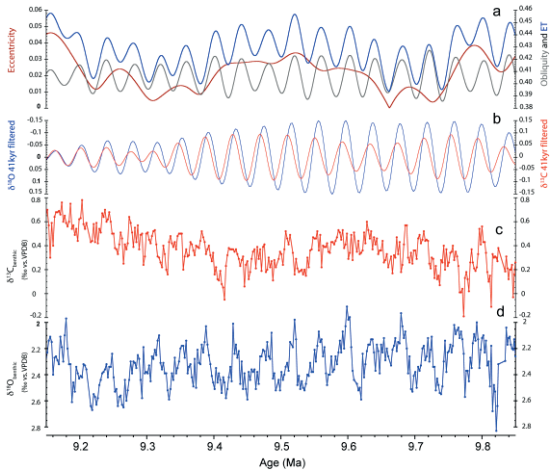

Figure 3. Details of benthic isotope data across 9.15-9.85 Ma; a. Eccentricity, obliquity and ET from Laskar et al. (2004); b. 41 kyr filtered δ13C and δ18O, Gaussian filter centered at frequency of 0.0243 with bandwidth of 0.004: c. δ13C: d. δ18O.

in internal climate dynamics driving rapid deglaciations and slower glaciations (Figure 3). Glacial expansion after

9.9 Ma also signals a major change in deep water ventilation. Whereas benthic $\delta^{18}O$ and $\delta^{13}C$ show weak co-variance on the obliquity band between 12.9 and 9.9 Ma, a distinct antiphase relationship is evident after 9.9 Ma with $\delta^{13}C$ lagging by ~7 kyr. This pattern is consistent with increased production of deep and intermediate waters in high latitudes during interglacials, resulting in a more vigorous meridional overturning circulation. Arguably, the East Antarctic ice sheet reached a new expansion threshold after 9.9 Ma, allowing development of a more „modern" circulation mode. A plausible scenario is that the ice sheet's margin became more responsive to changes in insolation and ocean heat flux controlling precipitation patterns, sea ice formation and glacial erosion, as the ice expanded to the coast after 9.9 Ma. In a manner reminiscent of Pleistocene glacial-interglacial cycles (Sigman et al., 2010), southward shifts in the position of Southern Hemisphere westerly winds during warmer intervals may have stimulated upwelling of cold, salty water and production of deep and intermediate waters after 9.9 Ma. However in contrast to late Pleistocene climate variability, late Miocene glacial-interglacial cycles were predominantly paced by obliquity, suggesting that increased latitudinal moisture transport controlled Antarctic ice expansion during periods of enhanced obliquity forcing. Additionally, declining atmospheric CO_2 probably played a pivotal role in setting favourable boundary conditions for long-term ice growth during the late Miocene.

References:

Holbourn, A. E., Kuhnt, W., Schulz, M., Flores, J.-A., and Andersen, N., 2007. Middle Miocene long-term climate evolution: Eccentricity modulation of the "Monterey" carbon-isotope excursion. Earth and Planetary Science Letters. 261, 534-550. http://dx.doi.org/10.1016/j.epsl.2007.07.026.

Laskar J., Robutel, P., Joutel, F., Gastineau, M., Correia, A. C. M., and Levrard, B., 2004. A long term numerical solution for the insolation quantities of the Earth. Astronomy and Astrophysics, 428, 261-285.

Loutre, M.-F., Paillard, D., Vimeux, F., and Cortijo, E., 2004. Does mean annual insolation have the potential to change the climate? Earth Planetary Science Letters, 221, 1-14.

Lyle, M., Barron, J., Bralower, T. J. ,Huber, M., Olivarez Lyle, A., Ravelo, A. C. Rea, D. K., and Wilson, P. A., 2008. Pacific Ocean and Cenozoic evolution of climate, Rev. Geophys., 46, RG2002, doi:10.1029/2005RG000190.

Sexton, P. F., Norris, R.D., Wilson, P.A., Pälike, H., Westerhold, T., Röhl, U., Bolton, C.T., and Gibbs, S., 2011. Eocene global warming events driven by ventilation of oceanic dissolved organic carbon. Nature, 471, 349 - 353.

Sigman, D.M., Hain, M.P., and Haug, G.H., 2010. The polar ocean and glacial cycles in atmospheric CO_2 concentration. Nature, 466, 47-55. jdoi:10.1038/nature09149.

Tian, J., Zhao, Q.H., Wang, P.X., Li, Q.Y., Cheng, X.R., 2008. Astronomically modulated Neogene sediment records from the 24 South China Sea. Paleoceanography 23, doi:10.1029/2007PA001552.

Wang, P. Prell, W. L. and Blum P. et al., 2000. Proceedings of the Ocean Drilling Program, Initial Reports, 184 [CD-ROM]. Available from: Ocean Drilling Program, Texas A&M University, College Station TX 77845-9547, USA.

IODP

Developing an early to middle Miocene benthic foraminiferal isotope chrono-stratigraphy across the Pacific „paleoequator transect" (IODP Expedition 320/321)

A. HOLBOURN[1], W. KUHNT[1], M. LYLE[2], N. ANDERSEN[3]

[1]Institute of Geosciences, Christian-Albrechts-University, D-24118 Kiel, Germany
[2]Department of Oceanography, Texas A&M University, College Station, Texas 77843, USA
[3]Leibniz Laboratory for Radiometric Dating and Stable Isotope Research, Christian-Albrechts-University, D-24118 Kiel, Germany

Our primary goals are to develop an early to middle Miocene (20-13 Ma) astronomically-calibrated benthic isotope chronostratigraphy in a "mega-splice" constructed from continuous and expanded sedimentary successions from multiple drill holes across the Pacific „paleoequator transect". The PEAT Expedition 320/321 (March to June

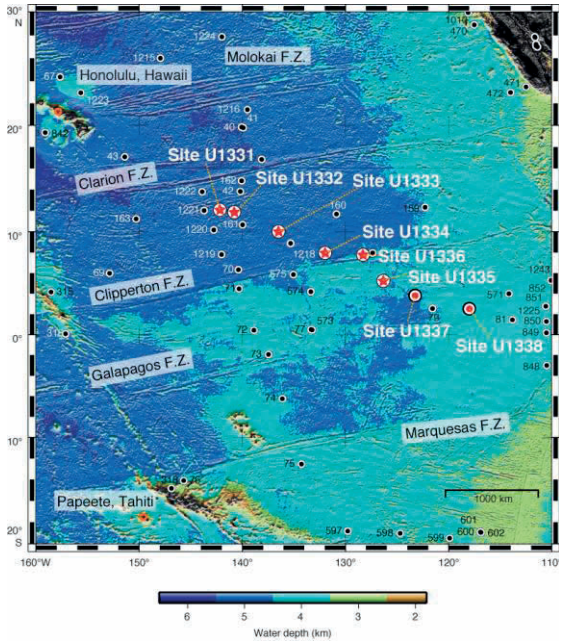

Figure 1. Location map of sites drilled during IODP Expedition 320/321 (from Pälike et al., 2010). Red stars = sites drilled during Expedition 320, red circles = sites drilled during Expedition 321, black circles = previous DSDP and ODP sites. F.Z. = fracture zone. Hawaii and Tahiti are also marked.

2009) targeted key time slices in the evolution of the Cenozoic climate at locations across the paleo-equator that were not deeply buried, thus allowing optimum accumulation and preservation of calcareous sediments (Pälike et al., 2010). Specific targets included the prominent oscillations in ice volume and/or ocean temperatures during the early Miocene leading on to the "Monterey Excursion" and Miocene Climatic Optimum followed by the punctuated expansion of ice sheets towards the end of the middle Miocene. Although these intervals were drilled during previous cruises, considerable information is still missing, as previous records are incomplete due to patchy core recovery and/or poor preservation of sedimentary successions, especially within the 20-16 Ma time interval, which is not yet firmly

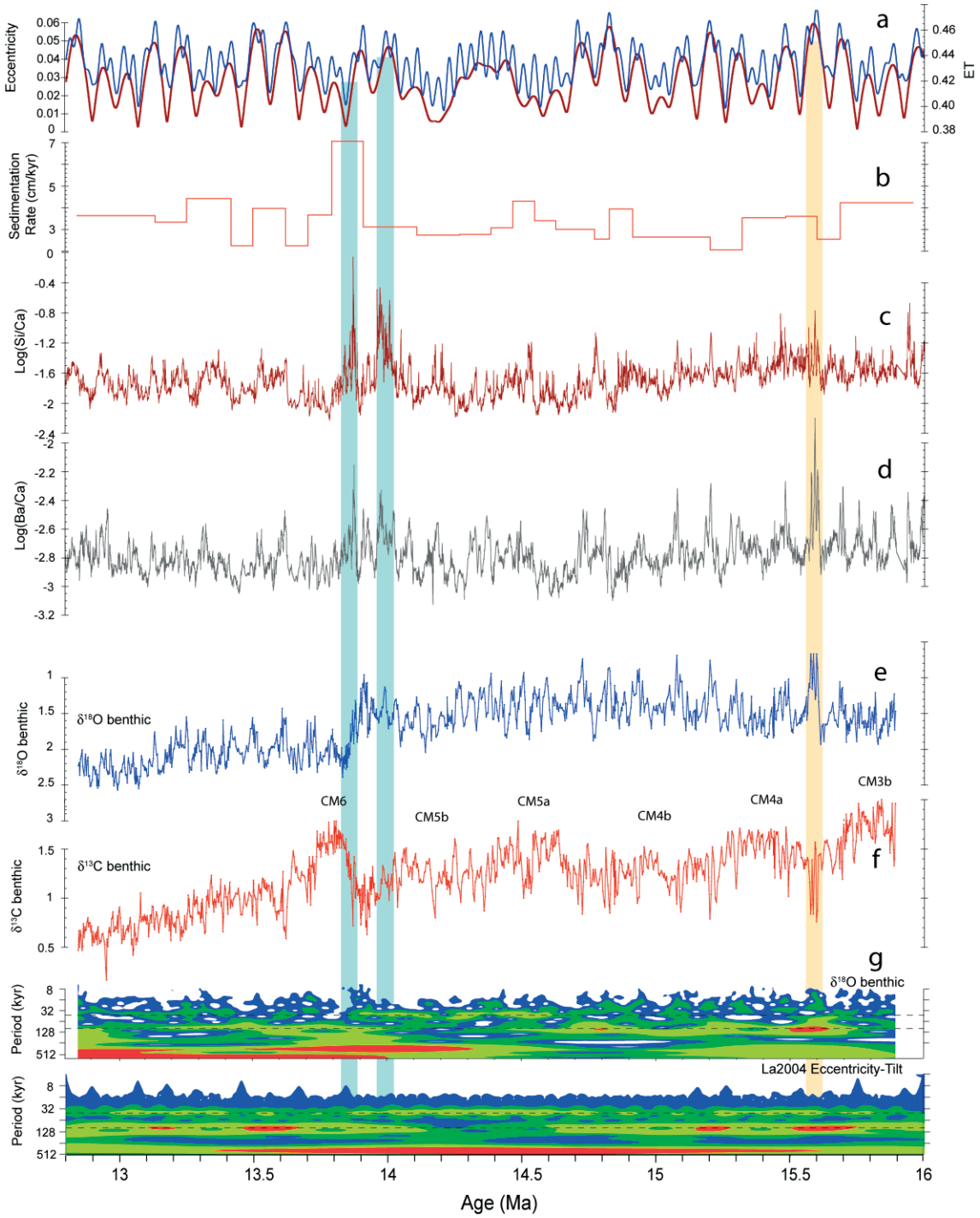

Figure 2. High-resolution middle Miocene climate records from equatorial Pacific IODP Site U1338; a. Eccentricity and ET from Laskar et al. (2004); b. Sedimentation rate between tuning tiepoints; c. XRF scanning Log(Si/Ca) data from Lyle et al. (in press); d. XRF scanning Log(Ba/Ca) data from Lyle et al. (in press); e. benthic δ18O; f. benthic δ13C; g. wavelet power spectrum of δ18O using a Morlet wavelet with 6 parameters, scale width of 0.01, and start scale of 2, contour levels represent more than 75% (red), 50% (yellow), 25% (green), and 5% (blue) of wavelet power; wavelet power spectrum of ET (same settings as for δ18O). Blue bands mark productivity spikes across main Mi-3 glacial expansion, orange band indicates "hyperthemal event" at 15.6 Ma.

anchored within the geological timescale and still requires major clarification.

We present high-resolution (1.5-3-kyr) benthic foraminiferal oxygen ($\delta^{18}O$) and carbon ($\delta^{13}C$) isotope data in a continuous middle Miocene sedimentary succession recovered at Integrated Ocean Drilling Program (IODP) Site U1338 in the equatorial Pacific Ocean (2° 30.469' N, 117° 58.178' W, 4200 m water depth; Figure 1). During the middle Miocene, IODP Site U1338 was located in paleodepths of ~3500 m within the equatorial zone (±2° of the Equator), ensuring optimum recovery of well-preserved carbonate-rich sediments at one of the most climate sensitive locations on Earth (Pälike et al., 2010). Sedimentation rates fluctuated between 2 and 4 cm/kyr, except over the main glacial expansion at 13.9-13.8 Ma, when rates increased to 7 cm/kyr. Thus, our isotope data allow unprecedented resolution of climate events (especially over the Climatic Optimum and Mi-3 glacial

expansion) and provide fresh insights into the pacing of Antarctic glaciation, the evolution of Pacific circulation and main drivers of climate change during the Grenhouse to Icehouse transition.

Material and methods

Cores were retrieved from multiple holes mainly with the APC coring system, thus ensuring optimum sediment recovery and preservation in IODP Site U1338. Our sediment samples were taken along the shipboard splice, constructed from correlation of magnetic susceptibility, NGR, GRA bulk density, L* data and scanned images (Pälike et al., 2010). Samples were oven dried at 40˚C and weighed before washing over a 63 µm sieve. Residues were dried at 40˚C on a sheet of filter paper, then weighed and sieved into appropriate size fractions for picking of foraminifers.

We measured $\delta^{18}O$ and $\delta^{13}C$ in epifaunal benthic foraminifers (Planulina wuellerstorfi and Cibicidoides mundulus) over the interval 331-436 mcd. Well-preserved tests were broken into large fragments, cleaned in alcohol in an ultrasonic bath, then dried at 40°C. Measurements were made with the Finnigan MAT 251 mass spectrometer at the Leibniz Laboratory, Kiel University. The instrument is coupled on-line to a Carbo-Kiel Device (Type I). Samples were reacted by individual acid addition (99% H_3PO_4 at 73°C). Standard external error is better than ±0.07 ‰ and ±0.05 ‰ for $\delta^{18}O$ and $\delta^{13}C$, respectively. Replicate measurements indicate mean reproducibility better than ±0.1 ‰ for $\delta^{18}O$ and $\delta^{13}C$. Results were calibrated using the National Institute of Standards and Technology (Gaithersburg, Maryland) carbonate isotope standard NBS 20 and NBS 19 and 18, and are reported on the Vienna-PeeDee belemnite (V-PDB) scale.

The benthic isotope signals are extremely well resolved and preserve original spectral characteristics in the depth domain, allowing us to apply a minimal tuning strategy in order to avoid artificial changes in sedimentation rates (Figure 2). We generated a new chronology in IODP Site U1338 by correlating the benthic foraminiferal $\delta^{18}O$ record to variations of the Earth's orbit (obliquity and eccentricity in Laskar et al., 2004) following the strategy outlined in Holbourn et al. (2007). We additionally performed time series analysis of core logging, coarse fraction residue >63 µm and XRF scanning data (Lyle et al., in press) over the middle Miocene interval to test the astronomically-calibrated chronostratigraphy, based on analysis of benthic isotope data.

Benthic foraminiferal stable isotopes

Benthic $\delta^{18}O$ exhibits remarkably high amplitude variability both on the eccentricity and obliquity bands at this deep equatorial Pacific location (~3500 m backtracked depth). This is particularly striking in the older 16-14.7 Ma interval, broadly corresponding to the Miocene Climatic Optimum, where $\delta^{18}O$ oscillates between ~0.7 and 1.9 ‰ (>1 ‰ amplitude variability). The amplitude variability in $\delta^{18}O$ declines to 0.8 ‰ over the stepped glacial expansion between 14.7 and 13.1 Ma. A further decline to 0.5 ‰ occurs between 13.1 and 12.8 Ma following the Mi-3 glacial shift. The amplitude variability in IODP Site U1338 falls within the range recorded at West Pacific ODP Site 1146 in shallower water depths (2000 m water depth), but is somewhat higher (on the obliquity band) than in Southeast Pacifc ODP Site 1237 (3000 m water depth).

Overall, the U1338 $\delta^{18}O$ series shows high coherence to high-resolution records from ODP Sites 1146 and 1237 (Holbourn et al., 2007), implying that variations indeed represent a global signal, primarily driven by Antarctic ice volume and Southern Hemisphere climate variability. Salient features of the $\delta^{18}O$ record are the enhanced response to obliquity between 14.6 and 14.2 Ma during an interval of low eccentricity (100 kyr) variability, the distinct, pulsed warming between 14.1 and 13.9 Ma during a period of renewed eccentricity forcing and the striking increase of 1.4 ‰ at 13.91-13.84 Ma, widely associated with Antarctic ice sheet expansion (Figure 2). The exceptional resolution of the $\delta^{18}O$ record, due to enhanced sedimentation rates in IODP Site U1338, reveals precessional (southern hemsiphere insolation) pacing across the major Mi-3 glacial shift at 13.91-13.84 Ma. A further remarkable feature is the resolution of individual peaks across the 15.6 Ma "hyperthermal event", which forms a main plateau with an abrupt onset and a more gradual decrease. Individual peaks within the plateau may correspond to maxima in precessional southern hemisphere insolation at high eccentricity.

Between 16 and 13.6 Ma, the $\delta^{13}C$ record exhibits high frequency fluctuations superposed on low frequency oscillations paced by 400 kyr eccentricity that are typical for the "Monterey Excursion" (Figure 2). Six main carbon isotope maxima (CM6 to CM3b) are clearly identified, confirming the carbon isotope stratigraphy previously developed in Site 1237 (Holbourn et al., 2007). Interestingly, CM3b (centered at 15.8 Ma) exhibits higher values than CM6, in contrast to records from shallower Pacific Sites 588, 1146, 1171 and 1237. This may reflect dampening of the $\delta^{13}C$ signal in IODP Site U1338, due to enhanced organic flux to the seafloor from intensified upwelling during CM6.

Orbitally-paced carbonate and organic flux fluctuations

XRF-derived carbonate and organic flux records indicate a strong orbital control on equatorial Pacific productivity and carbonate preservation over the middle Miocene (Figure 2). In particular, Log(Ba/Ca), Log(Si/Ca) exhibit a marked eccentricity beat between 16 and 14.6 Ma and between 13.8 and 13.1 Ma with eccentricity maxima reflected by peaks in the log ratios of these elements. We attribute these orbitally-modulated increases to decreased carbonate production/preservation during intervals of global warmth and reduced meridional overturning. However between 14.7 and 14.2 Ma (in the "obliquity world"), there is no clear phase relationship between $\delta^{18}O$ and XRF, suggesting an overall amelioration in carbonate preservation and deep water ventilation. The main glacial transition is characterized by two major spikes in Log(Ba/Ca), Log(Si/Ca), centered at 14.0 and at 13.9-13.8 Ma. The spike at 13.9-13.8 Ma is unusual, as it occurs during the phase of major ice growth at decreasing eccentricity and is accompanied by a massive increase in $\delta^{13}C$ at the onset of CM6. Furthermore, this interval is chracterized by a substantial increase in sedimentation rate (from ~3 to 7 cm/kyr), suggesting intensified terrigenous runoff from exposed shelves and increased biogenic silica production following the pronounced eustatic sea-level fall. A plausible scenario is that this spike reflects intensification of the Pacific equatorial upwelling and expansion an of the cold tongue, driven by stronger Pacific

meridional overturning circulation. We speculate that increased productivity in the equatorial eastern Pacific at the onset of CM6 contributed to atmospheric CO_2 drawdown, stimulating global cooling and favoring Southern Hemisphere ice expansion.

Outlook

We are currently completing stable isotope measurements in epifaunal benthic foraminifers (Planulina wuellerstorfi and Cibicidoides mundulus) over the early to middle Miocene interval in IODP Site U1337 (3° 50.009' N, 123° 12.352' W, 4463 m water depth; Figure 1). These results will be integrated with data from IODP Site U1338 to provide a continuous, high-resolution, astronomically-calibrated record over the interval 13-20 Ma. This work will contribute to improving the Cenozoic timescale, and will supply an essential chronological framework for future studies of Miocene climate, paleoceanography and evolutionary patterns. Our stable isotope records will also provide important information about ice volume fluctuations, Pacific deep-water characteristics and re-organizations in deep-water circulation associated with major climatic events (including the Miocene Climatic Optimum and Mi-1-3 glaciations). Ultimately, we will integrate our research with other postcruise studies to comprehensively explore the relationships between equatorial Pacific paleoproductivity, carbon isotope signals and the carbon cycle.

References:

Holbourn, A. E., Kuhnt, W., Schulz, M., Flores, J.-A., and Andersen, N., 2007. Middle Miocene long-term climate evolution: Eccentricity modulation of the "Monterey" carbon-isotope excursion. Earth and Planetary Science Letters. 261, 534-550. http://dx.doi.org/10.1016/j.epsl.2007.07.026.

Laskar J., Robutel, P., Joutel, F., Gastineau, M., Correia, A. C. M., and Levrard, B., 2004. A long term numerical solution for the insolation quantities of the Earth. Astronomy and Astrophysics, 428, 261-285.

Lyle, M., Olivarez Lyle, A., Gorgas, T., Holbourn, A., Westerhold, T., Hathorne, E., Kimoto, K. and Yamamoto, S., in press. Data report: raw and normalized elemental data along the Site U1338 splice from X-ray fluorescence scanning. In Pälike, H., Lyle, M., Nishi, H., Raffi, I., Gamage, K., Klaus, A., and the Expedition 320/321 Scientists, Proc. IODP, 320/321: Tokyo (Integrated Ocean Drilling Program Management International, Inc.).

Pälike, H., Lyle, M.W., Nishi, H., Raffi, I., Gamage, K., and Klaus, A., and the Expedition 320/321 Scientists, 2010. Proc. IODP, 320/321: Tokyo (Integrated Ocean Drilling Program Management International, Inc.). doi:10.2204/iodp.proc.320321.109.2010.

IODP

Petrological study of Basalts from Shatsky Rise Oceanic Plateau

(Site U1347, IODP Expedition 324)

A. HUSEN[1]*, R. R. ALMEEV[1], F. HOLTZ[1], J. KOEPKE[1], K.SHIMIZU[2], T.SANO[3], J.H.NATLAND[4]

[1]Institute of Mineralogy, Leibniz University of Hannover, Germany (*a.husen@mineralogie.uni-hannover.de)
[2]IFREE, JAMSTEC, Yokosuka, Japan
[3]National Museum of Nature and Science, Tokyo, Japan
[4]Rosenstiel School of Marine and Atmospheric Science, University of Miami, USA

Shatsky Rise Expedition 324

Large Igneous Provinces (LIPs) are constructs which are formed by enormous magma flux from the mantle to the lithosphere. They can be important indicators of fundamental processes of mantle convection and geodynamics, as well as major environmental changes and are crucial for understanding of the whole Earth system. It is widely accepted that oceanic plateaus arise from massive eruptions resulting from the arrival of a deep mantle plume head at the lithosphere. An alternative hypothesis invokes decompression melting of unusually fusible mantle beneath fast-spreading ridges.

Shatsky Rise is a unique oceanic plateau and a good object of study because it was formed in Late Jurassic and Early Cretaceous. In this period magnetic reversals preserved the evolution of the oceanic floor. Based on these magnetic isochrons it was possible to reconstruct Shatsky Rise's formation along the path of the Pacific-Farallon-Izanagi triple junction as described by e.g. Sager et al. (1999) and Nakanishi et al. (1999). They proposed an interaction of an arriving mantle plume with this spreading center. Mahoney et al. (2005) presented first geochemical data which contradicted the involvement of a mantle plume, because the isotopic and trace element data revealed rather MORB-like signatures. The major objective of the Integrated Oceanic Drilling Program Expedition 324

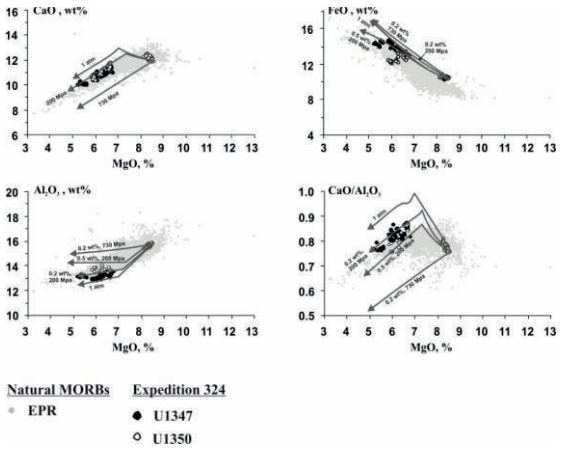

Figure 3: Compared to the natural EPR MORBs, the natural Shatsky Rise glasses are in the range of compositions but have high FeO and CaO/Al_2O_3 ratio. The calculated LLDs (COMAGMAT (Ariskin et al., 2004)) display the melt evolution during fractional crystallization. The best fit to the natural Shatsky Rise glasses is produced at 200 MPa.

(conducted in 2009) was to core the igneous rocks of Shatsky Rise to examine the age, physical volcanology, geochemistry, and tectonic evolution of this supervolcano (Sager et al., 2010, 2011).

Shatsky Rise consists of three distinct massifs (Tamu, Ori and Shirshov Massif), which are mostly constructed by massive flows and pillow lava basalts, with intercalated thin sedimentary layers. These three massifs are formed during different stages of Shatsky Rise evolution in the course of the northeast triple junction propagation. The most voluminous and the oldest massif is the TAMU Massif. Age and eruption volume are decreasing in the other massifs to the Northeast. Nakanishi et al. (1999) assumes an initial volcanism at the southwestern flank of the TAMU Massif. The younger (between M16 and M15) ORI Massif is located to the north of the TAMU Massif at the western side near the triple junction. The youngest (M16 - M15) and smallest Shishov Massif is located in the northeast of the ORI Massif. The northernmost construction of Papanian Ridge further propagates to the

Northeast, building an elongated extension of the Shatsky Rise and correspond to a waning of magmatic activity.

Recent post-cruise geochemical investigations of Shatsky Rise fresh glass samples (Sano et al., 2011; Shimizu et al., 2011) from four sites (U1346, U1347, U1348, U1350) revealed an existence of tholeiitic basalts broadly clustered into three geochemical magma groups - normal, low-Ti and high-K. Chemical compositions of the normal group are similar to those of N-MORB with slight depletion in HREE. The low-Ti group has slightly lower Ti, Fe, and Mn contents at a given MgO. The high-K basalts are characterized by distinctively high contents in K, Nb, and REEs, indicating that they are likely affected by enriched source mantle components (Sano et al., 2011).

TAMU Massif basalts: constraints from petrography, thermodynamic and experimental modeling

The samples from Shatsky Rise oceanic plateau rocks range in their composition from picritic basalts (15.6 wt% MgO) to more differentiated tholeiitic basalts (4.9-8 wt% MgO) located within the compositional field of East Pacific Rise MORBs. The glass compositions from Site U1347 and U1350 are shown in Fig. 1 (Sano et al, 2011). Rocks recovered in these drill cores are the least affected by alteration. The basalts from Site U1347 are more evolved (5.3-6.7 wt% MgO), whereas basalts from Site U1350 exhibit two compostional groups (first is similar to those from U1347, the second is more primitive having 8.1-8.5 wt% MgO). The higher-MgO rocks from U1350 have elevated FeO and low Al_2O_3 contents with decreasing MgO. The CaO/Al_2O_3 ratio increases in all basalts, indicating the melt evolution along Ol+Pl cotectic. The glass compositions from the more evolved rocks from both sites display depletion of FeO, CaO and Al_2O_3 concentrations with decreasing MgO. This results in a CaO/Al_2O_3 decrease, indicating the fractionation along Ol+Pl+Cpx cotectics.

In the course of our study we focused mainly on samples from the Site U1347 at TAMU Massif (77 thin sections, containing 41 quenched glasses). Here we present first results obtained after petrographical characterization of the cored samples, the chemical analyses of the glass rinds (for major elements and H_2O-CO_2), the chemical analyses of minerals and mineral intergrowths. Chemical data were also used to estimate pre-eruptive conditions of the basaltic magmas and to compare geochemical characteristics (obtained by other groups).

Methods

The major element compositions of the mineral phases are measured with the electron probe micro analyzer (EPMA) at the Institute of Mineralogy in Hannover (Cameca SX100). For mineral analyses a beam current of 15nA were used for a focused beam. The peak counting time was 10s for all elements (Si, Ti, Al, Fe, Mn, Mg, Ca, Na, K, Ni). Glasses were measured also with 10nA, using defocused beam size (5-10 µm). The counting times were 20 seconds for all major elements (Si, Ti, Al, Fe, Mn, Mg, Ca, Na, K). Cl and S were measured with 40nA for 60s.

Glass H_2O and CO_2 determinations were performed by Fourier Transformation IR (FTIR) spectroscopy (Bruker IFS88 FTIR, University of Hannover). For these measurements doubly polished glass fragments with a size of approximately 1mm³ from the natural chilled margins were used. For each core sample chips of 145-150 and 40-50 µm thickness were used. The thicknesses were measured with a digital micrometer (Mitutoyo, precision: ≤2µm). The spectrometer was coupled together with an IR-Scope II optical microscope. Before measuring the quality of the measured glass volume was controlled whether scratches, crystals or pores are present. (Operation conditions: MCT narrow range detector, globar light source and KBr beamsplitter)

The H_2O concentration was measured at the peak which is attributed to the OH stretch vibration (3550 cm^{-1}) with a typical molar absorptivity of 67 l/mol-cm for basaltic glasses (Stolper 1982). On each sample three spectra with a spot size of 100 x 100 µm were taken every spectrum was the average of 50 scans. The density was assumed to be a typical value for basalic glasses, 2815 g/l. The calculation of the H_2O concentrations was calculated depending on the peak height, which was determined referring a straight tangential base line.

Petrography

The samples cored at Site U1347 delivered mostly differentiated tholeiitic basalts from both massive flow and pillow units. In general, the rocks form Site U1347 are less altered, though sometimes the glasses show altered relicts. Some samples have veins with higher degree of alteration with calcite, zeolites or chlorite as alteration minerals. The textures and mineral assemblages are very similar in all lava flows. They are bordered by glassy rims, followed by a zone of transition, where crystallites form spherulitic bodies around phenocrysts. The inner parts are holocrystalline whith increasing crystal sizes to the core. The basalts show phenocrysts of Pl and Cpx within a matrix of intergranular textrure. Some samples show calcite pseudomorphs after Ol. There are three different groups of mineral associations: (1) coarse grained Pl phenocrysts/ glomerocrysts (up to 0.5 mm, discontinuously normal or multiple zoned) with many inclusions, (2) fine grained Pl and Cpx subphenocrysts which show evidence of undercooling (embayments, inclusions, skeletal growth) and form sometimes clots of radiate intergrowth (skeletal, columnar, discontinuously normal and/or sector zoned), (3) crypto- to microcrystalline groundmass, containing Mt, Pl, Cpx (dendritic and skeletal).

In the quenched glasses volatiles (H_2O, CO_2) were determined by FTIR spectroscopy. H_2O concentrations vary between 0.18 and 0.6 wt%. CO_2 concentrations are below the detection limit of the FTIR method (<50 ppm) indicating the degassing depths corresponding to pressures (<50MPa) (Shishkina et al. 2010). As shown in Fig. 1, the basaltic glasses from Site U1347 are evolved tholeiitic basalts (5.2-6.8 wt% MgO), corresponding in composition typical East Pacific Rise (EPR) MORBs. However they have very distinct high FeO and low SiO_2 and Al_2O_3 concentrations. Their CaO/Al_2O_3 ratios are amongst the highest known for MORBs, which may be related to their very low pressures of partial crystallization.

Geothermobarometry

To prove the assumption of low pressure cotectics for Shatsky Rise basalts, we used the COMAGMAT program to simulate conditions of partial crstallization following the method outlined in (Almeev et al., 2008). At first, assuming ideal fractional crystallization, we calculated liquid lines of descent (LLDs) of one of the most primitive basaltic glass compositions found so far (U1350A 24R2 31-33). We tried to reproduce the general trend of Shatsky

Rise glass compositions by varying initial pressure and H_2O content. In a second set of calulations, we simulated for individual glass compositions the conditions of multiply saturation (Ol+Pl+Cpx), assuming that the natural liquids experience crystallization along Ol+Pl+Cpx cotectics. The point of multiply saturation is believed to provide thermodynamic conditions and the composition in equilibrium with Ol+Pl+Cpx just before eruption. The knowledge about H_2O concentration is crucial for this approach because it strongly influences the liquidus of the melts.

Both approaches revealed low pressures and temperatures of the TAMU Massif magma storage system. Modeled LLDs for 200 MPa (0.2 wt% initial H_2O, QFM) reproduced roughly the natural glass compositions (Fig. 1). The calculated P-T conditions for Ol-Pl-Cpx multiply saturation range from 1110 to 1170°C and from 0 to 310 MPa, which represent the maximum values, since Ol is scarcely observed in natural Pl-Cpx-phyric lavas.

Based on the geochemical data, five groups of rocks were distinguished along the drilled profile (Sano et al., 2011). Their H_2O and MgO concentrations are compared to the lithological profile in Fig. 2, where the corresponding modeled thermodynamic conditions are displayed as well. Although the calculated temperatures and pressures vary in a relatively small range compared to the error of the COMAGMAT model (±15°C, ±100MPa), a clear trend for thermodynamic conditions is produced for the individual groups. Our data allow us to assume that there were different magmatic periods characterized by variations in eruption styles (massive flows or pillow lavas) and chemical compositions (including the regime of volatiles) which were also recorded in their P-T conditions of partial crystallization. These different events are chronological interupted by sedimentary layers. For example between group 4 and 3 the compositions shift to more primitive compositions and both temperature and pressure increase by 40°C and 150 MPa. The shift in P-T conditions is accompanied by a subsequent thick sedimentary layer, representing a discontinuity in the magmatic sequence, indicating different periods of mamga productiviy.

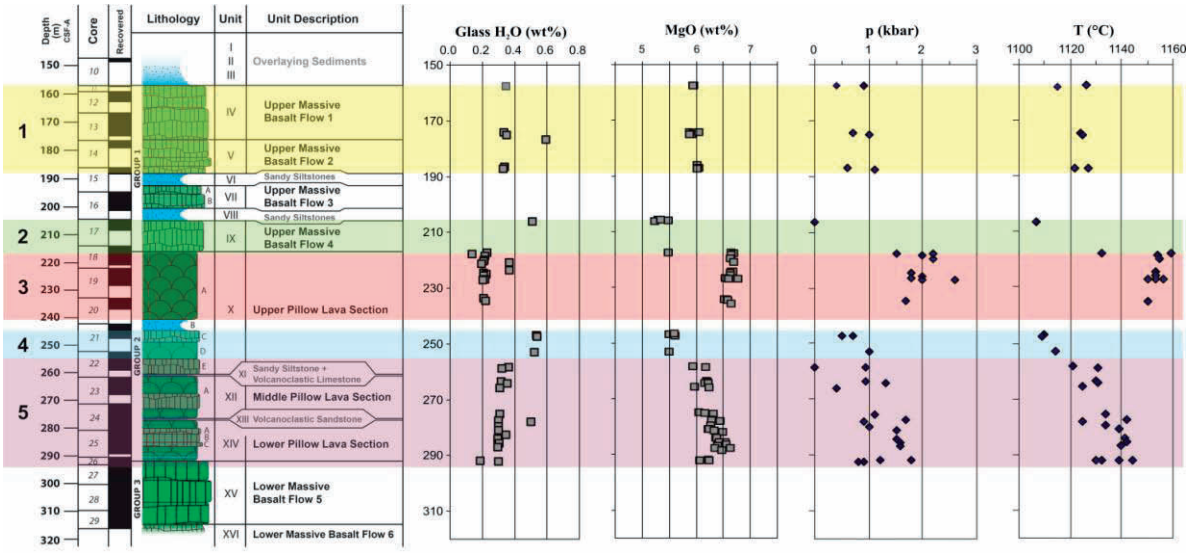

Figure 4: The geochemical groups (1-5) (Sano et al., 2011; Shimizu et al., 2011) correlate to the lithological units and represent destinct intervals of magmatic activity which produced basalts varying in eruption style, H_2O and major element concentrations and thermodynamic history.

It should be noted, that glass samples are rare in those units which are formed by massive flows. To estimate P-T conditions of glass-free samples we tried to develop and apply a new method for the estimation of thermodynamic parameters, using compositions recorded in phenocryst chemistry. We measured the compositions of coexisting Pl and Cpx (~30 samples studied), which often occur intimately intergrown in clots indicating simultaneous growth of these two minerals. During ongoing crystallization the mineral compositions evolve from high to low An (mol%) in Pl and high to low #mg in Cpx. The comparison of coexisting pairs (mol% An in Plag versus #mg in Cpx) shows two compositional evolutionary trends. Even though one trend can be reproduced as a result of ideal fractional crystallization at pressures between 0.5 and 3 kbar (simulated by COMAGMAT), the calculated mineral compositions do not correlate with their natural counterparts. Simulated Pl compositions have higher An content for given mg# in Cpx. This discrepancy and the second compositional trend are the objects of our ongoing investigations.

First experiments

In addition to the calculated models, we started to simulate crystallization processes experimentally. For this approach an appropriate method has to be applied to simulate nominally dry conditions at oxygen fugacities corresponding the quartz-fayalite-magnetite buffer (QFM), which correspond to the natural system. This was realized using graphite-lined double capsules (inner graphite and outer Pt capsules) which can maintain very low water activities (H_2O in melt <0.2 wt%). The oxygen fugacity was buffered by graphite-COH equilibrium in most runs.

Two samples representing different stages of magma evolution were used as starting materials: one natural glass (SR1347a, 7.4 wt% MgO) and one synthetic analogue of a natural glass composition (AH2, 8 wt% MgO). First experimental series were performed in an Internal Heated Pressure Vessel (IHPV) at 1175°C (±15°C) and at pressures of 100, 500 and 700 MPa (±5 MPa).

The natural mineral assemblage (Ol+Pl+Cpx) was reproduced only in AH2 at 500 and 700 MPa. In sample

SR1347a Pig crystallized together with Pl instead of Cpx and Ol at both 500 and 700 MPa. In all 100 MPa experiments we observed precipitation of pure Fe droplets indicating strongly reduced conditions. This observation supports the known strong pressure dependence of the graphite-COH buffer. Thus, for future low pressure experiments another technique to simulate crystallization at dry conditions has to be developed.

Conclusion

Our new data imply typical MORB-like characteristics for the TAMU Massif basalts. The glass compositions of the samples from Site U1347 and U1350 are in the field of EPR MORB and follow a trend which fits to typical MORB-type tholeiitic LLDs. However, considered collectively, tholeiitic basalts from Shatsky Rise (U1347A, U1350A) demonstrate compositions slightly off the trend of typical MORB (low SiO_2, high FeO). Preliminary results of geothermobarometry lead to the assumption that the magmas were stored at relatively low pressures (1atm-300 MPa). The mechanisms which led to the whole range of Shatsky Rise basalts cannot be attributed to fractional crystallization only. The presence of distinct groups of basalts, which differ in their geochemical characteristics implies the formation of individual magma batches, which were stored at shallow depth.

References

Almeev, R., F. Holtz, et al. (2008). "Depths of partial crystallization of H2O-bearing MORB: Phase equilibria simulations of basalts at the MAR near Ascension Island (7-11 degrees S)." Journal of Petrology 49(1): 25-45.

Ariskin, A.A., and Barmina, G.S. (2004) COMAGMAT: development of a magma crystallization model and its petrological applications. Geochemistry International, 42(Suppl. 1), S1–S157.

Mahoney, J. J., R. A. Duncan, et al. (2005). "Jurassic-Cretaceous boundary age and mid-ocean-ridge-type mantle source for Shatsky Rise." Geology 33(3): 185-188.

Nakanishi, M., W. W. Sager, et al. (1999). "Magnetic lineations within Shatsky Rise, northwest Pacific Ocean: Implications for hot spot-triple junction interaction and oceanic plateau formation." Journal of Geophysical Research 104(B4): 7539-7556.

Sager, W. W., J. Kim, et al. (1999). "Bathymetry of Shatsky Rise, northwest Pacific Ocean: Implications for ocean plateau development at a triple junction." Journal of Geophysical Research 104(B4): 7557-7576.

Sager, W.W., Sano, T., Geldmacher, J., and Expedition 324 Scientists. (2010) Expedition Reports Shatsky Rise Formation. Proceedings IODP, Vol. 324.

Sager, W.W., Sano, T., and Geldmacher, J. (2011) How Do Oceanic Plateaus Form? Clues From Drilling at Shatsky Rise. EOS, 92(5), 37-44.

Shimizu, K., Kimura, J.-I., Chang, Q., and Sano, T. (2011) Geochemical study of fresh volcanic glasses from ~145 Ma Shatsky Rise. Mineralogical Magazine (Goldschmidt Abstracts 2011), 75(3), 1861.

Shishkina, T. A., R. E. Botcharnikov, et al. (2010). "Solubility of H_2O- and CO_2-bearing fluids in tholeiitic basalts at pressures up to 500MPa." Chemical Geology 277: 115-125.

Stolper, E. (1982). "Water in silicate glasses: An infrared spectroscopic study." Contributions to Mineralogy and Petrology 81(1): 1-17.

ICDP

Frictional Behavior of the Alpine Fault, New Zealand, Sampled by DFDP Drilling

M.J. IKARI[1*], B.M. CARPENTER[2], A.J. KOPF[1°], C. MARONE[2], D.M. SAFFER[2], R. OBERHÄNSLI[3], V.G. TOY[4]

[1] MARUM, Universität Bremen, Leobener Str., 28359 Bremen, Germany
[2] Pennsylvania State University, Dept. of Geosciences, University Park, PA 16802, USA
[3] Universität Potsdam, Karl-Liebknecht-Str. 24, 14476 Potsdam, Germany
[4] University of Otago, Geology Dept., Leith Walk, Dunedin 9054, New Zealand
* mikari@marum.de, ° akopf@marum.de

The Alpine Fault, New Zealand, moved into the focus of ICDP research a few years ago when a workshop was held to plan for an ICDP drilling proposal. In parallel, groups in New Zealand (mostly GNS Science), the UK (Univ. Liverpool) and Germany (MARUM Bremen and Univ. Potsdam) sensed that there would be substantial benefit from drilling a pair of shallow (<200 m) pilot holes across the fault before the ICDP effort is started. The latter has now grown into a well perceived full drilling proposal, which is close to the transition into a drilling project (termed DFDP-2).

The pilot drilling, termed DFDP-1 (Deep Fault Drilling Project, Alpine Fault), took place in January/February 2011 near the world-class outcrop of Gaunt Creek and resulted into two shallow holes a few meters apart. Hole DFDP-1A was a little over 100 m deep, while hole DFDP-1B was >150 m deep. The principal slip surface of the Alpine Fault, separating Quarternary gravels from the overlying sequence of cataclasites, was recovered at ~90 m and 128 m, respectively (Figure 1). Core quality was beautiful in either case, and recovery was near perfect in that highly tectonized zone.

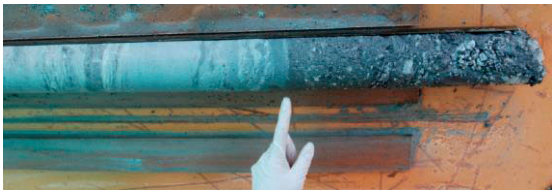

Figure 1: Principal slip surface of the Alpine Fault, identified in a core sample. PSS separates cataclasites from underlying gravel.

All cores underwent Multi-Sensor Core Logging as well as core description and are currently curated and stored at Univ. Otago, NZ. Sample requests were handled by a Sample Allocation Committee, and specimens of various kinds (rubble to whole core sections) were distributed among an international group of experts for further study. At MARUM, we received ~20 samples for frictional testing of the fault zone materials and rocks from the hanging wall and footwall. In addition, field campaigns served to get surface samples from outcrops of the Alpine Fault and adjacent rocks in various places on the South Island of NZ. The idea was to look at regional variability of the fault gouge and associated strata and how surface outcrops may differ from the drill core.

Specimens underwent geotechnical testing as dry powders in a triaxial direct shear apparatus as well as water-saturated in a rotary shear apparatus.

In the direct shear system, we measured the frictional properties of 8 wall rock samples recovered from the Alpine Fault during the first phase drilling, DFDP-1A, spanning a depth range of ~67-96 m. Additionally, we tested one outcrop sample of clay-rich material recovered from a surface exposure of the fault near Gaunt Creek to represent the actively shearing portion of the fault zone. All samples were powdered and remolded, and deformed in direct shear at room temperature and humidity. Two sets of tests were conducted: in the first set, the normal stress was increased in a stepwise fashion from 10-100 MPa, and sheared at a constant velocity of 11 µm/s in order to determine the failure envelope. In the second set of tests, each sample was sheared at a constant normal stress of 30 MPa at 11 µm/s until attainment of ~15 shear strain. We

then conducted a velocity-stepping procedure in the range 1-300 µm/s in order to measure rate-dependent frictional properties, and also a slide-hold-slide procedure in order to measure the rate of frictional healing with hold times ranging from 1-1000s.

We find that the strength of the wall rock samples is uniform, with friction ceofficients ranging from ~0.6-0.65. The outcrop sample representing the fault core, however, is slightly weaker with a coefficient of friction of ~0.5-0.6. Velocity-weakening behavior is consistently observed in the wall rock samples, however, the outcrop fault core sample exhibits velocity-strengthening. This indicates that seismic slip will likely be decelerated by the clay-rich material at the surface; however at depth it may be likely that the cataclasites and mylonites that compose the majority of the Alpine Fault assemblage are responsible for earthquake nucleation. Significant rates of healing are observed in all samples, suggesting that the fault easily regains its strength during interseismic periods.

Rotary shear tests at effective normal loads up to 20 MPa were carried out on six different outcrop samples spanning from Fault Creek, Saddle Creek, Hare Mare and Martyr River. The results confirm the general observation that clay-rich gouge shows velocity-strengthening behaviour. In the water-saturated experiments, however, friction coefficients drop significantly to between µ=0.27 - 0.38 (Fault Creek, Hare Mare) and 0.48 - 0.51 (Martyr River, Saddle Creek). While all samples show strain hardening during rotary testing (~45-60 shear strain), the phyllosilicate-rich gouge samples from Hare Mare and Gaunt Creek (base of gouge zone represents PSS) are weaker than the other materials and are characterised by velocity-strengthening. The data suggest that slip updip is likely aseismic whereas earthquake nucleation occurs within the cataclasites in the vicinity of the gouge surface.

Future laboratory work will cover dry rotary shear experiments for comparison between the two sets of experiments, and heated, water-satured direct shear tests at up to 200 MPa effective normal stress and temperatures well within those expected in the seismogenic zone to simulate expected conditions reached by DFDP-2 drilling by ICDP, or even deep drilling to ~4-5 km (DFDP-3) in a couple of years time.

IODP

Shear and Cohesive Strength of Sediments Approaching the Nankai Trough, NanTroSEIZE Sites C0011 and C0012, IODP Expeditions 322 and 333

M.J. IKARI*, A. HÜPERS, A.J. KOPF

[1]MARUM, Universität Bremen, Leobener Str., 28359 Bremen
*mikari@marum.de

In subduction zones, the shear strength of sediments controls the overall structure and geometry of the accretionary prism, and also controls faulting and fault slip behavior. We measure the shear strength of sediments on the subducting plate approaching the Nankai subduction zone offshore Japan, seaward of the deformation front. Samples were cores of intact material obtained from Sites C0011 and C0012 during IODP Expeditions 322 and 333 at depths of up to 406 mbsf. Each sample was sheared in a direct-shear apparatus at in-situ effective vertical stress conditions, calculated from shipboard density and porosity measurements. We also directly measure the cohesion of the sediment by measuring its shear strength with no applied effective normal stress ($\sigma n' = 0$). Two cohesion measurements were made in each experiment, one prior to shearing under load and one after shear displacements of ~8-10 mm. We interpret the cohesion measured after shearing under load to be the cohesive strength that exists throughout the shearing process, suggesting that in some cases the coefficient of internal friction should be used rather than the coefficient of sliding friction. For most samples, we observe a strong peak in the coefficient of friction at ~0.6 that decays to lower values of ~0.3. The low residual friction values are consistent with the clay-rich lithology of our samples, and the pronounced peak is characteristic of smectite, which represents ~40% of the bulk composition. In contrast, a sand-rich sample exhibited no peak, high friction, and high cohesion. This suggests active diagenesis resulting in advanced cementation and enhanced cohesive strength in this sample. Coulomb wedge theory dictates that the taper angle of accretionary wedges depends on the internal friction of the wedge, the basal sliding friction of the décollement, and the amount of excess pore pressure in these locations. Cohesion is typically neglected in such analyses. In the case of the Nankai subduction zone, cohesion should not negligible based on our experimental results. This is the case even along the décollement where active slip occurs, because even sheared sediment exhibits significant cohesion. Cohesion that is maintained during shear sliding is not considered in the classical Coulomb-Mohr failure criterion, therefore we present a modified failure law to account for this quantity. We suggest that high cohesive strength may affect wedge taper angle, faulting in the prism, and the amount of pore pressures that are maintained within the wedge and in the décollement. Ongoing experiments include continued cohesion and friction measurements of natural material sampled from the Nankai subduction zone during Integrated Ocean Drilling Program Expeditions 322 and 333.

ICDP

Carbon cycling at the Archean Proterozoic Transition

C. J. ILLING[1*], H. STRAUSS[1], R.E. SUMMONS[2], A.E. FALLICK[3] AND V.A. MELEZHIK[4,5]

[1] Institut für Geologie und Paläontologie, Westfälische Wilhelms-Universität, Münster, Germany
[2] Department of Earth, Atmospheric and Planetary Sciences, Massachusetts Institute of Technology, Cambridge, USA
[3] Scottish Universities Environmental Research Centre, Glasgow, United Kingdom
[4] Geological Survey of Norway, Trondheim, Norway
[5] Centre for Geobiology, University of Bergen, Bergen, Norway
[*]e-mail: christian.illing@uni-muenster.de

The global carbon cycle is strongly driven by the biological processes of carbon fixation and organic carbon recycling which in turn are affected by changes in environmental conditions. Proxies for such changes are potentially preserved in the carbon isotopic composition of carbonates ($\delta^{13}C_{carb}$) and organic matter ($\delta^{13}C_{org}$)(e.g. Des Marais, 2001).

The Archean-Paleoproterozoic transition (APT) represents a time interval in Earth history that witnessed fundamental changes in surface environmental conditions such as the oxygenation of Earth's atmosphere (i.e. the Great Oxidation Event – GOE, cf. Holland, 2006). Moreover, two of the earliest pertubations of the global carbon cycle happened during this time: the Lomagundi-Jatuli Event (Melezhik et al., 1999a; 2005; 2007) and the Shunga Event (Melezhik et al., 1999a; 2005; 2009). The former is characterized by the occurrence of ^{13}C enriched carbonates whereas the latter reflects the deposition of unprecedented amounts of organic matter. Both events have been preserved in the Paleoproterozoic sedimentary succession in Fennoscandia investigated by the multinational ICDP project FAR-DEEP (Fennoscandian Arctic Russia - Drilling Early Earth Project; Melezhik et al., 2005). The FAR-DEEP recovered fifteen drill cores with a total length of 3650 m. Cores were retrieved in three areas in northern Russia, namely the Imandra/Varzuga and Pechenga greenstone belts and the Onega Basin and cover a time interval of some 600 million years.

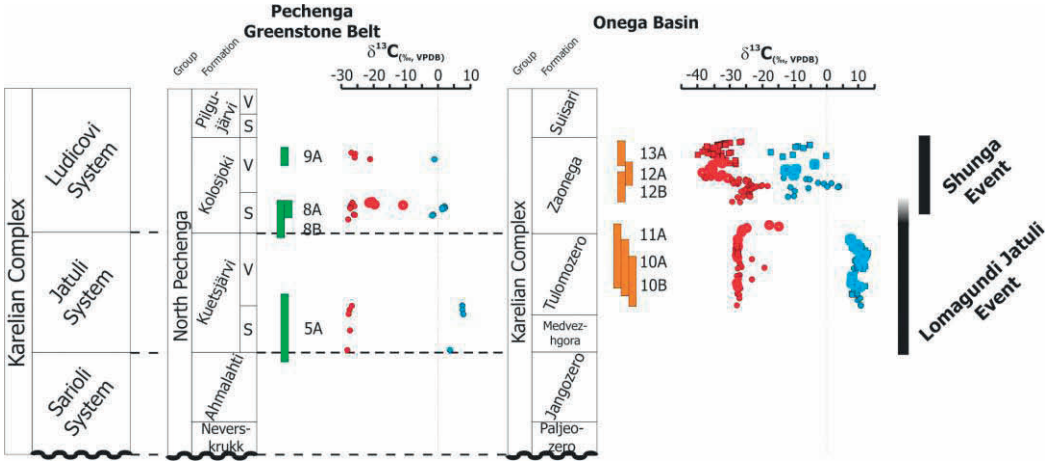

Figure 1: Carbon isotopic composition of bulk organic matter (δ13Corg; red) and whole-rock carbonate (δ13Ccarb; blue) for cores retrieved by FAR-DEEP from the Pechenga Greenstone Belt and the Onega Basin (chronostratigraphic correlation after Melezhik & Hanski, in preparation). Cored intervals are marked by coloured boxes (green: Pechenga Greenstone Belt, orange: Onega Basin; core numbers are listed next to it). The time interval of the Lomagundi Jatuli Event is marked on the right side.

During this work carbon isotopes dataset for sedimentary organic matter ($\delta^{13}C_{org}$) from all major sedimentary formations cored by FAR-DEEP have been measured. Moreover, organic carbon isotope analyses were paralleled by carbonate carbon isotope measurements, providing paired datasets for $\delta^{13}C_{org}$ and $\delta^{13}C_{carb}$. Thereby, the organic carbon isotopic composition mainly reflects the biological processes of primary production and recycling whereas the isotopic composition of carbonate carbon is a good proxy for the isotopic composition of atmospheric carbon dioxide. Important information in respect to the operation of the global carbon cycle can be gained from the isotopic difference ($\delta^{13}C$) between $\delta^{13}C_{carb}$ and $\delta^{13}C_{org}$. This parameter comprises the carbon isotope fractionation associated with biological carbon fixation, but has also archived any subsequent postdepositional alteration of this primary siganture.

The total variation in $\delta^{13}C_{org}$ recorded for the FAR-DEEP samples studied so far ranges between -40 and -17 ‰ which agrees well with previously published data for the observed period (e.g. Thomazo et al., 2009). Samples from the Imandra/Varzuga Greenstone Belt reveal a relatively constant isotope record, and neither of the above mentioned perturbations of the global carbon cycle is discernible from the record. The successions from the Pechenga Greenstone Belt and the Onega Basin cover the Shunga event and the Lomagundi-Jatuli Event (Fig. 1).

The Shunga Event is archived in drillcores 8A, 8B, and 9A (Kolosjoki Fm, Pechenga Greenstone Belt) and 11A (upper part) 12A, 12 B, and 13A (Zaonega Fm., Onega Basin). The succession hosting the Shunga Event includes a shift to negative $\delta^{13}C_{carb}$ values, and the carbon isotope record was described recently as the "Shunga-Francevillian" anomaly by Kump et al. (2011). These authors attribute this shift in $\delta^{13}C$ to oxidative weathering of organic-rich rocks (Kump et al., 2011).

The Kolosjoki and the Zaonega formations are underlain by the lower Kuetsjärvi Formation (core 5A, Pechenga Greenstone Belt) and the Tulomozero Formation (cores 10A, 10B, 11A, Onega Basin). They record the Lomagundi-Jatuli Event with its characteristically high $\delta^{13}C_{carb}$ values (up to + 12‰). Interestingly the $\delta^{13}C_{org}$ record is not changing compared to the succession prior and after the Lomagundi-Jatuli Event, causing significantly higher $\Delta^{13}C$ values (between 30 and 37‰) for this time interval.

The broadly parallel evolution of $\delta^{13}C_{org}$ and $\delta^{13}C_{carb}$ prior to and after this period indicates that respective perturbations affected the entire global carbon cycle, the apparent decoupling of both carbon isotope records during the time of the Lomagundi-Jatuli Event remains enigmatic. Brasier et al. (2010) studied the Tulomozero Formation carbonates and revealed the robustness of their isotopic composition. This makes a secondary overprint of this signal as the principal cause for this enigmatic temporal evolution unlikely.

Initially, the Lomagundi-Jatuli Event was thought to be caused by an enhanced deposition of organic matter linked to Earth's oxygenation. Consequently, in a steady-state system, this would mean that the atmospheric CO_2 becomes very enriched in ^{13}C. But as mentioned above the

examined succession shows a more or less constant organic carbon signal. The organic carbon isotopic record appears to be relatively robust against alteration, at least compared to other geochemical biosignatures. Even though it is important to keep in mind that high thermal maturity of organic matter is associated with a change in the isotopic composition that could overprint the original isotope signature. This would affect samples with low total organic carbon content (TOC) more than samples characterized by a higher TOC. However, new samples reveal no discernible correlation between a lower TOC and a higher $\delta^{13}C_{org}$ value (Fig. 2).

Considering that this succession resembles a more or less shallow-water environment, it is unlikely that the source for the biological fixed carbon is decoupled the atmospheric signal. Consequently, the carbon isotope enrichment recorded for the carbonates cannot be explained simply by an increased depletion of the carbon pool due to an extreme increase in the burial of organic matter. Another argument invoked to explain the Neoproterozoic excursions, like a much larger dissolved organic carbon pool (Rothman et al., 2003) is also not a likely explanation, since this would not explain the "decoupling" between the carbonate and the organic carbon isotope records observed here.

Other factors that might have caused or influenced $\Delta^{13}C$ include a higher pCO_2 that would lead to a higher biological fractionation, but also influence the ocean acidity or an increase in heterotrophy that would ultimately cause a depletion in $\delta^{13}C_{org}$.

A plausible assumption would be that the excursion records a higher bioproductivity and probably a higher burial, but not exclusively. The $\delta^{13}C_{org}$ record is very likely decreased by a higher secondary production and $\delta^{13}C_{carb}$ is locally amplified as reported earlier by Melezhik et al. (1999b). This explanation would also help to solve the paradox of an oxygen overshoot and the extreme demand in nutrients resulting from a model favoring a steady-state system with an extraordinary burial of organic matter, since it lowers the necessary fraction of organic carbon.

References:

Brasier, A. T., Fallick, A. E., Prave, A. R., Melezhik, V. A., and Lepland, A. (2011): Coastal sabkha dolomites and calcitised sulphates preserving the Lomagundi-Jatuli carbon isotope signal. Precambrian Research 189(1-2), 193–211.

Des Marais, D.J. (2001): Isotopic evolution of the biogeochemical carbon cycle during the Precambrian. Reviews in Mineralogy and Geochemistry 43, 555 – 578.

Holland, H.D. (2006) The oxygenation of the atmosphere and oceans. Philosophical Transactions of the Royal Society of London, Series B-Biological Sciences B361: 903-915.

Kump, L. R., Junium, C., Arthur, M. A., Brasier, A., Fallick, A., Melezhik, V., Lepland, A., et al. (2011): Isotopic evidence for massive oxidation of organic matter following the great oxidation event. Science, 334(6063), 1694–1696.

Melezhik, V.A., Fallick, A.E., Filipov, M.M. and Larson, O.(1999a): Karelian Shungite-an indication of 2000 Ma-year-old metamorphosed oil-shale and generation of petroleum: geology, lithology and geochemistry. Earth Sci. Reviews 47, 1 – 40.

Melezhik, V.A., Fallick, A.E., Medvedev, P.V. and Makarikhin, V.V. (1999b): Extreme δ13Ccarb enrichment in ca 2.0 Ga magnesite-stromatolite-dolomite-'red beds' association in a global context: a case for the worldwide signal enhanced by a local environment. Earth Sci. Reviews 48, 71 – 120.

Melezhik, V.A., Fallick, A.E., Hanski, E., Kump, L., Lepland, A. Prave, A. and Strauss, H. (2005): Emergence of the aerobic biosphere during the Archean-Proterozoic transition: Challenges of future research. GSA Today 15, 4 – 11.

Melezhik, V.A., Huhma,H., Condon, D.J., Fallick, A.E. and Whitehouse, M.J. (2007): Temporal constraints on the Paleoproterozoic Lomagundi-Jatuli carbon isotopic event. Geology 35, 655 – 658.

Melezhik, V.A., Fallick, A.E., Filipov, M.M., Lepland, A., Rychanik, D.V., Deines, J.E., Medvedev, P.V., Romashkin, A.E. and Strauss, H. (2009): Petroleum surface oil seeps from Palaeoproterozoic petrified giant oilfield. Terra Nova 21, 119 – 126.

Rothman, D., Hayes, J., and Summons, R.E. (2003): Dynamics of the Neoproterozoic carbon cycle. Proceedings of the National Academy of Sciences of the United States of America, 100(14), 8124–8129.

Thomazo, C., Pinti, D. L., Busigny, V., Ader, M., Hashizume, K., and Philippot, P. (2009): Biological activity and the Earth's surface evolution: Insights from carbon, sulfur, nitrogen and iron stable isotopes in the rock record. Comptes Rendus Palevol, 8(7), 665–678.

IODP

Late-stage mineral veins as recorders of fluid and temperature conditions in the footwall of an oceanic detachment fault (ODP Leg 304/305)

N. JÖNS[1*], W. BACH[1], M. ROSNER[1,2,3], B. PLESSEN[2]

[1]Department of Geosciences, University of Bremen, Germany (*correspondence: njoens@uni-bremen.de)
[2]Helmholtz-Zentrum Potsdam / GFZ, Potsdam, Germany
[3]FB Geowissenschaften, Freie Universität Bremen

Oceanic crust formed at slow- und ultraslow-spreading ridges (<55mm/yr half spreading rate) shows an anatomy that is distinct from layered cake-type crust formed at fast-spreading ridges. While the extension at fast-spreading ridges is accommodated by magmatism, slow-spread crust forms in a setting of tectonically driven extension with only episodic magmatism. Large-offset oceanic detachment faults and oceanic core complexes are characteristics of slow-spreading mid-ocean ridges. Here - in contrast to fast spreading environments - fault zones facilitate the influx of seawater-derived fluids into the deep crust, and interaction of these fluids with ultramafic, mafic or even felsic rocks at different temperatures leads to diverse types of fluid-rock interaction in depth, and a range of different types of hydrothermal systems at the seafloor. To understand this diversity and the effects of fluid-rock interaction on chemical and heat budgets, we study late-stage mineral veins that occur in samples from the Atlantis Massif.

The Atlantis Massif is an oceanic core complex situated at the Mid-Atlantic Ridge at ca. 30°N. IODP Leg 304/305 Hole U1309D drilled into the footwall of the detachment fault, which is related to exhumation of the core complex. It is mainly composed of gabbros and troctolites, with minor amounts of basaltic and ultramafic rocks. The 1416 m long drilled section is fractured and shows an intense retrograde overprint recorded by granulite- to zeolite-facies mineral assemblages. Late-stage mineral veins (consisting of anhydrite, calcite, prehnite or zeolite) formed from sub-seafloor fluid-rock interactions. In order to further our understanding of the fluid regime and temperature conditions in detachment fault systems, we performed a detailed mineral chemical and isotopic study of these mineral veins.

Syn- to postkinematic calcite veins are abundant. Calcite is characterized by low concentrations of incompatible elements (e.g., U, Li, Sr) and flat chondrite-normalized REE+Y patterns with positive Eu anomalies. The fluids from which the calcite precipitated were likely similar to basalt-hosted hight-T vents and no affinity to the nearby serpentinization-derived Lost City vent field is observed. The deep origin of the fluids is highlighted by low $^{87}Sr/^{86}Sr$ (0.704 to 0.708), mantle-like $\delta^{7}Li_{LSVEC}$ (+0.8 to +9.4‰) and $\delta^{13}C_{PDB}$ (-6 to -2‰). The $\delta^{18}O$ values point to calcite precipitation temperatures of 150-220°C.

Anhydrite and anhydrite + zeolite veins have $^{87}Sr/^{86}Sr$ values consistent with anhydrite formation from down-flowing seawater which had leached only minor amounts of Sr from the basement. The REE pattern of anhydrite veins indicate that admixed hydrothermal fluids at depth played a minor role. The deepest section of Hole 1309D is dominated by veins consisting of silicate minerals (prehnite, quartz, plagioclase). These veins indicate precipitation temperatures ranging from 270 to 145°C (estimated from $\delta^{18}O$ values). They are comparatively unradiogenic in $^{87}Sr/^{86}Sr$ (0.7033-0.7046) and demonstrate (in contrast to anhydrite) enhanced intensity of reactions between infiltration seawater and basement with increasing depth.

In summary, critical insights into the fluid regime and temperature conditions within the detachment fault footwall during formation of the Atlantis Massif oceanic core complex are provided by late-stage mineral veins from Leg 304/305 Site U1309D. The lack of systematic isotopic downhole trends does not allow for estimation of a geothermal gradient, but indicates that already conductively cooled basement fluids are responsible for precipitation of vein minerals. Furthermore, the fluid chemistry of the nearby Lost City vent field is dominated by ultramafic rocks, while the U1309D calcite veins point to fluids with affinities to basalt-hosted hydrothermal systems. This finding emphasizes that the heterogeneous composition of slow-spreading crust offers possibilities for pronounced differences in hydrothermal systems on small spatial and/or temporal scales. Additionally, although rocks below the detachment fault surface are strongly tectonized, the seawater influence on the fluids is insignificant and thus dominantly mantle carbon is sequestered within the examined calcite veins.

IODP

Late Campanian to Maastrichtian palaeoceanographic changes in the tropical Pacific

C. JUNG[1], S. VOIGT[1],O. FRIEDRICH[1], M. FRANK[2]

[1]Goethe-University Frankfurt, Institute of Geosciences, Altenhöferallee 1, 60438 Frankfurt am Main, Germany
[2]Helmholtz Centre for Ocean Research Kiel, GEOMAR,Wischhofstr. 1-3, 24148 Kiel, Germany

The latest Cretaceous was a period of long-term climate cooling succeeding the extreme warmth of the mid-Cretaceous greenhouse world. The cooling is mainly considered as a result of changes in ocean circulation due to plate-tectonic movements resulting in progressive deep-water exchange between the deep oceanic basins and a parallel drop in pCO_2 concentrations. The aim of this project is the reconstruction of changes in ocean circulation and deep-water formation in the tropical Pacific (Shatsky Rise) relative to carbon isotope events in the latest Campanian to late Maastrichtian carbon isotope events (CMBE and MME). The main objectives of this project are 1) to develop a high-resolution carbon isotope stratigraphy at Shatsky Rise (DSDP-Site 305, ODP-Site 1210B), 2) to reconstruct the history of changes in tropical surface- and deep-water temperatures, and 3) to decipher changes in ocean circulation and the source regions of different deep- and intermediate water masses.

A new high-resolution $\delta^{13}C$ record was measured for Site 1210B in order to improve the stratigraphic resolution. The new $\delta^{13}C$ record from Site 1210B allows for a detailed correlation with the previously generated $\delta^{13}C$ record of Site 305 that represents a deeper site at Shatsky Rise (Voigt et al. 2010). The correlation is validated by FO and LO ages of planktic foraminifera and calcareous nannoplankton and provides evidence for two major gaps below and above the CMBE of Site 305, each representing a 1 to 1.5 Ma long period of erosion and non-deposition.

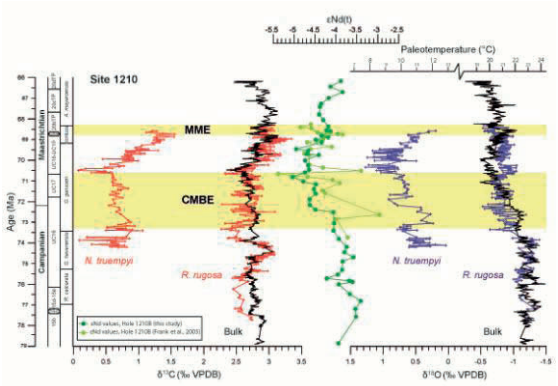

Figure 1. Compilation of bulk-carbonate and planktic and benthic foraminiferal $\delta^{13}C$ and $\delta^{18}O$ data together with Nd isotopes from sediment coatings (this project) and fish debris (Frank et al. 2005) at Site 1210B, Shatsky Rise.

The Campanian-Maastrichtian Boundary Event (CMBE) is characterized by a distinct long-lasting negative carbon isotope excursion and a short-term increase in oxygen isotopes recorded from the tropical Pacific, the Indian Ocean and the Southern Ocean. In fact, the first results of this project clearly show that the detection of sedimentary gaps is a serious issue in the paleoceanographic interpretation of deep-sea cores.

Another question addressed in our proposal was the occurrence of a late Campanian negative carbon isotope event (LCE) in the tropical Pacific. The new 1210B $\delta^{13}C$ bulk record does not show such a distinct carbon isotope excursion as it is recorded from European shelf records (sections in Gubbio, Italy, Norfolk, UK, Lägerdorf, N-Germany, Tercis, France; Voigt et al., 2010; Voigt et al., submitted). Possible reasons could be 1) regional effects restricted to locations in Europe or to shallower shelves, 2) a hiatus at Shatsky Rise, or 3) a much smaller magnitude of the event which makes it indistinguishable from the background noise.

The history of changes in surface- and deep water temperatures will be reconstruct by using stable oxygen and carbon isotopes. At Site 1210B, a total of 600 samples were processed to analyse the $\delta^{13}C$ and $\delta^{18}O$ of the planktic foraminifera *Rugoglobigerina rugosa* and the benthic foraminifera *Nuttallides truempyi*, representing the interval from the late Campanian up to the mid-Maastrichtian. Here, we present ~600 planktic and ~250 benthic isotope data (Figure 1). Oxygen isotopes are measured to reconstruct changes in surface- and deep-water temperatures, although the preservation of foraminiferal tests is not sufficient to calculate absolute temperatures.

Results show a positive excursion of benthic $\delta^{18}O$ values that indicates beginning bottom-water cooling during the CMBE and a temperature minimum after the event. The planktic $\delta^{18}O$ record shows constant

temperatures during and after the CMBE. This decoupling of bottom– and surface-water $\delta^{18}O$ changes during the CMBE provides a strong argument that possible buildups of ephemeral ice sheets in Antarctica are too small to modify the oxygen isotopic composition of seawater.

New insights about changes in ocean circulation comes from a second approach of the project, where ferromanganese-oxide coatings of bulk sediments are used as archive to analyse Nd isotopes from different Campanian-Maastrichtian sites in the tropical Pacific

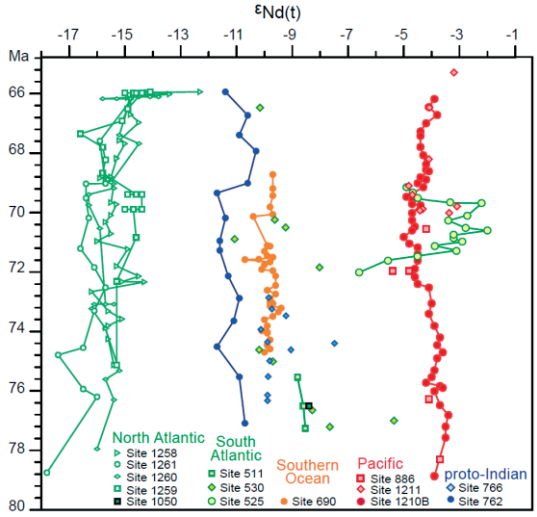

Figure 2: Summary of Late Cretaceous $\varepsilon_{Nd(t)}$ data for different oceanic basins. Data are from Frank et al. 2005, Robinson et al. 2010, MacLeod et al. 2011, and unpublished data of this project (DFG-projects VO 687/10 and Fr 1198/7)

(Shatsky Rise, Site 1210B), the proto-Indian (Exmouth Plateau, Site 762), the South-Atlantic (Walvis Ridge, Site 525) and the Southern Ocean (Maud Rise, Site 690). Ferromanganese coatings of sediment particles acquire bottom-water ε_{Nd} values during early seafloor diagenesis, and these records are generally insensitive to later alteration (Martin and Scher 2004, Gutjahr et al. 2007, Martin et al. 2010). This approach is rather new for Cretaceous sediments. It was demonstrated that the two archives, sediment coatings and fish debris, deliver indistinguishable results for Cretaceous sediments (Martin et al. 2010). Relatively high concentrations of Nd were extracted from the nannofossil chalks of Site 1210B. The low amount of detrital material reduces potential contamination effects by partial leaching of detrital particles. Nd isotopic results derived from sediment coatings at Site 1210B do not show a distinct difference in comparsion to previously published fish-debris derived data (Figure 1, Frank et al. 2005). This result is in good agreement with the observation of Martin et al. (2010) and offer the new opportunity to expand Nd isotopic studies as paleoceanographic tracer on longer timescales beyond the spatial and temporal limitations of the presence of fossil fish debris.

The Nd isotope record from 1210B show relative radiogenic Nd isotopic signatures for the tropical Pacific (εNd(t) = -3.4 to -5.0; Figure 1). Furthermore, a negative εNd excursion towards less radiogenic values is associated to the cooling of bottom waters at Shatsky Rise during and after the CMBE. This negative shift argues for the temporary presence of a cooler water mass with Southern Oceanic provenance that lasted about 3 Ma. The mode of ocean circulation in the latest Cretaceous is still a matter of debate. While some authors rejuvenated the idea of warm saline bottom water formation for the North Atlantic Ocean (MacLeod et al. 2011), others supposed the southern high latitudes as possible site of deep water formation. The new Nd isotope records from Site 690 and 762 confirm the idea of a "Southern Component Water" as oceanic deep water as stated by Robinson et al (2010). However, the Nd isotope record od Site 525 shows a complete different signal with very radiogenic values (εNd(t) = -6 to -3) that indicate the presence of a very local water mass derived from the weathering and/or hydrothermal alteration of volcanic rocks. According to these preliminary data, all investigated sites reveal a unique Nd-isotope signature in the Campanian-Maastrichtian that shows only restricted intermediate- to deep-water connections between ocean basins. Thus, the latest Cretaceous ocean circulation seems to be characterized by numerous and mostly local intermediate- to deep-water sources. Especially the Atlantic Ocean shows a broad spread of Nd-isotope values (Figure 2, 3), suggesting different source areas and weathering inputs for the regional intermediate- to deep-water masses. Based on the combination of the occurrence of numerous local source regions and the existence of oceanic barriers and silled basins, it has to be inferred that the late Cretaceous oceanic circulation system was significantly different from what we experience today.

References:

Frank, T.D., Thomas, D.J., Leckie, R.M., et al., 2005. The Maastrichtian record from Shatsky Rise (northwest Pacific): A tropical perspective on global ecological and oceanographic changes. Paleoceanography, 20, PA1008, doi:10.1029/2004PA001052.

Gutjahr, M., Frank, M., Stirling, C.H., Klemm, V., van de Flierdt, T. and Halliday, A.N., 2007. Reliable extraction of a deepwater trace metal isotope signal from Fe-Mn oxyhydroxide coatings of marine sediments. Chemical Geology, 242, 351-370.

MacLeod, K.G., Londono, C.I., Martin, E.E., Berrocoso, A.J., and Basak, C., 2011. Changes in North Atlantic circulation at the end of the Cretaceous greenhouse interval. Nature Geoscience 4, 779-782.

Martin, E.E., Blair, S.W., Kamenov, G.D., et al., 2010. Extraction of Nd isotopes from bulk deep sea sediments for paleoceanographic studies on Cenozoic time scales: Chemical Geology, v. 269, p. 414-431.

Martin, E.E., and Scher, H.D., 2004. Preservation of seawater Sr and Nd isotopes in fossil fish teeth: bad news and good news. Earth and Planetary Science Letters 220, 25-39.

Robinson, S.A., Murphy, D.P., Vance, D., and Thomas, D.J., 2010. Formation of "Southern Component Water" in the Late Cretaceous: Evidence from Nd-isotopes. Geology 38, 871-874.

Voigt, S., Gale, A., Jung, C., Jenkyns, H. Global correlation of Upper Campanian – Maastrichtian successions using carbon isotope stratigraphy: development of a new Maastrichtian timescale. Submitted to Newsletters on Stratigraphy.

Voigt, S., Schönfeld, J., 2010. Cyclostratigraphy of the reference section for the Cretaceous white chalk of northern Germany, Lägerdorf — Kronsmoor: a late Campanian-early Maastrichtian orbital time scale. Palaeogeography, Palaeoclimatology, Palaeoecology, 287, 67-80.

IODP

Polyphase serpentinization history of Mariana forearc mantle: observations on ultramafic clasts from ODP Leg 195, Site 1200

W.-A. KAHL[1]*, N. JÖNS[1], W. BACH[1], F. KLEIN[2]

[1]University of Bremen, 28359 Bremen, Germany
(*correspondence: wakahl@uni-bremen.de)
[2]Woods Hole Oceanographic Institution, Woods Hole, U.S.A.

Unraveling the geochemical consequences of seawater interactions with peridotite and the contribution of this process to lithosphere-ocean budgets is key to furthering our understanding of global geochemical cycles. Serpentinization of the oceanic lithospheric mantle is a widespread process, particularly along slow-spreading ridges, with significant consequences for rheology, chemistry and microbial habitability of the oceanic lithosphere. Under certain geologic conditions, serpentinization also occurs at intraoceanic convergent plate boundaries. Serpentinization of suprasubduction-zone mantle wedge can be observed in the mud volcanoes of the Mariana forearc, which are the only ones known to be active today.

In the forearc of the Mariana subduction zone system, numerous seamounts develop from extrusion of blueschist and serpentine mud. ODP Leg 195 drilled the South Chamorro seamount, where ultramafic clasts occur within the mud matrix. These clasts show a complex serpentinization history, which bears the potential for tracking the fluid history during uplift and cooling of mantle wedge rocks to the seafloor.

Pervasively serpentinized harzburgites, which are crosscut by different generations of late-stage veins, were examined. Relict primary minerals include olivine (X_{Mg}= 0.91-0.92) and orthopyroxene (X_{Mg}≈ 0.92). Magnesium-

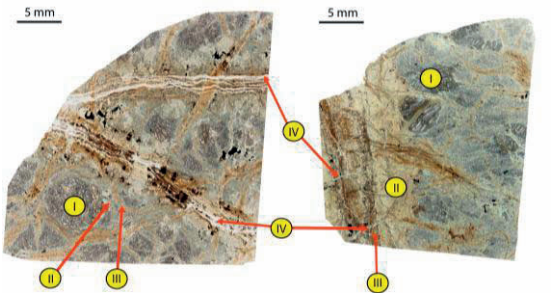

Fig. 1: Thin sections (plane-polarized light) of two clasts of serpentinized harzburgite carried by the mudflow matrix of South Chamorro seamount, a serpentine mud volcano of the Mariana forearc. Labels indicate the different stages of fluid infiltration.

rich (X_{Mg}= 0.95) clinopyroxene is present as exsolution lamellae in orthopyroxene and in symplectitic intergrowths with spinel (X_{Cr}= 0.48-0.59).

Multiple serpentinization steps are documented: (I) Pervasive serpentinization led to ubiquitous breakdown of olivine and formation of serpentine (X_{Mg}= 0.92-0.94) and magnetite. Orthopyroxene was replaced to lesser extent by serpentine (X_{Mg}≈ 0.90). Clinopyroxene remained stable during this stage. (II) The second hydration stage was bound to fractures crosscutting earlier serpentinization textures and is manifested as veins consisting of Mg-rich serpentine (X_{Mg}= 0.90-0.93). (III) Veins from stage II were re-activated and overprinted by serpentine + brucite assemblages. Replacement of magnetite is observed, leading to brucite with X_{Mg}≈ 0.80 and serpentine with X_{Mg}< 0.90. Furthermore, clinopyroxene breaks down and Fe-rich brucite (X_{Mg}≈ 0.60) forms. (IV) Finally, late discontinuous serpentine veins formed perpendicular to the stage II and III veins. Laser-ablation ICPMS trace element analyses show strongly variable concentrations of fluid mobile elements (Sr, Ba, Rb) and transition metals (Ni, Co, V). In addition, thermodyamic reaction path models are employed in developing plausible scenoarios for the origin of this succession of alteration and veining.

The compositional data and fabric relations of primary and secondary minerals indicate a multi-stage evolution of fluid-rock reactions in South Chamorro Seamount. The initial stages of serpentinization are related to aqueous solutions with high concentrations of silica, Sr, Ba, and Rb. During later stages, serpentinization assemblages are rich in brucite±hydrogarnet indicative of low silica activities in the intergranular fluids. Late-stage serpentine also lacks the enrichment in alkalies, Ba and Sr. We hypothesize that the fluids causing serpentinization are derived from the subducting slab. Being externally buffered by reactions with metabasaltic and sedimentary rocks, these fluids metasomatized the mantle upon intital serpentinization. Later stages of serpentinization took place further away from the subducting slab and within the feeding system of the mud volcano. Fluids were internally buffered by serpentinization reactions, leading to the formation of brucite. Late-stage serpentine is depleted in Rb, Ba, and Sr because these elements have been removed from the fluids in the course of increased fluid-rock reaction under decreasing temperatures. Thermodyamic calculations provide validation of this sequence and will allow us – in the next stage of this project – to investigate the production of hydrogen and potenital for CO_2 reduction during the various stages of fluid-rock interaction in the mantle wedge underlying the mud volcano.

IODP

Paleoproductivity controls on microbial abundance in marine subsurface sediments (IODP Exp. 320/321, PEAT)

J. KALLMEYER[1], D. LIEBRAND[2], M.W. LYLE[3], T. WESTERHOLD[4]

[1]University of Potsdam, Earth and Environmental Sciences, Germany
[2]National Oceanography Centre, Southampton, United Kingdom
[3]Texas A&M University, College Station, USA
[4]MARUM, Bremen, Germany

Despite the great variability in cell abundance between different sites (D'Hondt et al., 2009), it is generally observed that the abundance of cells in marine sediments declines linearly with depth when plotted on a log-log plot, reflecting the increasing recalcitrance of the sedimentary organic matter (Parkes et al., 2000). IODP Expeditions 320 and 321 (Paleocene-Eocene Age Transect, PEAT) retrieved long sediment drill cores in the Pacific equatorial upwelling area. The sites were selected in order to obtain sediment samples from the equatorial upwelling area in

different time intervals. Therefore, each core records a unique record of oceanic productivity over time.

The PEAT samples therefore represent a unique chance to get an understanding of whether changes of productivity are preserved over geologic timescales and if so, whether cell abundance can be used to trace changes in paleoproductivity.

Also, these cores offer a chance to study the influence of ongoing diagenetic (aka microbially mediated) processes on the distribution of microbial cells.

In high cell abundance sediments it was possible to enumerate the cells without any additional preparatory steps, but for most samples it was necessary to at least dissolve the carbonate minerals or extract the cells according to the method of Kallmeyer et al. (2008). Concentration of dissolved porewater compounds were measured on board JOIDES Resolution, solid phase Barium concentrations were quantified by XRF.

Between sites and with depth, microbial cell abundance varies by several orders of magnitude. Unlike most other cell abundance profiles, they show distinct kinks or bends, which correlate with local minima or maxima in geochemical or magnetic susceptibility profiles. These turning points can be related to either changes in paleoproductivity or ongoing diagenetic alteration of the sediment. Organic carbon content in these sediments is generally rather low and shows no correlation with cell abundance.

Our data show that cell distribution reflects conditions and processes of both past and present. However, in order to observe the controls of paleoproductivity and diagenetic processes on microbial cell abundance it is necessary to have good quality data with high depth resolution for all parameters.

References:

D'Hondt, S., Spivack, A.J., Pockalny, R., Fischer, J., Kallmeyer, J., Ferdelman, T.G., Abrams, L., Smith, D.C., Graham, D., Hasiuk, F., Schrum, H., and Stancin, A. (2009). Subseafloor sedimentary life in the South Pacific Gyre. Proceedings of the National Academy of Sciences of the United States of America 106, 11651-11656.

Kallmeyer, J., Smith, D.C., D'hondt, S.L., and Spivack, A.J. (2008). New cell extraction procedure applied to deep subsurface sediments. Limnology and Oceanography: Methods 6, 236-245.

Parkes, R.J., Cragg, B.A., and Wellsbury, P. (2000). Recent studies on bacterial populations and processes in subseafloor sediments: A review. Hydrogeology Journal 8, 11-28.

IODP

The early Pliocene constriction of the Central American Seaway (5-3.5 Ma): Interhemispheric ocean and climate linkages

C. KARAS[1,2], J. O. HERRLE[1,2], D. NÜRNBERG[3], R. TIEDEMANN[4]

[1] Goethe-University Frankfurt, D-60438, Frankfurt, Germany
[2] Biodiversity and Climate Research Centre (BIK-F), D-60325, Frankfurt, Germany
[3] Helmholtz Centre for Ocean Research Kiel (GEOMAR), D-24148 Kiel, Germany
[4] Alfred Wegener Institute for Polar and Marine Research, D-27568 Bremerhaven, Germany

We focus our studies on the paleoceanographic effects of the constriction of the Central American Seaway (CAS) on the North and South Atlantic Ocean during the early Pliocene epoch (~5-3.5 Ma). During ~4.8-4 Ma, a critical threshold in the closing history of the CAS was reached with a significantly restricted Caribbean-Pacific surface water exchange. This caused a thermocline shoaling in the equatorial east Pacific and increased the Atlantic Meridional Overturning Circulation transporting warm and more saline waters towards high northern latitudes.

For the first time recent simulation studies quantified this tectonic induced oceanographic changes. They predicted a distinct warming of the North Atlantic (up to 7°C) and a pronounced cooling of the Southern Hemisphere (~2°C) through "heat piracy" of the Northern Hemisphere. To test this hypothesis of an interhemispheric seesaw during the early Pliocene we selected Deep-Sea Drilling Project (DSDP) and Ocean Drilling Program (ODP) core sites 552A, 610A, 982, and U1313 in the North Atlantic and sites 357 and 516A in the South Atlantic Ocean sensitive to "heat piracy" from the Northern Hemisphere. We will conduct combined δ18O and Mg/Ca measurements of planktic foraminifera from surface and subsurface levels and δ13C analyses from benthic foraminifera to reconstruct the hydrography of the upper water column and deep water currents during the early Pliocene.

ICDP

Untersuchung der zeitlichen Veränderung der seismischen Geschwindigkeit im Schwarmbebengebiet Westböhmen/Vogtland

M.KEYSER, U. WEGLER

Bundesanstalt für Geowissenschaften und Rohstoffe, Stilleweg 2, 30655 Hannover, e-mail: Matthias.Keyser@bgr.de

Die Region Vogtland/Westböhmen ist durch das Auftreten von Erdbebenschwärmen gekennzeichnet. Dabei kommt es in einem Zeitraum von einem bis mehreren Monaten zum mehreren tausend Erdbeben auf kleinem Raum. Die typische Herdtiefe beträgt 6 km bis 12 km. Während des Auftretens von Schwarmbeben kann die Entgasung von Mantelfluiden beobachtet werden, wobei sich die Menge und Zusammensetzung der Gase sowie die Herdprozesse der Erdbeben zeitlich ändern. Hinweise auf die Triggerung von Erdbeben durch Fluide wurden durch Untersuchungen der Erdbebenherde gefunden. Fluideinlagerungen in der oberen Kruste und an der Krusten-Mantel-Grenze wurden als Erklärung vorgeschlagen, es fehlen aber bisher direkte Beobachtungen. Auch sind die Aufstiegswege der Fluide unbekannt. Die unbekannten Prozesse und Zusammenhänge machen das Eger Rift/Vogtland zu einem herausragenden Ort für wissenschaftliches Bohren.

Im Rahmen des Forschungsprojektes „Probing of Intra-continental magmatic activity: drilling the Eger Rift – International Continental Scientific Drilling Program" (PIER-ICDP) wird die zeitliche Veränderung der seismischen Geschwindigkeit in der oberen Kruste des Schwarmerdbebengebietes Westböhmen/Vogtland während der Schwarmbeben im Oktober 2008 untersucht. Dabei ist die Idee, dass durch aufsteigende Fluide während der Schwarmbeben die seismische Geschwindigkeit in der Quellregion verringert wird.

Die insgesamt 285 von der BGR lokalisierten Erdbeben mit Magnituden größer als ML 1.4 werden mit Codawelleninterferometrie (CWI) untersucht, um zeitliche

Veränderung in der seismischen Geschwindigkeit zu beobachten.

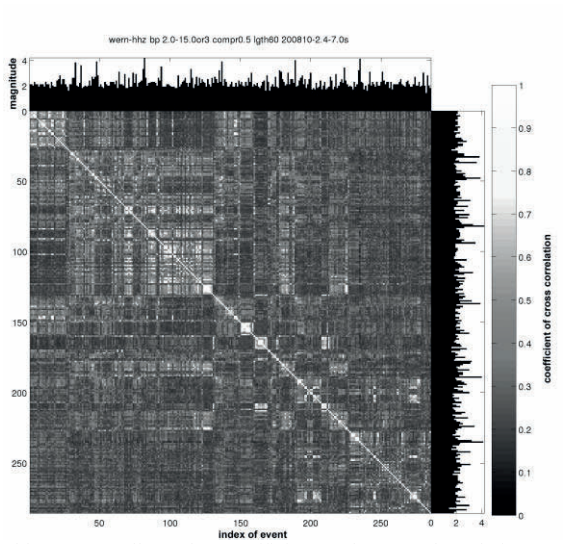

Abb. 1: Darstellung der Koeffizienten der Kreuzkorrelation zur Auswahl der Erdbebendubletten.

Die Analyse mittels CWI findet in zwei Schritten statt. Zuerst werden Erdbebendubletten (Erdbeben mit ähnlichen Wellenformen) ausgewählt, so dass von einem Abstand der Hypozentren von weniger als einem Viertel der seismischen Wellenlänge und ähnlicher Abstrahlcharakteristik beider Beben ausgegangen werden kann. Die Auswahl der Dubletten geschieht mittels Kreuzkorrelation eines Zeitfensters, in dem die Pg- und Sg-Welle der Beben enthalten sind. Diese Untersuchung wurde zunächst anhand der Komponenten Z, N und E der Station WERN, welche sich in ca. 9 km Entfernung von der Herdregion befindet, durchgeführt. Ist der Koeffizient der Kreuzkorrelation für alle drei Komponenten größer als 0.92 wird eine Erdbebendublette definiert. Schwarmbeben eignen sich gut für die Untersuchung mittels CWI, da sehr viele Erdbeben in kurzer Zeit in einem kleinen Volumen stattfinden, was bedeutet, dass viele Dubletten vorhanden sind. Abbildung 1 stellt grafisch die Koeffizienten der Kreuzkorrelation aller 285 Ereignisse beispielhaft an der Komponente Z der Station WERN dar. Dabei ist jedem Ereignis ein Index in zeitlicher Reihenfolge zugeordnet. Kleine Werte (dunkel) stehen dabei für geringe Ähnlichkeit und große Werte (hell) für hohe Ähnlichkeit. In der Diagonalen steht durchgängig der Wert von 1, hier wurde jedes Ereignis mit sich selbst korreliert.

In dem nächsten Schritt wird die eigentlich CWI angewandt. Dabei wird bei den gefundenen Dubletten die zeitliche Verschiebung der Codawellenformen gegeneinander bestimmt, aus der die zeitliche Änderung der seismischen Ausbreitungsgeschwindigkeit abgeleitet wird. Dies geschieht mittels Kreuzkorrelation in einem gleitenden Zeitfenster, mit welchem die Sg-Coda über eine länge von 60 Sekunden untersucht wird. Abbildung 2 zeigt das Ergebnis der CWI von zwei Ereignissen, welche 14 Tage auseinander liegen anhand der Z-Komponente der Station WERN. Oben sind die Wellenformen der zwei Ereignisse übereinander dargestellt, wobei der Zeitbereich des Pg- und Sg-Einsatzes sowie die Sg-Coda bei ca. 60 s vergrößert dargestellt ist. In der Mitte ist der Koeffizient der Kreuzkorrelation des gleitenden Zeitfensters über die gesamte Wellenform dargestellt und unten entsprechend die Verschiebung der Wellenformen im gleitenden Zeitfenster, aus welcher sich die zeitliche Änderung der seismischen Geschwindigkeit ablesen läßt. Es läßt sich leicht die hohe Ähnlichkeit und nicht vorhandene Verschiebung der Wellenformen zur Zeit des Pg- und Sg-Einsatzes sowie zur Zeit von ca. 60 s erkennen, was eine Konstanz der seismischen Geschwindigkeit zu den Herdzeiten beider Ereignisse bedeutet.

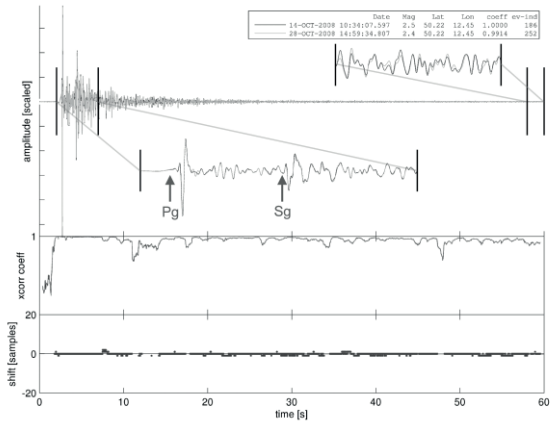

Abb.2: Codawelleninterferometrie von zwei Ereignissen, die zeitlich über 14 Tage auseinander liegen. Es läßt sich keine Änderung der seismischen Geschwindigkeit feststellen.

Nach den bisherigen Ergebnissen dieser Untersuchung können wir im Rahmen der Messgenauigkeit homogene Geschwindigkeitsänderungen von mehr als 0.04 % im Untersuchungsgebiet ausschließen. Dies entspricht einer absoluten Geschwindigkeitsänderung von 1.4 m/s bei einer angenommenen S-Wellengeschwindigkeit von 3500 m/s. Um statistisch signifikante Aussagen machen zu können, werden zukünftig noch weitere Stationen in die Untersuchung einbezogen. Auf dem Poster zeigen wir die bisherigen Ergebnisse, welche bislang keinen statistisch signifikanten Trend in der seismischen Geschwindigkeit zeigen.

IODP

Changes in North Atlantic deep water circulation during the past 4 Myr

N. KHÉLIFI[1], M. FRANK[1], D. NÜRNBERG[1]

[1]Helmholtz-Zentrum für Ozeanforschung Kiel (GEOMAR), Deutschland (nkhelifi@geomar.de)

Changes in northern North Atlantic deep water circulation during the past 4 million years (Ma) were studied at a suite of five IODP/ODP sites at water depths from 2400 to about 5000 m. Benthic $\delta^{13}C$ records at these sites oscillate in parallel around values lower than today by ~0.2 ‰ during interglacials and by ~0.7 ‰ during pronounced glacials of the late Pliocene warm period. However, Pliocene Mg/Ca-based deep-water temperatures were 2 to 3 °C higher than today during interglacials and near modern levels during glacial periods. The coeval changes in ventilation at a lower level than today may indicate a weaker difference between these warm water masses than today, which is probably caused by water

mixing in the northern North Atlantic. This is corroborated by ε_{Nd} bottom seawater values near -9 to -10 at all sites, which differs markedly from the modern situation characterized by clear differences in ε_{Nd} signatures between the water masses at these sites. Accordingly, the lesser ventilated, warm, and mixed water masses are most likely the result of the weaker overturning in the northern North Atlantic during that time of global warmth (Haywood and Valdes, 2004). After 1.6 Ma, benthic $\delta^{13}C$ records show a gradually improving ventilation, with pronounced glacial/interglacial oscillations, which came close to the modern-to-late-Pleistocene levels. This ventilation change in deep water masses was coeval with a clear divergence in ε_{Nd} of bottom water masses between the different sites towards modern signatures. This is apparently linked to a significant change in the sources of circulating deep waters in northern North Atlantic. Accordingly, the first reorganization of the deep circulation in northern North Atlantic towards the modern situation appears to have started only after ~1.6 Ma, most likely as a response to increases in the amplitude of the Earth's obliquity cycle during that time (Laskar et al., 1993).

References:
Haywood, A. M., and P. J. Valdes, 2004: Modelling Pliocene warmth: contribution of atmosphere, oceans and cryosphere, Earth and Planetary Science Letters, 218, 363–377.
Laskar, J., F. Joutel, and F. Boudin, 1993: Orbital, precessional, and insolation quantities for the Earth from –20 to +10 Myr, Astronomy and Astrophysics, 270, 522–533.

IODP

A combined numerical and experimental approach to constrain the dynamics of axial magma chambers beneath fast spreading ocean ridges

C. KIRCHNER[1], J. KOEPKE[1], H. BEHRENS[1]

[1] Institut für Mineralogie, Leibniz Universität Hannover, Callinstr. 3, 30167 Hannover, Germany, (c.kirchner@mineralogie.uni-hannover.de)

It has been confirmed by several studies that melt lenses above AMCs ("axial magma chamber") under fast spreading ocean ridges located at the boundary between lower and upper crust are dynamic systems with the potential to move up and down. Nevertheless, the time scales of these vertical movements are poorly constrained up to now with very rough estimations, varying between 10 and 100000 years. This project focuses on a close investigation on the gabbro/sheeted dike transition, which is part of a reference profile of the upper oceanic crust drilled by IODP multi-cruise mission „Superfast Spreading Crust"(Site 1256, equatorial East Pacific Rise). Of substantial interest is a specific horizon defined as CBL ("conductive boundary layer"), separating the AMC and the hydrothermally altered dikes. The ascent of the AMC leads to the formation of "granoblastic dikes" due to an intense contact metamorphic overprint under granulite facies conditions[Koepke et al. 2008]. In order to quantify the vertical oscillations of the AMC described above, we are applying tools of multi element diffusion profile modeling to relictic, zoned plagioclase phenocrysts within the granoblastic dikes, which were metamorphosed by the thermal imprint of the AMC (~1200°C) in a high position. Provided that the zoning patterns in the crystals studied are due to temperature-induced diffusion processes, the conditions of metamorphic overprint (temperature, volatile fugacities), and diffusion coefficients are known, the

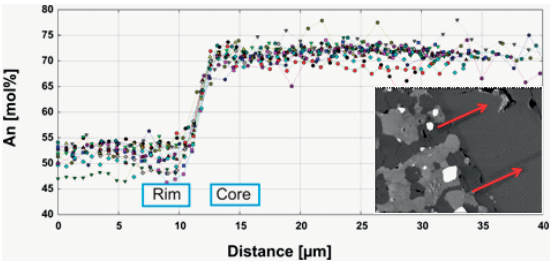

Figure 1. Backscattered electron image showing a relictic plagioclase with idiomorphic shape (medium grey) surrounded by plagioclase of the granoblastic matrix (dark grey) within a typical granoblastic dike drilled at Site 1256D (sample number 312-1256D-203-1-10-14) The red arrows mark the locations where the concentration profiles were measured with the electron microprobe. The light grey and withish phases are hornblende, pyroxene, and oxides of the granoblastic matrix (including products of secondary alteration).

detailed analysis and modeling of the concentration profiles allows us a quantification of the residence time of the heat source (AMC) in a high position and hence, temporal information about the vertical fluctuations of the AMC can be constrained. Here we report the current status of the project, including results as well as difficulties encountered during the diffusion modeling approach. Additionally, we also report about an experimental subproject, which is also part of this project.

At this stage of the project, we have collected more than 200 concentration profiles with a total number of analyses of approximately 10000 points with respect to CaAl-NaSi diffusion (An-Ab content and selected trace elements) in several relictic plagioclases with electron microprobe. This dataset was obtained in plagioclases within "wet" parageneses with hornblende present [for details see Koepke et al. 2008]. Just recently, we gained access to phenocryst bearing anhydrous samples, which were equilibrated at distinctly higher temperatures. We will obtain a new dataset of concentration profiles in these samples in order to evaluate the effect of different aH_2O and temperature conditions, as these parameters have great impact on the diffusivity of the elements. All concentration profiles have been measured perpendicular to the crystallographic c-axis of the crystals.Analysis of concentration profiles have been performed using a Cameca SX100 electron microprobe with standard operating conditions (beam current: 15nA, acceleration potential: 15KeV). The measurements were focused on the An-Ab and selected trace element contents of preselected, zoned plagioclase phenocrysts which survived the metamorphic overprint, but show now distinct concentration profiles induced by the diffusional reequilibration of the elements.

During the initial phase of the microprobe work, we realized that with standard operating conditions, we were not able to measure the An-concentration profiles with sufficient spatial resolution and precision. Since the diameter of the plagioclase volume irradiated by the electron beam can be estimated to ~ 1µm, and due to the fact that the profiles are very short (ranging from

approximately 4-10µm), we were not able to achieve a sufficient number of data points for a reliable fit of the profiles. Therefore, we made efforts to reduce the beam diameter by reducing the acceleration voltage of the microprobe from 15 to 8kV in subsequent analysis

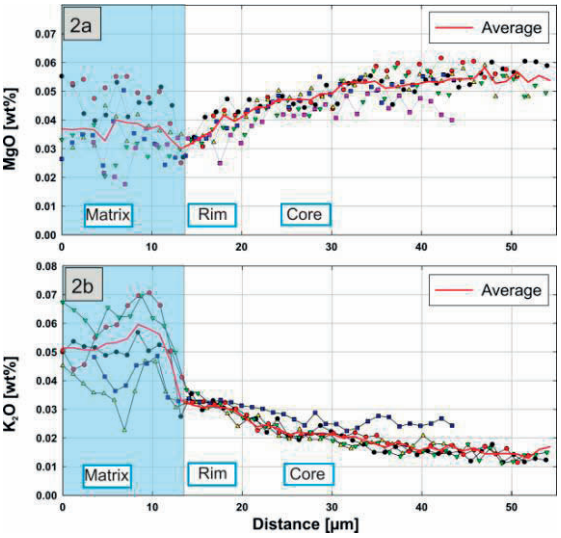

Figure 2. Compositional profiles starting from secondary plagioclases of the matrix into primary plagioclase phenocrysts. 2a: MgO-content, 2a: K2O-content. The red lines correspond to the average compositions used for the modeling.

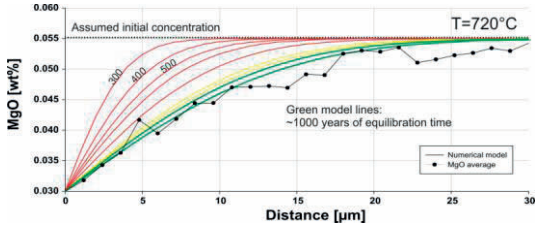

Figure 3. Comparison of average MgO profile (core) with various numerical calculations. Numbers above model curves indicate time in years of diffusive exchange. A homogeneous distribution of 0.055 wt% MgO has been assumed as initial concentration.

sessions. This modification resulted in a smaller excitation area at the sample surface revealing an improvement of the quality of the analyzed profile considerably. The measured An-profiles show the typical shape of diffusion profiles resulting from the exchange between plagioclase and matrix as presented in Figure 1. Trace element measurements were conducted with a high precision trace element setting, with high beam current of 40nA and counting times of 20 to 120s, in order to make the analysis of very low amounts of MgO and K_2O feasible.

Figure 2 shows selected trace-element profiles (MgO, K_2O) from matrix plagioclases into primary plagioclase phenocrysts. The data points within the matrix are often very irregularly and do probably not correspond to results of pure diffusional processes. It is likely that these parts of the profiles are influenced by transport processes proceeded on grain boundaries between the numerous secondary plagioclases.

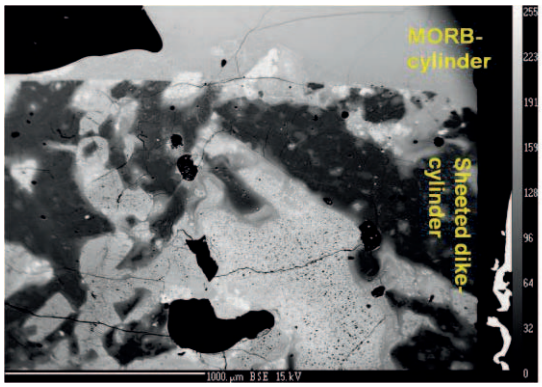

Figure 4: run product of test experiment. Large melt pools within the sheeted dikes can be observed at 1140°C and 20 min run duration.

Hence, only the data points within the phenocryst, in which we assume intracrystalline diffusion processes were taken into account for the modeling and subsequent time scale calculations.

The first calculations were conducted on the basis of the An-profiles (Fig. 1). The profiles were fitted with TableCurve2D using the appropriate solution of Fick´s second law (Crank, 1975) assuming constant diffusivity and an initially homogenous plagioclase (r^2=0.999). Diffusion modeling and numerical calculations based on CaAl-NaSi interdiffusion profiles yield average time scales less than 10000 years for the development of the profiles.On the other hand, calculations based on concentration profiles for Mg and K in plagioclase revealed rather different results: The durations extracted from these profiles are much shorter in the range of ~200-1000 years. These times scales are similar to the ones obtained by Gillis (2008). However, they do not fit to the much longer ones derived from the An-profiles in this study. Since most granoblastic dikes show effects of a late hydrothermal alteration, this discrepancy can possibly be explained by the fact that the profiles of the considerably faster diffusing Mg and K were possibly initialized by the peak metamorphism and can be attributed to subsequent second stage hydrothermal alteration processes, which has to be confirmed in the near future.

A requirement for the diffusion modeling method is the knowledge on initial concentration distribution of the elements. Concerning this parameter, we assumed a sharp concentration step for the An profiles and an homogeneous distribution of Mg and K within the crystal. Practically, a

Table 1: Composition of starting glass (MORB)

Oxide [wt%]	Na_2O	SiO_2	Al_2O_3	CaO	K_2O	TiO_2	FeO	MgO	MnO	P_2O_5	Total
	2.74	51.62	13.79	10.81	0.08	1.78	12.55	6.69	0.25	0.19	100.54
	(0.32)	(0.45)	(0.23)	(0.36)	(0.02)	(0.03)	(0.4)	(0.21)	(0.08)	(0.1)	
1 σ standard deviation are given in parenthesis											

discretized form of the suitable continuity equation (for details see Costa et al. 2008) in combination with the initial and boundary conditions, allows the calculation of concentration profiles for different durations, if diffusion coefficients are known. The calculations are performed by using the explicit finite difference method which is implemented into a Mathematica© notebook.

For the "wet" samples (see above) an equilibration temperature of 720°C was determined by thermometric measurements. As a first approximation, this static temperature has been used in the model. Figure 3 shows some preliminary profile calculations for MgO done by the explicit finite difference method. The results of the model also indicate short-time processes less than ~1000 years. In order to account for the heating and subsequent cooling of the samples, we are going to implement several reasonable T-t paths for the metamorphic overprint, in order to calculate much more realistic profiles.

Additionally to the diffusion modeling, an experimental project focused on melt/rock (MORB/granoblastic dike) reactions has just started. This subproject aims on the evaluation of the magmatic processes and the rates of assimilation caused by an upward burning of an axial melt lens through its overlying metamorphic lid.

In this context, we highly benefit from the direct access to natural samples both from the lower sheeted dikes and representive MORB drilled at IODP site 1256D. On the basis of chemical bulk-analyses we selected at least 4 different fresh MORB unaffected by the granoblastic overprint and 4 different samples from the lowermost sheeted dikes, which are intensively recrystallized to the granoblastic texture. The MORB starting material was subsequently ground and fused twice at 1 atm and 1600°C to get a dry, homogeneous glass. Before using, the starting material was checked carefully by electron microprobe for homogeneity and for major and trace element bulk composition (Tab. 1).

For the experiments, we applied an approach similar to the diffusion couple technique. 2mm long, one-side polished discs (Ø=5mm) were drilled from both starting materials (MORB/dike) and aligned in an AuPd-sample capsule with the polished sides at the contact. A series of time dependent experiments is in progress which are performed in IHPV (internally heated pressure vessels) near the liquidus temperature of the MORB melt (e.g., 1150°C), pressures of 100 MPa, fO_2: QFM+1.

At these conditions, two processes are expected: complex partial melting reactions in the granoblastic dikes will occur, possibly together with the crystallization of new minerals, making the detailed evaluation of newly formed phase compositions and relations feasible. Furthermore, the MORB melt will percolate through the granoblastic dike. By measuring the width of this reaction zone, we attempt to gain knowledge about the dissolution rates and hence, information about the amount of assimilation.

In a first test experiment we already aligned cylinders of MORB starting material with natural, hydrothermally altered sheeted dikes in an AuPd-sample capsule. The experiment was conducted for 20min in an IHPV at 1140°C, 100 MPa, fO_2: QFM+1. Figure 4 shows the interface between the two aligned sample cylinders of the experiment.

Even after these short run durations, vast partial melting reactions occurred within the sheeted dikes due to the breakdown and dehydration of water bearing minerals, while no reaction was observed within the MORB cylinder.

Due to that observation, a nearly anhydrous granoblastic dike rock will be used in upcoming experiments as starting material instead of hydrated sheeted dikes. This material will start to melt at considerably higher temperatures thus establishing more realistic conditionss.

To summarize, the combination of the modeling approach and the experimental study bears great potential to extent our knowledge on the dynamics of fast spreading ocean ridges and the underlying magmatic reactions, regarding processes like stoping, assimilation and contamination.

References:

Costa F, Dohmen R, Chakraborty S (2008) Time scales of magmatic processes from modeling the zoning patterns of crystals. Rev Mineralogy & Geochemistry 69: 545-594

Crank, J. (1975), The Mathematics of Diffusion, 414 pp., Oxford Univ. Press, Oxford, U. K.

Gillis KM (2008) The roof of an axial magma chamber: A hornfelsic heat exchanger. Geology 36: 299-302

Koepke et al. (2008), Petrography of the dike-gabbro transition at IODP Site 1256 (equatorial Pacific): The evolution of the granoblastic dikes, Geochem. Geophys. Geosyst., 9, Q07O09, doi:10.1029/2008GC001939.

ICDP

Forschungsbohrung im Thüringer Becken im Rahmen von INFLUINS

J. KLEY[1], N. KUKOWSKI[1], K.U. TOTSCHE[1] & INFLUINS-ARBEITSGRUPPE

[1]Friedrich-Schiller-Universität Jena, Institut für Geowissenschaften, Burgweg 11, 07749 Jena

Die Interaktion von tiefen und flachen Fluiden in Sedimentbecken ist das integrale Thema von INFLUINS, eines Projektverbundes der PROSIN-Initiative. Mit einem multidisziplinären Ansatz, der verschiedenste Teile der Geowissenschaften von der Geomikrobiologie über die Struktur- und Hydrogeologie, Geophysik und Mineralogie bis zur Fernerkundung umfasst, werden dabei fluidgesteuerte Prozesse auf ihren verschiedenen raum-zeitlichen Skalen vom Porenraum bis zum gesamten Becken untersucht. Das Zielgebiet von INFLUINS ist das Thüringer Becken, das aufgrund seiner relativ geringen Größe und recht guter Erschließung ein ideales Geolabor darstellt.

Ein zentrales Projekt im Rahmen von INFLUINS ist eine Forschungsbohrung mitten im Thüringer Becken nordöstlich von Erfurt. Zur Vorerkundung wurden 2011 reflexionsseismische Daten entlang von drei Profilen aufgenommen. Dabei liegt die avisierte Bohrung im Kreuzpunkt von zwei dieser Profile. Zusätzlich geht ein Profil über eine alte Bohrung, so dass sehr gute Möglichkeiten gegeben sind, die Tiefenlage wichtiger Reflektoren regional zuverlässig zu bestimmen. Im Rahmen der Bohrung sind bohrlochgeophysikalische Messungen, die Gewinnung von Kernstrecken und Pumpversuche geplant. Hier stellen wir das Gesamtprojekt sowie vor allem das Bohrvorhaben vor.

Dateninformationssystem für das GESEP Kern- und Probenlager

CAROLA KNEBEL[1,2], RONALD CONZE[1], FRANK KRYZIAK[3] UND ULRICH HARMS [1,2]

[1]Helmholtz-Zentrum Potsdam, Deutsches GeoForschungsZentrum GFZ
[2]German Scientific Earth Probing Consortium e.V. (GESEP)
[3]smartcube GmbH

Im Deutschen Forschungsbohrkonsortium GESEP e.V. haben sich geowissenschaftliche Institute mit Interesse an Forschungsbohrungen zusammengeschlossen. Infrastruktur aus dem marinen, terrestrischen und glazialen Bereich wird gemeinsam genutzt und weiter ausgebaut. Ein wichtiger Schritt ist die Kooperation der Bundesanstalt für Geowissenschaften und Rohstoffe (BGR) und des MARUM der Universität Bremen, ein nationales Bohrkernlager für kontinentale Bohrprojekte einzurichten, um wertvolles und wissenschaftlich bedeutsames Probenmaterial langfristig zu sichern und verfügbar zu machen.

Das GESEP Kernlager ist auf zwei Standorte verteilt: An der BGR-Außenstelle in Berlin-Spandau werden Proben und Kerne aus Festgesteinen gelagert, die keiner Kühlung bedürfen. Im Bremen Core Repository (BCR) am MARUM werden Sedimentkerne bei 4°C gelagert. Um internationalen Standards für Bohrkernlager, wie denen des Integrated Ocean Discovery Program (IODP) gerecht zu werden, ist das Kernlager mit entsprechender analytisch-apparativer Infrastruktur ausgestattet. Die Bohrkerne des ICDP-Projekts PALEOVAN aus dem Vansee in der Türkei mit 690 m Kerngewinn wurden bereits im MARUM adäquat dokumentiert, beprobt und eingelagert.

Um diese und zukünftige Proben und Daten dauerhaft der Wissenschaft zugänglich machen zu können, wird derzeitig ein Proben- und Informationssystem entwickelt. Hierfür wurden bei der Deutschen Forschungsgemeinschaft im Programm „Wissenschaftliche Literaturversorgungs- und Informationssysteme (LIS)“ Projektgelder genehmigt. Am Beispiel der mit dem Drilling Information System (DIS) bereits umfassend dokumentierten Bohrkerne und Daten von ICDP Projekten wird jetzt in einem ersten Schritt eine Kernlagerverwaltungssoftware (CurationDIS) entwickelt, mit der der Bestand des Kernlagers erfassbar und verwaltbar sowie Probenmaterial nach Programm und Expedition dokumentiert werden soll. Die Software wird so programmiert, dass auch andere Datenbestände integriert oder verbunden werden können. So soll u.a. ein einfacher und einheitlicher Zugang über das Internet zu möglichst vielen Proben und Daten ermöglicht werden. Im Rahmen des CurationDIS erhalten alle Proben einen eineindeutigen Identifikator, die sogenannte International GeoSample Number (IGSN). In einem zweiten Schritt wird ein Webportal entwickelt, in der die IGSN so genutzt werden und Proben bzw. Daten zitierbar sind wie bei DOIs mit Fachliteratur. Im Portal werden auch Suchwerkzeuge, eine elektronische Probenanforderung sowie die Nachverfolgung des Bearbeitungsstatus und Nach- bzw. Rückverfolgung einzelner Proben zur Verfügung stehen. Mit dem Portal werden über definierte Metadatenschnittstellen die Bestände des GESEP-Lagers und die anderer Bohrkernlager einbezogen sowie ein direkter Zugang zu Datenzentren wie PANGAEA eingerichtet.

IODP

Late Pliocene to early Pleistocene millennial-scale fluctuations in SST and stratification within the North Atlantic

MIRJAM KOCH[1*], OLIVER FRIEDRICH[1], PAUL WILSON[2]

[1]Institute for Geosciences, Goethe-University Frankfurt, Germany
*e-mail: Mi.Koch@em.uni-frankfurt.de
[2]National Oceanography Centre, School of Ocean and Earth Science, Southampton, UK

The late Pliocene to early Pleistocene (5.6–1.8 Ma) represents in many ways a key interval of Cenozoic palaeoceanography, including two major changes of the Earth system: the significant glaciation of the northern hemisphere, cluminating in a major expansion of Arctic ice sheets (Northern Hemisphere Glaciation, NHG) and the closure of the Panama Gateway. The impact of changes associated with the NHG on surface-water hydrology (SST and stratification) of the subpolar North Atlantic is, however, not fully understood yet. Given its proximity to the large dynamic ice-sheets of the northern hemisphere and the role in deep-water formation, however, the North Atlantic represents one of the climatically sensitive regions on Earth.

This study focuses on the combination of Mg/Ca and $\delta^{18}O$ analyses on planktic foraminifera in order to understand and reconstruct millennial-scale climate variability during the final stage of the NHG, especially marine oxygen isotope stages (MIS) 103-95 (late Pliocene to early Pleistocene, 2.6 to 2.4 Ma). In particular, this is relevant to better understand fluctuations in the magnitude of SST and stratification changes and their link to the intensification of NHG.

Stable isotope and Mg/Ca analyses have been carried out on the deep-dwelling planktic foraminiferal species Globorotalia crassaformis from IODP Site U1313 (North Atlantic, 41°N). This site is located at the base of the upper western flank of the Mid-Atlantic Ridge. It therefore is under direct influence of North Atlantic Deep Water and lies on the southerly limit of the so-called ‘IRD belt’. Samples are taken in millenial-scale resolution from 2.6 to 2.4 Ma, comprising isotope stages 103 to 95. Samples from this site were already used before to test the existence of a relationship between the emergence of large-amplitude millennial-scale climate oscillations and an intensification of glacial conditions during the intensification of NHG by measuring mixed-layer stable isotope data on the surface-dwelling planktic foraminifera Globigerinoides ruber. Comparison of our results with these surface-water data reveal relatively stable conditions in surface waters while intermediate waters show strong fluctuations on a glacial-interglacial time scale, most probably reflecting changing intermediate-water masses.

IODP

Campanian-Maastrichtian intermediate- to deep-water changes in the high latitudes: benthic foraminiferal evidence

MIRJAM C. KOCH*, OLIVER FRIEDRICH

Institute for Geosciences, Goethe-University Frankfurt, Germany,
*e-mail: mi.koch@em.uni-frankfurt.de

During the latest Cretaceous cooling phase, a positive shift in benthic foraminiferal $\delta^{18}O$ values lasting about 1.5 Ma (71.5-70 Ma) can be observed at a global scale (Campanian-Maastrichtian Boundary Event, CMBE). This $\delta^{18}O$ excursion is interpreted as being influenced by a change in intermediate- to deep-water circulation or by temporal build-up of Antarctic ice sheets. Here we test if benthic foraminiferal assemblages (BFA) from a southern high-latitudinal site near Antarctica (Ocean Drilling Program Site 690, Maud Rise, Weddell Sea, southern South Atlantic) are influenced by the CMBE. If the $\delta^{18}O$ transition reflects a change in intermediate- to deep-water circulation from low-latitude to high-latitude water masses, this change would result in cooler temperatures, higher oxygen concentration, and possibly lower organic-matter flux at the seafloor, resulting in a major BFA change. If, however, the $\delta^{18}O$ transition has mainly been triggered by ice formation, no considerable compositional difference in BFA would be expected. Our data (see Fig. 1 for detailed results of benthic foraminiferal assemblage counts) show a separation of the studied succession into two parts with distinctly different BFA. Species dominating the older part (73.0 to 70.5 Ma) tolerate less bottom-water oxygenation (e.g. Paralabamina hillebrandti) and are typical components of low-latitude assemblages (e.g. Reussella szajnochae). In contrast, the younger part (70.0 to 68.0 Ma) is characterized by species that indicate well-oxygenated bottom waters (e.g. Nuttallides truempyi) and species

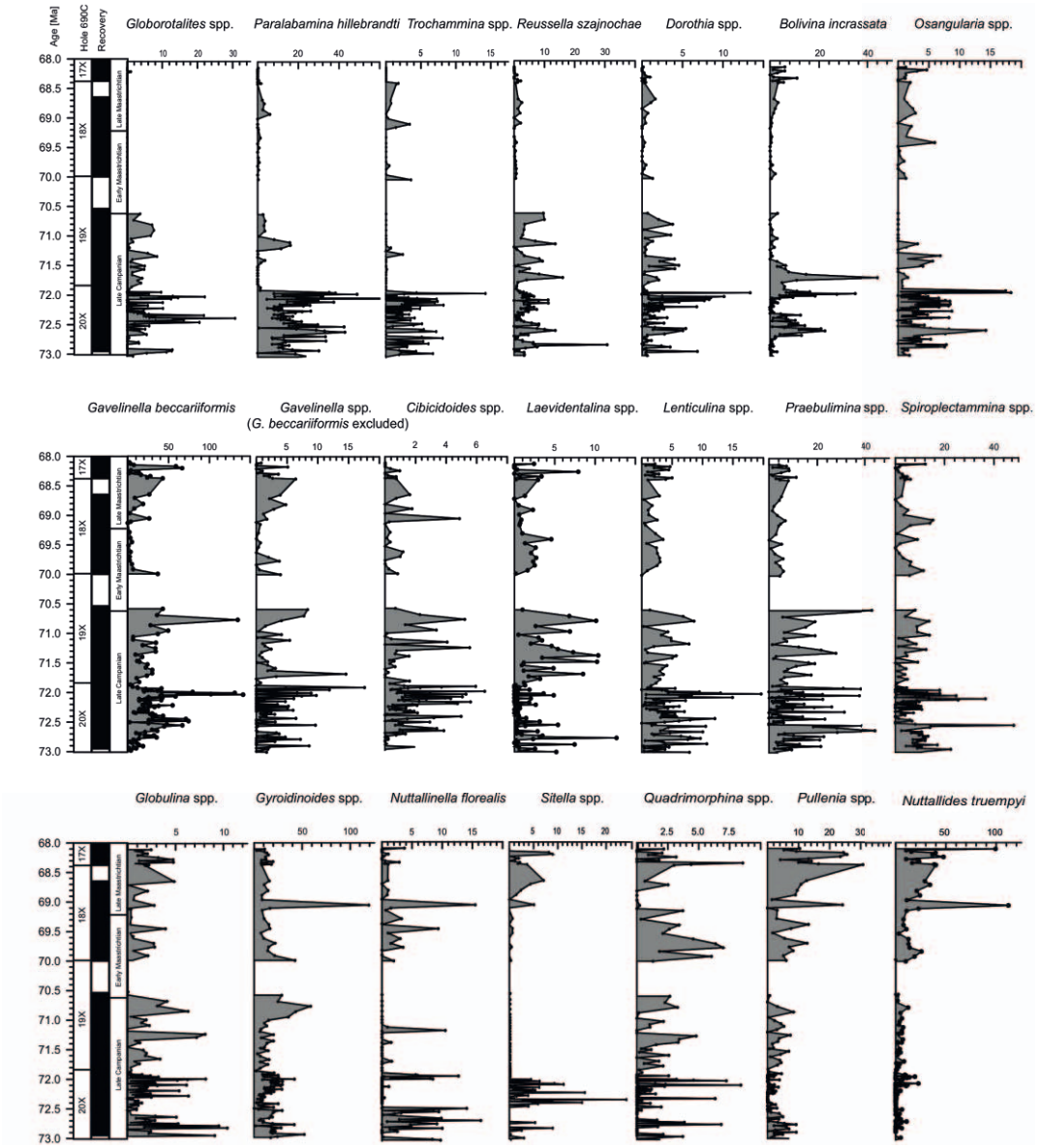

Figure 1. Absolute abundances of common (>1% of total fauna) benthic foraminiferal taxa (per gram of dried sediment) from ODP Site 690.

common in high-latitude assemblages (Pullenia spp.). We interpret the observed change in BFA towards a well-oxygenated environment to reflect the onset of a shift from

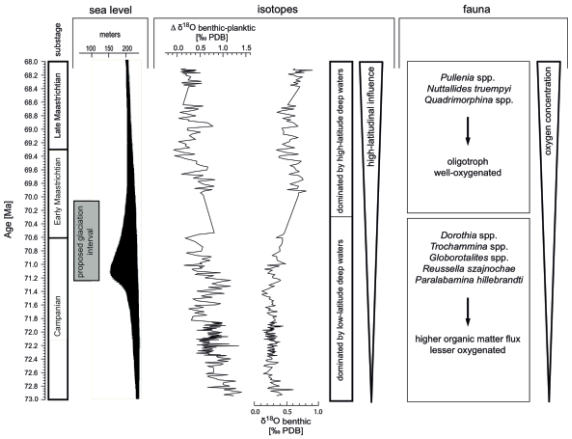

Figure 2. Comparison of proposed sea level reconstruction (after Barrera et al., 1997), Δδ18Obenthic-planktic and stable oxygen isotopes and their interpretation from Friedrich et al. (2009) with the dominant species of the benthic foraminiferal assemblage counts of ODP Site 690 and their environmental interpretation (this study). The grey bar indicates the proposed glaciation interval of Miller et al. (1999).

low-latitude towards high-latitude dominated intermediate- to deep-water sources (Fig.2). This implies that a change in oceanic circulation rather than ice volume was at least a major component of the CMBE.

References

Barrera, E., S. Savin, E. Thomas, and C. Jones (1997), Evidence for thermohaline-circulation reversals controlled by sea-level change in the latest Cretaceous, Geology, 25(8), 715.

Friedrich, O., J. Herrle, P. Wilson, M. Cooper, J. Erbacher, and C. Hemleben (2009), Early Maastrichtian carbon cycle perturbation and cooling event: Implications from the South Atlantic Ocean, Paleoceanography PA2211, 24(2).

Miller, K., E. Barrera, R. Olsson, P. Sugarman, and S. Savin (1999), Does ice drive early Maastrichtian eustasy?, Geology, 27(9), 783.

IODP

The Era of Mini-CORKS: Affordable Yet Fully Equipped Borehole Observatories for Long-term Monitoring of Geohazards

A. KOPF[1], S. HAMMERSCHMIDT[1], E.E. DAVIS[3], D. SAFFER[4], C.G. WHEAT[5], A. LABONTE[3], R. MELDRUM[3], M. HEESEMANN[3], R. MACDONALD[3], H. VILLINGER[2], T. FREUDENTHAL[1], V. RATMEYER[1], M. BERGENTHAL[1], J. RENKEN[1] AND G. WEFER[1]

[1] MARUM Research Center, University of Bremen, Leobener Str., 28359 Bremen, Germany
[2] Department of Geosciences, University of Bremen, Bremen, Germany
[3] Pacific Geoscience Centre, Geological Survey of Canada, British Columbia, Canada
[4] Department of Geosciences, Pennsylvania State University, Pennsylvania, USA
[5] Global Undersea Research Unit, University of Alaska Fairbanks, Alaska, USA

Borehole Observatories, so-called Circulation Obviation Retrofit Kits or CORKs, are a profound way to allow the re-establishment of in situ conditions in submarine boreholes and their subsequent monitoring for several months or even years. Since the first CORKs were installed almost 20 years ago, borehole observatories evolved from simple instruments providing only pressure and temperature sensors to multifunctional, interdisciplinary subseafloor laboratories, including fluid sampling devices (i.e. OsmoSampler, Jannasch et al., 2003), microbiological chambers (i.e. FLOCS, Orcutt et al., 2010) or strainmeter (e.g. Kopf et al., 2011). The scientific outcome, even of the more simple CORKs, is enormous. Recent studies showed that seismogenic activity at convergent margins, e.g. at the Nankai Trough, can be clearly correlated with pressure transients detected by borehole observatories (e.g. Davis et al., 2006; Davis et al., 2009). By monitoring in situ pressure, temperature and geochemistry over months or even years, it is generally possible to detect distinct changes in geochemical and isotope composition as well as strain (Bredehoeft, 1967; Davis et al., 2004) and relate these to seismogenic processes by comparing the data with volumetric strainmeter measurements or deformational events identified via GPS data (e.g. Solomon et al., 2009).

Unfortunately, despite their potential vital scientific outcome, several boreholes remained uninstrumented in the past, and were abandoned after drilling and coring were completed. This has several reasons: first of all, CORKs usually require a drillship for installation and subsequent ROV assignments for instrument maintenance and data download, which is not only a logistic but also a great financial effort. In addition to that, the increasing complexity of CORKs made them more affected by environmental constraints during and after the installation and by the installation procedure itself, which became noticeable in longer ship time and subsequently, again, in increased financial and logistic expenses.

Here we present three types if Mini-CORKs, which, instead of representing one step further to more complexity and higher expenses, are simpler yet provide a comprehensive set of measurements. As a regional example, the Nankai Trough accretionary prism is chosen, which started to form around 2.8 Ma years ago by subduction of the Philippine Sea Plate beneath the Eurasian Plate. In the past this led to repeated subduction thrust earthquakes of M8+, therefore this area was already chosen by the Deep Sea Drilling Project (DSDP), Ocean Drilling Project (ODP) and Integrated Ocean Drilling Project (IODP) for investigating the processes influencing the seismogenic activity. For this purpose, highly sophisticated CORKs were already installed, for instance the Advanced-CORK or the Seismo-CORK. Unfortunately, due to their complexity and the need for more ship time, IODP was forced to rely on third party funding. At the same time, not all sensors of the CORKs worked properly after the installation was completed. Consequently, the need for less complex and less expensive yet sufficiently equipped CORKs arose, which may be satisfied by the here presented alternatives.

One simple Mini-CORK is called the SmartPlug, which consists solely of two Paroscientific pressure and temperature sensors, one additional temperature sensor in the data logger housing and one autonomous ANTARES miniature temperature logger. The instrument is attached to a retrievable bridge plug, which seals the borehole and isolates the zone of interest from the overlying water column. Pressure and temperature measurements take place in a hydrostatic reference section and in the zone of

interest, where the sensors are connected to the formation via perforated casing screens. The SmartPlug was already installed at IODP Site C0010 during IODP Exp. 319 (Saffer et al., 2009), and after 15 months, got recovered during IODP Exp. 332 (Kopf et al., 2011). The data proved to be reliable in detecting incoming seismic and tsunami waves as well as low-pressure weather systems. Moreover, important assumptions could be made regarding the poroelastic properties of the surrounding formation.

The SmartPlug got replaced by a second, slightly advanced MiniCORK, the so-called GeniusPlug. It has the same simple design, but has a bulkhead extension at its lower part where an OsmoSampler and a FLOCS microbiological chamber are incorporated. Recovery is planned for 2012 or 2013 (associated with Exp 338).

Even simpler is the so-called MeBo-CORK, which was designed especially for the portable MARUM drill rig MeBo. The latter can drill to depths of up to 70 m and can be operated from any ship of opportunity. After coring, the upper part of the borehole remains cased, and is hydraulically sealed by an adapter which contains a hotstab hydraulic connection and an electrical connection. From this seal, pressure and temperature sensors are let down inside the borehole, where they monitor in situ pressure and temperature development. The MeBo-CORKs connect to these sensors via the hotstab connection, and can transmit the data via a telemetric unit, making time-consuming and costly recovery operations obsolete. Two MeBo-CORK designs will be available, one which can be installed directly by the MeBo, and one which replaces the first one and has to be installed by an ROV. At the same time, the second design consists of a seafloor unit, which has also the telemetric unit, battery packs, data logger and pressure transducers, but which allows adding further mission specific sensors and devices.

A first field test is envisaged for an expedition with R/V Sonne (SO-222) at the Nankai Trough in 2012, where the MeBo will drill into mud volcanoes piercing the Kumano forearc basin. These boreholes will be instrumented by MeBo-CORKs, thus allowing to observe pressure and temperature as well as fluid sampling over the whole monitoring period. Since mud volcanoes can serve as window to depth this may provide valuable insights into seismogenic processes of the underlying splay fault system or even the plate boundary megathrust.

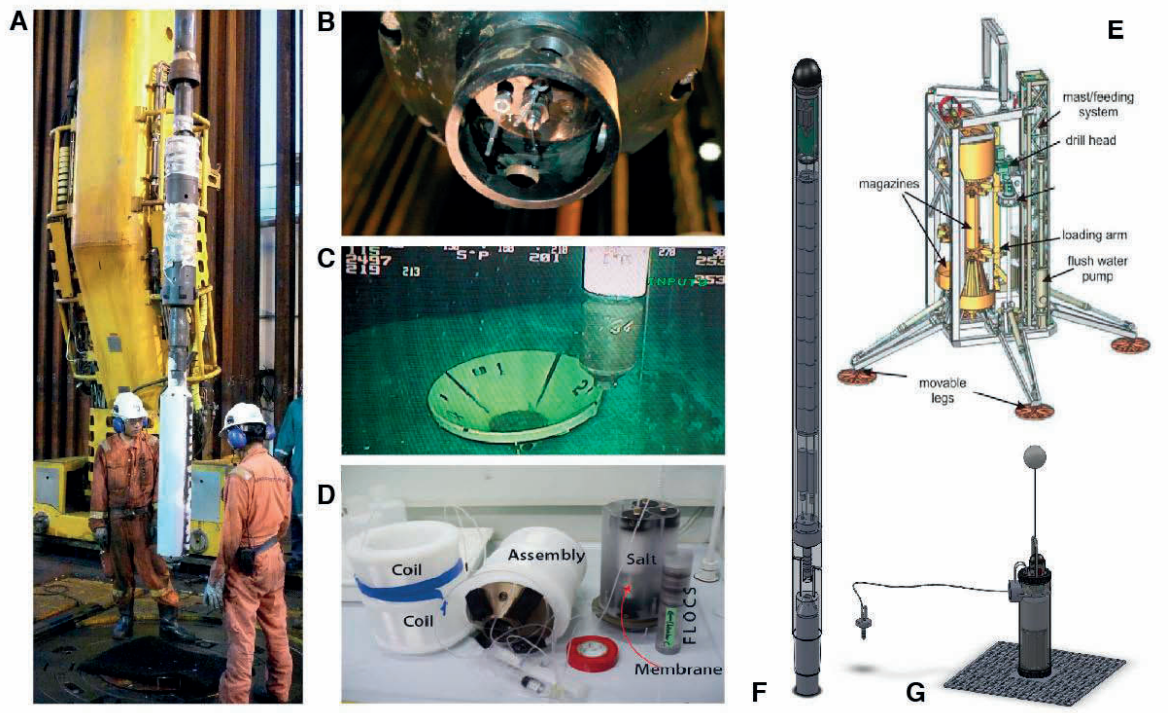

Illustrations of the SmartPlug (A), GeniusPlug (B-D) and MeBo seafloor drill (E) and associated MeBo-CORK components (F, G).

References:

Bredehoeft, J. D. (1967), Response of Well-Aquifer Systems to Earth Tides, J. Geophys. Res., 72(12), 3075-3087.

Davis, E., K. Becker, R. Dziak, J. Cassidy, K. Wang, and M. Lilley (2004), Hydrological response to a seafloor spreading episode on the Juan de Fuca ridge, Nature, 430(6997), 335-338.

Davis, E. E., K. Becker, K. Wang, K. Obara, Y. Ito, and M. Kinoshita (2006), A discrete episode of seismic and aseismic deformation of the Nankai trough subduction zone accretionary prism and incoming Philippine Sea plate, Earth and Planetary Science Letters, 242(1-2), 73-84.

Davis, E., K. Becker, K. Wang, and M. Kinoshita (2009), Co-seismic and post-seismic pore-fluid pressure changes in the Philippine Sea plate and Nankai decollement in response to a seismogenic strain event off Kii Peninsula, Japan, Earth, Planets and Space, 61(6), 9.

Jannasch, H., E.E. Davis,, M. Kastner, J. Morris, T. Pettigrew, J.N. Plant, E. Solomon, H. Villinger, and C.G. Wheat, (2003), CORK-II: long-term monitoring of fluid chemistry, fluxes, and hydrology in instrumented boreholes at the Costa Rica subduction zone., paper presented at Proceedings of the Ocean Drilling Program, Initial Reports, 205.

Kopf, A., E. Araki, S. Toczko, and the Expedition 332 Scientists (2011), NanTroSEIZE Stage 2: Riserless Observatory, Proceedings IODP, Exp 332: 190 pp. doi: 10.2204/iodp.proc.332.2011 (see: http://publications.iodp.org/proceedings/332/332title.htm)

Orcutt, B., C. G. Wheat, and K. J. Edwards (2010), Subseafloor Ocean Crust Microbial Observatories: Development of FLOCS (FLow-through Osmo Colonization System) and Evaluation of Borehole Construction Materials, Geomicrobiology Journal, 27(2), 143 - 157.

Saffer, D., L. McNeill, E. Araki, T. Byrne, N. Eguchi, S. Toczko, K. Takahashi and the Expedition 319 Scientists (2009), NanTroSEIZE Stage 2: NanTroSEIZE Riser/Riserless Observatory, IODP Preliminary Report, 319, 83 pp.

Solomon, E. A., M. Kastner, C. G. Wheat, H. Jannasch, G. Robertson, E. E. Davis, and J. D. Morris (2009), Long-term hydrogeochemical records in the oceanic basement and forearc prism at the Costa Rica subduction zone, Earth and Planetary Science Letters, 282(1-4), 240-251.

IODP

Sedimentology- and palynology-based reconstructions of environmental dynamics and sea-level development at the Miocene coast of New Jersey

KOTTHOFF, ULRICH[1*], MCCARTHY, FRANCINE M.G.[2], FANG, LINHAO.[3], HESSELBO, STEPHEN P.[3]

[1]Department of Geosciences, Hamburg University, Bundesstrasse 55, D-20146 Hamburg, Germany, e-mail: ulrich.kotthoff@uni-hamburg.de
[2]Department of Earth Sciences, Brock University, 500 Glenridge Avenue, St. Catharines, Ontario, L2S 3A1, Canada
[3]Department of Earth Sciences, University of Oxford, South Parks Road, Oxford, OX1 3AN, United Kingdom
*corresponding author

The major aims of IODP Expedition 313 are estimating amplitudes, rates and mechanisms of sea-level change and the evaluation of sequence stratigraphic facies models that predict depositional environments, sediment compositions, and stratal geometries in response to sea-level change. Cores from three sites (313-M0027A, M0028A, and M0029A; 45 to 67 km off the coast of New Jersey) from the New Jersey shallow shelf (water depth approximately 35 m) were retrieved during May to July 2009, using an ECORD "mission-specific" jack-up platform. The recovery rate for the three sites exceeded 80%; in total, more than 1300 m core length were achieved. The oldest sediments were recovered from Hole M0027A, and dated as late Eocene according to biostratigraphy, magnetostratigraphy and Sr-isotopy-based age estimates.

In the project presented here, the ratio between organic-walled dinoflagellate cysts and pollen grains found in late Eocene (Priabonian) to Miocene (Serravallian) sediments from Holes M0027A and M0029A are used to estimate the site-shoreline distance. The reconstructions of site-shoreline distance contribute to a pollen-transport model, allowing more reliable pollen-based reconstructions of the vegetation development in the hinterland of the New Jersey margin. The pollen data are complemented with $\delta^{13}C$ values measured from hand-picked phytoclasts for Hole M0029A.

While oak forests dominated the vegetation on the Atlantic Coastal Plain during the Eocene and Oligocene, the Miocene witnessed the spreading of hickory-oak forests. At the Aquitanian-Burdigalian boundary different hemlock (*Tsuga*) species were present in the hinterland of the New Jersey shelf, indicating humid, but probably relatively cool conditions. The interval of extraordinary-high *Tsuga* pollen percentages was also detected at site M0028A, and can be used as a biostratigraphic tie-point between the three sites. For the Early Miocene strata, the carbon-isotope values are anomalously heavy ~compared to oceanic records. On the basis of $\delta^{13}C$ and C/N ratios, the Early Miocene interval in Hole M0029A (~750 to 560 mbsf) is inferred to comprise reworked deposits. This interpretation is corrobated by a significantly stronger degradation of pollen grains and other palynomorphs within several samples from the Burdigalian, particularly around 640 mbsf, and by abundant reworked (pre-Neogene) dinocysts throughout the Burdigalian, but particularly around 730 m.

The spread of deciduous oaks and other broad-leaved tree taxa during the late Burdigalian points to warmer temperatures. Similarly to the "*Tsuga* horizon" found at the Aquitanian-Burdigalian boundary, an interval of particularly frequent elm-(*Ulmus*-) pollen grains can be used to identify the late Burdigalian in all three sites of IODP Expedition 313. During the Langhian to Tortonian, tree taxa such as Holly, Hickory, and Tupelo expanded as well as herbal taxa, the latter probably due to decrease in humidity.

During the Langhian, positive carbon-isotope excursions correspond to sandy strata, while negative carbon-isotope excursions correspond to clay-rich strata; whereas in the Burdigalian, there is no systematic relationship between isotope values and grain size. There is furthermore an apparent relationship between inferred eustatic sea-level change and carbon-isotope values of terrestrial organic matter for the Middle Miocene. For strata equivalent in age to the Middle Miocene Monterey Event, it is possible to correlate positive and negative carbon-isotope excursions in terrestrial organic matter to similar fluctuations recorded from oceanic carbonates globally.

ICDP

Pliocene and Pleistocene mass movement history and initial geochemistry of turbidites in Lake El'gygytgyn, Far East Russian Arctic

M. KUKKONEN[1], C. GEBHARDT[2], O. JUSCHUS[3], V. WENNRICH[1], T. COOK[4], M. MELLES[1] AND EL'GYGYTGYN SCIENTIFIC PARTY

[1] University of Cologne, Institute of Geology and Mineralogy, Cologne, Germany (maaret.kukkonen@uni-koeln.de)
[2] AWI Bremerhaven, Geosystems, Bremerhaven, Germany
[3] TU Berlin, Institute for Applied Geosciences, Berlin, Germany
[4] University of Massachusetts, Department of Geosciences, Amherst MA, USA

The 315-m long sediment record from ICDP Site 5011 at Lake El'gygytgyn (67° 30' N, 172° 5' E; 492 m asl; diameter 12 km; water depth 175 m) (Fig. 1), recovered in winter/spring 2009 from the 3.6 Ma old impact crater, provides a new key terrestrial record from the Arctic for the reconstruction of environmental and climatic history

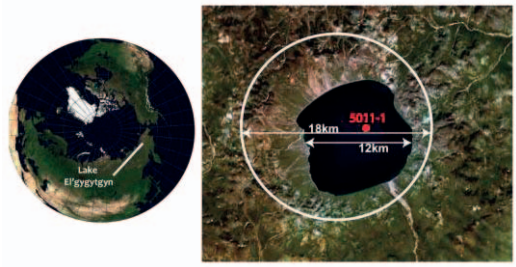

Fig. 1. Map of the northern hemisphere showing the location of Lake El'gygytgyn in the Far East Russian Arctic. White circle highlights the assumed crater rim and red dot indicates the coring site.

during the Quaternary and the Pliocene. Three parallel partly overlapping cores were obtained from the lake center, where a pre-site survey indicated undisturbed and layered sediments. On the lake slope, seismic survey and pilot cores have revealed thick debris flows thinning toward the lake centre. They vary in thickness between 3 and 20 m, and some of them show indications for partial erosion on their bases (Niessen et al. 2007). In 2003, one of

the discovered mass movement deposits was penetrated by two cores (Lz1039 and Lz1041) in order to investigate its characteristics and influence on the pelagic sedimentation in Lake El´gygytgyn (Juschus et al. 2009). Detailed investigation of these cores, as well as another, 16 m long core from the lake center (Lz1024), revealed that the acoustically transparent seismic unit consists of a basal debris flow deposit (debrite according to Gani 2004), which is directly overlain by a density flow deposit (densite) of wider distribution and further by a deposit settled from a suspension cloud (turbidite) that probably covers the entire lake floor.

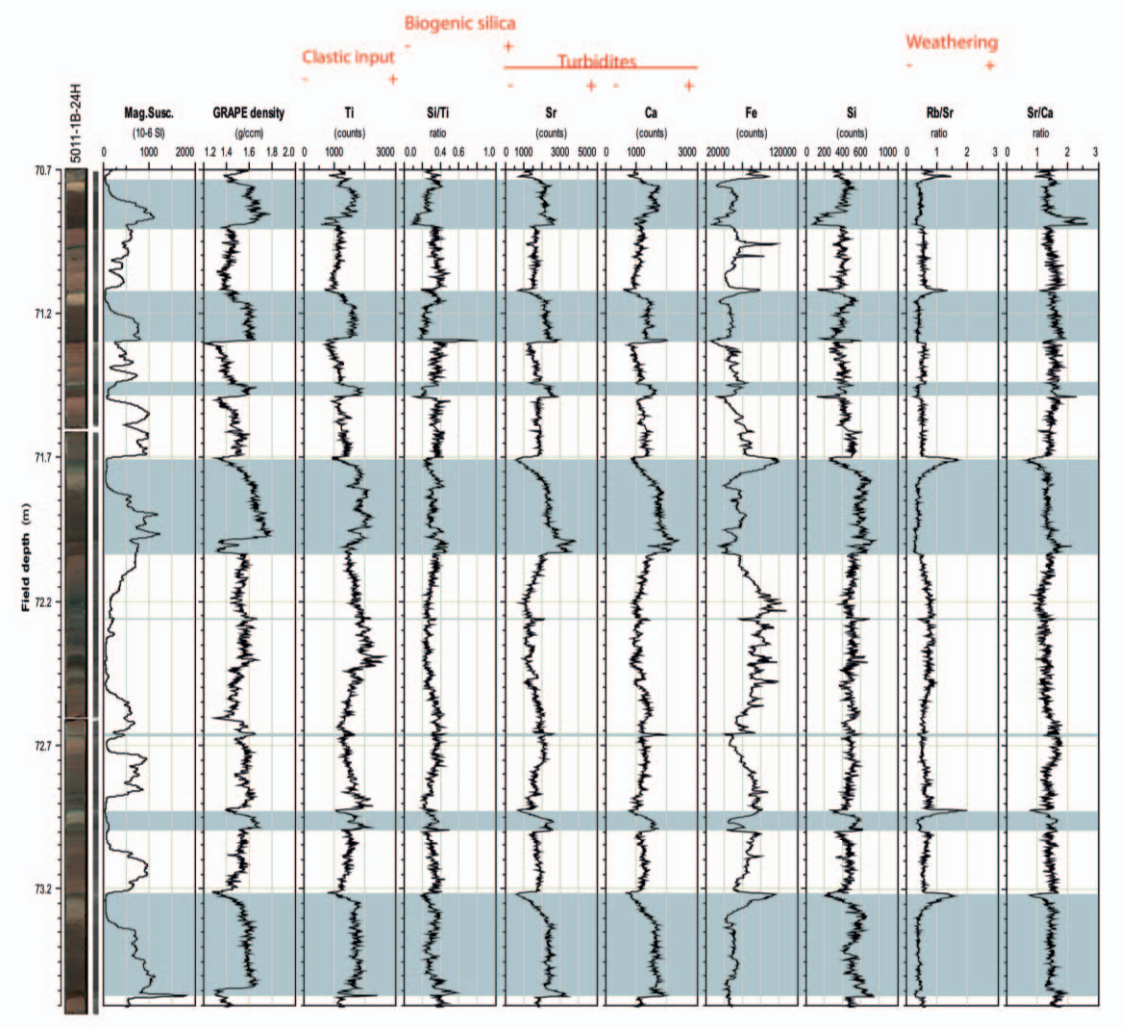

Fig. 2. Characteristics of turbidites (highlighted with greyish bars) in core run 5011-1B-24H with core scan, radiograph, magnetic susceptibility, GRAPE density and selected XRF-scanning data.

We present the results of identification and characterisation of mass movement deposits in the drill cores (5011-1A, 1B and 1C) from visual core descriptions and radiographs and compare them to high-resolution magnetic susceptibility and density measurements, as well as elemental analyses. Mass movement terminology is followed after Juschus et al. (2009), who used terms turbidite, densite and debrite as suggested by Gani (2004).

As in the pilot cores Lz1024 and PG1351 (Juschus et al. 2009), turbidites are the most abundant mass movement type throughout the drill cores. They show distinct fining upwards with a sharp contact to the underlying sediment. The fining upwards is either step-wise or diffuse, indicating possible differences in their deposition. No other sedimentary structures, such as lamination, are visually observed. Grain sizes vary from sand to clay and thicknesses from 2 mm to 55.3 cm in the Quaternary sediments and up to 95.3 cm in the Pliocene. The mean and median thicknesses of the Quaternary turbidites are, however, 6.3 cm and 2.9 cm, respectively. Magnetic susceptibility is in general high in the sandy and silty layers, the highest values are normally in the silty middle layer (Fig. 2). In the capping clayey silt layer magnetic susceptibility is lowest. Similarly, density is high in the middle silty layer and low in the topmost clayey silt layer. Density is also low in basal sandy layers (> 2 cm) of some thicker turbidites and it increases in the silty layer (Fig. 2 at 71.7-72.05 m). Such variation in density coincides in turbidites with fluctuations in magnetic susceptibility values and titanium counts in the silty layer, which might reflect grain size. Such turbidites may represent flood-induced hyperpycnal turbidites, which are inversely graded at their bases and overlain by a normal fining upwards sequence (Mulder et al. 2001, St. Onge et al. 2004).

Turbidites present a typical signal in chemical composition: Strontium (Sr) and Calcium (Ca), which are bound in feldspars, have high counts in the sandy and silty layers and are depleted in the clayey top (Fig. 2). Both

elements reflect primarily grain size, since they are enriched in sand to coarse silt (Francke 2010). Titanium (Ti) counts define clastic input to the lake, but since titanium is mostly enriched in coarse silt (Francke 2010), its counts can also show a minimum at the bases of turbidites due to the higher content of sand. Rb/Sr ratio is interpreted to reflect the weathering state and therefore highest values are reached in the clayey top of turbidites.

Physical properties of turbidites as well as differences in the nature of grading (diffuse vs. step-wise) indicate that not all turbidites are deposited from suspension clouds. The step-wise grading of the majority of the Lake El'gygytgyn turbidites suggests a sedimentation process, which differs from the sedimentation model suggested by Juschus et al (2009) and it may be a linked to a Bouma sequence (Bouma 1962). Turbidites with diffuse boundaries are interpreted to represent the end-results of slump events on the lake slope which through flow transformation have created suspension clouds that are deposited at the lake floor (Juschus et al. 2009). Thicknesses and grain-size distributions of turbidites in the Lake El'gygytgyn sediment record vary considerably. This may reflect different distances from the source area, as reported from several lakes in Switzerland by Sturm and Matter (1978) and Monecke et al. (2004) and from Lago Fagnano, Argentina (Waldmann et al. 2010). Grain-size measurements are ongoing to verify the nature of turbidite grading (Bouma 'sequence' vs. hyperpycnal turbidites).

Turbidites occur throughout the record and are intercalated in all pelagic facies, but are generally thinner in facies reflecting colder climate conditions, i.e. in finely (facies 1) or wavely laminated silt and clay (facies 2) (Cook et al. in prep., Wennrich et al. in prep.).

Densites, i.e. deposits of density flows, are well-sorted massive silty to sandy deposits without grading. They have sharp, likely erosional, bases. In contrast to the the pilot core Lz1024, where 3 densites were found within the 16-m long core, only 3 densites are presently identified in the drill cores. However, thin intrusions of massive sand are found intercalated in some slide and slump deposits.

Slide deposits consist of redeposited and multiplied pelagic fragments or event layers (turbidites). During sliding the source material stays widely undisturbed and can still be identified in the drill cores. Thicknesses vary between 160 and 275 cm. Slides have reached the lake floor only 3 times in the recoreved sediment record.

Folded pelagic sediments or event layers, such as tephras or turbidites are identified as slump deposits. The facies of the source material is still identifiable. Occasionally turbidites overlay slump deposits. Thicknesses vary between 44 and 380 cm. Both slides and slumps have not been described from the pilot cores (Juschus et al. 2009).

Debrites are grey poorly sorted deposits with fine gravel and sand in a silty matrix that have sharp boundaries to the underlying pelagic sediment. Thickesses vary between 30 cm and 2 m. Occasionally debrites can have inclusions of deformed silty material and be overlain by bended sediments. Debrites are often directly capped by turbidites. Debrites are deposited by debris flows, where the source material has been completely mixed. Debris flows occur on the lake slopes (Niessen et al. 2007) and can sometimes reach the deep lake basin. During their advance towards the lake floor, material is brought into suspension, from which the overlaying turbidite is deposited. Incorporated deformed silty material indicates possible erosion of pelagic sediments during flow advance towards the lake floor. Slumps possibly relate to debris flows on the lake slope, which deform the basin-plane sediments during their advance towards the lake centre.

The mass movement history of Lake El'gygytgyn is examined only for the time periods recovered with nearly 100 %, which are the complete Quaternary (sediment depth ca. 122 m) and parts of the Pliocene (between sediment depths 122 – 147 m and 275 – 315 m). Information concerning the youngest 10 turbidites is derived from the pilot core Lz1024 (Juschus et al. 2009) since these sediments were not recovered by the new cores 5011-1A to 1C.

In the Quaternary sediment record, corresponding to the upper ca. 122 m (Haltia-Hovi and Nowazcyk in prep.), approximately 240 mass movement deposits are identified. They comprise 35 % of the total sediment thickness. The mass movement deposits (and their portion to the total sediment thickness) are divided into 218 turbidites (11 %), 1 densite (0.1 %), 6 debrites (7 %), 8 slumps (11 %) and 3 slides (5 %). Turbidites account for 92 % of the number of all mass movement events but only 31 % of their thickness, reflecting the generally thinner nature of turbidites compared to other mass movement deposits. The portion of mass movements on the total sediment thickness is considerably higher than reported by Juschus et al. (2009) from the pilot cores Lz1024 and PG1351, which comprise the last ca. 300 and 250 ka (Nowaczyk et al. 2007, Juschus et al. 2007), with only 12.7 % and 7.1 % of mass movement deposits, respectively. This reflects a significant decrease in mass movement contribution to the sedimentation in central Lake El'gygytgyn in the course of the Quaternary. During Late and Middle Pleistocene only turbidites have reached the lake basin, with the exception of one slump (S34). However, turbidites comprise 10.2 % of core Lz1024, which correlates well with the percentage of turbidites in the entire Quaternary (11%). Thus, the decrease in mass movement deposition in the course of the Quaternary is widely independent of turbidites but mainly controlled by other types of mass movements. A mean rate of recurrence of mass movement events during the Quaternary is 11 ka. The Early Pleistocene is characterised by several slump events and debrites. There are also intervals with thicker or thinner turbidites, where all other mass movements are absent. Such intervals occur between 59 – 64 m, 70.7 – 74.5 m (thicker turbidites) and 74.5 – 80.7 m (turbidites < 20 cm). All debrites occur below 90 m, with the exception of one debrite at 34 m. The most significant mass movement event within the entire recovered sediment record in Lake El'gygytgyn is D195 between 91.3 – 95.5 m. This event consists of a basal debrite 2 m thick, overlain by a 1-m thick slump and finally capped by a 1-m thick turbidite.

In contrast to the Quaternary, Pliocene sediments were not fully recovered. We evaluate data from depths 122 – 147 m and 275 – 315 m, where the recovery is nearly perfect. Within the Late Pliocene sediments relative portion of mass movement deposits on the bulk sedimentation decreases significantly. Mass movement events in the upper Late Pliocene are dominated by turbidites. The lowermost 40 m of the sediment record covers the first 100 ka after the formation of the lake or even less, since the

sedimentation rate could have been much higher than the interpolated 44.5 cm/ka (Haltia-Hovi and Nowaczyk, in prep.). Several thick turbidites have reached the lake basin during this time period. The proportion of sand increases below 292 m indicating higher energies in the system. A transition zone to the impact rocks starts with gravel and stones of various lithologies in a sandy matrix at approximately 313 m.

In conclusion, mass movement events have frequently reached the coring site, which today is situated 4 km away from the nearest shore. Mass movement deposits constitute a significant amount of the sediment infill in Lake El'gygytgyn.Whilst turbidite frequence does not show significant variations throughout the record, their thicknesses as well as the occurrence of debrites and slumps, however, significantly decrease towards the upper part of the record, suggesting that the impact of mass movement on the pelagic sediment record has decreased over time.

References:

Bouma, A.H. (1962) Sedimentology of some flysch deposits. A graphic approach to facies interpretation. Elsevier, Amsterdam.

Cook, T.L., Wennrich, V., Kukkonen, M., Brigham-Grette, J. and Melles, M. (in prep.) Lithofacies classification and stratigraphy of pelagic sediments in Lake El'gygytgyn. Climate of the Past 2012.

Fedorov, G., Nolan, M., Brigham-Grette, J., Bolshiyanov, D., Schwamborn, G. and Juschus. O. (in prep.). Lake El'gygytgyn water and sediment balance components overview and its implications for the sedimentary record. Climate of the Past 2012.

Francke, A. (2010). Interdependency of grain-size and inorganic geochemistry of Lake El'gygytgyn, NE Siberia. Diploma Thesis. University of Cologne, Institute of Geology and Mineralogy.

Gani, M.R. (2004). From turbid to lucid: a straightforward approach to sediment gravity flows and their deposits. Sed. Rec., 2, 4–8.

Juschus O., Melles M., Gebhardt A.C. & Niessen F. (2009): Late Quaternary mass movement events in Lake El´gygytgyn, north-eastern Siberia. Sedimentology, 56, 2155-2174. DOI: 10.1111/j.1365-3091.2009.01074.x

Juschus O., Preusser, F., Melles M. and Radtke, U. 2007. Applying SAR-IRSL methodology for dating fine-grained sediments from Lake El'gygytgyn, nort-eastern Siberia. Quaternary Geochronology 2, 187-194.

Haltia-Hovi, E. and Nowaczyk, N. (in prep.) Paleomagnetic age constraints for the sediments from Lake El'gygytgyn (Northeastern Siberia) during the last 3.6 Myr. Climate of the Past 2012.

Melles M., Brigham-Grette J., Minyuk P., Koeberl C., Andreev A., Cook, T., Fedorov G., Gebhardt C., Haltia-Hovi E., Kukkonen M., Nowaczyk N., Schwamborn G., Wennrich V. & El'gygytgyn Scientific Party 2011. The El'gygytgyn Scientific Drilling Project – conquering Arctic challenges through continental drilling. Scientific Drilling, 11: 29-40. DOI: 10.2204/iodp.sd.11.03.2011.

Melles M., Brigham-Grette J., Glushkova O. Yu., Minyuk P., Nowaczyk N. R. & Hubberten H.-W. (2007): Sedimentary geochemistry of a pilot core from El´gygytgyn Lake - a sensitive record of climate variability in the East Siberian Arctic during the past three climate cycles. Journal of Paleolimnology, 37, 89-104.

Monecke, K., Anselmetti, F. S., Becker, A., Sturm, M. and Giardini, D. 2004. The record of historic earthquakes in lake sediments of Central Switzerland. Tectonophysics, 394: 21-40.

Mulder, T., Migeon, S., Savoye, B. and Faugéres J.-C. (2001) Inversely graded turbidite sequences in the deep Mediterranean: a record of deposits from flood-generated turbidity currents? Geo-Marine Letters 21: 86-93. DOI 10.1007/s003670100071

Niessen, F., Gebhardt, A.C., Kopsch, C. and Wagner, B. 2007. Seismic investigation of the El'gygytgyn impact crater lake Central Chukotka, NE Siberia: preliminary results. J. Pa- leolimnol., 37, 49–63.

Nowaczyk, N.R., Melles, M. and Minyuk, P. 2007. A revised age model for core PG1351 from Lake El'gygytgyn, Chukotka, based on magnetic susceptibility variations correlated to northern hemisphere insolation variations. Jounal of Paleolimnology 37, 65-76.

St-Onge, G., Mulder, T., Piper, D.J.W., Hillaire-Marcel, C. and Stoner, J.S. (2004). Earthquake and flood-induced turbidites in the Saguenay Fjord Québec: a Holocene paleoseismicity record. Quaternary Science Reviews, 23, 283-294

Sturm, M. and Matter, A. 1978. Turbidites and varves in Lake Brienz Switzerland: deposition of clastic detritus by density currents. Spec. Publs int. Ass. Sediment. 2, 147-168.

Waldmann, N., Anselmetti, F.S., Ariztegui, D., Austin, J.A. Jr., Pirouz, M., Moy, C.M. and Dunbar, R. 2010. Holocene mass-wasting events in Lago Fagnano, Tierra del Fuego (54° S): implications for paleoseismicity of the Magallanes-Fagnano transform fault. Basin Research 23, 171-190. DOI: 10.1111/j.1365-2117.2010.00489.x

Wennrich, V., Minyuk, P., Borkhodoev, V., Francke, A., Ritter, B., Brigham-Grette, J. and Melles, M. (in prep.) Pleistocene climate and environmental history of Lake El'gygytgyn, NE Russia based on high-resolution inorganic geochemistry data. Climate of the Past 2012.

IODP

Provenance and depositional processes of tephras and Tertiary volcaniclastic sandstones from IODP Expedition 322, Nankai Trough (KU 2685-1-1)

S. KUTTEROLF[1], A. FREUNDT[1], J.C. SCHINDLBECK[1]

[1]GEOMAR, Wischhofstr. 1-3, 24148 Kiel

During IODP Expedition 322 at the Nankai Trough, sediments down to the early Miocene have been drilled which allow to constrain the physical, compositional and structural characteristics of the subduction input into the seismogenic zone. Five lithologic units were identified at Site C0011, and six at Site C0012, based on sediment compositions, sediment textures, and sedimentary structures (henceforth for brevity referred to simply as "units"). More detailed descriptions and interpretations of the individual lithostratigraphic units as well as the used stratigraphical and sedimentological methods can be found in Underwood et al. (2010), Expedition 333 Scientists (2011). We have used samples from these expeditions and will use samples from other Nankai bore holes to:

- establish a Nankai-wide tephrostratigraphy including correlations with on land deposits.
- identify provenance sources comprising the Miocene to recent Japanese and Izu-Bonin arc segments.
- determine temporal and spatial variations in volcanic glass compositions since the Miocene.
- unravel depositional processes of the newly discovered middle Shikoku basin formation.

Additionally we initiated a strong collaboration with Rachel Scudder and Prof. Rick Murray from Boston University including a student exchange (R. Scudder to Germany in June 2012, J. Schindlbeck to Boston in July 2012) to work on samples from Nankai Trough Expeditions 322 and 333 to unravel the amount, provenance and influence of dispersed ash within the the sediment input. The American National Science Foundation already supports this collaboration with an approved proposal from Prof. Rick Murray (Position Rachel Scudder and analytical costs in Boston facilities). Both students will learn from each other and set the base for future colloborations. While Rachel Scudder will be made familiar with petrographic and micro-analytical methods, Julie Schindlbeck will learn to use the ICP-MS and to apply statistical analysis for geochemical data. Results from this project and other collaborations have been presented on international conferences (AGU 2010 and 2011, IUGG 2011 and 2nd post-cruise meeting in Barcelona 2011) and will be published within several contributions in the near future. The summary below is therefore a compilation of the research we are involved.

Major achievements in the last one and a half years are that our studies affirm the subdivison of the late Miocene lithologic Unit II (>7.07 to ~9.0 Ma) into two subunits by the abundance of volcanic glass shards, mineral and/or lithic contents. Whereas the upper subunit IIA consists of

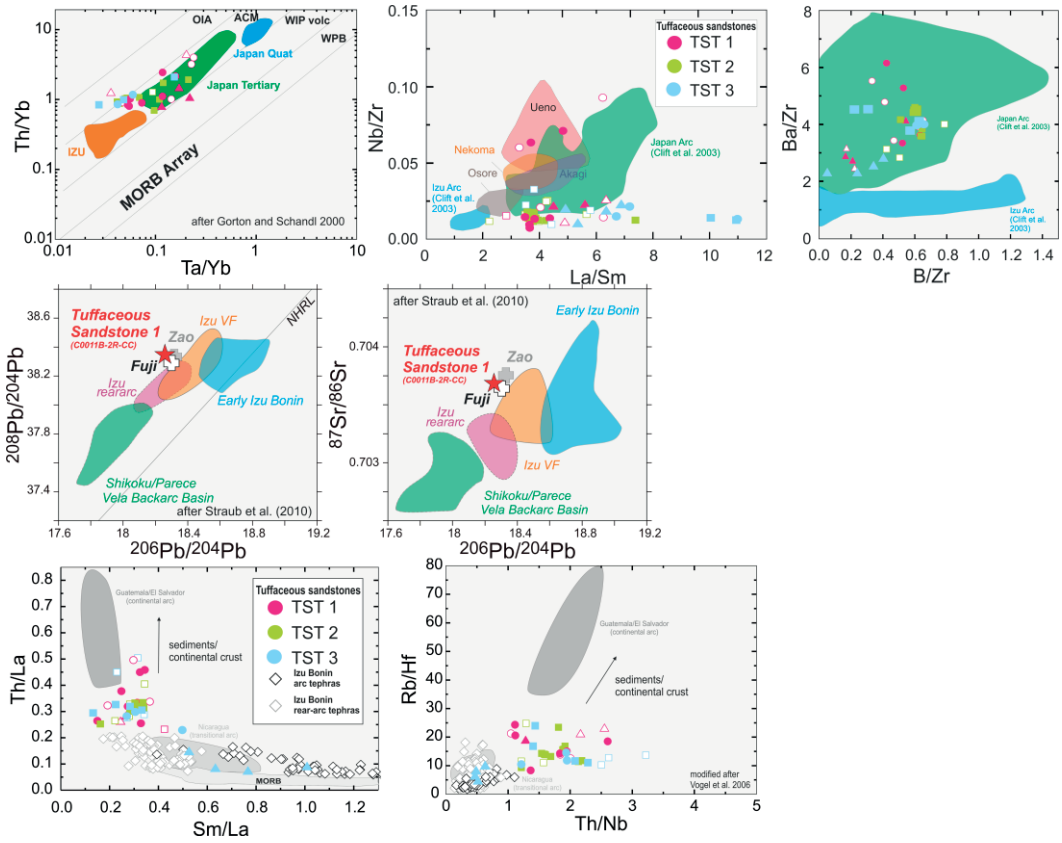

Figure A) upper panel: trace element ratios showing correlation to Japanese provenance; middle panel: isotope ratio of tuffaceous sandstone 1 (red star) in comparison to Izu-Bonin arc and rear arc as well as to Fuji and Zao volcano located in the vicinity of Izu Peninsula on the Japanese mainland. Lower panel: tuffaceous sandstone compositions in trace element diagrams indicating continental crust contamination.

silty claystone including three 1 to 10 meter thick interbeds of tuffaceous sandstones, unit IIB shows a transition from volcanoclastic sandstones at the top to normal sandstones at the base. Tuffaceous sandstones are characterized by their high amount (25 to 75%) of pyroclasts in their modal composition. Moreover, glass compositions show that the tuffaceous sandstones all derive from a similar source region, except the lowermost sandstone package that differs from the others. Magmatic compositions of both possible source regions, the Izu-Bonin back arc or the Japanese mainland, would be compatible with the moderate K_2O concentrations (2 to 3.5 wt%), but trace element ratios like Nb/Zr versus La/Sm , Th/Yb versus Ta/Yb or Ba/Zr versus B/Zr as well as isotope data favors the latter one (Fig. A). The Izu Bonin Arc can be excluded as a source due to generally lower potassium concentrations. Aditionally, glass trace element ratios like Th/La versus Sm/La, Rb/Hf versus Th/Nb or U/Th versus Th/Nb suggest a mantle source region lying below continental crust (Fig. A). Especially the lower sandstone packages of Unit IIa show convergence to Izu-Bonin rear arc signals whereas the mixture of those signals with clearly continental signal suggest the Japanese mainland (Izu Peninsula) at the collision zone between Izu Arc and the Japanese palaeo-arc to be the most likely provenance for the tuffaceous sandstones (see abstract Kutterolf et al.). This results are also assisted by the data from the provenance study of Scudder et al., who also see no significant ash proportion from an Izu–Bonin source within the background sediments of Unit IIa.

The three tuffaceous sandstone packages are build up by one to three density-graded units, interpreted as turbidity current deposits. For sandstone package 3, in contrast to 1 and 2, core pictures and thin section analyses indicate a subdivision in three units showing the same significant variations in top to bottom enrichment. This suggests three sedimentation events following each other in short time intervals. Modal analyses of 29 sandstone thin sections reveal systematic vertical changes within each bed. Generally low-density pyroclasts are enriched at the top (50-60 vol%) of each sandstone bed whereas dense lithic components (25-30 vol%) and minerals (25-30 vol%) as well as pumices with high amount of minerals are enriched at the bottom. The vertically varying abundance of various types of lithic fragments (sedimentary, volcanoclastic and metamorphic) suggests that these have also been segregated according to their respective densities (Fig. B). The highest amount of fine-grained matrix glass is found in the middle of each bed. Pumice and lithic fragments in the middle and upper parts of the sandstone beds carry ash coatings. Major and trace element glass-shard compositions in each sandstone package either have homogeneous composition or define a well-constrained compositional variation trend, implying that each package derived from a single pyroclastic deposit or a single eruptive event as opposed to gravity currents resulting from collapse of large, heterogeneous slope sections. Specifically the matrix glass-shard major element compositions are identical to the pumice clast composition in each tuffaceous sandstone bed assisting this interpretation (Fig. C). The compositions of amphibole and

pyroxene crystals differ only slightly between the

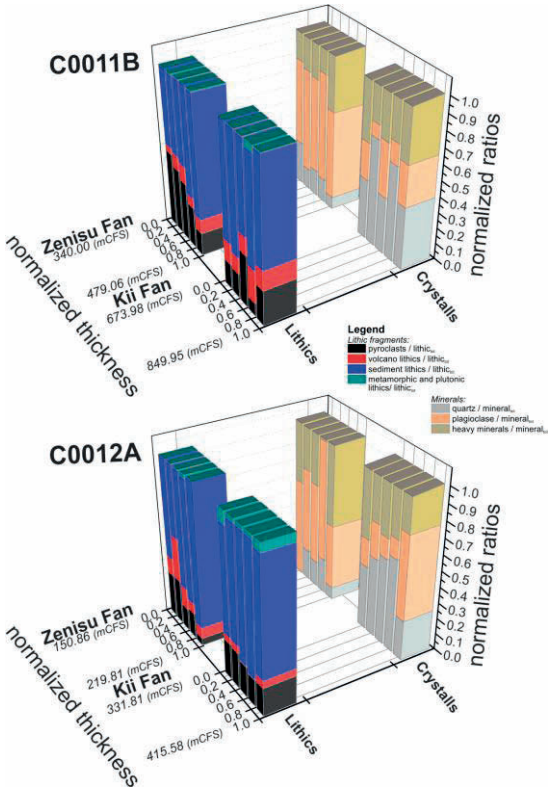

Figure B) Left: Pointcounting results of Unit II and IV showing the difference in component inventory within the stratigraphy.

sandstone packages (Fig. C). Application of the Ridolfi et al. (2009) thermobarometric calculations to amphiboles of sandstone packages 1 and 2 suggests that each of these was derived from a volcanic system comprising both a deep and a shallow magma reservoir. Thickness and massive density-graded structure, and characteristic glass composition of each sandstone bed as well as as their occurrence ~ 350 km from the Japanese mainland , the most likely source region, support emplacement by huge turbidity currents directly derived from major explosive volcanic eruptions, probably involving massive entrance of pyroclastic flows into the ocean (see abstract Schindlbeck et al.).

Beneath Unit II a monotoneous, volcanoclastic-poor, 9.1 to 12.7 Ma (middle to late Micocene) old sequence of silty claystones represents Unit III and is underlaid by bioturbated silty claystone with abundant interbeds of normally graded, dark gray clayey siltstone and fine-grained siliciclastic sandstone of Unit IV (middle Miocene, 12.2 to 13.5 Ma). The sediments are interpreted as deposits from muddy or sandy turbidity currents, respectively that are enriched in quartz (Fig. B).

In contrast, tuffaceous silty claystone and light gray tuff with minor occurrences of tuffaceous sandy siltstone are the dominant lithologies that can be found in Unit V at Site C0011 (~14 Ma). Results regarding their major element compositions correlate with the thick rhyolitic tuffs that were recovered at Site 808 from the Muroto transect of the Nankai Trough, which yielded an age of ~13.6 Ma (Taira et al., 1992).

Unit V (13.5 to 18.9 Ma) from Site C0012 is much better preserved and dominated by silty claystone. Coarser interbeds in the lower part of the unit consist of siliciclastic sandstone, volcaniclastic sandstone, and rare tuff. The sandstones, some show cross-laminae, plane-parallel laminae, convolute laminae, and soft-sediment sheath folds, appear to have two separate detrital provenances judging from point counting of smear slides and thin sections: (1) a volcanic source with fresh volcanic glass, together with relatively large amounts of feldspar, and (2) a siliciclastic source enriched in sedimentary lithic grains, quartz, and heavy minerals (including pyroxene, zircon and amphibole). The Outer Zone of southwest Japan (e.g.,

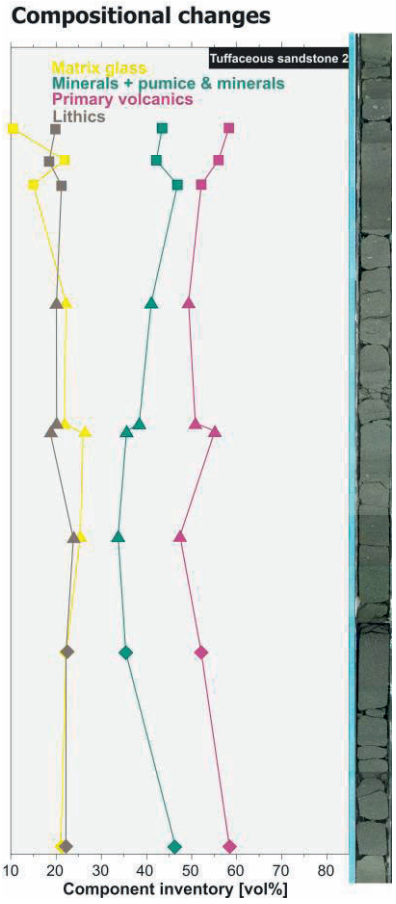

Figure B) Right: Varying components within the stratigraphy of tuffaceous sandstone II.

Shimanto Belt) is the likely siliciclastic source. Bulk XRD confirms that relative percentages of quartz and feldspar increase significantly in the coarse-grained strata, and XRF data show appreciable scatter in most of the major oxides because of lithologic/textural heterogeneity. These ranges of compositions, textures, and ages are also reminiscent of the older turbidite intervals and volcaniclastic-rich deposits at Site 1177 (Moore, et al., 2001).

Pickering et al. have combined our results, the results of the structural geology and logging-while-drilling with the seismic survey and interpreted the sediment successions as the result of three long-living submarine fan systems contributing to the basin evolution of the Shikoku Basin. Seismic interpretation suggests that the oldest fan (Kii Fan) has a more sheet-like geometry typical of depositional lobes, and petrographic data suggests that it was supplied

by sediment gravity flows fed from different sources from the north and east. The intermediate-age fan (Zenisu-daiichi Fan) appears channelized, recording more proximal

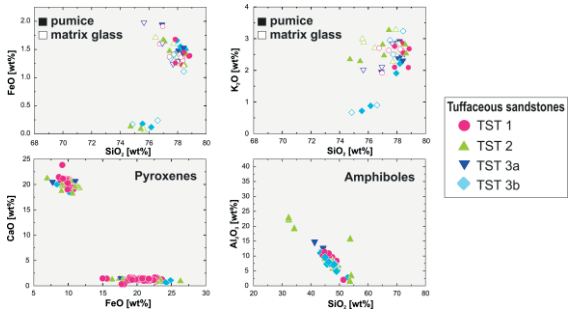

Figure C) Glass and mineral compositions of all tuffaceous sandstones showing homogenity within juvenile clasts and minerals.

middle-fan deposition at Expedition 322 sites. In contrast, the youngest fan (Zenisu-daini Fan) has sheet-like geometry that contains the thick-bedded and coarse-grained tuffaceous sandstones described above.

References:
Expedition 333 Scientists, 2011. NanTroSEIZE Stage 2: subduction inputs 2 and heat flow. IODP Prel. Rept., 333.
Ridolfi F, Renzulli A, Puerini M (2009) Stability and chemical equilibrium of amphibole in calc-alkaline magmas: an overview, new thermobarometric formulations and application to subduction-related volcanoes. Contrib Mineral Petrol, DOI 10.1007/s00410-009-0465-7.
Underwood, M.B., Saito, S., Kubo, Y., and the Expedition 322 Scientists, 2010. Expedition 322 summary. In Saito, S., Underwood, M.B., Kubo, Y., and the Expedition 322 Scientists, Proc. IODP, 322: Tokyo (Integrated Ocean Drilling Program Management International, Inc.).
Taira, A., Hill, I., Firth, J., Berner, U., Bruckmann, W., Byrne, T., Chabernaud, T., Fisher, A., Foucher, J.-P., Gamo, T., Gieskes, J., Hyndman, R., Karig, D., Kastner, M., Kato, Y., Lallemant, S., LU, R., Maltman, A., Moor, G., Moran, K., Olaffson, G., Owens, W., Pickering, K., Siena, F., Taylor, E., Underwood, M., Wilkinson, C., Yamano, M., and Zhang, J., 1992. Sediment deformation and hydrogeology of the Nankai Trough accretionary prism: synthesis of shipboard results of ODP Leg 131. Earth and Planetary Science Letters, 109, 431-450.
Moore, G.F., Taira, A., Klaus, A., et al., 2001. Proc. ODP, Init. Repts., 190: College Station, TX (Ocean Drilling Program).

IODP

Formation and origin of tuffaceous sandstones from IODP Expedition 322, Nankai Trough

S. KUTTEROLF[1], J. SCHINDLBECK[1], A. FREUNDT[1], R.P. SCUDDER[2], K.T. PICKERING[3], S. LABANIEH[4], H. NARUSE[5], M.B. UNDERWOOD[6], H. WU7[1]

[1]GEOMAR, Kiel, Germany
[2] Boston University, Boston, MA
[3] University College, London, United Kingdom
[4] University Joseph Fourier, Grenoble, France
[5] Chiba Univeristy, Chiba, Japan
[6] University of Missouri-Columbia, Columbia, MO
[7] China University of Geosciences, Beijing, China

During IODP Expedition 322 one major new discovery was an interval of tuffaceous and volcaniclastic sandstones, which has been defined as the middle Shikoku Basin facies. This lithologic Unit II is late Miocene (>7.07 to ~9.0 Ma) in age and can be divided into subunits by the abundance of volcanic glass shards, mineral and/or lithic contents and bulk-rock XRF data. The upper subunit IIA consists of moderately lithified and bioturbated silty claystone including three 1 to 10 meter thick interbeds of tuffaceous sandstones containing 35 to 60 vol% pyroclasts. Major and trace element glass-shard compositions in each sandstone package either have homogeneous compositions or define a well-constrained compositional variation trend, implying that each package derived from a single pyroclastic or a single eruptive event as opposed to gravity currents resulting from collapse of large, heterogeneous slope sections.

Moreover, glass compositions show that the tuffaceous sandstones came all from a similar source region at the Japanese mainland or the Izu Bonin arc. Magmatic compositions of both regions are partly compatible with major element data but elements like K_2O and TiO_2 show a clear deviation regarding the Izu-Bonin arc system as potential source area. Furthermore, trace elements, trace element ratios (Nb/Zr versus La/Sm , Th/Yb versus Ta/Yb or Ba/Zr versus B/Zr) and espacially isotopes probably indicate the origin at the collision zone between Izu-Bonin and Honshu arc on Izu-Peninsula. Aditionally, glass trace element ratios like Th/La versus Sm/La, Rb/Hf versus Th/Nb or U/Th versus Th/Nb suggest a mantle source region lying below continental crust which is inexistent below the Izu-Bonin arc.

The lower sandstone packages of Unit IIa show convergence to Izu-Bonin rear arc signals whereas the mixture of those signals with clearly continental signal again favors the Japanese mainland (Izu Peninsula) at the collision zone between Izu Arc and the Japanese palaeo-arc to be the most likely provenance for the tuffaceous sandstones, that are generated at least ~ 350 km away from the Shikoku Basin.

IODP

Introduction to a CRISP related proposal: Miocene to recent tephrostratigraphy and sediment variability offshore Central America: Evolution, Provenance and Cyclicities

S. KUTTEROLF[1], A. FREUNDT[1], J. SCHINDLBECK[1]

[1]GEOMAR, Wischhofstr. 1-3, 24148 Kiel

During IODP Expedition 334 offshore Costa Rica, sediments down to the early Miocene have been drilled which allow to constrain the physical, compositional and structural characteristics of sediments within an erosive subduction zone. A huge number of tephra layers (>170) has been collected during cruise 334 and were sampled from older Central American ODP/IODP cruises. Tephras that will be sampled during the second CRISP cruise offshore Central America will complement this record. Our project aims to correlate offshore and onland tephras for provenance in order to establish a tephrostratigraphic framework, which is supported by absolute age dating. Geochemical, petrological and volcanological characterization of these tephras and sediments will be used to constrain temporal and spatial changes in eruption processes, magnitudes and frequencies as well as subduction erosional processes along the Central American subduction zone and at the CRISP locations in particular. The major CRISP related questions are: When did the

Cocos Ridge collide with the Central American subduction zone? How did the ancient explosive Costa Rican volcanism evolve before collision? How is sediment

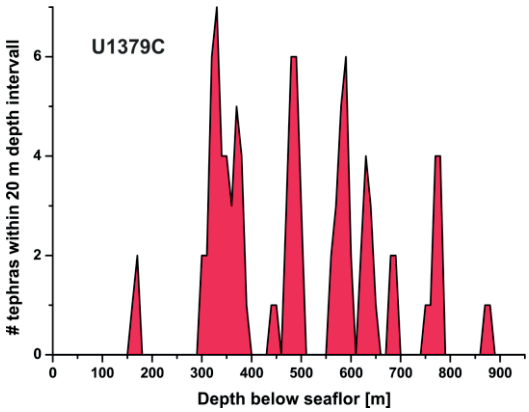

Figure 1: Variation in tephra abundance within Site U1379, probably suggesting cyclic behavior in the lower part of Southern Central American subduction volcanism

composition linked to temporal variations of subduction erosion? And what does the provenance of the ash layers on top of the Cocos Ridge tell us about explosive

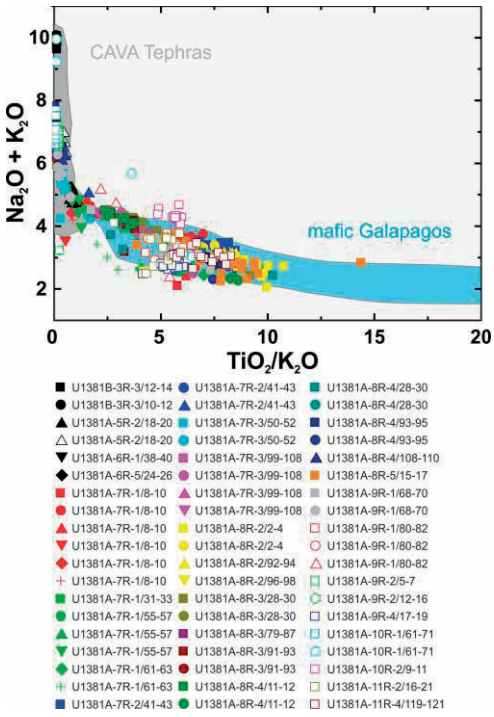

Figure 2: Discrimination diagram of total alkalis versus TiO_2/K_2O comparing Miocene to recent CRISP tephra compositions of Site 1381 from the incoming plate with Late Pleirsocene to recent Central American tephras as well as mafic rocks from Galapagos Hot Spot. Both source areas are captured by the CRISP tephras.

volcanism at the Galapagos Hotspot? In addition, our study will unravel hidden volcanic sources of the past, will evaluate the compositional and temporal relationships between subduction input and arc output along the whole Central American Volcanic Arc, and will investigate potentially cyclic behavior in subduction volcanism.

Cyclic behavior within the tephra record can very preliminarily suggested regarding the distribution pattern of tephra layers within Site 1379 sediment succession (see Figure 1). Additionally, first results of electron microprobe analysis of sediments from CRISP Site 1381 show that the tephras have a highly variable composition, ranging from relatively primitive basalts to trachytes and rhyolites. A first conducted provenance analysis based on major elements suggests that the first recovered tephra within the Pleistocene unit of Site U1381B at 22 m depth might be derived from one of the largest Costa Rican eruptions in the Quaternary, the 322 ka old Tiribi Tuff from Barva volcano. This results in a sedimentation rate of 6.8 cm/ka which is in agreement with Upper Pleistocene sedimentation rates on the incoming plate offshore Nicaragua. Within the Miocene sedimentary unit we can identify both, evolved tephras with low TiO_2/K_2O ratios (<2) comparable to Central American Arc tephras, as well as a series of evolved and primitive tephras with high TiO_2/K_2O ratios (>2.5) probably associated with the Galapagos Hot Spot volcanism (Figure 2).

IODP

Plio-Pleistocene evolution of nutrient cycling in the Benguela upwelling system: a chlorin-specific $\delta^{15}N$ approach

G. Leduc[1], N. Ogawa[2], S. Hisami[2], J. Etourneau[3], R. Schneider[1], N. Ohkouchi[2]

[1]Institute of Earth Sciences, Kiel University, Ludewig-Meyn Str. 10, Kiel, Germany
[2]Institute of Biogeosciences, JAMSTEC, 2-15 Natsuchima-cho, Yokosuka, Japan
[3]LOCEAN, Institut Pierre-Simon Laplace, 4 Place Jussieu, Paris, France

The Plio-Pleistocene climate evolution was marked by a transition from stable and warm conditions during the Pliocene toward colder conditions associated with the onset of pronounced glacial-interglacial cycles. A reduction of atmospheric CO_2 concentration was associated with this climate evolution (Pagani et al., 2010), but whether the driving mechanism responsible for such CO_2 drawdown was primarily triggered by increased surface ocean stratification at high latitudes (Haug et al., 1999) or increased biological pump at low latitudes (Etourneau et al., 2009) still remains uncertain. In the Benguela Upwelling System (BUS), the onset of the Plio-Pleistocene cooling co-occurred with extremely high accumulation rates of diatoms and biogenic opal, indicative of very high primary productivity during this time interval (Etourneau et al., 2009). As bulk $\delta^{15}N$ values were relatively low, ranging from 1 to 3‰ at this time, it is difficult to fully understand pathways of nutrient supply to sustain such high productivity. Here we have assessed the BUS nitrogen cycling by measuring $\delta^{15}N$ on chlorins to better determine and refine the nutrient supply to the BUS.

We have measured $\delta^{15}N$ on a suite of chlorophyll-derived chlorins (phaeophytin-a, pyrophaeophytin-a, Steryl-Chlorin esters, Chlorophyllone-a) extracted from ODP Site 1082 (northern BUS) and purified by HPLC prior to analysis on an ultra-sensitive elemental analyzer/isotope ratio mass spectrometer. We find that chlorin-specific compounds $\delta^{15}N$ are depleted by ~2 to 5‰ as compared to

the bulk $\delta^{15}N$ values, reflecting the effect of the isotopic fractionation occurring during biosynthetic partitioning of nitrogen within microalgae. This difference in $\delta^{15}N$ values between chlorins and bulk sediment however tends to decrease with age, indicating that other processes than nutrient cycling within the water column may have modified the isotopic signature of bulk sediment and/or of chlorins. We also detect more variability in chlorin $\delta^{15}N$ as compared to the $\delta^{15}N$ measured on bulk sediment, as already reported from other environmental settings (see e.g. Tyler et al., 2010). Overall, the chlorin-specific $\delta^{15}N$ values suggest little or no long-term changes in $\delta^{15}N$ associated with the Plio-Pleistocene climate transition.

It has been demonstrated that within particular sedimentary environments associated with high organic matter content such as in sapropel layers (Sachs and Repeta, 1999) and black shales deposited during Oceanic Anoxic Events (Ohkouchi et al., 2006) the bulk $\delta^{15}N$ signal can be significantly altered or hampered by diagenetic or heterotrophic processes. Therefore, if only the chlorin $\delta^{15}N$ is considered, it suggests that the mode of nutrient cycling in the BUS has experienced only little changes at the million-year timescale. Overall, the chlorin $\delta^{15}N$ values of ~0.5‰ (+/- 1.5‰) lead us to estimate an isotopic composition of the marine phytoplankton of ~6‰ if the isotopic integrity of the chlorin $\delta^{15}N$ remained unchanged over the last 3.5 Ma. Implications on the BUS nutrient cycling through the Pliocene-Pleistocene time interval will be discussed.

References:
Etourneau, J., et al. Pliocene-Pleistocene variability of upwelling activity, productivity, and nutrient cycling in the Benguela region. Geology, 37, 871-874 (2009).
Haug, G.H., et al. Onset of permanent stratification in the Subarctic Pacific Ocean. Nature, 401, 779-782 (1999).
Ohkouchi, N., et al. The importance of diazotrophic cyanobacteria as primary producers during Cretaceous Oceanic Anoxic Event 2. Biogeosciences 3, 467-478.
Pagani, M., et al. High Earth-system climate sensitivity determined from Pliocene carbon dioxide concentrations. Nature Geoscience, 3, 27-30 (2010).
Sachs, J.P., and D.J. Repeta, Oligotrophy and nitrogen fixation during eastern Mediterranean sapropel events. Science, 286, 2485-2488.
Tyler, J., et al. Tracking aquatic change using chlorin-specific carbon and nitrogen isotopes: The last glacial-interglacial transition in Lake Suigetsu. G-cubed, 11, Q09010, doi:10.1029/2010GC003186 (2010).

ICDP

The Siljan Meteorite Crater in central Sweden – an integral part of the Swedish Deep Drilling Program (SDDP)

O. LEHNERT[1], G. MEINHOLD[2], S.M. BERGSTRÖM[3], M. CALNER[4], J. O. R. EBBESTAD[5], S. EGENHOFF[6], Å.M. FRISK[7], A.E.S. HÖGSTRÖM[8] & J. MALETZ[9]

[1] GeoZentrum Nordbayern, Lithosphere Dynamics, University of Erlangen-Nürnberg, Schloßgarten 5, D-91054, Erlangen, Germany; lehnert@geol.uni-erlangen.de
[2] Department of Sedimentology & Environmental Geology, Geoscience Centre, University of Göttingen, Goldschmidtstrasse 3, D-37077 Göttingen, Germany, variscides@gmail.com
[3] School of Earth Sciences, Division of Earth History, The Ohio State University, 125 S. Oval Mall, Columbus, Ohio 443210; stig@geology.ohio-state.edu
[4] Department of Geology, Lund University, Sölvegatan 12, SE-223 62 Lund, Sweden; mikael.calner@geol.lu.se
[5] Museum of Evolution, Uppsala University, Norbyvägen 16, SE - 752 36 Uppsala, Sweden; jan-ove.ebbestad@em.uu.se
[6] Department of Geosciences, Colorado State University, 322 Natural Resources Building, Fort Collins, CO 80523-1482, USA; sven@warnercnr.colostate.edu
[7] Paläontologisches Institut und Museum, Karl Schmid-Strasse 4, 8006 Zürich, Switzerland; asa.frisk@pim.uzh.ch
[8] Tromsö University Museum, Natural Sciences, N-9037 Tromsö, Norway; anette.hogstrom@uit.no
[9] Institut für Geologische Wissenschaften, Freie Universität Berlin, Malteser Str. 74-100, Haus B, Raum 322, D-12249 Berlin, Germany; yorge@zedat.fu-berlin.de

New drill cores from the largest known impact structure in Europe, the Siljan crater, provide superb possibilities to reconstruct Early Palaeozoic marine environments and ecosystems, and to document changes in sedimentary facies, sea-level and palaeoclimate. The meteorite crater is a major target of the project Concentric Impact Structures in the Palaeozoic (CISP) in the framework of the Swedish Deep Drilling Program.

Studies of Ordovician and Silurian strata in the Siljan District have a long tradition and many scientific papers deal with the geology of the area. The Palaeozoic succession starts with the Tremadocian Obolus conglomerate, the youngest pre-Caledonian strata are Middle Silurian shales of the Nederberga Formation. However, exposures are limited, there are few continous sections, and the Early Palaeozoic sedimentary rocks resting on the Precambrian basement are incompletely investigated.

Detailed sedimentological and biostratigraphical studies of the cores and the Nittsjö trench together with analysis of the carbon isotope chemostratigraphy will allow intra- and intercontinental correlations and the dating of Caledonian movements. Our preliminary studies show that different and yet undefined facies belts are preserved in the Siljan District. The recent findings of palaeokarst in the area together with similar new findings in other parts of Baltoscandia reflect times of subaerial exposure of the basin regionally and challange the idea that the Baltoscandian basin was a deep and tranquil depositional environment.

Our preliminary data provide a first base for reinterpretations of this part of Sweden, previously regarded as representing a stable cratonic area unaffected by the Caledonian collision between Baltica and Laurentia. The erosional unconformity and the substantial hiatus between Middle Ordovician limestones and late Early Silurian shales in the western part of the crater suggests an extended period of uplift and erosion presumably related to flexural forebulge migration toward the east due to tectonic loading by the Caledonian nappes to the west. The Lower to Middle Ordovician carbonate succession is only about 21 m thick, with a sharp flooding surface on top of the Mid-Ordovician Holen Formation. The overlying siliciclastic succession (Upper Llandovery, based on graptolite data) comprises a minimum thickness of about 224 m. The sudden deepening after the eastward migration of the forebulge is indicated by rapid deposition of shales and shale/mudstones displaying unstable conditions expressed by megaslumps, debris flows, turbidites and several synsedimentary tectonic features. The intercalation of a sandstone unit reflects a strong regression in this shale basin followed by rapid transgression and deposition of dark, organic-rich shale and mudstone.

In contrast to this development, a classical Ordovician/Silurian carbonate/shale succession, well

known from other parts of Sweden, formed in the northern (Skattungbyn-Kallholn), northeastern (Furudal), and southeastern part (Boda) of the Siljan District. Detailed sampling of the cores for stable isotopes, thermal maturity, geochemistry, sediment provenance, facies and microfacies studies in the autumn of 2011 now helps in solving regional problems as well as stratigraphical and palaeogeographical questions.

ICDP

Seismic investigation of ancient Lake Ohrid (Macedonia/Albania) in preparation for the SCOPSCO ICDP-campaign.

K.LINDHORST[1], S.KRASTEL[1], T. SCHWENK[2], B. WAGNER[3]

[1] Helmholtz-Zentrum für Ozeanforschung Kiel (GEOMAR), Germany, klindhorst@geomar.de
[2] Fachbereich Geowissenschaften, Universität Bremen, Germany
[3] Institute für Geologie und Mineralogie, Universität Köln, Germany

The transboundary Lake Ohrid (Macedonia/Albania) represents an important archive to study the sedimentary evolution of a graben system over several million years (Figure 1). Lake Ohrid is not only considered to be the oldest, continuously existing lake in Europe but also host more than 210 endemic species which makes it a hotspot of biodiversity (Wilke and Albrecht, 2008). Its unique aquatic ecosystem was highlighted when Lake Ohrid was declared a UNESCO World Heritage Site in 1979. However, several factors such as the exact age and origin of the lake as well as the causes for the abundance of endemic species are still poorly understood.

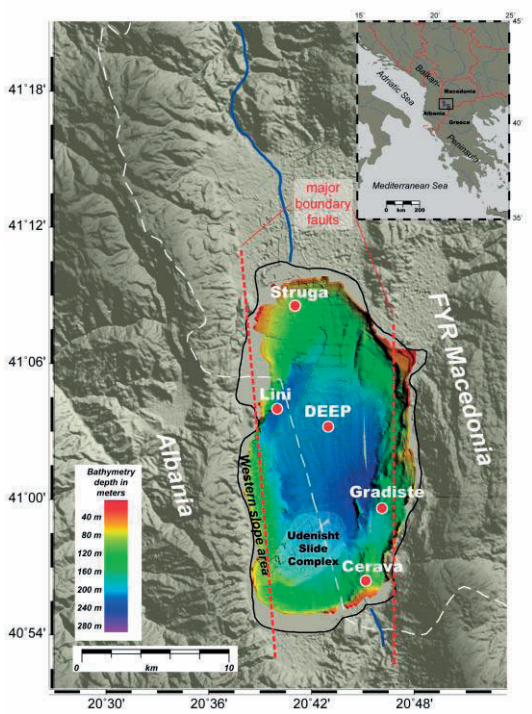

Figure 6: Bathymetry map of Lake Ohrid. Proposed sites are marked by the red dots.

A deep drilling campaign entitled SCOPSCO (Scientific Collaboration On Past Speciation Conditions in Lake Ohrid) approved by ICDP will take place in 2012 or 2013. Deep drilling will provide new insights on age and origin of Lake Ohrid as well as on major geological/environmental events and their impact on shaping an extraordinary degree of endemic biodiversity as a matter of global significance. In addition, a continuous record of paleoenvironmental history obtained from Lake Ohrid would provide an important database for historic climate changes as well as for volcanic activity within the northern Mediterranean region. As Lake Ohrid is located in a seismological active zone, a special interest is put on effects of major earthquakes and associated mass wasting events.

In order to select potential drill sites for the ICDP campaign, intense work was conducted on studying the morphological and sedimentary patterns of Lake Ohrid by means of multichannel seismic, sediment echo sounder, and bathymetric data; these data have been collected within several pre-site surveys between 2004 and 2009. Seismic profiles within the deep central basin of Lake Ohrid show thick undisturbed sediments overlying a rough basement (Figure 2). In this region no indications for a hiatus or major mass transport deposits are found. Hence it has been chosen as the most promising drill site (DEEP, see Figure 1) for collecting a long (>700 m) continuous and undisturbed archive; it is the key site for the entire drilling campaign. Major objectives to be addressed with this site include the age and origin of the lake, its environmental history, tephra deposition, and the link between evolutionary changes and geological events. Four additional drill sites in proximity to the shore will shed light on (i) major changes of the hydrological regime, (ii) ages of ancient clinoforms that are linked to lake level

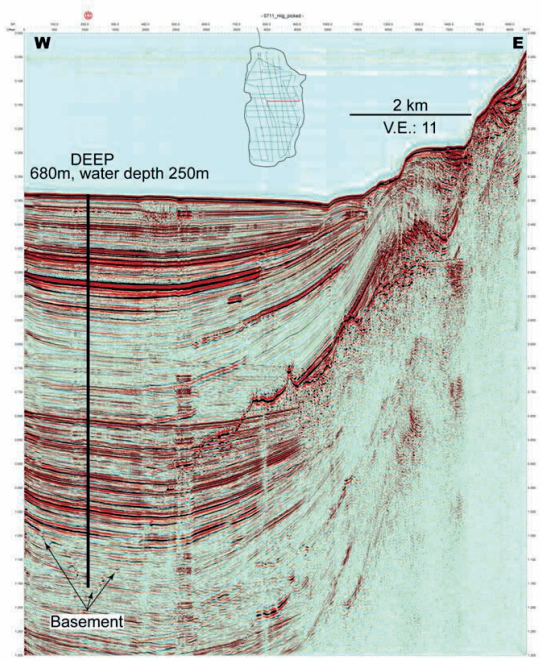

Figure 5: Multichannel seismic line crossing the DEEP-Site in the central basin of Lake Ohrid.

fluctuations, and (iii) neotectonic activity and associated mass wasting events.

Following a study in 2010 illustrating the importance of lake level fluctuations for geological and biological evolution of Lake Ohrid (Lindhorst et al., 2010), two drill

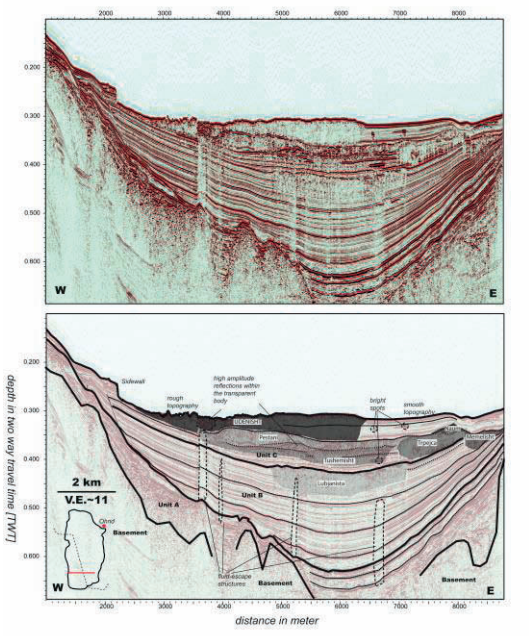

Figure 7: Bathymetry map of Lake Ohrid. Proposed sites are marked by the red dots.

sites were chosen in order to study clinoform structures identified on seismic data (Struga and Cerava, Figure 1). The proposed Struga site is close to the out flowing river Crni Drim at the northern part of Lake Ohrid. Buried clinoforms in this region indicate significant sediment input from the northern shore during a period of constant lake level, which might contradict a permanent drainage to the north. In the southern region five distinct clinoforms close to the Cerava Site indicate considerably lower lake levels in the past with subsequent sudden lake level rises, which is of major importance for the hydrological history of Lake Ohrid. Tracing reflections directly above or below the clinoforms is a first attempt of dating and allocating these events but deep drill cores are needed for exact age estimation and to reconstruct the subsidence history of the entire basin.

Lake Ohrid is located within a seismically active graben with two major boundary faults striking in a N-S direction on each side of the lake (Reicherter at al., 20011, Figure 1). A recent study of mass wasting events within Lake Ohrid suggest that slide bodies can be connected to seismic events within the region and therefore provide a promising possibility to assess paleaoseismicity of this active tectonic region (Lindhorst et al., 2012). On this account we selected two drill sites (Lini, Gradiste) on each side of Lake Ohrid in vicinity to the eastern and western major boundary fault zone in order to date major mass transport deposits and link them to the tectonic/earthquake history.

The Udenisht Slide Complex (USC) is a prominent mass wasting event that is detectable within acoustic data in the southwestern part of the lake (Lindhorst et al., 2012). This event was investigated in detail in order to reveal its age and its potential to trigger a tsunami within Lake Ohrid (Figure 3). Sediment echo sounder data suggest an undisturbed drape on top of slide deposits of maximal 30 cm. Assuming an accumulation rate of 0.2 mm/a for the Holocene (Wagner et al., 2009) we calculated a maximum age of 1500 years for the USC proofing that this particular slide event occurred within the late Holocene. Therefore the Udenisht slide event could have had a geological impact on the coastline while it was already populated. Our data allow reconstructing a two-phase landslide; the individual slide masses are characterized by volumes of less than 0.1 km3. The long run-out distance suggests a quickly disintegrating sediment mass. Based on these observations, we do not think that this slide triggered a significant tsunami. In addition, no historical report or geological evidence of waves that hit the shore line has been found so far.

Six additional transparent units older than the USC identified in the southwestern part of Lake Ohrid document the long history of mass wasting (Figure 3). The deepest slide (Lubjanista) has an estimated age greater than 500 kyr. No major mass movements older than 600 kyr are imaged on the seismic data. However only deep drill cores can provide substantial information needed for a reasonable time/depth conversion for future work.

References:

Albrecht, C., Wilke, T. (2008) Ancient Lake Ohrid: biodiversity and evolution, Hydrobiologia, 615, 103-140.

Lindhorst, K., Grün, M., Krastel, S., Schwenk, T. (2011) Mass wasting in Lake Ohrid (FYR Macedonia/Albania) – hydroacoustic analysis and its tsunamigenic potential. Submarine mass movements and their consequences. Advances in Natural and Technological Hazards Research, 31, Springer, 245-253

Lindhorst, K., Vogel, H., Krastel, S., Wagner, B., Hilgers, A., Zander, A., Schwenk, T., Wessels, M., Daut, G. (2010) Stratigraphic analysis of Lake Level Fluctuations in Lake Ohrid: An integration of high resolution hydro-acoustic data and sediment cores. Biogeosciences, 7, 3531–3548.

Reicherter, K., Hoffmann, N., Lindhorst, K., Krastel, S., Fernández-Steeger, T. (2011) Active basins and neotectonics: the Lake Ohrid (FYROM, Albania), ZDGG, Tectonics and Sedimentation, 162, 217-234.

Wagner, B., Lotter, A,. Nowaczky, N. et al. (2009) A 40,000-year record of environmental change from ancient Lake Ohrid (Albania and Macedonia). J. Paleolimnol., 41, 407-430.

ICDP

The extant ostracode fauna of Lake Ohrid – A key to anthropogenic and paleoenvironmental reconstructions

J. LORENSCHAT[1], F. VIEHBERG[2], B. SCHARF[3], A. SCHWALB[1]

[1]Institut für Geosysteme und Bioindikation, Technische Universität Braunschweig, Langer Kamp 19 c, 38106 Braunschweig, Germany (j.lorenschat@tu-bs.de)
[2]Institut für Geologie und Mineralogie, Universität zu Köln, Zülpicherstraße 49 a/b, 50674 Köln, Germany
[3]Ellhornstr. 21, 28195 Bremen, Germany

Recently, ancient Lake Ohrid (Republic of Macedonia/Albania) was selected as future coring site by the International Continental Scientific Drilling Program (ICDP) because of its high potential as paleoenvironmental archive (Wagner et al., 2008). The lake is characterized by a high degree in endemism and an unresolved geological history. Ostracodes, small crustaceans, which are environmentally sensitive bioindicators and preserve as fossils because of their calcitic shells, are abundant in at least the last two interglacial sediment sequences from Lake Ohrid. Thus, they provide a unique record to test the aquatic ecosystem response to environmental changes. It is of general importance to understand the ecology of individual ostracode species and species assemblages when working with subfossil and fossil assemblages. Because the ecology of ostracodes in Lake Ohrid is poorly known, the analyses of recent ostracode assemblages in Lake Ohrid are the basis for using ostracodes as bioindicators. For example, there is no information about ostracode diversity in water depths > 50 m. This is, however, of particular importance for the reconstruction of lake level changes from species assemblages and for interpreting ostracode assemblages form cores that will be retrieved within the frame of ICDP. Thus, we carried out seasonal samplings to unravel the ecology of ostracodes in Lake Ohrid by characterizing sediment and water parameters. Furthermore, we determined the degree of extinction due to anthropogenic pressure by the means of three sediment cores which were taken from 50 m water depth from polluted sites (nearby the cities of Struga (ST09; core length 49 cm) and Ohrid (OH09; core length 34 cm) on the northern and north-eastern shore) and from a pristine site (near Sveti Naum (SV09; core length 33 cm) at the south-eastern shore). Short cores were ^{210}Pb and ^{137}Cs dated, elemental composition was determined using XRF, CNS, and Mercury (Hg) Analyser, and sampled for ostracodes (every 1 cm, 50 g wet sediment). The constant initial concentration model was used to determine sediment ages. Sediment core CO1202 (spanning the past approximately 136 ka) was taken in September 2007 at 145 m water depth in the north-eastern basin of Lake Ohrid (Wagner et al., 2010).

Extant ostracode fauna:

A survey of living ostracodes and assemblage diversity based on 142 samples taken in Lake Ohrid provided 24 species belonging to seven families (Candonidae, Ilyocyprididae, Cyprididae, Leptocytheridae, Limnocytheridae, Cytherideidae, and Darwinulidae) and eleven genera (Candona, Fabaeformiscandona, Candonopsis, Cypria, Cyclocypris, Ilyocypris, Prionocypris, Leptocythere, Paralimnocythere, Cytherissa, and Darwinula) in Lake Ohrid. Another seven species were identified using empty carapaces and valves (Candona expansa, Candona hartmanni, Candona holmesi, Candona jordeae, Candona litoralis, Candona triangulata, and Paralimnocythere cf. umbonata). Ilyocypris bradyi and Prionocypris zenkeri were verified in the lake for the first time. Even in 280 m water depth living ostracodes were found (Candona hadzistei, Candona marginatoides, Candona media, Candona ovalis, Candona vidua, Fabaeformiscandona krstici, Cypria lacustris, Cypria obliqua, and Leptocythere karamani). Highest ostracode abundances occured in water depth < 50 m. The most common groups were the Candonidae, representing about 63% of all ostracode species in Lake Ohrid, and the Limnocytherinae (21%) so that the young ancient lake status is confirmed by the prevalence of species flocks of both groups (Frogley et al., 2002). The only real cosmopolitan species was Darwinula stevensoni. The presence of Leptocythere in Lake Ohrid, a genus that normally inhabits salt and brackish water, may hint at a marine origin of the lake. Eleven out of the 24 ostracode species were endemic to Lake Ohrid. In the catchment of Lake Ohrid 21 species were discovered out of which 14 also occurred in the lake itself.

The exact number of ostracode species in Lake Ohrid is so far unknown. Frogley & Preece (2004) reported 52 ostracode species in the lake and its catchment, meanwhile, Petkovski (2005, unpublished data) mentioned only 41 ostracode species for Lake Ohrid (excluding the catchment). Despite our intensive limnological and palaeolimnological study we found only 24 living species in the lake. For example, Petkovski (2005, unpublished data) affirmed four species of Leptocythere in Lake Ohrid (Leptocythere angulata, L. karamani, Leptocythere prespensis, and Leptocythere proboscidea) out of which we found only L. karamani. This could be an evidence for a recent species loss.

Anthropogenic impact on species assemblages:

The ostracode fauna of the three sediment cores closely resembles the modern species assemblages from Lake Ohrid. We identified a total of 27 ostracode species in the short cores (17 in ST09, 24 in OH09, and 18 in SV09). Only Candona sp.1 and Cypria sp. 1 were absent in surface sediments. The dominant species in ST09 and SV09 was Candona trapeziformis and in OH09 Candona media. Highest abundance of ostracodes occured in core OH09. Peaks in abundances appeared independently from changes in elemental compositions and there was a negative correlation between ostracode abundances and Shannon diversity index (mathematical measure of species diversity in a community). This diversity index was relatively constant in OH09 and ST09 but increased since 1980 in core SV09. The geoaccumulation index suggested uncontaminated to moderately contaminated levels of pollution at the three sites. Sedimentation rate was 0.083 cm yr $^{-1}$ near the city of Ohrid (sediment core spanning the past approximately 370 years), 0.4 cm yr^{-1} near the city of Struga (spanning the past approximately 85 years), and 0.46 cm yr^{-1} near Sveti Naum (spanning the past approximately 60 years). The dark color of top 4 cm from core OH09 suggested increasing eutrophication after 1970. The high C/N ratios in SV09 since 1981 were probably caused by the increase in tourist numbers and consequently the destruction of littoral habitats and increasing erosion.

Our results show an incipient eutrophication near the city of Ohrid after 1970 and a significant change in ostracode assemblages in SV09 after 1980 indicating environmental alteration. In 2010 Kostoski et al. warned about the „creeping biodiversity crisis“ of the last decades caused by major socio-politcal changes and human-meditated environmental changes.

Eemian and holocene ostracode assemblages:

A preliminary set of 118 samples from core CO1202 shows that ostracode valves were present in all interglacial samples of Eemian and Holocene age. We found only sporadically valves in the glacial sediments that are carbonate-free or have low carbonate contents (< 10 %). So far we identified 21 ostracode species (exclusively juveniles) out of which five species were not yet found in our recent sediment samples. In contrast, Belmecheri et al. (2009) reported only a total of 12 species from a sediment core spanning the past approx. 140 ka. In our cores, maximum number of species in a single sample was 11 (ca. 6.7 ka), and diversity during the Eemian was lower than during the Holocene. This also contradicts results by Belmecheri et al. (2009) who suggest that there is no significant change in species diversity between these two interglacial periods. These discrepancies also underline the need for accurate taxonomy. In general, the abundances of ostracodes were relativ low (max. 181 valves g^{-1}) which may be the result of the great water depth from where CO1202 was retrieved (145 m). Therefore, it would be ideal if during the upcoming ICDP deep drilling a core from a water depth < 50 m, where ostracodes and other organism occur in high abundances, would be retrieved.

References:

Belmecheri, S., Namiotko, T., Robert, C., von Grafenstein, U. & D.L. Danielopol, 2009. Climate controlled ostracod preservation in Lake Ohrid (Albania, Macedonia). Palaeogeography, Palaeoclimatology, Palaeoecology 277: 236-245.

Frogley, M.R., H.I. Griffiths & K. Martens, 2002. Modern and fossil ostracods from ancient lakes. Holmes, J. A. & A. Chivas (eds), The Ostracoda: Applications in Quaternary Research. American Geophysical Union, Washington DC: 167-184.

Frogley, M.R. & R.C. Preece, 2004. A faunistic review of the modern and fossil molluscan fauna from Lake Pamvotis, Ioannina, an ancient lake in NW Greece: implications for endemism in the Balkans. Griffiths, H.I., B. Kryštufek & J.M. Reed (eds), Balkan biodiversity: pattern and process in the European hotspot. Kluwer Academic Publishers, Dordrecht: 243-260.

Kostoski, G., C. Albrecht, S. Trajanovski & T. Wilke, 2010. A freshwater biodiversity hotspot under pressure – assessing threats and identifying conservation needs for ancient Lake Ohrid. Biogeosciences 7: 3999-4015.

Wagner, B., K. Reicherter, G. Daut, M. Wessels, A. Matzinger, A. Schwalb, Z. Spirkovski & M. Sanxhaku, 2008. The potential of Lake Ohrid for long-term paleoenvironmental reconstructions. Palaeogeography, Palaeoclimatology, Palaeoecology 259: 341-356.

Wagner, B., Vogel, H., Zanchetta, G. & R. Sulpizio, 2010. Environmental changes on the Balkans recorded in the sediments from lakes Prespa and Ohrid. Biogeosciences 7: 3365-3392.

IODP

A Pliocene-Pleistocene geochemical record from the Bering Sea (IODP Expedition 323, Site U1341) – Paleoenvironmental reconstructions and diagenetic processes

C. MÄRZ[1, 2], S.W. POULTON[2], L.M. WEHRMANN[3], S. ARNDT[4], B. SCHNETGER[1], T. WAGNER[2], H.-J. BRUMSACK[1]

[1]AG Mikrobiogeochemie, Institut für Chemie und Biologie des Meeres (ICBM), Postfach 2503, 26111 Oldenburg, Germany
[2]Biogeochemistry, School of Civil Engineering and Geoscience (CEG), Drummond Building, Newcastle University, NE1 7RU Newcastle upon Tyne, United Kingdom (corresponding author: christian.maerz@ncl.ac.uk)
[3]Department of Earth Sciences, University of California, Riverside, 900 University Avenue, Riverside, CA 92521, USA
[4]School of Geographical Sciences, University of Bristol, University Road, BS8 1SS Bristol, United Kingdom

In summer 2009, IODP Expedition 323 recovered the first continuous sediment records covering the last ~4.3 Ma from the Bering Sea (IODP Site U1341, Bowers Ridge, Figure 1; Expedition 323 Scientists, 2010; Takahashi et al., 2011). Onboard studies revealed that the sediment dominantly consists of a variable mixture of siliciclastic

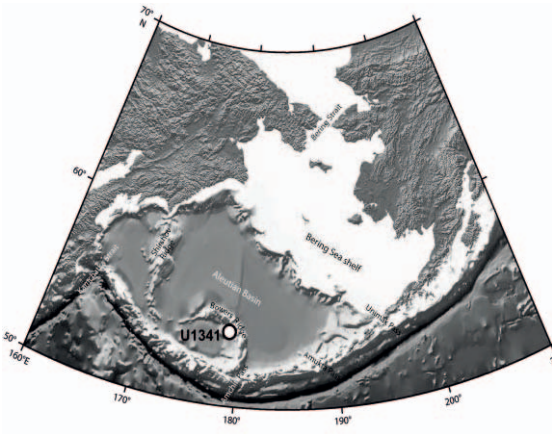

Figure 1: Location of IODP Site U1341 on Bowers Ridge, southern Bering Sea

clay/silt and biogenic opal, with minor amounts of biogenic/authigenic carbonate and volcanic ash, and was deposited with average sedimentation rates of 10-15 cm/ka. To resolve Pliocene-Pleistocene paleoenvironmental changes in the open Bering Sea (e.g. the amount and provenance of terrigenous material, paleoproductivity, bottom water redox conditions, diagenetic processes), the bulk chemical composition (C, S, major and minor elements) of ~190 freeze-dried ground sediment samples from Site U1341 was determined coulometrically, by thermal analysis, and by wavelength-dispersive X-ray fluorescence analysis (XRF). For a more precise quantification of trace element contents around the Pliocene-Pleistocene transition, ~35 selected samples were fully digested and analysed with a sector-field inductively coupled plasma mass spectrometer (ICP-MS). Around 100 of the samples were additionally subjected to a sequential P extraction procedure (modified after Ruttenberg, 1992; Schenau and De Lange, 2000; Latimer et al., 2006) to determine the associations of P with different sedimentary phases (e.g., fish bones, carbonates, Fe (oxyhydr)oxides, authigenic apatite, detrital apatite, biogenic opal).

Relatively low Al2O3 contents (~ 2-15 wt%) imply that terrigenous input (clay & silt) to the open marine Bowers Ridge was generally of minor importance, but there is a clear trend to higher Al2O3 contents in younger sediments (Figure 2). This increase of terrigenous material was most probably caused by the onset and intensification of the Northern Hemispheric Glaciation (NHG) and the related sea ice formation in the Bering Sea. The Al2O3 trend is inversely related to the SiO2 record, the latter documenting the overall reduced deposition of biogenic opal from the Middle Pliocene to the Holocene at Bowers

Ridge (Figure 2). The overall composition of this terrigenous sediment is similar to average continental crust, but a MgO-K2O-Al2O3 ternary diagram (Figure 3) shows an admixture of basaltic and especially andesitic material from adjacent volcanic rocks (Pribilof and Aleutian Islands). As shown by comparison with the Zr record, the Si enrichments at Site U1341 are not related to the increased deposition of sandy terrigenous material (Figure 3). Therefore, the Si-excess (Sixs) record (the calculated

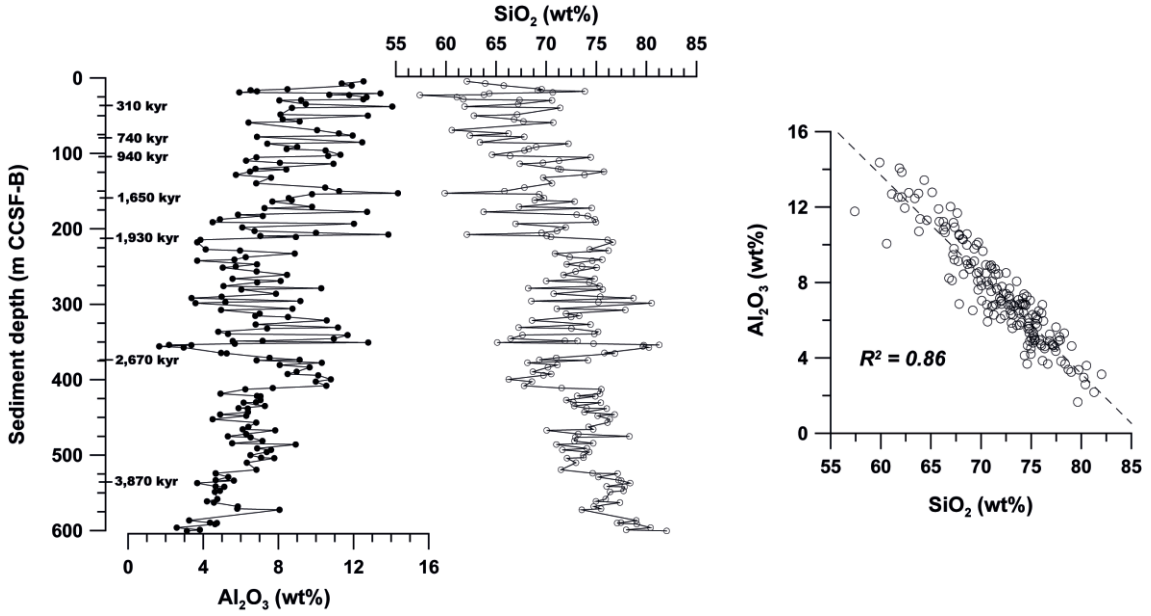

Figure 2: X-ray fluorescence records of Al_2O_3 (wt%) and SiO_2 (wt%) against sediment depth (m CCSF-B); Al_2O_3 - SiO_2 cross-plot.

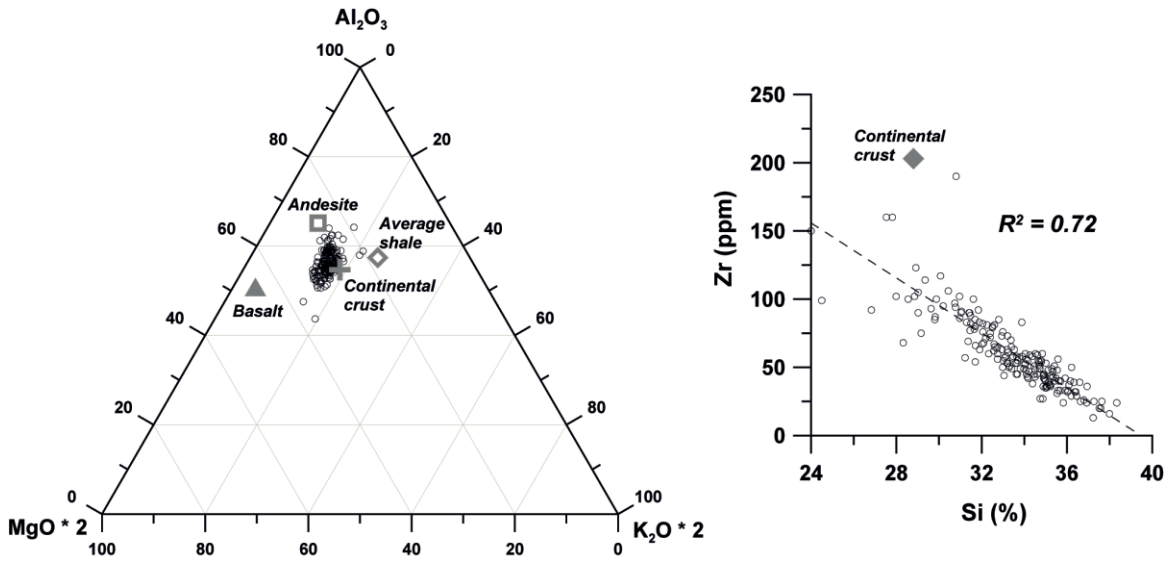

Figure 3: MgO-K_2O-Al_2O_3 ternary diagram with the Site U1341 samples (black circles) and the compositions of average basalt (triangle), andesite (square), continental crust (cross) and average shale (diamond); Zr - Si cross-plot.

non-detrital portion of total Si) can be applied as a proxy for biogenic opal deposition on Bowers Ridge.

The general Si enrichment in Bowers Ridge deposits reflects the importance of opal productivity since the Pliocene. But unlike sedimentary opal records from the open North Pacific (e.g., ODP Site 882; Haug et al., 1995, 1999), the Sixs record in the southern Bering Sea does not support a dramatic decrease in opal export to the sea floor after ~2.75 Ma (the Pliocene-Pleistocene transition) due to an intensification of the NHG. Instead, the Sixs record reached its highest peaks between ~2.7 and ~1.9 Ma BP, and only thereafter decreased to overall lower values. This early Pleistocene period of ~0.8 Ma duration was described as a phase of changing biogenic opal deposition patterns across the global ocean. While before ~2.7 Ma BP open marine, high-latitude areas (North Pacific, Southern Ocean) were the ocean regions with highest opal deposition, there was a global shift of opal deposition to Atlantic and Pacific upwelling regions (e.g., off California, Peru, Namibia; Cortese et al., 2004). In a similar way, the Bering Sea might have shifted from an "open marine high-latitude" setting to an "upwelling-type setting" around 2.7 Ma BP, resulting in a gradual rather than dramatic decline of biogenic opal deposition over the last ~4.3 Ma. An explanation for this paleoceanographic transition might be

the establishment of open North Pacific salinity stratification at ~2.75 Ma BP, suggested to have caused the "opal crash" at the Pliocene-Pleistocene boundary by preventing the upwelling of nutrients into the photic zone. As a consequence of shifting circulation regimes in the North Pacific, the nutrient-rich intermediate/deep North Pacific water masses could have been exported to the Bering Sea via the Kamtchatka Strait ("nutrient leakage"), upwelled at Bowers Ridge, and increased primary productivity. This scenario would explain our geochemical records, namely the increased opal deposition on Bowers Ridge after ~2.7 Ma BP.

There is also strong indication that biogeochemical element cycles at the sea floor were affected by this increase in opal productivity. The Early Pleistocene opal-rich sediment interval is not only significantly enriched in Cd, Mo and U (the most reliable indicators for anoxic to sulfidic bottom waters/surface sediments; Brumsack, 2006), but also in Ag that was recently suggested as a novel paleoproductivity proxy (McKay and Pedersen, 2008). This trace metal enrichment is exceptional, as most analysed samples are not significantly enriched in Mo, U or V, and only slightly depleted in Mn, indicating oxic-suboxic rather than anoxic bottom waters over the last ~4.3 Ma at Bowers Ridge. Notably, this trend might be biased due to the systematic exclusion of laminated biosilica-rich intervals during onboard sampling.

Further evidence for an exceptional paleoceanographic event after ~2.7 Ma BP comes from an independent biogeochemical reaction-transport modelling study. Based on geochemical analyses of pore waters (e.g., concentrations and S-isotopic composition of sulfate) and sediments (e.g., Sixs, Ba), this model supports a pulse of reactive organic matter export to the sea floor at Site U1341 following the Pliocene-Pleistocene transition. According to the model, this strong productivity pulse and the related reactive organic matter export strongly enhanced bacterial sulfate reduction rates, leading to complete sulfate depletion in the pore waters and most probably to the buildup of hydrogen sulfide in shallow sediments and bottom waters. These diagenetic processes did not only cause the trace metal enrichments reported above, but also the efficient remobilisation of biogenic Ba from this sediment interval, restricting its use as a paleoproductivity proxy. Interestingly, the pore water chemistry at Site U1341 is still adjusting to this productivity pulse millions of years after it occurred, as depicted in the pore water sulfate concentration and S isotope profiles.

According to our results, the Pliocene-Pleistocene paleoenvironmental record at Site U1341 is surprisingly different from the open North Pacific records (e.g., Haug et al., 1995, 1999), suggesting that the timing and sedimentological expression of an intensified NHG in the high northern latitudes might have been controlled more strongly by regional paleoceanographic parameters and processes. In addition, Site U1341 nicely exemplifies how non-steady state diagenetic processes induced by paleoenvironmental events can leave long-term imprints in the sediment and pore water compositions of marine sediments.

Another approach to reconstruct nutrient cycling in the water column and sediments at Site U1341 was sequential P extraction. Our results show that early diagenetic processes strongly overprinted the primary distribution and speciation of P throughout the sediment record. The quantitatively most important P phases at Site U1341 are authigenic and detrital apatite as well as opal-bound P. Fish remains, Fe-bound and organic P do not contribute significantly to the total P pool. Detrital apatite appears to be related to the input of terrigenous material by dust, currents, and/or sea ice. The high contribution of authigenic apatite results from a number of early diagenetic processes (e.g., organic matter degradation, recrystallisation) cummulatively referred to as "sink switching", transferring P from more labile fractions (e.g., Fe (oxyhydr)oxides, organic matter, fish remains) to stable and well-crystallised authigenic apatite. Although this "sink switching" limits our ability to reconstruct the original availability of P in the Bering Sea water column and its coupling to the Fe cycle, it might give insights into the diagenetic processes within the Bering Sea sediments and their controlling mechanisms.

Probably the most important finding of this study is that biogenic opal-bound P - a so far largely unrecognised reactive P pool (Latimer et al., 2006) - can in fact be an important sink for sedimentary P in biosilica-dominated marine regimes like the Bering Sea. At Site U1341, highest contents of this opal-bound P fraction seem to be directly related to maxima in the Sixs record (biogenic opal), while the highest contents of authigenic apatite seem to occur in the Al-rich (detrital) sediment intervals. The quantification of the opal-bound P fraction posed a methodological challenge, but it is supported by the good correlation of its record with Sixs, implying that the opal-bound P record might indeed document a primary depositional signal. The nature of the P pool remaining after the six extraction steps remains unclear, but as its downcore record correlates well with the Al contents, it might represent P bound in refractory silicate minerals. In conclusion, it appears that the Plio- and Pleistocene sediments on Bowers Ridge experienced a significant diagenetic transfer of formerly reactive and bioavailable P phases into more stable mineral phases, leading to more efficient long-term phosphate burial. Furthermore, not only authigenic apatite, but also opal-bound P constitute significant fractions of total reactive P in these opal-rich sediments.

References:

Brumsack, H.-J. (2006) The trace metal content of recent organic carbon-rich sediments: Implications for Cretaceous black shale formation. Palaeogeogr., Palaeoclimatol., Palaeoecol. 232, 344-361.

Cortese, G., Gersonde, R., Hillenbrand, C.-D., Kuhn, G. (2004) Opal sedimentation shifts in the World Ocean over the last 15 Myr. Earth Planet. Sci. Lett. 224, 509-527.

Expedition 323 Scientists (2010) Bering Sea Paleoceanography: Pliocene-Pleistocene paleoceanography and climate history of the Bering Sea. IODP Prel. Rept. 323, doi:10.2204/iodp.pr.323.2010.

Haug, G.H., Maslin, M.A., Sarntheim, M., Stax, R., Tiedemann, R. (1995) Evolution of northwest Pacific sedimentation patterns since 6 Ma (Site 882). In: Rea, D.K., Basov, I.A., Scholl, D.W., Allan, J.F. (Eds.) Proc. ODP Sci. Results 145: College Station, TX (Ocean Drilling Program), 293–314, doi:10.2973/odp.proc.sr.145.115.1995.

Haug, G.H., Sigman, D.M., Tiedemann, R., Pedersen, T.F., Sarntheim, M. (1999) Onset of permanent stratification in the subarctic Pacific Ocean. Nature 401, 779-782.

Latimer, J.C., Filippelli, G.M., Hendy, I., Newkirk, D.R. (2006) Opal-associated particulate phosphorus: implications for the marine P cycle. Geochim. Cosmochim. Acta 70, 3843-3854.

McKay, J.L., Pedersen, T.F. (2008) The accumulation of silver in marine sediments: a link to biogenic Ba and marine productivity. Global Biogeochem. Cyc. 22, GB4010, doi:10.1029/2007GB003136.

Ruttenberg, K.C. (1992) Development of a sequential extraction method for different forms of phosphorus in marine sediments. Limnol. Oceanogr. 37, 1460-1482.

Schenau, S.J., De Lange, G.J. (2000) A novel chemical method to quantify fish debris in marine sediments. Limnol. Oceanogr. 45, 963-971.
Takahashi, K., Ravelo, A.C., Alvarez Zarikian, C., Expedition 323 Scientists (2011) Proc. IODP 323, Tokyo (Integrated Ocean Drilling Program Management International, Inc.), doi:10.2204/iodp.proc.323.105.2010.

IODP

New Proposal: Comprehensive analysis of Atlantic Circulation during Heinrich-Events 1 & 2

A. MANGINI[1], B. ANTZ[1], J. LIPPOLD[1], H. SCHULZ[2]

[1]Heidelberger Akademie der Wissenschaften
[2]Universität Tübingen

Assessing past variations of the Atlantic Meridional Overturning Circulation (AMOC) is a major challenge for paleoceanography in order to provide possible scenarios of future climate changes. Such variations have a profound impact on the global climate system, as indicated by paleoclimate records. In particular, significant interest went into the question of how excessive freshwater input through melting of continental ice can affect AMOC vigour and, hence, heat supply to higher northern latitudes [Rahmstorf 2005]. In response to increasing greenhouse gases the possibility of a decreasing or even collapsing AMOC cannot be entirely excluded [Delworth et al. 2008]. Such forcing can be tested by investigating its behaviour during extreme iceberg discharge events into the open North Atlantic during the last glacial period, the so called Heinrich events (HE). It is believed that the freshening of the Atlantic Ocean at high latitudes resulted in a diminished relative influence of northern-source deep waters [McManus et al. 2004]. It has been recommended to improve the understanding of such past AMOC changes through the collection and analysis of the protactinium-231/thorium-230 proxy (Pa/Th), which most effectively document AMOC changes [Delworth et al. 2008; Lynch-Stieglitz et al. 2007].

^{231}Pa and ^{230}Th, both produced at a constant rate (activity ratio = 0.093) through radioactive decay from their parent isotopes ^{235}U and ^{234}U, scavenged onto sinking particles and measured in marine sediments have been increasingly used as a kinematic circulation proxy in the Atlantic Ocean over the past years [Gherardi et al. 2009; McManus et al. 2004]. Today the relatively vigorous renewal of waters in the deep Atlantic results in low ratios of Pa/Th in the underlaying sediments (< 0.093), but this ratio should increase if NADW production slows.

However, it is important to note, that besides AMOC the response of sedimentary Pa/Th on in the Atlantic Ocean is a function of water depth and latitude [Francois 2007; Gherardi et al. 2010]. Several former studies employed Pa/Th in order to derive past AMOC concentrated on a single core (and thus one single water depth) over a large time period. But interpretation of isolated sediment cores (even though in high time resolution) may be misleading. Due to this in a new approach a compilation of available Pa/Th data from the literature has already been accomplished, but obtained data for HE 1 (~ 17 ka) and HE 2 (~ 24 ka) do not allow deriving quantitative constraints due to the sparse coverage. Thus, the main task will comprise the collection of new sediment samples from very different locations and depths during HE 1 and HE 2. In addition the 2D box model developed by [Luo et al. 2010] will be a very valuable tool in order to understand past circulation behaviours in conjunction with the Pa/Th proxy. New measurements and Pa/Th data from the literature will allow modelling in order to obtain quantitative AMOC behaviour during Heinrich-Events 1 & 2.

The overarching goal of this proposed project is the qualitative and quantitative estimation of past AMOC modes in terms. By doing so we will also examine the lead/lag of AMOC in respect to Heinrich Event occurrences, by observing the unequal HE1 and HE2 in order to identify the underlying processes. By combining already compiled HE data with a high number of new measurements from IODP/ODP cores we aim to build up a comprehensive picture of the AMOC during these harshest times of the last deglaciation. We consider this approach of applying Pa/Th to be the most promising and effective in order to derive both geometry and strength of the past AMOC.

References:

Delworth, T., P. Clark, M. Holland, W. Johns, T. Kuhlbrodt, J. Lynch-Stieglitz, C. Morrill, R. Seager, A. Weaver and R. Zhang (2008). Chapter 4. The Potential for Abrupt Change in the Atlantic Meridional Overturning Circulation. Synthesis and Assessment Product 3.4 Report by the U.S. Climate Change Science Program, U.S. Geological Survey (USGS)
Francois, R. (2007). Paleoflux and paleocirculation from sediment 230Th and 231Pa/230Th. Proxies in Late Cenozoic Paleoceanography. C. H.-M. a. A. d. Vernal, Elsevier: 681-716.
Gherardi, J., L. Labeyrie, S. Nave, R. Francois, J. McManus and E. Cortijo, 2009. Glacial-interglacial circulation changes inferred from 231Pa/230Th sedimentary record in the North Atlantic region. Paleoceanography. 24: PA2204.
Gherardi, J., Y. Luo, R. Francois, J. McManus, S. Allen and L. Labeyrie, 2010. Reply to comment by S. Peacock on "Glacial-interglacial circulation changes inferred from 231Pa/230Th sedimentary record in the North Atlantic region". Paleoceanography. 25(PA2207).
Luo, Y., R. Francois and S. Allen, 2010. Sediment 231Pa/230Th as a recorder of the rate of the Atlantic meridional overturning circulation: insights from a 2-D model. Ocean Science. 6: 381–400.
Lynch-Stieglitz, J., J. Adkins, W. Curry, T. Dokken, I. Hall, J. Herguera, J. Hirschi, E. Ivanova, C. Kissel, O. Marchal, T. Marchitto, I. McCave, et al., 2007. Atlantic Meridional Overturning Circulation During the Last Glacial Maximum. Science. Vol. 316(no. 5821): pp. 66 - 69.
McManus, J., R. Francois, J. Gherardi, L. Keigwin and S. Brown-Leger, 2004. Collapse and rapid resumption of Atlantic meridional circulation linked to deglacial climate change. Nature. 428: 834-837.
Rahmstorf, 2005. Thermohaline circulation hysteresis: A model intercomparison. Geophys. Res. Lett. 32.

IODP

Evidence for long term cooling and short punctuated climate events at the Aptian-Albian boundary in the sub-tropical eastern Atlantic (Mazagan Plateau, DSDP Site 545)

A.MCANENA[1], J.O. HERRLE [2,3], A.GRIESAND[2,3], T. WAGNER[4], H.M.TALBOT[4], J.RETHEMEYER[1], P.HOFMANN[1]

[1]Department of Geology and Mineralogy, University of Cologne, 50674 Cologne, Germany,
[2]Institute of Geosciences, Goethe University Frankfurt, D-60438 Frankfurt am Main, Germany
[3]Biodiversity and Climate Research Centre (BIK-F), D-60325 Frankfurt, Germany
[4]School of Civil Engineering and Geosciences, Newcastle University, Newcastle Upon Tyne, NE1 7RU, United Kingdom,

Introduction

The mid Cretaceous (~120-90 Ma) represents a period of major global transition during the Mesozoic; where significant 'greenhouse' warming was associated with changes in volcanic, hydrothermal and tectonic activity

(Larson, 1991). The reorganisation of oceanic basins, in particular the opening of both the Equatorial Atlantic and Pacific Gateways (Poulson, 2003), led to oceanic paleocirculation, sea level, and stratification changes, with the development of an improved deep, intermediate and shallow water mass exchange. Alongside increased pCO_2, the interval defined by the late Aptian-early Albian

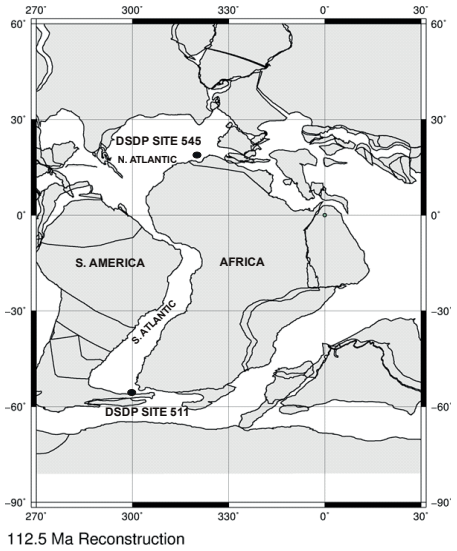

Figure 1: Paleogeographic reconstruction of late Aptian-early Albian (~112.5Ma; odsn.de/odsn/services/paleomap/adv_map.htm) DSDP Site 545 (Mazagan Plateau) and Site 511 (Falkland Plateau)

boundary (~112.5 Ma) experienced amplified global sea surface temperatures leading to subsequent variations in the global carbon cycle and significant changes to marine biota (Erba, 1994; Leckie et al., 2002; Herrle and Mutterlose, 2003; Huber and Leckie, 2011). Recent biostratigraphic and sedimentological studies suggest that short interludes of global cooling (Kemper, 1987) may have occurred during the late Aptian-early Albian (~112.5Ma). Evidence from ice rafted debris and the formation of glendonites in high latitude sites (e.g. Frakes and Francis, 1988) accompanies distinct evidence of cooling from planktic/benthic foraminifera and belemnite $\delta^{18}O$ records (Pirrie et al., 1995; Huber et al., 1995; Friedrich et al., 2012), bulk sediment isotopes (Clarke and Jenkyns, 1999: Voigt and Wiese, 2000) and calcareous nannofossil abundances (Erba, 1994; Herrle and Mutterlose, 2003; Mutterlose et al., 2009).Observed on a global scale, this evident cooling was proposed as a late Aptian 'cold snap' by Mutterlose et al., (2009), during times of equable warmth in the mid-Cretaceous. However, this event has so far not been constrained with quantifiable data, and the mechanisms of cooling in subtropical, low-mid latitude sites is unknown. We present the first high resolution study of north Atlantic sediments from the late Aptian-early Albian transition (DSDP Site 545, Mazagan Plateau, NW Africa) presenting $\delta^{13}C_{carb}$ isotope, sea surface temperature (TEX_{86}), bulk geochemical and calcareous nannofossil data, to constrain the late Aptian 'cold snap' and determine the environmental consequences this climatic variability induced. We also discuss the possible mechanisms and events which led to this prolonged period of cooling by examining a series of short term climate perturbations evident in both the isotope and sea surface temperature record.

Paleogeographic Setting and Methods

The Mazagan Plateau (Figure 1) is situated 200 km off NW Africa, in the eastern Atlantic Ocean, with cores recovered from DSDP Site 545 (Leg 79; Hinz et al., 1984). During the late Aptian-early Albian, Site 545 was located at a paleo-latitude of 20°N and a paleo-depth of ~2000m. Bulk geochemical data (TOC, $CaCO_3$ and elemental analysis of C/N/S) was collected and sub-samples taken for further analysis. Siliciclastic mineral composition and ocean redox was measured by X-ray fluorescence analysis. Bulk sediment isotopes ($\delta^{13}C_{carb}$) were analysed alongside GDGT (Glycerol Dibiphytanyl Glycerol Tetraether) derived TEX_{86} (Kim et al., 2010) to provide a sea surface temperature proxy to compare with the calcareous nannofossil record.

Results and Discussion

Figure 2 defines the late Aptian 'cold snap' as the interval between 415 and 450 mbsf in the Mazagan Plateau record, and is the climax of a more than 4 Ma long term cooling trend in the North Atlantic. The culmination of this long term cooling (decreasing from 32.5 to 27.5°C) indicates that at the lower boundary of the Upper Aptian 'cold snap', just prior to the late-Aptian- early Albian transition, sea surface temperatures stabilise for a short period of time. At 430 mbsf, a turning point is observed and SSTs begin to gradually recover to almost pre-event temperatures, which might signal the termination of the cold snap. Throughout this long term cooling trend, and towards the late Aptian- early Albian transition, sea surface temperatures becoming increasing variable, and superimposed upon the long term record is a series of short term climate perturbations, identifying where surface waters are either markedly cooler or warmer by ± 2oC. The most prominent of these excursions occurs at ~436 mbsf where a rapid increase (+ 5oC) is observed in the sea surface record, indicating a possible small hyperthermal event occurring within the 'cold snap' duration.

Corresponding to these sea surface temperature changes, positive and negative excursions of < 2‰ within the carbon isotope record are observed throughout the cooling event and into the boundary set for the 'cold snap'. The $\delta^{13}C_{carb}$ isotope value throughout the initial cooling of Mazagan Plateau is relatively stable (~1‰) before a rapid shift towards heavier isotope values is observed at ~465m (< 2‰). Into the 'cold snap', $\delta^{13}C_{carb}$ values become distinctly more variable, but still describe a distinct positive isotope excursion in the profile, shifting between 1 and 2.5‰ before heavier $\delta^{13}C$ values stabilise in the interval between 430 and 415mbsf. After the event, $\delta^{13}C_{carb}$ values begin to gradually decrease (between 2.5 to 1.75‰) before the major perturbation associated with OAE 1b is observed at ~390m. Several significant negative isotope excursions (< -1.5 ‰) are shown prior to and throughout the cooling event, most distinctly at 436 mbsf, 450 mbsf and 520 mbsf, the former of which corresponds directly to the hyperthermal event proposed in the sea surface temperature record. These short events represent short (50-150 ka) periods of successive warming or cooling in the north Atlantic, indicating climate variability during the late Aptian.

The long term cooling trend prior to the late Aptian 'cold snap' described in Figure 2 is also reflected in biostratigraphic data collected from calcareous nannofossil abundances. At the Mazagan Plateau, a 2 step bio-event occurs with significant repercussions for nannoconid and allowing only surface water exchange to occur (Wagner and Pletsch, 1999). Variable inflow of cooler and nutrient enriched intermediate and deep waters from the Cretaceous Pacific Gateway into the proto North Atlantic would have redirected water circulation from the western Pacific

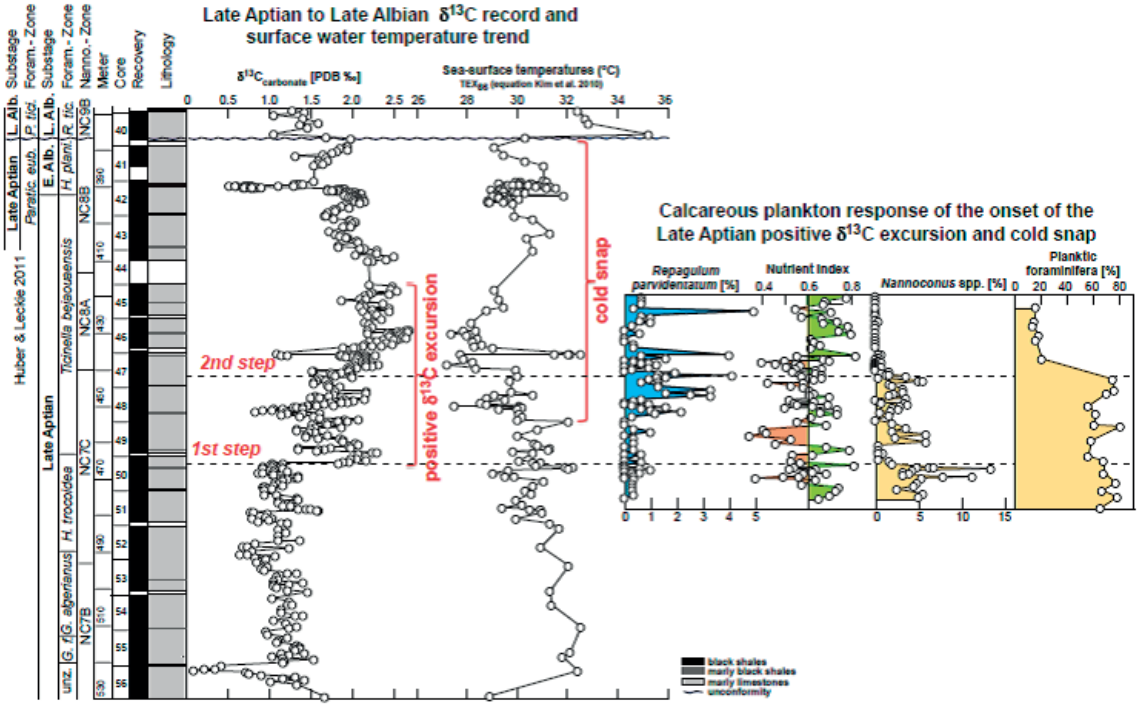

Figure 2: Bulk carbon isotope analysis and calcareous nannofossil data for DSDP Site 545: Long term trend and punctuated climate events observing significant cooling before the Upper Aptian "cold snap" (~425m), with multiple short term warming and cooling events comparable to isotopic excursions between 430 and 465 mbsf.

phytoplankton taxa evolution. A dramatic decrease in both warm water Nannoconus spp. and planktic foraminifera accompanies the cooling of sea surface temperatures in the north Atlantic prior to the Aptian-Albian transition, after which these species are not known to recover in such abundances. In parallel, a significant influx of cold water taxon Repagulum parvidentatum occurs, indicating the transgression of higher latitude, cooler surface waters into the north Atlantic at this time. Supporting evidence from bulk geochemical records capture the environmental effects of cooling in the north Atlantic. Indicators such as Si/Al, Na/Al and Mg/Al are below average shale values during the 'cold snap' event (~440 mbsf) and represent a decrease in coarse grain sediments and energy of the continental transport system. The ratio of Mg/Al is indicative of clay based minerals (e.g. palygorskite) generally observed in arid, dry conditions, and hence represents a transition from dry, arid conditions ideal of evaporation to a humid or wet climate with increased precipitation during the long term cooling of the north Atlantic.

We propose that both the long term cooling in the north Atlantic, and the expression of short term climate perturbations superimposed on this record, may have been triggered by the early opening of the Equatorial Atlantic and Pacific gateways (Barron, 1987). During the late Aptian-early Albian, only a shallow water connection between the north and south proto-Atlantic was formed, restricting intermediate and deep water circulation, and anticlockwise, focusing colder subsurface waters along the NW African margin. This exchange of cold intermediate- and surface waters from higher latitudes with the low latitude N. Atlantic at the Mazagan Plateau Site would have major consequences for surface water stratification and productivity as observed in the decrease of warm water calcareous nannofossils (Nannoconus spp.) and planktic foraminifera, occurring alongside the influx and bloom of cold water inferred nannofossil species, R. parvidentatum. We note, finally, that the multiple short term warming and cooling events evident during the long term cooling of the north Atlantic appear to culminate in a small hyperthermal event in the late Aptian. The rapid increase in SST by +5°C coinciding with a sharp negative $\delta^{13}C_{carb}$ excursion (~ 1.3‰) and a rapid drop in continental climate proxies (Zr/Al, Si/Al, Na/Al and K/Al ratios) argue for a period of significant African humidity consistent with geochemical signatures, which are well known for other hyperthermal events in the Paleogene-Mesozoic. This hyperthermal event in the late Aptian has not yet been described in other sites but may well be a precursor event to OAE1b.

What is currently still unclear, is whether the long term cooling observed is attributed to a local process in the north Atlantic; or if the trigger mechanism by which it occurs is global, and can therefore be measured in other sites from high latitudes or different basinal settings. Therefore, we also present the primary findings of a high resolution south Atlantic study from DSDP Site 511 (Falkland Plateau),

which describes the late Aptian-early Albian climate record complementary to the north Atlantic Mazagan Plateau Site 545. Previous data reported from Site 511 indicate that sea surface temperaturs at this low-latitude site are expected to range between 10-25°C (Huber et al. 1995) and hence are well within the calibration range of the TEX_{86} SST proxy (Kim et al., 2010) for comparison to the Mazagan Plateau. It is hoped from successful correlation of the carbon isotope record ($\delta^{13}C_{org}$ and $\delta^{13}C_{carb}$), TEX_{86}-derived sea surface temperatures and further calcareous nannofossil studies, that we may observe a comparable cooling trend in the south Atlantic record, and confirm and constrain the late Aptian 'cold snap' as a global event.

Conclusion

In conclusion, we present the first evidence of a long term cooling trend (< 5oC) in the north Atlantic, prior to the onset of the Upper Aptian 'cold snap' proposed by Herrle and Mutterlose (2003) and Mutterlose et al.,(2009). We observe a steady decrease in sea surface temperatures from 32.5oC to 27.5oC entering the 'cold snap' over a period of 1.5Ma. This supports the suggestion that significant interludes of global cooling occurred during mid-Cretaceous 'greenhouse' Earth as evident from ice rafted debris, and changes in the δ18O records of southern latitude bottom waters. The high resolution profile generated in this study proposes that late Aptian cooling was not only evident where ice formation may have cooled sea surface temperatures at high latitude sites, but also in subtropical low-mid latitudes; and that a specific trigger would be required to cool such environments, such as the opening of the Equatorial and Pacific Gateways to the north Atlantic ~112.5 Ma. There are numerous climate reponses which reflect the cooling of the north Atlantic also: the weakening of the transoprt system from continetal west Africa, as evident from the decrease of course grained material during the long term cooling event, and also the decrease of evaporite minerals such as palygorskite, indicating a change in climate from from arid and dry to one of increased precipitation. We also note serious changes to marine diversity and water stratification in the north Atlantic as a consequence of prolonged sea surface cooling and variations to paleo-circulation. The dramatic demise of nannoconids and planktic foraminifera alongside the parallel influx of cold water nannofossil taxa characterises critical changes in the evolution of the marine phyto-and zooplankton in the north Atlantic at this time.

References:

Barron, E.J., (1987). Palaeogeography, Palaeoclimatology, Palaeoecology, 59, 3-29.
Clarke L.J., Jenkyns H.C., (1999). Geology, 27, 699-702.
Erba E., (1994). Paleoceanography, 9, 483-501.
Frakes L.A., Francis J.E., (1988). Nature 333:547–549
Friedrich O., Norris R.D., Erbacher J., (2012). Geology, doi: 10.1130/G32701.1
Herrle O.J., Mutterlose J., (2003). Cretaceous Research, 24, 1-22.
Hinz, K.,Winterer, E.L. et al., (1984). Initial Reports of the Deep Sea Drilling Project 79, U.S. Government Printing Office, Washington
Huber B.T., Hodell D.A.,Hamilton C.P., (1995). Geological Society of America Bulletin, 107, 1164-1191.
Huber B.T., Leckie, R.M., (2011). Journal of Foraminiferal Research, 41, 53-95.
Kemper E (1987) Das Klima der Kreide-Zeit. Geol Jb A 96:5–185
Kim J.H., Van der Meer J., Schouten S., Helmke P., Willmott V., Sangiorgi F., Koc N., Hopmans E.C., Sinninghe Damste J.S., (2010). Geochimica et Cosmochimica Acta, 74, 4639-4654.
Larson, R.L., (1991). Geology, 19, 547-550.
Leckie R.M., Bralower T.J., Cashman R., (2002). Paleoceanography, 17, 13, 1-29.
Mutterlose J., Bornemann A., Herrle J.O., (2009). N.Jb. Geol. Palaont.Abh., 252, 217-225.
Pirrie D., Doyle P.,Marshall J.D., Ellis G., (1995). Journal of the Geological Society, London, 152, 739-742.
Poulsen C.J., Gendaszek A.S., Jacob R.L., (2003). Geology, 2003, 31, 115-118.
Voigt S., Weise F., (2000). Journal of the Geological Society, London, 157, 737-743.
Wagner T., Pletsch T., (1999). In: Cameron, N (ed.), Oil and gas habitats of the South Atlantic. Geological Society of London, Special Publication, London, 241-265.

IODP

Inorganic geochemical provenance analysis of Arctic Ocean sediments

A.-K. MEINHARDT[1], C. MÄRZ[2], R. STEIN[3], H.-J. BRUMSACK[1]

[1]AG Mikrobiogeochemie, Institut für Chemie und Biologie des Meeres (ICBM), Postfach 2503, 26111 Oldenburg, Germany
[2]Biogeochemistry, School of Civil Engineering and Geoscience (CEG), Drummond Building, Newcastle University, NE1 7RU Newcastle upon Tyne, United Kingdom
[3]Alfred Wegener Institut for Polar and Marine Research, Am Alten Hafen 26, 27568 Bremerhaven, Germany

In a preliminary study, we performed inorganic geochemical analyses of three sediment cores from the Mendeleev Ridge, which were recovered during RV Polarstern cruise ARK-XXIII/3 in 2008 (for lithology and tentative age model of ARK-XXIII/3 sediment cores see Stein et al., 2010). This study forms part of a proposed detailed provenance investigation of sediment cores from the central Arctic Ocean. Arctic marine sediments are frequently characterized by alternating dark brown and light olive brown layers. The composition and formation mechanism of these dark brown layers were recently studied by März et al. (2011). They applied inorganic geochemical methods to a sediment core recovered during the same cruise from the Mendeleev Ridge.. The dark brown layers are enriched in Mn and Fe (oxyhydr)oxides and certain trace metals (Co, Cu, Mo and Ni), and most likely represent climatic signals: Metal enrichments were formed primarily via enhanced riverine input during warmer periods. Trace metal scavenging in the water column played an important role, but a potential diagenetic overprint was discussed as well. In our investigated sediment cores, Mn- and Fe-rich layers associated with trace metal enrichments are also visible and corroborate the results of März et al. (2011). Some of the layers are also characterized by specific element patterns related to terrigenous input (e.g. Si, Zr, Ca and Mg). These elements bear a large potential for provenance analyses. One frequently used parameter for provenance analyses in the Arctic Ocean is the detrital carbonate content, which serves as a proxy for trace ice-rafted debris (IRD) layers that largely consist of dolomite ($CaMg(CO_3)_2$). The likely source area of this material is the Canadian Archipelago (Stein et al., 2010 and references therein). The vertical distribution of the dolomite-associated elements Ca, Mg, and TIC in our investigated cores shows similar patterns with distinct peaks, which is in accordance with findings of März et al. (2011). The down-core positions and intensities of the dolomite peaks vary in each core, indicating different sedimentation rates and the varying influence of the Beaufort Gyre on different parts of the Arctic Ocean. This dominant current system in the Amerasian Basin is responsible for the delivery of coarse-grained material to the studied core locations. Paleoenvironmental and/or paleoclimatic changes are documented by geochemical

proxies in the geolocial record, and sediment geochemistry may provide valuable information about potential changes in source areas and current systems. In a previous study of a sediment core from the Lomonosov Ridge (IODP Exp. 302, ACEX), März et al. (2010) identified inorganic geochemical signals specifically related to the western Siberian Putoran Massif. The overall low K/Al ratios in our sediment cores from the Mendeleev Ridge suggest that this location has been influenced by clay minerals from western Siberia as well. The chemical composition of certain layers differs from the overall down-core profile and indicates changes in the input of material to the Mendeleev Ridge. We intend to expand our study to longer sediment cores to assess the paleoenvironmental evolution of the Arctic Ocean. For detailed provenance analyses, more sediment cores need to be studied by inorganic geochemical methods to determine the specific element enrichment/depletion patterns of specific time intervals like the last glacial/interglacial cycle, which is neccessary to define distinct source areas. The proposed expansion includes the determination of a wide range of elements to find new proxies for these distinct source areas. In this context, we emphazise the use of Nd isotopes, which are used to trace water masses. The Nd isotopic compositions of several Arctic rivers and water masses like the Barents Sea are well-defined and can be applied to central Arctic Ocean sediments to determine the likely source areas. Our study will also provide a geochemical data basis that may help in the planning of future drilling projects in the Arctic Ocean and the interpretation of deep sediment cores.

References:
März, C., Schnetger, B., Brumsack, H.-J. (2010) Palaeoenvironmental implications of Cenozoic sediments from the central Arctic Ocean (IODP Expedition 302) using inorganic geochemistry. Palaeoceanography 25, PA3206, doi:10.1029/2009PA001860.
März, C., Stratmann, A., Matthiessen, J., Meinhardt, A.-K., Eckert, S., Schnetger, B., Vogt, C., Stein, R., Brumsack, H.-J. (2011) Manganese-rich brown layers in Arctic Ocean sediments: Composition, formation mechanism, and diagenetic overprint. Geochim. Cosmochim. Acta 75, 7668-7687.
Stein, R., Matthiessen, J., Niessen, F., Krylov, R., Nam, S., and Bazhenova, E., 2010. Towards a Better (Litho-) Stratigraphy and Reconstruction of Quaternary Paleoenvironment in the Amerasian Basin (Arctic Ocean). Polarforschung 79 (2), 97-121.

ICDP

Resolving sedimentary sulphur cycling during the Shunga Event (early Palaeoproterozoic) with sulphur isotopes

D. MEISTER[1], H. STRAUSS[1], V.A. MELEZHIK[2,3], A. LEPLAND[2]

[1]Westfälische Wilhelms-Universität Münster, Institut für Geologie und Paläontologie, Münster, Germany
[2]Geological Survey of Norway (NGU), Trondheim, Norway
[3]University of Bergen, Centre of Geobiology, Bergen, Norway

The early Palaeoproterozoic is an important time period marked by several fundamental environmental changes of global nature like the oxygenation of Earth's atmosphere at c. 2.4 Ga (Great Oxidation Event, cf. Holland 1999) causing enhanced terrestrial sulphide weathering and subsequent delivery of sulphate to the ocean. The enhanced input of sulphate into the ocean water most likely resulted in an increased role of sulphate reducing bacteria in the microbial turnover of sedimentary organic matter which is archived in the isotopic signature of sulphur bearing minerals embedded in the Palaeoproterozoic sediments.

In the aftermath of the Lomagundi-Jatuli Event (e.g. Melezhik et al. 1999b) during which isotopically heavy

Fig. 1: Map of the study area (modified after Melezhik et al. 1999a).

carbonates accumulated, sediments were deposited during the Shunga-Event at c. 2.05 Ga (Hannah 2008) which were characterized by unprecedented amounts of organic matter.

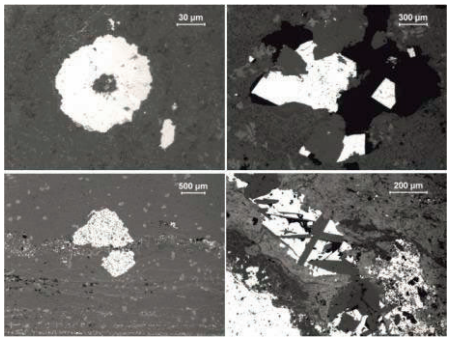

Fig. 2: Some polished section images of different iron sulphide morphologies in drillcores 12A, 12B and 13A.

The data presented here base on analyses of drillcore material from the Fennoscandia Arctic Russia – Drilling Early Earth Project (FAR DEEP). The drilling location is situated near Shunga, which is north of Petrozavodsk near the Onega Lake in NW Russia (Fig. 1). Some 744 m of "shungite" drillcore from three drillholes within the c. 2.05 Ga old Zaonega Formation (ZF) were recovered. Results focus on samples from drillcores 12A, 12B and 13A. Drillcore 13A ranges in depth from 0 to 240 m below surface and 12A and 12B belong to the same lithological profile with 12A covering the uppermost core meters to a depth of ~95 m and 12B covering the core from a depth of 95 m to 500 m below surface. The main objective of this project is to resolve sedimentary sulphur cycling during the early Palaeoproterozoic with sulphur isotopes and related geochemical markers.

It was suggested that rhythmically bedded sedimentary rocks of the ZF were deposited in a low-energy, non-euxinic environment (Melezhik et al. 1999a). They are of typically black to grey colour due to the great amount of organic matter which is most likely of algal or bacterial

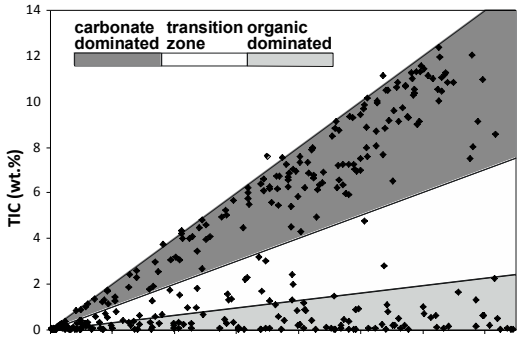

Fig. 3: TIC content plotted against TC content (drillcore 12A and 12B).

origin (Melezhik et al. 1999a). The rocks deposited during the Shunga Event underwent diagenesis under greenschist facies conditions during the 1.8 Ga Svecofennian orogeny (Melezhik et al. 1999a). Iron sulphides are very common in

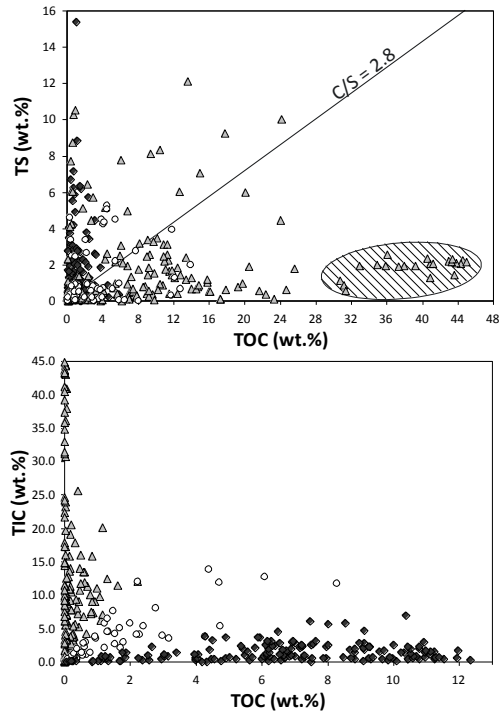

Fig. 4: Scatter plot of TS versus TOC and TIC versus TOC. Upper diagramm: line marks Holocene normal marine Corg/Ssulphide ratio. The hatched field marks samples where bitumen migration is suggested. Carbonate dominated samples are displayed in dark grey/diamonds, organic dominated samples in light grey/triangles and transitional samples in white/circles.

these sediments and show a high variability in their habitus (Fig. 2) with pyrite being the most prevalent iron sulphide. The complex pattern of the iron sulphide morphologies (cf. Fig. 2) and their geochemical characteristics can trace back to the nature of marine sulphur-cycling, to different sulphide or sulphate generation stages, late-diagenetic processes (e.g. migration of solutes) and organic matter degradation accompanying the generation and migration of bitumen within the sediments of the ZF (Melezhik et al. 2009) as a result of postdepositional processes. The migrated petrified hydrocarbons (termed as Shungite, personal information V.A. Melezhik) complicate the interpretation of the collected dataset in terms of primary versus secondary pyrite formation. Therefore, it is of major interest to assess the different aforementioned processes.

Initially, sulphur and carbon contents were measured, in the following expressed as total sulphur (TS), total carbon (TC) and total inorganic carbon (TIC) abundances in bulk rock samples (Figs. 3, 4) with a CS MAT 5500 in Münster. Sedimentary rocks with an increased total sulphur content (TS) usually (but not always) show an enrichment in the total organic content (TOC). They interbed with high-TIC/TC-dominated rocks in a relatively close pattern. A first attempt was made to separate types of different geochemical characteristics by correlating TIC versus TC content. The TIC versus TC plot (Fig. 3) defines three data populations: carbonate dominated rocks (TIC/TC 0.5-1), organic carbon (C_{org}) dominated rocks (TIC/TC <0.15 and a third population with transitional TIC/TC ratios. Mean values for TS (wt.%) are 1.34 for carbonate dominated

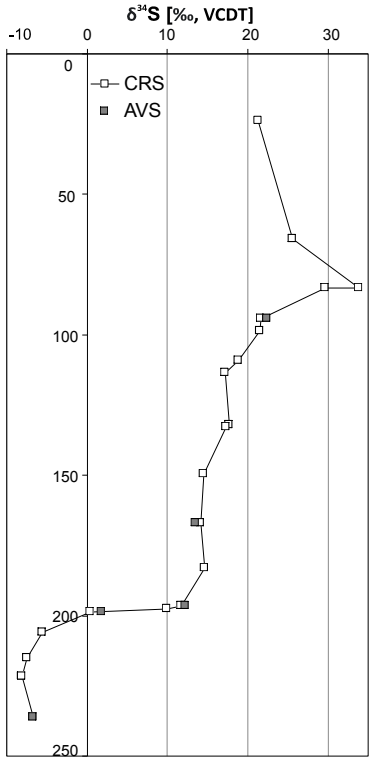

Fig. 5: $\delta^{34}S$ depth profile of drillcore 13A.

rocks, 1.36 for the transition zone and 1.98 for organic carbon dominated rocks.

Allthough a staightforward correlation between sedimentary rocks with a higher TOC and a higher sulphur content is discernible in figure 7, but no general correlation between the TS and TOC content could be illustrated (Fig. 4). Carbonate dominated as well as C_{org} dominated rocks show higher maximum values for TS vs. TOC values compared to the transition zone. A group of high TOC and low TS samples could be identified (hatched ellipse). These

samples likely reflect hydrocarbons that migrated through the sediments postdepositionally. But this theory still awaits microscopical verification on handsamples and (polished and thin) sections.

Sulphur isotopes represent an important fingerprint in the rock record for tracing sulphur sources and prevailing reaction pathways. Figures 5 and 6 show the $\delta^{34}S$ values for drillcores 12A, 12B and 13A, determined for different sulphur species after sequential extraction of acid volatile sulphur (monosulphides), chromium reducible sulphur

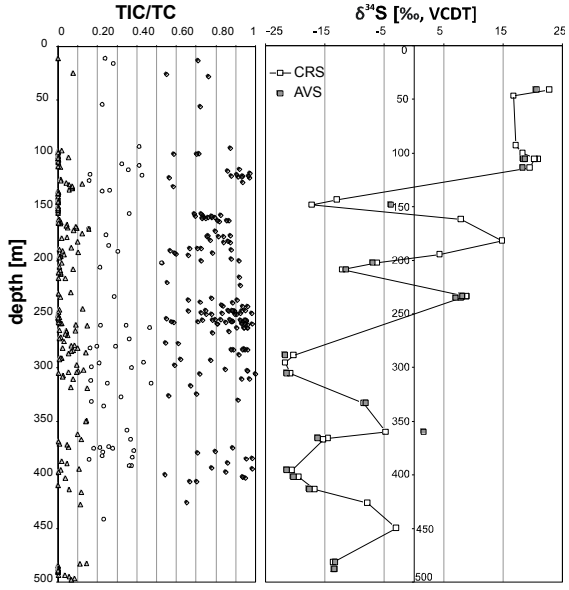

Fig. 6: Profiles of drillcore 12A and 12B. From left to right: TIC/TC ratio and $\delta^{34}S$ values against depth.

(pyrite and elemental), sulphate sulphur and organically bound sulphur (extraction method after Poulten & Canfield

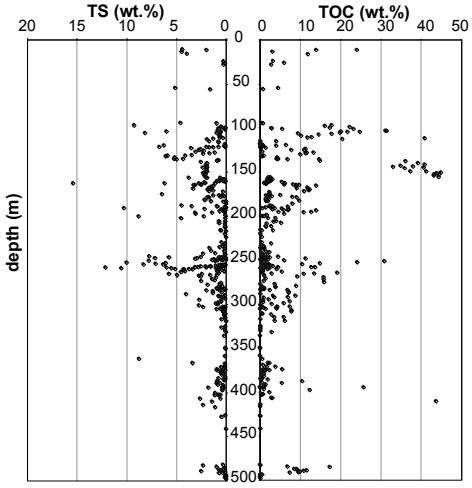

Fig. 7: Profiles of drillcore 12A and 12B. TOC and TS values against depth.

2005). Isotope values for the chromium reducible fraction (pyrite) vary within a wide range from -21.7 to +22.8 ‰ VCDT for drillcores 12A and 12B and from -6.4 to +14.8 ‰ VCDT for drillcore 13A which suggests bacterially mediated sulphate reduction (e.g. Habicht et al. 1998). In both profiles, a general positive shift (Fig. 5 and 6) up-section is discernible, which can be interpreted as a change towards a limited sulphate supply and subsequently, successively heavier $\delta^{34}S$ signature of the residue. In sedimentary environments, two crucial sulphur isotope fractionating pathways are likely to take place: thermochemical fractionation and biological fractionation (bacterial sulphate reduction, sulphide oxidation and/or disproportionation, Habicht et al. 1998). Alternatively, the organic-rich sediments could form an environment for thermochemical sulphate reduction (Machel et al. 1995). In order to distinguish these two processes, supplementary isotopic and elemental analyses will be required.

To get a deeper insight into ocean water chemistry, iron and the differentiation of its redox states and mineralogical fractionation are commonly used parameters. As described in papers of e.g. Raiswell & Canfield (2012), Li et al. (2010) and Shen et al. (2002), there is a strong correlation between the oxygenation characteristics of the ocean water chemistry and the abundance of total iron (FeT), pyrite iron (FePy) and highly reactive iron (FeHR = Fe_{pyrite}+ $Fe_{magnetite}$+ Fe_{oxides}+ $Fe_{carbonates}$, Poulten et al. 2004) in the sediments and can provide an additional indication of the nature of iron and sulphur cycling.

In addition, the diagenetic history of sulphur cycling will be studied through high-spatial sulphur isotope analysis on single grain scale at the NORDSIM ion probe facility in Stockholm. Moreover, multiple sulphur isotope analysis (^{33}S and ^{36}S) will be performed.

Acknowledgements: This project forms part of the Fennoscandian Arctic Russia – Drilling Early Earth Project (FAR-DEEP). Financial support through the Deutsche Forschungsgemeinschaft (STR281/35) is gratefully acknowledged.

References:

Habicht, K.S., Canfield, D.E., Rethmeier, J. (1998). Sulphur isotope fractionation during bacterial reduction and disproportionation of thiosulphate and sulfite. Geochimica et Cosmochimica Acta 62 (15): 2585-2595.

Hannah, J.L. (2008). Re-Os geochronology of a 2.05 Ga fossil oil field near Shunga, Karelia, NW Russia. Abstract, 33rd International Geological Congress, Oslo, 2008, 6-14 August

Holland, H.D. (1999). When did the Earth's atmosphere become oxic? The Geochemical News 100: 20-22.

Li, C., Love, G.D., Lyons, T.W., Fike, D.A., Sessions, A.L., Chu, X. (2010). A stratified redox model for the Ediacaran ocean. Science 328: 80-83.

Machel, H.G., Krouse, H.R. and Sassen, R. (1995). Products and distinguishing criteria of bacterial and thermochemical sulphate reduction. Applied Geochemistry 10: 373-389.

Melezhik, V.A., Fallick, A.E, Filippov, M. M. Larsen, O. (1999a). Karelian shungite - an indication of 2.0-Ga-old metamorphosed oil-shale and generation of petroleum: geology, lithology and geochemistry. Earth-Science Reviews 47: 1-40.

Melezhik, V.A., Fallick, A.E., Filippov, M.M., Lepland, A., Rychanchik, D.V., Deines, Y.E., Medvedev, P.V., Romashkin, A.E., Strauss, H. (2009). Petroleum surface oil seeps from a Palaeoproterozoic petrified giant oilfield. Terra Nova 21: 119–126.

Melezhik, V.A., Fallick, A.E., Medvedev, P.V., Makarikhin, V.V. (1999b). Extreme 13Ccarb enrichment in ca. 2.0 Ga magnesite-stromatolite-dolomite-`red beds´ association in a global context: A case for the world-wide signal enhanced by a local environment: Earth-Science Reviews 48: 71–120.

Poulten, S.W. & Canfield , D.E. (2005). Development of a sequential extraction procedure for iron: implications for iron partitioning in continentally derived particulates. Chemical Geology 214: 209-221.

Poulten, S.W., Fralick, P.F., Canfield, D.E. (2004). The transition to a sulphidic ocean ~1.84 billion years ago: Nature 431: 173-177.

Raiswell, R., Canfield, D.E. (2012). The iron biogeochemical cycle past and present. European Association of Geochemistry, Geochemical Perspectives 1.

Shen, Y., Canfield, D.E., Knoll, A.H. (2002). Middle proterozoic ocean chemistry: evidence from the McArthur basin, northern Australia. American Journal of Science 302: 81-109.

IODP

Fractionation of highly siderophile elements in the lower oceanic crust at ODP Site 735b, SW Indian Ridge

C. MEYER[1], H. BECKER[1]

[1]Freie Universität Berlin, Insitut für Geologische Wissenschaften, Malteser Straße 74 – 100, 12249 Berlin

The processes that lead to the strong fractionation of highly siderophile elements (HSE, the platinum group elements, rhenium and gold) in the crust are not well understood. Compared to the mantle, abundances of some HSE in gabbroic oceanic crust and ocean ridge basalts are lower by a factor of 1000 or more, with Re, Au and Pd being more abundant than Os, Ir, Ru or Rh. The causes of the large variability of HSE ratios also remain enigmatic. Because most erupting basalts are sulphide saturated it has been suggested that the highly variable abundances of the HSE in basalts may reflect sulfide fractionation processes in the deeper oceanic crust (e.g. Hertogen et al. 1980). The detailed processes of magmatic HSE fractionation between the crust and the mantle is still an unresolved major question, particularly because of the limited availability of HSE data and systematic work on lower crustal rocks. Samples from ODP Site 735b, legs 118 and 176, a 1500 m section of tectonically exhumed middle to lower oceanic crust at the SW Indian Ridge, were analyzed for abundances of HSE and Os isotopic composition to study magmatic fractionation of the HSE in the deeper oceanic crust.

For reconnaissance study, 30 samples characterized by little alteration were selected to cover a range of lithologies, including olivine gabbro, gabbro, troctolitic gabbro, troctolite and disseminated oxide gabbro and oxide gabbro. Samples provided by the core repository were abraded to remove potential surface contamination, crushed and ground to powder in an agate disk mill. Up to 2.5 g of powder was digested in inverse aqua regia in a high pressure asher at 320 °C. HSE separation and analyses methods follow those established previously in our lab (Fischer-Gödde et al. 2011; Gleißner et al. 2012). Total chemistry blanks are 1.4 pg Os, 18 pg Re, 2 pg Ir, 30 pg Pt, 90 pg Pd, 9 pg Ru, 2 pg Rh and 4 pg Au.

In a Re-Os isochrone diagram, the most radiogenic samples (with large errors) plot along a 11 Ma reference line, in good agreement to the crustal age of site 735 B of 11 to 12 Ma (Dick et al. 1991). Two troctolitic gabbros and 3 olivine gabbros with 187Os/188Os of 0.14 to 0.24 display a different linear trend that yields an apparent age of 244 ± 77 Ma, with an initial 187Os/188Os of 0.126 ± 0.022. In an 187Os/188Os-1/Os diagram, a binary mixing relationship is not evident for these samples and 187Os/188Os does not correlate with Mg# or Cr #. The significance of this date is thus not clear. More data is required to address this issue.

CI-chondrite normalized abundances of HSE in the lower crustal rocks cover a wide range of abundances (at the most extreme 10-3 to 10-7 x CI chondrite for Os), with relatively high abundances of all HSE in some troctolitic gabbros to more fractionated HSE patterns and much lower abundances of Os, Ir, Ru, Rh and Pt in other lithologies. Of all HSE, Re is the least variable, with typical abundances in gabbros of 0.2-0.5 ppb, considerably lower than in most MORB (Schiano et al. 1997). These results are broadly consistent with previous Re concentration data obtained by NiS fire assay digestion on integrated strip samples from the same site (Blusztajn et al. 2000). Gold concentrations in most analyzed samples are typically < 0.1 ppb. Gold is more strongly depleted than Re compared to MORB (Keays and Scott 1976) and most mantle rocks (Fischer-Gödde et al. 2011). This would imply that Au is more incompatible than Re during fractional crystallization, at least in this section of oceanic crust.

Some HSE ratios display large and systematic variations over several orders of magnitude with other HSE ratios or lithophile fractionation indices. From HSE abundance and ratio data, it appears that olivine gabbros behave as a coherent group, whereas troctolitic gabbros may reflect more complex processes. HSE abundances, Au/Ir, Pd/Ir and Os/Ir in olivine gabbro reach values >100 at high MgO, Mg#, Ni and Cr abundances and decrease to < 1 with decreasing Mg#, Cr, Ni and MgO. As yet, little data is available for troctolitic gabbros (n = 3), but the evolution appears to follow different trajectories for some ratios, in particular increasing Au/Ir and Pd/Ir with decreasing Mg# and Cr. In the most primitive troctolitic gabbro, the enrichment of Pd over Au is more pronounced than in olivine gabbros and the HSE pattern is similar to HSE patterns of fertile peridotite (Fischer-Gödde et al. 2011).

The progressive depletion of HSE in olivine gabbros may be related to fractional crystallization from progressively evolved basic melts. This process appears to result in a strong increase in Re/Os from olivine gabbro via gabbro to leuco gabbro and a strong decrease of Au/Ir, Pd/Ir and Os/Ir. Consequently, while Re/Os in melts increase during fractional crystallization, Au/Ir, Pd/Ir and Os/Ir decrease.

The different behavior of the troctolite data hint at a different origin, possibly involving hybridization of early lower crustal cumulates or mantle tectonite by infiltrating basic melt (Renna and Tribuzio, 2011)

References:
Dick, H.J.B. et al. 1991: In: Von Herzen, R.P. et al. (Ed), Proceedings of the ODP, Scientific Results Leg 118.
Hertogen J. et al. 1980: Geochimica et Cosmochimica Acta, 44, p. 2125 – 2143.
Blusztajn et al. 2000: Chemical Geology, 168, p.113 – 122.
Keays and Scott, 1976: Economic Geology, 71 No , p. 705 – 718.
Fischer-Gödde et al., 2011: Chemical Geology, 280, p. 365 – 383.
Gleißner et al., 2012: Chemical Geology, article in press.
Renna and Tribuzio, 2011: Journal of Petrology, 52, No. 9, p. 1763 – 1790.
Schiano et al. 1997: Earth and Planetary Science Letters, 150, p. 363 – 379.

IODP

Changes of benthic foraminiferal assemblages across the Middle Eocene climatic optimum (MECO) in the North Atlantic (OPD Site 1051, Blake Plateau)

I. MOEBIUS[1], O. FRIEDRICH[1], K.M. EDGAR[2]

[1] Institute for Geosciences, Goethe University Frankfurt, Altenhöferallee 1, 60438 Frankfurt am Main, Germany
[2] School of Earth and Ocean Science, Cardiff University, Park Place, Cardiff CF103AT, United Kingdom

The middle to late Eocene (49-34 Ma) represents a time period characterized by global cooling of ocean temperatures. Superimposed on this general cooling trend

is a short-lived warming event, the Middle Eocene climatic optimum (MECO). Oxygen isotope data suggest a duration of ~750 kyrs with peak temperatures around 40.1 Ma. Despite ongoing research within the last few years, little is known about the causation of this climatic reversal and its effects on marine ecosystems. Furthermore, research mainly focused on southern high-latitude and mid-latitude regions. Therefore, the MECO event is well documented in the Southern Ocean, but it's influence on the northern mid- and high-latitudes are still poorly understood.

To increase the global understanding of the processes across the event, we chose ODP Site 1051 in the North Atlantic (Blake Plateau, 30°N) for this study. Material from that location was used for a benthic foraminiferal assemblage analysis to investigate the effects of the MECO warming event on the benthic ecosystem. Benthic foraminifera from 36 samples across the MECO, as well as 8 samples before and 9 samples after the excursion were investigated in order to obtain a high-resolution record (1 m resolution during the MECO event, 2 m resolution before and after, respectively).
The results reveal that benthic foraminiferal assemblages undergo marked changes during the warming event at Site 1051. This is interpreted as a response to rising bottom-water temperatures as indicated by the increasing benthic foraminiferal ∂18O values. A marked shift from epifaunal species to infaunal species parallels the climatic trend. The correlation between the stable isotope record and the changes in species assemblages across the MECO event suggest a causal relationship of species abundance with organic matter flux and oxygen consumption.

ICDP

Peering into the Cradle of Life: multiple sulphur isotopes reveal insights into environmental conditions and early sulphur metabolism some 3.5 Ga ago

A. MONTINARO[1], H. STRAUSS[1], P. MASON[2], C. MÜNCKER[3], U. SCHWARZ-SCHAMPERA[4]

[1] Institut für Geologie und Paläntologie, Westfälische Wilhelms-Universität Münster, Münster, Germany
[2] Department of Earth Science, Utrecht University, Utrecht, The Netherlands
[3] Institut für Geologie und Mineralogie, Universität zu Köln, Köln, Germany
[4] Bundesanstalt für Geowissenschaften und Rohstoffe, Hannover, Germany

During the early stages of Earth's evolution, environmental conditions were much different from today. Early Earth was characterized by a predominance of oceanic over continental crust, more vigorous mantle convection and presumably warmer surface temperatures (Knauth, 2005). The early atmosphere was reducing with abundant carbon dioxide and methane but largely devoid of oxygen (<10-5 PAL – present atmospheric level), while the ocean was anoxic (Holland, 2002). Hence, life emerged and evolved under seemingly inhospitable environmental conditions. Evidence for early life on Earth derives from different proofs: microfossils, stromatolites and chemofossils, i.e. chemical and isotopic signatures related to metabolic pathways. In particular, the stable isotopes of key elements of life, i.e. C, N and S have been utilized successfully for tracing life in Earth's respective archive: the sedimentary rock record.

One of the most intriguing questions in Earth and Life Sciences is where, when and under what conditions life emerged on our planet. This multinational and multidisciplinary ICDP project aims at investigating which

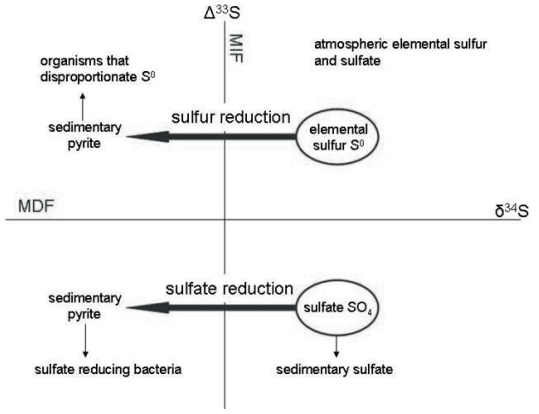

Fig. 1 Two metabolic pathways followed by early organisms.

environmental conditions existed when life emerged and evolved on our planet. A systematic and comprehensive multiple sulphur isotope (32S, 33S, 34S, and 36S) study should be used for the characterization of the

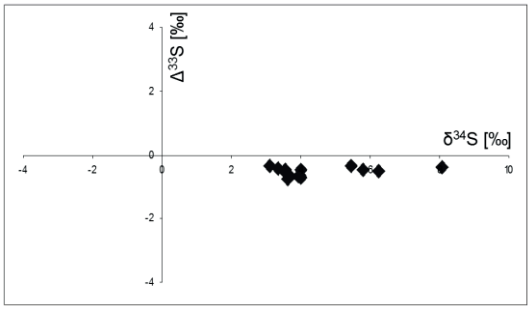

Fig. 2 Multiple sulphur isotope data for barite from the Barberton Greenstone Belt

environmental and the redox conditions in particular. The record of well preserved rock successions from the earliest part of Earth history is rather limited. The 3.55 – 3.23 billion years old Barberton Greenstone Belt in South Africa represents one of the oldest well preserved rock successions from the earliest part of Earth history. This greenstone belt is characterised by a sequence of volcanic and sedimentary rocks and is one of the oldest well preserved successions that has archived environmental conditions prevailing at the surface of our young planet.

This research should yield insights into the geochemical boundary conditions under which life emerged. A multiple sulphur isotope approach will be utilized in order to constrain environmental conditions and identify some of the prevailing metabolic pathways in early Archean habitats. The isotopic composition of sedimentary pyrite reflects the (bio)geochemical conditions during its formation and allows identifying the prevailing metabolic pathways of microbial sulphur cycling (Fig. 1). The minor isotopes ($\delta^{33}S$, $\delta^{36}S$) identify an atmospheric source of sulphur compounds whereas the traditional $\delta^{34}S$ values

reflect microbial sulphur metabolism. Generally, bacteria prefer the lighter isotope for their metabolism, allowing the precipitation of 34S-depleted pyrite.

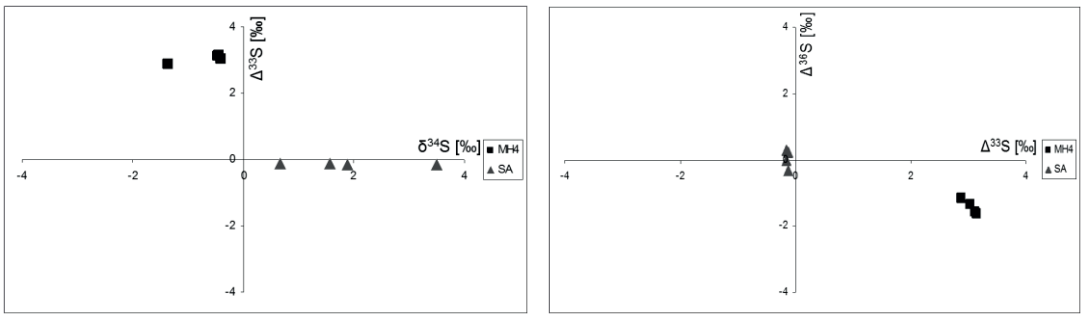

Fig. 3 Multiple sulphur isotope data for massive sulphides from the Bien Venue Prospect (SA) and the Mhlati deposit (MH4)

Unfortunately, due to drilling delays, no samples from the ICDP drill cores have become available yet for research. For this reason, other samples with relevance to the project were analyzed.

Barite from the Mapepe Formation, which is part of the 3.23-3.26 Ga old Fig Tree Group in the Barberton Greenstone Belt, have been studied in collaboration with Dr. Paul Mason, (University of Utrecht, The Netherland).

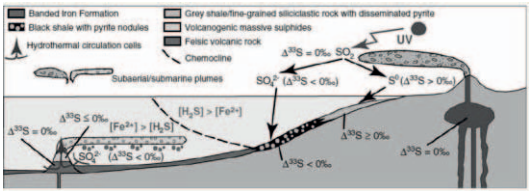

Fig. 4 Sulfur isotope composition of depositional environments influenced by mass independent fractionation in the Archean anoxic ocean and atmosphere (Bekker et al., 2009, modified)

The sulphur isotopic composition ($\delta^{34}S$) varies between 2.9 and 7.7‰ (avg. 4.0 ± 1.0‰; n=39) (Fig. 2) and the oxygen isotopic composition (δ18O) displays a range between 7.6 and 13.0‰ (avg. 10.3 ± 1.4‰; n=35). Multiple sulphur isotope data fit well with results obtained during previous studies (e.g., Farquhar et al., 2000; Bao et al., 2007; Strauss and Gutzmer, unpublished). The sulphur isotope study reveals mass-independent fractionation signal with $\delta^{33}S$ values around an average of -0.530‰ (range: -0.771 to -0.343‰) (Fig 2). One of the key questions which arises from this research is whether this barite reflects the sulphur isotopic composition of the Archean seawater and the overall evolution of the ocean-atmosphere system.

Massive sulphides, from the volcano-sedimentary succession in the Barberton Greenstone Belt were studied in collaboration with Dr. Ulrich Schwarz-Schampera (Bundesanstalt für Geowissenschaften und Rohstoffe, Hannover). Samples come from two different deposits: the Bien Venue Prospect (Fig. 3, triangles) and the Mhlati deposit (Fig 3, squares). The Bien Venue sulphides are characterized by $\delta^{34}S$ values ranging from 0.7 to 3.5‰, while all Mhlati sulphides display slightly negative $\delta^{34}S$ values between -1.2 and -0.1‰. All results are close to the 0‰ and could resemble a juvenile sulfur source. In contrast, both sample sets show totally different $\Delta^{33}S$ values. Samples from the Mhlati deposit yielded a range from 2.657 to 3.152‰ while the Bien Venue Prospect samples vary between -0.160 and -0.130‰, thus defining two different populations. $\delta^{33}S$ values represent a mass-dependent fractionation signal in the Bien Venue samples ($\delta^{33}S = 0 \pm 0.25$‰), while the Mhlati deposit displays a sizeable mass-independent sulphur isotope fractionation. Besides, the sulphides from the Mhlati deposit (squares) show a linear negative correlation between the $\delta^{33}S$ and $\delta^{36}S$ values, typical for Archean sedimentary sulphides.

Komatiites and tholeiites from the type locality at the Komati River, Barberton Greenstone Belt (samples from Prof. Carsten Müncker, Universität zu Köln) were studied for their multiple sulphur isotope geochemistry. Five out of six samples are characterized by $\delta^{33}S$ values between -0.200 and -0.090‰, i.e. very close to 0‰, that could resemble a juvenile sulfur source. $\delta^{33}S$ values are small but clearly negative and represent the mass-dependent fractionation line. $\delta^{34}S$ values for these samples range from

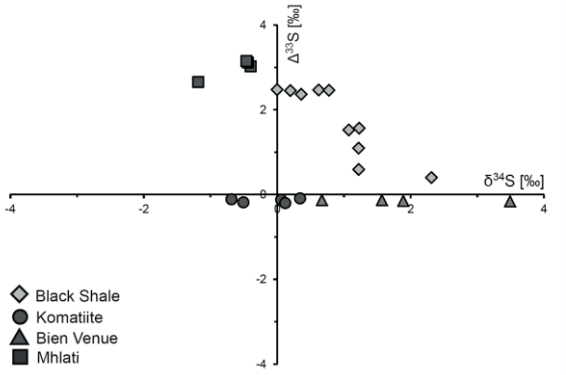

Fig. 5 Multiple sulphur isotope data for massive sulphides from the Barberton Greenstone Belt (source of Fig Tree Group black

-0.69 to 0.34‰. These values are also close to the sulphur isotopic composition of mantle sulphur. However, one sample shows a $\delta^{33}S$ value of -0.507‰, which reflects mass-independent sulphur isotope fractionation, and a $\delta^{34}S$ value of +5.0‰.

Some preliminary conclusions can be drawn with respect to the sulphur source and the possible pathways of sulphur turnover. Barite is characterized by $\delta^{33}S$ and $\delta^{34}S$ results that are very different from those for komatiites and massive sulphides. $\delta^{33}S$ values in barite (average of -0.530‰) represent mass-independently fractionated sulphur which reflects the atmospheric signal. This is due to the ultraviolet photolysis of volcanogenic SO_2 (Fig. 4). Ultraviolet photolysis of atmospheric SO_2 generates

elemental sulphur with positive $\delta^{33}S$, and sulfate with negative $\delta^{33}S$, i.e. clearly mass-independently fractionated sulphur compounds (Bekker et al, 2009; Farquhar et al., 2010). Both products are being transferred to Earth surface environments, thereby delivering distinctly different sulphur isotope signals.

The preservation of distinctly different $\delta^{33}S$ signals into the sedimentary realm is possible only under anoxic atmospheric conditions, with a maximum level of atmospheric oxygen of 10^{-5} PAL (Pavlov and Kasting, 2002). Komatiites and the massive sulphides from the Bien Venue prospect are indeed characterized by comparable $\delta^{34}S$ and $\delta^{33}S$ values, which suggests a common sulphur supply, specifically a juvenile source. On the contrary, massive sulphides from the Mhlati deposit are significantly different in their multiple sulfur isotopic composition. Results appear to define a mixing line between the komatiites population and the barite data (Fig. 5).

Acknowledgements: Financial support from the Deutsche Forschungsgemeinschaft (DFG Str 281/36) is gratefully acknowledged.

References:

Bao, H., Rumble III, D., Lowe, D.R., 2007. The five stable isotope compositions of Fig Tree barites: implications on sulphur cycle in ca. 3.2 Ga oceans. Geochim. Cosmochim. Acta 71: 4868-4879.

Bekker, A., Barley, M.E., Fiorentini, M. L., Rouxel O.J., Rumble, D., Beresford, S.W., 2009. Atmospheric sulfur in Archean Komatiite-hosted Nickel deposits. Science 326, 1086-1098.

Farquhar J., Bao H.,Thiemens M., 2000. Atmospheric Influence of Earth's Earliest Sulfur Cycle. Science 289 no. 5480, 756-758.

Holland, H.D., 2002, Volcanic gases, black smokers, and the Great Oxidation Event. Geochim. Cosmochim. Acta 66: 3811-3826.

Knauth, L.P., 2005. Temperature and salinity history of Precambrian ocean: implications for the course of microbial evolution. Palaeogeogr. Palaeclimat. Palaeoecol. 219: 53-69.

Pavlov, A.A., and Kasting, J.F., 2002. Mass-independent fractionation of sulphur isotopes in Archaean sediments: strong evidence for an anoxic Archaean atmosphere. Astrobiology 2: 27-41.

ICDP

Towards timescales of assimilation and magma mixing in the Large Igneous Province of Snake River Plain-Yellowstone, northwest United States.

D. MORGAVI[1], C. P. DE CAMPOS[1], D. PERUGINI[2], W. ERTEL-ÍNGRISCH[1], Y. LAVALLÉE[1,] K-U. HESS AND D. B. DINGWELL[1]

[1] Dept. Earth and Environmental Sciences, Ludwig-Maximilian-University (LMU), Theresienstrasse 41/III, 80333 München, Germany. (morgavi@min.uni-muenchen.de)

[2] Dept. Earth Sciences, University of Perugia, Piazza Universitá, 06100 Perugia, Italy

The Snake River Plain (SRP) presents a unique opportunity to study the impact of a hot-spot-related thermal anomaly on the continental crust and the subsequent development of magma reservoirs. As a reservoir forms, primitive magma batches induce crustal melting, assimilation, and therefore mixing through differentiation processes. Mixing caused by a recharge of a more primitive magma is expected to be accompanied by heating of the reservoir which may obstruct crystal fractionation and thus, precede it. Due to the complexity of the mixing process, especially in multicomponent silicate melts, understanding and interpreting mixing related data require detailed analytical, experimental and numerical studies.

In this work we present results from a series of mixing experiments using both synthetic and natural melts with extreme viscosity ratios (Fig. 1) at super-liquidus temperatures, low Reynolds number (Re around 10^{-7}) and atmospheric pressure. The progress in our experimental mixing campaign started with eight density-driven mixing experiments; and continued with two long-lasting Taylor-Couette mixing experiments. Due to the uncertainties of the starting configuration for the above mentioned experiments, it became obvious that we needed to develop a new technique to investigate mixing processes. For this purpose we developed and built a new experimental setup, called the Journal Bearing System (De Campos et al., 2011). In a first experimental run we performed three chaotic mixing experiments with synthetic melts, and then we run five chaotic mixing experiments with natural melts. All experimental steps have been followed by analytical studies of major and trace elements. Here we focus in detail on the experiments done with the new chaotic mixing device presenting the results with synthetic melts and natural melts collected from the SRP volcanic province.

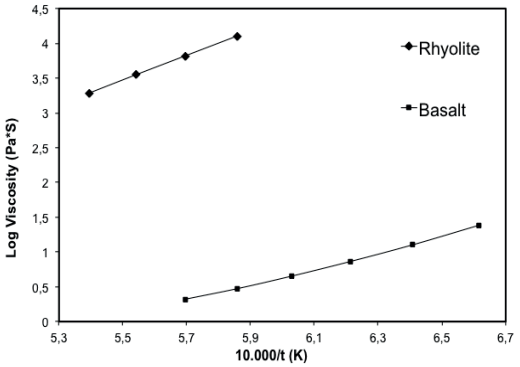

Figure 1: The plot below shows the viscosity-temperature relationship between the basaltic and the rhyolitic natural end-member used in the chaotic mixing experiments and highlights the extreme viscosity contrast.

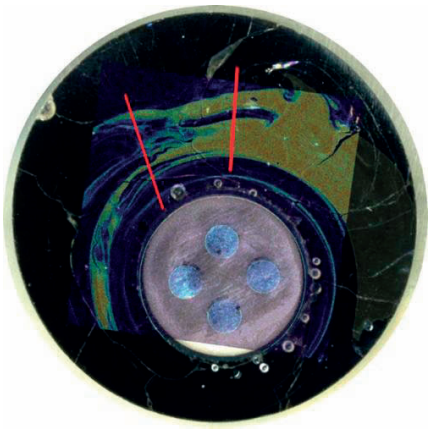

Figure 2: The picture below shows a representative slice (radius 11mm) obtained from quenching one of chaotic mixing experiments at 1,400°C. Lines 1 and 2, in red, correspond to the analyzed transects crossing the filaments. The colored square is a superposed geochemical map depicting the distribution of MgO. Note the variance of concentrations represented by changing shades and colors (Blue representing the rhyolite and yellow the basalt)

Chaotic fluid-dynamic conditions are known to enhance mixing efficiency (Swanson & Ottino., 1990). This was our starting background to develop and build a new apparatus to perform chaotic mixing experiments using fluids with a high viscosity contrast. The setup consists of an outer and an inner cylinder, which is located off-center with respect to the former (fig.2). The motion of the two cylinders are independent and their rotation at given angular velocities, trigger chaotic mixing processes with variable degree of chaoticity (De Campos et al., 2011, Morgavi et al., submit. to Chemical Geology). For the first experiments with the new device, two end-members, with silicate melt compositions were synthesized: (i) a peralkaline haplogranite and (ii) a haplobasalt (anorthite-diopside). Experimental conditions were kept 'extreme', since most of melt fraction consisted of a high-viscosity melt (95%) and small amounts of lower viscosity mafic melt (5%). Such a configuration was chosen to test the ability of our device to function under severe conditions, which could mimic SRP-like conditions. The next goal was then testing the assimilation of restricted volumes of basalts by large amounts of rhyolite.

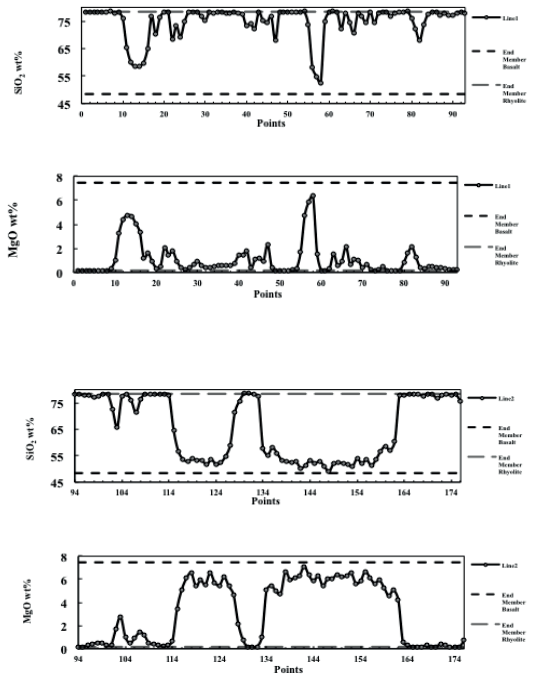

Figure 3: Show the variability of major elements along the analyzed transects. (SiO_2 and MgO). In general element variability exhibits an oscillatory pattern with compositional "hills and valleys" corresponding to the presence of filaments of the two melts. The velocity of compositional transition between filaments depends on the thickness of the filaments: the larger the filament thickness, the sharper the copositional variation. This is the reflection of the interplay between physical stretching and folding and chemical diffusion at the onset of mixing.

Five experimental runs were performed with natural melts under identical run condition as those used in the previous chaotic mixing experiments. Experiments were performed using natural samples from the Bruneau Jarbidge eruptive center (SRP). The melt proportions have been kept identical (basalt 20%, rhyolite 80%) for all the experiments, only temperature and protocols have been changed. Time duration ranges from 1 to 4 hours according to the different protocols.

First optical investigations shows that the basaltic melt was dispersed within the rhyolitc melt due to stretching and folding dynamics generated by the applied experimental protocol (fig. 2). These bands strongly modulate the chemical exchanges between the end-members, leading to regions with extremely variable heterogeneities.

For the investigation of the mobility of major and trace elements across the band interfaces, electron microprobe (EMP), and Laser Ablation ICP-MS measurements were performed. To understand in detail how chaotic mixing develops in space and time, we applied three different approaches: 1) Numerical simulation of the time evolution of the mixing process; 2) first return maps to visualize the evolution of compositional fields (Morgavi et al., submit. to Chemical Geology); and 3) the quantification of rate of homogenization by using the relaxation of concentration variance during the mixing process (Perugini et al., and Morgavi et al., submit. to Chemical Geology).

Results from these experiments are in good agreement with those from chaotic mixing experiments with synthetic silicate melts, such as anorthite-diopside and haplogranite (Morgavi et al., submit. to Chemical Geology; De Campos et al., 2011).

The different configurations used to mix produced a differential modulation of mixing patterns resulting in different mixing efficiencies. This is due to the mobility of the different chemical elements along chaotic flow fields. This process is responsible for strongly non-linear correlations in inter-elemental plots. All experimental results confirm the interplay between advection (convection) and diffusion as the controlling parameters for mixing silicate melts. Another important result is the experimental proof of an additional fractionation mechanism: the diffusive fractionation process (Perugini et al., 2006, 2008; De Campos et al., 2008, 2011, Morgavi et al., submit. to Chemical Geology).

In natural environments, depending on geometric and fluid dynamics constraints, different mixing efficiencies should also be expected. Thus, before any geochemical modeling, petrologists should carefully evaluate each case study. The conceptual and methodological approach emerged from this work can, in principle, be applied to any natural examples in order to estimate the time-scales and degree of magma mixing and assimilation evidenced across volcanic rocks/deposits. First applications of this model are found in Perugini et al. (2010, submit. to Chemical Geology).

From a preliminary comparison between geochemical data from SRP rhyolites and our experimental data, we can suggest that assimilation of small proportions of basalt can reproduce most of the geochemical variation found in natural SRP rhyolites. Taking into account the diversity and complexity of the physico-chemical processes involved, this procedure could provide decisive pieces of the puzzle portraying the evolution of magmas in the SRP system. At a further research stage, we also intend to apply the methods presented here to evaluate times-scales of assimilation along the SRP. For this purpose, new samples from the intermediate-drilling region will contribute to unravel the hidden history of magmatic reservoirs along the hot-spot track.

In conclusion, despite the limitation still persisting in the replication of magma mixing processes by laboratory experiments, we are confident that the approach presented in this work is a valid step towards a better understanding of the complexity of this natural phenomena.

References:
De Campos C.P., Dingwell D.B., Perugini D., Civetta L., Fehr T. K., 2008 Chemical Geology. 256 (3-4), 185-195
De Campos, C. P., Ertel-Ingrisch, W., Perugini, D., Dingwell, D. B. and Giampiero. P., 2010. In: Skiadas, C. H. and Dimotilakis, I., Eds. Chaotic Systems Theory and Applications. Int. Publ. Com. pp 51-58.
De Campos C.P, Perugini D., Ertel-Ingrisch W., Dingwell D.B. & Poli G., 2011 Contribution. Mineral. Petrology., 161, 863-881.
Morgavi D., Perugini D., De Campos C.P., Ertel-Ingrish W., Lavallee Y., Morgan L., Dingwell D.B, submit. to Chem. Geol.
Perugini D., De Campos C. P., Dorfman A., Dingwell D.B., submit to Chem. Geol.
Swanson & Ottino., 1990 Journal of Fluids Mechanics. 213, 227-249
Perugini D., Petrelli M & Poli G., 2006 Earth and Planetary. Science.Letters 243 (3-4) 669-680
Perugini D., De Campos C. P., Dingwell D. B., Petrelli M. and Poli, G 2008 Chemical Geology. 256, 146-157

ICDP

Average 1-D P and S wave Velocity Model for NW Bohemia/Vogtland

S. MOUSAVI[1], M. KORN[1], D. RÖSSLER[2], K. BAUER[3]

[1]Institut für Geophysik und Geologie, Universität Leipzig, Talstraße 25, 04103 Leipzig
[2]DTU Space, Technical University of Denmark, 2800 Kgs. Lyngby, Dänemark
[3]Deutsches Geoforshcungszentrum Helmholtz-Zentrum Potsdam

Joint inversion for hypocentral parameters and seismic P and S wave velocities is nowadays a state of the art tool to obtain high-resolution images of seismically active regions. Our study aims to compute a 3-D P and S velocity model for the NW Bohemia/Vogtland region at the border between Czech republic and Germany between 49.7º to 50.5ºN and 11.7º to 13º W using body wave travel time tomography. The resulting images can then be compared to the results of ambient- noise surface wave tomography and to reflection seismic images that will be obtained from parallel investigations.

Data for this study are first arrival onset times of P and S waves from natural local earthquakes in the years 2000-2010. The data were taken from permanent networks WEBNET, KRASNET, BAYERNNETZ, SXNET, Thuringian network and from temporary networks BOHEMA, PASSEQ and other institutions data like GFZ and University of Potsdam. The data archive consists of more than 1500 events recorded by up to 120 stations. As 700 of them have magnitudes lower than 0.5 S waves can be detected much easier than P and the number of S waves arrival times are in majority. The hypocentral depths are mostly between 6 and 12 km and are distributed all over the region.

Up to now we derived an average 1-D velocity model using VELEST (Kissling et al. 1994) performing a simultaneous inversion of location and velocity strucgture. It will serve as a starting model for a 3-D travel time tomography that will be done in future. Finally we compare the VELEST model with other studies (e.g. Malek et al. 2004, 2005).

Kissling, E., W.L. Ellsworth, D. Eberhart-Phillips, and U. Kradolfer: Initial reference models in local earthquake tomography, J. Geophys. Res., 99, 19635-19646, 1994.
Malek, J., Jansky, O., Novotny, O., Rössler, D: Vertically inhomogeneous models of the upper crustal structure in the West-Bohemian seismoactive region inferred from the CELEBRATION 2000 refraction data. Stud. Geophys. Geod., 48 (2004), 709−730.
Malek, J., Horalek, J., Jansky, J.: One-dimensional qP-wave velocity model of the upper crust from the West-Bohemia/Vogtland earthquake swarm region. Stud. Geophys. Geod., 49 (2005), 501−524.

IODP

Seismic reflection data of the Eirik Drift: A first step to decipher the Neogene development of the Western Boundary Undercurrent (WBUC)

A. MÜLLER-MICHAELIS[1], G. UENZELMANN-NEBEN[1]

[1]Alfred-Wegener-Institut für Polar- und Meeresforschung, Am Alten Hafen 26, 27568 Bremerhaven

The Eirik Drift off the southern tip of Greenland contains sedimentary records since the Miocene. This archive of depositional processes has been shaped by the Western Boundary Undercurrent (WBUC), the Greenland ice sheet, and material input from the Labrador Sea through the Davis Strait. The WBUC is a main contribution to the lower branch of the global Thermohaline Circulation, which determines the world's climate. Therefore, changes in strength and direction of the WBUC are closely connected to climate changes.

The high-resolution multichannel seismic reflection

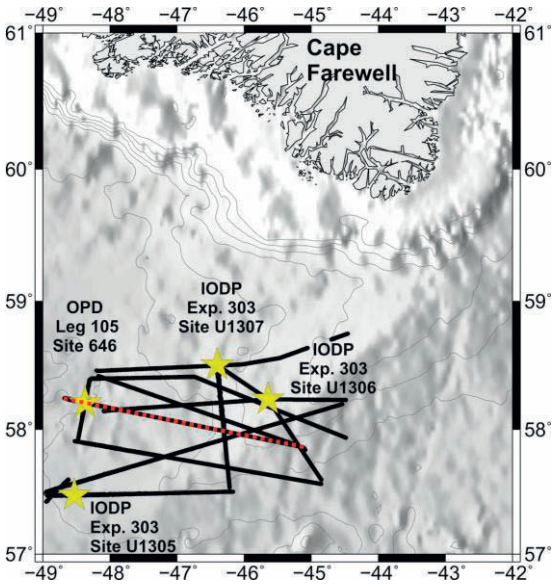

Figure 1: Bathymetric map (Smith and Sandwell, 1997) of the vicinity of the Eirik Drift south of Cape Farewell (Greenland) showing the locations of the seismic profiles (black lines) and the ODP/IODP Sites (yellow stars). The red dashed line highlights the location of profile AWI-20090004 presented in Figure 2.

data network collected during RV Maria S. Merian cruise MSM 12/2 connected ODP Leg 105 Site 646 and IODP Expedition 303 Sites U1305, U1306, and U1307 (Fig. 1). The seismic reflection data were incorporated with geological information from the ODP and IODP sites to deduce information on the development of the WBUC as

well as the dimensions and expansion/retreat of the Greenland ice sheet and a much clearer understanding of the evolution of the climate southwest of Greenland.

After correlating synthetic seismograms based on density and P-wave velocity data from ODP Leg 105 Site 646 and IODP Expedition 303 Sites U1305, U1306, and U1307 with the processed seismic reflection data we identified four seismic units and the reflectors defined by Arthur et al. (1989) (Table 1; Fig. 2).

Reflectors/Seismic Units	Age	Paleoceanographic History
SU I		weakening of deep currents
R1	2.5 Ma	onset of ice rafting
SU II		strong deep currents
erosional unconformity	4.5 Ma	initiation of strong deep currents local erosion
SU III		increasing deep currents
R2	5.6 Ma	higher carbonate content
SU III		onset of Denmark Strait Overflow Water weak deep currents
R3/R4	7.5 Ma	change in water mass characteristics increased sedimentation rate
SU IV		corrosive, southern sourced bottom water

Table 1: Compilation of defined seismic stratigraphy (seismic units SU I - IV), seismic reflector (R1 - R3/R4) nomenclature and Paleoceanographic history at ODP Leg 105 Site 646 following Arthur et al. (1989).

Figure 2 shows seismic profile AWI-20090004 (red dashed line in Fig. 1) as an example with the location of ODP Leg 105 Site 646 and the identified reflectors and units (Table 1). Tracking of both reflectors and units leads to information about the redistribution of the WBUC in the vicinity of the Eirik Drift during the Neogene.

Seismic unit IV (SU IV; > 7.5 Ma) is bounded by the acoustic basement (brown) and the reflector doublet R3/R4 (blue). SU IV shows a high sediment accumulation at the main drift mound in the east (CDP 66-5000), more than twice as high as the more uniform thickness in the west (CDP 5000-12780). This indicates a strong deep current influence in northward direction at the western flank of the main mound (~ CDP 5000) depositing the sediments to the right of the flow. In this phase it is believed that the water masses are mainly of southern origin before a more modern pattern of the WBUC was established at the R3/R4 boundary (~8.2-7.5 Ma) (Kaminski et al., 1989). SU III (7.5-4.5 Ma) is bounded by reflector doublet R3/R4 (blue; 7.5 Ma) and the erosional unconformity (orange; 4.5 Ma) and is subdivided by reflector R2 (red dashed; 5.6 Ma). The lower part of SU III (7.5 - 5.6 Ma) is acoustically transparent and of uniform thickness in the west (CDP 8000-12780) and thins towards the western flank of the main mound (CDP 5000) with no deposition on top of the main mound. This indicates a decreased deep current influence, not strong enough to deposit sediments on top of the main mound. We observe a thinning of the unit at CDP 5000, which we interpret to represent erosion due to the

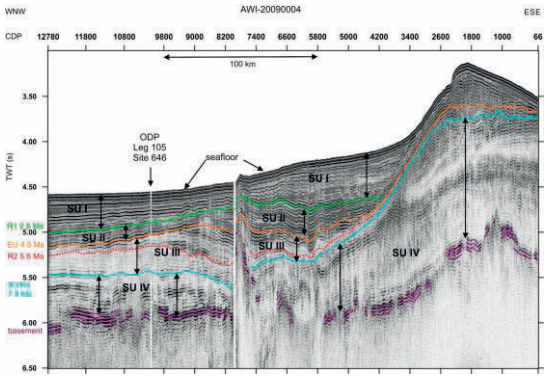

Figure 2: Seismic profile AWI-20090004 (red dashed line in Fig. 1) including the location of ODP Leg 105 Site 646 and the identified reflectors and units. R1 (green), erosional unconformity (orange), R2 (red dashed), R3/R4 (blue) and the acoustic basement (brown). The solid reflectors comprise the seismic units SU I - SU IV.

location of the current core. The upper part of SU III (5.6 - 4.5 Ma) shows two depositional centers, one on top of the main mound (CDP 66-2600) and one in the center of the profile (CDP 5000-10000). This distribution of the sediments suggests that the deep current divided into two northward-directed branches located near CDP 4000 and CDP 11000. This deposition pattern and the higher amplitudes within this unit suggest increased deep current activity. Some reflectors wedge out at the upper boundary (CDP 9000-10000), which indicate erosion at the erosional unconformity caused by strong deep currents. SU II (4.5 - 2.5 Ma) is bordered by the erosional unconformity and reflector R1 (green; 2.5 Ma) and consists of high amplitude reflectors. The shape of SU II still points towards still two branches of the deep current. These probably shifted upslope towards CDPs 3500 and 9500, respectively. SU I (< 2.5 Ma) comprises the interval between reflector R1 and the seafloor. The almost uniform thickness of SU I in the west (CDP 4000-12780) suggests that the western branch of the WBUC ceased at formation of reflector R1 with the onset of ice rafting under glacial conditions. The main branch of the deep current weakened and shallows towards CDP 3000 under a glacial regime.

The changes in deposition of sediments are assigned to changes in direction and strength of the WBUC in the vicinity of the Eirik Drift. Based on our data drift building started before 7.5 Ma. This is in contrast to Arthur et al.'s (1989) observation, who dated the onset of drift building at 4.5 Ma based on ODP Leg 105 Site 646 results and seismic reflection data in the vicinity of this ODP Site in the west of our investigation area. In the time interval 7.5 - 5.6 Ma our observation indicate a weak WBUC, followed by increasing WBUC activity and the separation of the WBUC into two branches (5.6 - 4.5 Ma). At 4.5 Ma we observe strong WBUC activity with local erosion and the two branches of the WBUC are preserved and move upslope in the transitional phase to a glacial regime. With the onset of ice rafting and the glacial regime at 2.5 Ma the western branch of the WBUC cannot be detected any

longer and is interpreted to weaken and shallow. This is correlated with major changes in the Thermohaline Circulation as deep-water formation was restricted and intermittent during the Pleistocene and shifted to intermediate water depth (Glacial North Atlantic Intermediate Water; Sarnthein et al., 2000).

References:
Arthur, M., Srivastava, S. P., Kaminski, M., Jarrad, R. and Osler, J., 1989. Seismic stratigraphy and history of deep circulation and sediment drift development in Baffin Bay and the Labrador Sea. In: Srivastava, S. P., Arthur, M. and Clement, B. (eds) Proceedings of the Ocean Drilling Program, Scientific Results, 105, Ocean Drilling Program, College Station. TX, 957-988.
Kaminski, M. A., Grandstein, F. M., Scott, D. B. and MacKinnon, K. D., 1989. Neogene benthic foraminifera biostratigraphy and deep-water history of sites 645, 646 and 647, Baffin Bay and Labrador Sea. In: Srivastava, S. P., Arthur, M. and Clement, B. (eds) Proceedings of the Ocean Drilling Program, Scientific Results, 105, Ocean Drilling Program, College Station. TX, 731-747.
Sarnthein, M. S. et al., 2000. In: Schäfer, P. R., Ritzau, W., Schlüter, M. and Thiede, J. (eds) The Northern North Atlantic: A Changing Environment, Springer Berlin, 365-410.
Shipboard Scientific Party, 1987. Site 646. In: Srivastava, S. P., Arthur, M., Clement, B. et al. (eds) Init. Repts, Ocean Drilling Program, College Station, TX, 419-674.
Shipboard Scientific Party, 2005. North Atlantic Climate: Ice-sheet-ocean-atmosphere interactions on millennial timescales during the late Neogene-Quaternary using a paleointensity-assisted chronology for the North Atlantic. Expedition 303 Preliminary Report, Site U1305, Site U1306, Site U1307, Integrated Ocean Drilling Program, Washington, D.C., 21-28.
Smith, W. H. S. and Sandwell, D. T., 1997. Global Sea Floor Topography from Satellite Altimetry and Ship Depth Soundings. Science, 277, 1956-1962.

ICDP

The "Wadi Gideah" cross section in the Southern Oman ophiolite: a reference profile for the fast-spreading oceanic crust?

MÜLLER, T. [1*], WOLFF, P.E. [1], KOEPKE, J. [1], GARBE-SCHÖNBERG, D. [2], STRAUSS, H. [3]

[1]Institut für Mineralogie, Leibniz University of Hannover, Germany
[2] Institut für Geowissenschaften, University of Kiel, Germany
[3] Institut für Geologie und Paläontologie, University of Münster, Germany
correspondence: t.mueller@mineralogie.uni–hannover.de

Ocean crust formed at fast–spreading rates exhibits a relatively uniform seismic stratigraphy and is regarded as layered and relatively homogeneous, in contrast to oceanic crust generated at slow–spreading ridges. Importantly, theoretical models on magmatic accretion of the oceanic crust, thermal models, mass balance calculations for the whole ocean crust, or general alteration models only exist for fast–spreading systems. However, due to the lack of exposures and drilled sections of the deep basement of fast–spread crust, most models for fast–spread crust are not tested up to date by using natural samples. Therefore, it is necessary to perform complementary studies of ophiolites, in particular the Oman ophiolite, which is regarded to present the best example of fast–spreading oceanic crust on land, and which played a vital role in developing crucial paradigms for understanding sea floor spreading.

During February 2010 we undertook a detailed field campaign on the Wadi Gideah, which is located in the Wadi–Tayin Massif in the southern part of the Oman ophiolite in order to sample a complete section through the whole ophiolite. The southern massifs of the Oman ophiolite are regarded as the best area for studying primary "normal" fast-spreading ridge processes, where the so-called "late-stage magmatism" is widely absent. Up to now, our profile contains more than 100 samples from mantle peridotites, gabbros to dikes and lavas. This profile is representative for fast–spread oceanic crust both in terms of completeness of the crust–forming structural components and in coherence of geochemical and petrological data to be obtained, thus well–suited for shedding light on crustal accretion processes and the evolution of primary and secondary geochemical cycles of fast–spreading oceanic crust. In

order to obtain data sets as coherent as possible (major and trace elements, isotopes, and microanalytical results), we will follow a concept to perform all analytical investigations on the same samples. Our study follows an approach of an US working group in the late 1970s to obtain a complete profile through the Oman ophiolite (Pallister & Hopson, 1981, J. Geophys. Res. 86) in the same Wadi.

In this study we present our data obtained so far, in order to present geochemical and petrological logs of the Wadi-Gideah section. Main interest at this stage of the project is to focus on the mineral chemical evolution as well as the bulk major/trace element compositional evolution.

By evaluating the structural data obtained during our field campaign, we were able to reconstruct the layered stratigraphy of a virtually undeformed oceanic crust with a thickness of approximately 6 km. We identified the main lithologies from top to bottom (estimated thickness in parentheses): pillow lava (600 m), sheeted dikes (1300 m), varitextured gabbro (400 m), foliated gabbro (1600 m), layered gabbro (2200 m) resting upon a very thin MOHO transition zone (< 50 m) on the mantle sequence.

First results based on electron microprobe analyses of the constituent mineral phases of the gabbroic section reveal very homogeneous compositions in the layered gabbro section: XMg olivine 0.76 to 0.82; XMg clinopyroxene 0.82 to 0.91; An content plagioclase 79-85 mol%. The mineral compositions of the foliated gabbros show more scattering and are slightly more evolved: XMg olivine 0.65 to 0.74; XMg clinopyroxene 0.74 to 0.87; An content plagioclase 62-82 mol%. In the varitextured gabbro the variation in the compositions are more pronounced with the trend to more evolved compositions (e.g. An content plagioclase 60 to 85 mol%).

Far–reaching goals include to elaborate a complete mass balance and to establish the whole evolution of the hydrothermal alteration cycles (by using Sr, O, S, and other suitable isotopes).

Finally, the Oman reference profile provides scientific support for the "Oman Ophiolite Drilling Project" (lead PI: Peter Kelemen) within the ICDP (International Continental Scientific Drilling Program) and also for the IODP (Integrated Ocean Drilling Program) drilling at Site 1256 (equatorial Pacific) where a complete section from the lavas through the sheeted dikes down to the uppermost gabbros is available.

ICDP

Reflection seismic investigation of the geodynamically active West-Bohemia/Vogtland region

N. MULLICK[1], S. BUSKE[1], S. SHAPIRO[2], P. WIGGER2, B. RŮŽEK3, J. HORÁLEK[3], P. HRUBCOVÁ[3], T. FISCHER[4]

[1]TU Bergakademie Freiberg, Institute of Geophysics and Geoinformatics, 09596 Freiberg, nirjhar.mullick@geophysik.tu-freiberg.de
[2]Freie Universität Berlin, Department of Geophysics, Malteserstrasse 74-100, 12249 Berlin
[3]Institute of Geophysics of the Academy of Sciences of the Czech Republic, Boční II/1401, 141 31 Prague 4, Czech Republic
[4]Institute of Hydrogeology, Engineering Geology and Applied Geophysics, Charles University, Albertov 6, 128 43 Praha 2, Czech Republic

The West Bohemia-Vogtland region in central Europe attracts much scientific interest due to recurrent earthquake swarms and continuous emission of CO_2 dominated fluid from the subsurface. Seismological and geochemical studies reveal 1) significant upper mantle derived content

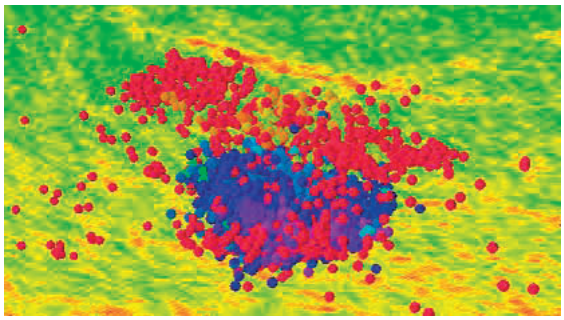

Fig. 1: Reprocessing result of the 9HR profile

of the emitted fluid, 2) an updoming of the Moho below that area 3) possible existence of a magmatic fluid reservoir in the upper mantle and 4) fluid activity as a possible trigger for the swarm earthquakes. In this study the subsurface structure beneath the region is investigated by reprocessing the deep reflection seismic profile 9HR, which runs closely east almost parallel to the earthquake swarm. The migrated image (Fig. 1) confirms the

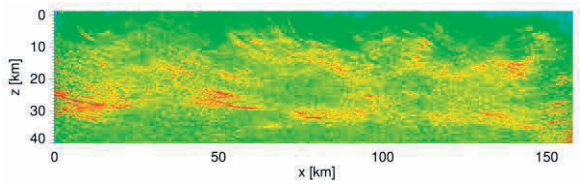

Fig. 2: Bright spot versus earthquake swarm locations.

upwelling of the Moho known from receiver function studies. Directly below one of the major gas escape centres, channel like fault structures are observed which seem to have their roots at the Moho. They may represent deep reaching degassing channels that allow direct transport of mantle-derived fluid. A region of diffused reflectivity is observed that extends from the Moho and ends immediately below the main cluster of the swarm earthquake hypocenters. The upper boundary of the swarm earthquakes is clearly marked by a prominent high-amplitude reflector (bright spot) (Fig. 2). Together with the gas-escape related observations these features suggest that fluids ascend from the Moho upward through fractured rock and generate swarm earthquakes. These fluids are then blocked by near surface non-permeable rocks directly above the swarm earthquake region, thereby causing the bright spot, while they escape unblocked at the gas escape centres where such a barrier may not exist. A comparison of the spatiotemporal evolution of the recent swarms in the years 2000 and 2008 with the subsurface reflectivity shows that in both cases the swarm activity initiates at the upper edge of the highly diffuse reflectivity zone, moves upward, bends at the bright spot above and finally stops after travelling a few kilometers along the bright spot. This correlation may indicate the movement of an overpressured trapped fluid forcing its way into a less permeable volume above it and thereby generating earthquakes swarms. These observations and in particular their joint interpretation give new insight into the causes and driving mechanisms of earthquake swarms in the West Bohemia-Vogtland region.

IODP

Interactions between surface water characteristics and ice-rafting events in the mid-latitude North Atlantic during the last one million years

B.D.A. NAAFS[1], J. HEFTER[1], R. STEIN[1]

1Alfred Wegener Institute for Polar and Marine Research, Department of Marine Geology and Paleontology, D-27568 Bremerhaven, Germany

One of the most dramatic examples of millennial-scale climate change during the last glacial cycle is the episodic collapse of the large continental ice sheets circum the North Atlantic during so-called Heinrich Events of which six took place between 70 and 14 thousand years (ka) (Heinrich, 1988; Bond et al., 1992; Broecker et al., 1992; Hemming, 2004). During the recent years, several studies have reported the occurrence of Heinrich(-like) Events during older glacials periods as well (e.g., Hodell et al., 2008; Stein et al., 2009; Naafs et al., 2011; Channell et al., 2012). However, little is know about the origin (e.g., Hudson area) of these older Heinrich(-like) Events or their influence on surface water characteristics in the North Atlantic. Here we report results from a high-resolution multi-proxy study using both inorganic and organic geochemical proxies and material from Integrated Ocean Drilling Program (IODP) Site U1313 covering the last 1 million years. The results for the first time demonstrate that the Heinrich(-like) Events in older glacials had a similar source as those from the last glacial and thus indicate comparable configurations of the circum-Atlantic ice sheets and a common triggering mechanisms during the various glacials. However, the impact of the different Heinrich(-like) Events on surface water characteristics (sea surface temperature and productivity) varied between glacials, highlighting the complex interaction between millennial-scale climate variability and surface water characteristics in the North Atlantic.

References:
Bond, G., Heinrich, H., Broecker, W., Labeyrie, L., McManus, J., et al., 1992. Evidence for massive discharges of icebergs into the North Atlantic ocean during the last glacial period. Nature 360 (6401), pp. 245-249
Broecker, W., Bond, G., Klas, M., Clark, E., McManus, J., 1992. Origin of the northern Atlantic's Heinrich events. Climate Dynamics 6 (3), pp. 265-273. doi: 10.1007/BF00193540
Channell, J.E.T., Hodell, D.A., Romero, O., Hillaire-Marcel, C., de Vernal, A., et al., 2012. A 750-kyr detrital-layer stratigraphy for the North Atlantic (IODP Sites U1302-U1303, Orphan Knoll, Labrador Sea). Earth and Planetary Science Letters 317-318, pp. 218-230. doi: 10.1016/j.epsl.2011.11.029
Heinrich, H., 1988. Origin and consequences of cyclic ice rafting in the Northeast Atlantic Ocean during the past 130,000 years. Quaternary Research 29 (2), pp. 142-152. doi: 10.1016/0033-5894(88)90057-9
Hemming, S.R., 2004. Heinrich events: Massive late Pleistocene detritus layers of the North Atlantic and their global climate imprint. Review of Geophysics 42 (1), p. RG1005. doi: 10.1029/2003rg000128
Hodell, D.A., Channell, J.E.T., Curtis, J.H., Romero, O.E., Röhl, U., 2008. Onset of "Hudson Strait" Heinrich events in the eastern North Atlantic at the end of the middle Pleistocene transition (~640 ka)? Paleoceanography 23, p. PA4218. doi: 10.1029/2008PA001591
Naafs, B.D.A., Hefter, J., Ferretti, P., Stein, R., Haug, G.H., 2011. Sea surface temperatures did not control the first occurrence of Hudson Strait Heinrich Events during MIS 16. Paleoceanography 26, p. PA4201. doi: 10.1029/2011PA002135
Stein, R., Hefter, J., Grützner, J., Voelker, A., Naafs, B.D.A., 2009. Variability of surface-water characteristics and Heinrich-like Events in the Pleistocene mid-latitude North Atlantic Ocean: Biomarker and XRD records from IODP Site U1313 (MIS 16-9). Paleoceanography 24, p. PA2203. doi: 10.1029/2008PA001639

ICDP

First results of the ICDP Dead Sea Deep Drilling Project and its potential for high-resolution studies

I. NEUGEBAUER[1], U. FRANK[1], P. DULSKI[1], M.J. SCHWAB[1], N. NOWACZYK[1], A. BRAUER[1] AND DSDDP SCIENTIFIC PARTY*

[1]GFZ German Research Centre for Geosciences, Section 5.2 Climate Dynamics and Landscape Evolution, Telegrafenberg, D-14473 Potsdam, Germany
*The complete list of scientists involved in the DSDDP project can be found at http://www.icdp-online.org

Introduction

Located at the deepest continental point on earth, the Dead Sea Basin (DSB) has been periodically filled by several water bodies during the Pleistocene (Stein, 2001). The lake level of the Holocene Dead Sea currently lies ~425 m below mean sea level. The DSB is situated in a tectonically active region, the Dead Sea Rift zone, which has been a major source of historic earthquakes. Various studies in the last decades have proven the Dead Sea and its precursors' sediments as being excellent archives of paleo-environmental, tectonic and seismological information of the Middle East region. Having great importance for ancient human development the DSB further provides the opportunity to study the influence of environmental changes on the human history in the Dead Sea and Jordan region. However, previous drilling efforts at outcrops (e.g. Migowski et al., 2004; Fig. 1 – coring project 1997) and in the deep basin (Heim et al., 1997) achieved neither continuous nor deep sediment records due to depositional gaps and hard halite sequences, respectively. In the last decade scientists from Israel, Germany, the USA and Switzerland set up a deep basin drilling campaign in the Dead Sea. The major objective of this ICDP-based campaign was to recover a continuous high-resolution record of the DSB for the past several glacial-interglacial cycles. Main research goals are to reconstruct the environmental, seismic, tectonic and magnetic history of the region and to study the physical properties of the Dead Sea sediments including salt. A high-resolution chronology will be established by AMS radiocarbon and U-series dating supported by varve counting in selected intervals..

Drilling campaign

The ICDP Dead Sea Drilling took place in winter 2010-2011. In total, ~720 m of sediment cores have been recovered from three sites (Fig. 1, sites 5017-1, -2, -3) in the northern deep basin of the Dead Sea. Site 5017-1 is located in the deepest part of the basin at a water depth of 300 m. Sites 5017-2 and 5017-3 are situated in a shallow bay close to the western Dead Sea margin at a water of ~11 m and 2 m, respectively. The longest core (5017-1-A) reaches down to 456 m below lake floor (m blf). Several shorter cores from the same site allowed for creating a composite profile for the upper ~80 m. At the second site (5017-2) only ~10 m of sediment cores have been recovered, whereas from the third site (5017-3) another long sediment core (~340 m blf) is available. Downhole logging has been performed for the holes 5017-1-A and 5017-1-C from the deep site and for the second deep hole (5017-3-C).

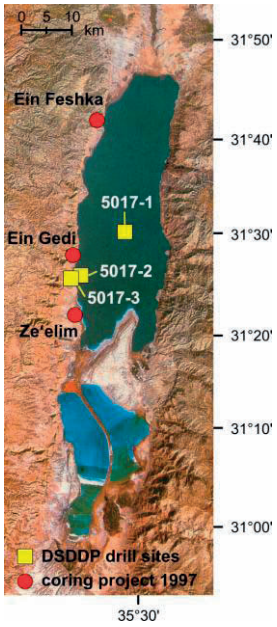

Figure 1: coring sites of the ICDP DSDDP and the 1997-coring locations at the western shore of the Dead Sea

Sediment record

From initial interpretation of sedimentological and petrophysical data of the longest core, it is estimated that the record covers the last ~200 ka including the Zeelim (Holocene), Lisan (last Glacial) (Stein, 2001) and Samra (last Interglacial; Waldmann et al., 2009) formations and the later part of the Amora Formation (penultimate Glacial; Torfstein et al., 2009). Magnetic susceptibility and gamma ray values strongly fluctuate during the Interglacial intervals, while constantly low values have been measured in the Glacial sequences (Fig. 2). The recovered sediments are composed of clayey-silty detrital mud, alternated with authigenic aragonite laminae during the glacial Lisan and Amora formations (Fig. 2). These sequences are further characterised by the occurrence of native sulfur

concretions, prominent gypsum layers, frequent folding or slumping structures and sections of a dark-greenish colour. During the Holocene Zeelim and last Interglacial Samra sequences salt-dominated sediments, either as massive halite or salty mud, and homogeneous to laminated detrital muds have been deposited. Gypsum and aragonite layers are ubiquitous (Fig. 2).

Sediment composition

A first glimpse into the fraction of the magnetic carrier minerals in the Dead Sea sediments was obtained by Scanning Electron Microscopy (SEM) and in-line energy dispersive X-ray spectroscopy analyses on magnetic extracts. These extracts were prepared from dark sediment layers with high magnetic susceptibilities from the Holocene and Lisan formation, deposited at sites 5017-1 and -3. Whereas the Holocene sediments are dominated by fine grained greigite, coarse grained magnetite and some pyrite, the paramagnetic pyrite becomes prominent in the Lisan sediments, thus explaining the distinct decrease in magnetic susceptibility during this interval. Less frequent components of the extracts are barite, zircon and coccoliths.

High-resolution micro-facies analyses

Generally, deposition of sediments in the Dead Sea basin is strongly related to precipitation (Enzel et al., 2008). During wetter intervals the deposition of alternating detrital clay and authigenic aragonite is favoured, while evaporites (e.g., halite and gypsum) precipitate in times of increased aridity and lower lake stands. For high-resolution studies of small-scale climate changes a late Holocene ca. 14 m long section, spanning the time from ~2 to 4 ka BP, and a section from the upper Lisan Formation (~15-17 ka BP, ca. 9 m long) have been chosen for detailed comparison. These intervals have been analysed by µXRF element scanning (step-size 200 µm) and magnetic susceptibility measurements (step-size 1 mm). Petrographic thin section preparation for microscopic layer thickness measurements is ongoing. For the late Holocene sequence (ca. 11-28 m composite depth) the composite profile of site 5017-1 is used, whereas only cores of hole 5017-1-A are available for the upper Lisan interval (ca. 88-99 m blf). Both sequences are composed of detrital, aragonite and gypsum layer-successions that are interrupted by frequently occurring mm to 70 cm thick turbidites (Fig. 3). In the lower half of the analysed Holocene sequence laminated sections further alternate with halite deposits indicating low, flickering lake levels. The late Lisan sequence is characterized by two prominent ~10 cm and ~20 cm thick gypsum layers and is followed by a massive halite sequence that defines the final stage of an extreme decrease of the Dead Sea level before the transition to the Holocene.

Outlook

In the framework of the ICDP Dead Sea Deep Drilling Project analyses of the sedimentation processes in the deep basin during late Holocene and Lateglacial times and of magnetic carrier mineral analyses are ongoing. The results will be compared to sediment profiles from the western margin of the Dead Sea (see Fig. 1), where the same methods will be applied. This offers a great potential for developing high-resolution timeseries of climatic change and depicting single extreme events like floods, droughts and dust storms. A second focus of investigation will be on the genesis of the Fe-sulfide greigite in the Dead Sea sediments by rock magnetic means, since former studies revealed that greigite formation is strongly enhanced during wet climatic phases. A detailed comparison of the rock magnetic records, with the results from micro-facies and micro-XRF scanning, will thus contribute to the identification of periods of increased aridity/humidity and event layers.

References:

Enzel, Y., Amit, R., Dayan, U., Crouvi, O., Kahana, R., Ziv., B., Sharon, D., 2008. The climatic and physiographic controls of the eastern Mediterranean over the late Pleistocene climates in the southern Levant and its neighboring deserts. Global and Planetary Change 60, 165-192.

Heim, C., Nowaczyk, N.R., Negendank, J.F.W., Leroy, S.A.G., Ben-Avraham, Z., 1997. Near East Desertification: Evidence from the Dead Sea. Naturwissenschaften 84, 398-401.

Migowski, C., Agnon, A., Bookman, R., Negendank, J.F.W., Stein, M., 2004. Recurrence pattern of Holocene earthquakes along the Dead Sea transform revealed by varve-counting and radiocarbon dating of lacustrine sediments. Earth Planet. Sci. Lett. 222, 301-314.

Stein, M., 2001. The sedimentary and geochemical record of Neogene-Quaternary water bodies in the Dead Sea basin – inferences for the regional paleoclimatic history. J. Paleolimnol. 26, 271-282.

Torfstein, A., Haase-Schramm, A., Waldmann, N., Kolodny, Y., Stein, M., 2009. U-series and oxygen isotope chronology of the mid-Pleistocene Lake Amora (Dead Sea basin). Geochimica et Cosmochimica Acta 73, 2603-2630.

Waldmann, N., Stein., M., Ariztegui, D., Starinsky, A., 2009. Stratigraphy, depositional environments and level reconstruction of the last interglacial Lake Samra in the Dead Sea basin. Quaternary Research 72, 1-15.

ICDP

Geochemistry of gases in spring waters along the Alpine Fault, South Island of New Zealand

S. NIEDERMANN[1], M. ZIMMER[1], J. ERZINGER[1], S.C. COX[2], C.D. MENZIES[3], D.A. TEAGLE[3]

[1]Helmholtz-Zentrum Potsdam – Deutsches GeoForschungsZentrum GFZ, Telegrafenberg, D-14473 Postdam, Germany
[2]GNS Science, Private Bag 1930, Dunedin 9054, New Zealand
[3]School of Ocean and Earth Science, University of Southampton, European Way, Southampton SO14 3ZH, United Kingdom

The Alpine Fault on the South Island of New Zealand is a major oblique-slip feature, with right-lateral strike-slip rates of 27 ± 5 mm/a and >10 mm/a dip-slip that accommodates over half of Australia-Pacific plate motion, causing rapid uplift of the Southern Alps on its southeast hanging wall. No major earthquakes have occurred on the fault in historic time, but it last ruptured around 1717 AD and is thought to fail at recurrence intervals of 200–400 years, It is globally significant and similar in character to the San Andreas Fault in America or the North Anatolian Fault in Turkey. However, the Alpine Fault is unique in the fact that rapid uplift and mountain building has exhumed fault rocks from depth, and uplift continues to restrict earthquake activity to depths that are shallower than normal. New Zealand is a unique natural laboratory to investigate deep crustal tectonic processes because once-deeply buried rocks (>25 km) now crop out along the Alpine Fault.

Rocks southeast of the Alpine Fault are exhumed at rates faster than they can cool, resulting in a disturbed thermal regime in the shallow crust, and development of geothermal circulation and warm springs without related volcanic activity. Crushed rocks uplifted within the Alpine Fault zone (mylonite, cataclasite, schist) carry widespread evidence of alteration by fluids, with formation of clay and

other minerals showing different generations of cross-cutting relationships. The high heat flow and clay alteration have potential to weaken the Alpine Fault, but it is unclear whether or not the fault will rupture through the zone of weakness, and hence generate very large M7-8

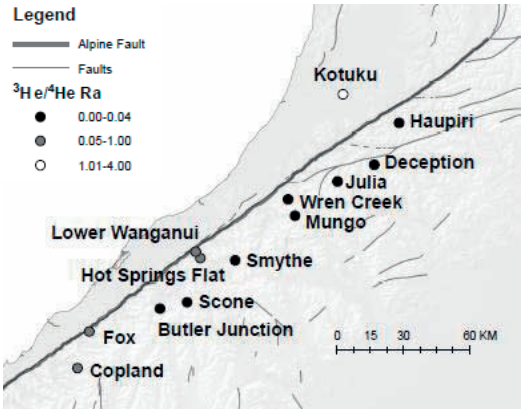

Fig. 1: Locations of sampled springs along the Alpine Fault, South Island of New Zealand. 3He/4He ratios are indicated by the shading of symbols; they imply that the occurrence of mantle fluids is restricted to the immediate vicinity of the fault, except for Copland and Kotuku springs (see text).

earthquakes, or become slowed through the zone and result in multiple numbers of smaller earthquakes. Because the seismic cycle is fundamentally controlled by fluids and fluid circulation, improved knowledge of fluid circulation in the shallow crust is paramount to understanding earthquake processes on the Alpine Fault or any other major fault.

In the context of the ICDP project for scientific drilling into the Alpine Fault (Deep Fault Drilling Project DFDP), we have started a regional investigation of the gas composition in spring waters from the vicinity of the fault. Free gas was sampled at Copland, Fox River, Hot Spring Flat, and Mungo springs, while nine other springs provided water samples that were degassed in the lab. We have determined the abundances of major and trace gas components (CO_2, N_2, CH_4, Ar, He etc.) and the elemental and isotopic compositions of the noble gases (He, Ne, Ar, Kr, Xe). Nitrogen is the most abundant gas in most springs, CO_2 concentrations vary from <0.1% to >96%, and CH_4 contributes up to 13%. Helium concentrations are up to ~500 ppm. $^3He/^4He$ ratios are generally highest (up to 0.81 Ra, where Ra is the atmopsheric $^3He/^4He$ ratio of 1.39×10^{-6}) close to the fault and decrease to radiogenic values (<0.04 Ra) to the southeast at distances of a few kilometers from the fault (Fig. 1). There are just two exceptions: Copland Spring (0.42 Ra) is located some 12 km from the fault, and is characterized by the highest gas flow and the highest CO_2 content of all springs studied in this work. At Kotuku Spring, the only location available for sampling to the northwest of the fault (i.e., on the Australian plate), a particularly high $^3He/^4He$ ratio of ~3.1 Ra is observed despite low gas flow and ~17 km distance from the fault. Obviously, mantle fluids can penetrate the thick crust beneath the Southern Alps directly at the fault and may be diverted away from it only where major passageways through the crust exist. It remains to be seen whether the high $^3He/^4He$ ratio of Kotuku indicates a distinct fluid origin on the northwest side of the fault in general or is just a local feature. In any case, our data will serve as a basis of comparison for results that will be obtained during the DFDP.

IODP

Mississippi paleo-freshwater discharge into the northern Gulf of Mexico and related Loop Current dynamics – results from IODP Site U1319A, RV METEOR and IMAGES cores

D. NÜRNBERG[1], A. KUJAU[2], A. BAHR[3], C. KARAS[3]

[1]Helmholtz-Zentrum für Ozeanforschung Kiel (GEOMAR), Wischhofstr. 1-3, D-24148 Kiel
[2]Institute of Geology, Universitätsstr. 150, D-44801 Bochum
[3]Institute of Geosciences, Goethe University Frankfurt, Altenhoeferallee 1, D-60438 Frankfurt

We here present (isotope)geochemical and sedimentological data from marine sediment cores from the northern Gulf of Mexico to approximate the temporally and spatially varying terrigenous sediment contribution via the Mississippi River and the related spread of freshwater over the last glacial-interglacial cycles, with specific focus on the last deglaciation. Our study is based on cores from southwest of the Mississippi delta (IODP Site U1319A Brazos-Trinity Basin), from ~90 km southeast off the River delta (M78-181), and from the DeSoto Canyon to the east of the delta (MD02-2576 and 2575). The geochemical signature of the eastern cores closely matches that of the Mississippi catchment area rather than those of the Alabama and Mobile River catchments. In particular, the siliciclastic major element potassium (K), estimated from calibrated XRF core scanning, serves as a suitable proxy for Mississippi River sediment discharge, becoming less concentrated with distance from the delta.

The K variability suggests enhanced glacial phase terrigenous influx triggered by strengthened fluvial runoff and changing fluvial and ice sheet dynamics. Mississippi River influx was at a maximum during glacial MIS 2/3, late MIS 8 and MIS 10, reflected by sedimentation rates being 4 to 5 times higher than in the Holocene. Late glacial to deglacial fluvial sediment supply, however, decreased abruptly at ca. 20 ka at our easternmost core location (MD02-2576), and ca. 2 kyr later at our core location closest to the Mississippi Delta, implying a gradual westward shift of the Mississippi outflow. Due to synchronous changes in sea-surface temperatures, we hypothesize an increasing impact of the northward extending Loop Current on the Mississippi outflow pattern.

Combined stable oxygen isotope and element ratios from shallow and deep-dwelling as well as benthic foraminifers allow to approximate paleosalinity, and hence to follow the dispersal of freshwater across the Gulf of Mexico. According to our data, significant Mississippi freshwater discharge events appeared during the last glacial and even during Termination II, but were mostly confound to the southwest of the Mississippi River delta (IODP Site U1319A). The prominent discharge event during Heinrich 1 and the Boelling/Alleroed warm period is also observed at core location M78-181, but not further to the east. Notably, sediment supply during these megadischarge events is insignificant compared to full glacial conditions,

suggesting that signals of freshwater and sediment supply became decoupled.

Holocene changes of Mississippi discharge are closely related to the sea-surface temperature and salinity development in the northern Gulf, most likely amplified by the migration of the Innertropical Convergence Zone, related dislocations of the Hadley Cell, and changes in climatic zones.

IODP

The evolution of the Hawaiian Hotspot: Ar/Ar geochronology and geochemistry of the Hawaiian-Emperor Seamount Chain

J. O'Connor[1], M. Regelous[1], K. Haase[1], K. Hoernle[2], F. Hauff[2], M. Portnyagin[2], R. Werner[2]

[1]GeoZentrum Nordbayern, Universität Erlangen-Nürnberg, Schloßgarten 5, D-91054 Erlangen, Germany
[2]GEOMAR | Helmholtz Centre for Ocean Research, Wischhofstr. 1-3, 24148 Kiel, Germany

Most of the seamounts and volcanic ridges on the ocean floor are hypothesised to form at hotspots that are the surface expression of mantle plumes - hot mantle upwelling from a mantle boundary layer. Morgan's model proposed that the migration of tectonic plates over fixed mantle plumes would generate parallel chains of matching age-progressive volcanoes such as the Hawaiian-Emperor that reflect the direction and speed of plate motion. Moreover, when a tectonic plate changes direction its seamount trails should all develop bends at the same time such as the Hawaiian-Emperor Bend. The type example of such a long-lived, age-progressive intraplate volcanic chain is the Hawaiian-Emperor Seamount Chain (HESC). While the HESC has long been explained by Morgan's concept of Pacific Plate drift over a fixed melting anomaly ('hotspot' or 'plume') in the mantle, recent paleomagnetic data for Emperor Seamount (ODP Leg 197) lavas show that the Hawaiian hotspot drifted southwards between 80 and 50 Ma. The origin of the conspicuous 'bend' in the HESC is therefore debated; it may record the time at which the Hawaiian plume ceased to drift, or it may result from a change in Pacific Plate motion at 50 Ma, or a combination of both processes. Furthermore, geochemical studies of lavas from HESC volcanoes have shown that there have been systematic temporal changes in the composition of Hawaiian volcanism since 80 Ma. The origin of these changes is unclear - proposed mechanisms include hotspot-ridge interaction, and variable degrees of mantle melting controlled by differences in lithosphere thickness. Testing these hypotheses requires accurate age and geochemical data for individual volcanoes along the chain. The age progression along the Emperor Seamount Chain (ESC) is currently very poorly known. Using our recently improved sample preparation and dating techniques we will determine high-precision ages for cleaned plagioclase separates from 50 samples from 19 DSDP-ODP drillsites and new dredge sites on 6 seamounts which cover the critical northern 1200 km of the HESC, where lava compositions and volcano paleolatitudes changed most rapidly. Previous attempts to date the lavas at these sites have been unsuccessful, because these studies were carried out on highly altered, whole-rock samples. We will determine also trace element and isotope composition of 50 accurately-dated lava samples from 15 seamounts from the central 1250 km of the HESC, for which geochemical data are almost completely lacking. This dataset will define

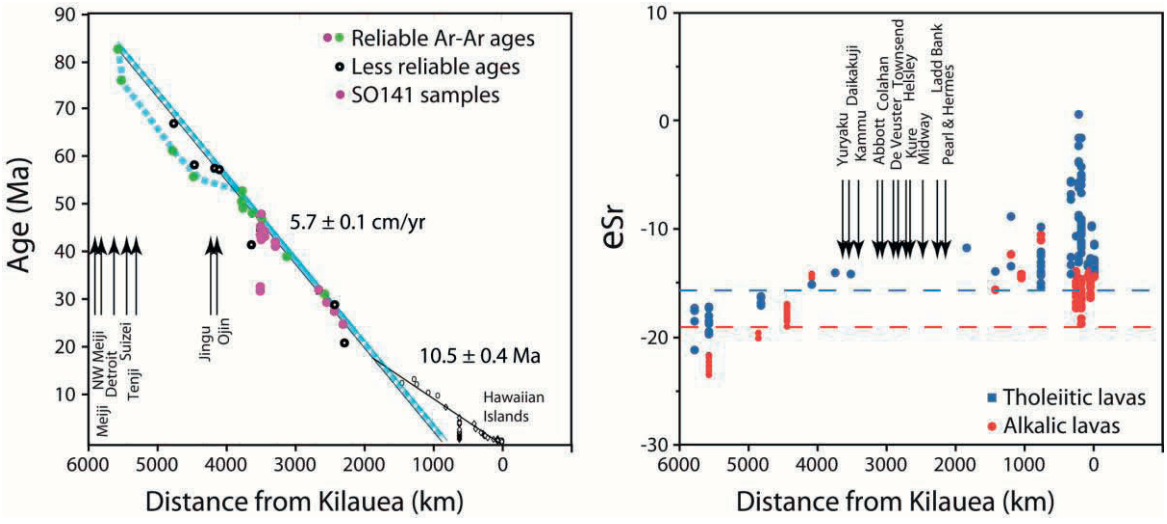

Fig. 1. Left panel shows new and published isotopic ages for Hawaiian-Emperor Seamounts plotted against distance along the seamount chain from Kilauea Volcano (O'Connor et al., manuscript in prep.). The long thick line is a linear distance vs. age slope fitted to the oldest ages for volcanoes along the 1900 km section of the chain between Ōjin and Jingū and Pearl & Hermes Atoll. The non-linear dashed line is an alternative age-distance relation. Arrows show locations of seamounts to be analysed in this project that will establish which of these very different models is correct. Our new sample set for Ar-Ar dating covers the critical period 55-90 Ma, during which the composition of magmatism changed from depleted to more enriched similar to young lavas from the Hawaiian Islands. Right panel shows the geochemical evolution of Hawaiian magmatism with time. Lavas from the oldest Emperor Seamounts >4500 km from Kilauea have low $^{87}Sr/^{86}Sr$ ratios, also low concentrations of incompatible elements and are unlike younger lavas from the HESC and Hawaiian Islands. Arrows show locations of seamounts to be analysed in this project that will test models proposed to explain this difference. Our new results will more than double the existing sample set for Hawaiian volcanoes older than 28 Ma by providing new ages for 50 samples from Meiji to Ojin and geochemical data for 50 samples from Yuryaku to Pearl & Hermes Reef (age data recently obtained by O'Connor et al., in prep.).

accurately the rate of age-progression along the HESC, the duration of magmatism on individual volcanoes, and the geochemical evolution of magmatism between 90 and 28 Ma. We will combine our new dataset for the HESC with data being obtained for recently recovered IODP Leg 330 samples from the Louisville Seamounts to reconstruct the distance between coeval volcanoes along these two primary hotspots in sufficient detail to quantify their relative motion and whether this drift can be related to surface tectonic factors. We will test models for the origin of intraplate magmatism, determine the degree of hotspot fixity and the origin of the HESC 'bend', examine the role of deformation in young rejuvenated stage magmatism in the Pacific and the influence of spreading ridges and lithosphere age on the compositions of intraplate lavas. These goals fall within the IODP priority theme 'Earth Connections: Deep Processes and Their Impact on Earth's Surface Environment'.

ICDP

Stable isotopes of carbonate from the ICDP-site Laguna Potrok Aike reflect hydrological changes in Patagonia

MARKUS OEHLERICH[1], CHRISTOPH MAYR[1,2,3], ANDREAS LÜCKE [4], ANNETTE HAHN[5], CHRISTIAN OHLENDORF[5], BERND ZOLITSCHKA[5] AND THE PASADO SCIENCE TEAM[6]

[1]Dept. of Earth and Environmental Sciences, Ludwig-Maximilians Universität Munich, D-80333 Munich, Germany
[2]Geo-Bio-Center, Ludwig-Maximilians Universität München, D-80333 Munich, Germany
[3]present address: Institute of Geography, Friedrich-Alexander-Universität Erlangen-Nürnberg, D-91054 Erlangen, Germany
[4]Institute of Bio- and Geosciences, IBG-3: Agrosphere, Forschungszentrum Jülich, D-52425 Jülich, Germany
[5]GEOPOLAR, Institute of Geography, University of Bremen, D-28359 Bremen, Germany
[6] PASADO Science Team as cited at: http://www.icdp-online.org/front_content.php?idcat=1494

Stable isotopes ($\delta^{18}O$ and $\delta^{13}C$) of lacustrine carbonates provide a paleotemperature and hydrological archive. The 106 m composite profile from the lake center of Laguna Potrok Aike (52°S, 70°W; 116 m asl; diameter: 3.5 km, water-depth: 100 m) bears the potential to investigate a high-resolution paleoclimate record in the zone of the Southern Hemisphere westerlies of the last 51 cal kyrs BP (Kliem et al., 2012). The polymictic, closed lake is located in the Patagonian steppe and mainly controlled by ground water inflow and evaporation rates.

However, carbonates in Laguna Potrok Aike consist of µm-sized calcite crystals dispersed in clayey to silty matrix. The low carbonate content in the sediments of Laguna Potrok Aike, especially before 9.2 kcal BP, challenge careful pre-treatment procedures and sample selection. After thorough testing of frequently used pre-treatment methods we decided to measure untreated bulk samples, because these treatments caused obviously artificial isotope shifts. The TIC/TOC ratio was found in tests with synthetic organic-carbonate mixtures to be of importance for providing reliable carbonate isotope data (Oehlerich et al., in prep.). A TIC/TOC ratio of ≥ 0.3 was found as an approximate threshold for providing a reliable isotope value for Laguna Potrok Aike's bulk sediment. Given this limitation the carbonate isotope record of Laguna Potrok Aike is restricted to the period after 9.2 cal. kyrs BP, a short period in the transition from the Holocene to the Late Glacial, and only a few samples from the Glacial (Fig. 1). The preliminary stable isotope records of the ICDP-cores (site 5022-2) and previously taken piston cores (PTA03-12/13) show similar fluctuations in this time period (Fig. 1). The Holocene $\delta^{18}O$ maximum of the carbonates centred around 8 cal. kyrs BP is matched by highest $\delta^{15}N$ values that represent increased soil erosion during that time (Mayr et al., 2009). Maximum TIC and far-distance transported Andean Forest pollen (Mayr et al., 2007; not shown) indicate a drought period with extreme low lake levels

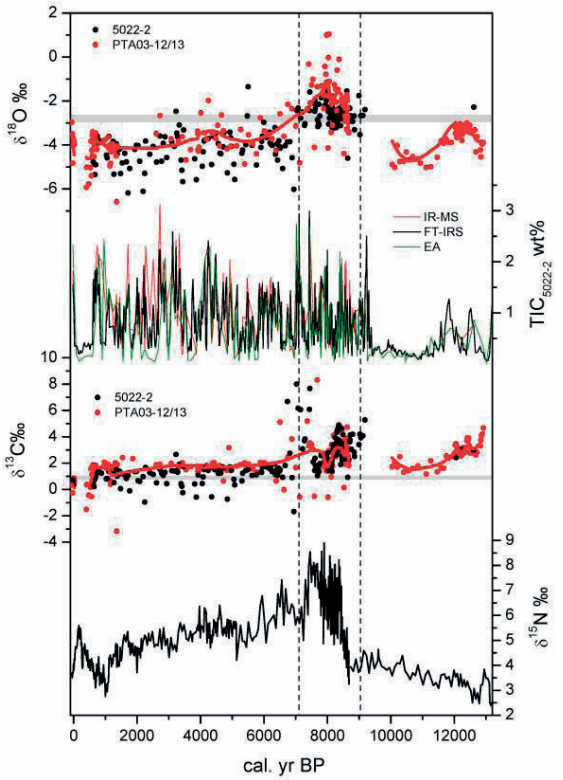

Fig. 1 $\delta^{18}O$ and $\delta^{13}C$ values of carbonates from Laguna Potrok Aike from ICDP core 5022-2 (black dots) versus PASADO age model V.3 (Kliem et al., 2012) compared to isotope data from piston cores (PTA 03/12-13, red dots, SALSA age model from Haberzettl et al., 2007). Red line represent 10-point FFT filtered piston core data. The grey bars in the graphs are $\delta^{18}O$ and $\delta^{13}C$, respectively, for modern ikaite-derived calcite formed in the lake water during austral winter 2008. For comparison total inorganic carbon (TIC) analysed with different methods (Hahn et al. 2012 and unpublished data) and $\delta^{15}N$ values from piston cores (Mayr et al., 2009 versus SALSA age model) is shown.

(Anselmetti et al., 2007). Relative increases of $\delta^{18}O$ around 12.4 and 8.0 cal. kyr BP represent drought periods while periods with low $\delta^{18}O$ and TIC, such as around 0.4 cal. kyrs BP, reflect more humid periods. Thus, the $\delta^{18}O$ record can be interpreted as proxy for hydrological rather than temperature variations.

Further investigations were carried out on the origin of the sedimentary carbonate in Laguna Potrok Aike. As catchment rocks are carbonate-free, the carbonates were precipitated in the water column or within the sediments. The carbonates in the uppermost sediment layer show good isotopic agreement with modern carbonates precipitated in the lake pointing to a precipitation within the water column. However, the enormously high phosphorus

concentration (1.3-3.6 mg L^{-1}, Zolitschka et al., 2006) inhibits the primary formation of unhydrated calcium carbonate phases like calcite and aragonite (Bischoff et al. 1993). Instead, the formation of ikaite ($CaCO_3 \cdot 6H_2O$), a hydrated calcium carbonate mineral precipitating only at temperatures below 5°C, was observed at Laguna Potrok Aike during winter (Oehlerich et al., 2012). Thus, Laguna Potrok Aike is one of the very few sites in the world where lacustrine ikaite precipitates. After air exposure and/or rising temperature ikaite at Laguna Potrok Aike rapidly transforms to calcite powder. The abundantly present crystals of less than 10 µm in the profundal sediment cores from Laguna Potrok Aike are very likely the product of ikaite disintegration.

Acknowledgements

This study is supported by the International Continental Scientific Drilling Program (ICDP) in the framework of the "Potrok Aike Maar Lake Sediment Archive Drilling Project" (PASADO). Funding for drilling was provided by the ICDP, the German Science Foundation (DFG grants ZO-102/11-1,2), the Swiss National Funds (SNF), the Natural Sciences and Engineering Research Council of Canada (NSERC), the Swedish Vetenskapsradet (VR) and the University of Bremen. Funding by the DFG Priority Programme ICDP MA 4235/4-1 and MA 4235/4-2 is gratefully acknowledged.

For their invaluable help in field logistics we thank the staff of INTA Santa Cruz, the Moreteau family and the DOSECC drilling crew.

References:

Anselmetti, F.S., Ariztegui, D., De Batist, M., Gebhardt, A.C., Haberzettl, T., Niessen, F., Ohlendorf, C., Zolitschka, B. (2009). Environmental history of southern Patagonia unravelled by the seismic stratigraphy of Laguna Potrok Aike. Sedimentology 56: 873-892.

Bischoff, J.L., Stine, S., Rosenbauer, R.J., Fitzpatrick, J.A., Stafford Jr., T.W., 1993. Ikaite precipitation by mixing of shoreline springs and lake water, Mono Lake California, USA. Geochimica et Cosmochimica Acta 57, 3855-3865.

Haberzettl, T., Corbella, H., Fey, M., Janssen, S., Lu¨ cke, A., Mayr, A., Ohlendorf, C., Schabitz, F., Schleser, G.H., Wille, M., Wulf, S. and Zolitschka, B. (2007). Late Glacial and Holocene wet-dry cycles in southern Patagonia-Chronology, sedimentology and geochemistry of a lacustrine sediment record from Laguna Potrok Aike (Argentina). The Holocene 17, 297-310.

Hahn, A., P. Kliem, C. Ohlendorf, B. Zolitschka, P. Rosén and the PASADO science team (2012). Climate induced changes in the content of carbonaceous and organic matter of sediments from Laguna Potrok Aike (Argentina) during the past 50 ka inferred from infrared spectroscopy. Quaternary Science Reviews, submitted.

Kliem, P., D. Enters, A. Hahn, C. Ohlendorf, A. Lisé-Pronovost, G. St-Onge, S. Wastegård, B. Zolitschka and the PASADO science team (2012). Lithology, radiocarbon chronology and sedimentological interpretation of the lacustrine record from Laguna Potrok Aike, southern Patagonia. Quaternary Science Reviews, submitted.

Mayr, C., Wille, M., Haberzettl, T., Fey, M., Janssen, S., Lücke, A., Ohlendorf, C., Oliva, G., Schäbitz, F., Schleser, G.H. & Zolitschka, B. (2007). Holocene variability of the Southern Hemisphere westerlies in Argentinean Patagonia (52°S). Quaternary Science Reviews 26, 579-584.

Mayr, C., L cke, A., Maidana, N.I., Wille, M., Haberzettl, T., Corbella, H., Ohlendorf, C., Schäbitz, F., Fey, M., Janssen, S., Zolitschka, B. (2009). Isotopic fingerprints on lacustrine organic matter from Laguna Potrok Aike (southern Patagonia, Argentina) reflectenvironmental changes during the last 16,000 years. Journal of Paleolimnology 42, 81-416.

Oehlerich, M., Mayr, C.C., Griesshaber, E., L cke, A., Oeckler, O.M., Ohlendorf, C., Schmahl W.W. & Zolitschka, B. (2012). Ikaite precipitation in a lacustrine environment – implications for paleoclimatic studies using carbonates from Laguna Potrok Aike (Patagonia, Argentina). Quaternary Science Reviews, submitted.

Oehlerich, M., Mayr, C.C., L cke, A. and Wissel, H. (2012). Effect of CO_2 release from OM on carbonate stable isotope analyses. Rapid Communication in Mass Spectrometry, In preparation.

olitschka, B., Sch bitz, F., L cke, A., Corbella, H., Ercolano, B., Fey, M., Haberzettl, T., Janssen, S., Maidana, N., Mayr, C., Ohlendorf, M., Oliva, G., Paez, M.M., Schleser, G.H., Soto, J., Tiberi, P., Wille, M. (2006). Crater lakes of the Pali Aike Volcanic Field as key sites for paleoclimatic and paleoecological reconstructions in southern Patagonia, Argentinia. Journal of South American Earth Sciences 21, 294-309.

ICDP

Identification of eolian input at the Laguna Potrok Aike drill site, Patagonia PASADO-Eolian (Project bundle PASADO-support 3)

C.OHLENDORF[1], C.GEBHARDT[2] AND THE PASADO SCIENCE TEAM [3]

[1] Geopolar, Institute of Geography, University of Bremen, Germany (ohlen@uni-bremen.de)
[2] Alfred Wegener Institute for Polar and Marine Research, Bremerhaven, Germany
[3] PASADO Science Team as cited at: http://www.icdp-online.org/front_content.php?idcat=1494

In the past decades, there was an ongoing discussion about the impact of dust in the southern hemisphere. Detailed investigations of the Antarctic ice cores have resulted in several publications that deal with long-distance dust transport. Fingerprint analyses of the dust components revealed Southern South America (SSA) with its extended dry areas as the major source for dust in the higher latitudes of the southern hemisphere. Dust is mostly related to strength and direction of the wind systems and thus to paleoclimatic changes. SSA is mainly influenced by the Southern Hemisphere Westerlies (SHW) that shift in latitudinal position between glacial and interglacial times, thus influencing the amount of dust that is mobilized. Our study site Laguna Potrok Aike is a lake situated in the middle of the source area of dust and thus offers the unique opportunity to investigate a dust record that allows to better understand the migration of the SHW and the associated paleoclimatic changes. In this lake, a lacustrine deep drilling campaign (PASADO) was carried out in 2008 (Zolitschka et al. 2009). The cores recovered during the PASADO deep drilling hold a paleoclimatic record of the past ~51 ka. Magnetic susceptibility was used in marine cores to trace eolian input (e.g. Pugh et al. 2009). For Laguna Potrok Aike, the same approch was proposed (Haberzettl et al. 2008, 2009). However, this lake is situated in a large volcanic field, and grains carrying magnetic susceptibility presumeably are not exclusively of eolian origin. Hence, grains that are carriers of magnetic susceptibility do not necessarily have to travel long distance as with wind input, but could derive from the nearby hinterland and be transported e. g. by rivers. It is thus questionable whether magnetic susceptibility can be used without any constraint as a measure for eolian input in this terrestrial record. Studies on eolian material in Southern South America have shown that the chemical composition of these grains is quite distinct (e.g. Gaiero, 2007; Gaiero et al., 2004; Tripaldi et al., 2010).

Within the scope of the project PASADO-Eolian, we are thus attempting to characterize the specific fingerprint of eolian material in the lacustrine record in order to distinguish it from e.g. riverine material. Such a fingerprint however cannot be reduced to a single characteristic such as geochemical composition or magnetic susceptibility, but needs a combination of both, including also information on the respective grain size distribution and the grain surface morphology. In order to reach this goal, geochemical and sediment-physical analyses (including XRF/XRD analyses,

determination of grain size distribution, magnetic susceptibility measurements, and scanning electron microscope analyses) are applied on both, the whole sample and on grain-size-separated fractions of the samples.

In a first step, 76 samples representative of all different lithologies encountered in the sediment sequence were taken from the 106 m long PASADO Site 2 composite profile. On fresh samples, magnetic susceptibility was measured and the element composition was determined by XRF-scanning. After freeze drying, physical, chemical and mineralogical sediment properties were determined. Each sample was then separated into six grain size classes by sieve and sedimentation techniques, and the same parameters were determined for each fraction separately. Based on a cluster analysis of the collected data, samples for SEM analyses were selected. SEM techniques were then used to verify the eolian origin of grains. The aim of this approach is to isolate the fingerprint of the eolian sediment fraction in terms of their grain size, physical and chemical composition. A first evaluation of the dataset indicates that the magnetic susceptibility signal of the original bulk samples is not solely representing the grain size of the sediments as is often the case. For instance, samples with high sand percentages show average susceptibility values and low total Fe counts. However, considering only the silt fraction of these samples, high values of magnetic susceptibility and high Fe counts are observed. Hence, unmixing of the signal stored in the sedimentary record of Laguna Potrok Aike with statistical tools (multivariate statistics, mostly cluster and principle component analyses) is a necesseary step to characterize the eolian fraction. Once the eolian input is characterized, we will investigate the entire core record for the eolian fraction to get a high-resolution dust record for the Southern South American terrestrial realm for the past approximately 51 ka BP. This record can then be compared with marine records from the nearby South Atlantic, but also e.g. with IODP drill sites from the Chilean side of the Andes, i.e. from the Pacific, and with ice core records from Antarctica. All these archives record the dust transported from Patagonia and are thus perfect for studies of wind patterns and paleoclimate change in the higher latitudes of the southern hemisphere.

References:
Gaiero, D.M., 2007. Dust provenance in Antarctic ice during glacial periods: From where in South America? Geophys. Res. Lett., 34: L17707.
Gaiero, D. M., Depetris, P.J., Pobst, J.-L., Bidart, S. M., Leleyter, L., 2004. The signature of river- and wind-borne materials exported from Patagonia to the southern latitudes: a view from REEs and implications for paleoclimatic interpretations. Earth and Planetary Science Letters, 219:357-376
Haberzettl, T., B. Kück, S. Wulf, F. Anselmetti, D. Ariztegui, C. Corbella, M. Fey, S. Janssen, A. Lücke, C. Mayr, C. Ohlendorf, F. Schäbitz, G. Schleser, M. Wille, B. Zolitschka (2008). Hydrological variability and explosive volcanic activity in southeastern Patagonia during Oxygen Isotope Stage 3 and the Holocene inferred from lake sediments of Laguna Potrok Aike, Argentina. Palaeogeography, Palaeoclimatology, Palaeoecology, 259: 213-229.
Haberzettl, T., Anselmetti, F. S., Bowen, S. W., Fey, M., Mayr, C., Zolitschka, B., Ariztegui, D., Mauz, B., Ohlendorf, C., Kastner, S., Lücke, A., Schäbitz, F., Wille, M., 2009. Late Pleistocene dust deposition in the Patagonian steppe - extending and refining the paleoenvironmental and tephrochronological record from Laguna Potrok Aike back to 55 ka. Quaternary Science Reviews 28:2927-2939.
Pugh, R.S., McCave, I.N., Hillenbrand, C.D., Kuhn, G., 2009. Circum-Antarctic age modelling of Quaternary marine cores under the Antarctic circumpolar current: ice-core dust-magnetic correlation. Earth and Planetary Science Letters 284, 113–123.
Tripaldi, A., Ciccioli, P.L., Alonso, M.S. and Forman, S.L., 2010. Petrography and geochemistry of late Quaternary dune fields of western Argentina: Provenance of aeolian materials in southern South America. Aeolian Research, 2: 33-48.
Zolitschka, B., Anselmetti, F., Ariztegui, D., Corbella, H., Francus, P., Ohlendorf, C., Schäbitz, F. and the PASADO Scientific Drilling Team (2009). The Laguna Potrok Aike Scientific Drilling Project PASADO (ICDP Expedition 5022). Scientific Drilling 8: 29-33.

IODP

The Pliocene Closure of the Central American Seaway: reconstructing surface-, intermediate-, and deep-water connections.

A. OSBORNE[1], M. FRANK[1], R. TIEDEMANN[2] , R. STUMPF[1]

[1]GEOMAR | Helmholtz-Zentrum für Ozeanforschung Kiel, Wischhofstr. 1-3, 24148 Kiel
[2]AWI, Alfred-Wegener-Institut für Polar- und Meeresforschung, Am Alten Hafen 26, 27568 Bremerhaven.

The closure of the Central American Seaway and the associated reorganisation of deep-ocean circulation have been controversially reported as contributing to both a warming and a cooling of global climate. A resulting increase in moisture supply to the northern hemisphere may have been an important precondition for the inception of Northern Hemisphere Glaciation. A robust timeframe for the closure of this major ocean gateway is essential for understanding its direct and indirect effects on global climate. Here we use radiogenic isotopes of Nd and Pb to reconstruct the history of shallow, intermediate and deep water connections between the Caribbean Sea and the eastern Equatorial Pacific Ocean from 5.0 to 2.0 million years ago. Surface water exchange is characterised using the Nd isotope composition of planktonic foraminiferal calcite. The Nd and Pb isotope compositions of early diagenetic ferromanganese coatings of the same sediment samples are employed to determine intermediate and deep water exchange.

A core-top survey compares εNd in surface sediments from either side of the Isthmus of Panama and finds a difference of $\geq$ 5.5 epsilon units between the Pacific and Caribbean sites, consistent with published data from ferromanganese crusts (Reynolds et al. 1999, Frank et al. 1999, 2006). Our downcore results indicate that Caribbean Intermediate Water continued to diverge from a relatively constant Pacific deepwater Nd composition from 5.0 to 2.0 Ma. A more rapid restriction of mixing is inferred between 4 and 3.5 Ma, clearly preceeding a major increase in ice-rafted-debris north of Iceland (Jansen et al. 2000). Interpretations of the records benefit from the wealth of multiproxy data already published from Pacific ODP site 1241 and Caribbean sites 999 and 1000, e.g. Steph et al. 2006, Groeneveld et al. 2008.

References:
Frank et al. 1999, Geology 27, 1147-1150.
Frank et al. 2006, G^3 7, doi:10.1029/2005GC001140.
Groeneveld et al., 2008, G^3 9 Q01P23.
Jansen et al. 2000, Paleoceanography 15, 709-721.
Reynolds et al. 1999, EPSL 173, 381-396.
Steph et al., 2006, Paleoceanography 21 PA4221.

IODP

Reconstruction of oceanic calcium isotope variations during the late Paleogene

ST. PABICH[1], K. RABE[1], N. GUSSONE[1], B.M.A. TEICHERT[2]

[1] Westfälische Wilhelms-Universität Münster, Institut für Mineralogie, Münster, Germany
[2] Westfälische Wilhelms-Universität Münster, Institut für Geologie und Paläontologie, Münster, Germany

One important aim in earth science is, to understand and reconstruct the oceanic chemical and isotopic evolution over geologic time to gain a better understanding of earth's climate changes. One element that is especially important in this context is Ca. Its variations in concentration that have been observed over time are controlled by weathering, carbonate sedimentation and CO_2 concentration of the atmosphere. Imbalances in the input and output of Ca to the ocean will cause a shift in the Ca isotopic composition (Farkas et al. 2007). Therefore, the Ca isotopic composition of paleo-seawater, recorded in biominerals, is an ideal tool to study changes in the Ca budget of the ocean. During the Phanerozoic, significant variations in the isotopic composition of marine Ca have occurred (De La Rocha and DePaolo 2000; Farkas et al. 2007). Especially the Cenozoic is known as a time of extreme climates and rapid climate changes expressed in a rapidly shifting carbonate compensation depth (CCD) (Zachos et al. 2001).

The PEAT drilling program (Exp. 320 and 321) recovered a unique, well-preserved Cenozoic carbonate record (Pälike et al. 2010, Lyle et al. 2010) providing an excellent archive of extreme Cenozoic climate variability. The aim of this study is to use this record and establish a reliable, high resolution $\delta^{44/40}$Ca paleo-seawater record for the Late Paleogene between 45 Ma and 23 Ma and model changes in the Ca budget through time in response to major paleoceanographic fluctuations in the global carbonate cycle, as expressed in dramatic CCD fluctuations.

The sediment samples were first characterised in terms of their calcareous microfossil content, in order to select the most appropriate Ca isotope archive for our seawater reconstructions. Based on occurrence, isotope fractionation behaviour and preservation, we chose the benthic foraminifers Nuttalides spp., Gyroidinoides sp., Cibicidoides subhaidingerii, Cibicidoides mundulus and Cibicidoides grimsdalei from size-fraction >63µm for $\delta^{44/40}$Ca measurements. Foraminifer tests were hand-picked under the binocular and cleaned individually following the method described in Gussone and Filipsson (2010). An aliquot of each sample was mixed with a $^{42}Ca/^{43}Ca$ double-spike to correct isotope fractionation during measurements (Gussone et al. 2011) prior to the isotope analysis by thermal ionisation mass spectrometry.

Generally, our first results suggest considerable differences in the Ca isotope record of benthic foraminifers during the Eocene and the Oligocene. The different Ca isotope trends seem to be related to differences in the C-cycle, expressed in the carbonate preservation and CCD. While the Eocene sedimentation is characterised by a strong variability in CCD, leading to rapids changes in the carbonate content of the sediments and the occurrence of several carbonate accumulation events (CAE), the Oligocene sediments show uniformly high carbonate contents. The different $CaCO_3$ dynamic of the Eocene and Oligocene is also reflected in the Ca isotope ratios of benthic foraminifers, showing a constant long-term isotope value and excursions to higher values during phases of CCD highstand. This latter feature is interpreted according to Gussone and Filipsson (2010) as a reduction of Ca isotope fractionation at low carbonate saturation during formation of the foraminifer test. The Ca isotope values of the seawater were rather invariant. The long-term Ca budget seems hence to be rather little affected by the prominent CAEs. The Ca isotope ratios of the Oligocene record in contrast, indicates a slight increase in $\delta^{44/40}$Ca of the seawater by ~0.3‰ during the Oligocene, which is consistent with a continuous carbonate deposition and successive decrease in dissolved Ca in the ocean.

References:
De La Rocha C.L., DePaolo D.J. (2000) Isotopic evidence for variations in the marine calcium cycle over the Cenozoic. Science 289: 1176-1178
Farkas J., Böhm F., Wallmann K., Blenkinsop J., Eisenhauer A., van Geldern R., Munneke A., Voigt S., Veizer J. (2007) Calcium isotope record of Phanerozoic oceans: Implications for chemical evolution of seawater and its causative mechanisms. Geochimica et Cosmochimica Acta 71, 5117 – 5134
Gussone N. and Filipsson H.L. (2010) Calcium isotope ratios in calcitic tests of benthic Foraminifers. Earth and Planetary Science Letters 290, 108 - 117
Gussone, N., Nehrke, G. and Teichert, B.M.A. (2011) Calcium isotope fractionation in ikaite and vaterite. Chemical Geology 285, 194-202.
Lyle M., Pälike H., Nishi H., Raffi I., Gamage K., Klaus A. and the IODP Expeditions 320/321 Scientific Party (2010) The Pacific Equatorial Age Transect, IODP Expeditions 320 and 321: Building a 50-Million-Year-Long Environmental Record of the Equatorial Pacific Ocean. Scientific Drilling 9, 4 - 15
Pälike H., Lyle M., Nishi H., Raffi I., Gamage K., Klaus A. and the IODP Expeditions 320/321 Scientists (2010) Expedition 320/321 summary. Proc. IODP, 320/321: Tokyo (Integrated Ocean Drilling Program ManagementInternational, Inc.)
Zachos J., Pagani M., Sloan L., Thomas E., Billups K. (2001) Trends, Rhythms, and Aberrations in Global Climate 65 Ma to Present. Science 292: 686 - 693

IODP

Import, accumulation, and export of sediments into a shelf canyon: Insights from the head of the Swatch of No Ground offshore the Ganges-Brahmaputra Delta, (Bangladesh)

L. PALAMENGHI[2,*], V. SPIEß[1], T. SCHWENK1, H.-R. KUDRASS[3] , C. FRANCE-LANORD[4].

[1]Department of Geosciences, University of Bremen, Klagenfurter Str. 28359 Bremen, Germany.
[2] Bremen International Graduate School for Marine Sciences (GLOMAR), University of Bremen, Leobener Straße, 28359 Bremen, Germany
* contact:lupala@uni–bremen.de
[3] MARUM — Center for Marine Environmental Sciences, University of Bremen, Leobener Straße, 28359 Bremen, Germany
[4]CRPG, Centre de Recherches Pe´trologiques et Ge´ochimiques, 15 rue Notre Dame des Pauvres, 54501 Vandoeuvre le`s Nancy, France.

Transport and sedimentation processes at canyon heads are addressed as key determining factors for the architectural style of deposits accumulating in deepwater. Their understanding is crucial for the reconstruction of depositional history and tectonic and climatic forcing inherent to a continental margin and its terrestrial sediment source (Posamentier et al., 1991; Pirmez et al., 2000; Covoult and Graham, 2011). As part of our long term research strategy, we studied multiple facets of the world's largest source-to-sink system, which connects monsoon-

related precipitation and Himalayan erosion with river transport by Ganges, Brahmaputra and Meghna to the deposition in a terrestrial and a subaqueous delta, but also to the large Swatch of No Ground shelf canyon, which both bypasses and accumulates huge sediment volumes.

For deciphering terrestrial processes, sediment fluxes and climatic and tectonic controls by drilling in the Ganges-Brahmaputra depositional system, the acting processes must be identified to adequately utilize the sedimentary archive. As a follow-up of the pending ODP proposal 'Bengal Fan' for drilling a transect across the whole Bengal Fan at 8°N back to 10 million years in time, we initiated a research project closer to the sediment source on the slope and shelf of Bangladesh to get access to variations on shorter time scales, namely to decadal to centennial time scales for deposits on the shelf and within the canyon floor.

In this context, we believe that our recent findings on the interaction of the delta front with the Swatch of No Ground (SoNG) on the Bangladesh shelf can significantly help to understand the role of the main Quaternary head of the Bengal Fan channel levee complex and its depositioinal history. This study will focus on the upper SoNG in Bangladesh territorial waters, particularly on the establishment of the sediment transport pathway within the SoNG during a base level normal regression, the filling architecture and some insights on the filling style.

During the Holocene the subaqueous delta sigmoidal clinoform has prograded on the Bengal Shelf and consequently the sediments building the bottomset deposits were the first to deliver sediment into the canyon head. Three V-shaped channels serve as feeders to the canyon. These three channels meander in the foreset beds and become straight in the lower canyon head where the bottomset beds are nowadays downlapping from the rim onto the canyon thalweg. Around the water depth of 350 mbsl the three channels converge into a single channel. With increasing distance from the canyon head the channelized deposits significantly reduce their negative relief from 45-50 m to 5-10 m in the upper SoNG with respect to the surrounding thalweg .

The near surface stratigraphy of the channelized deposits consists of a stacked parallel to subparallel sequence of approximately 10 units. These stacked sequences are counted by the condensed section that separates them and the thickness of each individual unit ranges from a few to tens of meters. Their internal acoustic facies is persistently transparent. The seismic facies reveals amplitudes higher than in the side deposits, where facies is mostly chaotic with occasional internal reflections. Most of these homogenous units terminate where the thalweg slope angle decreases with exception of two thicker units, MTD-1 and MTD-2, which reach the southernmost part of surveyed area and seem to even continue further downslope.

On the flanks of the channelized deposits, the near surface deposits of the SoNG thalweg are unchannelized and densely stratified (Facies Ia, Kottke et al., 2003). Their averaged amplitude is significantly weaker. The unchannelized deposits were sampled by 4 cores of more than 10 m length. These cores consist of graded sand-silt-clay layers interpreted as tempestites which closely correlate with the historical record of cyclones of the northern Bay of Bengal (Kudrass et al., 1998; Michels et al., 2003).

The pattern of channelized deposits (high amplitude) versus unchannelized (weaker amplitude) extends down to a depth of 750-1000 mbsf and the base surface appears very smooth compared to the present day seafloor and the underlying unit shows a completely different signature.

The widespread occurrence of the two massive units, MTD-1 and MTD-2, may indicate the influence of earthquakes as a trigger. According to the average sedimentation rate of 20 cm/yr, derived for the upper 10 meters, these units were formed 170 years ago (MTD-1) and 320 years ago (MTD-2). The may correlate with two massive subduction earthquakes, which occurred in this time period in 1762 (Chittagong Earthquake, Magnitude 8.8) and in 1892 (Great India Earthquake, Magnitude 8.7).

Based on the conditions of net sediment deposition, it is concluded that the main filling architecture of the canyon may consist of unchannelized sheet flow tempestites (Straub et al., 2009) derived from diffusive dispersion processes from the bottomset. On the long term SoNG developement such deposits can be stratigraphically interpreted as internal levee (Kane et al., 2011). Intensified sediment flux during severe storms and large floods might have initiated repetitive channelized debris flows in the foreset bed region which, if sufficiently diluted, might become transitional toward turbidity currents and are therefore recorded as erosive event on the internal levee. The vertical succession of debrites forms a downslope sediment reservoir which will be possibly reworked when base level requires an adjustment toward a new equilibrium state. The MTD-1 and MTD-2 units might have been the result of an even more complex gravity flow, which may have been sufficient in volume to bypass sediment into the deep-sea: initially a liquefaction flow (in situ shock deformation) might have destabilized the slope depositing a seismite; with some time lag, a debris flow might have propagated downslope, also producing a turbidity current due to the shear on the front and at the upper surface.

Studying multiple cores from proximal to distal environments of the SoNG, it might be possible to evaluate the lower frequency gravity flow propagation in the channelized deposits with respect to the higher frequency ones recorded in the internal levee. As a future outlook, this approach may help to establish to what extent a deep-sea turbiditic system respond to processes taking place in the sedimentary prism itself (autocyclicity) and to processes mainly caused by variations external to the system (allocyclicity)

These preliminary results on the fill pattern and sediment volume found in the Swatch of No Ground indicate that these units represent a relatively short time period of rapid sediment accumulation, constructing semi-uniform packages from constant annual sedimentation intercalated by severe cyclones, extreme floods and earthquake-triggered massive units. At this stage we consider the SoNG as a suitable drilling target which provides a direct archive of terrestrial sediment fluxes and processes, which can be properly deciphered if the above described temporal and facies changes are considered.

References

Covoult, J.A., and Graham, S.A., 2011.Submarine fans at all sea level: Tectono-morphologic and climatic controls on the terrigenous sediment delivery to deep sea fan. Geology 38, 939-942

Kane, I.A., and Hodgson, D.M., al., 2011. Sedimentological criteria to differentiate submarine channel levee subenvironment: exhumed examples from the Rosario Fm. (Upper Cretaceous) of Baja California, Mexico, and Fort Brown Fm. (Permian), Karoo Basin, S. Africa. Mar. Petr. Geol. 28, 807-823.

Kottke, B., T. Schwenk, M. Breitzke, M. Wiedecke, H.R. Kudrass, and V. Spiess (2003) Acoustic Facies and Depositional Processes in the Upper Submarine Canyon Swatch of No Ground (Bay of Bengal). Deep-Sea Research II, 50, 979-1001. Pirmez et al., 2000;

Kudrass, H.R., Michels, K.H., Wiedicke, M., Suckow, A., 1998. Cyclones and tides as feeders of a submarine canyon off Bangladesh. Geology 26, 715–718.

Michels, K.H., Suckow, A., Breitzke, M., Kudrass, H.R., Kottke, B., (2003). Sediment transport in the shelf canyon ''Swatch of No Ground'' (Bay of Bengal). Deep-Sea Research II 50, 1003–1022.

Posamentier, H.W., Erskine, R.D., Mitchum, Jr., 1991. Models for submarine deposition within a sequence-staratigraphic framework. In: Weimer, P., and Links, M.H., (Eds) Seismic Facies and sedimentary processes of submarine fans and turbidite systems. Springer Verlag, 127-136.

Straub K.M., and Mohring, D., 2009. Constructional canyons built by sheet-like turbidity currents: observations from offshore Brunei Darussalam. J.S.R. 79, 24-39.

ICDP

Long continental pollen record of the last ca. 500 ka in eastern Anatolia – First palynological results from Lake Van cores obtained in 2010

NADINE PICKARSKI [1], *, GEORG HEUMANN [1], THOMAS LITT [1]

[1] University of Bonn, Steinmann Institute for Geology, Paleontology and Mineralogy, Nussallee 8, D-53115 Bonn, Germany

Lake Van is located in a climatically sensitive semiarid and tectonically active region in Eastern Anatolia, Turkey. It is a key site to reconstruct terrestrial paleoecology and paleoclimate in the Near East during the Quaternary. Lake Van is the largest soda lake (surface area 3.570 km²) and the fourth largest terminal lake in the world (volume 607 km3). The maximum water depth is 460 m and the maximum length is 130 km WSW-ENE. The present lake level is at an elevation of 1,646 m above mean sea level. The northern and eastern part of Lake Van is mainly characterized by steppe vegetation related to the so-called Irano-Turanian plant geographical territory. In contrast, some remnants of deciduous oak forests can be observed mainly in the Bitlis Massive, SW of the lake. We present preliminary palynological results of a long continental sedimentary record obtained during a coring campaign supported by the International Continental Scientific Drilling Program (ICDP) in summer 2010. The composite profile from the Ahlat Ridge, the most important site for paleoclimatological studies (total length of ca. 218 m), yields a continuous paleoclimate archive encompassing ca. 500.000 years. The record is partly characterized by annually laminated sediments. By using pollen analysis, several glacial and interglacial/ interstadial periods can be observed. The warm stages can be identified based on higher amounts of pollen from thermophilous trees such as deciduous oak. In addition to the current interglacial stage (MIS 1), pronounced warm phases coincide with past interglacials probably correlative to MIS 5, 7, 9 and 11 or 13. Cold stages are characterized by pollen types related to steppe plants such as Artemisia, chenopods and grasses. The glacial-interglacial cycles as reflected in the palynological data are in broad agreement with those of stable oxygen isotope analyses based on autigenic carbonate of the lacustrine sediments (bulk). Caused by the state of the art, more detailed information will be given to the last 130,000 years.

IODP

Fluid entrapment and release from sediments intruded by volcanic sills, Newfoundland Margin

T. PLETSCH[1], J. KUS[1], R. PETSCHICK[2]

[1]Federal Institute for Geosciences and Natural Resources (BGR), Stilleweg 2, 30655 Hannover, Germany, thomas.pletsch@bgr.de

[2]Institute of Geoscience, Goethe-Universität Frankfurt, Altenhöferallee 1, 60438 Frankfurt/M, Germany, petschick@em.uni-frankfurt.de

Ocean Drilling Program Hole 1276A, at the toe of the SE facing Newfoundland Margin, provided access to more than 600 m of mid-Cretaceous, deep-marine, organic-rich mudstones with two intercalated volcanic sills near the base of the hole. A 10 m basaltic sill, dated as 105 Ma, was recovered at 1612 m below seafloor. Another sill, at least 17 m thick and recovered some 100 m deeper in the section, is 8 M.y. younger than the upper sill. Undercompacted, plastic, high-porosity sediments recovered from between the two sills yielded elevated concentrations of gaseous hydrocarbons.

Metamorphic minerals and textures characterise the narrow contact zones between sills and host sediment. Further away from the narrow metamorphic contact zones, the thermal aureole of the sills is recorded by unusual gradients in the alteration of organic and mineral components. In the poorly compacted, gas-bearing interval, however, organic maturity indicators reach a minimum where clay mineral assemblages indicate substantial alteration This discrepancy may be related to the unusually elevated porosity: Whereas overlying sediment was compacted to a porosity around 20%, porosity values up to 44% were retained in the gas-bearing interval. Pore-water overpressure may have delayed the maturation of organic matter whereas mineral transformation was probably favoured by ion supply from alteration near the underlying sill through the open pore framework.

Elevated concentrations of gaseous hydrocarbons were likely generated at the lower sill contact or in the underlying sedimentary section. Numerical simulation suggests that pore pressure build-up beneath the upper sill is strong enough to overcome its tensile strength. Mineralised veins within the metamorphic contact zone are thought to have precipitated from fluids that escaped from the compartment between the sills when pressure exceeded the strength of the overlying seal.

The intercalation of undercompacted sediments with sills creates a high-amplitude seismic reflector that covers much of the proximal Newfoundland Basin. We expect that sills and adjacent, normally compacted shales, created extensive, vertically stacked fluid barriers. Where pressure build-up was sufficient, fracturing of the sills allowed for intermittent fluid release, wheras other sills may remain unbreached.

IODP

The impact of water mass interfaces on sedimentary processes at continental slopes - A comparison of the Argentine Margin and the IODP Leg 339 contourite study area in the Gulf of Cadiz

B. PREU[1], F.J. HERNÁNDEZ-MOLINA[2], T. SCHWENK[1], R. VIOLANTE[3], M. PATERLINI[4], A. PIOLA[3], S. KRASTEL[4] AND V. SPIEß[1]

[1] MARUM – Center for Marine Environmental Sciences, University of Bremen, D-28359 Bremen, Germany
[2] Facultad de Ciencias de Mar, Univerisdad de Vigo, Vigo, Spain
[3] Servicio de Hidrografia Naval (SHN), Buenos Aires, Argentina
[4] GEOMAR | Helmholtz Centre for Ocean Research Kiel, Germany

The influence of along-slope transport processes on continental slope architecture, sedimentary deposits and therefore on paleoclimatic and paleoceanographic archives were described in several regions of the world's ocean. While in early studies only the deposits, called contourites, were described and analyzed, modern approaches consider both depositional and erosive features, which together form so-called Contourite Depositional Systems (CDS).

Based on a morphosedimentary analysis, combining morphological observations with sedimentary patterns, structures, depocenters and processes, it can be demonstrated that the architecture of complete margin segments is dominated by bottom current influence rather than by classical margin-shaping (predominantly downslope) processes. As a consequence, an intimate relationship exists between sedimentation and structures and processes in the water column as the distribution of water masses, current velocities, turbulent energy at water mass boundaries, internal waves, suspension load etc..

As part of a long-term research strategy we have chosen the continental margin offshore Argentine and Uruguay to study this relationship, as the margin is known to be influenced by Antarctic Bottom Water, North Atlantic Deep Water and northward and southward flowing surface currents, which have left a peculiar margin architecture. This became evident during a pre-site survey for the IODP proposal 'Malvinas Confluence' (R/V Meteor Cruise M49/2, 2001), where appropriate sites were difficult to find due to widespread erosion, alternating with contouritic sediment bodies. Subsequent refinement of the database with another R/V Meteor Cruise (M78/3, 2009) led to the development of an evolutionary concept for the continental margin of the Rio de la Plata River, which may be even generally applicable to other current-dominated continental margins.

To further refine and validate the concept, an ideal continuation of this research would include the ongoing drilling activities in the Gulf of Cadiz contourite study area during IODP Leg 339. Here a similar data set of subsurface multichannel and echosounder data can be compared with newly acquired hydroacoustic water column information, which may create the linkage between transport mechanisms for particles and accomodation space availability in a dynamic current-controlled depositional system.Argentine Margin

The morphosedimentary analysis of the northern Argentine margin based on seismoacoustic and hydroacoustic data has revealed the presence of a major CDS and evidence for erosive and depositional features as well as mass transport deposits of high lateral variability. Three major terraces were identified located in 500-600 m (La Plata Terrace), 1100-1300 m (Ewing Terrace) and 3500 m (Necochea Terrace) water depth, respectively. At least the shallowest two are connected upslope to particularly steep erosional slopes. In 2000-2900 m water depth, the influence of downslope processes can be identified based on their hummocky surface and their chaotic seismic expression.

The margin shape including erosive and depositional features changes distinctly in the center of the study area close to the Mar del Plata Submarine Canyon. While the La Plata Terrace narrows from south to north, the Ewing Terrace widens. Seaward, gravitational deposits in the northern part of the study area show slope parallel incisions identified as current induced furrows.

Correlation of the morpho-sedimentary features with the surrounding oceanographic regime revealed a clear relation between the terraces and the water masses. The location and evolution of terraces along the Argentine margin can be related to distinct water mass interfaces. While the La Plata Terrace correlates to the Brazil Current (BC)/Antarctic Intermediate Water (AAIW) interface, the Ewing Terrace is located at the AAIW/Upper Circumpolar Deep Water (UCDW) transition. The Necochea Terrace is probably located at the LCDW/Antarctic Bottom Water (AABW) interface during glacial times.

The presence of these terraces along water mass interfaces suggests turbulent energy associated to these zones as initial mechanism for terrace formation. These erosive processes might be enhanced due to processes related to internal wave generation. Once the first smaller incision is carved into the margin, locally the currents will be enforced along the steeper segments of the slope. In contrast, calmer, tabular conditions will dominate along the terraces. The combination of both flow patterns results in a cutting-back of the margin and therefore in a widening of the terrace over time. Through time the terrace may reach a size, when the seaward boundary of the terrace is distal to the high velocity pattern focused along the steeper parts of the slope. This will result in the formation of contourite drifts.

Drift formation on the Ewing Terrace goes along as well with a decrease in suspended particle concentration in the water column. While the fast flowing AAIW due to its large transport capacity carries vast amounts of particles, the UCDW is characterized by low particle concentrations, which indicates a fallout of particles in this water level and the formation of contourites. This correlation can be shown by point measurements in turbidity using an optical nephelometer or by 18 kHz parametric echosounder data, which clearly indicate a decrease in particle concentrations from 1000 m water depth towards greater depth

Gulf of Cadiz

Most recently, IODP leg 339 drilled the sedimentary deposits of the Gulf of Cadiz CDS, which is located within the Mediterranean Outflow Water (MOW). Comparable to the Argentine margin, this CDS is as well characterized by the presence major contourites terraces. Hydrographic and hydroacoustic data sets imaging nepheloid layers within the water column reveal that these terraces are located in close proximity to the interface between the upper and lower branch of the MOW. Consequently, the sedimentary processes controlling drift formation in the Gulf of Cadiz

might be as well susceptible to the variations in the oceanographic setting not only induced by varying flow velocities but as well by vertical migration of the interface between the MOW's upper and lower core. Future analysis of 18 kHz parametric echosounder data might reveal a potential relationship between unequal sediment transport capacity of the upper and lower branch of the MOW and therefore, allow to decipher their different impact on sedimentary processes in the Gulf of Cadiz, in particular in the area of the newly drilled IODP boreholes U1388 through U1390.

IODP

Reconstruction of the onset and development of the Agulhas Current from contourite deposits at a proposed SAFARI drill site in front of Limpopo River, Mozambique margin

B. PREU[1], S. WENAU[1], V. SPIEß[1], T. SCHWENK[1], R. SCHNEIDER[2]

[1]Department of Geosciences, University of Bremen, D-28359 Bremen, Germany
[2]Institute for Geosciences, Christian-Albrechts-Universität zu Kiel, D-24118 Kiel, Germany

The Indian Ocean and its western boundary currents play a key role in the global redistribution of mass, heat, freshwater and other properties. Especially the Agulhas Current (AC), which is one of the strongest surface currents of the modern ocean, forms a major inter-ocean exchange system by linking the Indian and Atlantic Ocean. The main focus of this study is the analysis of sediment deposits formed under the influence of the Mozambique Current (MC), which represents one of the main water sources for the AC. Multichannel seismic data, which were collected on the shelf in front and southeast of the Limpopo River mouth during R/V Meteor Cruises M63/1 (2005) and M75/3 (2008), image the internal geometry of the shelf area and the Inharrime Terrace located in water depths between 150 and 500 m. In this region the MC and the East Madagascar Current (EMC) merge forming the AC, which is mainly characterized by deep reaching eddies delivered by the MC and EMC (Lutjeharms, 2006).

In the course of the SAFARI IODP drilling proposal, a detailed study of the depositional system related to the Limpopo River was carried out to identify suitable drill sites in the region. This included the vicinity of the river mouth, transport processes on the shelf, the role of the stationary Delagoa Bight eddy and the contourite-type of deposition on the Inharrime Terrace. It turned out to be essentail to gain a sufficient understanding of lateral transport processes driven by shelf currents, by small-scale and large-scale eddy circulation and by the Agulhas current, which both drives and interacts with the other currents. While a depocenter in front of the Limpopo river was lacking both at the cost and on the slope, terrestrial material nowadays seems to be incorporated into the contourites.

Based on the analysis of the regional seismic and echosounder data set, several contouritic units could be identified on the Inharrime Terrace. It revealed the presence of four major seismic units bounded by regional discontininuities (Preu et al., 2011), which control the slope architecture at the proposed drilling sites LIM-01 and LIM-02. The presence of these major discontinuities allow correlations with previously published regional stratigraphic models based on borehole and seismic data (Dingle et al., 1978; Martin et al., 1982), and conseqeuently to allocate ages to each seismic unit.

Seismic Unit 1 (Fig. 1) with a thickness of ~500 ms TWT is located ~1000 ms TWT under the crest of the Inharrime Terrace. This sedimentary unit was deposited between the late Cretaceous and the Oligocene/Early Miocene. The overall sediment accumulation pattern indicates hemipelagic sedimentation on top of basement irregularities with sediment thickness increasing landwards. Thus, the unit appears to represent a period of absent or low contour current activity.

On top of Seismic Unit 1, three major drift sequences can be identified. The deepest drift (Seismic Unit 2, Fig. 1) shows a mounded morphology with a maximum thickness of ~350 ms TWT and is interpreted as a plastered drift formed between the Late Oligocene and the Middle Miocene (~ 16.5 Ma). Subsequently, a major depocenter shift is detectable towards the northeast of the study area forming a new drift with ~500 ms TWT thickness, representing another large change in the local hydrodynamic regime (Seismic Unit 3, Fig.1). The Early-Middle Miocene initiation of drift accumulations is considered to mark the onset or intensification of the MC, which correlates with results from the Zambezi River delta reconstruction (Walford et al., 2005). The shifting of sediment depocenter towards the northeast is related to the onset of the modern lee eddy system at the Inharrime Terrace. This lee eddy results in a coast-parallel counter current, which transports sediments shelf-parallel eastward along the coast (Flemming, 1981). The influence on sedimentary processes becomes evident from multichannel seismic, high frequency echosounder and multibeam data documenting the shelf architecture and modern sediment dispersal on the shelf. The shelf architecture is dominated by prominent unconformities which show the influence of strong currents acting on the shelf. These currents may be

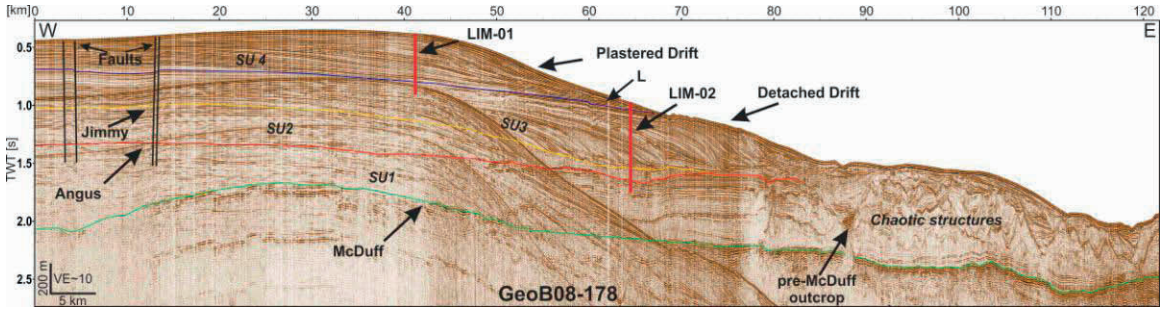

Figure 1: Seismic profile GeoB08-178 is an example of the internal geometry of the central part of the Inharrime Terrace

related to the AC lee eddy affecting the area. Modern sediment dispersal from the Limpopo River mouth is affected by this eastward-directed coast-parallel current as well as remnant coastal dunes formed during the last interglacial. These remnant ridges hamper sediment transport to the outer shelf and promote eastward current-induced transport. Similar remnant dune generations may have been present on the shelf during earlier glacial cycles, affecting sediment transport in a similar way as today. Sediment from the Limpopo River mouth may thus be transported eastwards towards the Inharrime Terrace and may account for a terrigenous fraction incorporated into the drift bodies.

Seismic Unit 4 with a maximum thickness of ~500 ms TWT forms the modern seafloor morphology with a crest-like feature striking NE-SW along the central part of the Inharrime Terrace (Fig.1). This plastered drift represents the modern conditions in the transition between MC and AC. It is concluded that this sedimentary complex is formed mainly under the influence of upwelling of Antarctic Intermediate Water (Martin et al. 1982) resulting from the interaction of the semi-stationary lee eddy system and the slope morphology in the study area (Lutjeharms and Da Silva, 1988).

As shown above, the deposits of the Inharrime Terrace encompass a terrestrial component, originating from the Limpopo River, and a marine fraction, which is related to the upwelling of Antacrtic Intermediate Water. The overall shape of the terrace and its depocenters are controlled by the flow intensity of the MC. Consequently, the sedimentary sequences of the Inharrime Terrace form an excellent archive to study both, the climatic variations in the hinterland and the evolution of the MC as a major source of the AC.

References:

Dingle, R. V. et al. (1978): Bathymetry and stratigraphy of the northern Natal Valley (SW Indian Ocean): A preliminary account. Marine Geology, 28: 89-106.

Flemming, B. W. (1981): Factors controlling shelf sediment dispersal along the southeast African continental margin. Marine Geology, 42: 259-277.

Lutjeharms, J. R. E. and Da Silva, A. J. (1988): The Delagoa Bight eddy. Deep Sea Research Part A., Oceanographic Research Papers, 35: 619-634.

Martin, A. K. (1981): The influence of the Agulhas Current on the physiographic development of the northernmost Natal Valley (S.W. Indian Ocean). Marine Geology, 39: 259-276.

Preu et al. (2011): Evidence for current-controlled sedimentation along the southern Mozambique continental margin since Early Miocene times. Geo-Marine Letters, 31 (5-6): 427-435.

Walford, H. L. et al. (2005): Solid sediment load history of the Zambezi Delta. Earth and Planetary Science Letters, 238: 49-63.

IODP

Viral impact on microbiology and geochemistry of extremely nutrient-depleted sediments

F. PREUSS, T. ENGELHARDT, H. CYPIONKA, B. ENGELEN

Institut für Chemie und Biologie des Meeres, Carl-von-Ossietzky Universität Oldenburg,
Carl-von-Ossietzky Straße 9-11, D-26111 Oldenburg, Germany,
http://www.pmbio.icbm.de

Microbiological and molecular analysis of the marine deep-subsurface has opened a new window to microbial ecology and biogeochemistry. However, the deep subseafloor biosphere remains among the least-understood habitats on Earth. Despite recent advances to describe general patterns in the diversity and distribution of functional and taxonomic groups, the extent and character of subsurface life throughout most parts of the oceans remains unknown. The absence of knowledge is largely due to ignorance of subseafloor life in the major ocean gyres.

Mid-ocean gyres represent the most oligotrophic marine ecosystems comprising about 48% of the world´s oceans. An extremely low primary productivity leads to rather low cell numbers and diminished microbial activities within the water column and the sediments below. While sub-seafloor life has mostly been studied at continental margins, mid-ocean gyres are unexplored, so far. The largest of these oceanic provinces, the South Pacific Gyre, was now investigated during IODP Exp. 329. The assessement of microbial abundances, diversity and activities will lead to a more comprehensive picture of the global deep-subseafloor biosphere.

In this project, we will identify if viral lysis could provide labile organic compounds to this extremely nutrient-depleted ecosystem and if viruses might be the main controling factor for the abundance and diversity of indigenous microorganisms. Therefore, we will isolate subseafloor microorganisms and identify the prophages within their genome. The morphological and phylogenetic diversity of these phages will be analysed in detail. Viral counts will be determined to calculate a global distribution within the subsurface. In comparison to our previous studies on benthic viruses from continental margin sites (Engelhardt et al., 2011), we will obtain more realistic estimates for the viral loop as a factor for sustaining the deep biosphere.

The overall goal of the project is to understand the role of phages for biogeochemical cycling, microbial abundance and diversity in sediments of the extremely nutrient-depleted mid-ocean gyres. The viral abundance will be determined and compared to previously investigated ocean margin sites. It will be tested if cell lysis might support microbial life in providing nutrients for indigenous microorganisms.

The following questions will be addressed:

What are the viral numbers in the sediments of the South Pacific Gyre? Will we find a different ratio of cell numbers vs. viral counts in comparison to the relatively nutrient-rich ocean margin sites? Is the analysis of viruses a reliable tool as an indirect indicator for subseafloor life?

Do isolates obtained from these sediments contain prophages within their genome? When host cells are under severe starvation, is the percentage of infected cells different to those isolated from “high activity sites”

What is the effect of the viral shunt on these nutrient-limited sediments? Is the lytic activity affected by these extreme environmental conditions. Can viral lysis provide essential nutrients for deep subsurface populations?

The integration of the viral component into the biogeochemical model for subsurface sediments of the South Pacific Gyre is important to understand the recycling of labile organic matter within this habitat. The fact that the number of viruses exceeds the number of prokaryotic cells by more than one order of magnitude might be advantageous on the microbial description of sediment layers in which the cell numbers are below the detection limit.

References:
Engelhardt T, Sahlberg M, Cypionka H, Engelen B (2011) Induction of prophages from deep-subseafloor bacteria. Environm Microbiol Rep 3:459–465

IODP

Intermediate water mass history at a cold-water coral habitat in the North Atlantic: Geochemical signals from IODP Site 1317

J. RADDATZ[1], M. FRANK[1], V. LIEBETRAU[1] AND W-CHR. DULLO[1]

[1] GEOMAR | Helmholtz-Zentrum für Ozeanforschung Kiel, Wischhofstr. 1-3, 24148 Kiel, Germany

The Integrated Ocean Drilling Program (IODP) Expedition 307 sailed in 2005 in order to drill, for the first time, the entire sediment body of a huge cold-water coral carbonate mound in the Porcupine Seabight, NE Atlantic. In general, cold-water corals and hence carbonate mound initiation and development in the Porcupine Seabight was most likely dependent on changes in the interaction between intermediate water masses, such as the Mediterranean Outflow Water (MOW) and the Eastern North Atlantic Water (ENAW, Raddatz et al. 2011)

The main aim of this research project is the reconstruction of the inflowing intermediate water masses (MOW, ENAW). For this purpose we propose to use the neodymium isotope composition of past water masses extracted from samples of cold-water coral Lophelia pertusa recovered from IODP Site 1317. These investigations will improve our understanding of the role and trigger mechanisms of intermediate water mass dynamics, circulation, and potential admixture (MOW, Bay of Biscay) in relation to the colonization of cold-water corals in the Porcupine Seabight around 3 Ma ago, as well as during the Pleistocene and Holocene when further carbonate mounds developed.

Four major questions of this study are: Was mound initiation and subsequent development controlled by the reintroduction of MOW? Have the different stages of mound growth been affected by variations in strength and flow path of intermediate water masses and or/vertical displacements of MOW? How has MOW interacted with the ENAW? Have both water masses been present at the site of coral growth throughout the time of mound growth or have there been shifts in their relative proportions? Finally this study will provide new insights into the long-term control mechanisms of cold-water coral carbonate mound growth in the entire North Atlantic.

Raddatz, J., Rüggeberg, A., Margreth, S. und Dullo, W- Chr. and the IODP Expedition 307 Scientific Party, 2011. *Paleoenvironmental reconstruction of Challenger Mound initiation in the Porcupine Seabight, NE Atlantic* Marine Geology, 282. pp. 79-90. DOI 10.1016/j.margeo.2010.10.019.

ICDP

The El´gygytgyn Impact structure-Expedition to the crater and stratigraphy of the impactites at the ICDP-drillcore

U. RASCHKE, W. U. REIMOLD, R. T. SCHMITT AND P. ZAAG

Museum für Naturkunde – Leibniz Institute at Humboldt University Berlin, Invalidenstr. 43, D-10115 Berlin, Germany (ulli.raschke@mfn-berlin.de)

Introduction: El´gygytgyn (67°30'N and 17°05'E), a 3.6 Ma [1], 18-km-diameter crater, is located in the Late Mesozoic Ochotsk-Chukotsky Volcanic Belt of Northeast Siberia. The complex crater was formed in a 86-89 Ma [2-5] old siliceous volcanic target [6,7]. In 2009 a ~ 500 m long drill core was drilled by ICDP at Lake El'gygytgyn. The project had two main purposes: to investigate the sedimentary crater fill for information about the paleoclimatic record for the high Arctic latitudes and to investigate the effects of the impact event on the felsic volcanic target [8]. The El'gygytgyn crater is one of only three known terrestrial impact structures in volcanic areas. We curated the 200 m long impactite section of the El'gygytgyn drill core D1c at the Museum f r Naturkunde, Berlin. After that we began detailed petrographic and geochemical analyses of the impactites. For a better understanding of the drill core impactite rocks we have to compare this material with information from the literature

Figure 1:Stratigraphic coloum of the drilled impact rocks

are limited; only a small record of the regional country rocks exists in collections and only a part of the crater rim is documented in literature. In mid-2011 a joint expedition from several different institutes (Alfred-Wegener-Institute, Potsdam; Arctic and Antartic Research Institute, St. Petersburg, University of Cologne, Museum für Naturkunde, Berlin) visited the impact structure. This gave us the unique opportunity to investigate the geology of the eastern half of the crater rim in order to complete the

geological map of the crater structure and to obtain samples from traverses in this area.

Methods: By now we have studied some 140 polished thin sections of core samples and a further 35 from country rocks (collections of the MfN and a handful from the 2011 crater expedition). Optical microscopy was used for lithological classification and first shock deformation analysis. We have also carried out XRF-analyses. These

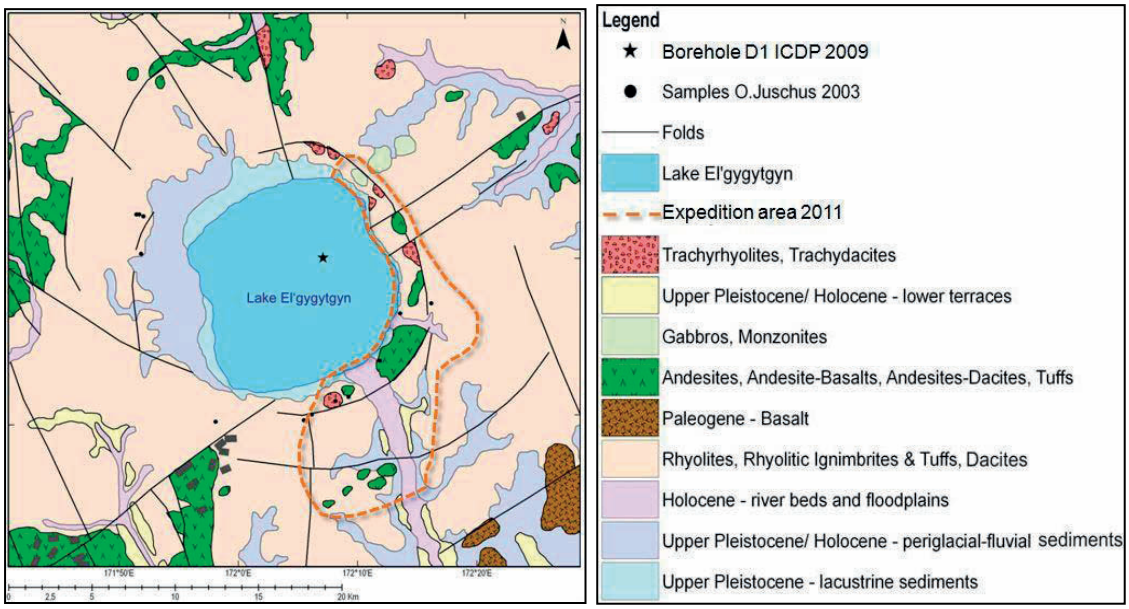

Figure 2: Geological map of the El´gygytgyn-crater

Figure 3,4: Blocks of impact melt breccia with “schlieren”

Figure 5: reddish tuffite, fine-grained with lamination

Figure 6: coarse-grained deposits

enable us to measure bulk-and trace elements of 150 samples, 115 among them from the drill core. Here we distinguished between clasts and matrix of the impact rocks. Furthermore we plan to use the EMPA and REM for the determination of the melt content and composition and to study the alteration minerals.

Drill core stratigraphy: The 200 m sequence of impact rocks in the El'gygytgyn drill core D1c can be divided into four main lithologies (see fig.1). The uppermost layer (316-328 m) is formed of reworked suevite, a mixture of sediments (clay to sand) and polymict impact breccia with clasts, which belong to the different target lithologies. They often show strong shock metamorphism (esp. pumice-like texture). The underlying unit is the suevite (329-390 m). This polymict impact breccia contains impact melt particles and is therefore classified as a suevite. Other shock features comprise diaplectic glass (often surrounded by melt) and shocked minerals. Additionally we found within this unit four shatter cones. Clasts and matrix grain sizes range from silt to stone (>0,002 mm to 20 cm). The identified clast lithologies comprises a wide range of volcanic rocks, some of which resemble the lithology of the bedrock sequence. At 333 and 383 m we found some ca. 3 m thick subunits which represent incorporated blocks of volcanic rocks. Our guess is that the upper block could be a part of the upper bedrock sequence. The lower block appears to belong to the greenish brecciated bedrock from the lowermost part of the bedrocks. The bedrock sequence could be distinguished in an upper unit (390 – 422 m) and a lower unit from 422 to 517 m (end of the bore hole). The upper bedrock unit is strongly altered ranging in color from dark grey to dark green and contain some veins of white to reddish calcite. The altered volcanic rock shows a fluidal texture and contains phenocrysts of feldspar, quartz and the mafic minerals biotite and amphibole. Shocked minerals are very rare. The lower bedrock unit is of rhyodacitic chemical composition. Volcanic melt particles (up to 1 cm in width and 2 to 6 cm long) occur frequently and contain fine-grained phenocrysts embedded in a brownish glassy matrix. These particles are depleted pumice fragments. This unit was named therefore "well welded ignimbrite". Beside this, phenocrysts of plagioclase, alkali feldspar, quartz, biotite and amphibole were observed, and the fine-grained groundmass is composed of the same minerals. The shock metamorphic overprint of this unit is weak (< 10 GPa). Nevertheless, the whole unit is brecciated and fractured, with a common abundance in the upper part and less to the end of the unit. These fractures are orientated with an angle of 30-45° in the upper part and increasing to ~ 75° in the lower part. Hydrothermal alteration occurred along the whole length of this unit, but is less intense than in the upper bedrock unit. Fractures are filled sometimes with zeolites and calcites. At 471 m we found a vein (~ 70 cm) of polymict reddish breccias with greenish to blackish clasts in cm-size. Within this vein shock features (PF and PDF) occur.

Expedition to the crater: In preparation for the expedition we wrote a proposal to the DFG - SPP 1006 (Re 528-12/1) to obtain financial support for this trip and the analyses of the samples. We started on the 13th of July 2011 and arrived on the 18th of August 2011. After a more or less problematic arrival at the crater lake we spent 26 days in the field. Our activities were strongly limited by the weather conditions which included a snowstorm at the beginning of August. Beside this, the overwhelming part of the widely, deeply eroded (denudation) landscape is covered with low bushes and grasses. Only a few places with higher morphological gradients allowed us to study the rocks. Here it was shown that the rocks are strongly weathered by the arctic frost blasting. Nevertheless, we worked at 45 outcrops from the NE-part to the SE-part of the crater rim. Additionally, we made a special short trip downstream along the Emnyvaam-river to collect samples outside the crater rim.

Preliminary results of the expedition: At this time we can give only a short summary of the results of the petrographic and geochemical analyses; the main sample suite of the expedition arrived in Berlin in Mid-January 2012. The available samples from the crater region show that the rocks of the crater rim are generally not strongly shock metamorphosed. However we did find some rocks resembling impact melt rocks occurring in large blocks (~ 1.5 m in diameter) on the eastern shore of the lake (see fig.3,4). Beside this we discovered an entirely unknown outcrop on the southern edge of the crater rim. At this place occur different suites of phreatomagmatic rocks. On top there are fine-grained reddish tuffs (see fig.5), below that occur a suite of coarse-graind, grey deposits (see fig.6).These volcanic target rock types have never been documented before.

During the first analysis of these new lithologies we did not found evidence of shock effects. Nevertheless, the collected sample suite on this expedition increases significantly the available range of target rocks for further investigations (see fig.7).

Outlook: The petrographic and geochemical analysis

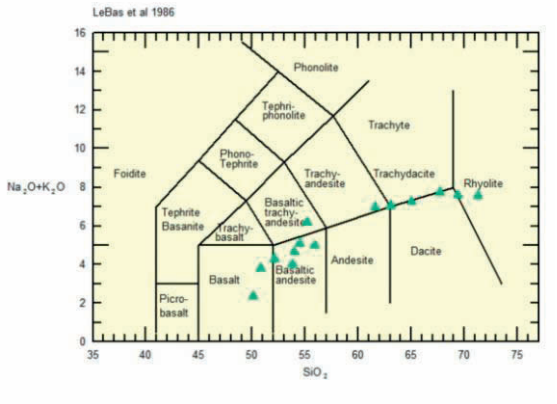

Figure 7: XRF bulk rock analysis of first specimens => the same trend as for the drill core samples

of the whole sample suite of the samples is still in progress. Together with our study of the drilled rocks, these will enable us to acquire a profound knowledge of the regional target rocks and of the rocks which were metamorphosed by the impact. Furthermore, we will be able to refresh the original Russian geological map of 1975. We will also carry out about PGE-analyses to determine the projectile components from samples of impact-melt-breccia. Beside this, we have collected oriented samples for paleomagnetic analysis (collaboration with KIT). Additionally, we have measured the magnetic susceptibility of the country rocks in the field.

Acknowledgements: Both projects are funded by DFG (expedition grant RE 528/12-1, drill core project grant RE 528/10-1). G. Schwamborn (AWI) and G. Federov (AARI) are thanked for support during the expedition. Drilling and logistics were supported by ICDP, the US National Science Foundation, the German Ministry of Research and Education, the Russian Academy of Sciences, and the Austrian Ministry for Science and Research.

References:
[1] Layer, P. (2000) Meteoritics & Planet. Sci, v. 35, p. 591–599;
[2] Beliy, V.F. (1969) Nauk. Dumka Press 138 p;
[3] Beliy, V.F. (1982) Tichookean. Geol., no. 5, p. 85–92;
[4] Feldman,V.I. et al., (1981), Marak., A.A., ed., Impactites: Moscow St. Univ. Press, p. 70–92
[5] Ispolatov,V.O. et al., (2004), The Journal of Geol., 2004, volume 112, p. 369–377;
[6] Gurov, E.P. et al., (1979), LPS X, p. 479–481;
[7] Gurov, E.P. & Gurova, E.P. (1991), Nauk. Dumka Press, 160 p;
[8] Melles et al. (2003), Ber. Polarforsch. Meeresfosch.509,ISSN 1618-3193;

IODP

Trace elements in carbonate veins

S. RAUSCH[1], W. BACH[1], F. BÖHM[2], A. KLÜGEL[1]

[1] Geoscience Department, University of Bremen, Germany; srausch@uni-bremen.de / akluegel@uni-bremen.de / wbach@uni-bremen.de
[2] GEOMAR, Helmholtz-Zentrum für Ozeanforschung, 24148 Kiel, Germany; fboehm@ifm-geomar.de

Calcium carbonate precipitates in veins during circulation of seawater through the basaltic ocean crust. This mechanism provides a significant sink of CO_2 in the global carbon cycle (Alt and Teagle, 1999). We have used carbonate infill in veins, vesicles and breccias to better determine the magnitude of carbonate formation and the processes of low-temperature alteration of the oceanic crust in ridge flank systems. Carbonate veins that formed with no or little basement interaction are reliable indicators for Mg/Ca and Sr/Ca of past seawater (Coggon et al. 2010, Rausch et al, submitted). In addition, carbonate veins can be used to study chemical exchange processes between seawater and the ocean crust.

We present laser-ablation ICP-MS analyses of trace element concentrations in carbonate veins, focussing on transects measured across single veins. Determining the element variablity in veins may provide insights into the evolution of the seawater-basalt system, in particular in terms of intensity of interaction with the host basalt and changes in redox conditions in the fluid during carbonate precipitation. The carbonates investigated are from DSDP (Sites 332, 333, 335, 395, 396, 407, 417, 418, 553) and ODP drill holes (Sites 801, 1149, 1224 and 896) and are mainly calcite. Aragonite was found in two cores (409, 504); dolomite and Fe- and Mn-rich carbonates are rare and have been excluded from this study.

Fig.1a and b shows that carbonate veins reveal a global positive correlation in Mg/Ca vs. Sr/Ca plots. This trend is largely due to seawater compositional changes from low Mg/Ca and Sr/Ca in the Mesozoic and Paleogene to high values in the modern ocean. Considerable variations in these ratios within single veins indicate that additional mechanisms play a role. We have examined dependencies of these ratios on precipitation rate, exchange with basement rocks, and crystal chemical effects. Variation of precipitation rates cannot explain the positive correlation because Mg incorporation is independent of precipitation rates (Morse and Bender, 1990). Interactions with basement remove Mg from and add Ca to the migrating fluid, while Sr concentrations change only slightly.

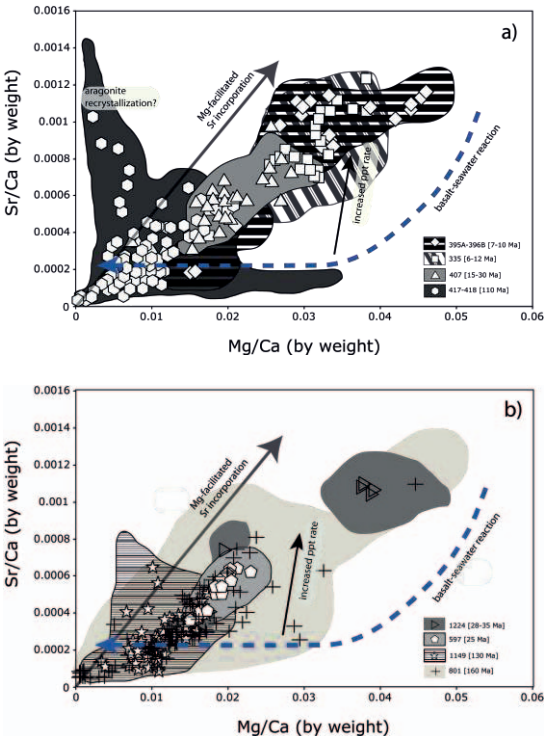

Fig. 1a and b: Sr/Ca versus Mg/Ca ratios of calcites a) in the North Atlantic and b) in the Pacific. The gray and striped fields encompass laser ICP MS trace element analyses for the different sites. The symbols represent average compositions of veins or of growth zones within veins. Most analyses plot along a major trend interpreted to reflect compositional changes of seawater in the past 180 Ma. The effects of interaction with basement (trend fitted through data from Coggon et al., 2004, dashed line), fractionation due to different rate dependencies of partitioning (Morse and Bender, 1990, black arrow), and crystal chemical controls of Sr partitioning into calcite with variably Mg concentrations (Carpenter and Lohmann, 1992) are also shown (gray arrow); ppt = precipitation.

Experimental work (e.g. Mucci and Morse, 1983) suggests some co-variation between Mg/Ca and Sr/Ca, whereupon high concentrations of Mg lead to an increase in Sr partitioning between calcite and the fluid. By using a relation proposed by Carpenter and Lohman (1992) we calculated the slope of a trend caused by this feedback mechanism. This slope is identical to that displayed by within-vein variability. Neither partitioning or rate effects nor basement interactions cause trends that match the observed variations. This finding corroborates the interpretation of Coggon et al. (2010) that this trend reflects compositional changes of seawater through time. The aforementioned effects, however, add considerable scatter to the trend and need to be corrected for reconstructing seawater compositions (Rausch et al., submitted).

We have also analyzed calcite veins for elements that are depleted in seawater but relatively abundant in basalt (e.g., Mn, Ba, REEs, Y, etc.). These elements are sensitive recorders of seawater-basement interaction, the extent of

which is expected to be greatest in sites where recharge of circulation seawater is restricted and basement fluids have long residence times in crustal aquifers. In contrast, in places where recharge rates are large (i.e., open circulation), residence times of circulating seawater are short and the fluid is little affected by reactions with basalt. For instance, the Y/Ho ratio of carbonate veins responds to even minor extents of exchange with basement, because Ho and Y concentrations of seawater are 5-6 orders of magnitude lower than those of basalt, and the Y/Ho ratio of seawater (70) is much higher than that of basalt (28). Our combined analyses of ~75 veins indicate a major range of Y/Ho from 25 to 90, indicating highly variable intensities of basement-seawater interaction.

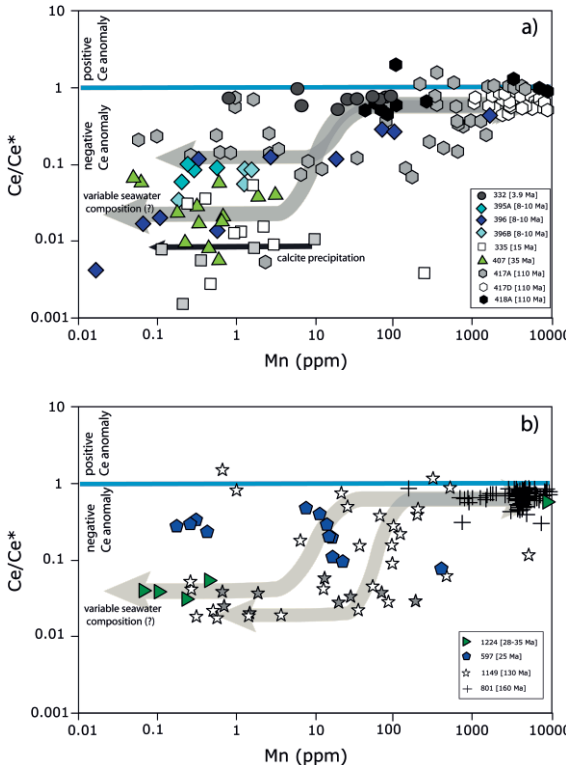

Fig. 2a and b: Ce/Ce* versus Mn concentration in carbonate veins. a) in the North Atlantic and b) in the Pacific. The thin arrow indicates the trajectories during calcite precipitation, whereas the thicker arrows represent schematic mixing lines between basalt and seawater. Ce/Ce* is normalized to PAAS (Post-Archean average Australian shale, Taylor and McLennan 1985)

We have used Sr isotope ratios of calcite veins to distinguish between open versus closed circulation basement sites. Because the $^{87}Sr/^{86}Sr$ ratio of global seawater has strongly increased during the past 40 Ma (McArthur et al., 2004), the $^{87}Sr/^{86}Sr$ ratio in carbonate veins can be compared with this record to estimate their formation age (Hart et al., 1994). Carbonates veins that have higher $^{87}Sr/^{86}Sr$ than contemporaneous seawater indicate a formation age considerably younger than the age of the basement host rocks. These sites (in particular 335, 395, 396, 407, 1224) were open for circulating of fresh seawater on long time scales. In contrast, samples with $^{87}Sr/^{86}Sr$ identical to or below that of contemporaneous seawater indicate hydrothermal uptake of Sr from the basaltic basement (Sites: 332, 333, 409, 418, 801) and indicate significant exchange with basement.

The PAAS-normalized rare earth element (REE) patterns of the investigated carbonate veins define two distinct groups, one with a pronounced negative Ce anomaly ($Ce/Ce^*=3Ce/[2La + 1Nd] << 1$) and a second group with $Ce/Ce^* \approx 1$. Compared to other REEs, cerium is typically depleted in oxic seawater, hence a Ce depletion in the carbonates is an indication of oxidative conditions during carbonate precipitation. Negative Ce anomalies are commonly observed in carbonates from veins with high $^{87}Sr/^{86}Sr$ (i.e., sites with open circulation). In contrast, carbonates from sites where low $^{87}Sr/^{86}Sr$ ratios indicate considerable exchange with basement show elevated REE contents without a pronounced Ce anomaly, suggesting that the basement had considerably higher REE concentrations (cf. Wheat et al., 2002). Suboxic to anoxic conditions likely prevail in case of restricted circulation where exchange with the ocean is strongly limited. Manganese is another element with a redox-sensitive behaviour. In a diagram of Ce/Ce* versus Mn (Fig.2a and b) we observe that samples showing the most intense interaction with the basement (i.e. low $^{87}Sr/^{86}Sr$) cluster at $Ce/Ce^* \approx 1$ and high concentrations of Mn. In contrast, other samples with a pronounced Ce anomaly show widely variable Mn contents. Much of this variation can be related to basement interaction with circulating seawater to variable extents, as indicated by basalt-seawater mixing lines in Fig. 2. A caveat of using seawater as an endmember is that its composition has changed over time. The most dramatic changes can be expected for the case of oceanic anoxic events (OAE), which impose changed redox conditions and thus would also lead to variable Ce/Ce* and Mn contents of precipitating carbonates. Remarkably, only sites where basement is overlain by basal sediments indicating anoxia (1149 and 417), show a strongly bimodal distribution of Ce/Ce* values. We hypothesize that the basement was open for circulating seawater throughout the duration of the OAE and that the carbonate veins record the change in ocean redox chemistry.

References:

Alt, J.C., Teagle, D.A.H., 1999. The uptake of carbon during alteration of ocean crust. Geochimica et Cosmochimica Acta 63, 1527-1535.

Carpenter, S. J. and Lohmann, K. C., 1992. Sr/Mg ratios of modern marine calcite: Empirical indicators of ocean chemistry and precipitation rate. Geochim. Cosmochim. Acta 56 (5), 1837-1849.

Coggon, R.M., Teagle, D.A.H., Cooper, M.J., Vanko, D.A., 2004. Linking basement carbonate vein compositions to porewater geochemistry across the eastern flank of the Juan de Fuca Ridge, ODP Leg 168. Earth and Planetary Science Letters 219, 111-128.

Coggon, R.M., Teagle, D.A.H., Smith-Duque, C.E., Alt, J.C., Cooper, M.J., 2010. Reconstructing past seawater Mg/Ca and Sr/Ca from mid-ocean ridge flank calcium carbonate veins. Science 327, 1114-1117.

Hart, S. R., J. Blusztajn, et al., 1994. fluid circulation in the oceanic crust: Contrast beween volcanic and plutonic regimes. Journal of Geophysical Research 99: 3163-3173.

McArthur, J.M., Howarth, R.J., 2004. Strontium isotope stratigraphy, in: Gradstein, F., Ogg, J.G., Smith, A. (Eds.), A Geological Time Scale, 1st ed, Cambridge, pp. 96-105.

Morse, J. W. and M. L. Bender, 1990. Partition coefficients in calcite: Examination of factors influencing the validity of experimental results and their application to natural systems. Chemical Geology 82 (0), 265-277.

Mucci, A. and J. W. Morse, 1983. The incorporation of Mg2+ and Sr2+ into calcite overgrowths: influences of growth rate and solution composition. Geochimica et Cosmochimica Acta 47 (2), 217-233.

Rausch, S., Böhm, F., Eisenhauer A., Klügel, A., Bach, W. Calcium carbonate veins in ocean crust record a threefold increase of seawater Mg/Ca in the past 30 Million years, submitted

Taylor, S.R. and McLennan, S.M., 1985. The Continental Crust: Its Composition and Evolution. Blackwell Scientific Publications, Oxford, 312 pp.

Wheat, C. G., M. J. Mottl, et al., 2002. Trace element and REE composition of a low-temperature ridge-flank hydrothermal spring. Geochimica et Cosmochimica Acta 66(21): 3693-3705.

IODP

Macroevolutionary patterns in Antarctic Neogene radiolarians

J. RENAUDIE[1], D. LAZARUS[1]

[1]Museum für Naturkunde, Leibniz-Institut für Evolutions- und Biodiversitätsforschung an der Humboldt Universität zu Berlin, Invalidenstraße 43, 10115 Berlin.
johan.renaudie@mfn-berlin.de

Introduction

Reconstructing paleodiversity has become a major theme in paleobiology, based on compilations of taxa occurrences from the published literature. To circumvent numerous biases caused by the incompleteness (most species are not preserved) and misrepresentativity of this fossil data (variable sample size, differential preservation among species, habitat or environment, etc), a large number of statistical methods to produce such reconstructions have arisen in the literature.

prior published data (DSDP-ODP Antarctic radiolarian reports), as an empirical test of the accuracy of paleobiologic methods.

Using a whole-fauna dataset to test the accuracy of paleodiversity reconstitutions

To obtain a taxonomically-complete dataset, we began with a full taxonomic reexamination of the Southern Ocean Neogene radiolarian fauna. We then counted the 492 species recognized in 98 samples - Atlantic sector (ODP Leg 113) and Kerguelen Plateau (ODP Legs 119, 120 and 183). Approximately 7000 specimens were counted in each sample. Extrapolations using methods such as ACE (Chao & Lee, 1992) suggests that more than 80% of the species preserved at each level are recovered in our counted data.

We compared the diversity pattern observed in our whole-fauna dataset (Figure 1) to that of (Lazarus, 2002) in which three independent data sets (Caulet 1991; Abelmann 1992; Lazarus 1992), from ODP Legs 119 and 120, were carefully cleaned (removal of reworked specimens, use of an uniform taxonomy) but processed without subsampling,

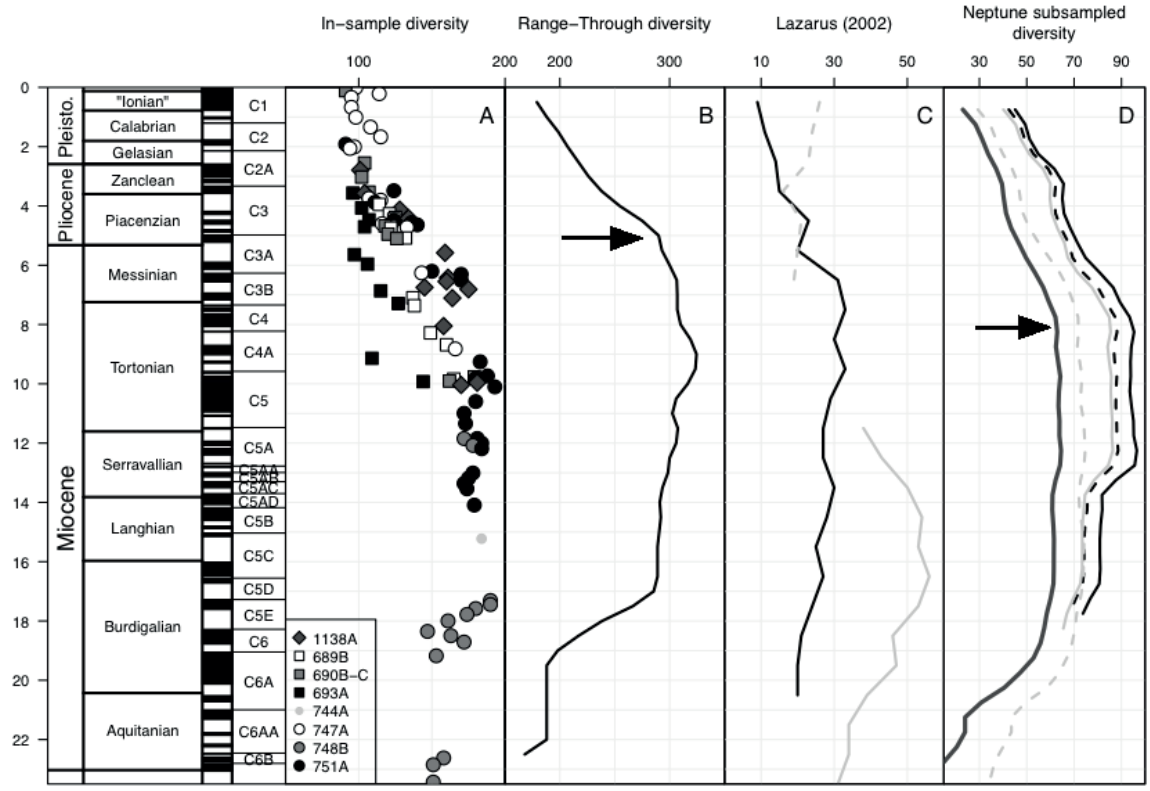

Figure 1: Antarctic Neogene radiolarian diversity. A and B: Respectively, in-sample species richness and range-through diversity in our whole-fauna dataset. C: Diversity curves previously published in Lazarus (2002). D: Diversity computed from the Neptune dataset with five different type of subsampling: UW (black line), OW (dashed black line), CR (light grey line), O2W (dashed light grey line) and SQS (bold dark grey line). Arrows show location of diversity drops.

More than 90% of the living and fossil Neogene polycystine (e.g. siliceous) radiolarian species are considered to be preserved; samples from the deep-sea sediments often contain ca 103 to 105 specimens per gram dry sediments, thus allowing a constantly large sample size. The biggest bias in this material is therefore the recording effort, that has been historically low, compared to what the material actually allows (Lazarus, 2011).

We collected a quantitative, taxonomically-complete dataset of Antarctic radiolarians in numerous samples ranging from 23 to 0 Ma. We compare the diversity trend retrieved by our dataset to ones produced using 'classical' diversity reconstructions based only on compilations of

based on species' first and last occurences; and to a Antarctic Neogene dataset extracted from the Neptune database (which contains most microfossils inventories published in the context of the DSDP/ODP drilling campaign; Lazarus, 1994). This dataset was analysed using standard paleobiologic methods: classical rarefaction (CR), unweighted by-list (UW), occurence-weighted by-list (OW), occurence-squared-weighted by-list (O2W) and 'Shareholder Quorum' (SQS) subsamplings.

Although the subsampled Neptune dataset is successful in retrieving the main diversity trend seen in our dataset (Fig. 1), two major differences can be seen: an artefactual

increase at ca. 13 Ma and a significant lag of 3 My for the late Miocene diversity drop (seen at ca. 5 Ma in our dataset).

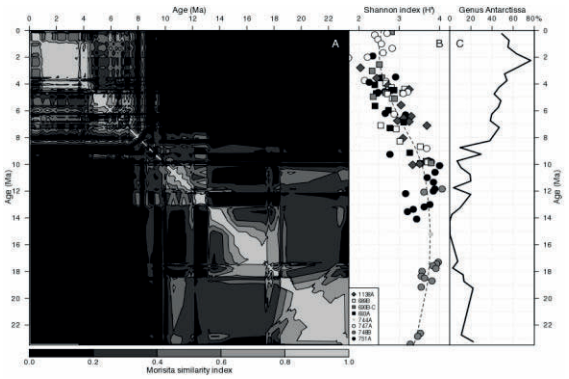

Figure 2: Ecological summary. A: Sample-by-sample similarity plot, using here the Morisita-Horn index: the color key represents the value of the index, while the x and y-axis both represents time (in Ma). B: Evenness (here, Shannon H' index) for studied samples. C: Mean relative abundance in each time bin of the species of genus *Antarctissa*.

Such a divergence could be due to the common use (in the data contained in databases such as Neptune) of checklists of biostratigraphic markers instead of true fauna inventories:subsampling data pre-screened to emphasise only a small subset of species. Distorted diversity reconstructions can also come from mixing of diversity and relative abundance signals: as can be seen on Figure 2, the fauna underwent a major ecological turnover at ca. 8 Ma (Fig. 2), from a relatively equitable fauna to one heavily dominated by species of the nasselarian genus Antarctissa. This turnover was not associated with any extinction or origination event. Yet, all subsampled diversities start dropping during this event, as increasingly common Antarctissa reduce sampling of rarer species in the rest of the fauna.

Environmental context to the observed macroevolutionary pattern

The ecological turnover seems to be contemporaneous with two other Southern Ocean events (Fig. 3): an abrupt shift in the benthic carbon isotope signal known as the Late Miocene Carbon Shift (though poorly understood, it is likely to be linked to the development of a modern interbasinal $\partial^{13}C$ gradient and, to some extent, to the growth of the West Antarctic Ice Sheet and the initiation of the modern bottom water formation process) and the replacement of coccolith dominated phytoplankton by, first, at ca. 15 Ma, a microflora where coccoliths and diatoms cohabited and, then, at ca. 8 Ma, by a microflora dominated by diatoms.

Although change in bottom waters might have affected the radiolarians, it is more likely that they were affected by the changes in the phytoplankton. In this scenario, species which preferentially fed on calcareous nannoplankton decreased in relative abundance in favor of species more specialized in diatom grazing. Of course, those two hypotheses are not mutually exclusive.

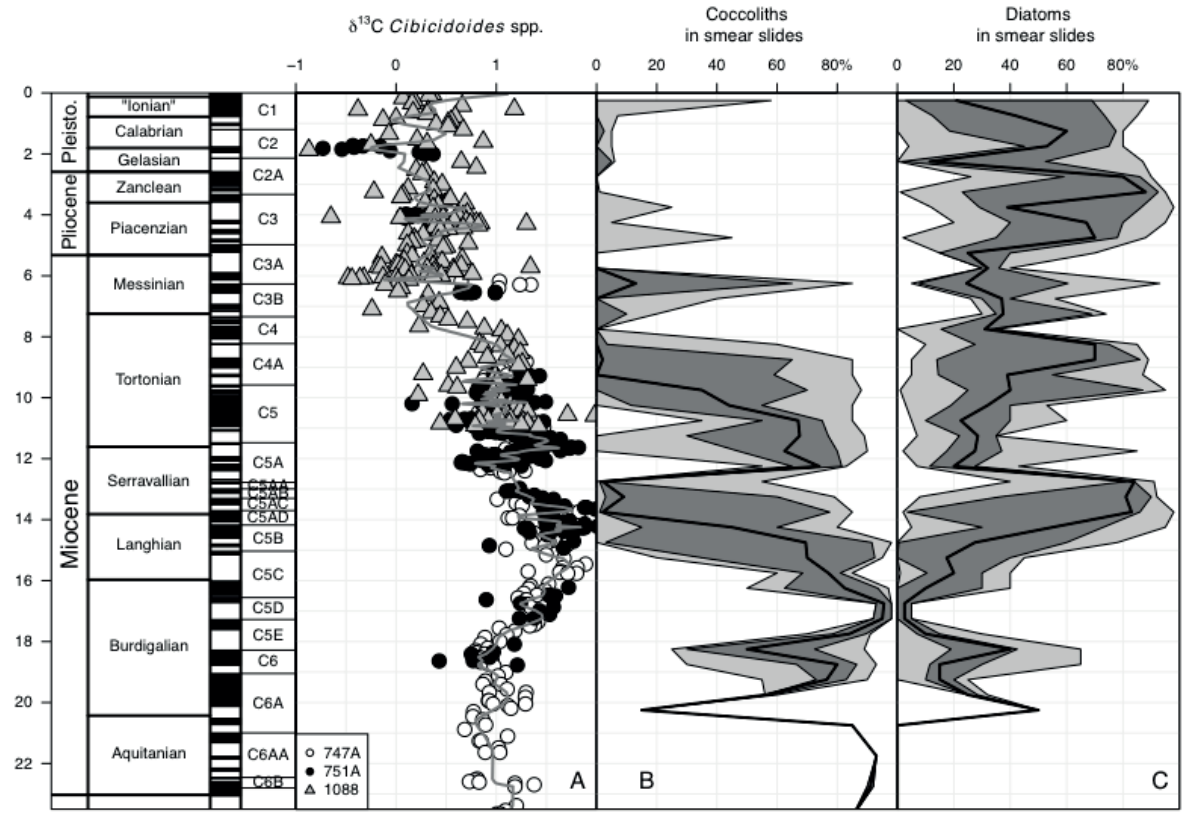

Figure 3: Environmental context. A. $\partial^{13}C$ *Cibicidoides* spp. (benthic foraminifera) from Leg 120 Site 747A (Wright & Miller, 1992) and site 751A (Mackensen et al., 1992) on the Kerguelen Plateau and from Leg 177 Site 1088 (Billups, 2002) in the subantarctic Atlantic, in per mil. B and C. Relative abundance of, respectively, calcareous nannofossils and diatoms in smear slides, as reported in the core descriptions of Legs 113 and 120. Bold black line represents the median value, the dark grey area encompasses the range between the first to the third quartiles of the values and the light grey area the range between the smallest and the highest value.

Outlook

The final phase of our project consists of an analysis of the same whole-fauna dataset using modern methods such as CONOP to increase biostratigraphic resolution in Antarctic Neogene sediments. Although this phase is well underway, additional counting will continue throughout most of the first semester of 2012 to increase the sample density of each site and, hence, resolve the order sequence of the numerous new bioevents.

References:

Abelmann, A., 1992. Early to Middle Miocene radiolarian stratigraphy of the Kerguelen Plateau, leg 120. In Wise, S. W. Jr et al. (Eds), Proceedings of the Ocean Drilling Program, Scientific Results, College Station, TX (Ocean Drilling Program), 120: 757-783.

Billups, K., 2002. Late Miocene through early Pliocene deep water circulation and climate change viewed from the sub-antarctic South Atlantic. Palaeogeography, Palaeoclimatology, Palaeoecology, 185: 287-307.

Caulet, J.-P., 1991. Radiolarians from the Kerguelen Plateau, ODP Eg 119. In Barron, J. and Larsen, B. (Eds), Proceedings of the Ocean Drilling Program, Scientific Results, College Station, TX (Ocean Drilling Program), 119: 513-546.

Chao, A. and S.-M. Lee, 1992. Estimating the number of classes via sample coverage. Journal of the American Statistical Association, 87(417): 210-217.

Lazarus, D. B., 1992. Antarctic Neogene radiolarians from the Kerguelen Plateau, Legs 119 and 120. In Wise, S. W. Jr et al. (Eds), Proceedings of the Ocean Drilling Program, Scientific Results, College Station, TX (Ocean Drilling Program), 120: 785-809.

Lazarus, D. B., 2002. Environmental control of diversity, evolutionary rates and taxa longevities in Antarctic Neogene Radiolaria. Palaeontologia Electronica, 5(1): 32pp.

Lazarus, D. B. 2011. The deep-sea microfossil record of macroevolutionary change in plankton and its study. In McGowan, A. J. and Smith, A. B. (Eds) Comparing the Geological and Fossil Records: implications for biodiversity studies. Geol. Soc. London Spec. Pub. 358: 141-166.

Mackensen, A., E. Barrera and H.-W. Hubberten, 1992. Neogene circulation in the Southern Indian Ocean: evidence from benthic foraminifers, carbonate data and stable isotope analyses (Site 751). In Wise, S. W. Jr et al. (Eds), Proceedings of the Ocean Drilling Program, Scientific Results, College Station, TX (Ocean Drilling Program), 120: 867-878.

Wright, J. D. and K. G. Miller, 1992. Miocene stable isotope stratigraphy, site 747, Kerguelen Plateau. In Wise, S. W. Jr et al. (Eds), Proceedings of the Ocean Drilling Program, Scientific Results, College Station, TX (Ocean Drilling Program), 120: 8

ICDP

The redox state of ocean and atmosphere in the Paleoproterozoic constrained by sulfur isotope data from ICDP FAR-DEEP drillcores

M. REUSCHEL, H. STRAUSS

Westfälische Wilhelms-Universität Münster, Institut für Geologie und Paläontologie, Münster (Germany)

The Paleoproterozoic eon (2.5-1.6 Ga) is characterized by substantial changes in tectonics and climate. However the most important change is a substantial rise in atmospheric oxygen concentration in the earliest Paleoproterozoic initiating the irreversible oxygenation of our planet, which led to severe changes in the (bio-) geochemical cycling of redox sensitive elements. Paleoproterozoic sedimentary rocks from the Fennoscandian Shield have been the target of this study to track the redox conditions of atmosphere and ocean after the first major rise in atmospheric oxygen concentration. The Russian part of the Fennoscandian Shield provides exceptional sedimentary and volcanic successions, spanning nearly 600 Ma of Earth history and providing therefore a unique record of the Paleoproterozoic eon, which could help to further investigate the geotectonic, climatic and biochemical changes during that time (Melezhik et al., 2005). In summer 2007, the ICDP FAR-DEEP (Fennoscandian Arctic Russia - Drilling Early Earth Project) drilled 15 holes in three areas of the Fennoscandian Shield. Two of these areas are situated on the Kola Peninsula, notably in the Pechenga Greenstone

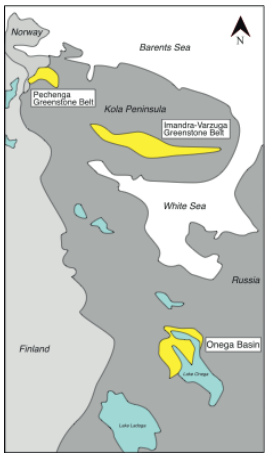

Fig. 1 Map of the Russian part of the Fennoscandian Shield. The working areas are highlighted in yellow.

Belt located in the north-west, close to the Norwegian boarder, and in the Imandra/Varzuga Greenstone Belt, in the south-east. The third drilling area, the Onega palaeobasin, is located in Karelia (Fig 1).

The loss of the mass independent fractionated sulfur isotopes (MIF-S) is thought to reflect the rise in atmospheric oxygen, because MIF-S can only be produced,

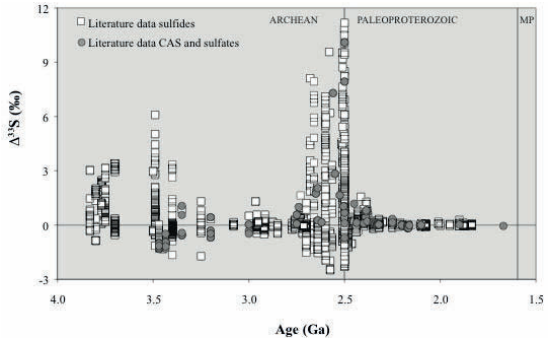

Fig. 2 Temporal evolution of $\Delta^{33}S$ recorded in sedimentary sulfides and sulfates (plot modified after Farquahr et al., 2010). Source of sulfate data: Reuschel et al., 2012; Domagal-Goldman et al., 2009; Guo et al., 2009; Shen et al., 2001, 2008, 2009; Johnston et al., 2005; Bao et al., 2007; Farquhar et al., 2000 (CAS= carbonate associated sulfate, MP=Mesoproterozoic)

transferred and archived in Earth surface environments in an anoxic atmosphere and hydrosphere (Farquhar et al., 2000, 2002; Pavlov and Kasting, 2002). As a further consequence of the Earth's atmospheric oxygenation and the concomitant onset of oxidative weathering of sulfides, the oceanic sulfate concentration began to rise. This process significantly affected the sulfur cycling in the marine realm. With the increasing availability of sulfate in the oceanic water column, the microbial turnover of sulfate, associated with a significant mass dependent sulfur isotope fractionation (MDF-S), became more and more

important and altered the sulfur isotope composition of water column sulfate and the reduced sulfur pool, both preserved in sedimentary sulfate and sulfide minerals.

Mineralogical (e.g., the absence of detrital pyrite in paleosols) and geochemical evidence (traditional sulfur isotopes, trace metal abundances) indicate a rise in atmospheric oxygen concentration in the early Paleoproterozoic. However, the loss of the (MIF-S) in

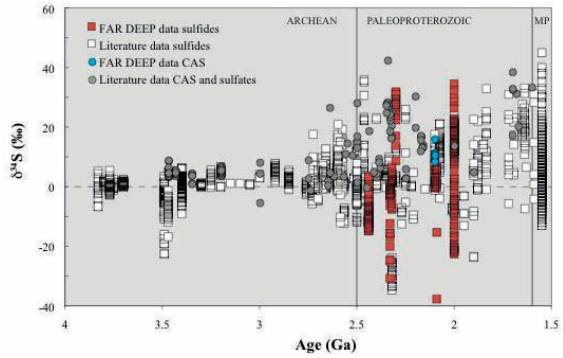

Fig. 3 Temporal evolution of $\delta^{34}S$ recorded in sedimentary sulfides and sulfates (Source of data: sulfides: modified after Canfield and Farquhar, 2009; sulfates: Reuschel et al., 2012; Domagal-Goldman et al., 2009; Guo et al., 2009; Shen et al., 2001, 2008, 2009; Johnston et al., 2005; Bao et al., 2007; Farquhar et al., 2000). (MP=Mesoproterozoic, CAS= carbonate associated sulfate)

sedimentary sulfur species is by now the most reliable tool for reconstructing the past atmospheric oxygen concentrations. The loss of the MIF-S and thus the rise in atmospheric oxygen above 10^{-5} PAL (Pavlov and Kasting, 2002; present atmospheric level) is thought to have occurred between 2.45 and 2.32 Ga (Fig. 2; Bekker et al., 2004; Mojzsis et al., 2003; Williford et al., 2011). A review about the published multiple sulfur isotope datasets points to uncertainties associated with the timing of the loss of MIF, but shows also a broad agreement that the loss of MIF-S occurred during the first global glacial event, the Huronian Glaciation. Respective successions from North America and South Africa indicate the loss of MIF between the second and third glacial interval (Guo et al., 2009; Papineau et al., 2007; Reuschel et al., in press, Fig.2).

A total of 3650 m of drill cores has been stored and archived at the Norwegian Geological Survey in Trondheim. To date, more than 300 samples (archive samples and selected research samples) have been studied for their sulfur geochemistry, including total sulfur abundances and sulfur isotope measurements for acid volatile sulfur (AVS), pyrite sulfur and carbonate-associated sulfate (CAS). The results of sulfur isotope measurements from pyrites are shown in Fig. 3, together with existing sulfide and sulfate sulfur isotope data from the literature. The sulfur isotope data have been generated from 12 FAR-DEEP drillcores, representing 6 different sedimentary formations ranging in age between 2.44 and c. 2.0 Ga. A distinct stratigraphic trend can be observed, with the sulfides of the oldest formation (Seidorechka Sedimentary Formation) displaying only minor variability in their sulfur isotopic composition ($\delta^{34}S$ ranges between -15 and +3 permill). In contrast, the formations younger than c. 2.3 Ga (Polisarka, Umba, Kolsajoki, Kuetsjärvi and Zaonega Formation) exhibit a broad range in $\delta^{34}S$ between -38 and +35 per mill (Fig. 3). This is in very good agreement with existing sulfur isotope data from time equivalent formations all over the globe.

The increasing variability in $\delta^{34}S_{sulfide}$ is the consequence of a growing seawater sulfate reservoir and enhanced microbial turnover of the sulfate. After the rise in atmospheric oxygen above 10^{-5} PAL between 2.45 and 2.32 Ga, the oceans have been continuously fed with sulfate by the enhanced oxidative weathering of continental sulfide minerals. The growing availably of sulfate in the ocean stimulated the microbial sulfate reduction, which is associated with a significant sulfur isotope fractionation effect, i.e., sulfate molecules with the lighter sulfur isotope (^{32}S) are preferentially used during microbial sulfate reduction. As a consequence, the seawater sulfate reservoir gets depleted in ^{32}S and therefore more positive in its sulfur isotopic composition with respect to the average Archean seawater sulfate (which is near zero). In contrast, the reduced sulfur reservoir, if ultimately stored as pyrite in the sediments will be enriched in ^{32}S, carrying more negative sulfur isotopic compositions.

The 2.1 Ga Tulomozero Formation (CAS data shown as blue circles in Fig. 3) consists of marine shallow water carbonates and sulfate evaporites, which are now mostly present as pseudomorphs after sulfate evaporites. The formation was the target for a sulfur isotope study to constrain the evolution of the seawater sulfate reservoir in the Paleoproterozoic (Reuschel et al., 2012) after the rise in atmospheric oxygen. For that purpose, sulfate has been extracted from carbonates across the entire formational thickness and measured for its sulfur isotopic composition. In addition, relics of sulfate minerals in pseudomorphs after sulfate evaporites (gypsum) have been used to measure sulfur isotopic compositions in situ using secondary ion mass spectrometry (SIMS). Although only present as pseudomorphs, the large occurrence of sulfate evaporites as observed from the Tulomozero Formation suggests a seawater sulfate concentration above 2.5 mM and reveals the presence of a substantial seawater sulfate reservoir at the time of deposition of the Tulomozero Formation. This is consistent with previous suggestions based on observations from other locations, e.g., the 2.2 Ga Lucknow Formation (Schröder et al., 2008). CAS displays remarkably constant sulfur isotopic compositions, which are comparable to $\delta^{34}S$ values measured in situ for sulfate relicts in pseudomorphs after sulfates (not shown in Fig.3, but see Reuschel et al., 2012). The data indicate a temporal and spatial homogeneity of the initial water column sulfate pool. Furthermore, the range in $\delta^{34}S$ of the Tulomozero sulfates agrees well with the data obtained for sulfates of similar age, suggesting a globally homogenous seawater sulfate pool with respect to its sulfur isotopic composition. The seawater sulfur isotopic composition obtained from the sulfates of the Tulomozero Formation is in the rage of +10 ‰, which indicates that bacterial sulfate reduction shifted the $\delta^{34}S$ of the global seawater sulfate away form zero (as suggested for the Archean) to more positive values. The homogeneity of the sulfur isotope data throughout the formation indicates a sulfur cycling in balance, and ultimately a minimum residence time of sulfate in the ocean of 5 Ma, estimated from the depositional time of the carbonate rocks. Moreover, the widespread deposition of sulfate evaporites is not only evidence for a sizeable seawater sulfate reservoir, but indicates also oxygenated

surface waters in the Mid-Paleoproterozoic ocean (Reuschel et al., 2012).

References:
Bekker, A., Holland, H.D., Wang, P.L., Rumble, D., Stein, H.J., Hannah, J.L., Coetzee, L.L., Beukes, N.J. (2004) Dating the rise of atmospheric oxygen. Nature 427. 117-120.
Domagal-Goldman, S.D., Kasting, J.F., Johnston, D.T., and Farquhar, J. (2008) Organic haze, glaciations and multiple sulfur isotopes in the Mid-Archean Era. Earth and Planetary Science Letters 269, 29–40.
Farquhar, J., Bao, H.M., Thiemens, M. (2000) Atmospheric influence of Earth's earliest sulfur cycle. Science 289, 756–758.
Farquar, J., Zerkle, A.L., Bekker, A. (2010) Geological constraints on the origin of oxygenic photosynthesis. Photosynth. Res. 107, 11-36.
Guo, Q., Strauss, H., Kaufman, A.J., Schröder, S., Gutzmer, J., Wing, B., Baker, M.A., Bekker, A., Jin, Q., Kim, S., Farquhar, J. (2009) Reconstructing Earth's surface oxidation across the Archean Paleoproterozoic transition. Geology 37, 399-402.
Johnston, D.T., Wing, B.A., Farquhar, J., Kaufman, A.J., Strauss, H., Lyons, T.W., Kah, L.C., Canfield, D.E. (2005) Active microbial sulphur disproportionation in the Mesoproterozoic. Science 310, 1477–1479.
Melezhik, V.A., Fallick, A.E., Hanski, E.J., Lepland, A., Prave, A.R., Strauss, H. (2005) Emergence of the aerobic biosphere during the Archean-Proterozoic
transition: Challenges of future research. GSA Today 15, 4.
Mojzsis, S.J., Coath, C.D., Greenwood, J.P., McKeegan, K.D., Harrison, T.M. (2003) Mass-independent isotope effects in Archean (2.5 to 3.8 Ga) sedimentary sulphides determined by ion microprobe analysis. GCA 67, 1635-1658.
Papineau, D., Mojzsis, S.J. Schmitt, A.K. (2007) Multiple sulfur isotopes from Paleoproterozoic interglacial sediments and the rise of the atmospheric oxygen. EPSL 255, 188-212.
Pavlov, A.A., Kasting, J.F. (2002) Mass-independent fractionation of sulfur isotopes in Archean sediments: strong evidence for an anoxic Archean atmosphere.
Astrobiology 2, 27–41.
Schroeder, S. Bekker, A. Beukes, N.J., Strauss, H., van Niekerk, H.S. (2008) Rise in seawater sulphate concentration associated with Paleoproterozoic positive carbon excursion: evidence from sulphate evaporites in then 2.2-2.1 Gyr shallow marine Lucknow Formation, South Africa. Terra Nova 20, 108-117.
Reuschel, M., Strauss, H., Lepland, A. The end of mass-independent fractionation of sulfur isotopes In: V.A. Melezhik, A.E. Fallick, L. Kump, A. Lepland, A.R. Prave, H.Strauss (Editors), Reading the Archive of Earth's oxygenation, Springer.(accepted for publication)
Reuschel, M., Whitehouse M., Strauss, H., Lepland, A., Melezhik, V. (2012) Isotopic evidence for a sizeable seawater sulfate reservoir at 2.0 Ga. Prec. Res. 192-195, 78-88.
Shen, Y., Buick, R., Canfield, D.E. (2001) Isotopic evidence for microbial sulphate reduction in the early Archaean era. Nature 410, 77-81.
Shen, B., Xiao, S., Kaufman, A.J., Bao, H, Zhou, C., Wang, H. (2008) Stratification and mixing of a post glacial Neoproterozoic ocean: evidence from carbon
and sulfur isotopes in a cap dolostone from Northwest China. EPSL 265, 209-228.
Shen, Y.N., Farquhar, J., Masterson, A., Kaufman, A.J., Buick, R. (2009) Evaluating the role of microbial sulfate reduction in the early Archean using quadruple isotope systematics. EPSL 279, 383-391.
Williford K.H., van Kranendonk M.J., Ushikubo T., Kozdon R. and Valley J. (2011) Constraining atmospheric oxygen and seawater sulfate concentrations during Paleoproterozoic glaciation: in situ sulfur three isotope microanalysis of pyrite from the Turee Creek Group, Western Australia. GCA 75, 5686-5705.

IODP

New high-resolution Paleogene records from the Wilkes Land Margin, Antarctica

U. RÖHL[1], P. K. BIJL[2], F. JIMÉNEZ[3], J. PROSS[4], L. CONTRERAS[4], L. TAUXE[5], S.M. BOHATY[6], J. BENDLE[7], H. BRINKHUIS[2] AND IODP EXPEDITION 318 SCIENTISTS.

[1]MARUM - Center for Marine Environmental Sciences, University of Bremen, Bremen, Germany.
[2]Utrecht University, Utrecht, The Netherlands; [3]University Granada, Spain; [4]University of Frankfurt, Germany; [5]Scripps Institution of Oceanography, La Jolla, USA; [6]National Oceanography Centre, University of Southampton, UK; [7]University of Glasgow, UK.

Expedition 318 operated at seven sites in direct proximity to the Antarctic continent and resulted in the recovery of about 2000 m of upper Eocene to Holocene sediments. Four sites were drilled on the Wilkes Land rise (U1355, U1356, U1359, and U1361) and three sites on the Wilkes Land shelf (U1357, U1358, and U1360) at water depths between ~400 and 4000 meters below sea-level (mbsl). Together, the cores record the past ~53 m.y. of Antarctic history. The cores document the evolution of the Wilkes Land Antarctic margin from an ice-free greenhouse Antarctica to the present-day icehouse conditions, including the onset and erosional consequences of the first glaciation and the subsequent dynamics of the waxing and waning ice sheets.

We present a high-resolution cyclostratigraphy for the early Eocene drillcores from the Wilkes Land Margin Site U1356. This site were situated in a mid-shelf setting during the early Eocene and are characterized by a superb magnetostratigraphy and a robust biostratigraphic age control. Our investigation includes XRF core scanning and collection of bulk geochemical data via ICP-MS as well as bulk organic carbon isotope ratios ($\delta^{13}C_{org}$) in combination with the concentration of total organic carbon (TOC). The Lower Eocene at Site U1356 consists of well-developed cyclic claystones that span the interval of magnetochron C24, which makes this succession ideal to re-evaluate the early Eocene part of the Geomagnetic Polarity Time Scale (GPTS) and to provide new insights into the environmental responses as well as orbital configuration of early Eocene climatic cycles.

The early Eocene Greenhouse interval (~56–49 Ma) was punctuated by multiple transient global warming events, or hyperthermals—the most prominent of which being the Paleocene-Eocene Thermal Maximum (PETM). Many of the thermal maxima identified in Eocene records exhibit negative carbon isotope excursions (CIEs), carbonate dissolution horizons, and biotic perturbations, although of reduced magnitude and duration relative to the PETM. It is unclear, however, which of these events are normal carbon-cycle variations that occurred at orbital frequencies and which are exceptional events outside the normal range of Eocene carbon-cycle variability. We hope to address these questions through multi-proxy analysis of the early Eocene strata recovered at Site U1356.
Several lines of investigation on the Wilkes Land cores are ongoing. High-resolution XRF scanner data will be calibrated by integrating XRF and ICP-MS data from discrete samples. New records from Wilkes Land Oligocene cores will also be used toward a cyclostratigraphic integration with orbitally-tuned Pacific records. Additionally, X-ray CT analysis undertaken on selected core sections will contribute to a detailed reconstruction of the nature and distribution of ice-rafted debris (IRD) in earliest Oligocene sediments.

ICDP

Paleoclimate reconstruction for East Africa, the region of human origins: First results from Chew Bahir basin, Ethiopia, an ICDP site in the context of the "Hominid Sites and Paleolakes Drilling Project" (HSPDP)

F. SCHÄBITZ[1], M. TRAUTH[2], V. FÖRSTER[1], H. LAMB[3], A. ASRAT[4] & M. UMER[4]

[1] University of Cologne, Seminar for Geography and Education; Gronewaldstrasse 2; 50931 Cologne; Germany
[2] University of Potsdam, Institute of Earth and Environmental Science; Germany
[3] Aberystwyth University, Institute of Geography and Earth Sciences, Aberystwyth SY23 [3]DB, U.K.
[4] Addis Ababa University, Department of Earth Sciences; P. O. Box 1176, Addis Ababa, Ethiopia

The driving forces of human evolution and dispersal in East Africa are still not completely understood. Different hypotheses, based on palaeoenvironmental information from marine and lacustrine archives, have been presented during recent decades. Detailed consideration raises more questions: was drought the key triggering climatic factor or were several short time transitions between wet and dry climate responsible for evolutionary steps and human dispersal? What is the role of tectonic change? The HSPDP aims to deliver new answers to these questions by investigating six sites in East Africa, the so-called cradle of mankind. This presentation will give an overview of the main research questions of HSPDP, while briefly introducing the sites. We have cored six sites in the Chew Bahir basin, which forms the transition zone between the Main Ethiopian Rift to the North and the Omo-Turkana basin to the south. Sediments up to a depth of 19 m were retrieved along a west-east transect through this tectonic basin. These sediments cover about 50 ka and give hints of several wet-dry cycles. First results show that the last of these cycles, the "African Humid Period" (14-5 ka cal BP), is well represented, and even short term variations like Heinrich events and D/O cycles have left their traces in the sediment record. These findings prove the great potential of this basin for deeper drilling by the ICDP.

IODP

Unravelling the palaeoecology of Pliocene and Pleistocene dinoflagellate cysts

STIJN DE SCHEPPER[1], EVA I. FISCHER[2], JEROEN GROENEVELD[3], MARTIN J. HEAD[2] AND J. MATTHIESSEN[4]

[1] Department of Earth Science, University of Bergen, Allégaten 41, N-5007 Bergen, Norway, +4755583576, stijn.deschepper@geo.uib.no. Previously at Fachbereich Geowissenschaften, Universität Bremen.
[2] Department of Earth Sciences, Brock University, 500 Glenridge Avenue, St. Catharines, Ontario L2S 3A1, Canada
[3] Fachbereich Geowissenschaften, Universität Bremen, Postfach 330440, D-28334 Bremen, Germany
[4] Alfred Wegener Institute, Columbusstraße, D-27568 Bremerhaven, Germany

The (palaeo)autecological preferences of extant and extinct dinoflagellate cysts have been determined by comparing Late Pliocene and Early Pleistocene dinoflagellate cyst assemblage with geochemical data of planktonic foraminifera from the same sample. Our database contains >200 dinoflagellate cyst samples from four North Atlantic IODP/DSDP sites that are calibrated to Mg/Ca ratios of Globigerina bulloides as a measure of sea surface temperature.

This palaeo-database is compared with modern North Atlantic and global datasets. The focus lies in the relationship between Mg/Ca-based (i.e. spring–summer) sea-surface temperatures ($SST_{Mg/Ca}$) and dinoflagellate cyst relative abundances. In general, extant species are shown to have comparable spring–summer sea surface temperature ranges in the past ($SST_{Mg/Ca}$) and today (from World Ocean Atlas 2005, Locarnini et al., 2006), demonstrating that our approach is valid for inferring spring–summer sea surface temperature ranges for extinct species. For example, Habibacysta tectata represents $SST_{Mg/Ca}$ values between 10 and 15 °C when it exceeds 30% of the assemblage, and Invertocysta lacrymosa exceeds 15% when $SST_{Mg/Ca}$ values are between 18.6 and 23.5 °C. However, comparing Pliocene and Pleistocene $SST_{Mg/Ca}$ values with present day summer values for the extant Impagidinium pallidum suggests a greater tolerance of higher temperatures in the past. This species occupies more than 5% of the assemblage at $SST_{Mg/Ca}$ values of 11.6–17.9 °C in the Pliocene and Pleistocene, whereas present day summer sea surface temperatures are around −1.7 to 6.9 °C. This observation questions the value of Impagidinium pallidum as reliable indicator of cold waters in older deposits, and may explain its bipolar distribution.

References:

Locarnini, R.A., Mishonov, A.V., Antonov, J.I., Boyer, T.P., Garcia, H.E., 2006. World Ocean Atlas 2005, Volume 1: Temperature. In: Levitus, S. (Ed.), NOAA Atlas NESDIS 61. U.S. Government Printing Office, Washington, D.C., p. 182.

IODP

Emplacement processes of tuffaceous sandstones at IODP Site C0011B, Nankai Trough, derived from modal analysis

J.C. SCHINDLBECK[1], S. KUTTEROLF[1], A. FREUNDT[1]

[1]GEOMAR, Wischhofstr. 1-3, 24148 Kiel

Tuffaceous sandstones are characterized by their high amount (25 to 75%) of pyroclasts in their modal composition. During IODP Expedition 322 three interbeds of tuffaceous sandstones have been found within a moderately lithified and bioturbated silty claystone sequence in the late Miocene (>7.07 to ~9.0 Ma) upper part of the middle Shikoku Basin facies. Of the three sandstones, units 1 and 2 are single beds whereas unit 3 is composed of three beds.

Modal analyses of 29 sandstone thin sections reveal systematic vertical changes within each bed. Generally low-density pyroclasts are enriched at the top (50-60 vol%) of each sandstone bed whereas dense lithic components (25-30 vol%) and minerals (25-30 vol%) are enriched at the bottom. The vertically varying abundance of various types of lithic fragments (sedimentary, volcanoclastic and metamorphic) suggests that these have also been segregated according to their respective densities. The highest amount of fine-grained matrix glass is found in the middle of each bed. Pumice and lithic fragments in the

middle and upper parts of the sandstone beds carry ash coatings. For sandstone package 3, in contrast to 1 and 2, core pictures and thin section analyses indicate a subdivision in three units showing the same significant variations in top to bottom enrichment. This suggests three sedimentation events following each other in short time intervals.

Glass and mineral chemistry of each sandstone bed show no significant vertical variations. Specifically the matrix glass-shard major element compositions are identical to the pumice clast composition in each tuffaceous sandstone bed. The compositions of amphibole and pyroxene crystals differ only slightly between the sandstone packages. Application of the Ridolfi et al. (2009) thermobarometric calculations to amphiboles of sandstone packages 1 and 2 suggests that each of these was derived from a volcanic system comprising both a deep and a shallow magma reservoir.

Thickness and massive density-graded structure, and characteristic glass composition of each sandstone bed as well as as their occurrence ~ 350 km from mainland Japan, the most likely source region, support emplacement by huge turbidity currents directly derived from major explosive volcanic eruptions, probably involving massive entrance of pyroclastic flows into the ocean.

References:
Ridolfi F, Renzulli A, Puerini M (2009) Stability and chemical equilibrium of amphibole in calc-alkaline magmas: an overview, new thermobarometric formulations and application to subduction-related volcanoes. Contrib Mineral Petrol, DOI 10.1007/s00410-009-0465-7.

IODP

Middle through Late Miocene climate variability in the Nordic Seas as recorded by marine palynomorphs

M. SCHRECK, M. MEHEUST, M. MATTHIESSEN, R. STEIN

Alfred Wegener Institute for Polar and Marine Research

Continuous Neogene high northern latitude paleoclimate records with an unequivocal age model that allow tackling Miocene climate variability are rare. Moreover, owing to a generally low carbonate deposition/preservation and scarcity of calcareous microfossils in these Neogene sediments most previous studies have focussed on reconstructing the paleoceanographic and paleoclimatic history of the Nordic Seas since the onset of large-scale Northern Hemisphere glaciations and thus the Miocene paleoenvironmental evolution still remains enigmatic.

ODP Hole 907A in the Iceland Sea is located close to the growing Greenland and Iceland ice sheets and experienced the effects of sea-ice cover, migrating wind fronts and ocean currents, and its continuous middle through late Miocene sediment sequence and a pristine paleomagnetic record predisposes it for detailed investigations on the response of the Nordic Seas to major Neogene climate deteriorations. To bypass the virtual absence of biogenic carbonates, marine palynomorphs (dinoflagellate cysts, prasinophyte algae and acritarchs) have been utilized for detailed paleoenvironmental reconstructions as they are continuously present within this time-interval and show relatively high abundance and diversity in the high northern latitudes hemipelagic sediments. In addition, an initial low-resolution alkenone-based sea surface temperature record has been generated for this interval to provide first constrains on the thermal evolution of the Nordic Seas.

The analysed sequence is characterized by a general long-term trend from a diverse middle Miocene palynomorph assemblage towards the impoverished assemblages of the latest Miocene accompanied by a somewhat gradual decrease of SSTs being as high as 20°C at ~ 13.5 Ma to around 7°C by ~ 6 Ma, both clearly reflecting the prevailing Neogene cooling. However, superimposed on this trend several short-term changes in diversity, abundance and assemblage composition have punctuated the long-term decline. Different assemblages, distinctive suites of acmes, and significant extinction events have been identified, proving considerable changes in the physical characteristics of surface water masses that reflect both, globally recognized features such as the Miocene isotope events (Mi-events), and more regional events such as the onset of an East Greenland Current precursor and its subsequent strengthening. A significant late Miocene cooling is revealed by low dinoflagellate cyst diversity and productivity, and an acme of the endemic cold-water acritarch Decahedrella martinheadii that may be related to the reorganisation of ocean circulation due to the final restriction of deep-water exchange across the Panama Isthmus. This cooling is confirmed by a SST decline of ~ 5°C across this interval.

The identified paleoceanographic and paleoclimatic signals provide new insights into the paleoenvironmental evolution of the Nordic Seas during middle through late Miocene times and suggest that major adjustments of the climate system occurred prior to 4 Ma in the Iceland Sea, well before the onset of large-scale glaciations on Greenland.

IODP

Synchrotron texture analysis of naturally and experimentally deformed water-rich sediments from the Nankai Trough offshore Japan

KAI SCHUMANN[1], MICHAEL STIPP[1], BERND LEISS[2], JAN H. BEHRMANN[1]

[1]GEOMAR, Helmholtz-Zentrum für Ozeanforschung Kiel, Wischhofstr. 1-3, D-24148 Kiel
[2]Geowissenschaftliches Zentrum der Universität Göttingen (GZG), Goldschmidtstr.3, D-37077 Göttingen

Texture analysis of clays and clay rich sediments using standard X-ray goniometry is problematic due to artifacts from sample cutting, high water content and polishing, as well as from severe beam defocussing effects at small 2-theta angles. Because of the short wave lengths (in the range of 0.12 Å) and high energy, synchrotron radiation is a versatile tool for fast multi-mineral phase texture analysis. In contrast to X-ray goniometry, larger sample volumes can be measured, as the synchrotron beam has a penetration depth at mm- to cm-scale, depending on the material. This effectively reduces the surface effects. We have carried out synchrotron texture analysis on a set of mudstone samples from the Nankai trough and accretionary prism offshore Japan. The samples were recovered by

IODP expeditions 315, 316 and 333 of the NanTroSEIZE project from a depth range between 25 mbsf (meters below seafloor) and 522 mbsf. Two different groups were analyzed: First, samples were taken as recovered from drilling; second, samples were additionally experimentally deformed in a triaxial deformation apparatus at Kiel University up to axial strains of 46%. Accompanying petrographic and fabric analysis yielded data on composition, grain size, microstructure, and strain. On average, the samples are uniform silty clays composed of approximately 40% clays, 25% quartz, 25% feldspar, and 10% calcite. Grain size fractions range from clay to fine sand, with the clay fraction making up 65-85% of the sample volumes.

Synchotron texture measurements were carried out at the DORIS W2 beam line of the "Deutsches Elektronen Synchrotron" (DESY) in Hamburg, Germany. In order to determine complete pole figures sample cylinders of 2 cm in diameter and 2 cm in length were measured in a phi angle-range from -90 to +90° in 5° steps. A MAR 345 image plate detector was installed at a distance of 1.30 m behind the samples. The detector data were analysed with the help of the MAUD software package (Lutterotti et al., 1997). To fit theoretical spectra to the measured data, background level, sample detector distance, wavelength as well as the necessary cell parameters were set. An E-WIMV algorithm (modified from the WIMV algorithm of Matthies and Vinel, 1982) was used for texture calculation.

Rietveld refinement results using MAUD show that the compositions of the Expedition 333 samples from the incoming plate differ from the relatively uniform Expedition 315 and 316 samples of the accretionary prism. The differences in composition are mirrored by differences in texture. For example specimen 333-C0012C-4H-5 (25 mbsf) is mainly composed of quartz and feldspar (68%) and 24% illite with the illite showing a weak preferred orientation. The accretionary prism samples display textures for illite, kaolinite and montmorillonite. In the depth range between 90 mbsf (sample 315-C0001E-11H-1) and 220 mbsf (sample 316-C0006E-30X-1) there is not a strong change in the degree of crystallographic preferred orientation. One important observation is that the textures relate to bedding parallel compaction rather than to tectonic deformation, as in zones of steep bedding (see Kinoshita et al., 2009) the maxima of poles to basal reflections of the sheet silicates remain at high angles to bedding The synchroton textures can be compared with the shape preferred orientations of sheet silicates seen in scanning electron micrographs (BSE images) of the Expedition 315 and 316 samples.

The results reflect a pioneering effort to use sychrotron radiation to analyze the textures of weakly deformed, highly porous, water-rich material in order to achieve quantitative full 3D texture characterization. Our data are a proof of concept, because the problem can be solved much easier in more compacted and stronger deformed material.

References

Lutterotti, L., Bortolotti, M., Ischia, G., Lonardelli, I. and Wenk, H.-R. (2007). Z. Kristallogr.,Suppl. 26, 125-130, 2007.

Matthies, S. and Vinel, G. (1982). Phys. Star. Sol. (b) 112, Klll-Kll4.

Kinoshita, M.; Tobin, H.; Ashi, J.; Kimura, G.; Lallemant, S.; Screaton, E.; Curewitz, D.; Masago, H.; Moe, K.; and the Expedition 314/315/316 Scientists (2009): Proceedings of the Integrated Ocean Drilling Program, Volume 314/315/316

ICDP

Magma storage conditions and degassing processes of low-K and high-Al island-arc tholeiites: Experimental constraints for Mutnovsky volcano, Kamchatka

T. SHISHKINA[1], R. ALMEEV[1], R. BOTCHARNIKOV[1], F. HOLTZ[1], M. PORTNYAGIN[2]

[1]Institut für Mineralogie, Leibniz Universität Hannover, Callinstrasse 3, 30167 Hannover, Germany
[2]Helmholtz-Zentrum für Ozeanforschung Kiel (GEOMAR) Wischhofstrasse 1-3, Geb.12, 24148 Kiel, Germany

Introduction

Mutnovsky volcano is located in the southern part of the Eastern volcanic front of Kamchatka peninsula (Russia). The mafic lavas of the volcano are typical island arc high-Al, low-K tholeiitic basalts. Mutnovsky is the object of a proposed ICDP drilling project which is focused on the investigation of the interaction between active magmatic and adjacent hydrothermal systems. It has two central scientific issues: (1) the identification of magmatic component in fluids proximal to conduits and (2) the determination of the overall volatile and thermal budget of the Mutnovsky volcano.

The experimental data and natural observations obtained in the course of our DFG-project should provide new constraints on the magma storage conditions, especially on the pressures (depths), temperatures and volatile contents in the magma chamber of Mutnovsky volcano. The project consists of three main parts: (1) experimental study of the H_2O-CO_2 solubilities in basaltic melts relevant to Mutnovsky primitive magmas, since H_2O and CO_2 contents in magmas can be used as indexes of magma storage conditions; (2) determination of pre-eruptive conditions and depths of basaltic magma chamber beneath Mutnovsky volcano based on crystallization experiments; and (3) the study of natural samples: petrography and mineralogy of the rocks and compositions and volatile abundances in glass inclusions in minerals.

The data obtained for Mutnovsky volcano have a broad application and can be used to constrain a general genetic model for the formation of island arc tholeiitic series and will provide estimates on the budget and contribution of magmatic volatiles to the magmatic-hydrothermal volcanic systems.

1. Experimental investigation of solubility of H_2O and CO_2 in mafic melts

This part of the project is devoted to the quantitative determination on H_2O-CO_2 solubility in mafic melts in the range of pressures of 50 to 900 MPa. Experiments were conducted in an internally heated pressure vessel (IHPV) at pressures of 50 to 900 MPa and temperature of 1200 or 1250ºC with Ar as pressure-medium. Run products were analysed by different methods (IR, KFT, electron microprobe, colorimetry).

At first we performed experiments with natural low-K high Al tholeiitic basalt from Mutnovsky volcano. The solubility of H_2O in equilibrium with pure H_2O fluid increases from about 2.2 wt.% at 50 MPa to about 12.8 wt.% at 900 MPa. The concentration of CO_2 increases from about 200 to 5000 ppm in glasses which were in equilibrium with the most CO_2-rich fluids (Shishkina et al., 2010). The solubility plot (Fig. 1a) constructed from the

performed experiments can be used as a tool for the evaluation of magma storage conditions and for the reconstruction of the dynamics of magma degassing for natural basaltic glasses. H_2O-CO_2 contents in the melt inclusions in olivines from Mutnovsky were analysed (see part 3) and are reported on the solubility diagram in Fig. 1a.

Additionally we have investigated the effect of the anhydrous composition on the solubilities of H_2O and CO_2 in mafic melts with different compositions varying from from MORB to nephelenite (Shishkina et al., submitted). Our results confirm the strong effect of melt composition on the solubility of CO_2: at 500 MPa mafic melts coexisting with nearly pure CO_2 fluids can dissolve from around 0.32 to more than 0.90 wt% CO_2 as melt composition changes from tholeiitic to nephelenitic. H_2O solubility changes are comparatively small (in relative variation): from 8.8 to 9.5 wt.% for the same compositional range.

The correlation between solubility of CO_2 and melt composition is best described by the compositional parameterization proposed by Dixon (1997) taking into account structural parameters and the Gibbs free energy of carbonation reactions for the different cations. The obtained relationship can be described by an exponential function for every pressure (see example for 100MPa at Fig. 1b; Shishkina et al., submitted)

2. Crystallization experiments

Experimental investigation of phase relations in the Mutnovsky parental magma provided quantitative information on the influence of pressure, aH_2O and fO_2 on stability fields of oxide and silicate phases, as well as on evolutionary trends of island-arc tholeiitic magma of Mutnovsky volcano.

We have conducted two sets of crystallization experiments on the tholeiitic basalt (sample N72) previously investigated for H_2O-CO_2 solubilities (part 1): at 300 MPa and 100 MPa and in range of 950-1200°C. All experiments have been carried out in an IHPV at intrinsic oxygen fugacity, corresponding to the value of QFM+3.3 at water-saturated conditions, and to ~QFM at nominally dry conditions. In general, with decreasing temperature, the crystallization sequence in melts containing ~ 3 wt% H_2O is as follows: Mt → Mt + Pl → Mt + Pl + Ol → Mt + Pl + Ol + CPx→ Mt + Pl + Cpx + Opx, where Cpx and Opx are high and low-Ca pyroxene respectively.

The compositions of minerals and residual glasses observed in the crystallisation experiments were measured by electron microprobe and were compared with natural rock samples from Mutnovsky volcano (see part 3).

3. Study of natural samples from Mutnovsky volcano

Rock samples from Mutnovsky volcano representative for the current project were collected during a fieldwork in 2009. We have sampled several young fresh cinder cones on the south-west slope of Mutnovsky volcano. The lavas of these cones are composed of clinopyroxene-olivine-plagioclase-bearing basalts (8 wt.% MgO, 50 wt.% SiO_2). For studying melt inclusions in olivines we collected basaltic tephra (pieces of scoria and ash) from holocene eruptions of Mutnovsky. Due to the explosive eruption and rapid cooling, olivines from tephra usually contain naturally quenched glassy inclusions with well preserved pre-eruptive volatile abundances.

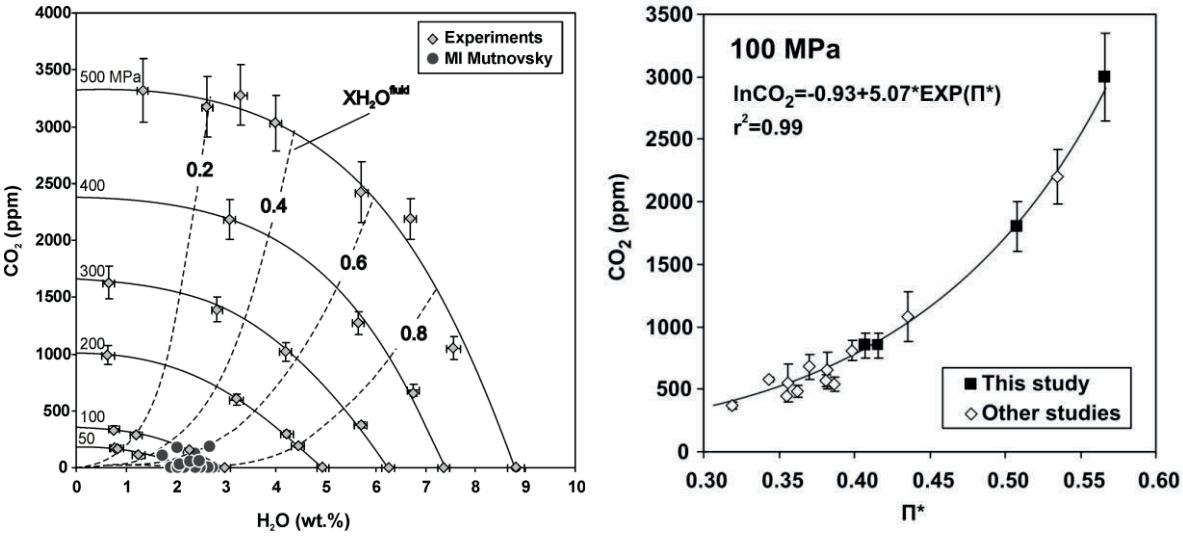

Fig. 1. a) Solubility plot for H_2O- and CO_2-bearing fluids in basaltic melts at 1250°C and pressures from 50 to 500 MPa. The solid lines represent isobars, the dashed lines are isopleths of constant fluid composition for the melts saturated with H_2O-CO_2-bearing fluids. Dark grey circles are compositions of melt inclusions in olivine from Mutnovsky volcano (see part 3). b) Dependence of CO_2 solubility in natural silicate melts coexisting with pure CO_2 fluids on the compositional parameter Π* (see text) at 100 MPa.

Mineral associations and their compositions have been studied in basaltic lavas and tephras from Mutnovsky volcano. The most abundant rocks among the eruptive products of the last stage of Mutnovsky activity are Ol-Plag-(±CPx)-basalts. Compositions of phenocrysts are quite similar between studied lava and tephra samples and in general are in a range of: An85-94 for plagioclase, Fo72-84 for olivine, Mg# 74-81 for Cpx (Fig. 3).

Glass inclusions from tephra of Mutnovsky volcano (with diameter more than 20 μm in olivines (Fo 75-80)) were studied using different methods. Major-element compositions as well as S and Cl content were determined by electron microprobe. H_2O and CO_2 concentrations were determined by SIMS in Yaroslavl`, Russia and in Nancy,

France. S^{+6}/S^{-2} proportions in the glasses were determined by XANES (Karlsruhe, Germany).

The studied melt inclusions have basaltic compositions and overlap with the general petrochemical trend of Mutnovsky volcanic series, indicating that they are evolved

4. Magma storage and pre-eruptive conditions for Mutnovsky volcano

From the combination of the natural and experimental observations we can derive several hypotheses on magma storage and pre-eruptive conditions for Mutnovsky.

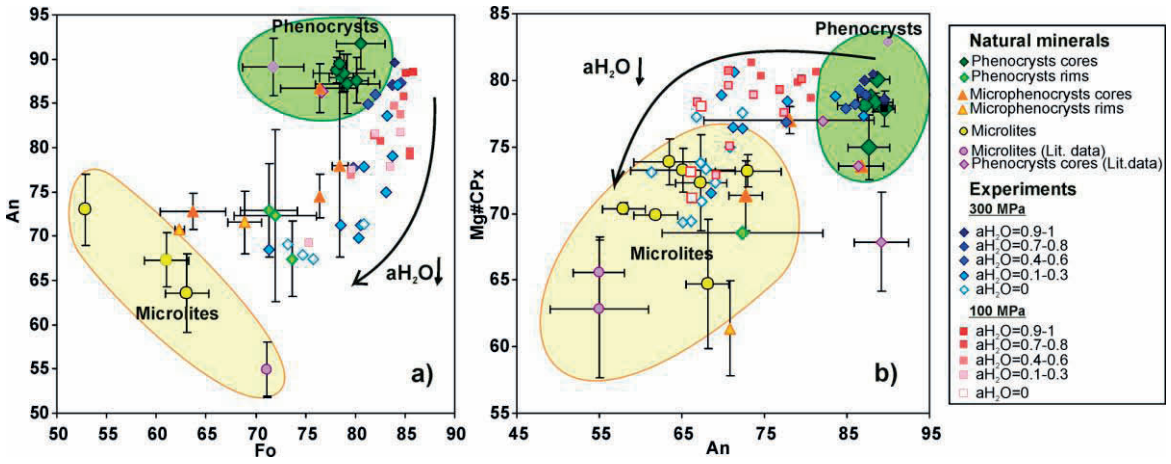

Fig. 3. Compositions of natural and experimentally produced mineral assemblages: a) coexisting olivines and plagioclases, b) coexisting plagioclases and Ca-pyroxenes.

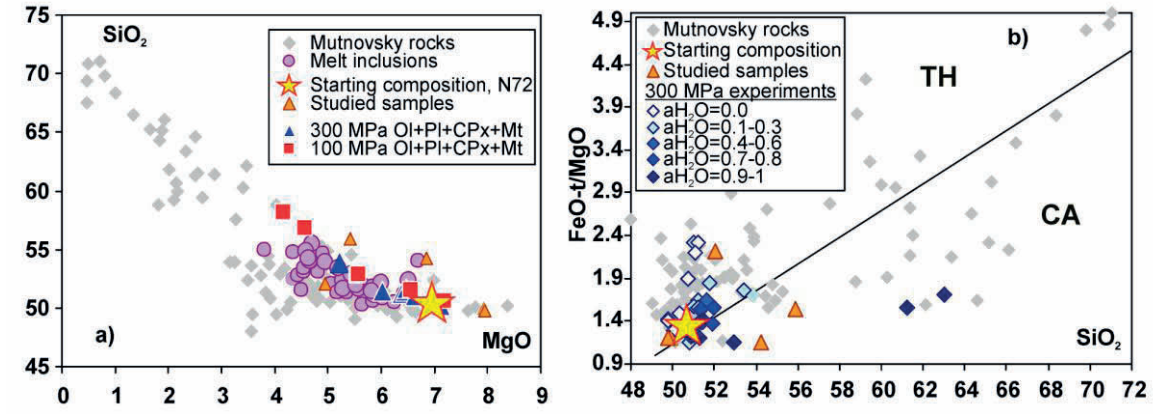

Fig. 4. Compositions of natural volcanic rocks (grey diamonds), melt inclusions in olivines (circles) in comparison with residual melts produced in experiments at 300 and 100 MPa (symbol description is in the legends).

derivates of the parental Mutnovsky melts, formed by crystallisation processes (Fig. 4a). The inclusions contain 1.7-2.7 wt.% H_2O and 0-180 ppm CO_2. Using the diagram in Fig.1a, these values indicate that most of the studied inclusions were trapped into olivines at relatively low pressures (less then 110 MPa), implying that differentiation processes involving the crystallization of olivine and magma storage occurred at shallow depths (less then 3 km). Moreover, values of H_2O analysed in melt inclusions are similar to the H_2O contents in experimental residual melts coexisting with the Ol+Pl+CPx+Mt association.

Data on S^{+6}/S^{-2} ratios in the natural glasses were used for the calculations of the oxygen fugacity according to the method described by Jugo et al. (2010). In the glass inclusions of Mutnovsky, $S^{6+}/\Sigma S$ vary from 0.4 to 1, which corresponds to fO2 in the range of QFM+0.9 to QFM+1.7. These fO2 values are in a good agreement with previous estimations of redox conditions for island arc magma systems.

1) Mutnovsky volcanic series (at least from basalts to andesites) can be reproduced by differentiation of basaltic melt (7.0 wt.% MgO, 50.1 wt.% SiO_2) at both studied pressures of 100 and 300 MPa (Fig. 4a). The parental magma must contain relatively high amounts of water (at least 1.5 - 2.0 wt.% H_2O), which corresponds to water activity (aH_2O) higher than 0.2 at 300 MPa or 0.4 at 100 MPa and redox conditions of QFM+1.7 to QFM +3.5 at 300 MPa and QFM+3 to QFM+3.5 at 100 MPa. Relatively water-poor conditions (2 to 4 wt.% H_2O) favor the delayed crystallization of magnetite and the early beginning of crystallization of plagioclase. This causes a weak enrichment of residual melt in FeO-tot and TiO_2 and a depletion of Al_2O_3 in the early stages of crystallization of basaltic melt, which is typical for a significant part of Mutnovsky rocks (island arc tholeiitic trend) (Fig. 4b). Another part of the volcanic rocks might be a product of crystallization of very H_2O-rich basaltic magma with early crystallization of magnetite which prevent any FeO-tot and TiO_2-enrichment (these natural samples plot on the

discriminant line between tholeiitic (TH) and calc-alkaline (CA) fields of the Miyashiro diagram or in the field of calc-alkaline rocks for most evolved species (Fig. 4b).

2) The best conditions for simultaneous crystallization of Plag+Ol+CPx assemblage of natural phenocrysts (An 85-94, Fo72-84, Mg#CPx74-81) were found in experiments at 300 MPa pressure (corresponding to depth of about 9km) (Fig. 3). Parental melt must contain 2 to 5 wt.% H_2O, which corresponds to water activity between 0.3 and 0.9 at 300 MPa. And an oxygen fugacity of QFM+2.2. to QFM+2.7. According to the experiments, crystallization of Plag+Ol+CPx from H_2O-bearing melt will happen in a temperature interval of 1025-1075°C. Magnetite is always stable together with silicates at these conditions.

3) We suggest the presense of a relatively shallow magma chamber (magma storage reservoir) below Mutnovsky volcano located ot a depth of about 1.5 – 3 km, filled with partially degassed magma containing 1.5-2.5 wt.% H_2O. The crystallization of this magma produces the association of high-Ca-plagioclase (An 84-90) and olivine (Fo 84-86) phenocrysts at temperatures in the range 1050-1075°C. Th eruption of this magma produces basaltic lava flows or tephra deposits in case of rapid ascend and explosive eruption. Strong hydrothermal activity in the crater of Mutnovsky also requires a constant input of heat, which can derive from a hot magma body located not far from the surface.

4) The crucial role of water in crystallization process is shown again in our experiments on phase relations in basaltic melt. The crystallization of nominally dry melts is characterized by early stabilization of silicates: Plag+Ol and CPx and by the absence of magnetite crystallization. This leads to significant enrichment of residual melts in FeO-tot (and TiO_2) and produces typical tholeiitic differentiation trend. In melts containing at least 1.5-2.0 wt.% H_2O at 100 and 300 MPa early crystallization of magnetite and delayed crystallization of silicates (plagioclase) prevents FeO-tot enrichment and produces calc-alkaline differentiation trends (Fig. 4b).

This research was supported by the German Science Foundation (DFG project Ho1337/21) and Europlanet Ri TNA program, grant 228319.

References:

Dixon, J.E. (1997) Degassing of alkali basalts. American Mineralogist, 82, 368-378.

Jugo, P.J., Wilke, M., and Botcharnikov, R.E. (2010) Sulfur K-edge XANES analysis of natural and synthetic basaltic glasses: Implications for S speciation and S content as function of oxygen fugacity, Geochim. Cosmochim. Acta 74, 5926-5938

Shishkina, T., Botcharnikov, R.E., Holtz, F., Almeev, R.R., and Portnyagin, M. (2010) Solubility of H2O and CO2-bearing fluids in tholeiitic basalts at pressures up to 500 MPa Chemical Geology 277, 115-125

Shishkina, T., Botcharnikov, R., Jazva, A., Jakubiak, A., Holtz, F., Almeev, R. and Wilke, M. (submitted) Compositional and pressure effects on the solubility of H2O and CO2 in mafic melts, submitted to American Mineralogist

ICDP

Carbonation of porous volcanic rocks by interaction with fluids at Unzen volcano, Japan

A. V.SIMONYAN[1], S.DULTZ[1,2], H. BEHRENS[1], J. FIEBIG[3] AND K. VOGES[1]

[1]Institute of Mineralogy, Leibniz University of Hannover, Callinstr. 3, D-30167 Hannover
[2]Institute of Soil Science, Leibniz University of Hannover, Herrenhäuser Str. 2, D-30419 Hannover
[3]Institute for Geosciences, J.W. Goethe University of Frankfurt, Altenhöferallee 1, D-60438 Frankfurt am Main

Unzen is a large composite volcano of dacite to andesite composition, characterized by non-explosive activity throughout its history. The Unzen drilling project was the first attempt to get insights into the mechanisms of volcanic eruptions by drilling into an active volcano shortly after eruption. The strong alteration of drilled rocks with large amounts of secondary minerals such as carbonates, chlorite and pyrite, supposed to be products of reactions of discharged volcanic fluids with the host rocks, inspired us to use the drilling cores in combination with experimental

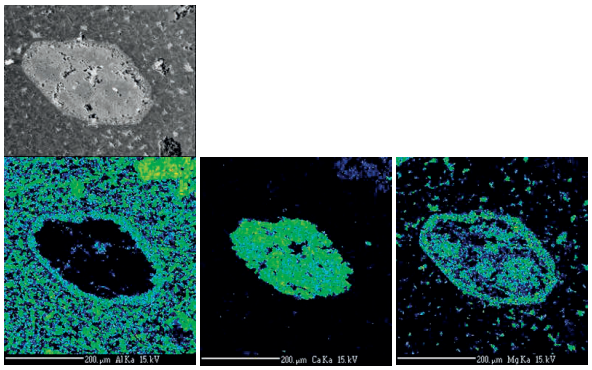

Fig. 1. Back scattered electron image of amphibole alteration in a polished section of sample C13-2-10 and element maps for Al (left), Ca (middle) and Mg (right) obtained by electron microprobe. The presence of different mineral phases in the samples together with aggregates of layer silicates is a challenge for image analysis, where it is tried to separate the regions of pores and carbonates.

work to have closer look on the mechanisms of fluid-rock interaction, in particular the carbonation and decarbonation of rocks. This research is not only important for understanding the deep degassing of volcanoes, but it has also major impacts for storage of CO_2 in cavities or in porous/brecciated volcanic rocks. For instance, the formation of carbonate immobilizes CO_2 and may strongly change the permeability of rocks by closing open paths.

Observations on thin sections

From microprobe investigations and back scattered electron images it is visible that amphiboles are strongly altered in all samples. The largest contents of Ca,Mg-carbonates were determined by image analyses in the samples C13-C16. The content of carbonate is up to 15 wt.%. These rocks were sampled at depth of 1975-2000 m in the magmatic conduit of Unzen. The most abundant phenocrysts in the rocks are plagioclases and amphiboles, whereby plagioclases are much more stable against alteration. Alteration of amphiboles is related to the formation of two types of carbonates, i.e., Ca-rich and Mg-rich, quartz, fine-grained muscovite and chlorite (Fig. 1).

Also pyrite and rutile were detected. Carbonates are also observed in cracks and pores of the groundmass.

Pore volume and pore size distribution, specific surface area, connectivity of the pore system

Pore volume of connected pores and the distribution of pore sizes were determined by mercury intrusion porosimetry (MIP). The pore size distribution was calculated from the minimum pressure required to fill pores of a certain radius with Hg by using the Washburn equation. The specific surface area (SSA) was calculated from the pore volume and the distribution of pore sizes. Further information about SSA and pore volume of fine pores in the range from 0.5 nm to 200 nm were determined by N2-adsorption methods. The SSA varies from 0.4 for unaltered dacite to 1.0÷5.0 (m^2/g) for altered core samples.

The inflection points on the branchs in cumulative normalized (volume-based) pore size distribution of the altered and unaltered samples determined by MIP show the broad maxima in the sub-micrometer range. The most frequent pore sizes for coherent altered dacites are observed in the range between 30 and 400 nm, whereas unaltered dacite has pores in the range from 100 nm to 10 µm. For the brecciated dacite three inflection points are observed indicating difference in density and structure compared to the other samples and implying that this sample can potentially have different transport properties. For the altered samples and unaltered dacite the difference in pore size distribution both for micropores and mesopores is obvious and different control of diffusion transport is observed. The shape of hysteresis obtained in adsorption-desorption isotherms for altered samples is relatively sharp and associated with both slit-shaped (pores are open on all sides) and the wedge-shaped pores with narrow necks at one or both open ends. A maximum in the pore size distribution by N_2-adsorption in altered core samples was observed at 3 - 5 nm. For the unaltered dacite the proportion of micropores is insignificant. In a modification of MIP, Hg was replaced by a alloy Wood`s metal, which solidifies below 78°C. It allows visualization of pore structure, cracks and dissolution textures in polished sections using back scattered electron (BSE) images. The white colour in the images corresponds to pores filled with the alloy. BSE shows that interconnected porosity is characteristic for all samples from Unzen volcano, where a marked tortuosity of the pores is visible. The intrusion of the alloy results in an excellent contrast for the layer silicates, suggested a chronological sequence of formation of chlorite. Altered rims of amphibole, which contain chlorite, have very high porosity while the cores, formed mainly by carbonates, are very dense.

3D microtomography and image analysis

X-ray tomographic microscopy approach, based on a synchrotron-based light source, provided a possibility for 3D visualization of natural and experimental samples with a high spatial resolution of 0.4-0.7 µm voxel size. The assignment of different areas obtained by cluster analysis to pores and mineral phases was based on microscopic observations and the amount of carbonates and pores quantified in the samples. Carbonates are not only observed in altered hornblende phenocrysts but also finely distributed in the matrix of the rock. The pore volume was found to be underestimated by image analysis. For the sample shown in Figures 3 and 4, pore volume determined by Hg-porosimetry is 3.2 vol.%, whereas with image analysis it is only one third of this value. This underestimation can be assigned to the fact that small pores less than the pixel width of 350 nm and pores, which were not fully imaged within one pixel, are not detectable by image analysis. Nevertheless the coarser pores which might be of highest importance for mass transport can be visualized.

3-D tomography and subsequent image analysis from dacitic samples resulted in a relatively high number of separate pore systems which is in opposite to the findings by Wood`s metal intrusion, where pores were observed to be well connected. Obviously the X-ray tomographic microscopy approach, even performed in a synchrotron-based light source with a relatively high spatial resolution of 0.7 µm pixel width is not sufficient to resolve small pore spaces and, hence, only larger pores are represented. Although the separation of pores is apparently excellent in the greyscale histograms, some uncertainty for their quantification arise if voxels share pores and minerals in addition to noise due to the physical property of the tomographic apparatus. Small pores less than the voxel size of 0.73 µm and pores which were not fully imaged within one voxel are not detectable by image analysis. According to mercury porosimetry samples have high shares of pores below a pore radius of 0.1 µm, suggesting that only the coarser fraction of pores is imaged by tomography. Out of this reason, relatively high numbers of separate pores were observed and porosity, quantified by tomography tends to be underestimated. Here more sophisticated methods such as the Focused Ion Beam (FIB) technique combined with high resolution scanning electron microscopy may help to improve visualization of fine pore structures.

Analyses of stable isotopes

The investigated amphiboles exhibit a quite homogeneous oxygen isotopic composition, with their $\delta^{18}O$ vs VSMOW varying between 6.6 and 7.0‰. Considering that the $\delta^{18}O_{VSMOW}$ of recent and historic dacite lava at Unzen varies between 8.0 and 8.9‰, the measured $\delta^{18}O_{VSMOW}$ values point to a primary magmatic origin of the hornblende. From oxygen isotope analysis alone, however, we cannot exclude secondary alteration of the hornblende at low water/rock ratios, because at low water/rock ratios the oxygen isotopic composition of the exchanging hornblende would remain unaffected.

The carbonate carbon isotopic composition varies between –4.7 and –6.4‰ vs VPDB, whereas its oxygen isotopic composition ranges from 6.0 to 9.1‰ vs VSMOW. Carbonate $\delta^{13}C_{VPDB}$ values are identical to those measured for the magmatic CO_2 discharging at Unzen volcano ($\delta^{13}C_{VPDB}$ = –3.9 to –6.4‰; Ohba et al., 2008; Shinohara et al., 2008), whereas carbonate $\delta^{18}O_{VSMOW}$ values are indistinguishable from those reported for fumarolic water vapor (7.4‰ < $\delta^{18}O_{VSMOW}$ < 10.0‰; Ohba et al., 2008) and primary volcanic rocks (6.9‰ < $\delta^{18}O_{VSMOW}$ < 8.9‰, Ohba et al., 2008). Carbonate $\delta^{18}O_{VSMOW}$ values are, however, different from those characteristic for the local meteoric water ($\delta^{18}O_{VSMOW}$ ~ –6‰; Mizota & Kusakabe, 1994). It, therefore, appears that magmatic CO_2 and primary silicates provide the sources for the carbonate carbon and carbonate oxygen, respectively.

Hydrogen isotope composition of unaltered amphiboles shows typical magmatic signatures (δD= –48‰) without any evidence for late- or post-magmatic contamination by

meteoric waters. The analysis of several altered samples showed in general homogeneous isotopic composition for each sample and indicates that presumably chlorite or matrix glass are the main water-bearing phases in samples (the bulk δD values vary in the range from –84 to –92‰). The high δD values for the alteration products are difficult to explain by reaction of magmatic amphiboles with magmatic water. Most likely the hydrogen signature is caused by meteoric water. However, the data base for hydrogen isotope fractionation at low temperature is poor and, hence, we can not completely rule out a magmatic origin of water bond in alteration products.

Carbonation reactions at hydrothermal conditions

The results of a series of experiments in different systems, i.e., dacite or pure amphibole + H_2O, $H_2C_2O_4{\cdot}2H_2O$, $Ag_2C_2O_4$, Pl, $CaCO_3$ in different proportions conducted at T=150–700°C and at P=100–500 MPa show that amphiboles do participate in exchange reactions with the formation of new mineral phases. However, the efficiency of carbonation reaction on amphiboles is relatively small and only tiny carbonate phases could be qualitatively identified by EDX (Fig. 6a).

Raman spectroscopy confirms that carbonates are indeed present as secondary phases in altered products (Fig. 6b) and new phases on the surface of amphibole crystals after hydrothermal experiments (Fig. 6c) have spectral characteristics similar to natural calcite. However, more work is needed to optimize the spectroscopic method for analyses of the small phases in experimental products.

The effective diffusion of water in porous Unzen volcanic rocks is 2 - 3 orders of magnitude slower than the diffusion of protons and 1.5 – 2.5 orders of magnitude slower than diffusion of H_2O and D_2O in liquid water (Mills, 1973), indicating that porosity and pore characteristics exsert a significant control on the efectiveness of mass transfer in volcanic rocks.

References:
Mills, 1973; Mizota and Kusakabe, 1994; Ohba et al., 2008; Shinohara et al., 2008.

IODP

The End of the CO2–Age with first Steps towards Earthquake–Prevention as Side–Effect

PETER P. SMOLKA

[1]University Münster, smolka@uni–muenster.de

Warm El–Nino–type tropical oceans in co–existence with arctic sea–ice produce cold snow–rich winters on northern hemisphere continents, similar to pliocene conditions. A mild effect of this was seen in winter 2010/2011. An approach to Pliocene conditions with large permanent El Ninos in coexistencewith Arctic sea ice will become unaffordable. The same applies to large volcanic eruptions or meteoritic impacts (YD) and their impact on energy–costs.

Limited fossil fuels, including Uranium (40 years), require replacement of nuclear energy and coal. Therefore an unlimited cheap source of energy is provided by ultra–deep wells (10–14 km, in Japan 50–70 km possible) with a large diameter (2 m) that are drilled by melting an outer ring of 2 cm, three segments 120° each, cutting the base every 3–9 meters and transporting the core–segments in a row, one after the other, by a stafette–system that runs at the wall (no drill–string needed). Wall–segments and other material, including cooling–substances for the electronics, are transported by the stafette–system downward. The drilling–device runs without moving parts. Based on the melting–energy for beta–quartz and the respective number of moles of the slim ring, the slim three radii and a slim base that is cut off every about 3 meters, only about 30000 MWh electricity are needed to drill 10 km at a speed of 1 m/min. The speed is limited by the stafette–system. Limiting agens is only the temperature, not the depth (no friction of a drillstring, very low steel–costs).

In geothermally cold areas with 300°C at 10 km depth 100 MW are produced by one large main–well and 200–300 sidetracks each at 4 km length and 0.5 m diameter. At 3 Ct/kWh downpayment (current steel–costs) is done in about 4 years if an old coal or nuclear powerstation exists or 7 years if everything must be new such as in Fukushima/Japan. Afterwards costs are below 1.8 Ct/kWh.

The water/steam flows in a closed(!) system. Because there are no fracs of the rocks no(!) (small) earthquakes occur.

The needed large surface (to compensate low thermal conductivity of rock) is arrived at by the many sidetrack–wells. If the steel–wall is left away (toothrails for the stafette–system) plus steel–net against rockfall, costs and thermal properties optimize.

Economic deep geothermal wells can thus be drilled almost anywhere, also in NW Europe (submitted/pending German and one US patent(s)).

Heat–exchangers can after electricity–generation cool the steam down. This way the steam can be used for heating cities, also in geothermally cold areas (no heatpump needed, just using steam in Germany as in Iceland): Dependency on oil for heating can reduce. Oil will thus last longer.

What is disastrous for energy–generation, releasing tensions and creating earthquakes, can be used technologically: In regions with tectonic tensions (California, Japan, Haiti, Auckland) by pressing water or, in deep settings, a cheap liquid metal into rock, fracs, that weaken the rock, can be induced intentionally. If the rock is weakened sufficiently, then normally an earthquake is released, as is observed sometimes in connection with production from gas–fields. Thus tensions can be released *controlled* by many small earthquakes or even changed *controlled* to creep. By using a few very deep main–wells and many sidetrack–wells this is economically feasible (saved costs of destroyed cities).

As the limiting agens for the new drilling–method is only the temperature (no friction by a drill string, no mechanical forces), by using high–tech ceramics as wall–segments, 650–750 °C (seismogenic zone in Japan) can be reached in a second step.

First such experiments should be done in Japan as there houses are built strong. Releasing a bigger earthqake by error will in Japan not cause problems. In addition a first such experiment can be done in Haiti: In the 17th century two big earthquakes ocurred in about 20 years distance. Now again only a part of the tensions is released. In addition rebuilding is slow. If, by such an experiment, tensions are released intentionally while people still live in tents, a possible error will be no problem too.

Released tensions in one place may build up tensions "further down". Thus in the future detailed large–scale FEM studies, that will require large 3D datasets, will be needed. This way progress in many fields will be enhanced by this method.

By this method, creating intentionally many small(!) earthquakes/creep by a few big (cheap) main wells and many (cheaper) sidetrack–wells in the future catastrophic earthquakes / tsunamis might be avoided by changing them to many small earthquakes. In case of open–hole solutions (toothrails plus steel–nets against rockfall) thermal properties and costs can be enhanced as well. To reduce costs for earthquake–prevention the respective wells can be used in addition for electrcity–generation and heating.

For the IODP/ICDP the same method (melting a very slim outer diameter, cutting the base off every 9 meters) can be used to build a piston–corer for high–quality cores in hardrock. Thus drilling the Moho (one of the launching–targets that lead to the DSDP) at a high quality, in case of non–ductile rocks, comes now into reach. The tool will be pushed down while melting without any rotation like a slow piston–corer. Vertical push–forces can be generated by the lowest segment directly above the corer. Befoore "cutting" (melting) the base off the core can be held by short needles or ribbons that pierce from the wall of the core–barrel. This way the base–part can operate without vertical forces (feasibility). By using ionprobe–microbveam arrays andor spectral libraries (incident "normal" / "polarized" light) core–analysis can be semi–automated. This way large datasets that are needed for future 3D FEM–studies, much later in connection with mantle models, come into reach. As the earths mantle is much larger than the atmosphere experience from climate modeling / paleooceanography can be used for future mantle models.

IODP

The partial decoupling of source and sink in the current-controlled sediment dispersal systems on the East African and Northern Madagascar continental margin – The Agulhas Current Depositional Systems and the SAFARI Proposal

V. Spieß[2,1], B. Preu[1], S. Wenau[2,1], T. Schwenk[2,1], L. Palamenghi[2], R. Schneider[3]

[1]MARUM – Center for Marine Environmental Sciences, University of Bremen, D-28359 Bremen, Germany
[2]Department of Geosciences, University of Bremen, D-28359 Bremen, Germany
[3]Institute for Geosciences, Christian-Albrechts-Universität zu Kiel, D-24118 Kiel, Germany

The relationship between a sedimentary deposit and the source of its accumulated particles is intimately linked to the processes of transport. While classical river-delta-slope systems are quite common, the presence of coast- and slope-parallel current systems can modify sediment dispersal patterns significantly. In front of river systems, shelf currents may lead to non-deposition on the shelf, may result in a shift of maximum sediment transport across the shelf break and again in a slope-parallel shift of the depocenter on the upper slope. As a function of current patterns on shelf and slope, current strength, sea level, shelf morphology and riverine sediment input, the resulting dispersal pattern can reveal a high degree of complexity. It may even lead to an almost complete decoupling of sediment source and depocenters on shelf, slope and in basins.

As a result of a recent IODP pre-site survey (SAFARI, Hall et al.) on the East African continental margin off Mozambique and Madagascar during R/V Meteor Cruises M63/1 and M75/3, sedimentary deposits were investigated with high-resolution multichannel seismics, sediment echosounder, multibeam and acoustic water column imaging to study the impact of the Agulhas and Madagascar currents on the slope sedimentation.

Widespread contourite bodies on the upper and middle slope as well as stationary eddy systems related to the continental margin structure have controlled presence and shifts of depocenters during the last 15 million years, revealing a rich history of current activity as part of the global conveyor belt in conjunction with the storage of terrestrial signals from riverine sources. Deciphering these archives, however, will require an advanced understanding of the sediment dispersal from seismoacoustic mapping of sedimentary units.

First results from several study areas reveal also an intimate link between changes in sea level and sediment dispersal, being further complicated by the persistence of widespread continuous Pleistocene dune fields on the inner shelf off Limpopo, which seem to a larger extent inhibit sedimentation on the upper slope, guiding sediment onto an outer terrace, where sedimentation occurs under strong control of the Agulhas current. Off the Mozambique river, a wider shelf, starved of sediments, supports the NE-directed sediment transport, feeding the Mozambique Channel as well as the Madagascar contour current, which in turn builds up widespread contourites in front of the Mozambique river. While the contourites accumulate mainly due to the shape of the shelf break, they lack a causal relationship to the riverine input. On the Northern Madagascar slope, strongest interaction of terrigenuous sediment input occurs in intermediate water depths, where complex drift bodies develop in the vicinity of major canyon systems.

With respect to the SAFARI drilling proposal, which traces the Agulhas current southward from the Mozambique Channel towards Capetown, the widespread occurrence of contourite bodies, suitable for deep drilling, is favourable due to the mixing terrestrial signals into the marine archive with these contourites. To establish a precise relationship between terrestrial source and depositional sink, an understanding of the acting processes is crucial, and may only be established by a dedicated geophysical and geological investigation, as it had been carried out for the northern SAFARI sites.

IODP

Authigenic Mn-Fe-rich contaminant phases on foraminiferal tests: Possible implications for Pliocene and Miocene Mg/Ca temperature reconstructions

S. STEINKE, C. KWIATKOWSKI, J. GROENEVELD

MARUM – Center for Marine Environmental Sciences, University of Bremen, Leobener Strasse, 28359 Bremen, Germany

One of the most common techniques being used to reconstruct sea surface temperatures (SST) is Mg/Ca of planktonic foraminiferal shells. Uncertainties in interpreting Mg/Ca data can arise from post-depositional, selective/partial dissolution and salinity effects on the shell Mg/Ca ratios. In addition, the occurrence of syn-sedimentary and post-depositional Mn-Fe-rich oxyhydroxide precipitates and Mn-Fe-rich carbonate coatings can exert a significant control on Mg/Ca ratios, resulting in elevated Mg/Ca ratios and by inference overestimated SSTs. For that reason, rigorous cleaning procedures have been introduced to remove secondary contaminant phases e.g. clays and/or Mn-Fe rich coatings, potentially present on foraminiferal shells (e.g. Boyle, 1983; Barker et al., 2003).

Non-reductively cleaned Miocene samples of Ocean Drilling Program (ODP) Site 1146 (northern South China Sea) show average Mn/Ca ratios of 1.41 mmol/mol and average Fe/Ca ratios of 0.85 mmol/mol. Similarly, non-reductively cleaned Pliocene samples of ODP Site 999 (Caribbean Sea) show average Mn/Ca ratios of 1.70 mmol/mol and average Fe/Ca ratios of 0.30 mmol/mol. These values are distinctly higher than the 0.1 mmol/mol Mn/Ca and Fe/Ca ratios given by Barker et al. (2003) for clean, uncontaminated foraminiferal tests. Although high Fe/Ca ratios were detected, it is assumed that the Mg/Ca analyses were unaffected by contaminant clay particles because Al was found to be under the detection limit of the ICP-OES technique. Instead, high Fe/Ca and Mn/Ca ratios might be the result of Mn-Fe-oxyhydroxides and/or Mn-Fe carbonates present on the planktonic foraminiferal tests (e.g. Boyle, 1983).

We have performed different cleaning experiments including an additional reductive cleaning step in order to test the potential influence of Mn-Fe contaminant phases on the Mg/Ca temperature estimates. The reductive cleaning step was performed after the oxidative step of the Barker et al. (2003) cleaning procedure. In a first experiment, as a reductive cleaning reagent a mixture of hydroxylamine and sodium acetate solution has been used. In a second experiment, we used a hydrazine/ammonium citrate solution as a reductive cleaning reagent. The results of the two experiments using an additional reductive cleaning step revealed a 6.1–21.7% and 5.9-14.0 % decrease in Mn/Ca and Fe/Ca, respectively, when compared to the non-reductively cleaned samples. More importantly, no clear difference is seen between "non-reductive-cleaned" and "reductive-cleaned" samples in terms of Mg/Ca ratios of the different experiments. Therefore we suggest that our Mg/Ca ratios and thus our Pliocene and Miocene SST estimates are not contaminated by Mn-Fe-oxyhydroxides rich in Mg and as such, there is no a priori reason to include an additional reductive cleaning step for these samples. Our experiments further indicate the presence of Mn-Fe-rich phases present on the foraminiferal that cannot be fully removed with our applied cleaning procedure. Our experiments do not exclude that (1) additional phases which are not removed with these cleaning steps, like Mn/Fe-carbonates, could affect the Mg/Ca, (2) reduction is able to remove Mg-rich contaminant phases in sediments from different settings (Pena et al., 2005).

References:

Barker, S., Greaves, M., Elderfield, H. (2003). A study of cleaning procedures used for foraminiferal Mg/Ca paleothermometry. Geochemistry, Geophysics, Geosystems 4, doi:10.1029/2003GC000559.

Boyle, E.A. (1983). Manganese carbonate overgrowths on foraminifera tests. Geochimica et Cosmochimica Acta 47, 1815–1819.

Pena, L.D., Calvo, E., Cacho, I., Eggins, S., Pelejero, C. (2005). Identification and removal of Mn-Mg-rich contaminant phases on foraminiferal tests: Implications for Mg/Ca past temperature reconstructions. Geochemistry, Geophysics, Geosystems 6, doi:10.1029/2005GC000930.

ICDP

The climatic, volcanic and geodynamic evolution of the Lake Van-Nemrut-Süphan system (Anatolia) over the past ca. 550-600 000 years
A progress report based on a study of the products of explosive volcanism on land and in the lake

M. SUMITA[1], H.-U. SCHMINCKE[1], PALEOVAN SCIENTIFIC TEAM

[1] Helmholtz-Zentrum für Ozeanforschung (GEOMAR), Wischhofstr. 1, 24148 Kiel, Germany

Introduction

Alkaline Lake Van and adjacent active stratovolcanoes Nemrut and Süphan represent a coupled system that evolved over ca. 550-600 000 years. The origin and evolution of the closed lake basin and the climatic history reflected in its sediment fill cannot be understood and reconstructed temporally at high resolution without broadly understanding that of both volcanoes, especially that of Nemrut, the volcano having supplied much of the ca. 20-25 % of volcanic fraction in the drilled sediments. The importance of tephra layers for the Paleovan drilling project lies in (a) their enormous stratigraphic value, (b) basic information to infer erupted magma volumes and reconstruct paleowind directions, (c) correlating sediments between holes and drill sites via distinct tephra layers, (d) establishing a temporal framework ($^{40}Ar/^{39}Ar$ ages of alkali feldspars), (e) supply of alkali elements from the unstable glass and probable CO_2-degassing to the lake pore water and (f) suggesting complex genetic and temporal relationships between geodynamic activity, especially earthquakes and volcanic eruptions thus aiding hazard assessment of the area.

Our project encompasses 2 major subprojects: (A) a pre-site survey focussing on documenting the explosive evolution of both volcanoes and (B) analysis of the cores drilled into Lake Van in 2010 at Site 1 (Northern Basin: 142 m blf) and Site 2 (Ahlat Ridge: ca. 218 m blf).

Work on subproject-A preceded that on subproject-B to provide basic stratigraphic/compositional and temporal patterns of explosive volcanic activity that occurred throughout the entire sediment column drilled to basement.

In other words, the success of subproject-B with respect to the items listed above depends significantally on the results of subproject-A. Field and laboratory work in subproject-A will be largely completed in 2012 while that in subproject B began with opening and sampling of the cores in January-February 2011 and is our present focus.

Our combined contributions of subprojects -A and -B to the Paleovan Project include:

Mass, composition, distribution and facies of tephra in the cores of sites 1 and 2

Most of the tephra that is easily recognizable macroscopically, occurs as distinct layers a mm or less to, more rarely, a few cm thick, sandwiched in fine-grained laminated/varved or turbiditic sediments. We are presently revising a list of ca. close to 300 tephra layers proposed by Stockhecke (pers. comm. 2012) for Site 2 and estimate the total to be close to 350. In view of the higher abundance of tephra layers in the Site 1 cores (see below), the total number of discrete explosive events over the past ca. 550-600 000 years recorded in Lake Van probably exceeds 500 which would translate into 1 explosive eruption/1 ka. Because microtephra studies have not yet been carried out by us, this is a minimum number, also considering that tephra from an unknown number of explosive eruptions were not deposited at sites 1 and 2. Two eruptions from Nemrut occurred in historic times.

A few thick tephra units, some up to several m thick, consist dominantly of pumice lapilli generally <5cm in diameter, rock fragments and variable amounts of ash-sized tephra. Some intervals are represented by drilling gaps, the largest one up 15 m thick (holes 2D, 2F, 2G) between ca. 117 and 132 m blf, because of nonrecovery of unconsolidated pumice lapilli. The gap also shows up very well in the logging data (Wonik et al. pers. comm. 2012). One prominent basaltic hyaloclastic tephra unit drilled at Site 2 is up to 4.63 m thick at Hole 2B (including the slumped part), 2.01 m thick at Hole 2D and 2.02 m thick at Hole 2E.

Turbidites are mostly <10 cm but some are up to several dcm thick. They make up >50 % of the drilled sediments at Site 1 and are the reason why overall sedimentation rates at Site 1 are about 3-4 times (>1 m/1ka) those at Ahlat Ridge (0.25-0.5 m/1ka) as deduced by correlation of distinct tephra layers between sites. Turbidites also dominate in some cores at Site 2. Turbidites studied by us (grain size, lithology) consist largely of volcanic particles. The total number of turbidites in the 142 m cored at Site 1 is estimated as ca. 800. By taking into account non-recovered intervals, the total number of volcaniclastic turbidites generated over ca 100-110 ka (our present age estimate of the drilled base at Site 1) may exceed 1000. The turbidites are interpreted to have generally been generated by downslope slumping of tephra accumulated higher up on the slope. Earthquakes and tectonic movements along the boundary fault of the northwestern edge of Lake Van are plausible triggers of turbidites, as are major storms and excess sediment supply from rivers and temporarily active canyons as also reflected in rounded clasts in some. Turbidites consisting of homogeneous angular pumice lapilli and compositionally homogeneous shards may, however, be the direct result of eruptions, resp. eruption-related slope overloading. Some turbidites are interpreted as being transformed from pyroclastic flows and debris avalanhes that entered the lake. There are turbidites including abundant ostracodes probably transported from shallower parts of the lake.

Contrasting tephra accumulation in Site 1 vs. Site 2. Tephra layer T-16 of the short cores (Sumita et al., 2008), with a varve age of ca. 13.585 a (Heumann, pers. comm. 2011) occurs at 6.2 m blf (Hole 2A (6.33 m at Hole 2D) but at 20.27 m blf at Hole 1A (20.78 m at Hole 1C) reflecting sedimentation rates ca. 3.5 times those at Site 2. The number of tephra layers is estimated as about twice as high at Site 1 (ca. 30) than at Site 2 (16) in this interval. Moreover, the thickness of discrete tephra layers is greater at Site 1 compared to Site 2 with the possible exception of tephra layers derived from Süphan. There are several reasons for this contrast. For one, the northern basin is much closer to the maximum thickness (fan axis) of many fallout fans sourced in Nemrut volcano as determined from land data, SW wind directions having dominated in the past (see below). Secondly, individual tephra layers are also better preserved in the northern basin than at Ahlat Ridge where they would have been prone to removal by erosion more easily while rapid burial by turbidites would have favored their preservation at Site 1.

Discrete sub-mm tephra layers (microtephra) occur in the cores but the very time-consuming detailed analysis and documentation of their number and composition is deferred priority being to analyze the overwhelming number of macroscopic tephra layers.

An unknown mass of dispersed tephra in the very fine ash (silt size and smaller) fraction is contained in background carbonate sediments as documented by variably replaced very small glass shards that we have recognized microscopically. Whether or not the breakdown products of the glass have significantly influenced pore water compositions or not is uncertain (see also below).

Clearly reworked older volcaniclastic sands making up the basement sediments at Site 2 in the freshwater section are derived from older volcanics resp. volcaniclastic sediments (see also below).

The total mass of volcanic particles in the sediment column at both sites is estimated to amout to roughly 20-25 % by volume, also taking into account drilling gaps, no recovery being generally due to thick pumice-rich tephra units.

Composition and source of tephra in the sediments

Several mostly trachytic-rhyolitic (Nemrut) resp. dacitic-rhyolitic (Süphan) and minor more mafic major fallout and pyroclastic flow deposits have been recognized in the cores by (1) sedimentological characteristics (grain size, thickness etc), (2) distinct mineralogical and chemical compostion and (3) stratigraphic position. The ages of such prominent marker beds are inferred from the age of the correlative land deposits dated (subproject-A).

Nemrut volcano (alkaline to peralkaline, intraplate) has probably supplied more than 90 % of all tephra particles in the cores.

Tephra derived from Süphan (subduction-related composition) is of lesser volume but has been recognized throughout the cores.

Huge basaltic Incekaya system straddling the southwestern boundary land-lake and depositing a >2 m thick hyaloclastite layer in the lake ca. 25 km from source

Intralake eruptive centers of intermediate to trachytic composition.

Tephra sourced in distant eruptive centers, e.g. central Anatolia or even the eastern Mediterranean area has not yet been definitely recognized but is suspected to be represented by several white very fine-grained ash layers.

Transport and depositional mechanisms of tephra deposited in the lake

On land we have now recognized some 40 distinct fallout tephra units – compared to none known prior to subproject-A – and some 12 ignimbrites (pyroclastic flow deposits) compared to about 2 mentioned in the literature. Moreover, we have found impresssive debris avalanche deposits close to the lake shore at the foot of both volcanoes. Dominantly wind-reworked fine-grained intervals separate tephra layers in all land sections and represent a major source for reworked volcanic particles in lake Van.

Fallout deposits in the drilled sediments are most easy to recognize, many showing inverse size grading because of the lower settling velocity of pumice lapilli compared to crystals and rock fragments. The interpretation of thin fine-grained apparent fallout tephra layers as deposited by (1) airborne fallout following explosive eruptions, (2) fallout from co-ignimbrite ash clouds, (3) distal turbidites generated by either pyroclastic flows or (4) debris avalanches, (5) grinding within pumice rafts (see below) or by (6) wind transport (reworked) is generally difficult and under study.

Pyroclastic flows entering a water body are known to separate into several fractions traveling on the lake bottom (dense bed load), suspension part sheared-off the bedload at changes in bottom gradient and above the water surface (highly dilute fraction). A major separation already occurs on land between an ash cloud (co-ignimbrite) traveling close to ground but above the main hot bed load. These ground-hugging ash clouds may also separate from the bed load and spread along the lake surface but can also rise many kilometers to tens of km into the atmosphere prior to settling. Fine tephra may also move close to the seabed together with pumice lapilli populations of the proclastic flow which is transformed into turbidite under water. In any case, both pumice lapilli and ash-sized tephra may eventually be sedimented together resulting in highly complex facies. We correlate two prominent thick marker beds recovered to Upper Pumice (UP) (ca. 30 ka old) and Lower Pumice (LP) (ca. 76 ka). UP (3-4 m thick) occurs at ca. 60 m blf at Site 1 and 15 m blf at Site 2. LP occurs at 100 m blf at Site 1 and 30 m blf at Site 2 and is 1.5-2.7 m thick. Both are interpreted by us as having resulted from both fallout and pyroclastic flow.

Pumice-raft-generated fine-grained tephra deposits. A new type of fine-grained tephra is here proposed based on our study of UP, LP and other units. Pumice from fallout or flows is known to form closely-packed pumice rafts on the surface of the sea or lakes. The constant abrasion - accentuated in the Lake Van basin because of the strong wind fields postulated by us as reflected in common narrow tephra depositional lobes - produces significant rounding of pumice lapilli, the abraded fine-gained tephra settling to the bottom earlier than water-logged pumice. Pumice rafts must have formed many times on the surface of Lake Van following each major explosive eruption. Basic conditions for the formation of sustained rafts are (a) the large volume of many fallout eruptions, thicknesses exceeding 10 m in the near-shore area, and (b) sustained supply of pumice to the lake by washing down from the steep mountains enclosing much of the lake basin except at its eastern end. Such pumice rafts could have covered the lake surface for years and must have been very productive mills for generating abundant fine-grained tephra. Pumice rounding in both UP and LP and older pumice deposits in the cores and associated fine-grained tephra is tentatively interpreted by us as representing such raft deposits.

High-resolution dating of the Lake Van sediment column, correlation with the global MIS framework, clustering of volcanic eruptions in time, preceding seismic unrest and hazard implications

Of prime interest to the Paleovan consortium is a precise age structure of the sediment column in order to allow direct correlation with the global MIS framework and thus to be able to date climate changes at high resolution. In our experience, the complexity of obtaining well-supported precise physical ages is commonly not entirely appreciated as reflected in the not uncommon failure of scientists and groups who neglect to follow the basic rules of a fundamental approach essential to reliable dating.

A solidly based and high-resolution age framework of the sediments drilled cannot be derived from the tephra layers drilled, for several reasons. Alkali feldspars of sufficient size, composition (radiogenic yield), amount and quality (freshness, absence of inclusions, lack of strong zoning or corrosion etc) are not present in 90% or more of the tephra layers drilled, most layers being in the mm thickness range. Moreover, distinguishing unequivocal primary from reworked and contaminated tephra layers requires painstaking work, not uncommonly with ambiguous results.

For these reasons, the essential prerequisite for building up a reliable age framework of the cores is to first carefully work out a tephrostratigraphic framework in the cores based on a range of criteria (thickness, grain size, qualitatiave and quantitative mineral assemblages, glass and bulk chemical composition etc) which is in progress, some major markers dated on land having already been identified in the cores. Correlation of the core-based tephrostratigraphy so derived with the reconstructed and dated onland tephrostratigraphy (now nearing completion) will then allow a preliminary temporal structure of the core. This framework is then adjusted by dating those drilled tephra layers that contain a suitable alkali feldspar suite (age data of the next batch of more thoroughly treated and selected alkali feldspars across the cores submitted in September 2011 being expected to be completed in March/April 2012). The time from opening the cores (February 2011) to being able to present a well-founded high resolution temporal framework throughout the entire sediment column drilled that allows fine-scale correlation to the MIS scale takes 2-3 years.

Earlier in 2011 we have obtained ages from only marginally suited cc samples (small sample size, rough treatment of core catcher samples) from the lower ca 70 m at Site 2 available prior to core opening, ages ranging from ca. 330 to ca. 570 ka. These preliminary ages – with high standard deviations on account of the quality of only moderately suited samples – , first presented by us to the Paleovan community in June 2010 – enabled many groups in the Paleovan consortium to seriously begin to speculate

on identifying marine isotope stages in the entire sediment column drilled, briefly published in EOS (Litt et al. 2011).

Tephra layers are not distributed statistically, neither in the field nor throughout the cores but occur in clusters suggesting distinct periods of eruptive swarms lasting hundreds to thousands of years separated by periods of reduced explosive activity. We interpret this episodic explosive volcanic behavior as being basically controlled by magma production/supply rates modulated and triggered by e.g. regionally controlled (North Anatolian fault system) tectonic and by seismic activity.

An excellent example is a group of up to 5 (Site 2) to 7 (Site 1) tephra layers a few mm to ca. 40 mm thick, the thickest occurring in the lower center of the group, which were laid down through a time interval of ca. 1000 years (varve ages, Heumann pers. comm 2011). This cluster of tephra layers is compositionally clearly derived from Süphan based on glass composition and abundance of biotite phenocrysts while tephra layers stratigraphically above and below are dominantly Nemrut-derived (Sumita et al. 2000). Nonvolcanic sediments underlying this cluster show small-scale faulting interpreted by us as caused by seismic shocks, the zone of deformation ending in Hole 2E at ca. 6.03 m blf. The distance between the lowest tephra layers of the Süphan cluster and the estimated top of the deformation zone is 45 cm. The zone of deformation begins in 2E at ca. 20 m blf but is especially prominent between 14 and 8 m blf. We tentatively interpret this deformation as caused by regional earthquakes that preceded the eruptions of Süphan volcano by several hundred years and may have activated the rise of magma pockets to higher levels in the edifice.

Our data show that Süphan volcano - in contrast to Nemrut - is characterized by small-volume explosive eruptions of phenocryst clots-rich dacite/andesite and an extreme disequilibrium mineral assemblage, interpreted as resulting from a complex magma chamber/magma pathway structure and small magma reservoirs as well as the high viscosity of the magmas due to high silica and abundance of phenocrysts. In other words, the volcano appears to grow preferentially from within by subvolcanic intrusions and domes, a behavior also reflected in large-volume debris avalanche deposits interpreted as due to more common flank oversteepening by subvolcanic intrusions. We speculate that the dominance of turbidites in the sediments drilled at Site 1 may be related to the dynamic behavior of Süphan volcano.

In stark contrast, Nemrut explosive products throughout the past at least 400 ka are characterized by equilibrium phenocryst assemblages and low viscosity alkaline to peralkaline magma compositions. The episodicity of large-volume mostly rhyolitic explosive eruptions at 20-40 ka intervals separated by smaller trachytic eruptions may indicate a dominant mode of relatively constant magma supply from depth, periods of small-volume moderately high differentiation punctuated by episodic large volume eruptions of highly evolved magma having accumulated to a critical threshold volume.

In other words, eruptions of Nemrut may be triggered preferentially by internal forcing while we tentatively interpret the cluster of (small) Süphan eruptions over ca 1000 years (see above) as generated by external triggers possibly related to preceding long lasting earthquake activity.

We speculate that the probability of future explosive eruptions especially of Süphan volcano has increased following the devastating magnitude 7 earthquake on October 24 2011 in the viciniy of the city of Van.

Secular changes in tephra layer/mass supply and/or composition throughout the cores (Site 2)

Changes in source location and composition of tephra throughout the past ca. 550-600 ka drilled could provide (a) important clues for the overall volcanic evolution of the area, (b) change in supply of highly alkaline fine-grained tephra as factors influencing water composition, (c) wind direction and (d) tectonic evolution of the lake basin.

Incomplete data at hand suggest that basaltic hyaloclastites are most common in the lowermost ca 30 m at (Site 2), the initial fresh water stage of Lake Van. These basalts are probably mostly locally derived from centers within the lake which, however, might have been much smaller at that stage, intra- and extralake eruptive centers being then difficult to distinguish from each other. The ability of dense (Fe-rich) basaltic magma to erupt at the surface commonly decreases with the evolution of large evolved volcanoes because of the density lid building up over time in the main central magms reservoir (Nemrut system). We thus speculate that the relatively high abundance of early basalt tephra does indeed mirror an early growth stage of Nemrut volcano.

Overall tephra supply – except for the likely local derivation (see above) – appears to increase in time irregularly from the lower part of Site 2 (ca. 150-200 m blf) to the upper 50 m. This evolution most likely mirrors the development of the adjacent volcanic systems. If supported by further especially compositional and age data, this would indicate a strong temporal and genetic link between the birth and growth of Nemrut volcano and Lake Van.

Nature and age of the basement drilled at site 2 and age and origin of the closure of the lake Van basin and thus the onset of the alkaline soda lake development: volcanic or tectonic forcing?

The rounded polymict clasts of the basal slightly consolidated and well-sorted epiclastic fresh water volcanic sediments at the base of Site 2 petrographically resemble the >200m thick strongly faulted continental red beds on which the town of Ahlat has been built. These sediments vary strongly lithologically but consist basically of reworked and variously altered volcanic and subvolcanic rock fragments and single crystals varying widely in composition.

Single feldspar crystals from the basal sand drilled yielded ages ranging from ca 2 to 16 Ma, in accord with, and slightly extending, the age of Miocene volcanics erupted over wide areas in eastern Anatolia north of Lake Van, previously thought to be no older than 12 Ma (Pearce et al., 1990).

The composition of this basement suggests that the floor of lake Van in this area was faulted down by several hundred meters (and subsequently (?) uplifted to form Ahlat Ridge).

The boundary between the Miocene continental sediments and the metamorphic Bitlis Massif directly south of the lake must thus lie further south in the lake.

Major climate changes caused e.g. by uplift of mountain belts such as the Andes or Himalaya are well known illustrating that evaluation of geodynamic aspects is not peripheral in a research project with a paleoclimate

mandate. The cause and timing of isolation of Lake Van – and of the tectonic basin in general - has been one of the main issues in previous Lake Van studies. No convincing model has, however, been proposed sofar. Previous speculations that eruption of a lava flow (e.g. Degens et al., 1984) from Nemrut volcano cut off the drainage to ancient Murat river, a tributary to Euphrates, was never substantiated. During the early stages of this project we have speculated (Sumita and Schmincke 2010) that, instead, thick ignimbrites underlying the high plateau south of Tatvan and the Muş Basin and a debris avalanche from Kirkor dome cut off the outlet of an ancient river. Kuzucuoğlu et al. (2010) thought that a former outlet of Lake Van was dammed by an ignimbrite c. 100-130 ka ago. Our discovery of uplifted carbonate sediments interlayered with tephra (ca. 220 ka old) along the 5 km long Halepkalesi tectonic belt (Sumita and Schmincke, 2011) clearly shows, however, that lake alkalinity and thus isolation of the lake must have developed long before 200 ka.

Based on the oldest ages of subaerial tephra from Nemrut obtained by us so far and our ages from the lower part of the sediment sequence drilled at Site 2 makes us think that growth of the entire Nemrut edifice including its prograding flanks in the hinge area between the Muş and Van pull-apart graben structures caused the isolation of the Van Basin and consequently its alkalinity, inception of the isolation of the lake basin thus dating to ca. 450-500 ka.

Paleoclimate proxies inferred from onland tephra deposits and precise dating of climate oscillations reflected in fast rise and fall of lake level.

Paleoclimate proxies in widespread land-based tephra deposits are especially valuable in the case of the Van system because climate evolution mirrored in these proxies is representative for much larger regions than the lake basin and some such as prevailing wind directions are only poorly mirrored in the sediment cores.

Reconstruction of approximate dominant paleowind directions based on the axes of partial isopach maps of 15 fallout lobes reflect dominant SW-NE paleowind directions over the past 300 000 years but more westerly directions also occur, possibly especially between ca. 300 and 400 ka.

These SW-NE paleowind directions are supported by the generally greater thickness of (Nemrut-derived) correlated fallout tephra layers in the northern drill Site 1 compared to the more southerly Site 2.

Whether or not the apparent decrease of tephra layers, especially those of Nemrut-derivation, in the lower part of the core (below ca 150 m at Site 2) is the result of changing wind directions through time, lower explosivity of Nemrut or due to stronger Süphan- vs. Nemrut-explosive activity between ca. 400 and 600 ka is not yet known.

Evidence for a period of pronounced wet and warm conditions and high-resolution correlation. A fossil swamp deposit interlayered with diatomites and tephra layers characterized by a rare phenocryst mineralogy (aenigmatite) was found in an intramontane basin ca 25 km southeast of Nemrut Volcano. These deposits are overlain by fallout deposits of the ca. 80-90 (?) ka old large-volume basaltic Incekaya volcanic system also erupted during a period of dense vegetation (roots, tree molds etc) below and above the thick deposits. Significantly, up to ca. 2.5 m thick hyaloclastites – the thickest bed of basaltic tephra at both sites – were drilled at holes 2B, 2D, and 2E at Site 2 where they are sandwiched between laminated sediments reflecting warm climate conditions. The correlation of these hyaloclastites with the Incekaya eruptive center is thus strongly supported by three independant lines of evidence: (a) the only large-volume basaltic eruption on land, (b) the warm climate at the time of eruption and (c) the occurrence of rare aenigmatite-bearing tephra below the drilled hyaloclastite.

A temporal history of overall dry vs. wet climate reconstructed from weathering intensity of tephra deposits is equivocal because of the strong orographic contrast between the dry subdued topography north-northwest and the wet precipituous mountaineous region south of Lake Van. Moderately well-developed paleosols are more strongly developed in fallout deposits south of the lake.

The fall-rise-fall of lake level prior to, and following, emplacement of the youngest thick fallout pumice deposit UP (Upper Pumice) was dated precisely at ca. 30 ka at 3 different localities. Lake level was significantly lower than at present by several tens of m since UP and preceding fallout sheets were deposited on dry land in near-shore sections. Shortly after eruption of UP, lake level rose quickly, inundating, eroding and reworking most of UP – being >10 m thick in nearby quarries at higher elevation. The erosional remnant of UP and some 8 m of overlying shallow water-reworked volcaniclastic sediments fell dry again which we speculate occurred at ca 20 ka. We tentatively correlate the rapid rise in lake level as due to the known strong precipitation in the eastern Mediterranean at this time (Kuzucuoglo et al., 2010) and subsequent fall of lake level by dry conditions at about 20 ka.

Alteration of tephra and geochemical significance of time-dependant mass influx of alkaline tephra on the evolution of the lake alkalinity

In our preceding study of the short cores (Sumita et al. 2008), we found the lowermost layer encountered (T 16, varve age ca. 13 585 varve years) to be moderately strongly zeolitized. Prior to drilling, we thus expected that alteration (hydration and/or more advanced zeolitization) would increase downward at least in fine-grained volcanic sediments. Volcanic glass in coarse-grained highly permeable sediments is commonly less affected by alteration. To our surprise, fresh glass ranging from rhyolite to basalt in composition is quite fresh in most tephra layers even near the base of the sediment lake fill. Mafic phenocryst phases (orthopyroxene, olivine) show pronounced coxcomb dissolution in the lowermost fresh water sediments, however.

Massive influx of alkaline fine-grained tephra into the lake, alkaline groundwater from beneath the volcanoes and possibly intra-lake hydrothermal springs – e.g. CO2 – degassing - may have contributed significantly to the alkaline character of Lake Van as much as climate.

Conclusion

Field and analytical pre-site work on tephra deposits on land , chiefly resulting from Nemrut explosive eruptions over the past 400 ka, provides the fundamental framework for the broad-based high-resolution analysis of the stratigraphy, facies, chemical and mineralogical composition and age of many tens of tephra layers in Lake Van cores from sites 1 and 2. Initial results on prominent tephra layers, each several meters thick, in the upper part of the cores and preliminary ages – as old as ca 550-600 ka -, obtained on core catcher samples from the lower part of

Site 1 cores has provided the Paleovan consortium with critical information to initiate evaluation of various types of data within more quantitative boundary conditions. The bulk of the results of our ongoing analytical work, will, however, be forthcoming throughout 2012 and will be presented in work shops planned for Vienna (EUG, April 2012) and Kiel (September/October 2012).

References:
Degens ET, Wong H, Kempe S, Kurtman F (1984) A geological study of Lake Van, eastern Turkey. Geol Rundsch 73: 701-734
Kuzucuoglo C, Christol A, Moiralis D, Dogu A, Akköprü E, Fort M, Brunstein D, Zorer H, Fontugne M, Karabiyikoglu M, Scaillet S, Reyss J-L, Guillou H (2010) Formation of the Upper Pleistocene terraces of Lake Van (Turkey). J Quat Sci 25: 1124-1137
Litt T, Anselmetti FS, Çağatay N, Kipfer R, Krastel S, Schmincke H-U, PaleoVan scientific team (2011) A 500,000 year-long sedimentary archive drilled in Eastern Anatolia (Turkey): The PaleoVan Drilling Project. EOS, Am Geophys Union
Pearce JA, Bender JF, de Long SE, Kidd WSF, Low PJ, Guåner Y, Saroglu F, Yilmaz Y, Moorbath S, Mitchell JG (1990) Genesis of collisional volcanism in Eastern Anatolia, Turkey. J Volcanol Geotherm Res 44: 189-229
Sumita M, Schmincke H-U (2010) Onland tephra record around Lake Van as a stratigraphic, compositional, temporal and alteration framework for the Paleovan drilling project. Abs IODP-ICDP Kolloquium 2010 (Frankfurt)
Sumita M, Schmincke H-U (2011) Structural, volcanic, temporal, compositional and environmental evolution of explosive volcanism of Nemrut and Süphan volcanic systems, sources for the tephra framework of Lake Van sediments (Anatolia). Abs IODP-ICDP Kolloquium 2011 (Muünster)
Sumita M, Schmincke H-U, Litt T, Heumann G, Krastel S (2008) Impact of Tephra input into Lake Van (Turkey). Abs IAVCEI General Assembly (Reykjavik, Iceland)

IODP

Methane-induced carbonates along the Cascadia Margin: Faithful recorders of fluctuations in methane seepage due to global climate changes?

B.M.A.TEICHERT[1]

[1] Westfälische Wilhelms-Universität Münster, Institut für Geologie und Paläontologie, Münster, Germany, barbara.teichert@uni-muenster.de

The Cascadia Margin has been studied thoroughly with ODP (Legs 146 and 204) and IODP Expeditions (Exp. 311) with respect to the occurrence of gas hydrates within the hemipelagic silts and clays and sandy turbidites forming the accretionary wedge. As the sediments of the prism, which have been scraped off the subducting plate, are consolidated, dewatering and expulsion of fluids occurs. The faults and fractures that are associated with this tectonic deformation act as conduits for the upward moving fluids. The seafloor expressions of such deep rooted faults or other fluid pathways are active methane seeps with characteristic microbes, chemosynthetic communities and methane-induced authigenic carbonates. At Hydrate Ridge, in the southern part of the Cascadia Margin, these authigenic carbonates even form above-seafloor expressions so-called chemoherms (Teichert et al. 2005). Previous studies have shown that they are ideal recorders of the history of methane seepage over time and that they indicate episodic times of enhanced methane seepage due to sealevel variations associated with glacial/interglacial cycles (Teichert et al. 2003). This observation has also been discussed for fossil methane seeps reaching as far back as the Mesozoic (Kiel et al. 2009).

The goal of this project will be to verify whether the global climate signal that is recorded in methane-induced carbonates at Hydrate Ridge can be traced along the Cascadia Margin in authigenic carbonates that were, unlike at Hydrate Ridge, precipitated within the sediments of the accretionary wedge. Abundant authigenic carbonates were sampled in a transect across the northern Cascadia Margin during IODP Expedition 311. Complex mineralogical compositions and paragenesis ranging from aragonite, calcite, Mg-calcite, Ca-dolomite to dolomite and siderite indicate a highly variable geochemical environment of their formation. Distinct horizons of extensive carbonate formations with depth clearly show that authigenic carbonate formation and therefore also methane seepage was episodic in the past. The question that has to be answered is if these events of enhanced carbonate formation were triggered through rather local processes or if the can be linked to the southern Cascadia Margin and thus global climate changes.

References:
Teichert, B.M.A., Eisenhauer, A., Bohrmann, G., Haase-Schramm, A., Bock, B., Linke, P. (2003) U/Th systematics and ages of authigenic carbonates from Hydrate Ridge, Cascadia convergent margin: recorders of fluid composition and sealevel changes. Geochimica et Cosmochimica Acta, 67, 3845-3857.
Teichert, B.M.A., Bohrmann, G., Suess, E. (2005) Chemoherms on Hydrate Ridge - Unique microbially-mediated carbonate build-ups growing into the water column. Palaeogeography, Palaeoclimatology, Palaeoecology, 227, 67-85.
Kiel, S. (2009) Global hydrocarbon seep-carbonate precipitation correlates with deep-water temperatures and eustatic sea-level fluctuations since the Late Jurassic. Terra Nova, 21, 279-284.

IODP

Plio- and Pleistocene evolution of the water mass exchange and erosional input in the Norwegian-Greenland Seas

CLAUDIA TESCHNER[1], MARTIN FRANK[1], BRIAN A. HALEY[2], JOCHEN KNIES[3]

[1]Helmholtz-Zentrum für Ozeanforschung Kiel (GEOMAR),Wischhofstrasse 1-3, 24148 Kiel, Germany
[2]COAS, College of Oceanic and Atmospheric Sciences, Oregon State University, Corvallis, OR 97331-5503
[3]Geological Survey of Norway, NO-7491 Trondheim, Norway

The Arctic Ocean and Norwegian-Greenland Seas (NGS) have played an important role for the thermohaline circulation and the development of climate. Besides the Labrador Sea, the NGS is presently the most important area for deep water formation in the Northern Atlantic Ocean. Therefore it is essential to better understand variations of the circulation in the Arctic Ocean and Nordic Seas in the past, in particular the Plio-Pleistocene period, during which significant climatic changes occurred. These include the onset and intensification of the Northern Hemisphere Glaciation, starting 2.82 to ~2.7 Ma (Sarnthein et al., 2009; Lisiecki & Raymo, 2005) and the Mid Pleistocene Transition (1.5 – 0.5 Ma) (Lisiecki & Raymo, 2005). To reconstruct the water mass mixing and erosional input we use the radiogenic isotope composition of neodymium (Nd) and lead (Pb), which we apply to three sediment cores (ODP Sites 911 from the Fram Strait, 907 from the NGS and 984 from the northernmost Atlantic).

The first analyses were performed on sediment samples from ODP site 911 (leg 151, in 900 m water depth). The

stratigraphy of this core is complicated to establish and has been subject of past and ongoing studies by Knies et al. (2002, 2007, 2009). Due to the low amount of biogenic material (e.g. foraminifera) it is mostly not possible to apply paleoceanographic standard methods like δ18O and δ13C analyses. Hence, the leaching method of Gutjahr et al. (2007) to extract the Nd, Pb and Sr isotopic composition of past bottom water from early diagenetic metal oxide coatings on the sediment particles was modified by eliminating the carbonate dissolving step, due to the low carbonate content in this core. The 87Sr/86Sr ratio was monitored to support the reliable extraction deep water signal was extracted.

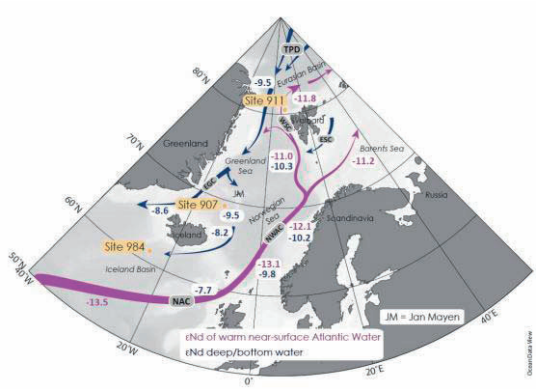

Figure 1: Map of the North Atlantic and Norwegian-Greenland Seas with Site locations, schematic flowpaths and εNd signatures of major currents (Aagard et al. 1985, Hansen & Østerhus 2000). Purple arrows indicate the warm inflowing Atlantic water, the dark blue arrows represent the cold outflowing polar deep water and the deep waters in the Norwegian-Greenland Seas (Lacan & Jeandel, 2004; Anderson et al., 2008).

Site 911 is located NW of Svalbard on the southeastern slope of the Yermak Plateau in the Fram Strait. Today this location is strongly influenced by the inflow of Atlantic water from the NGS. The Norwegian Atlantic Current (NWAC), flowing along the west coast of Norway towards Svalbard has a present day εNd of -11.0 ± 0.2 at a location slightly south of Svalbard (Lacan & Jeandel, 2004) and shows somewhat less radiogenic values of -11.8 ± 0.4 north of Svalbard in shallower water depths (Andersson et al., 2008) (Fig. 1). The deep waters flowing from the Arctic Ocean into the NGS through the western Fram Strait are characterized by εNd values of -9.5 ± 0.4 (Andersson et al., 2008). The core location is thus well suited to study the variability of the water mass exchange between the Arctic Ocean and the NGS and to reconstruct erosional inputs over the past 5 Ma. The analyses of the core top sample of ODP Site 911 resulted in Nd isotope signatures (εNd = -11 ± 0.2) close to present day values observed in the Atlantic water inflow (Lacan & Jeandel, 2004) which documents reliable extraction of the deep water signature and which is supported by Sr isotope signatures very close to seawater in the same leachates. Based on these results downcore samples covering the proposed time period of the past 5 million years were analysed.

The down core Nd isotope data vary between εNd = -7 to -12 ± 0.3. Over the past 5 million years the Nd isotope record does not show a pronounced trend with time (Fig. 2), which contrasts with the Nd isotope record of the central Arctic Ocean and the global benthic $\delta^{18}O$ record (Lisiecki & Raymo, 2005). The Nd isotope record of deep waters on Yermak Plateau ranges between the more radiogenic values of the central Arctic Ocean (εNd = -5.3

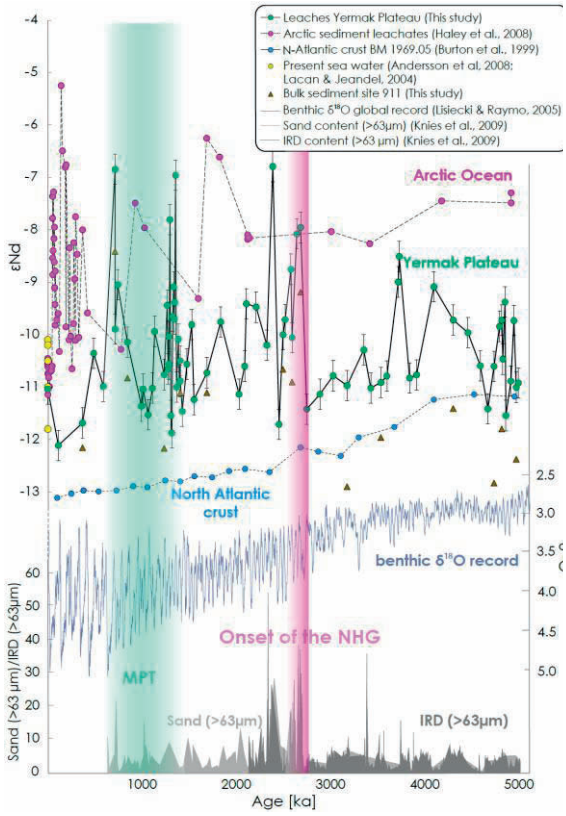

Figure 2: Comparison of the new Nd isotope data of Site 911 with Leg 302 (Haley et al., 2008) and other paleo environmental records. The green symbols shows the newly acquired deep water Nd isotope data leached from the sediments of Site 911 and the brown triangles shows the Site 911 εNd data of the bulk sediments. Pink dots: central Arctic sediments of Leg 302 (Haley et al., 2008a); yellow symbols: Nd isotopic composition of waters from different depths north of Svalbard (Andersson et al., 2008); blue symbols: western North Atlantic crusts (Reynolds et al., 1999), blue curve in the background: global oxygen isotope stacked of Lisiecki and Raymo (2005), gray areas: sand and IRD from Site 911 (Knies et al., 2009).

to -11) and the less radiogenic values of the NW Atlantic Fe-Mn- crusts (εNd = -11.2 to -13) reflecting the NADW signal (Reynolds et al., 1999), which indicates prevailing mixing of water masses from the Arctic Ocean and the Norwegian-Greenland Seas. However, the εNd values display a high variability, in particular since the beginning of the Northern Hemisphere Glaciation, which roughly coincided with the occurrence of significant peaks in the IRD- and sand-content. Four shifts of about 2 to 3 εNd units to more radiogenic values are observed in the isotopic record during glacial periods around 0.72 Ma, 1.36 Ma, 2.4 Ma and 2.69 Ma (Fig.2). These shifts indicate major inflow of waters influenced by highly radiogenic source areas, either by the Icelandic basalts in the south or by the Siberian Putorana flood basalts in the hinterland of the Kara/Laptev Sea region. In case the latter was the source region, the radiogenic isotope signal was supplied either (1) by brine-water production resulting from increased sea-ice formation at the edges of ice sheets grounding on large areas of the Kara Sea and Novaya Zemlya shelves (Haley et al., 2008a) or (2) by sea ice formed on the shelves and carrying lithic grains with Fe-Mn coatings obtained on the shelf and transported via the Siberian branch of the

Transpolar drift (Pfirman et al., 1997). All four peaks were accompanied by more positive Nd isotope signatures of the detrital sediment particles indicating a contemporaneously enhanced sediment supply from the above Siberian shelf regions, which supports the hypothesis of the sea ice transported particles.

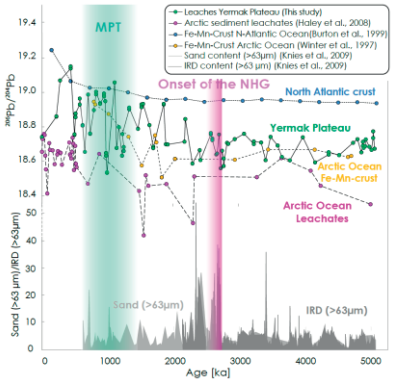

Figure 3: Comparison of the newly obtained Pb isotope data of Site 911 with other records. The green symbols show the deep water Pb-isotope data leached from the sediments. Pink circles: central Arctic Leg 302 (Haley et al., 2008a), yellow: Fe-Mn-micronodule record from the Alpha ridge (Winter et al., 1997), blue symbols: crusts from the western North Atlantic bathed in NADW (Reynolds et al., 1999), grey areas: sand/IRD content in % of total weight.

The radiogenic Pb isotope compositions at Site 911 evolved from 206Pb/204Pb ratios between 18.55 and 18.75 prior to 2.2 Ma to generally more radiogenic values between 18.5 and 19.15 thereafter (Fig. 3). In contrast to Nd, the higher resolution variability, which was particularly pronounced after 2.2 Ma does not seem to systematically correlate with changes in IRD inputs and thus changes in glacial/interglacial ice sheet extent and ocean circulation. The general increase after 2.2 Ma closely resembles the Pb isotope evolution of the deep Arctic Ocean as recorded by sedimentary ferromanganese micronodules (Winter et al., 1997) and the Pb isotope evolution of North Atlantic Deep water in the North Atlantic as recorded by ferromanganese crusts (Burton et al., 1997; Reynolds et al., 1999). In contrast to the central Arctic Ocean record from the Lomonosov Ridge, which has been under the influence of weathering inputs from Siberia over the past 5 million years (Haley et al., 2008b), this indicates that the Pb isotope composition of deep waters in the Fram Strait has been increasingly dominated by highly radiogenic Pb isotope signatures resulting from incongruent weathering and preferential release of radiogenic Pb originating from glacially weathering old continental landmasses, such as Northern Canada, Greenland, or parts of Svalbard over the past 2 Ma.For Sites 907 and 984 the leaching method to extract the seawater derived radiogenic Nd and Pb isotope signatures from the early diagenetic ferromanganese coatings of the sediments after Gutjahr et al. (2007) was extensively tested with different concentrations of leach solutions and eliminating the carbonate dissolution and was improved by comparison of core top data to the modern dissolved bottom water Nd isotope signatures in the same areas (Lacan and Jeandel, 2004; Andersson et al., 2008). Furthermore, we extracted and analyzed the seawater Nd isotope data from ferromanganese coatings of the carbonate shells of planktonic foraminifera.

Site 984 is located in 1650 m water depth and is currently influenced by the Iceland-Scotland Overflow waters flowing from the Nordic Seas across the Iceland-Faroer Ridge and carrying a Nd isotope signature of -7.3 to -9.9 (Lacan & Jeandel, 2004). Although the Sr isotope data obtained on the leachates surface sample are close to seawater and apparently confirm the seawater origin of the Nd isotope signatures, the leached Nd isotope compositions are far too radiogenic (+3.9 ± 0.3) compared to the existing NGS water data, which is most probably caused by partial dissolution of volcanic glass particles, causing a contamination with radiogenic Nd. Therefore, we decided to analyse carbonate shells of planktonic foraminifera applying the cleaning methods of Vance et al. (1999, 2004). The foraminiferal data are less radiogenic (between 0 ± 0.4 and -3.9 ± 0.4) than the leachates but still more

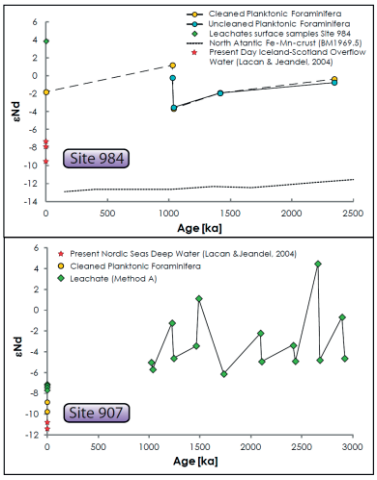

Figure 4: Comparison of Nd isotope data obtained from sediment leachates, foraminifera, and nearby deep waters for Sites 907 and 984.

radiogenic than the expected present day deep water values near this area (Lacan & Jeandel, 2004). This may also be caused by glass particles not fully removed from the foraminifera shells, because either the chambers were not fully opened due to the small size of the foraminifera (63 – 200 µm) or because the volcanic glass particles stuck to the pores of the shells.

A similar observation was made at Site 907 where the leachates are also at least 3 εNd units more radiogenic than expected. The data of the cleaned planktonic foraminifera of a sediment core near to Site 907 yielded plausible results for the reconstruction of the Nd isotopic composition of the bottom water. However, it was not possible to extract enough planktonic foraminifera from Site 907 to obtain reliable Nd isotope compositions. Therefore we are going to leach the sediment of two other cores from the Nordic Seas (Site 986 and Site 644) and one from the North Atlantic Ocean (Site 982) to extract Nd-, Sr- and Pb-isotopic composition of past seawater for a better understanding of past water mass exchange between the Norwegian-Greenland Seas and the North Atlantic Ocean.

References:

Aagaard, K., Swift, J.H., Carmack, E.C. (1985) Thermohaline Circulation in the Arctic Mediterranean Seas. Journal of Geophysical Research 90, 4833-4846.

Andersson, P., D. Porcelli, M. Frank et al. (2008) Neodymium isotopes in seawater from the Barents Sea and Fram Strait Arctic-Atlantic gateways. Geoc. Cosmoc. Acta, 72, 2854-2867.
Burton K.W., H.-F. Ling and R.K. O'Nions (1997) Closure of the Central American Isthmus and its effect on deepwater formation in the North Atlantic. Nature, 386, 382-385.
Gutjahr, M., M. Frank, C. H. Stirling et al. (2007) Reliable extraction of a deepwater trace metal isotope signal from Fe-Mn oxyhydroxide coatings of marine sediments. Chem. Geol., 242, 351– 370.
Haley B. A., M. Frank, R.F. Spielhagen and A. Eisenhauer (2008a) Influence of brine formation on Arctic Ocean circulation over the past 15 million years. Nat. Geosci. 1, 68–72.
Haley B.A., M. Frank, R.F. Spielhagen and J. Fietzke (2008b) Radiogenic isotope record of Arctic Ocean circulation and weathering inputs of the past 15 million years. Paleoc., 23, PA1S13.
Hansen, B. and S. Østerhus (2000) North Atlantic-Nordic Seas Exchanges. Progress in Oceanography, 45, 109-208.
Knies, J., J. Matthiessen, A. Mackensen et al. (2007) Effects of Arctic freshwater forcing on thermohaline circulation during the Pleistocene. Geology, 35, 1075-1078.
Knies, J., J. Matthiessen, C. Vogt et al. (2002) Evidence of 'Mid-Pliocene (~3 Ma) global warmth' in the eastern Arctic Ocean and Implications for the Svalbard/Barents Sea ice sheet during the late Pliocene and early Pleistocene (~3 – 1.7 Ma). Boreas, 31, 82-93.
Knies, J., J. Matthiessen, C. Vogt et al. (2009) The Plio-Pleistocene glaciation of the Barent Sea-Svalbard region: a new model based on revised chronostratigraphy. Quat. Sci. Rev., 28, 812-829.
Lacan, F. and C. Jeandel (2004) Neodymium isotopic composition and rare earth element concentrations in the deep and intermediate Nordic Seas: Constrains on the Iceland Scotland Overflow Water signature. Geochem. Geophy. Geosyst. , 5.
Lisiecki, L.E., and M.E. Raymo (2005) A Pliocene-Pleistocene stack of 57 globally distributed benthic δ18O records. Paleocean., 20.
Pfirman, S., Colony, R., Nürnberg, et al. (1997) Reconstructing the origin and trajectory of drifting Arctic sea ice. J. of Geophy. Res. 102, 12,575-12,586.
Reynolds, B.C., M. Frank and R.K. O'Nions (1999) Nd- and Pb-isotope time series from Atlantic ferromanganese crusts: Implications for changes in provenance and paleocirculation over the last 8 Myr. Earth. Planet. Sci. Lett., 173, 381-396.
Sarnthein, M., G. Bartoli, M. Prange, et al., 2009: Mid-Pliocene shifts in ocean overturning circulation and the onset of Quaternary-style climates, Climates of the Past, 5, pp. 269–283.
Vance, D. and K. Burton (1999) Neodymium isotopes in planktonic foraminifera: a record of the response of continental weathering and ocean circulation rates to climate change. Earth and Planetary Science Letters, 173, 365-379.
Vance, D., Scrivner, A.E. and P. Beney (2004) The use of foraminifera as a record of the past neodymium isotope composition of seawater. Paleoc., 19, PA2009
Winter, B., C. M. Johnson, and D. L. Clark (1997) Strontium, neodymium and lead isotope variations of authigenic silicate sediment components from the late Cenozoic Arctic Ocean: Implications for sediment provenance and the source of trace metals in sea water. Geochim. Cosmochim. Acta, 61, 4181– 4200.

IODP

The Agulhas Ridge: Its role as a barrier to the exchange of water masses between high and low latitudes

G. UENZELMANN-NEBEN[1]

[1]Alfred-Wegener-Institut für Polar- und Meeresforschung, Am Alten Hafen 26, 27568 Bremerhaven, Germany

The Agulhas Ridge forms a topographic anomaly within the Agulhas Falkland Fracture Zone, South Atlantic, and in this way represents a barrier to the exchange of water masses and hence energy and salt between high and low latitudes. The exchange of energy and salt plays a critical role in the stability and variability of the global oceanic circulation and thus has a strong impact on climate. Variations in the local ocean circulation, mainly Circumpolar Deepwater and Agulhas Rings, are archived in the structure and distribution sedimentary deposits. High resolution seismic reflection collected during RV Maria S. Merian cruise MSM 19/2 image those sedimentary deposits will be analysed invoking information from ODP Leg 177 Sites 1088-1090 and lead to information on modifications of depositional style and environment. This will allow the development of a self-consistent model for the development of the oceanic circulation and hence climate.

IODP

Preliminary results of the palynological study of Pliocene sediments off north-western Africa

FRANCESCA VALLÉ[1*], LYDIE DUPONT [1]

[1]MARUM - Center for Marine Enivironmental Sciences, University of Bremen, Leobener Strasse D28359, Bremen

The variability of the Atlantic meridional overturning circulation is supposed to be a driving force for climate changes in north-western Africa during the Quaternary (Mulitza et al. 2008). To test this hypothesis for the Pliocene, we specifically investigated the Mid-Pliocene Warm Period defined between 3-3.3 Ma (Dowsett, 2007) to compare this period with the previous one. Modelling studies suggest that during the Mid-Pliocene Warm Period, the final closure of the Central American Seaway strengthened the Atlantic meridional overturning circulation enhancing the heat advection to high northern latitudes and increasing the precipitation in north-western Africa (Lunt et al. 2007, Salzmann et al. 2008). As a result of more humid conditions, Mid-Pliocene woodlands and tropical savannahs extended northwards far into the today's arid regions.

Here we present the preliminary results of a palynological study of well-dated marine sediments retrieved offshore north- western Africa at ODP Site 659 (18°05'N 21°02'W; 3071 m water depth). ODP Site 659 is located outside the upwelling area under the distal Canary Current and is reached by the North Atlantic Deep Water. The site also lies directly under the main stream of the Saharan Air Layer which carries dust, plant waxes, and pollen out of the African continent.

We studied the pollen and dinoflagellates cyst contents of two time slices: one from 2.9 to 3.6 Ma (imbedding the Mid-Pliocene Warm Period) and the other between 4.6 and 4.9 Ma to look at the different terrestrial and oceanic conditions before and after the closure of the Central American Seaway. Although the dust record of ODP Site 659 showed pulses of high terrestrial input all the way back to 5 Ma, the pollen content is extremely low in the Early Pliocene and the preservation of the palynomorphs is poor. We speculate that the poor pollen preservation is due to higher oxygen content of the North Atlantic bottom water during periods of less vigorous North Atlantic Deep Water formation; something that seems to be corroborated by the carbon stable isotopes of ODP Site 659.
Additionally we ran XRF scanning of the sediment cores to compare our pollen record with element ratios (in particularly Fe/Ca and Ti/Ca) that can be used as indication of terrestrial input at the marine site.

References:
Dowsett H. J., 2007. The PRISM palaeoclimate reconstruction and Pliocene sea-surface temperatures. In Williams M, Haywood, A.M., Gregory, F.J. & Schmidt, D.N,(eds). Deep-Time perspectives on Climate Change: Marrying the Signal from Computer Models and Biological

proxies. The Micropaleontological Society, Special Publication. The Geological Society, London: 459-480.
Lunt, D.J., Valdes, P.J., Haywood, A.M., & Rutt, I.C., 2007. Closure of the Panama Seaway during the Pliocene: implications for climate and Northern Hemisphere glaciations. Climate Dynamics, 30: 1-18.
Mulitza, S., Prange, M., Stuut, J-B., Zabel, M., Von Dobeneck, T., Itambi, A.C., Nizou, J., Schulz, M., & Wefer, G., 2008. Sahel megadrougths triggered by glacial slowdowns of Atlantic meridional overturning circulation. Paleoceanography, 23, PA4206: 1-11.
Salzmann, U., Haywood, A.M., Lunt, D.J., Valdes, P.J., & Hill, D.J., 2008. A new global biome reconstruction and data-model comparison for the Middle Pliocene. Global Ecology and Biogeography, 17: 423-447.

ICDP

Three-Component Magnetic Logging in the Outokumpu Borehole

C.VIRGIL[1], A.HÖRDT[1], S.EHMANN[1], M. LEVEN[2], E. STEVELING[2]

[1] Institut für Geophysik und Extraterrestrische Physik, Technische Universität Braunschweig, Germany (c.virgil@tu-bs.de)
[2] Institut für Geophysik, Universität Göttingen, Germany

Borehole magnetic data can be used for several tasks, like the localization of ferro-magnetic objects, determination of apparent polar wander curves, and the computation of the magnetisation of rock units. However, using only total field or horizontal and vertical field components with these applications often gives ambiguous results. To reduce this ambiguity, three-component borehole magnetics can be used, which provides important additional information, including the declination of the magnetic field.

The "Göttinger Bohrloch Magnetometer" (GBM) comprises three fluxgate magnetometers and three orthogonal aligned fibre optic gyros (FOGs). The FOGs have the benefit of a very small drift per hour (approx. 2 °/h) in combination with a high resolution (9·10-5 degree per increment). With these sensors, the vector of the magnetic field along with the tool rotation can be recorded continuously during the measurement. Using the high precision gyro data, we can compute the vector of the magnetic anomaly with respect to the Earth's reference frame North, East and Downwards.

In September 2008, the GBM was successfully applied in the Outokumpu Deep Drill Hole (OKU R2500), Finland. OKU R2500 was drilled during 2004-2005 to a total depth of 2516 m. The aim of this project was the understanding of the ore formation process and the tectonic evolution in the Outokumpu mining region. The ore is hosted in the so-called Outokumpu assemblage, consisting of black shales, serpentinite and skarn rock. Due to magnetite and pyrrhotite minerals hosted in the serpentinite, borehole magnetics is well suited for a structural interpretation of the assemblage.

With the GBM, we carried out six measurements to a maximum depth of 1440 m. Based on the comparison of these logs, the estimated precision of the reorientation of the magnetic field is 0.8° in azimuthal direction and 0.1° in inclination. We further computed the borehole path using the FOG data and the depth information. Here, the relative error with respect to the maximum depth is 0.3 %. The vector information of the magnetic anomalies was used to compute the magnetization of rock units in the environment of the borehole via numerical simulations. Due to the strong heterogeneity of the Outokumpu region, we used two models with different length scales.

The first length scale is related to the drilled-through Outokumpu-assemblage in the direct vicinity (< 50 m) of the borehole. Between 1300 m and 1440 m, there are three distinct magnetized sections. Each section was individually modelled by a set of elliptically-shaped cylinders with arbitrary magnetization. By trial-and-error inversion, we could obtain extent, orientation and the depth dependent magnetization vector for each section. Using supplementary susceptibility data, we further computed the natural remanent magnetization vector (NRM). The estimated accuracy in this model is 6° in inclination and 12° in declination.

The first section (1328 m – 1338 m) is nearly horizontally aligned. The inclination and declination of the NRM agree reasonably well with the paleo-field direction at the estimated time of magnetization (1.9 Ga). The second section (1359 m – 1371 m) is tilted by 45° to the South. Here, the direction of the NRM vector differs strongly from the paleo-field data. This indicates a post magnetization movement of the corresponding rock units. The third section (1403 m – 1424 m) is again horizontally aligned with a good agreement between NRM inclination and paleo-field inclination. However, the difference in declination between NRM and paleo-field suggests a rotation after receiving the magnetization.

The NRM data of this model could further be used to reorient core samples. Using the borehole path, derived from the GBM measurements, the GBM NRM data could be projected into the borehole reference frame. In this frame, the NRM measured on core samples (eg. Dietze et al. 2011) could be compared with the GBM data and be rotated to fit these. Using core samples with a minimum magnetization of 0.5 A/m, the estimated accuracy of the reorientation is 20°.

The second model describes the geological structure of the surrounding (< 1 km) of the drill site. To reduce the ambiguity in interpretation, we use seismic profiles (Kukkonen et al. 2006) to locate different rock units. By this joint interpretation we were able to link the seismic reflectivity with magnetic properties. This yields an estimate of the mineralogy for rock units away from the borehole path, which were not cored.

References

Dietze, F., Kontny, A., 2011, A Study of Rock Magnetic Properties of Serpentinites from the Outokumpu Deep Drill Hole, Finland., in Outokumpu Deep Drilling Project 2003-2010, (Hg.) I. T. Kukkonen, Geological Survey of Finland, special Paper 51, 133-155
Kukkonen, I. T., Heikkinen, P., Ekdahl, E., Hjelt, S.-E., Yliniemi, J., Jalkanen, E., 2006, F. W. G., 2006, Aquisition and geophysical characteristics of reflection seismic data on FIRE transects, Fennoscandian Shield, in Finish Reflection Experiment 2001-2005, (Hg.) I. T. Kukkonen, R. Lahtinen, Geological Survey of Finland, special Paper 43, 13-43

IODP

Carbonate diagenesis in the Pacific Equatorial Age Transect (PEAT) Sites and the preservation of geochemical signals in foraminifera

J. VOIGT[1], E.C. HATHORNE[1], M. FRANK[1]

[1]Helmholtz-Zentrum für Ozeanforschung Kiel (GEOMAR), Wischhofstr. 1-3, 24148 Kiel, Germany

The trace element and isotopic compositions of the calcite shells (tests) of foraminifera preserved in marine sediments are widely used for reconstructions of oceanic and climatic conditions in the past. However, ancient tests can be altered after deposition by a process where the original biogenic calcite is replaced by secondary (inorganic) calcite which adopts the form of the foraminifera tests. Therefore, it is very important to quantitatively understand changes in the elemental and isotopic composition of the tests caused by this recrystallisation process. Here we present initial results from a study of recrystallisation in sediments from IODP Expedition 320/321 Pacific Equatorial Age Transect (PEAT), where sediments of similar age and initial composition have been subjected to different diagenetic histories. This natural diagenesis laboratory is ideal for the study of recrystallisation and the preservation of geochemical proxies in foraminifera.

Radiogenic Sr ($^{87}Sr/^{86}Sr$) isotopes of bulk carbonate leachates and the associated pore waters generally suggest recrystallisation occurred relatively quickly as values are indistinguishable (within 2σ uncertainties) from the contemporaneous seawater (McArthur et al. 2001). Notable exceptions include Site U1336 where in sediments older than
15 Ma the pore waters have lower $^{87}Sr/^{86}Sr$ ratios than contemporaneous seawater, most likely resulting from upward diffusion of Sr from recrystallised older carbonates. In sediments older than 20.3 Ma the carbonate $^{87}Sr/^{86}Sr$ ratios of Site U1336 exhibit lower values than contemporaneous seawater indicating the incorporation of Sr dissolved from older/deeper carbonates. At Site U1338 the Sr isotope signal of the pore waters from sediments older than 9.5 Ma increases with depth from the upward diffusion of relatively modern seawater in the basement. The deepest bulk carbonate sample from Site U1334 appears to have incorporated some of the younger Sr from the pore waters suggesting persistent diagenetic alteration.

Furthermore, as less Sr is incorporated into inorganic calcite, the lower Sr/Ca ratios of bulk carbonates from Site U1336 suggest more extensive diagenetic alteration compared to the other PEAT sites.

Although the recrystallisation of bulk carbonates is well documented, the fate of foraminiferal chemistry is potentially different. To investigate this, laser ablation ICP-MS element/Ca ratio depth profiles were obtained through planktonic foraminifera tests of Globigerina venezuelana from Site U1336 and U1338 for two time intervals (13.9 Ma and 15.5 Ma). The depth profiling technique reveals heterogeneity of trace elements across the wall of the foraminifera test with Mg/Ca and Mn/Ca ratios increasing from the outer to the inner calcite. These patterns are comparable to those reported for modern foraminifera from sediment traps (Hathorne et al. 2009). The Mg/Ca ratios are similar for both sites and time intervals. The absolute values are also comparable to modern foraminifera implying that any change in Mg/Ca from diagenesis is small or the foraminifera retain most of their original Mg/Ca signal. The Mn/Ca ratios show a large difference between the inner and the outer calcite up to a factor of 10 through the test wall. Although the absolute values are different, the observed trend in Mg/Ca and Mn/Ca ratios for the PEAT sites are similar to modern foraminifera suggesting that the original geochemical proxy signal is retained. Additionally, Sr/Ca ratios show little heterogeneity and fluctuate around 1.1-1.2 mmol/mol as observed for modern tests (Hathorne et al. 2009). The Sr/Ca ratios exhibit no difference between the sites and time intervals indicating that foraminifera react differently during recrystallisation diagenesis to bulk sediments that consist mostly of calcareous nannofossils. Although many more samples need to be analysed from more time intervals across the different sites, these first results suggest foraminiferal geochemistry is relatively robust to recrystallisation diagenesis.

References:
Hathorne et al. (2009)
McArthur et al. (2001)

IODP

Unlocking the secrets of slow slip by drilling at the northern Hikurangi subduction margin, New Zealand: Riserless drilling to sample and monitor the forearc and subducting section

L. WALLACE[1], N. KUKOWSKI[2], & HIKURANGI-WORKING GROUP

[1]GNS Science - Te Pu Ao, 1 Fairway Drive. Avalon, PO Box 30-368, Lower Hutt, New Zealand 5010
[2]Friedrich-Schiller-Universität Jena, Institut für Geowissenschaften, Burgweg 11, 07749 Jena, Germany

Slow slip events (SSEs), or 'silent earthquakes' which have much longer rupture times than ordinary earthquakes, have been recently detected at many Pacific Rim subduction margins. Rupture duration is much longer than for ordinary earthquakes, and SSEs result in crustal movements with velocities 1–100 times background tectonic levels, such that so far GPS has been the best way to detect them. The mechanism for slow slip initiation is poorly understood, but thought to be related either to fluid processes or to the transition between velocity strengthening and velocity-weakening behaviour.

Slow slip events at the Northern Hikurangi subduction margin, New Zealand, recur every two years, and thus provide an excellent setting to monitor changes in deformation rate, in situ conditions, and rock physical properties surrounding the SSE source area throughout a slow slip cycle. The Hikurangi margin is well known from many seismic reflection and other geophysical and geological surveys. Sampling material from the sedimentary section and oceanic basement of the subducting plate, and from the primary active thrust in the outer wedge near the trench will reveal the rock properties, composition, and lithological and structural character of the material that is transported downdip to the known SSE

source region, and in the case of the shallow fault zone, may even lie within the SSE rupture area.

Therefore we submitted a riserless proposal as a cornerstone to a recently submitted complex drilling project (MDP) proposal that outlines a plan for IODP drilling to discern the mechanisms behind subduction zone slow slip events (SSEs) by drilling at northern Hikurangi. Sampling of the upper plate and subducting section via shallow drilling (300-1200 m), and installing of borehole observatories are key components of this project. These riserless boreholes are designed to address three fundamental scientific objectives: (1) characterize the state and composition of the incoming plate and shallow plate boundary fault near the trench, which comprise the protolith and initial conditions for fault zone rock at greater depth; (2) characterize material properties and stress conditions in the upper plate above the fault that hosts slow slip; and (3) install borehole observatory instruments to monitor a transect of holes that span the region of the fault where repeated slow slip events have been documented. The proposed borehole observatories focus on monitoring deformation, seismicity and evolution of physical and chemical properties throughout the SSE cycle. Together, data from these riserless boreholes and observatories will test a suite of hypotheses about the fundamental mechanics and behavior of slow slip events, and their relationship to great earthquakes along the subduction interface.

IODP

IODP Scientific Earth Drilling Information Service

H.-J. WALLRABE-ADAMS[1], M. DIEPENBROEK[1], H. GROBE[2], R. HUBER[1], U. SCHINDLER[1], J. COLLIER[3]

[1]MARUM - Center for Marine Environmental Sciences, Univ. of Bremen, Germany
[2]Alfred Wegener Institute for Polar and Marine Research, Bremerhaven, Germany
[3] IODP-MI, Tokyo, Japan

The Integrated Ocean Drilling Program (IODP) has set up a web-based information service (Scientific Earth Drilling Information Service, SEDIS, http://sedis.iodp.org), which integrates the data of the three IODP implementing organizations from the United States (USIO), Japan (CDEX) and Europe with Canada (ESO). The SEDIS portal provides information on ODP, DSDP and IODP expeditions, publications and data. Moreover, post-cruise data has been collected and published via the portal. A thesaurus supports information and data searches. Data sets can be downloaded as tab-delimited text files.

SEDIS is also being prepared to include other IODP relevant scientific drilling data from terrestrial or lake drilling programs. The portal is designed to integrate available scientific data via metadata by employing international standards for metadata, data exchange and transfer.

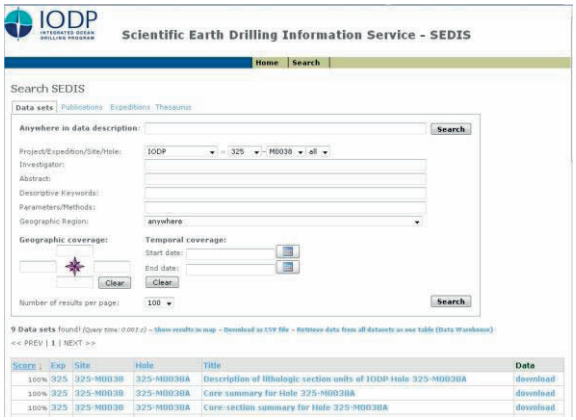

Screen shot of SEDIS search page.

IODP

Bipolar synchronicity for the termination of the Last Glacial Maximum

M.E. WEBER[1], P.U. CLARK[2], W. RICKEN[1], J.X. MITROVICA[3], S.W. HOSTETLER[4], D. SPRENK[1], G. KUHN[5]

[1]Institute of Geology and Mineralogy, University of Cologne, Zuelpicher Str. 49a, 50674 Cologne, Germany
[2]College of Earth, Ocean, and Atmospheric Sciences, Oregon State University, Corvallis, OR 97331, USA
[3]Department of Earth and Planetary Sciences, Harvard University, Cambridge, MA 02138, USA
[4]U.S. Geological Survey, College of Earth, Ocean, and Atmospheric Sciences, Oregon State University, Corvallis, OR 97331, USA
[5]Alfred Wegener Institute for Polar and Marine Research, Helmholtz Association, Am Alten Hafen 26, 27568 Bremerhaven, Germany

The timing of the last maximum extent of the Antarctic ice sheets relative to those in the Northern Hemisphere remains poorly understood because only a few findings with robust chronologies exist for Antarctic ice sheets. We developed a chronology for the Weddell Sea sector of the East Antarctic ice sheet that, combined with ages from other Antarctic ice-sheet sectors, indicates the advance to their maximum extent at 29 –28 ka, and retreat from their maximum extent at 19 ka was nearly synchronous with Northern Hemisphere ice sheets (Weber et al., 2011).

As for the deglaciation, previous modeling studies suggest a late ice-sheet retreat, starting around 14 ka BP and ending around 7 ka BP with a large impact of an unstable West Antarctic Ice Sheet (WAIS) and a small impact of a stable East Antarctic Ice Sheet (EAIS). However, the Weddell Sea sites studied here, provide evidence that specifically the EAIS responded much earlier around 19 ka, and again, around 16 ka, possibly provided a significant contribution to the last sea-level rise, and was much more dynamic than previously thought.

Recently, we have developed high-resolution chronologies for deep-sea sites from the Scotia Sea (Weber et al., in press) by correlating magnetic susceptibility to the non sea-salt Ca^{2+} flux of the EDML ice core. Both components are proxies for atmospheric dust. Preliminary work on these cores confirms our results insofar as we detected iceberg routing through the Scotia Sea at the same time as ice-sheet retreat in the Weddell Sea. Accordingly, a

precursory ice-rafted debris signal occurred around 19 ka, whereas massive iceberg routing commenced around 16.5 ka.

Using the results of an atmospheric general circulation we conclude that surface climate forcing of Antarctic ice mass balance would likely cause an opposite response, whereby a warming climate would increase accumulation but not surface melting. Furthermore, our new data support teleconnections involving a sea-level fingerprint forced from Northern Hemisphere ice sheets as indicated by gravitational modeling. Also, changes in North Atlantic Deepwater formation and attendant heat flux to Antarctic grounding lines may have contributed to synchronizing the hemispheric ice sheets.

References:
Weber, M.E., Clark, P. U., Ricken, W., Mitrovica, J. X., Hostetler, S. W., and Kuhn, G. (2011): Interhemispheric ice-sheet synchronicity during the Last Glacial Maximum. – Science, 334, 1265-1269, doi: 10.1126:science.1209299
Weber, M.E., Kuhn, G., Sprenk, D., Rolf, C., Ohlwein, C., and Wicken, W. (in press): Dust transport from Patagonia to Antarctica – a new stratigraphic approach from the Scotia Sea and its implications for the last glacial cycle. Quaternary Science Reviews, doi: 10.1016/j.quascirev.2012.01.016.

IODP

New insights on Middle to Late Eocene Carbon Cycle Dynamics from high-resolution geochemical records (IODP Exp 320/321 and ODP Leg 199)

T. WESTERHOLD[1], U. RÖHL[1], K. EDGAR[2], M. LYLE[3], H. PÄLIKE[4], R. WILKENS[5], P. WILSON[4], J. ZACHOS[6]

[1]MARUM - Center for Marine Environmental Sciences, University of Bremen, 28359 Germany
[2]Cardiff University, UK
[3]Texas A&M Univ., USA
[4]National Oceanography Centre, Southampton, UK
[5]Univ. Hawaii, Honolulu HI 96822, USA
[6]University of California, Santa Cruz, California, USA

The Eocene/Oligocene transition ~34 million years ago was a critical turning point in Earth's climatic history. A warm, high-diversity greenhouse world of the early Eocene ceded to the glacial, icehouse conditions of the early Oligocene (Zachos et al. 2001; Koeberl and Montanari, 2009). In contrast, up to today the extent and stability of land ice in the "doubthouse" world (Prothero et al., 2003) of the middle and late Eocene remain uncertain (Prentice and Matthews, 1988, Ehrmann and Mackensen, 1992; Miller et al., 1991; Zachos et al., 1994, 1996; Tripati et al., 2005; Edgar et al., 2007; Burgess et al. 2008). This interval in Earth's history is critical to test climatic and evolutionary hypotheses about the Eocene deterioration (Zachos et al., 2001). The stratigraphy of the Eocene/Oligocene transition events, the relationship between them and the stability of the precursor late Eocene climate remain subjects of debate (e.g., Coxall et al., 2005; Edgar et al., 2007; Katz et al., 2008).

Key records that provide a new depth transect for several Cenozoic key horizons for the late Eocene and Oligocene epochs are those recovered by Ocean Drilling Program (ODP) Leg 199 (Lyle et al. 2002; Lyle and Wilson 2006) and Integrated Ocean Drilling Program (IODP) Expedition 320/321 (Lyle et al. 2010; Pälike et al. 2010) . Stable isotope records from Site 1218 for example allowed the astronomical calibration of the entire Oligocene. However, due to the lack of carbonate in Leg 199 drill sites a detailed time control available for the Oligocene could not be achíeved for the late Eocene. Relatively recently, IODP Expedition 320/321 recovered sediments that provide a new depth transect for several Cenozoic key horizons, such as the Eocene/Oligocene transition and the Middle Eocene Climate Optimum (MECO) at Sites U1331-U1334. Especially the carbonate bearing Sites U1333 and U1334 are excellent to gain new information with superb age control on middle to late Eocene carbon cycle dynamics from the world's largest ocean.

During the late Eocene seven Carbonate Accumulation Events (CAEs) at ODP Site 1218 and 1219 in the equatorial Pacific have been identified, each characterized by high-carbonate burial, a relatively deep Carbonate Compensation Depth (CCD), and oxygen isotope values demonstrating relatively cool global conditions (Lyle et al. 2005). Between these events large CCD excursions of 1200 - 1500 m have been found. In contrast, Neogene CCD variations in the equatorial Pacific were only in the order of 200 m or less (Lyle et al. 2008). The CAEs have been linked to events of global cooling (Lyle et al. 2005, Tripati et al. 2005) that lead to elevated primary productivity and carbonate production in the equatorial region. The main driver for the strong CCD fluctuations was interpreted to represent different carbon reservoirs in the carbon cycle interacting with climate (Lyle et al. 2005). However, the data resolution was limited and a precise age model was still lacking both essential to unravel the ultimate causes of the CAEs as well as their potential relation to orbital cycles.

With our project we are working on a reconstruction of the highly dynamic late Eocene carbon cycle at high resolution. Prerequesite is to acquire very high resolution records (e.g., calcium carbonate) over a depth transect and construct an accurate orbitally calibrated time scale. Here we present Ca and Fe intensity data from XRF scanning of more than 1200 meters of sediment cores from ODP Leg 199 (Sites 1218-1220) and IODP Exp. 320 (Sites U1331-U1334) spanning magnetic polarity chrons C13n to C20n (34 to 44 Ma). The records from Exp. 320 and Leg 199 provide pronounced cyclic sediments in combination with exceptionally good paleomagnetics for magnetic polarity chrons C12n to C20n. Prior to time series analysis we correlated and integrated XRF core scanning data, shipboard physical property and biomagnetostratigraphic data for the interval of magnetic polarity chrons C12n to C19n of Leg 199 (Sites 1218, 1219, 1220) and Exp. 320 (Sites U1331, U1332, U1333, and U1334) in detail (Westerhold et al. 2012). We then used high resolution Fe intensity data to establish a stratigraphic framework based on the identification of the stable long eccentricity cycle (405 kyr) and subsequently applied orbital tuning of the records.

Integration of calcium (Ca) intensity data from XRF core scanning of Leg 199 and Exp. 320 data provide the ideal basis to reconstruct calcium carbonate records over a depth transect through time at unprecedented resolution. XRF core scanning Ca elemental intensity data have been transferred into carbonate records using $CaCO_3$ values analyzed on discrete samples. We have carefully chosen 188 samples from Sites 1218, 1219, 1220, U1331, U1332,

U1333, and U1334 and analyzed those with the Portable

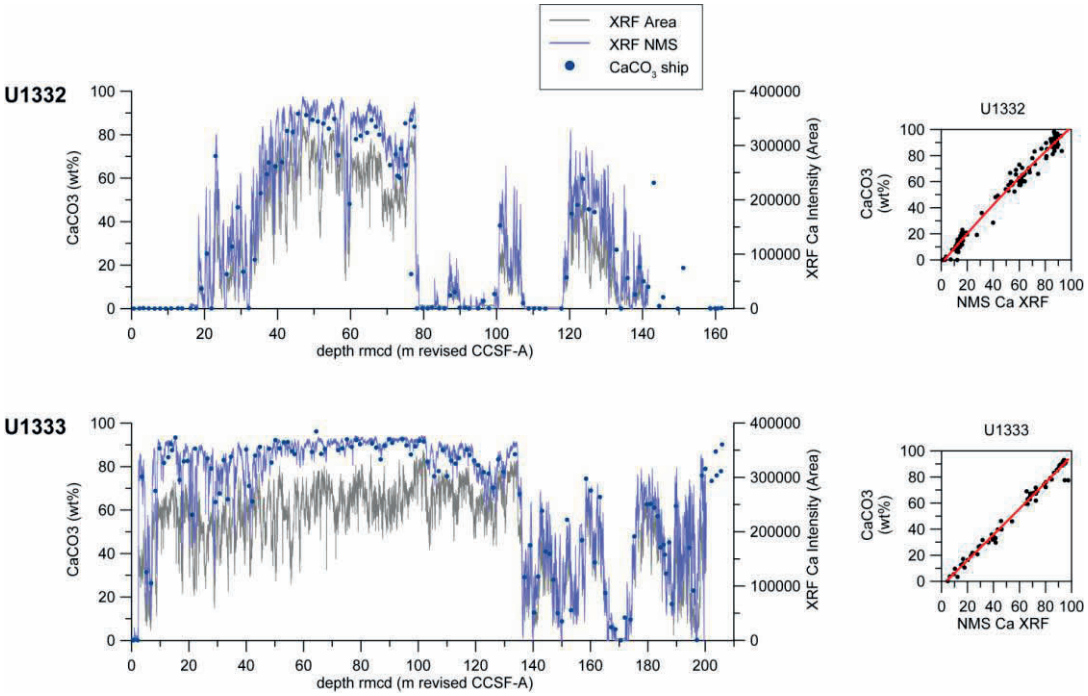

Figure 1. Comparison of raw XRF core scanning Ca intensity data (gray line) with calibrated NMS Ca XRF data (blue line) and shipboard coulometric data (blue dots) for IODP Sites U1332 and U1333. To the right calibration plots for IODP Sites U1332 and U1333 to calibrate Normalized Median-Scaled (NMS) XRF core scanning Ca intensity data (NMS Ca XRF) using coulometric CaCO3 data for the Eocene-Oligocene Transition following the approach of Lyle et al. (in press). Polynomial regression formulas are applied to transfer the NMS Ca XRF data into $CaCO_3$ wt% data. The NMS Ca XRF data are calculated from the XRF core scanning Ca intensity data and the EDF XRF sample data obtained in the first phase of our project. Especially at U1333 the NMS procedure significantly enhances the reliability of $CaCO_3$ wt% estimates by eliminating variability caused by differences in porosity, cracks, coring disturbance and geochemical density alterations.

Energy Dispersive Polarization X-ray fluorescence analyzer (EDP-XRF) at MARUM for the elemental composition (see Figure 1). After calibration we used these data as well as geochemical data for Leg 199 Sites 1218 and 1219 (e.g. $CaCO_3$, Ba, Si, organic carbon and stable isotopes data) to test the calibrated XRF core scanning data.

The depth transect including seven sites significantly contributes to an improved spatial view of the CAE's in the equatorial Pacific and reveals a highly dynamic middle to late Eocene environment. The CAE's are expressed as sharp carbonate fluctuations at ~35, 37.5, 39, 41, 44, 46 Ma across Sites U1331-U1334 and 1218, followed by a sharp transition into much higher carbonate accumulation rates from the Eocene into the Oligocene. In combination with a newly developed cyclostratigraphic age model our new depth transect indicates that the CAE's might be related to fluctuations in the very long eccentricity cycle suggesting a close connection to long-term variations in the carbon cycle.

In detail we will show: (1) examples of detailed time series analysis of the integrated Leg 199 and Exp. 320 sites and the cyclostratigraphy based on the identification of the stable long eccentricity cycle (405 kyr). (2) calibration of the XRF core scanning intensities with data for discrete samples acquired by the Portable Energy Dispersive Polarization X-ray Fluores-cence analyzer (EDP-XRF) at MARUM and crosscheck with other geochemical data (incl. shipboard $CaCO_3$) (see Figure 1). (3) Calcium carbonate records across a depth transect from 45 to 30 Ma characterising the CAE's. (4) First bulk isotopes data from U1333 and U1334.

References:

Burgess, C. E., P. N. Pearson, C. H. Lear, H. E. G. Morgans, L. Handley, R. D. Pancost, and S. Schouten (2008), Middle Eocene climate cyclicity in the southern Pacific: Implications for global ice volume, Geology, 36(8), 651-654.

Coxall, H. K., P. A. Wilson, H. Pälike, C. H. Lear, and J. Backman (2005), Rapid stepwise onset of Antarctic glaciation and deeper calcite compensation in the Pacific Ocean, Nature, 433(7021), 53-57.

Edgar, K. M., P. A. Wilson, P. F. Sexton, and Y. Suganuma (2007), No extreme bipolar glaciation during the main Eocene calcite compensation shift, Nature, 448(7156), 908-911.

Ehrmann, W. U., and A. Mackensen (1992), Sedimentological evidence for the formation of an East Antarctic ice sheet in Eocene/Oligocene time, Palaeogeography, Palaeoclimatology, Palaeoecology, 93(1-2), 85-112.

Katz, M. E., K. G. Miller, J. D. Wright, B. S. Wade, J. V. Browning, B. S. Cramer, and Y. Rosenthal (2008), Stepwise transition from the Eocene greenhouse to the Oligocene icehouse, Nature Geosci, 1(5), 329-334.

Koeberl, C., and A. Montanari (2009), The Late Eocene Earth - Hothouse, Icehouse and Impacts, 322 pp.

Lyle, M., and P. A. Wilson (2006), Leg 199 synthesis: Evolution of the equatorial Pacific in the early Cenozoic, 39 pp.

Lyle, M., P. A. Wilson, T. R. Janecek, and et al. (2002), Proc. ODP, Init. Repts., 199: College Station, TX (Ocean Drilling Program).

Lyle, M., A. Olivarez Lyle, J. Backman, and A. Tripati (2005), Biogenic sedimentation in the Eocene equatorial Pacific - the stuttering greenhouse and Eocene carbonate compensation depth, in Proc. ODP, Sci. Results, 199: College Station, TX (Ocean Drilling Program), edited by P. A. Wilson, M. Lyle and J. V. Firth, pp. 1-35.

Lyle, M., H. Pälike, H. Nishi, I. Raffi, K. Gamage, A. Klaus, and and the IODP Expeditions 320/321 Science Party (2010), The Pacific Equatorial Age Transect, IODP Expeditions 320 and 321: building a 50-million-year-long environmental record of the equatorial Pacific Ocean, Scientific Drilling, 9, 4-15.

Lyle, M., Olivarez Lyle, A., Gorgas, T., Holbourn, A., Westerhold, T., Hathorne, E., Kimoto, K., Yamamoto S., in press. Data report: raw and normalized elemental data along the U1338 splice from X-ray Fluorescence scanning. In Pälike, H., Lyle, M., Nishi, H., Raffi, I., Gamage, K., Klaus, A., and the Expedition 320/321 Scientists, Proc. IODP, 320/321: Tokyo (Integrated Ocean Drilling Program Management International, Inc.).

Miller, K. G., J. D. Wright, and R. G. Fairbanks (1991), Unlocking the icehouse: Oligocene-miocene oxygen isotope, eustacy, and margin erosion., Journal of Geophysical Research, 96, 6829-6848.
Pälike, H., H. Nishi, M. Lyle, I. Raffi, K. Gamage, A. Klaus, and the Expedition 320/321 Scientists (2010), Proc. IODP, 320/321: Tokyo (Integrated Ocean Drilling Program Management International, Inc.).
Prentice, M. L., and R. K. Matthews (1988), Cenozoic ice-volume history: Development of a composite oxygen isotope record, Geology, 16(11), 963-966.
Prothero, D. R., L. C. Ivany, and E. A. Nesbitt (2003), From greenhouse to icehouse: The marine Eocene-Oligocene transition, Columbia University Press, New York.
Tripati, A., and H. Elderfield (2005), Deep-Sea Temperature and Circulation Changes at the Paleocene-Eocene Thermal Maximum, Science, 308(5730), 1894-1898.
Westerhold, T., et al. (2012), Revised composite depth scales and integration of IODP Sites U1331-U1334 and ODP Sites 1218-1220, in Proc. IODP, 320/321: Tokyo (Integrated Ocean Drilling Program Management International, Inc.), edited by H. Pälike, M. Lyle, H. Nishi, I. Raffi, K. Gamage, A. Klaus and and the Expedition 320/321 Scientists.
Zachos, J., M. Pagani, L. Sloan, E. Thomas, and K. Billups (2001), Trends, Rhythms, and Aberrations in Global Climate 65 Ma to Present, Science, 292, 686-693.
Zachos, J. C., L. D. Stott, and K. C. Lohmann (1994), Evolution of early Cenozoic marine temperatures, Paleoceanography, 9(353-387).
Zachos, J. C., T. M. Quinn, and K. A. Salamy (1996), High-resolution (104 years) deep-sea foraminiferal stable isotpe records of the Eocene-Oligocene climate transition, Paleoceanography, 11(251-266).

ICDP

Comparison of pollen profiles with the dust proxy from the Antarctic ice core EPICA Dome C since 51.1 ka cal BP

M. WILLE[1], F. SCHÄBITZ[1], THE PASADO SCIENCE TEAM[2]

[1]University of Cologne, Seminar for Geography and Education, Gronewaldstr. 2, 50931 Cologne
[2]http://dc-app1-02.gfz-potsdam.de/site/contacts/contacts-search-all?select=3&term=pasado

The pollen analytical section of the ICDP-PASADO CoreCatcher Project (DFG SCHA 472/12) is in its final stage. Two core catcher profiles (sample resolution: 3m) have been analyzed to help to identify the most promising sediment record to provide a composite core of the ICDP-PASADO deep drilling at Laguna Potrok Aike. This maar lake, located at 52°S 70°W in the Province of Santa Cruz, Argentina, is one of the few permanent lakes in the area, providing a unique continuous lacustrine record of the climatic and ecological history. The two analyzed pollen records from holes 1D and 2C show considerable differences in quality. The record of hole 1D has several gaps because of low pollen content probably associated with the generally coarser-grained sediments. Although the almost continuous record of hole 2C is better suited for interpretation, major changes are recognized in both pollen records. In total, 65 pollen, 11 spores, 5 algal and 15 other non-pollen-palynomorph types were identified in the core catcher pollen records (Recasens et al. 2011).

Both core catcher pollen records witness climatic changes since the Late Pleistocene and indicate that the study area was covered with Patagonian Steppe vegetation during the last 51.1 ka cal BP (dating: Kliem et al. submitted). The oldest part of both pollen records, corresponding to glacial times, shows a pollen assemblage of dry steppe in the catchment area of Laguna Potrok Aike. In contrast, Nothofagus pollen originates in the Andes ca. 60 km to the west. Fire activity seemed to be comparable with Holocene times. We interpret this pollen signal as glacial, because of a higher contribution of dwarf shrubs, indicating conditions drier than today. However in the Andean area Nothofagus was present probably as shrubs as it occurs today close to its lower temperature limits. Around 80 m conditions changed to considerably lower temperatures and probably lower humidity than before. The uppermost parts of the pollen records confirm the already well-known and well-dated spread of Nothofagus forest in the Andes (Wille et al., 2007). We interpret this pollen signal as a warming with a contemporaneous increase in humidity during the Lateglacial and earliest Holocene times.

As the PASADO composite profile from site 2 (5022-CP2) became available in the course of the project, our focus changed to this record to provide a more detailed picture over the vegetation and climate history of the last 51.1 ka cal BP. At the end of this project a pollen record with 32 cm spatial resolution will be available. In total, 84

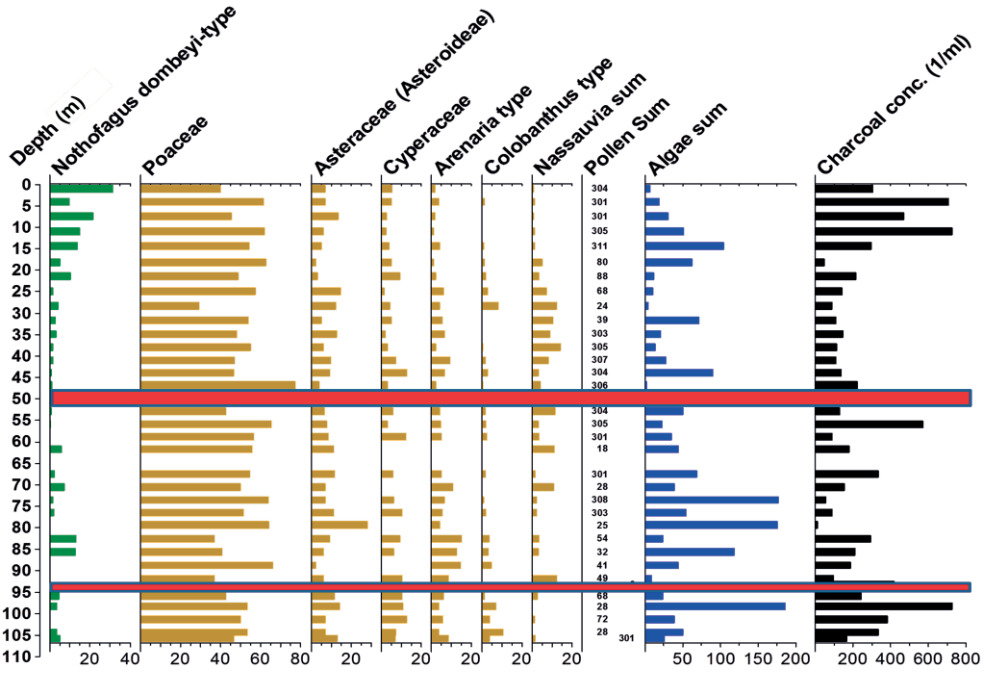

Fig 1: Pollen percentage diagram of selected taxa from core catcher samples of drill site 2C at Laguna Potrok Aike, southern Argentina.

pollen, 14 spores, 5 algal and 17 other non-pollen-palynomorph types were identified in this composite pollen record so far.

The pollen analyses of the composite profile support core catcher results documenting that southern Patagonia was dominated by grass steppe during the last 51.1 ka cal BP. However the much higher resolution already shows some considerable dynamics in the paleo-vegetation. For the first time a comparison with durst records from Antarctica is worthwhile, as it is well known that the dust in Antarctic ice cores originates from Patagonia (eg. Delmonte et al. 2002). A detailed interpretation and integration into the results from other proxies will be the future task. However, a preliminary interpretation based on pollen can be given already here:

The lowermost section of the pollen record shows steppe vegetation with a considerable amount of shrubby taxa and reduced dominance of grasses. The contribution of the Andean taxa reaches Late Glacial values. The dust concentration in this section is low. In summary the vegetation in Patagonia was relatively dense probably due to sufficient available moisture and/or wind speed was low. The following section (50-32 ka cal BP) shows a glacial pollen signal with low contribution of Andean taxa. Dust supply is increased but still relatively low. It is remarkable that the increase of dust transport to Antarctica is synchronous to a period with higher amounts of charcoal in Laguna Potrok Aike. This might be the start of cooler and significantly drier conditions. It was shown that fires become more frequent in times when a transition to drier conditions occurs (e.g. Huber et al. 2004). The following period (30-20 cal ka BP) shows the lowest amounts of grasses and highest values of the drought indicator Nassauvia. It is likely that this period is the coldest and driest section of the record. The Late Glacial and Holocene pollen spectra since 18 ka cal BP show the published vegetation dynamics caused by an increase of temperature and humidity (Wille et al. 2007).

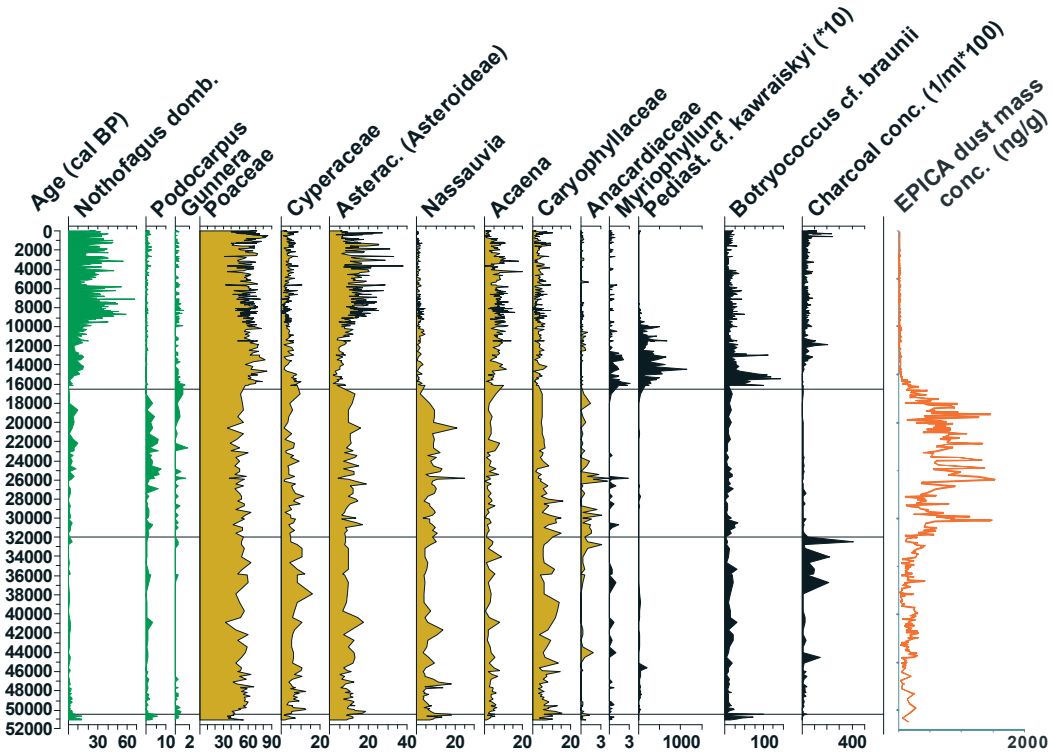

Fig. 2: Pollen percentage diagram of selected taxa of the PASADO composite core at Laguna Potrok Aike, southern Argentina in comparison to the EPICA dust mass concentration profile (Lambert et al. 2008). Core section 16-0 ka is taken from the synchronized SALSA pollen record (Wille et al. 2007) due to its better resolution. Steppe taxa: yellow; Andean taxa: green.

References

Delmonte, B., Petit, J.R., Maggi, V. 2002. LGM-Holocene changes and Holocene millennial-scale oscillations of dust particles in the EPICA Dome C ice core, East Antarctica. Annals of Glaciology 35: 306-312.

Kliem, P., D. Enters, A. Hahn, C. Ohlendorf, A. Lisé-Pronovost, G. St-Onge, S. Wastegård, B. Zolitschka and the PASADO science team 2012. Lithology, radiocarbon chronology and sedimentological interpretation of the lacustrine record from Laguna Potrok Aike, southern Patagonia. Quaternary Science Reviews, submitted.

Lambert, F., Delmonte, B., Petit, J.R., Bigler, M., Kaufmann, P.R., Hutterli, M.A., Stocker, T.F., Ruth, U., Steffensen, J.P., Maggi, V., 2008. Dust-climate couplings over the past 800,000 years from the EPICA Dome C ice core. Nature, Vol. 452: 616-619. doi:10.1038/nature06763.

Recasens, C., Ariztegui, D., Gebhardt, C., Gogorza, C., Haberzettl, T., Hahn, A., Kliem, P., Lisé-Pronovost, A., Lücke, A., Maidana, N., Mayr, C., Ohlendorf, C., Schäbitz, F., St-Onge, G., Wille, M., Zolitschka, B. and the PASADO science team 2011. New insights into paleoenvironmental changes in Laguna Potrok Aike, southern Patagonia, since the Late Pleistocene: The PASADO multiproxy record. The Holocene, doi: 10.1177/0959683611429833.

Wille, M., Maidana, N.I., Schäbitz, F., Fey, M., Haberzettl, T., Janssen, S., Lücke, A., Mayr, C., Ohlendorf, C., Schleser, G.H., Zolitschka, B. 2007. Vegetation and climate dynamics in southern South America: The microfossil record of Laguna Potrok Aike, Santa Cruz, Argentina. Review of Palaeobotany and Palynology 146: 234-246.

ICDP

Environmental instability at the last Glacial – Interglacial transition in Patagonia, Argentina: the stable isotope record of bulk sedimentary organic matter from Laguna Potrok Aike

JIAYUN ZHU[1*], ANDREAS LÜCKE[1], HOLGER WISSEL[1], CHRISTOPH MAYR[2,3], CHRISTIAN OHLENDORF[4], BERND ZOLITSCHKA[4] AND THE PASADO SCIENCE TEAM[5]

[1]Institute of Bio- and Geosciences, IBG-3: Agrosphere, Research Center Jülich, D-52428 Jülich, Germany,
[2]GeoBio-Center and Dept. of Earth and Environmental Sciences, University of Munich, D-80333 Munich, Germany,
[3]Institute of Geography, University of Erlangen-Nürnberg, D-91054 Erlangen, Germany,
[4]GEOPOLAR, Institute of Geography, University of Bremen, D-28359 Bremen, Germany,
[5]PASADO science team as listed at http://www.icdp-online.org/front_content.php?idcat=1494

An investigation of stable isotope ($\delta^{13}C_{TOC}$ and $\delta^{15}N_{TN}$) and elemental parameters (TOC, TN contents and TOC/TN ratios) of bulk organic matter (<200 µm) from sediment cores recovered from the Patagonian maar lake Laguna Potrok Aike (Argentina) (Fig. 1) in the framework of the ICDP deep drilling project PASADO has provided insights into past changes in lake primary productivity and environmental conditions in South Patagonia throughout the last Glacial – Interglacial transition (Zhu et al. submitted).

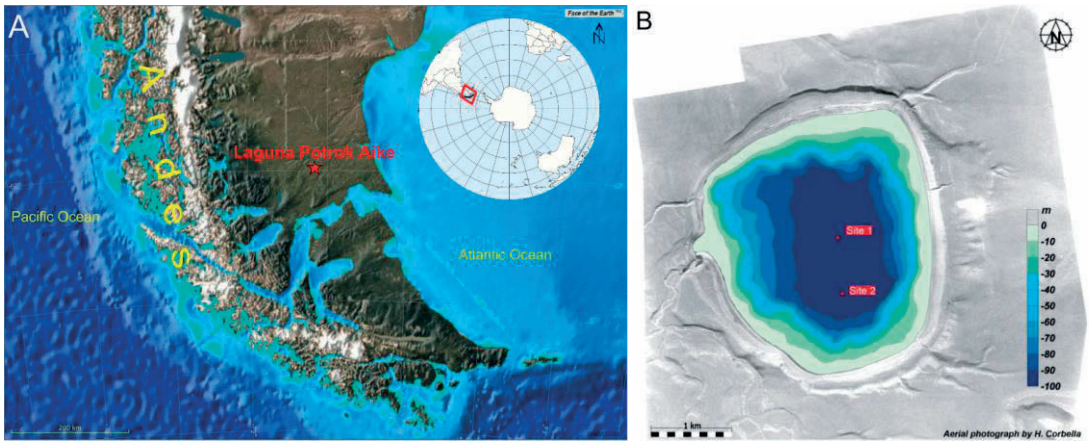

Fig. 1: A) Location of Laguna Potrok Aike (red star) in South Patagonia in the relief map modified from http://jules.unavco.org/voyager/EarthScope. Red frame marked in the inserted map (source: Sean Baker/Wikipedia) shows the location of South Patagonia on the Southern Hemisphere. B) Drilling sites in 2008 in the aerial photography of Laguna Potrok Aike with bathymetry.

We used the samples collected from the 106 m long Site 2 composite profile 5022-2CP (Ohlendorf et al. 2011) which covers the last 51,000 years according to the age-depth model (version 3) established by Kliem et al. (submitted). For analysis we chose the composite depth from 30 to 10 m covering the period between ca. 26,100 – 8,400 cal. years BP including the Last Glacial Maximum (LGM) and the last glacial-interglacial transition. Around 600 samples with 2 cm spatial resolution from sections with undisturbed sediments were measured contiguously with an average temporal resolution of 28 years (Fig. 2). In addition, about 100 samples from sections with re-deposited sediments were measured at 8 cm intervals for carbon and at 16 cm intervals for nitrogen isotope analyses, respectively (Fig. 2).

Stratigraphically constrained cluster analyses of all proxy parameters suggest four main phases. From ca. 26,100 to 17,300 cal. years BP (phase 1), lake phytoplankton was presumably the predominant organic matter source in an aquatic environment with low primary productivity rates. At around 17,300 cal. years BP, an abrupt and distinct shift of isotopic and elemental values indicates that the lacustrine system underwent a rapid reorganization. Lake primary productivity (phytoplankton and aquatic macrophytes) shows higher levels albeit with large variations during most of the deglaciation until 13,000 cal. years BP (phase 2). The main causes for this development can be seen in improved growing conditions for primary producers because of deglacial warming in combination with expedient availability of nutrients and likely calm wind conditions. After 13,000 cal. years BP (phase 3), decreased $\delta^{13}C_{TOC}$ values, TOC, TN contents and TOC/TN ratios indicated that the lake approached a new state with reduced primary productivity probably induced by unfavorable growing conditions for primary producers like strengthened winds and reduced nutrient availability. The steady increase in $\delta^{15}N_{TN}$ values suggests limitation of nitrate supply for growth of primary producers resulting from a nutrient shortage after the preceding phase with high productivity. Nitrate limitation and consequent decreased lacustrine primary productivity may continue into the early Holocene (10,970 – 8,400 cal. years BP, phase 4) as reflected by isotopic and elemental values.

It is clear to distinguish phase 1 with low lacustrine primary productivity under LGM conditions from the later phases with high, varied productivity (Fig. 3). Deglaciation warming and improved growth conditions led to a distinct and large shift of lake productivity from phase 1 to phase 2 as there was possibly a relatively sufficient nutrient reserve in Laguna Potrok Aike directly after the glacial phase with little consumption. The primary productivity in Laguna Potrok Aike reached the maximum at around 14,000 cal. years BP (Fig. 2). Simultaneously, the nutrients availability, particularly nitrate, could likely start to become reduced with persistent enhancement in the primary productivity. After 13,000 cal. years BP, lake primary productivity declined progressively documented

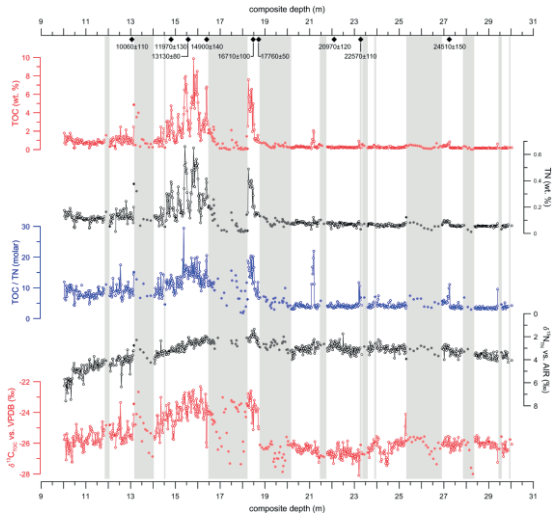

Fig. 2: Downcore changes in carbon and nitrogen isotope compositions, TOC and TN contents (wt. %) and TOC/TN ratios during the investigated period (ca. 10 – 30 m cd) for core 5022-2CP from Laguna Potrok Aike. Measured samples from sections with undisturbed as well as from redeposited sediments defined by Kliem et al. (submitted) are plotted. Composite depths of sections with redeposited sediments are marked by grey bars. Note inverse scale of $\delta^{15}N_{TN}$ values. Black diamonds with numbers on the upper depth scale show the depths of AMS radiocarbon ages (cal. years BP) with error (1σ) given by Kliem et al. (submitted, Tab. 2).

This may explain the negative relationship between carbon and nitrogen isotope compositions over the course of the late Glacial and the early Holocene (Fig. 3, upper left).

The timing of the onset of the last deglacial warming in the southern hemisphere is illustrated in Antarctic ice cores and Southern Ocean sediments at around 17,000 – 19,000 cal. years BP (e.g. Sachs et al. 2001, EPICA 2006, Jouzel et al. 2007, Lamy et al. 2007). Moraine records (e.g. McCulloch et al. 2005, Sugden et al. 2005, Kilian et al. 2007, Kaplan et al. 2008) and palynological evidences from the peat bog records in South Patagonia (e.g. McCulloch & Davies 2001, Markgraf & Huber 2010) have confirmed the terrestrial response to the initial warming signal which also caused the increase in the bio-productivity and the shift from phase 1 to phase 2 in Laguna Potrok Aike. McCulloch et al. (2000) suggested two steps of deglacial warming influencing southern South America at 17,600 and 11,400 cal. years BP. Since in southern Patagonia temperature changes primarily control effective moisture (Markgraf & Huber 2010), that has in turn large impact on the lake-system, both steps can be associated with changes in primary productivity in Laguna Potrok Aike at the onset of phase 2 and phase 4, respectively. A warming induced polewards shift of southern westerlies could take several thousand years to their latitudes today centered on 50° S (McCulloch et al. 2000) corresponding to the windier conditions since around

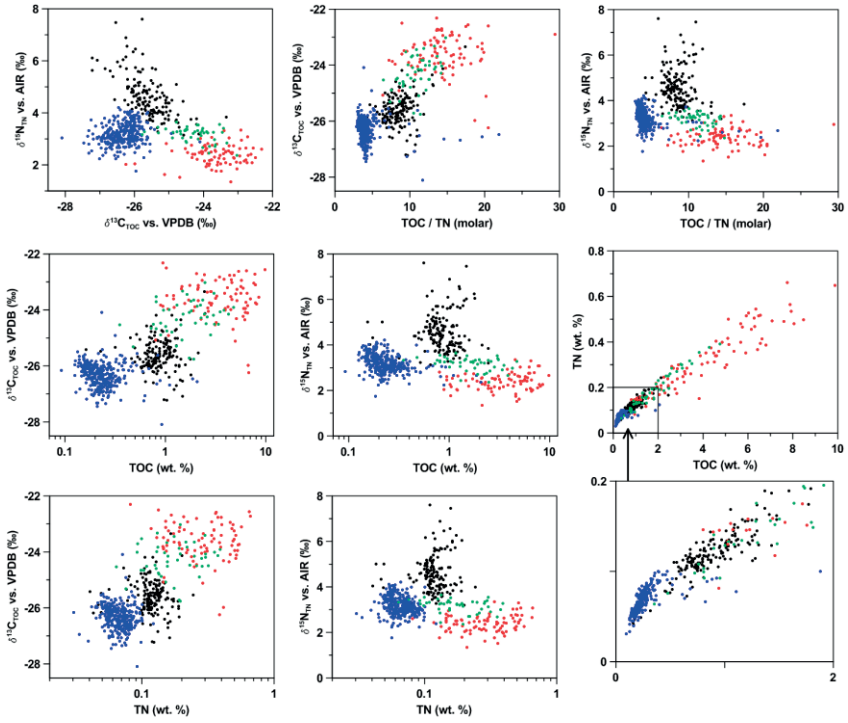

Fig. 3: Cross-plots of the measured proxy parameters for the four main phases (blue: phase 1, 26,075 – 17,300 cal. years BP; red: phase 2, 17,300 – 13,000 cal. years BP; green: phase 3, 13,000 – 10,970 cal. years BP; black: phase 4, 10,970 – 8,400 cal. years BP). The cross-plot of TOC and TN is enlarged in the lower right. Low correlations on the intra-phase scale can be observed, however there are visible inter-phase relationships among the proxy parameters.

by the inter-phase positive relationship between $\delta^{13}C_{TOC}$ values and elemental parameters like TOC, TN contents and TOC/TN ratios (Fig. 3). Under conditions of nitrate limitation, the declined discrimination against ^{15}N by algal assimilation can result in ^{15}N enriched algal organic matter.

13,000 cal. years BP in the Laguna Potrok Aike area. The in Antarctic ice core well illustrated Antarctic Cold Reversal (ACR) (Stenni et al. 2010) is not reflected by our geochemical data. The primary productivity in late-glacial Laguna Potrok Aike appears to be mainly controlled by the

nutrient availability as long as temperature was not low enough to influence the primary producers substantially. However, more investigations particularly comparisons with other proxies in Laguna Potrok Aike are needed to gain a better understanding of the connection between the lake response and the Antarctic signal.

References:

EPICA community members (2006): One-to-one coupling of glacial climate variability in Greenland and Antarctica. – Nature, 444: 195-198.

Jouzel, J., Masson-Delmotte, V., Cattani, O., Dreyfus, G., Falourd, S., Hoffmann, G., Minster, B., Nouet, J., Barnola, J.M., Chappellaz, J., Fischer, H., Gallet, J.C., Johnsen, S., Leuenberger, M., Loulergue, L., Luethi, D., Oerter, H., Parrenin, F., Raisbeck, G., Raynaud, D., Schilt, A., Schwander, J., Selmo, E., Souchez, R., Spahni, R., Stauffer, B., Steffensen, J.P., Stenni, B., Stocker, T.F., Tison, J.L., Werner, M. & Wolff, E.W. (2007): Orbital and millennial Antarctic climate variability over the past 800,000 years. – Science, 317: 793-796.

Kaplan, M., Fogwill, C., Sugden, D., Hulton, N., Kubik, P. & Freeman, S. (2008): Southern Patagonian glacial chronology for the Last Glacial period and implications for Southern Ocean climate. – Quaternary Science Reviews, 27: 284-294.

Kilian, R., Schneider, C., Koch, J., Fesq-Martin, M., Biester, H., Casassa, G., Arévalo, M., Wendt, G., Baeza, O. & Behrmann, J. (2007): Palaeoecological contraints on late Glacial and Holocene ice retreat in the Southern Andes (53°S). – Global and Planetary Change, 59: 49-66.

Kliem, P., Enters, D., Hahn, A., Ohlendorf. C., Wastegård, S., Zolitschka, B. and the PASADO science team (submitted): Lithology, absolute dating and hydrological interpretation of a 51,000 year old lacustrine record, Laguna Potrok Aike (Patagonia). - Quaternary Science Reviews.

Lamy, F., Kaiser, J., Arz, H.W., Hebbeln, D., Ninnemann, U., Timm, O., Timmermann, A. & Toggweiler, J.R. (2007): Modulation of the bipolar seesaw in the Southeast Pacific during Termination 1. - Earth and Planetary Science Letters, 259: 400-413.

Markgraf, V. & Huber, U. (2010): Late and postglacial vegetation and fire history in Southern Patagonia and Tierra del Fuego. - Palaeogeography, Palaeoclimatology, Palaeoecology, 297: 351-366.

McCulloch, R., Bentley, M., Purves, R., Hulton, R., Sugden, D. & Clapperton, C. (2000): Climatic inferences from glacial and palaeoecological evidence at the last glacial termination, southern South America. – Journal of Quaternary Science, 15: 409-417.

McCulloch, R., & Davies, S. (2001): Late-glacial and Holocene palaeoenvironmental change in the central Strait of Magellan, southern Patagonia. – Palaeogeography, Palaeoclimatology, Palaeoecology, 173: 143-173.

McCulloch, R., Fogwill, C., Sugden, D., Bentley, M. & Kubik, P. (2005): Chronology of the last glaciations in central Strait of Magellan and Bahía Inútil, southernmost South America. – Geografiska Annaler, 87 A: 289-312.

Ohlendorf, C., Gebhardt, C., Hahn, A., Kliem, P., Zolitschka, B. and PASADO science team. (2011): The PASADO core processing strategy – A proposed new protocol for sediment core treatment in multidisciplinary lake drilling projects. – Sedimentary Geology, 239: 104-115.

Sachs, J., Anderson, R. & Lehman, S. (2001): Glacial Surface Temperatures of the Southeast Atlantic Ocean. – Science, 293: 2077-2079.

Stenni, B., Buiron, D., Frezzotti, M., Albani, S., Barbante, C., Bard, E., Barnola, J.M., Baroni, M., Baumgartner, M., Bonazza, M., Capron, E., Castellano, E., Chappellaz, J., Delmonte, B., Falourd, S., Genoni, L., Iacumin, P., Jouzel, J., Kipfstuhl, S., Landais, A., Lemieux-Dudon, B., Maggi, V., Masson-Delmotte, V., Mazzola, C., Minster, B., Montagnat, M., Mulvaney, R., Narcisi, B., Oerter, H., Parrenin, F., Petit, J.R., Ritz, C., Scarchilli, C., Schilt, A., Schüpbach, S., Schwander, J., Selmo, E., Severi, M., Stocker, T.F. & Udisti, R. (2011): Expression of the bipolar see-saw in Antarctic climate records during the last deglaciation. - Nature Geoscience, 4: 46-49.

Sugden, D., Bentley, M., Fogwill, C., Hulton, N., McCulloch, R. & Purves, R. (2005): Late-Glacial glacier events in southernmost South America: a blend of 'northern' and 'southern' hemispheric climatic signals? – Geografiska Annaler, 85 A: 273-288.

Zhu, J., Lücke, A., Wissel, H., Mayr, C., Ohlendorf, C., Zolitschka, B. and PASADO science team. (submitted): Environmental instability at the last Glacial – Interglacial transition in Patagonia, Argentina: the stable isotope record of bulk sedimentary organic matter from Laguna Potrok Aike. – Quaternary Science Reviews.

IODP

Deciphering Oligocene climate dynamics using benthic and planktic foraminifera from Site U1334 (IODP Expedition 320)

J. ZIRKEL[1,2], J. O. HERRLE[1,2], H. PÄLIKE[3], D. LIEBRAND[3]

[1]Goethe-University Frankfurt, Institute of Geosciences, D-60438 Frankfurt, Germany
[2]Biodiversity and Climate Research Centre (BIK-F), D-60325 Frankfurt, Germany
[3]School of Ocean and Earth Sciences, University of Southampton, S014 3ZH, United Kingdom

The Oligocene is a critical epoch of the Cenozoic as it marks the initiation of Antarctic ice sheets and consequently the "icehouse" world, which continues to the present day. To document the evolution of the Antarctic ice sheet, it is indispensable to assess and quantify changes in the ocean circulation pattern and the intensity of Pacific equatorial upwelling since the initiation of southern hemisphere ice caps during the Eocene-Oligocene boundary. This project aims at deciphering the mode, tempo, and amplitude of Oligocene glaciation events to unravel the dynamics of Oligocene climate and its impact on equatorial paleoproductivity at orbital to suborbital time-scales from the Central Eastern Pacific Ocean (CEPO). The main focus will be on environmental/climate end-member representatives: the mid-Oligocene Oi-2b maximum glaciation event (~27 Ma) and the weak late Oligocene Oi-2c glaciation event (~24 Ma), using new material from IODP Expedition 320 (Site U1334) of the "Pacific Equatorial Age Transect" (PEAT). These intervals will be studied in high resolution over an interval of ~1Ma. Methods will include a combined approach of benthic (Oridorsalis umbonatus, Cibicidoides grimsdalei and Cibicidoides havanensis) and planktic (Globoquadrina venezuelana) foraminifera oxygen and carbon isotopes as well as trace element geochemistry (Mg/Ca ratios) to reconstruct bottom water temperatures and to calculate ice volume and sea level changes, respectively. In addition, benthic foraminifera accumulation rates and the $\Delta\delta 13C$ of epi- and infaunal benthic foraminifera as indicators for organic matter flux and the $\Delta\delta 13C$ of benthic and planktic foraminifera will be applied to ascertain the strength of the equatorial upwelling as well as the ocean stratification in the Pacific Ocean, the largest reservoir of water, heat, nutrients, and CO2 on Earth.

ICDP

Hydrological variability of the last 50 ka recorded in Laguna Potrok Aike (Pali Aike Volcanic Field, Argentina)

B. ZOLITSCHKA[1], C. OHLENDORF[1], J.-P. BUYLAERT[3], A.C. GEBHARDT[2], A. HAHN[1], P. KLIEM[1], C. MAYR[4,5], S. WASTEGÅRD[6] AND THE PASADO SCIENCE TEAM[7]

[1] Institute of Geography (Geopolar), University of Bremen, Germany – zoli@uni-bremen.de
[2] Alfred Wegener Institute of Polar and Marine Research, Bremerhaven, Germany
[3] Nordic Laboratory for Luminescence Dating, Aarhus University, Denmark
[4] Dept. of Earth and Environmental Sciences, University of Munich, Germany
[5] Institute of Geography, University of Erlangen-Nürnberg, Germany
[6] Department of Physical Geography and Quaternary Geology, Stockholm University, Sweden
[7] PASADO Science Team as cited at: http://www.icdp-online.org/front_content.php?idcat=1494

Semiarid conditions are prevailing at Laguna Potrok Aike (52°S, 70°W; 116 m asl; diameter: 3.5 km, water-depth: 100 m), a currently terminal maar lake in the steppe of southern Patagonia (Coronato et al., 2012; Fig. 1). Here depositional processes are dominantly controlled by the inflow-to-evaporation ratio, a direct function of climate (Ohlendorf et al., 2012). In this climatic zone it is expected that the lake experienced distinct hydrological changes

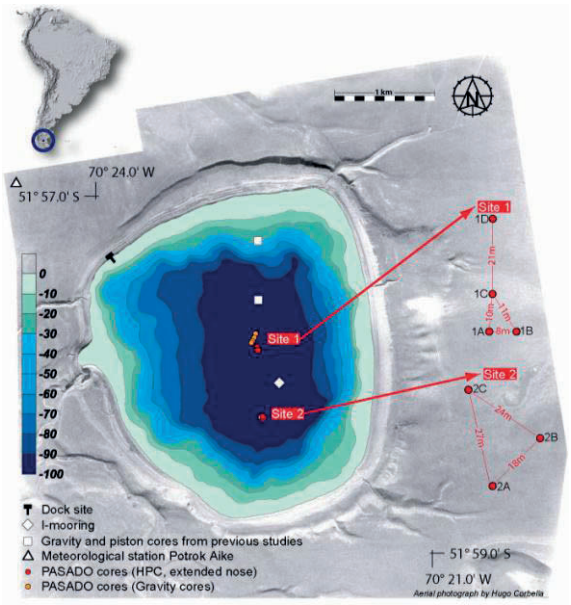

Fig. 1 – Bathymetric map of Laguna Potrok Aike with indicated drilling positions of ICDP expedition 5022 – PASADO (site 1 and site 2). The location of the studied site in South America is shown as insert.

during its history from open to terminal lake conditions, especially at glacial/interglacial temporal scales. The past hydrological variability could have ranged from a freshwater lake with an outflow in which solutes were diluted on the one end to a saline lake where dissolved loads tended to build up over time and increased salinity as well as pH caused the formation of chemical precipitates on the other end. Such distinct changes are reflected in the chemical composition of sediments. Additionally, terminal lakes are characterized by rapid water-depth and shoreline fluctuations resulting from variations in lake area and water volume. These in turn are the trigger for processes of sediment re-deposition and, sometimes, even desiccation of lakes (Kliem et al., 2012a).

Four seismic surveys (Anselmetti et al., 2009; Gebhardt et al., 2011) and a stratigraphic record based on 51 AMS 14C dates (Kliem et al., 2012b) obtained in the framework of ICDP expedition 5022 "Potrok Aike Maar

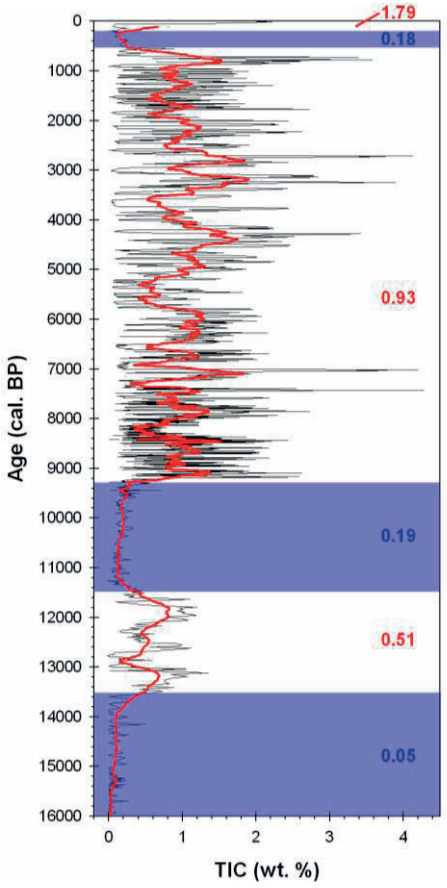

Fig. 2 – Total inorganic carbon (TIC) versus time (PASADO age model V.3 according to Kliem et al., 2012b) as a proxy for increased alkalinity of the lake water causing precipitation of carbonates linked to lake level low stands. Periods when the threshold for formation of carbonates was not passed (i.e. higher lake levels) are shaded in blue. TIC data are plotted as thin line with their 21-point running mean as a red line (data according to Haberzettl et al., 2007). Numbers given at the right relate to mean TIC concentrations for the respective time periods. The mean TIC value is 0.04% for the time before 16 kcal. BP (not shown, according to Recasens et al., 2012).

Lake Sediment Archive Drilling Project" (PASADO: Zolitschka et al., 2009) provide a database to compare the 106 m composite profile from the lake centre (site 2; Fig. 1) with piston cores from the lake shoulder (Haberzettl et al. 2008, 2009) and outcrops in the catchment (Kliem et al., 2012a). Based on event correlation using distinct volcanic ash layers with unique geochemical composition (Wastegard et al., 2012) and additional optically stimulated luminescence (OSL) dates on feldspars (Buylaert et al., 2012), lake core and outcrop sediment records are firmly

linked. Moreover, this approach allows to match the sediment record with water levels during the past ca. 50 kyrs providing evidence for lake level variations up to 200 m (Kliem et al., 2012a). Seismic reflection data even points to very low lake levels before ca. 55 kcal BP (Gebhardt et al., 2012). This is supported by dune-like structures in the eastern lake basin unconformably overlain by a series of paleo-shorelines as interpreted from seismic records. This suggests a rapidly rising lake level after a period of desiccation. Flooding of the lake basin ended with freshwater lake conditions established a couple of millennia later which continued until the early Late Glacial (Fig. 2).

The end of the Pleistocene is characterized by transitions between clastic-dominated (high inflow lake conditions, perhaps with an outflow) and carbonate-rich (end lake conditions) sediments (Jouve et al., 2012; Zhu et al., 2012; Fig. 2). During the late Pleistocene (13.5-11.5 kcal BP) carbonate is precipitated biologically, e.g. as shells of the green algea Phacotus, whereas at the transition from the Late Glacial to the early Holocene (11.5-9.3 kcal BP) clastic sediments regain dominance. Since 9.3 kcal BP intense carbonate precipitation (up to 35% calcite) is recorded that continues until today with one marked interruption during the neoglacial "Little Ice Age" (Haberzettl et al., 2007).

Such geochemical changes are related to hydrological variability which is probably caused by (1) changes in runoff due to permafrost sealing of the ground during the Pleistocene (Kliem et al., 2012a), (2) changes in intensity and position of the Southern Hemispheric Westerlies linked to variations in precipitation and wind-induced evaporation (Ohlendorf et al., 2012; Pollock & Bush, 2012) and (3) the Glacial to Holocene temperature increase (Toggweiler, 2009).

Acknowledgements

This study is supported by the International Continental Scientific Drilling Program (ICDP) in the framework of the "Potrok Aike Maar Lake Sediment Archive Drilling Project" (PASADO). Funding for drilling was provided by the ICDP, the German Science Foundation (DFG grants ZO-102/11-1,2), the Swiss National Funds (SNF), the Natural Sciences and Engineering Research Council of Canada (NSERC), the Swedish Vetenskapsradet (VR) and the University of Bremen.

For their invaluable help in field logistics we thank the staff of INTA Santa Cruz, the Moreteau family and the DOSECC drilling crew.

References:

Anselmetti, F.S., Ariztegui, D., De Batist, M., Gebhardt, A.C., Haberzettl, T., Niessen, F., Ohlendorf, C., Zolitschka, B. (2009). Environmental history of southern Patagonia unravelled by the seismic stratigraphy of Laguna Potrok Aike. Sedimentology 56: 873-892.

Buylaert, J.P., Murray, A.S., Gebhardt C., Sohbati, R., Ohlendorf, C., Thiel, C., Zolitschka, B. (2012). Luminescence dating of the PASADO core 5022-1D from Laguna Potrok Aike (Argentina) using IRSL signals from feldspar. Quaternary Science Reviews, submitted.

Coronato, A., Ercolano, B., Corbella, H., Tiberi, P. (2012). Glacial, fluvial and volcanic landscape evolution in the Laguna Potrok Aike maar area, southernmost Patagonia, Argentina. Quaternary Science Reviews, submitted.

Fortin, D., Francus, P., Gebhardt, A.C., Hahn, A., Kliem, P., Lisé-Pronovost, A., Royshowdury, R., Labrie, G., St-Onge, G. and the PASADO Science Team (2012). Destructive and non-destructive density determination: method comparison and evaluation from the Laguna Potrok Aike sedimentary record. Quaternary Science Reviews, submitted.

Gebhardt, A.C., De Batist, M., Niessen, F., Anselmetti, F.S., Ariztegui, D., Haberzettl, T., Kopsch, C., Ohlendorf, C., Zolitschka, B. (2011). Deciphering lake and maar geometries from seismic refraction and reflection surveys in Laguna Potrok Aike (southern Patagonia, Argentina). Journal of Volcanology and Geothermal Research 201: 357-363.

Gebhardt, A.C., Ohlendorf, C., Niessen, F., De Batist, M., Anselmetti, F.S., Ariztegui, D., Kliem, P., Wastegård, S., Zolitschka, B. (2012). Seismic evidence of up to 200 m lake-level change in Southern Patagonia since MIS4. Sedimentology, in press. http://dx.doi.org/10.1111/j.1365-3091.2011.01296.x

Haberzettl, T., Corbella, H., Fey, M., Janssen, S., Lücke, A., Mayr, C., Ohlendorf, C., Schäbitz, F., Schleser, G.-H., Wessel, E., Wille, M., Wulf, S., Zolitschka, B. (2007). A continuous 16,000 year sediment record from Laguna Potrok Aike, southern Patagonia (Argentina): Sedimentology, chronology, geochemistry. The Holocene 17: 297-310.

Haberzettl, T., B. Kück, S. Wulf, F. Anselmetti, D. Ariztegui, C. Corbella, M. Fey, S. Janssen, A. Lücke, C. Mayr, C. Ohlendorf, F. Schäbitz, G. Schleser, M. Wille, B. Zolitschka (2008). Hydrological variability and explosive volcanic activity in southeastern Patagonia during Oxygen Isotope Stage 3 and the Holocene inferred from lake sediments of Laguna Potrok Aike, Argentina. Palaeogeography, Palaeoclimatology, Palaeoecology, 259: 213-229.

Haberzettl, T., F.S. Anselmetti, S.W. Bowen, M. Fey, C. Mayr, B. Zolitschka, D, Ariztegui, B. Mauz, C. Ohlendorf, S. Kastner, A. Lücke, F. Schäbitz, M. Wille (2009). Late Pleistocene dust deposition in the Patagonian steppe - extending and refining the paleoenvironmental and tephrochronological record from Laguna Potrok Aike back to 55 ka. Quaternary Science Reviews 28/25-26: 2927-2939.

Hahn, A., P. Kliem, C. Ohlendorf, B. Zolitschka, P. Rosén and the PASADO science team (2012). Climate induced changes in the content of carbonaceous and organic matter of sediments from Laguna Potrok Aike (Argentina) during the past 50 ka inferred from infrared spectroscopy. Quaternary Science Reviews, submitted.

Jouve, G., Francus, P., Lamoureux, S., Provencher-Nolet, L., Hahn, A., Haberzettl, T., Fortin, D., Nuttin, L., and the PASADO Science Team (2012). Microsedimentological characterization using image analysis and XRF as indicators of sedimentary processes and climatic changes during the Late Glacial at Laguna Potrok Aike, Santa Cruz, Argentina. Quaternary Science Reviews, submitted.

Kliem, P., Buylaert, J.P., Hahn, A., Mayr, C., Murray, A., Ohlendorf, C., Veres, D., Wastegård, S., Zolitschka, B. and the PASADO science team (2012a). Magnitude, geomorphologic response and climate links of lake level oscillations at Laguna Potrok Aike, Patagonian steppe (Argentina) . Quaternary Science Reviews, submitted.

Kliem, P., D. Enters, A. Hahn, C. Ohlendorf, A. Lisé-Pronovost, G. St-Onge, S. Wastegård, B. Zolitschka and the PASADO science team (2012b). Lithology, radiocarbon chronology and sedimentological interpretation of the lacustrine record from Laguna Potrok Aike, southern Patagonia. Quaternary Science Reviews, submitted.

Ohlendorf, O., M. Fey, C. Gebhardt, T. Haberzettl, A. Lücke, C. Mayr, F. Schäbitz, M. Wille and B. Zolitschka (2012). Mechanisms of lake-level change at Laguna Potrok Aike (Argentina) - Insights from hydrological balance calculations. Quaternary Science Reviews, submitted.

Pollock, E.W. & Bush, A.B.G. (2012). Atmospheric simulations of the present and past climate of southern South America. Quaternary Science Reviews, submitted.

Recasens, C., D. Ariztegui, C. Gebhardt, C. Gogorza, T. Haberzettl, A. Hahn, P. Kliem, A. Lisé-Pronovost, A. Lücke, NI. Maidana, C. Mayr, C. Ohlendorf, F. Schäbitz, G. St-Onge, M. Wille, B. Zolitschka and the PASADO Science Team (2012). New insights into paleoenvironmental changes in Laguna Potrok Aike, Southern Patagonia, since the Late Pleistocene: the PASADO multiproxy record. The Holocene, in press.

Toggweiler, J.R. (2009). Shifting Westerlies. Science 323: 1434-1435.

Wastegård, S. Veres, D., Kliem, P., Ohlendorf, C., Zolitschka, B. and the PASADO science team (2012). Towards a late Quaternary tephrochronological framework for the southernmost part of South America – the Laguna Potrok Aike tephra record. Quaternary Science Reviews, submitted.

Zhu, J., A. Lücke, H. Wissel, C. Mayr, C. Ohlendorf, B. Zolitschka and the PASADO science team (2012). Environmental instability at the last Glacial – Interglacial transition in Patagonia, Argentina: the stable isotope record of bulk sedimentary organic matter from Laguna Potrok Aike. Quaternary Science Reviews, submitted.

Zolitschka, B., Anselmetti, F., Ariztegui, D., Corbella, H., Francus, P., Ohlendorf, C., Schäbitz, F. and the PASADO Scientific Drilling Team (2009). The Laguna Potrok Aike Scientific Drilling Project PASADO (ICDP Expedition 5022). Scientific Drilling 8: 29-33.

IODP

Evaluating Calcium isotopes as proxy for early diagenetic processes in marine porewaters

B.M.A.TEICHERT [1], C. OCKERT[2], N. GUSSONE[2]

[1]Westfälische Wilhelms-Universität Münster, Institut für Geologie und Paläontologie, Münster, Germany
[2]Westfälische Wilhelms-Universität Münster, Institut für Mineralogie, Münster, Germany

ODP/IODP expeditions have provided during the last years unique sample material to study the porewater Calcium isotope geochemistry in different marine sedimentary settings (Fantle and DePaolo, 2007; Teichert et al., 2009; Turchyn and DePaolo, 2011). In carbonate sediments, dissolution and recrystallization are the dominating processes that can be identified through the Ca isotopic composition of porewater and bulk carbonate enabling even the determination of rates. In clastic dominated settings, the dominating processes are less well understood and seem to be more complicated due to different superimposed processes. The decrease of Ca concentration in the porewater within the upper 100 meters is a general observation and has been agreed on to be the result of authigenic carbonate formation within the sediments. However, the corresponding heavy Ca isotope signal, the predicted result of carbonate formation, has in most locations not been observed. A process had been proposed to overprint this signal with a distinct light signature (Teichert et al., 2009), the release of adsorbed light Ca isotopes from clay minerals. Quite recently, the results from experiments with clay minerals (Ockert et al., in rev.) enable us to clearly monitor this process of cation exchange as a function of clay mineralogy and abundance. It also reveals a significant additional pool of Ca to the porewater which is released if the equilibrium between dissolved and adsorbed Ca is affected by authigenic calcium carbonate formation or ammonium production during organic matter remineralization. The new results offer the unique possibility to observe and characterize the two most dominating processes influencing Ca geochemistry in the upper 100 meters of clastic dominated sequences – the release of light Ca isotopes from clay minerals and authigenic calcium carbonate precipitation – and their interplay.

References:

Fantle, M. S. and DePaolo, D. J., 2007. Ca isotopes in carbonate sediment and pore fluid from ODP Site 807A: The Ca2+(aq)-calcite equilibrium fractionation factor and calcite recrystallization rates in Pleistocene sediments. Geochim. Cosmochim. Acta 71, 2524-2546.

Ockert, C., Gussone, N., Kaufhold, S., Teichert, B. M. A., in review. Isotope fractionation during Ca exchange on clay minerals in a marine environment. Geochim. Cosmochim. Acta.

Ockert, C., Teichert, B. M. A., Gussone, N., in prep. Ca isotope fractionation in marine porewaters: The effect calcium carbonate precipitation, dissolution and cation exchange. Earth Planet. Sc. Lett.

Teichert, B. M. A., Gussone, N., Torres, M. E., 2009. Controls on calcium isotope fractionation in sedimentary porewaters. Earth Planet. Sc. Lett. 279, 373-382.

Turchyn, A. V. and DePaolo, D. J., 2011. Calcium isotope evidence for suppression of carbonate dissolution in carbonate-bearing organic-rich sediments. Geochim. Cosmochim. Acta. 75, 7081-7098.